THE ROLE OF EPIGENETIC MODIFICATIONS IN CANCER PROGRESSION

EDITED BY: Lei Chang, Hongquan Zhang, Atsushi Fujimura, Hanna Lucie Sladitschek and Hailong Pei

PUBLISHED IN: Frontiers in Oncology and Frontiers in Cell and Developmental Biology

frontiers Research Topics

frontiers

ISSN 1664-8714
ISBN 978-2-88966-492-4
DOI 10.3389/978-2-88966-492-4

About Frontiers

Frontiers is more than just an open-access publisher of scholarly articles: it is a pioneering approach to the world of academia, radically improving the way scholarly research is managed. The grand vision of Frontiers is a world where all people have an equal opportunity to seek, share and generate knowledge. Frontiers provides immediate and permanent online open access to all its publications, but this alone is not enough to realize our grand goals.

Frontiers Journal Series

The Frontiers Journal Series is a multi-tier and interdisciplinary set of open-access, online journals, promising a paradigm shift from the current review, selection and dissemination processes in academic publishing. All Frontiers journals are driven by researchers for researchers; therefore, they constitute a service to the scholarly community. At the same time, the Frontiers Journal Series operates on a revolutionary invention, the tiered publishing system, initially addressing specific communities of scholars, and gradually climbing up to broader public understanding, thus serving the interests of the lay society, too.

Dedication to Quality

Each Frontiers article is a landmark of the highest quality, thanks to genuinely collaborative interactions between authors and review editors, who include some of the world's best academicians. Research must be certified by peers before entering a stream of knowledge that may eventually reach the public - and shape society; therefore, Frontiers only applies the most rigorous and unbiased reviews.
Frontiers revolutionizes research publishing by freely delivering the most outstanding research, evaluated with no bias from both the academic and social point of view. By applying the most advanced information technologies, Frontiers is catapulting scholarly publishing into a new generation.

What are Frontiers Research Topics?

Frontiers Research Topics are very popular trademarks of the Frontiers Journals Series: they are collections of at least ten articles, all centered on a particular subject. With their unique mix of varied contributions from Original Research to Review Articles, Frontiers Research Topics unify the most influential researchers, the latest key findings and historical advances in a hot research area! Find out more on how to host your own Frontiers Research Topic or contribute to one as an author by contacting the Frontiers Editorial Office: frontiersin.org/about/contact

THE ROLE OF EPIGENETIC MODIFICATIONS IN CANCER PROGRESSION

Topic Editors:
Lei Chang, Soochow University Medical College (SUMC), China
Hongquan Zhang, Peking University Health Science Centre, China
Atsushi Fujimura, Okayama University, Japan
Hanna Lucie Sladitschek, University of Padua, Italy
Hailong Pei, Soochow University, China

Citation: Chang, L., Zhang, H., Fujimura, A., Sladitschek, H. L., Pei, H., eds. (2021). The Role of Epigenetic Modifications in Cancer Progression. Lausanne: Frontiers Media SA. doi: 10.3389/978-2-88966-492-4

Table of Contents

frontiers in Oncology

EDITORIAL
published: 08 January 2021
doi: 10.3389/fonc.2020.617178

Editorial: The Role of Epigenetic Modifications in Cancer Progression

Atsushi Fujimura[1*], *Hailong Pei*[2], *Hongquan Zhang*[3], *Hanna Lucie Sladitschek*[4] *and Lei Chang*[2*]

[1] Department of Cellular Physiology, Okayama University Graduate School of Medicine, Dentistry, and Pharmaceutical Sciences; Neutron Therapy Research Center, Okayama University, Okayama, Japan, [2] State Key Laboratory of Radiation Medicine and Protection, School of Radiation Medicine and Protection, Collaborative Innovation Center of Radiation Medicine of Jiangsu Higher Education Institutions, Medical College of Soochow University, Suzhou, China, [3] Department of Human Anatomy, Histology and Embryology, Key Laboratory of Carcinogenesis and Translational Research, Ministry of Education, and State Key Laboratory of Natural and Biomimetic Drugs, Peking University Health Science Center, Beijing, China, [4] Department of Molecular Medicine, University of Padua, Padua, Italy

Keywords: chromatin remodeling, histone modifications, noncoding RNAs, microRNA, long noncoding RNA

Editorial on the Research Topic

The Role of Epigenetic Modifications in Cancer Progression

Epigenetics describes multimodal molecular mechanisms that confer a certain phenotype on cell without a change in genotype (1). Chromatin remodelers (e.g. SWI/SNF complex) control opening and shutting a gateway for transcription factors to access genomic loci, and chemical modifications on chromatins (e.g. DNA methylation and histone modifications) regulate transcriptional activities, both resulting in a large-scale alteration of transcriptional landscape (2, 3). Small noncoding RNAs also modulate a transcriptome by targeting a large number of sequence-matched mRNAs and sustain an epigenetic state by triggering and maintaining epigenetic gene silencing of chromatin modifier (4).

In the post-genomic era, epigenetic regulations have been widely investigated to understand the molecular mechanisms underlying transcriptional addiction and phenotypic diversity in cancer cells. In this Research Topic, we have organized a collection of reviews and original research articles that shed light on the epigenetic regulations of cancer cell identity and fate. Chemical modifications in histone proteins, such as acetylation, methylation, phosphorylation, and ubiquitination, alter the structure of chromatin and renew the transcriptional landscape. Since the manner of histone modifications is often dysregulated in cancer, understanding the molecular mechanism by which the modifications contribute to cancer progression is important. Illiano et al. describe that targeting histone lysine demethylases (KDMs) JMJD3/UTX complex by chemical inhibitor, GSKJ4 reduces proliferation activity by downregulating CREB stability in acute myeloid leukemia cells. Lin et al. report that a histone demethylase KDM5c, which specifically demethylates trimethylated and dimethylated H3K4, promotes proliferation activity in colon cancer cells.

During the acquisition of malignant traits, such as metastatic capacity, stemness/dormancy, and therapy-resistance, cells become addicted to a transcriptional mode that is peculiar to cancer. As described by Carvalho and supported by a growing body of evidence, tumor initiation is closely associated with the acquisition of a stem-like state (5). Oncogenic signals drive the rewiring of transcriptional networks and epigenetic states in cells, resulting in a constitutively active expression of stem cell-related genes, such as SOX2, MYC, NANOG, etc. BRACHYURY is one of the well-known stem cell factors. Chen M. et al. introduce the molecular regulation and biological aspects of BRACHYURY in cancer cells, and summarize the clinical relevance in various kinds of cancer. Xu et al. report that BRACHYURY regulates cell cycle and

Edited and reviewed by:
Paolo Pinton,
University of Ferrara, Italy

***Correspondence:**
Atsushi Fujimura
atsushi.fujimura@okayama-u.ac.jp
Lei Chang
changlei@suda.edu.cn

Specialty section:
This article was submitted to Molecular and Cellular Oncology, a section of the journal Frontiers in Oncology

Received: *14 October 2020*
Accepted: *27 November 2020*
Published: *08 January 2021*

Citation:
Fujimura A, Pei H, Zhang H, Sladitschek HL and Chang L (2021) Editorial: The Role of Epigenetic Modifications in Cancer Progression. Front. Oncol. 10:617178. doi: 10.3389/fonc.2020.617178

apoptotic cell death program. In the regulation of a dormant state of cancer cells, Guo et al. describe that ARF-like GTPase 14 (ARL14) controls dormancy in lung adenocarcinoma. Although the concept of dormancy is controversial in cancer biology, there is an increasing body of evidence that cancer stem cells go to a dormant state in a certain niche and several cues awake them to reactivate cancer stem cell-related traits (6). This concept explains, for example, the late-onset bone metastasis from breast cancer.

Cancer stem cells have been identified by the specific expressions of marker protein (e.g. CD133 in glioma, CD44 in breast cancer, etc.) and characterized with self-renewal capacity, tumor-initiating potential, and their malignant behaviors (e.g. epithelial-mesenchymal transition (EMT), metastasis, therapy-resistance, etc.). In the process of the acquisition of the cancer stem cell-related traits, epigenetic reprogramming is considered to play pivotal roles. Shen et al. report that ALKBH4 acts as a suppressor of EMT program and reduces invasion and metastasis of cancer cells. Mechanistically, ALKBH4 controls the levels of histone H3K4me3 modification by interacting with a methyltransferase WDR5.

Therapy-resistance is a clinically important aspect of cancer stem cells. Romero-Garcia et al. describe the roles of DNA methylation in chemoresistance and a wide variety of modified genomic loci in several types of cancer, and summarize the anti-cancer drugs related to the resistance triggered by the methylations. Quagliano et al. describe the hallmarks of epigenetic alteration-induced therapy resistance, and introduce several chemical compounds that inhibit the activities of epigenetic modifiers. They further summarize the possible effects of these inhibitors and the molecular targets in various types of cancer. Chen Q. et al. describe that Annexin A6 (ANXA6) contributes to radioresistance in nasopharyngeal cancer. Mechanistically, ANXA6 inhibits PI3K/AKT/mTOR signaling pathway and thus induces cell-protective autophagy. Chen B. et al. describe that gene silencing or chemical inhibition of CDK8 reduces radioresistance in colorectal cancer.

Implications of RNAs in epigenetic regulations are widely recognized in cancer biology. For example, modifications on RNAs are emerging hallmarks of the genes under epigenetic control. N^6-methyladenosine modification in mRNAs promotes the stability and translation efficiency of these mRNAs, resulting in a dynamic alteration of gene expressions and, thus, cancer cell behavior. The process of this modification and the mode of gene expression are similar to those of DNA modifications: there are Writers, Erasers, and Readers regarding N^6-methyladenosine. Lu et al. describe the molecular process in detail and summarize the impacts in the development of hepatocellular carcinoma. Yu et al. describe each modifier's characteristic in detail and summarize their implications in various types of cancer. Noncoding RNAs are also important for cancer epigenetics. Xu et al. describe that long noncoding RNA LINC-PINT suppresses cellular proliferation of melanoma cells. They provide the evidence that LINC-PINT recruits a histone methylase EZH2 (enhancer of zeste homolog 2) to the loci of proliferation-related genes like PCNA. Zou et al. describe the significance of single-nucleotide variants in long intergenic non-protein coding RNAs. Wang et al. demonstrate microRNA miR-27a targets EGFR and its phosphorylation, resulting in suppression of cutaneous squamous cell carcinoma. As one of the emerging evidence that RNA editors are important for epigenetic regulation in cancer, Chen J. et al. report a large number of RNA editing sites, which are associated with hepatocellular carcinoma.

AUTHOR CONTRIBUTIONS

AF and LC wrote the manuscript. All authors contributed to the article and approved the submitted version.

FUNDING

LC is supported by National Natural Science Foundation of China (Grants No: 31971165), the Fok Ying-Tong Education Foundation, China (Grants No: 171017), the Natural Science Foundation of Jiangsu Province (Grants No: KB20191422). AF is supported by Grant-in-Aid for Scientific Research from the Ministry of Education, Culture, Sports, Sciences, and Technology of Japan (20K07618) and the Japan Agency for Medical Research and Development (AMED) (18072932 and 20318557) (AF).

REFERENCES

1. Meissner A. Epigenetic modifications in pluripotent and differentiated cells. *Nat Biotechnol* (2010) 28(10):1079–88. doi: 10.1038/nbt.1684
2. Petty E, Pillus L. Balancing chromatin remodeling and histone modifications in transcription. *Trends Genet* (2013) 29(11):621–9. doi: 10.1016/j.tig.2013.06.006
3. Azad GK, Swagatika S, Kumawat M, Kumawat R, Tomar RS. Modifying Chromatin by Histone Tail Clipping. *J Mol Biol* (2018) 430(18 Pt B):3051–67. doi: 10.1016/j.jmb.2018.07.013
4. Duempelmann L, Skribbe M, Bühler M. Small RNAs in the Transgenerational Inheritance of Epigenetic Information. *Trends Genet* (2020) 36(3):203–14. doi: 10.1016/j.tig.2019.12.001
5. Zanconato F, Cordenonsi M, Piccolo S. YAP/TAZ at the Roots of Cancer. *Cancer Cell* (2016) 29(6):783–803. doi: 10.1016/j.ccell.2016.05.005
6. De Angelis ML, Francescangeli F, La Torre F, Zeuner A. Stem Cell Plasticity and Dormancy in the Development of Cancer Therapy Resistance. *Front Oncol* (2019) 9:626. doi: 10.3389/fonc.2019.00626

Conflict of Interest: The authors declare that the research was conducted in the absence of any commercial or financial relationships that could be construed as a potential conflict of interest.

frontiers in Cell and Developmental Biology

ORIGINAL RESEARCH
published: 15 October 2019
doi: 10.3389/fcell.2019.00238

Silencing of *ARL14* Gene Induces Lung Adenocarcinoma Cells to a Dormant State

Fei Guo, Dexiao Yuan, Junling Zhang, Hang Zhang, Chen Wang, Lin Zhu, Jianghong Zhang, Yan Pan and Chunlin Shao**

Institute of Radiation Medicine, Fudan University, Shanghai, China

Recently, a growing number of ADP ribosylation factor (ARF) family members has been suggested to be critical in tumorigenesis. However, the effects of most ARF members on lung adenocarcinoma pathogenesis are still not well disclosed yet. In this study, *ARF-like GTPase 14 (ARL14)* was screened as an important prognostic factor of lung adenocarcinoma from The Cancer Genome Atlas (TCGA) database and validated by our *in vitro* experiments. It was found that silencing of *ARL14* gene inhibited cell proliferation and the abilities of cell migration and invasion, and it also attenuated radiation damage of lung adenocarcinoma cells but had no effect on the proliferation of normal lung cells. Notably, *ARL14* siRNA blocked the extracellular signal-regulated kinase (ERK)/p38 signaling pathway and induced cell cycle arrest in G0 phase, ultimately leading to cell dormancy. Moreover, *ARL14* siRNA enhanced the expression of *cell death activator DFFA-like effector* (*CIDEC*) that had opposite roles in cell proliferation and migration to *ALR14*. Collectively, our results suggest that *ARL14* has an important role in the pathogenesis of lung adenocarcinoma through CIDEC/ERK/p38 signaling pathway, and thus it could be applied as a new candidate of prognosis indicator and/or therapeutic target of lung adenocarcinoma.

Keywords: *ARL14*, *CIDEC*, ERK/p38, lung cancer dormancy, radiation

OPEN ACCESS

Edited by:
Lei Chang,
Soochow University Medical College (SUMC), China

Reviewed by:
Guan Jian,
Southern Medical University, China
Yamei Tang,
Sun Yat-sen University, China

****Correspondence:***
Yan Pan
swallowpan@fudan.edu.cn
Chunlin Shao
clshao@shmu.edu.cn

Specialty section:
This article was submitted to Molecular and Cellular Oncology, a section of the journal Frontiers in Cell and Developmental Biology

Received: *27 August 2019*
Accepted: *01 October 2019*
Published: *15 October 2019*

Citation:
Guo F, Yuan D, Zhang J, Zhang H, Wang C, Zhu L, Zhang J, Pan Y and Shao C (2019) Silencing of ARL14 Gene Induces Lung Adenocarcinoma Cells to a Dormant State. Front. Cell Dev. Biol. 7:238. doi: 10.3389/fcell.2019.00238

INTRODUCTION

With the development of diagnostic techniques and treatment strategies, significant improvements have been made in the quality of life of patients with lung cancer; however, malignant lung tumors still show the highest morbidity and mortality rates among cancer types (Siegel et al., 2017), with only 16.8% of patients surviving for 5 years after diagnosis (Ridge et al., 2013). Given the variability between pathology and etiology, lung cancer can be subdivided into non-small cell lung cancer (NSCLC) and small cell lung cancer (SCLC) (Sharma et al., 2007; Cheng et al., 2015). Approximately 40% of all lung cancer cases are lung adenocarcinoma, which is the most common type of NSCLC (Xue et al., 2018). The prognosis of patients with lung adenocarcinoma is extremely poor because of the lack of effective treatment measures against metastatic lung cancer. Therefore, studies to determine the molecular mechanisms governing the oncogenesis and metastasis process of lung adenocarcinoma are urgently needed.

ADP ribosylation factor-like GTPase 14 (*ARL14*), also known as *ARF7*, belongs to the ADP ribosylation factor (ARF) family of GTP-binding proteins of the Ras superfamily and it is the closest homolog of *ARL11* (Yendamuri et al., 2007). The *ARL11* polymorphisms Trp149Stop and Cys148Arg have been shown to be associated with a high risk of familial cancers, such as breast,

ovarian, colorectal, and hematological malignancies, among others (Calin et al., 2005; Frank et al., 2006; Masojc et al., 2006; Siltanen et al., 2008; Yang et al., 2009; Hamadou et al., 2017). *ARL11* was also reported as a novel tumor suppressor gene in lung and prostate cancer (Yendamuri et al., 2007, 2008; Siltanen et al., 2013). However, the function of *ARL14* in the formation and progression of human cancer is unknown.

This study was conducted to determine the function and possible underlying mechanisms of *ARL14* in lung adenocarcinoma tumorigenesis. Our results revealed the contribution of *ARL14* in lung adenocarcinoma tumorigenesis and suggested that *ARL14* might have potential implication as a diagnostic biomarker and therapeutic target for lung adenocarcinoma.

MATERIALS AND METHODS

Cell Culture and Irradiation

Human lung bronchial epithelial BEAS-2B cells and human lung cancer PC9 cells were obtained as gifts from the Nanjing Medical University and School of Life Sciences of Fudan University, respectively. They were cultured in Dulbecco's Modified Eagle Medium (DMEM). Human non-small-cell lung cancer A549 cells and human lung fibroblast MRC-5 cells were purchased from Shanghai Cell Bank (Shanghai, China) and cultured in DMEM and α-modified Eagle medium (MEM), respectively. All cells were cultured with suitable medium contained 10% fetal bovine serum (FBS, Gibco, Invitrogen, United States), 100 U/ml penicillin and 100 μg/ml streptomycin, and incubated at 37°C and 5% CO_2 atmosphere. For irradiation treatment, cells were exposed to different doses of γ-rays as described previously (He et al., 2014).

Transient Transfection of SiRNA

Short interfering RNAs (siRNAs) against *ARL14*, cell death activator DFFA-like effector (*CIDEC*) and their negative controls (RiboBio Biotechnology, Guangzhou, China) were transfected into cells with lipofectamine 2000 (Invitrogen, Carlsbad, CA, United States) following the manufacturer's protocol. The target sequences of these transiently transfected siRNAs are listed in **Supplementary Table S1**.

Cell Growth and Cloning Efficiency Assays

Following siRNA transfection for 24 h, 1000 cells/well were plated into a 96-well plate and incubated for 24, 48, 72, 96, or 120 h and then measured by Cell Counting Kit-8 assay (CCK-8, Dojindo Laboratories, Kumamoto, Japan) at an absorbance of 450 nm. For the cloning efficiency assay, 200–300 cells/well were seeded into six-well culture plates and grown for 10–14 days. The number of colonies containing more than 50 cells was counted and normalized to corresponding control.

Radiation Sensitivity Assay

After siRNA transfection for 24 h, 1500–2500 cells/well from all groups were plated onto a 96-well plate and incubated for 24 h. After irradiation with γ-ray at 0, 2, 4, and 8 Gy, the cells were further cultured for 96 h and then issued for cell proliferation assay described above.

Cell Migration and Invasion Assay

In vitro transwell assays were performed to assess cell migration and invasion abilities as previously described (Pan et al., 2016). Briefly, for the migration assays, 5–7 × 10^4 serum-starved cells were cultured with serum-free medium in a upper insert dish containing enormous 8-μm-diameter pores in its bottom membrane (Corning Inc., Corning, NY, United States) companied with a 6-well plate chamber filled with DMEM containing 10% FBS. For the invasion assays, the above insert dish was replaced with one coated with 1 μg/mL Matrigel (Corning). After 24 h of culture, the cells were fixed with 100% methanol for 30 min and stained with crystal violet staining solution (Beyotime, Shanghai, China) for 25 min. Cells on the upper surface of the insert dish bottom were carefully removed using a wet cotton swab and those that had migrated through the membrane were photographed and counted in five random fields (×10) using an inverted microscope.

Western Blot Assay

Western blot analysis for specific protein expression was performed as previously described (Wang et al., 2017). The antibodies used in this study are listed in **Supplementary Table S2**.

Immunofluorescence Assay of Ki67 Protein

For all groups, 2–4 × 10^4 cells plated on culture slides were incubated for 48 h at 37°C in 5% CO_2, and then the exponentially growing cells were fixed with immune staining fix solution and treated with enhanced immunostaining permeabilization buffer for 15 min at room temperature. Next, non-specific antibody binding sites were blocked with QuickBlock™ blocking buffer for immunological staining for 1 h. Ki67 primary antibody at appropriate dilutions was added and incubated at 4°C overnight followed by further incubation for 1 h at room temperature in the dark with Alexa Fluor® 594 goat anti-mouse IgG (H + L) (Thermo Fisher Scientific, Waltham, MA, United States). Finally, the cell nuclei were counterstained with DAPI Fluromount-G™ (Southern Biotech, Birmingham, AL, United States) for 5 min. The Ki67 positive cells were examined using a Zeiss Axioplan fluorescence microscope (Oberkochen, Germany).

RNA Isolation and Quantitative Real-Time PCR Analysis

Total RNA was isolated from cells using a MiniBEST Universal RNA Extraction Kit (Takara, Shiga, Japan). Reverse transcription and real-time PCR (qRT-PCR) were performed with PrimeScript™ RT Master Mix (Perfect Real Time, Takara) and SYBR® Premix Ex Taq™ II (Tli RNaseH Plus, Takara) following the manufacturer's instructions. The gene-specific primers are shown in **Supplementary Table S3**. The relative

expression level of mRNA was examined as the inverse log of the delta CT and normalized to the reference gene, β-actin.

Cell-Cycle Analyses

Following siRNA transfection and 8 Gy γ-ray radiation treatment, the cells were grown in an incubator with 5% CO_2 at 37°C for 24 h and then collected, fixed in 70% cold ethanol, and stored at −20°C overnight. The cell pellets were washed twice with 1 × phosphate-buffered saline and centrifuged at 1000 × *g* and 4°C for 10 min, following by staining with a cell cycle kit (BD Biosciences, Franklin Lakes, NJ, United States) according to the manufacturer's instructions. The total cellular DNA content was analyzed with a flow cytometer (Beckman, Brea, CA, United States) by acquiring data for at least 10,000 events.

Gene Set Enrichment Analysis (GSEA)

Gene set enrichment analysis (GSEA 3.0)[1] was used to explore potential KEGG pathway and GO analysis within the Molecular Signatures Database (MSigDB 6.0) of c2 (curated gene sets) and c5 (GO gene sets). Setting *ARL14* gene expression levels as population phenotypes in GSEA, we analyzed gene expression omics predictions and assessed related pathways in lung adenocarcinoma. A nominal *P*-value <0.05 and false discovery rate (FDR) <0.25 of the enrichment gene sets in the analysis were considered statistically significant. The theory and process of GSEA have been described previously (Subramanian et al., 2005).

Statistical Analysis

All data were obtained from 3 to 5 independent experiments and presented as the means ± SE. Statistical analyses were analyzed with Student's *t*-tests using SPSS 19.0 software (SPSS, Inc., Chicago, IL, United States). $P < 0.05$ was considered to be statistically significant difference between treatment groups.

RESULTS

ARL14 Is a Candidate Prognostic Factor for Lung Adenocarcinoma

Analyzing the data of lung adenocarcinoma samples and matched normal control tissues obtained from The Cancer Genome Atlas (TCGA) online resource, we found that the mRNA expression of *ARL14* in lung adenocarcinoma samples was significantly higher than that in the matched normal tissues (**Figure 1A**, $N = 57$, fold change = 2.3, $P = 1.23E-06$), and the expression of *ARL14* in adenocarcinoma had a very strong negative correlation with the overall survival of those lung cancer patients (**Figure 1B**, $N = 482$, $P = 4.12E-04$). In comparison with the mean level, the lower level of *ARL14* mRNA corresponds to the higher survival. Our measurement further confirmed that the expression levels of *ARL14* in lung adenocarcinoma cells (A549 and PC9) were higher than that in normal lung cells (BEAS-2B and MRC-5) (**Figure 1C**), which is consistent with the results obtained from TCGA cohort. Therefore, *ARL14* might become a candidate prognostic factor of lung adenocarcinoma development and is worthy of further investigation of its function.

Knockdown of *ARL14* Suppresses Proliferation, Migration, and Invasion of Lung Adenocarcinoma Cells

To investigate the functions of *ARL14* in lung adenocarcinoma cells, *ARL14* gene expression in A549 and PC9 cells was interfered with siRNA and the silencing effect was detected by qRT-PCR and Western blot assays. As shown in **Figures 1D,E**, siARL14-1 (hereafter called siARL14) had the most effective efficiency in knock-down *ARL14* expression and thus was applied for the following studies. It was found that siARL14 significantly inhibited cell proliferation (**Figure 1F**) and cell colony formation ability (**Figure 1G**) for both A549 and PC9 tumor cells. In addition, siARL14 also effectively suppressed the expression of *ARL14* in normal lung cells MRC-5 and BEAS-2B (**Figures 1H,I**), however, it had no influence on the proliferation and cloning efficiency of both normal lung cells (**Figures 1J,K**). These results suggest that *ARL14* may have some special function in cancer cells, which could influence the outcome of radiotherapy. To confirm this hypothesis, we studied the influence of siARL14 on radiation responses of lung adenocarcinoma cells. Results showed that cell proliferations of A549 and PC9 were decreased by γ-ray irradiation in a dose dependent manner, but this decrease was effectively weakened when *ARL14* was knocked down in these cells (**Figure 1L**). In addition, radiation reduced the abilities of migration and invasion of A549 and PC9 cells but it had no obvious influence on the migration and invasion of siARL14-transfected cells although siARL14 itself suppressed cell migration and invasiveness (**Figures 1M,N**).

Knockdown of *ARL14* Induces Lung Adenocarcinoma Cells to Dormancy

Uncontrolled proliferation is a well-established hallmark of cancer cells. Nearly all human cancers have deregulated control in cell-cycle progress. G0 phase is an important check-point when cells decide to begin proliferation or remain quiescence. We monitored the cell cycle distribution by flow cytometer at 24 h after irradiation and found that A549 and PC9 cells were arrested in G2/M phase in accompany with a reduction of cells in G1 phase (**Figure 2A** and **Supplementary Table S4**). When the cells were transfected with siARL14, radiation-induced G2/M arrest was effectively released, especially for A549 cells. In fact, silencing of *ARL14* expression resulted in G0/G1 phase accumulation of A549 cells (**Figure 2A**).

Ki67 protein is an indicator of cell proliferation (Bruno and Darzynkiewicz, 1992). Our immunofluorescence experimental results showed that about 80% cells in the logarithmic growth population of A549 and PC9 had positive Ki67 expression, but when the cells were interfered with siARL14, the ratios of Ki67-positive cells were obviously decreased in both cell lines (**Figures 2B,C**), indicating cell proliferation ability was attenuated by siARL14.

Imbalance of extracellular signal-regulated kinase (ERK)/p38 signaling activities has also been suggested to determine

[1] http://software.broadinstitute.org/gsea/index.jsp

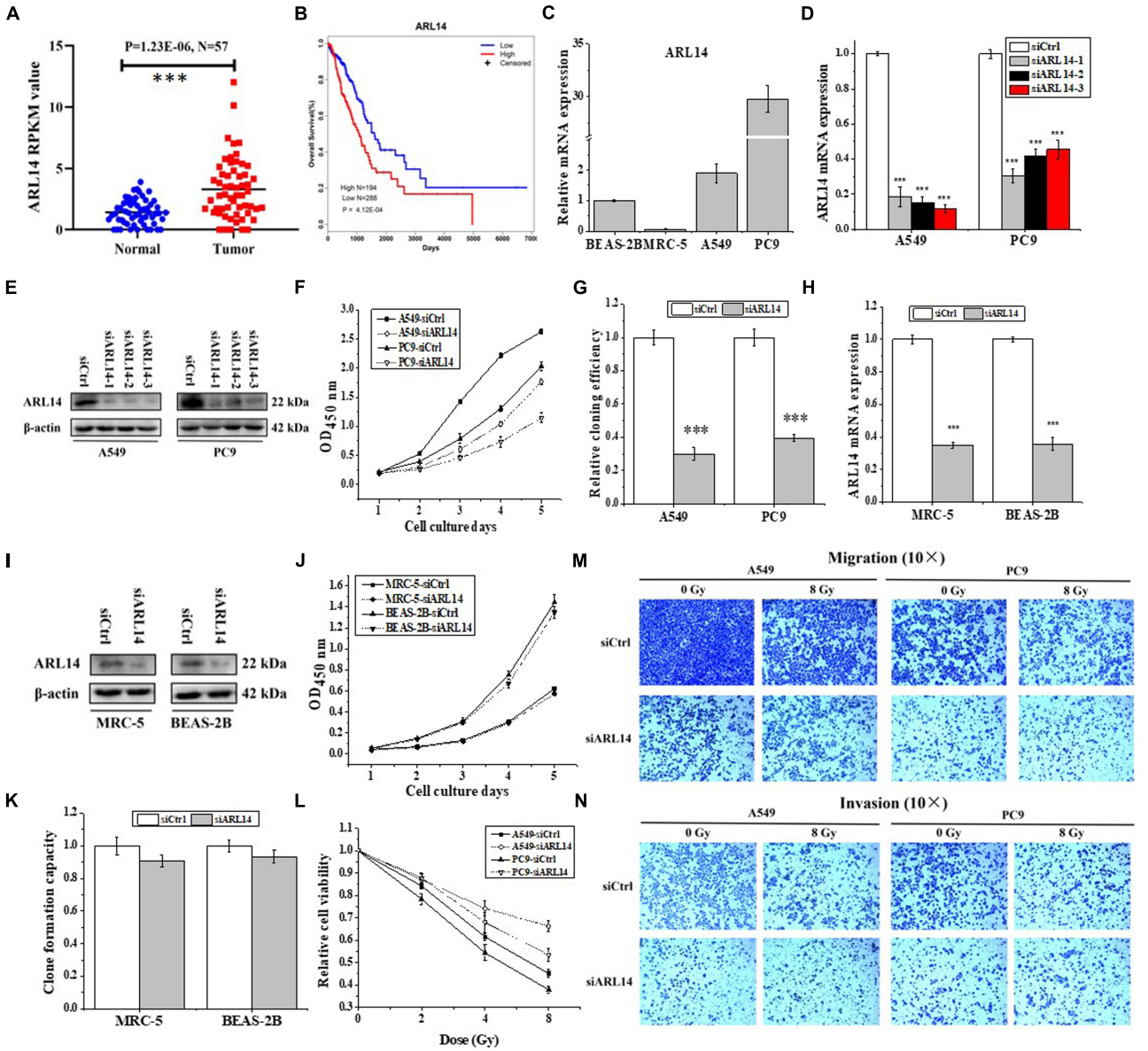

FIGURE 1 | *ARL14* is a potential prognostic biomarker for lung adenocarcinoma and contributes to proliferation, radiosensitivity, migration, and invasion of lung adenocarcinoma cells. **(A)** The expression levels of *ARL14* mRNA in lung adenocarcinoma samples and matched normal control tissues ($N = 57$) in the TCGA cohort. **(B)** Kaplan–Meier analysis of the correlation between *ARL14* level and overall survival of lung adenocarcinoma patients with high ($N = 194$) and low ($N = 288$) *ARL14* expression in the TCGA cohort. Cut-off value for evaluation of *ARL14* mRNA level was the mean expression of 482 lung adenocarcinoma samples. **(C)** The expression levels of *ARL14* mRNA in BEAS-2B, MRC-5, A549, and PC9 cells. **(D,E)** The expressions of *ARL14* mRNA **(D)** and protein **(E)** were reduced in A549 and PC9 cells transfected with *ARL14* siRNAs for 48 h. **(F,G)** Silencing of *ARL14* decreased proliferation **(F)** and cloning efficiency **(G)** of A549 and PC9 cells significantly. **(H,I)** The expressions of *ARL14* mRNA **(H)** and protein **(I)** in MRC-5 and BEAS-2B cells transfected with *ARL14* siRNAs for 48 h. **(J,K)** Silencing of *ARL14* had no significant influence on proliferation **(J)** and cloning efficiency **(K)** of MRC-5 and BEAS-2B cells. **(L)** The dose responses of the viability of A549 and PC9 cells with or without *si*ARL14 transfection. **(M,N)** The migration and invasion activities of A549 and PC9 cells with or without *ARL14* siRNA transfection. After siRNA transfection, cells were irradiated with 8 Gy γ-rays. $^{***}P < 0.001$ compared with the corresponding control.

carcinoma cell proliferation or dormancy (Aguirre-Ghiso et al., 2001, 2003; Ranganathan et al., 2006). We wonder whether ERK and p38 signaling pathways are regulated by *ARL14* in lung adenocarcinoma cells. It was found that when *ARL14* in A549 and PC9 cells was silenced, both total protein and its phosphorylation level of ERK1/2 were increased and p-p38 protein was activated (**Figure 2D**). A high level of ERK1/2 activity contributes to the promotion of cell proliferation (Aguirre-Ghiso et al., 2001, 2003; Lents et al., 2002; Ranganathan et al., 2006; Chambard et al., 2007). But here silencing *ARL14* caused a distinct decreased cell proliferation, indicating that the ERK signaling pathway is blocked by knockdown of *ARL14* expression, which

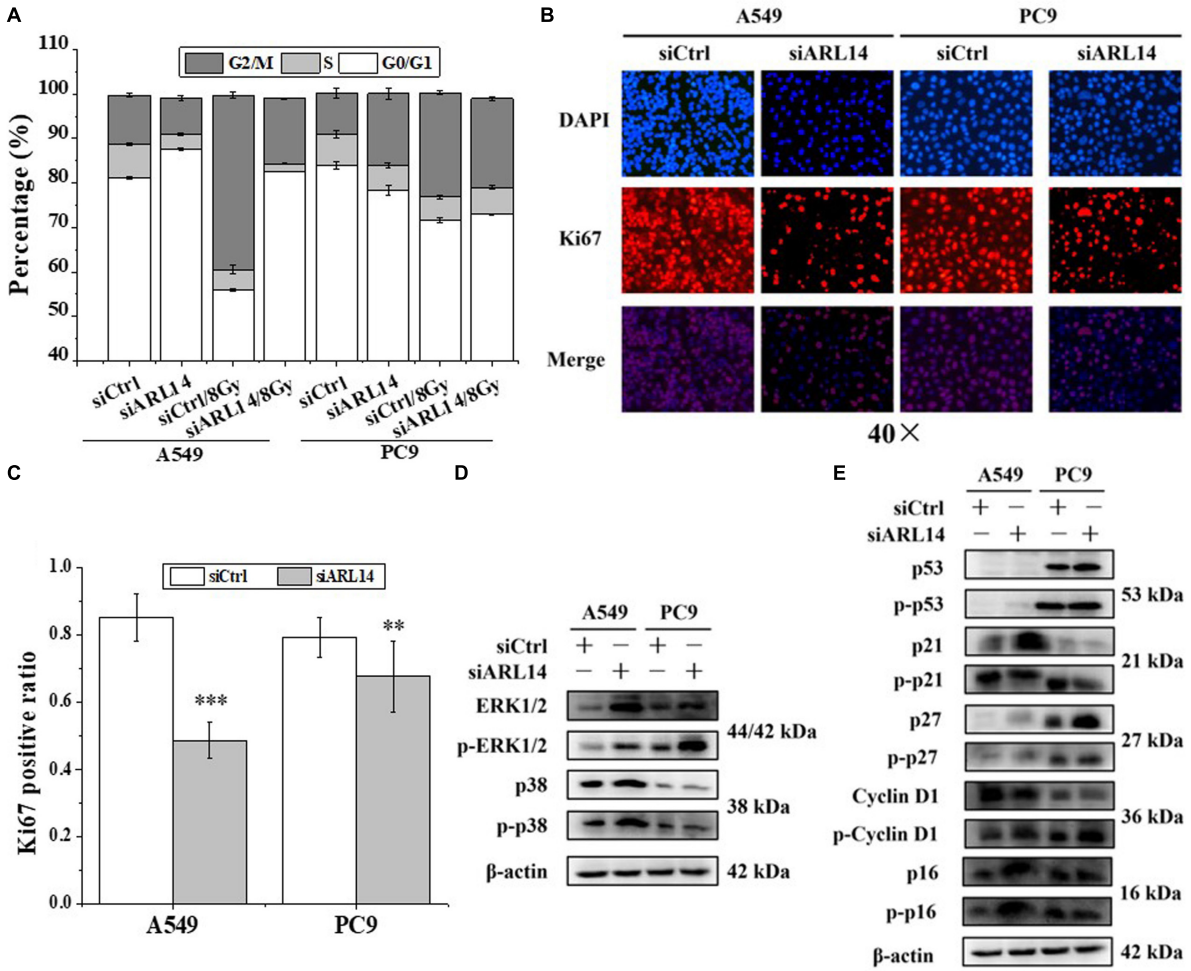

FIGURE 2 | Down-regulation of *ARL14* expression induced quiescence of lung adenocarcinoma cells in G0/G1 phase and inhibited cell proliferation. **(A)** Effects of *ARL14* siRNA on cell cycle distribution and radiation-induced G2/M phase arrest of A549 and PC9 cells. **(B,C)** Ki67 positive ratio in A549 and PC9 cell population transfected with *ARL14* siRNA. **(D,E)** The proteins and their phosphorylation levels of ERK and p38 **(D)**, p16, cyclin D1, p27, p21, and p53 **(E)** in A549 and PC9 cell population transfected with *ARL14* siRNA and its negative control. $^{**}P < 0.01$ and $^{***}P < 0.001$ compared with the corresponding control.

resulted in the accumulation of ERK and its phosphorylation. To verifying this, we examined whether p21 and cyclin D1 were affected by siARL14. Results showed that when *ARL14* expressions in A549 and PC9 cells were silenced, the expressions of cyclin D1 protein and its phosphorylation level were both increased. However, the p21 protein and its phosphorylation level were upregulated in A549 cells but downregulated in PC9 cells (**Figure 2E**). Because the cell dormancy after siARL14 transfection was observed in both A549 and PC9 cells according to above Ki67 immunofluorescence assay, we predicted that other cell cycle associated factors may also play important roles in siARL14-induced cell cycle arrest and cell dormancy, such as p16 (Barkan et al., 2008; Sosa et al., 2011), p27 (Barkan et al., 2008; Cackowski et al., 2017; Fluegen et al., 2017; Liu et al., 2018), and p53 (Nagayama et al., 2000; Sosa et al., 2011; Dai et al., 2016). Indeed, our further assay demonstrated that, after siARL14 transfection, both p16, p27 and p53 protein and their phosphorylation levels were upregulated in PC9 cells, and p16 and p27 were upregulated in A549 cells that had abnormal status of p53 (**Figure 2E**).

CIDEC Is a Downstream Gene of *ARL14*

Seldom study has evaluated the transcriptional regulation of *ARL14* in human cancers. GSEA is a useful tool to reveal the corresponding pathway and regulation mechanism of specific genes (Li et al., 2018), particularly those with unknown functions (Liu et al., 2016). Therefore, the GSEA of 594 RNA-seq data of lung adenocarcinoma from TCGA was performed to gain the insights of interaction networks of *ARL14*. The results suggested that 5850 genes are co-expressed with *ARL14* (**Supplementary Data Sheet S1**) and the pathways of both positively and negatively correlated with *ARL14* are mostly related to metabolism and immune system (**Supplementary Tables S5**, **S6**). Because the absolute magnitude of the correlation index of genes involved in the pathways negatively correlated with *ARL14* were much lower than 0.2 ($P < 0.05$), we focused

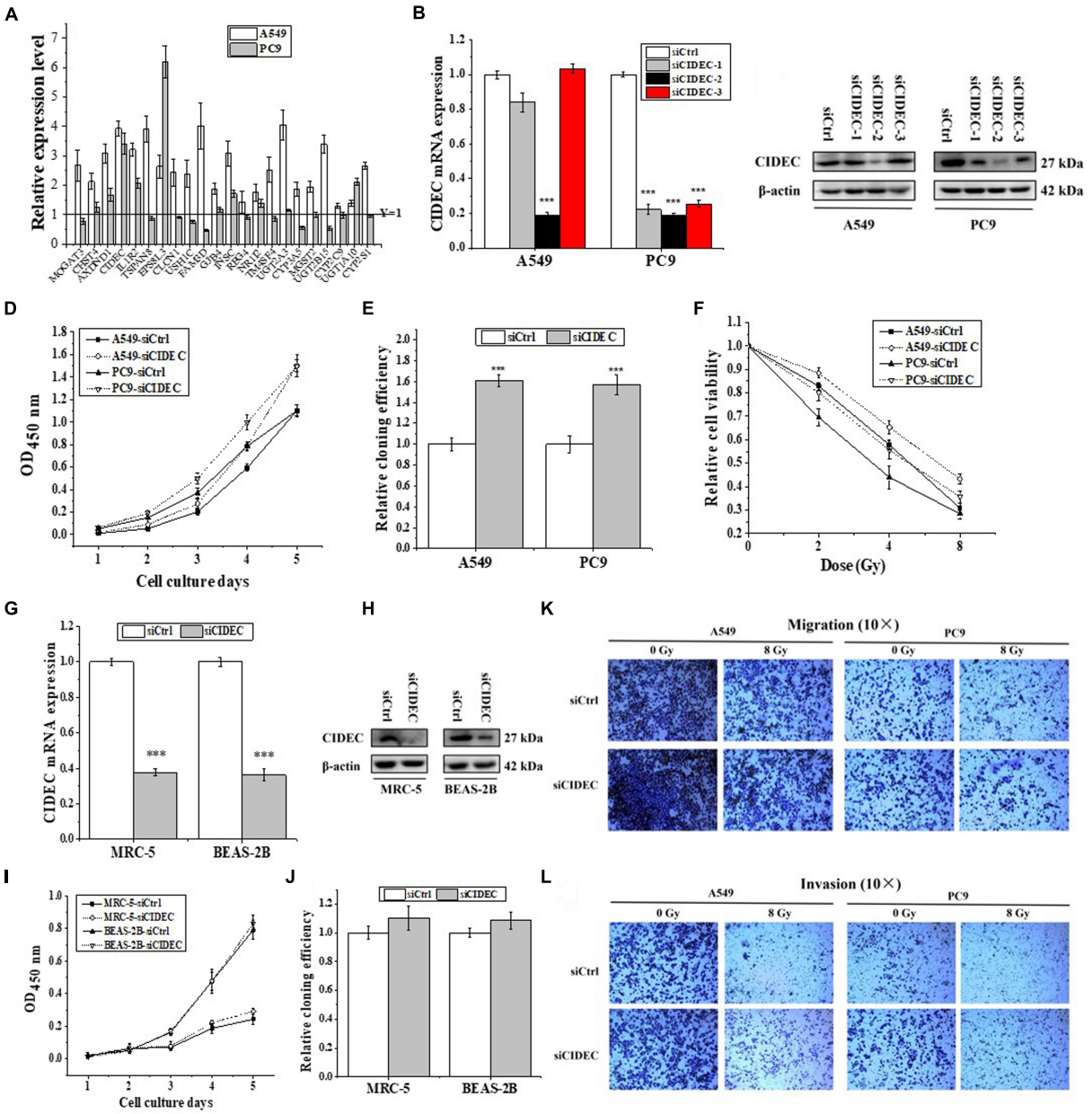

FIGURE 3 | *CIDEC* is a downstream gene of *ARL14* and contributes to proliferation, radiosensitivity, migration and invasion of lung adenocarcinoma cells. **(A)** The candidate genes negatively correlated with *ARL14* analyzed from GESA database and their relative expression levels of mRNA were measured in A549 and PC9 cells transfected with *ARL14* siRNA. **(B,C)** The expressions of *CIDEC* mRNA **(B)** and protein **(C)** in A549 and PC9 cells transfected with *CIDEC* siRNAs for 48 h. **(D–F)** Silencing of *CIDEC* increased proliferation **(D)**, cloning efficiency **(E)**, and radioresistance **(F)** of A549 and PC9 cells. **(G,H)** The expressions of *CIDEC* mRNA **(G)** and protein **(H)** were reduced in MRC-5 and BEASA-2B cells transfected with *CIDEC* siRNAs for 48 h. **(I,J)** Silencing of *CIDEC* had no significant influence on proliferation **(I)** and cloning efficiency **(J)** of MRC-5 and BEAS-2B cells. **(K,L)** The migration and invasion activities of A549 and PC9 cells with or without *CIDEC* siRNA transfection. After siRNA transfection, cells were irradiated with 8 Gy γ-rays. $^{**}P < 0.01$ and $^{***}P < 0.001$ compared with the corresponding control.

only on the pathways positively correlated with *ARL14* and examined the mRNA expressions of 22 top-ranking protein encoding genes (**Supplementary Data Sheet S1**). It was found that only the expressions of *AXDND1*, *CIDEC*, *IL1R2*, *EPS8L3*, and *INSC* genes were significant increased (fold-change > 1.5) in both A549 and PC9 cells after *ARL14* silencing (**Figure 3A**), indicating that these gene may be downstream of *ARL14*. **Figure 3A** also showed that *CIDEC* and *EPS8L3* had the highest expressions and the biggest changes in both cell lines, since the function of EPS8L3 protein is still unknown, we focused on the relationship between *ARL14* and *CIDEC*, which has a correlation coefficient of 0.7756 (**Supplementary Data Sheet S1**).

To further determine the relationship between *ARL14* and *CIDEC*, the function of *CIDEC* in tumor proliferation

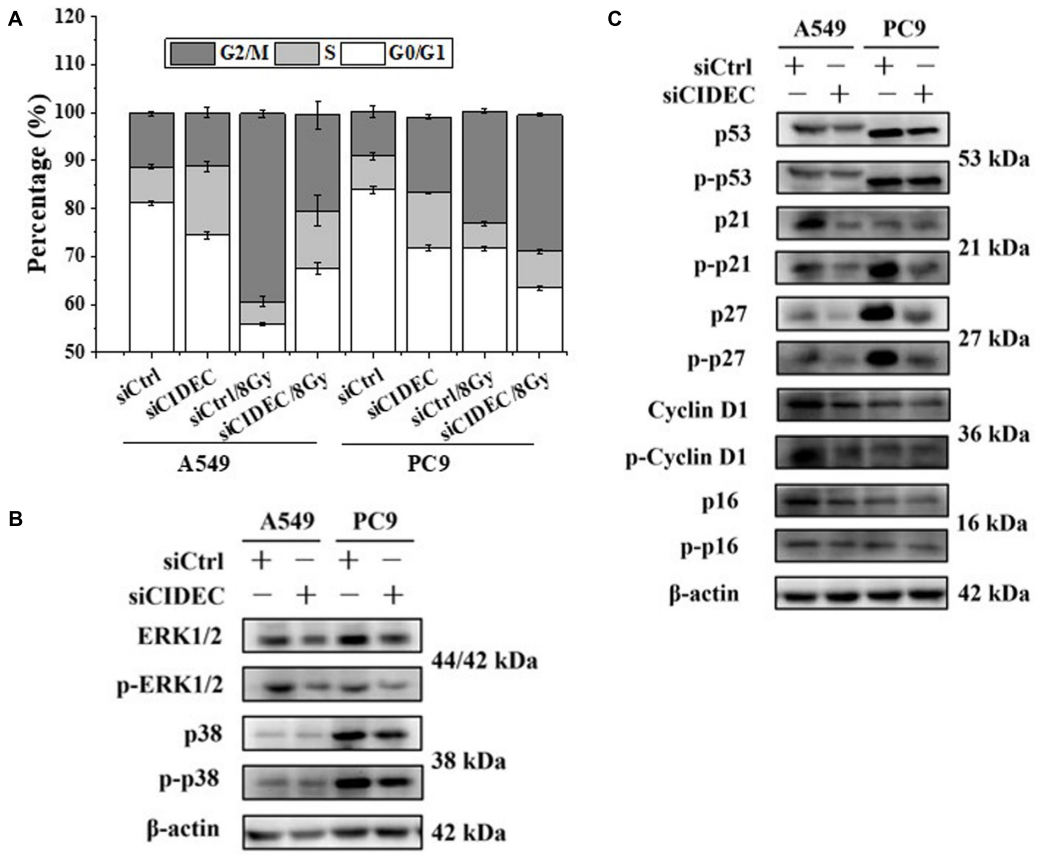

FIGURE 4 | Down-regulation of *CIDEC* expression contributes to the distribution of cell cycle and the expression of cell cycle-related proteins in A549 and PC9 cells. **(A)** Effects of *CIDEC* siRNA on the cell cycle distribution and radiation-induced G2/M phase arrest of A549 and PC9 cells. **(B,C)** The proteins and their phosphorylation levels of ERK and p38 **(B)**, p16, cyclin D1, p27, p21, and p53 **(C)** in A549 and PC9 cell population transfected with *CIDEC* siRNA and its negative control. After siRNA transfection, cells were irradiated with 8 Gy γ-rays.

was then detected. We transfected A549 and PC9 cells with siRNAs against *CIDEC* and the silencing effect were evaluated by qRT-PCR and Western blot assays (**Figures 3B,C**). The sequence siCIDEC2 (hereafter named siCIDEC) had the most effective efficiency in silencing *CIDEC* gene and thus applied for further experiments. It was found that siCIDEC significantly increased cell proliferation, clone formation and radiation resistance of A549 and PC9 cells (**Figures 3D–F**). Interestingly, although siCIDEC also reduced the expressions of *CIDEC* gene and protein in both MRC-5 and BEAS-2B cells (**Figures 3G,H**), it had no significant influence in cell proliferation and clone formation of these normal cells (**Figures 3I,J**). In addition, silencing of *CIDEC* expression could increase cell migration and invasion and further partly recovered radiation-reduced metastasis ability of both A549 and PC9 cells (**Figures 3K,L**). Accordingly, *CIDEC* has opposite roles in cell proliferation and migration to *ALR14* in lung adenocarcinoma cells.

In addition, cell cycle analysis revealed that silencing of *CIDEC* attenuated the accumulation of cell cycle arrested at G2/M phase of irradiated A549 cells but increased the accumulation of PC9 cells arrested at S-phase (**Figure 4A** and **Supplementary Table S4**). Western blot assay shows that the protein and phosphorylation levels of p38 and ERK1/2 and their downstream proteins p16, p21, p27, p53, and cyclin D1 were all down-regulated in A549 and PC9 cells after siCIDEC transfection (**Figures 4B,C**), which also had a conversed pattern in comparison with that in *ARL14* silencing cells.

DISCUSSION

ARL14 is located on human chromosome 13q14.2, a region closely related to several cancers including lung cancer (Ninomiya et al., 2013; Du et al., 2018) and involved in multidrug resistance in cancer treatment (Litviakov et al., 2016). The *ARL14* gene encodes a protein member of the Ras super-family composed of 196 amino acids which is involved in apoptotic signaling and several regulatory pathways (Kahn et al., 1992), indicating its usefulness as a marker for predicting tumor progression and prognosis. We found that *ARL14* had significantly different levels between lung adenocarcinoma samples and matched normal control tissues as well between lung adenocarcinoma cells and normal lung cells, and *ARL14*

level is associated with the prognosis of lung adenocarcinoma. Moreover, silencing *ARL14* inhibited the proliferation, migration and invasion of lung adenocarcinoma cells but it had no influence on the proliferation of normal lung cells. Therefore, *ARL14* may be applied as an ideal prognostic biomarker and therapeutic target of lung adenocarcinoma.

Our pilot study showed that, when the lung adenocarcinoma A549 cells were transferred with a lentiviral expression vector of *ARL14* gene, the cell cloning efficiency became very low (<5%) and the cell proliferation was almost total inhibited, indicating that the silencing *ARL14* by lentivirus causes growth arrest and dormancy of lung adenocarcinoma cells. Therefore, this study just transiently transferred siARL14 into lung adenocarcinoma cells and normal lung cells to knock-down *ARL14* expression and found that the percentage of G0/G1-phase cells was increased and the protein level of Ki67 was downregulated in *ARL14* knockdown lung adenocarcinoma cells.

CIDEC, a member of the cell-death-inducing DFF45-like effectors family (Liang et al., 2003), is located on human chromosome 3p25, a region associated with a high frequency of loss of heterozygosity in a wide range of tumor tissues. This region plays an important role in the pathogenesis of lung cancer (Graziano et al., 1991). However, few studies of *CIDEC* expression in cancer cells have been reported. Min et al. (2011) found that *CIDEC* expression was decreased in hepatocellular carcinoma tissue compared with its adjacent normal tissues, and overexpression of *CIDEC* inhibited the proliferation of SMMC-7721 cells. In agreement with those studies, our results showed that *CIDEC* silencing promoted cell proliferation, while *ARL14* silencing inhibited proliferation and upregulated *CIDEC* expression in lung adenocarcinoma cells. Moreover, *CIDEC* and *ARL14* had opposite effects on the expressions of proliferation-related proteins and the migration and invasion capacities of lung adenocarcinoma cells. These results supply an evidence that *CIDEC* is downstream of *ARL14* and has antagonistic effect on the biological function of *ARL14*.

Overall, our results demonstrate that silencing *ARL14* can block ERK1/2 and p38 signaling and stimulates its downstream gene *CIDEC* expression, which further activates their downstream effectors of p16, p21, p27, p53, and cyclin D1, resulting in cell cycle arrest of the lung cancer cells. These findings should have implication in identifying the predictive biomarker and treatment targets for lung adenocarcinoma.

DATA AVAILABILITY STATEMENT

The datasets generated for this study are available on request to the corresponding author.

AUTHOR CONTRIBUTIONS

FG, DY, and CS: conceptualization. FG, JuZ, HZ, CW, LZ, and JiZ: methodology. FG, DY, and JuZ: formal analysis. FG and DY: investigation. FG: draft writing. YP and CS: review and editing. FG: visualization. CS: project administration. YP and CS: funding acquisition. CS: supervision.

FUNDING

This work was supported by the National Key R&D Program of China (Grant Number 2017YFC0108604) and the National Natural Science Foundation of China (Grant Numbers 31770910, 31570850, and 11775052).

SUPPLEMENTARY MATERIAL

The Supplementary Material for this article can be found online at: https://www.frontiersin.org/articles/10.3389/fcell.2019.00238/full#supplementary-material

REFERENCES

Aguirre-Ghiso, J. A., Estrada, Y., Liu, D., and Ossowski, L. (2003). ERK(MAPK) activity as a determinant of tumor growth and dormancy; regulation by p38(SAPK). *Cancer Res.* 63, 1684–1695.

Aguirre-Ghiso, J. A., Liu, D., Mignatti, A., Kovalski, K., and Ossowski, L. (2001). Urokinase receptor and fibronectin regulate the ERK(MAPK) to p38(MAPK) activity ratios that determine carcinoma cell proliferation or dormancy in vivo. *Mol. Biol. Cell* 12, 863–879. doi: 10.1091/mbc.12.4.863

Barkan, D., Kleinman, H., Simmons, J. L., Asmussen, H., Kamaraju, A. K., Hoenorhoff, M. J., et al. (2008). Inhibition of metastatic outgrowth from single dormant tumor cells by targeting the cytoskeleton. *Cancer Res.* 68, 6241–6250. doi: 10.1158/0008-5472.can-07-6849

Bruno, S., and Darzynkiewicz, Z. (1992). Cell cycle dependent expression and stability of the nuclear protein detected by Ki-67 antibody in HL-60 cells. *Cell Prolif.* 25, 31–40. doi: 10.1111/j.1365-2184.1992.tb01435.x

Cackowski, F. C., Eber, M. R., Rhee, J., Decker, A. M., Yumoto, K., Berry, J. E., et al. (2017). Mer tyrosine kinase regulates disseminated prostate cancer cellular dormancy. *J. Cell. Biochem.* 118, 891–902. doi: 10.1002/jcb.25768

Calin, G. A., Trapasso, F., Shimizu, M., Dumitru, C. D., Yendamuri, S., Godwin, A. K., et al. (2005). Familial cancer associated with a polymorphism in ARLTS1. *N. Engl. J. Med.* 352, 1667–1676. doi: 10.1056/NEJMoa042280

Chambard, J. C., Lefloch, R., Pouyssegur, J., and Lenormand, P. (2007). ERK implication in cell cycle regulation. *Biochim. Biophys. Acta* 1773, 1299–1310. doi: 10.1016/j.bbamcr.2006.11.010

Cheng, H., Shcherba, M., Kandavelou, K., Liang, Y., Liu, H., and Perez-Soler, R. (2015). Emerging drugs for squamous cell lung cancer. *Expert Opin. Emerg. Drugs* 20, 149–160. doi: 10.1517/14728214.2015.1001365

Dai, Y., Wang, L., Tang, J., Cao, P., Luo, Z., Sun, J., et al. (2016). Activation of anaphase-promoting complex by p53 induces a state of dormancy in cancer cells against chemotherapeutic stress. *Oncotarget* 7, 25478–25492. doi: 10.18632/oncotarget.8172

Du, M., Thompson, J., Fisher, H., Zhang, P., Huang, C. C., and Wang, L. (2018). Genomic alterations of plasma cell-free DNAs in small cell lung cancer and their clinical relevance. *Lung cancer*120, 113–121. doi: 10.1016/j.lungcan.2018.04.008

Fluegen, G., Avivar-Valderas, A., Wang, Y., Padgen, M. R., Williams, J. K., Nobre, A. R., et al. (2017). Phenotypic heterogeneity of disseminated tumour cells is preset by primary tumour hypoxic microenvironments. *Nat. Cell Biol.* 19, 120–132. doi: 10.1038/ncb3465

Frank, B., Hemminki, K., Brenner, H., Hoffmeister, M., Chang-Claude, J., and Burwinkel, B. (2006). ARLTS1 variants and risk of colorectal cancer. *Cancer Lett.* 244, 172–175. doi: 10.1016/j.canlet.2005.12.006

Graziano, S. L., Pfeifer, A. M., Testa, J. R., Mark, G. E., Johnson, B. E., Hallinan, E. J., et al. (1991). Involvement of the RAF1 locus, at band 3p25, in the 3p deletion of small-cell lung cancer. *Genes Chromosomes Cancer* 3, 283–293. doi: 10.1002/gcc.2870030407

Hamadou, W. S., Besbes, S., Mani, R., Bourdon, V., Ben Youssef, Y., Achour, B., et al. (2017). ARLTS1, potential candidate gene in familial aggregation of hematological malignancies. *Bull. Cancer* 104, 123–127. doi: 10.1016/j.bulcan.2016.10.016

He, M., Dong, C., Konishi, T., Tu, W., Liu, W., Shiomi, N., et al. (2014). Differential effects of p53 on bystander phenotypes induced by gamma ray and high LET heavy ion radiation. *Life Sci. Space Res.* 1, 53–59. doi: 10.1016/j.lssr.2014.02.003

Kahn, R. A., Der, C. J., and Bokoch, G. M. (1992). The ras superfamily of GTP-binding proteins: guidelines on nomenclature. *FASEB J.* 6, 2512–2513. doi: 10.1096/fasebj.6.8.1592203

Lents, N. H., Keenan, S. M., Bellone, C., and Baldassare, J. J. (2002). Stimulation of the Raf/MEK/ERK cascade is necessary and sufficient for activation and Thr-160 phosphorylation of a nuclear-targeted CDK2. *J. Biol. Chem.* 277, 47469–47475. doi: 10.1074/jbc.M207425200

Li, Y., Deng, L., Zhao, X., Li, B., Ren, D., Yu, L., et al. (2018). Tripartite motif-containing 37 (TRIM37) promotes the aggressiveness of non-small-cell lung cancer cells by activating the NF-kappaB pathway. *J. Pathol.* 246, 366–378. doi: 10.1002/path.5144

Liang, L., Zhao, M., Xu, Z., Yokoyama, K. K., and Li, T. (2003). Molecular cloning and characterization of CIDE-3, a novel member of the cell-death-inducing DNA-fragmentation-factor (DFF45)-like effector family. *Biochem. J.* 370, 195–203. doi: 10.1042/BJ20020656

Litviakov, N. V., Cherdyntseva, N. V., Tsyganov, M. M., Slonimskaya, E. M., Ibragimova, M. K., Kazantseva, P. V., et al. (2016). Deletions of multidrug resistance gene loci in breast cancer leads to the down-regulation of its expression and predict tumor response to neoadjuvant chemotherapy. *Oncotarget* 7, 7829–7841. doi: 10.18632/oncotarget.6953

Liu, Y., Lv, J., Liu, J., Liang, X., Jin, X., Xie, J., et al. (2018). STAT3/p53 pathway activation disrupts IFN-beta-induced dormancy in tumor-repopulating cells. *J. Clin. Invest.* 128, 1057–1073. doi: 10.1172/JCI96329

Liu, Y. Z., Yang, H., Cao, J., Jiang, Y. Y., Hao, J. J., Xu, X., et al. (2016). KIAA1522 is a novel prognostic biomarker in patients with non-small cell lung cancer. *Sci. Rep.* 6:24786. doi: 10.1038/srep24786

Masojc, B., Mierzejewski, M., Cybulski, C., van de Wetering, T., Debniak, T., Gorski, B., et al. (2006). Cancer familial aggregation (CFA) and G446A polymorphism in ARLTS1 gene. *Breast Cancer Res. Treat.* 99, 59–62. doi: 10.1007/s10549-006-9180-9185

Min, J., Zhang, W., Gu, Y., Hong, L., Yao, L., Li, F., et al. (2011). CIDE-3 interacts with lipopolysaccharide-induced tumor necrosis factor, and overexpression increases apoptosis in hepatocellular carcinoma. *Med. Oncol.* 28(Suppl. 1), S219–S227. doi: 10.1007/s12032-010-9702-9701

Nagayama, Y., Shigematsu, K., Namba, H., Zeki, K., Yamashita, S., and Niwa, M. (2000). Inhibition of angiogenesis and tumorigenesis, and induction of dormancy by p53 in a p53-null thyroid carcinoma cell line in vivo. *Anticancer. Res.* 20, 2723–2728.

Ninomiya, H., Kato, M., Sanada, M., Takeuchi, K., Inamura, K., Motoi, N., et al. (2013). Allelotypes of lung adenocarcinomas featuring ALK fusion demonstrate fewer onco- and suppressor gene changes. *BMC Cancer* 13:8. doi: 10.1186/1471-2407-13-18

Pan, Y., Zhou, C., Yuan, D., Zhang, J., and Shao, C. (2016). Radiation exposure promotes hepatocarcinoma cell invasion through epithelial mesenchymal transition mediated by H2S/CSE pathway. *Radiat. Res.* 185, 96–105. doi: 10.1667/rr14177.1

Ranganathan, A. C., Adam, A. P., and Aguirre-Ghiso, J. A. (2006). Opposing roles of mitogenic and stress signaling pathways in the induction of cancer dormancy. *Cell Cycle* 5, 1799–1807. doi: 10.4161/cc.5.16.3109

Ridge, C. A., McErlean, A. M., and Ginsberg, M. S. (2013). Epidemiology of lung cancer. *Semin. Int. Radiol.* 30, 93–98. doi: 10.1055/s-0033-1342949

Sharma, S. V., Bell, D. W., Settleman, J., and Haber, D. A. (2007). Epidermal growth factor receptor mutations in lung cancer. *Nat. Rev. Cancer.* 7, 169–181. doi: 10.1038/nrc2088

Siegel, R. L., Miller, K. D., and Jemal, A. (2017). Cancer statistics, 2017. *Cancer J. Clin.* 67, 7–30. doi: 10.3322/caac.21387

Siltanen, S., Fischer, D., Rantapero, T., Laitinen, V., Mpindi, J. P., Kallioniemi, O., et al. (2013). ARLTS1 and prostate cancer risk–analysis of expression and regulation. *PLoS One* 8:e72040. doi: 10.1371/journal.pone.0072040

Siltanen, S., Syrjakoski, K., Fagerholm, R., Ikonen, T., Lipman, P., Mallott, J., et al. (2008). ARLTS1 germline variants and the risk for breast, prostate, and colorectal cancer. *Eur. J. Hum. Genet.* 16, 983–991. doi: 10.1038/ejhg.2008.43

Sosa, M. S., Avivar-Valderas, A., Bragado, P., Wen, H. C., and Aguirre-Ghiso, J. A. (2011). ERK1/2 and p38alpha/beta signaling in tumor cell quiescence: opportunities to control dormant residual disease. *Clin. Cancer Res.* 17, 5850–5857. doi: 10.1158/1078-0432.ccr-10-2574

Subramanian, A., Tamayo, P., Mootha, V. K., Mukherjee, S., Ebert, B. L., Gillette, M. A., et al. (2005). Gene set enrichment analysis: a knowledge-based approach for interpreting genome-wide expression profiles. *Proc. Natl. Acad. Sci. U.S.A.* 102, 15545–15550. doi: 10.1073/pnas.0506580102

Wang, P., Yuan, D., Guo, F., Chen, X., Zhu, L., Zhang, H., et al. (2017). Chromatin remodeling modulates radiosensitivity of the daughter cells derived from cell population exposed to low- and high-LET irradiation. *Oncotarget* 8, 52823–52836. doi: 10.18632/oncotarget.17275

Xue, X., Fei, X., Hou, W., Zhang, Y., Liu, L., and Hu, R. (2018). miR-342-3p suppresses cell proliferation and migration by targeting AGR2 in non-small cell lung cancer. *Cancer Lett.* 412, 170–178. doi: 10.1016/j.canlet.2017.10.024

Yang, X. Y., Yu, H., Xi, M. R., Yang, K. X., Pan, X. L., Hu, M., et al. (2009). Association of the ARLTS1 variants with familial ovarian cancer risk in China. *Int. J. Gynecol. Cancer* 19, 585–590. doi: 10.1111/IGC.0b013e3181a39d03

Yendamuri, S., Trapasso, F., and Calin, G. A. (2008). ARLTS1 - a novel tumor suppressor gene. *Cancer Lett.* 264, 11–20. doi: 10.1016/j.canlet.2008.02.021

Yendamuri, S., Trapasso, F., Ferracin, M., Cesari, R., Sevignani, C., Shimizu, M., et al. (2007). Tumor suppressor functions of ARLTS1 in lung cancers. *Cancer Res.* 67, 7738–7745. doi: 10.1158/0008-5472.can-07-1481

Conflict of Interest: The authors declare that the research was conducted in the absence of any commercial or financial relationships that could be construed as a potential conflict of interest.

frontiers in Oncology

REVIEW
published: 19 December 2019
doi: 10.3389/fonc.2019.01407

N^6-Methyladenosine: A Novel RNA Imprint in Human Cancer

Sihui Yu[1†], *Xi Li*[1†], *Shiyun Liu*[2], *Rui Yang*[1], *Xiangnan Liu*[1] *and Sufang Wu*[1*]

[1] Department of Obstetrics and Gynecology, Shanghai General Hospital, Shanghai Jiao Tong University School of Medicine, Shanghai, China, [2] Department of Urology, Shanghai General Hospital, Shanghai Jiao Tong University School of Medicine, Shanghai, China

N^6-Methyladenosine (m^{6}A), a pervasive posttranscriptional modification which is reversible, has been among hotspot issues in the past several years. The balance of intracellular m^{6}A levels is dynamically maintained by methyltransferase complex and demethylases. Meanwhile, m^{6}A reader proteins specifically recognize modified residues and convey messages so as to set up an efficient and orderly network of m^{6}A regulation. The m^{6}A mark has proved to affect every step of RNA life cycle, from processing in nucleus to translation or degradation in cytoplasm. Subsequently, disorders in m^{6}A methylation are directly related to aberrant RNA metabolism, which results in tumorigenesis and altered drug response. Therefore, uncovering the underlying mechanism of m^{6}A in oncogenic transformation and tumor progression seeks opportunities for novel targets in cancer therapy. In this review, we conclude the extensive impact of m^{6}A on RNA metabolism and highlight its relevance with human cancer, implicating the far-reaching value in clinical application.

Keywords: epitranscriptome, RNA methylation, m^{6}A, posttranscriptional control, human cancer

OPEN ACCESS

Edited by:
Hailong Pei,
Soochow University, China

Reviewed by:
Jia Meng,
Xi'an Jiaotong-Liverpool University, China
Kwok-Ming Yao,
The University of Hong Kong, Hong Kong

****Correspondence:***
Sufang Wu
wsf_sfph@sjtu.edu.cn

† These authors have contributed equally to this work

Specialty section:
This article was submitted to Molecular and Cellular Oncology, a section of the journal Frontiers in Oncology

Received: *21 October 2019*
Accepted: *27 November 2019*
Published: *19 December 2019*

Citation:
Yu S, Li X, Liu S, Yang R, Liu X and Wu S (2019) N^6-Methyladenosine: A Novel RNA Imprint in Human Cancer. Front. Oncol. 9:1407. doi: 10.3389/fonc.2019.01407

INTRODUCTION

N^6-methyladenosine (m^{6}A), which refers to the addition of methyl groups to the N-6 position of the adenosine residue, is a pervasive posttranscriptional RNA internal modification of eukaryotes (1). Since its first discovery in the 1970s, m^{6}A had remained an uncharted territory due to technical bottlenecks (2). The stagnation ended in 2011, when the fat mass and obesity-associated protein (FTO) was revealed to exhibit demethylation activity on m^{6}A-modified RNAs (3). The m^{6}A mark was thus identified as a reversible process, which generated refueled passion in this field. To date, scientists have confirmed multiple m^{6}A regulatory enzymes and classified them as "writers," "erasers," and "readers" (4).

With the availability of high-throughput sequencing technique, scientists are nowadays capable of detecting m^{6}A methylation at transcriptome-wide level (5, 6). m^{6}A sites are mainly enriched near stop codons, in 3′-untranslated regions (3′-UTRs) and within long internal exons. Besides messenger RNAs (mRNAs) and long non-coding RNAs, a wide range of circular RNAs (circRNAs) generated by back splice events also undergoes m^{6}A modification (7). The m^{6}A-circRNAs frequently arise from exons that are void of m^{6}A peaks in mRNAs. This chemical mark is evolutionarily conserved and falls within a consensus motif RRACH (R = G/A, A = m^{6}A, H = A/C/U) (5, 6, 8). What is more, m^{6}A RNA methylation poses a broad control on RNA metabolism including alternative splicing, subcellular localization, and translational regulation (9). The impact of m^{6}A regulatory enzymes on RNA processes may further interplay with tumor biology, which will be respectively discussed in this review.

m^{6}A REGULATORY ENZYMES WORK IN A COOPERATIVE MANNER

The m^{6}A regulatory enzymes work cooperatively to maintain the balance of intracellular m^{6}A levels (4) (**Figure 1**). m^{6}A "writers" composing the methyltransferase complex catalyze this modification positively. This decoration could be reversed by m^{6}A "erasers" harboring demethylase activity. Meanwhile, m^{6}A "readers" specifically recognize modified residues and convey messages so as to set up an efficient and orderly network of m^{6}A regulation.

The m^{6}A methyltransferase complex is mainly comprised of methyltransferase-like 3 (METTL3), METTL14, and Wilms' tumor 1-associating protein (WTAP), which regulate the distribution of m^{6}A in coordination (10). METTL3 serves as the core component, while METTL14 is integrated with METTL3 as a stable heterodimer and catalyzes m^{6}A RNA methylation through synergistic effect (10, 11). WTAP anchors METTL3–METTL14 complex to target RNAs and promotes its accumulation in nuclear speckles (8). Since WTAP harbors no methyltransferase activity, this regulatory subunit takes effect on the premise of functional m^{6}A methylation complex (12). Scientists have also reported some other proteins that modulate the cellular m^{6}A landscape cooperatively. METTL16, a newly defined m^{6}A writer targeting U6 spliceosomal small nuclear RNA, also regulates S-adenosylmethionine homeostasis by inducing the expression of S-adenosylmethionine synthetase upon methionine starvation (13–16).

The m^{6}A erasers discovered so far involve two candidates, FTO and AlkB homolog 5 (ALKBH5). FTO was initially proved to regulate energy homeostasis and is positively related to risk of obesity (17, 18). ALKBH5 is a homolog of FTO, and they both belong to the Fe(II)- and oxoglutarate-dependent AlkB oxygenase family (17–19). In the m^{6}A circuit, FTO and ALKBH5 identify m^{6}A-modified nuclear RNAs as substrate and catalyze removal of m^{6}A mark (3, 19).

The reader proteins specifically recognize m^{6}A decoration to sort mRNAs for quicker metabolism to further perform biological functions (4). Among these readers, YT521-B homology (YTH) domain proteins are the best documented, including YTH domain family proteins (YTHDF1–3) and YTH domain containing proteins (YTHDC1–2) (20–25). YTHDF1–3 and YTHDC2 are cytoplasmic readers, while YTHDC1 mainly operates in the nucleus. Insulin-like growth factor 2 mRNA-binding proteins (IGF2BP1–3) is a distinct family of readers with K homology (KH) domains to recognize m^{6}A (26). More potential m^{6}A readers are under exploration, such as heterogeneous nuclear ribonucleoprotein A2/B1 (HNRNPA2B1) and eukaryotic initiation factor 3 (eIF3) (27, 28).

m^{6}A REGULATES RNA METABOLISM IN PHYSIOLOGICAL CONDITIONS

The RNA life cycle comprises RNA processing, export, and translation or degradation. Formidable evidence has shown that m^{6}A and its regulatory enzymes take part in every step of RNA metabolism. Generally speaking, the writers and erasers dictate m^{6}A levels in specific targets, which are decoded by the readers to accelerate RNA process and translate into distinct functions.

RNA Processing in Nucleus

WTAP favors the positioning of METTL3–METTL14 complex in nuclear speckles that are sites associated with RNA processing and transcription (10). As a result, WTAP modulates alternative splicing and gene expression. Similarly, ALKBH5 colocalizes with nuclear speckles, and m^{6}A erasure mediated by ALKBH5 is critical for correct splicing, preventing longer 3′-UTR mRNAs from quick degradation during spermiogenesis (29).

YTHDC1 binds m^{6}A-modified pre-mRNAs and affects RNA binding affinity of splicing factors (30). Under normal circumstances, YTHDC1 promotes mRNA binding of SRSF3 while antagonizing that of SRSF10, predominantly triggering exon inclusion of targeted mRNAs (31) (**Figure 1**). In addition, YTHDC1 interacts with pre-mRNA 3′ end processing factors such as CPSF6 and determines the length of 3′-UTR where lie many microRNAs (miRNAs) target sites (25). Given that miRNAs pair to mRNAs of protein-coding genes and repress them at posttranscriptional level, YTHDC1 regulates mRNA stability and translation efficiency indirectly (25, 32).

Meanwhile, m^{6}A mark induced by METTL3 on primary miRNAs could be recognized by adaptor readers such as HNRNPA2B1 (27, 33). The microprocessor protein DGCR8 is then recruited to specific precursor miRNAs and encourages their processing into mature miRNAs.

mRNA Export From Nucleus to Cytoplasm

In addition to alternative splicing and exon inclusion, YTHDC1 favors export of methylated mRNAs from nucleus to cytoplasm by the aid of SRSF3, indirectly triggering translation via increased cytoplasmic abundance of targets (34) (**Figure 1**).

Consistently, *Alkbh5* deficiency in male mice lifts m^{6}A levels and facilitates mRNA export to cytoplasm (35, 36). Cytoplasmic levels of mRNAs critical for proper spermatogenic maturation are altered, leading to aberrant spermatogenesis and apoptosis. Thus, it appears that m^{6}A exerts complex roles on subsequent effect of mRNA export. In addition, the latest findings show that Fragile X mental retardation protein, a newly identified m^{6}A reader protein, is also capable of facilitating the nuclear export of m^{6}A-marked transcripts through directly binding to a collection of m^{6}A sites on target mRNAs (37).

mRNA Translation or Degradation in Cytoplasm

After nuclear export, m^{6}A-modified RNAs will be sorted into different groups depending on diverse readers and then undergo a fast-tracking metabolism for translation or dedicated degradation. This process helps to generate adequate protein for urgent demand or rapidly degrade mRNAs in necessity (2).

YTHDF1 binds m^{6}A-modified RNAs and promotes ribosome loading via recruiting initiation factors (eIFs) that are pivotal in the rate-limiting step of translation (20) (**Figure 1**). Accordingly, YTHDF1 facilitates translation efficiency and protein synthesis. Other readers including YTHDC2, IGF2BPs, and eIF3 also bind

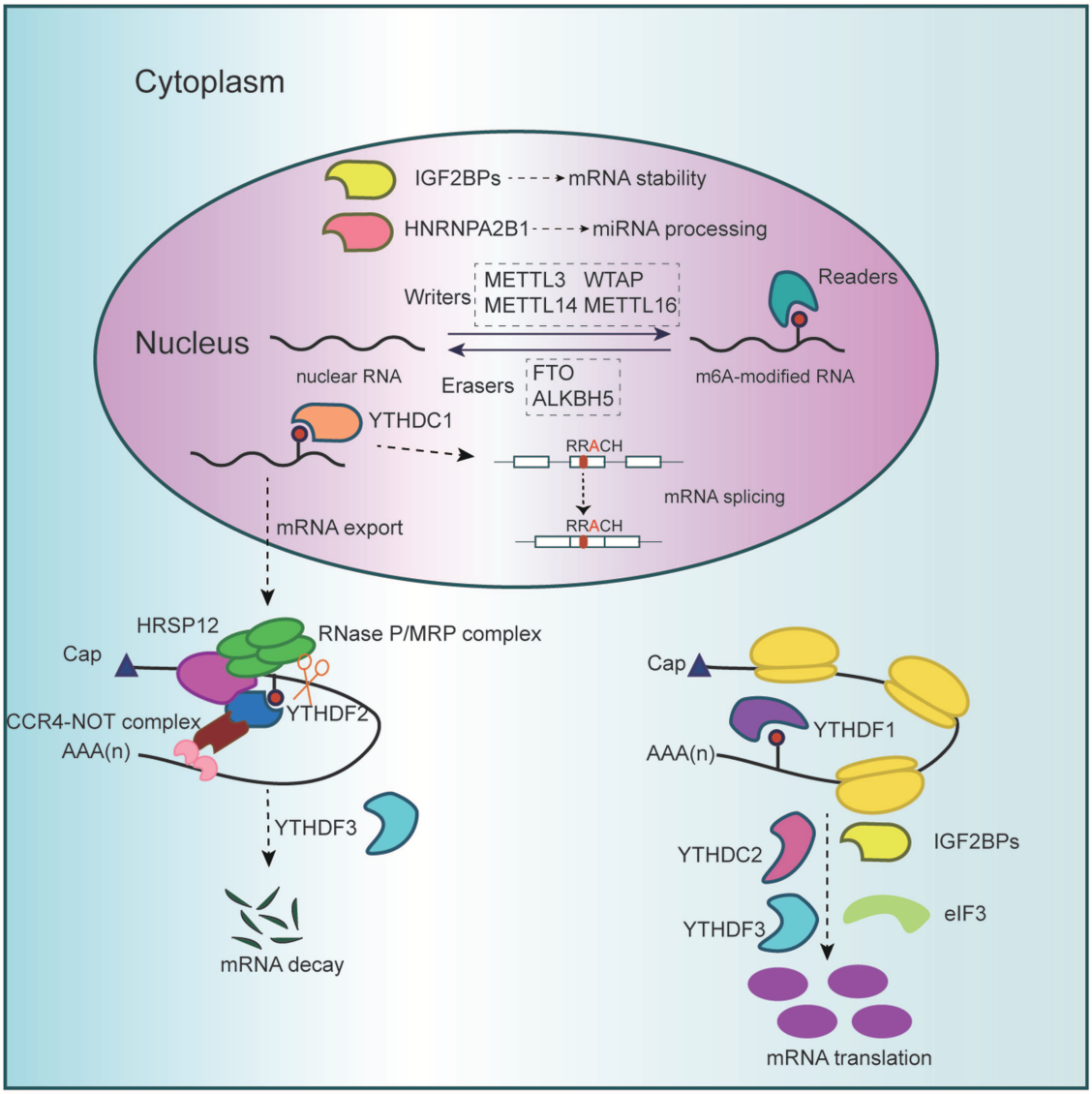

FIGURE 1 | Schematic diagram of RNA m^{6}A methylation. The methyltransferase complex (METTL3, METTL14, WTAP, and METTL16), which catalyzes methylation at the N6 position adenosine, and the demethylases (FTO and ALKBH5), which remove methyl groups, dynamically regulate cellular m^{6}A levels in the nucleus. Besides, m^{6}A modification could be specifically recognized and bound by diverse reader proteins. Nuclear m^{6}A readers promote miRNA processing while affecting mRNA splicing, stability, and export. Cytoplasmic readers mediate m^{6}A-marked mRNA translation and degradation.

m^{6}A at its consensus motif to enhance translation efficiency (23, 24, 26, 28).

On the contrary, YTHDF2 mediates m^{6}A-containing RNA decay, thus regulating gene expression and cell fate (21). YTHDF2 knockdown results in accumulation of untranslated target mRNAs, thereby reducing translation efficiency. Specifically speaking, carboxy-terminal domain of YTHDF2 selectively binds to m^{6}A-modified mRNA, while amino-terminal domain localizes the YTHDF2–mRNA complex to RNA decay sites. Recently, the molecular mechanism underpinning YTHDF2-directed RNA decay has been expounded. m^{6}A-containing linear and circular RNAs undergo endoribonucleolytic cleavage through YTHDF2-HRSP12-RNase P/MRP axis, coupled to CCR4-NOT complex-mediated deadenylating pathway (38) (**Figure 1**). In addition, a recent study reported that multivalent m^{6}A-modified RNAs could promote the phase separation of YTHDFs and that phase separation of m^{6}A and YTHDF2 might participate in cellular response to stresses, despite the uncertainty of its specific role (39).

After nuclear export of methylated RNAs, YTHDF3 tunes their delivery before YTHDF1 and YTHDF2, especially partitioning their shared targets (22). YTHDF3 accelerates translation or decay of m^{6}A-containing mRNAs in synergy

with YTHDF1 and YTHDF2. By the way, a broad range of circular RNAs generated by pre-mRNA back splicing in human transcriptome has coding potential and bears m^{6}A modification (40). YTHDF3 drives protein translation from these circRNAs in a cap-independent fashion.

Except for the YTHDF family members, SND1, a putative m^{6}A reader of the "royal family" also binds to m^{6}A modification of *ORF50* RNA and stabilizes the transcript, which favors the replication of Kaposi's sarcoma-associated herpesvirus (41).

m^{6}A POSES CONTROL ON TUMORIGENESIS AND CANCER PROGRESSION

Researchers have involved m^{6}A decoration in the development of human diseases. Mechanistically, m^{6}A could alter the expression of mRNAs encoding various regulators such as transcription factors and function as either barrier or facilitator of malignant transition in tumor cells. In this section, we respectively state the variable roles of m^{6}A in tumorigenesis and cancer progression based on different m^{6}A regulatory enzymes (**Table 1**).

m^{6}A Writers

METTL3

In glioblastoma stem cells (GSCs), Cui et al. knocked down METTL3 to hinder m^{6}A enrichment, and they also observed enhanced growth, self-renewal of GSCs, and tumor progression (42). In this process, oncogenes such as *ADAM19, EPHA3*, and *KLF4* were upregulated, while expression of tumor suppressors involving *CDKN2A*, *BRCA2*, and *TP53I11* were impeded. On the contrary, another study argued that METTL3 plays an oncogenic role in glioblastoma via methylating 3′-UTR of *SOX2* mRNA, which encodes transcription factors enabling the regain of stem-like properties and efficient DNA repair (43). The m^{6}A modification enhances the stability of *SOX2* mRNA. Accordingly, silencing of METTL3 interrupts SOX2-dependent DNA repair, impairs GSC maintenance, and delays tumor propagation *in vivo*. Different target mRNAs of m^{6}A mark, genetic, and non-genetic heterogeneity of cancer stem cells (CSCs) shall account for the controversy. Studies in normal stem cells have also been performed to complement the results, which are quite different. In adult neural stem cells, depletion of METTL3 reduces m^{6}A levels on transcripts of histone methyltransferase *EZH2* and inhibits its protein expression (73). Scientists reported that m^{6}A depletion not only suppressed cell growth but also blocked neuronal development and morphological maturation. This conclusion also implicates certain crosslink between m^{6}A mark and histone modification.

Besides, additional studies have verified the role of METTL3 in oncogenic transformation of various tumors. For instance, METTL3 depletion sensitizes pancreatic cancer cells to anticancer agents such as gemcitabine, 5-fluorouracil, cisplatin, and irradiation (44).

The METTL3-induced m^{6}A mark also drives malignant progression in breast tumor in aid of hepatitis B X-interacting protein (*HBXIP*), an oncogene in breast cancer cells (45). METTL3 lifts the mRNA and protein levels of *HBXIP*, which in turn promotes the expression of METTL3 and forms a positive feedback loop. The m^{6}A regulation in mRNA stability could have a bearing on this procedure.

Scientists have also reported in bladder cancer that METTL3 accelerates the processing of pri-miR221/222 via recognition by DGCR8 (46). Subsequently, mature miR221/222 restrains the expression of the antioncogene *PTEN* and ultimately boosts tumor growth both *in vitro* and *in vivo*. Based on the preferential m^{6}A recognition by YTHDF1, METTL3 also facilitates translation of oncogene *CDCP1*, which plays a pivotal role in bladder cancer progression (47). Simultaneously, this biological process exerts synergistic effect with chemical carcinogens in malignant transformation of uroepithelial cells.

In human lung cancer, gain-of-function study of METTL3 motivates cell growth and invasion, giving rise to tumors of larger size in mouse xenografts (48, 49). METTL3 was found to bind m^{6}A sites near the stop codon of specific mRNAs and recruit eIF3 to translation initiation complex in the 5′ end, which mediates mRNA circularization and ribosome recycling. In this way, METTL3 directly promotes efficient translation of onco-proteins involving BRD4, EGFR, and TAZ. Notably, the methyltransferase activity and m^{6}A-binding readers are proved to be uncoupled. This finding proposes a novel model of METTL3 in translational control, and the molecular determinants, such as the specificity of target mRNAs and localization of m^{6}A peaks, are worth in-depth investigation.

In acute myeloid leukemia cells (AMLs), the abundance of METTL3 is elevated compared to that in normal hematopoietic stem/progenitor cells (HSPCs) (50). Cell proliferation is inhibited along with depletion of this enzyme, and leukemogenesis is also delayed *in vivo*. Besides, METTL3 level is negatively relevant to the status of differentiation and apoptosis in AML cells. Inactivation of AKT induced by METTL3 overexpression contributes partially to the block of differentiation in an m^{6}A-independent manner. Further research suggests that METTL3 promotes the translation of functional proteins regulating cell cycle progression and apoptosis, such as c-MYC and BCL2. A later study instructed that METTL3 is recruited by the CAATT-box binding protein CEBPZ to promoters of active genes and mediates m^{6}A methylation within coding regions of target transcripts (51). Translation of genes necessary for AML is thus enhanced via relieved ribosome stalling. As a result, an alternative mechanism of METTL3 in translational regulation has been put forward.

In hepatocellular carcinoma (HCC), METTL3 is significantly upregulated and indicates poor prognosis (52). Mechanistically, METTL3 promotes HCC growth and invasiveness by repressing the expression of suppressor of cytokine signaling 2 (*SOCS2*), a tumor suppressor in HCC, through m^{6}A-YTHDF2-dependent mRNA degradation.

Nevertheless, expression of METTL3 is reduced in endometrial carcinoma, which stimulates AKT signaling and promotes tumor growth and invasiveness both *in vitro* and *in vivo* (53). Mechanistically, lower expression of METTL3 reduces m^{6}A methylation, restrains YTHDF1-promoted translation of

TABLE 1 | The summary of roles of m^{6}A subunits in tumor formation and progression.

Candidate	Tumor tissues or cell lines	Function	Mechanism	References
METTL3 and METTL14	Glioblastoma stem cells (GSCs)	Tumor suppressor	Reduces oncogene (*ADAM19*, *EPHA3*, *KLF4*) and upregulates tumor suppressor (*CDKN2A*, *BRCA2*, *TP53I11*) expression, inhibits GSC growth, self-renewal *in vitro*, and glioblastoma progression *in vivo*	(42)
METTL3	Glioma stem-like cells (GSCs)	Oncogene	Enhances *SOX2* mRNA stability, contributes to efficient DNA repair and GSC maintenance, promotes tumor propagation *in vivo*	(43)
METTL3	Pancreatic cancer cells	Oncogene	Induces resistance to anticancer reagents such as GEM, 5-fluorouracil, cisplatin, and irradiation	(44)
METTL3	Breast cancer tissues	Oncogene	Lifts expression of *HBXIP*, accelerates cell proliferation, and inhibits apoptosis	(45)
METTL3	Bladder cancer tissues and cell lines	Oncogene	Promotes *CDCP1* translation and inhibits *PTEN* expression through positively modulating pri-miR221/222 process, enhances cell proliferation, invasion, and survival *in vitro* and *in vivo*	(46, 47)
METTL3	Lung adenocarcinoma tissues	Oncogene	Recruits eIF3 to translation initiation complex, promotes translation of oncogenes including *BRD4*, *EGFR* and the Hippo pathway effector *TAZ*, enhances cell growth, survival, and invasion	(48, 49)
METTL3	Acute myeloid leukemia cells	Oncogene	Enhances translation of *c-MYC*, *BCL2*, and *PTEN* mRNAs, blocks cell differentiation and apoptosis, promotes leukemia progression	(50, 51)
METTL3	Hepatocellular carcinoma tissues	Oncogene	Destabilizes *SOCS2* mRNA through YTHDF2-mediated degradation, enhances HCC growth and metastasis, indicates poor prognosis of HCC	(52)
METTL3 and METTL14	Endometrial tumor tissues	Tumor suppressor	Upregulates PHLPP2 expression and downregulates mTORC2 expression, attenuates AKT activity, inhibits cell proliferation, migration, and *in vivo* tumor growth	(53)
METTL14	Hepatocellular carcinoma tissues	Tumor suppressor	Enhances recognition of pri-miR126 by DGCR8 and processing to mature miRNA, suppresses tumor metastasis *in vitro* and *in vivo*	(54)
METTL14	Acute myeloid leukemia cells	Oncogene	Enhances stability and translation of *MYB* and *MYC* mRNA, blocks myeloid differentiation, contributes to maintenance and self-renewal of LSCs/LICs	(55)
WTAP	Renal cell carcinoma tissues and cell lines	Oncogene	Stabilizes the transcript and promotes *CDK2* expression, enhances cell proliferation *in vitro* and tumorigenesis *in vivo*, indicates poor prognosis	(56)
WTAP	Pancreatic cancer	Oncogene	Stabilizes *Fak* mRNA, activates Fak-PI3K-AKT and Fak-Src-GRB2-Erk1/2 pathways, promotes migration/invasion both *in vitro* and *in vivo*	(57)
FTO	Glioblastoma stem cells (GSCs)	Oncogene	Induces expression of oncogenes (*ADAM19*, *EPHA3*, *KLF4*), promotes GSC growth, self-renewal *in vitro* and brain tumor development *in vivo*	(42)
FTO	Breast cancer tissues and cell lines	Oncogene	Induces degradation of *BNIP3* mRNA, bursts tumor growth and metastasis *in vitro* and *in vivo*, suggests poor clinical outcome	(58)
FTO	Acute myeloid leukemia cells	Oncogene	Represses expression of *ASB2* and *RARA*, enhances cell proliferation *in vitro*, promotes leukemogenesis *in vivo*, blocks ATRA-induced cell differentiation	(59)
FTO	Acute myeloid leukemia cells	Oncogene	Increases *MYC/CEBPA* transcript levels and associated pathways, promotes leukemia cell proliferation/viability *in vitro*, enhances AML progression *in vivo* and shrinks mice survival	(60)
FTO/ALKBH5	*BRCA*-mutated epithelial ovarian cancer cells	Tumor suppressor	Destabilizes *FZD10* mRNA, inhibits Wnt/β-catenin, enhances cell sensitivity to PARP inhibitors	(61)
ALKBH5	Hypoxic breast cancer cells	Oncogene	Stabilizes *NANOG* mRNAs, induces breast cancer stem cell (BCSC) enrichment, promotes tumor initiation	(62)
ALKBH5	Glioblastoma stem-like cells (GSCs)	Oncogene	Enhances *FOXM1* expression, promotes GSCs proliferation *in vitro* and tumorigenesis *in vivo*	(63)
YTHDF1	Colorectal cancer tissues	Oncogene	Promotes cell proliferation, enhances resistance to fluorouracil and oxaliplatin	(64)
YTHDF1	Ocular melanoma	Tumor suppressor	Promotes the translation of *HINT2* mRNA, inhibits tumor progression *in vitro* and *in vivo*	(65)
YTHDF1	Nonsmall cell lung cancer cells	Oncogene/tumor suppressor	Promotes translation of CDK–cyclin complex and enhances tumor growth under normoxia condition; sensitizes cancer cells to cisplatin through reduced Nrf2-AKR1C1, the clearance system of reactive oxygen species (ROS)	(66)
YTHDF2	Hepatocellular carcinoma cells	Tumor suppressor	Promote degradation of *EGFR* mRNA, inhibits extracellular-signal-regulated kinase/mitogen-activated protein kinase signaling, suppresses cell proliferation and tumor growth *in vitro* and *in vivo*; represses inflammation and vascular abnormalization *via IL11* and *SERPINE2* mRNA decay, promotes metastasis	(67, 68)

(Continued)

TABLE 1 | Continued

Candidate	Tumor tissues or cell lines	Function	Mechanism	References
YTHDF2	Acute myeloid leukemia cells	Oncogene	Downregulates TNFR2, facilitates LSC development and AML propagation	(69)
YTHDC2	Colon cancer tissues	Oncogene	Facilitates translation of *HIF-1α* and *Twist1* mRNA in hypoxia, promotes cancer metastasis	(70)
IGF2BP1-3	Cervical and liver cancer cells	Oncogene	Enhances mRNA stability and translation, upregulates oncogenic genes such as *MYC*, facilitates tumor growth and invasiveness	(26)
IGF2BP1	Ovarian, liver, and lung cancer cells	Oncogene	Impairs miRNA-directed decay of *SRF* mRNA, enhances serum response factor (SRF)-driven transcription, sustains expression of *PDLIM7*, and *FOXK1*, promotes tumor growth and invasion	(71)
IGF2BP2	Colorectal tumor tissues	Oncogene	Stabilizes *HMGA2* mRNA by forming a circNSUN2/IGF2BP2/*HMGA2* ternary complex, promotes colorectal liver metastasis both *in vitro* and *in vivo*	(72)

PHLPP2, a negative AKT regulator, while dampens YTHDF2-promoted decay of transcripts encoding mTORC2, which is a positive AKT regulator.

In a nutshell, METTL3 modulates the expression of oncogenes and tumor suppressor genes primarily at posttranscriptional levels, including mRNA stability and translational process. Consequently, different downstream targets of METTL3 and the dominant cancer-related pathways involved in the process bring about the discrepancy in cell fate of different tumors.

METTL14

As is the case of METTL3 in glioblastoma, METTL14 depletion facilitates the malignant phenotype, characterized by upregulated oncogenes such as *ADAM19* and reduced expression of tumor suppressors such as *CDKN2A* (42). Meanwhile, loss-of-function mutation of METTL14 in endometrial tumor also diminishes m^{6}A methylation, inhibits YTHDF1-mediated translation of PHLPP2, and impedes YTHDF2-related mRNA decay of mTORC2, both of which regulate AKT pathway, as aforementioned in METTL3 (53). Subsequently, cell proliferation and tumorigenicity of endometrial tumors are increased, along with AKT stimulation.

Furthermore, m^{6}A modification is suppressed in HCC tissues, and METTL14 downregulation suggests poor prognosis for recurrence-free survival (54). In HCC, METTL14 restrains metastasis by enhancing pri-miR126 process into mature miRNA in a DGCR8-dependent manner. This result is opposite to the conclusion drawn by Chen et al. in primary HCC tissues that m^{6}A is significantly increased and overexpression of METTL3 promotes liver carcinogenesis through m^{6}A-YTHDF2-dependent degradation of *SOCS2* mRNAs (52). The controversy may be attributed to complex factors, including different reader proteins to sort mRNA transcripts, as well as distinct tumor samples and methodology of m^{6}A detection.

However, the opposite conclusion has been drawn in hematopoietic diseases. In normal HSPCs and AML cells carrying t(11q23), t(15;17), or t(8;21), METTL14 is overexpressed and exerts oncogenic role through m^{6}A signal by positively manipulating the stability and translation of *MYB* and *MYC* mRNA (55). This result is partially overlapped with the impact of METTL3 in AML, and might be explained by alternative reading process mediated by IGF2BPs, for an example. METTL14 undertakes an essential role in self-renewal of leukemia stem/initiation cells (LSCs/LICs) and AML progression (55). Silencing of METTL14 facilitates differentiation of both normal HSPCs and AML cells while repressing AML cell survival.

WTAP

In cancerous tissues of glioblastoma and cholangiocarcinoma, WTAP is overexpressed and promotes cell migration and invasion (74, 75). However, the regulation WTAP exerts on cell proliferation is cell-type specific. In AML, WTAP supports tumor growth but arrests differentiation of leukemia cells (76).

In renal cell carcinoma, WTAP indicates poor survival of patients, and knockdown of WTAP impedes cell proliferation *in vitro* and tumorigenesis *in vivo* (56). Mechanistically, WTAP binds to 3′-UTR of cyclin-dependent protein kinase 2 (*CDK2*) mRNAs and stabilizes the transcripts, lifting CDK2 protein level. As a key regulator of cell cycle, upregulation of CDK2 enables cell to cross the G1/S limit and initiates DNA replication. Similarly, in pancreatic cancer, WTAP promotes cell migration, invasion, and chemoresistance to gemcitabine via stabilizing focal adhesion kinase (*Fak*) mRNA and subsequently activating Fak-PI3K-AKT and Fak-Src-GRB2-Erk1/2 pathways (57).

To the best of our knowledge, WTAP promotes tumorigenic change in a variety of tumors. However, the underlying mechanism remains elusive. Future researches are required to unveil whether the regulatory role of WTAP in m^{6}A decoration is linked to these biological processes.

m^{6}A Erasers

FTO

A number of studies have attested to the tumorigenic role of FTO in various sorts of cancers. In endometrial carcinoma, β-estradiol induces expression of FTO and mediates cell growth and invasion (77). In addition, FTO inhibitor has been reported to abolish the expression of oncogenes such as *ADAM19* and to suppress GSC growth, self-renewal *in vitro*, and tumor development *in vivo* (42).

Silencing of FTO also attenuates cell growth and metastasis in breast cancer (58). Mechanistically, FTO disturbs the expression of *BNIP3*, a proapoptotic gene, both in mRNA and protein levels, via demethylating m^{6}A residues in 3′-UTR. On the other hand, YTHDF2 binding has proved to be uncoupled.

FTO is also significantly overexpressed in AMLs with t(11q23)/MLL rearrangements, t(15;17)/PML-RARA, FLT3-ITD, or NPM1 mutations (59). Reducing m^{6}A levels in *ASB2* and *RARA* mRNAs, FTO destabilizes the transcripts and, as a result, enhances leukemogenesis while blocks cell differentiation induced by all-trans-retinoic acid (ATRA) in these AML subtypes. Besides, researches also precluded YTHDF1/2 as readers regulating the stability of *ASB2* and *RARA* mRNAs.

Interestingly, R-2-hydroxyglutarate (R-2HG), a metabolic product in isocitrate dehydrogenase mutant cancers such as AML, is similar to α-KG structurally and competitively represses Fe (II)/α-KG-dependent dioxygenases (60). Thus, FTO could be suppressed by R-2HG in sensitive leukemia cells to elevate global m^{6}A RNA modification, which destabilizes the *MYC/CEBPA* transcripts and reduces their expression. As a crucial transcription factor in leukemogenesis, CEBPA being inhibited further inactivates FTO as a feedback loop and reinforces the growth-suppressive effect. Compared with METTL14 which promotes *MYC* mRNA stability via modulating m^{6}A abundance on 3′-terminal exons, FTO enhances MYC expression by demethylating m^{6}A sites on 5′-terminal and internal exons, which inhibits the YTHDF2-mediated RNA decay (55, 60).

However, in epithelial ovarian cancers (EOC) with *BRCA* mutation, downregulation of FTO confers resistance to PARP inhibitors such as Olaparib, with m^{6}A enrichment in 3′-UTR regions of *FZD10* and increased mRNA stability (61). FZD10 positively upregulates Wnt/β-catenin pathway and further promotes activity of homologous recombination. Meanwhile, stabilization of *FZD10* mRNA is mainly caused by the predominant effect of IGF2BP2, also overexpressed in resistant cells.

Obviously, when FTO mediates deprivation of m^{6}A signaling that is previously recognized by readers promoting mRNA stability, corresponding mRNA levels would be impaired. On the contrary, protein-coding mRNAs would be upregulated if FTO prevents YTHDF2-mediated mRNA decay via m^{6}A erasure. In this way, different binding proteins and downstream targets regulate the trend of tumor growth in coordination.

ALKBH5

Similar to FTO in *BRCA*-mutated EOC, expression of ALKBH5 is also inhibited, which activates Wnt/β-catenin pathway via stabilizing *FZD10* mRNA and renders cell resistance to Olaparib (61).

However, all sites subject to m^{6}A modification are not equally critical, since they are chosen to be involved in different biological pathways. ALKBH5 may play distinct roles from FTO due to their preference in molecular substrates. In hypoxic breast cancer cells, ALKBH5 demethylates *NANOG* mRNA and elevates the protein level via reduced mRNA decay, on the premise of hypoxia-inducible factors (HIFs) (62). As a pluripotency factor, upregulation of NANOG leads to enrichment of breast CSCs (BCSCs). Otherwise, ALKBH5 knockdown inhibits NANOG expression, reduces BCSC population, and impairs tumor formation *in vivo*.

Similarly, in glioblastoma, GSCs proliferation and tumor formation is disrupted upon ALKBH5 inhibition (63). Owing to enzymatic activity of ALKBH5, the nascent transcripts encoding FOXM1, a transcription factor, are stabilized and thus increases expression of relevant protein. Besides, interplay between ALKBH5 and FOXM1 can be enhanced by a non-coding RNA antisense to FOXM1 (*FOXM1-AS*).

m^{6}A Readers

YTHDF1

In colorectal cancer tissues, c-Myc drives the expression of YTHDF1 transcriptionally, and high level of YTHDF1 suggests poor prognosis in patients (64). Knockdown of YTHDF1 hinders cell proliferation and renders sensitization to fluorouracil and oxaliplatin. However, the detailed mechanism remains unknown.

Notably, YTHDF1 recognizes m^{6}A-marked transcripts of lysosomal proteases and promotes translation of lysosomal cathepsins in dendritic cells, which favors antigen degradation (78). Cross-presentation of engulfed neoantigens and cross-priming of CD8$^+$ T cells are then suppressed, contributing to the immune evasion and incomplete tumor elimination.

On the other hand, in ocular melanoma, YTHDF1 promotes the translation of m^{6}A-containing *HINT2* mRNA, a tumor suppressor (65). Scientists reported decreased m^{6}A levels in these tumor samples, which was significantly correlated with tumor progression both *in vitro* and *in vivo*. Therefore, specific m^{6}A-modified targets of YTHDF1 might vary according to the cellular context, resulting in different functions of YTHDF1 in various tumors.

Interestingly, a recently released study demonstrated the critical and contradictory role of YTHDF1 in hypoxia adaptation and pathogenesis of non-small cell lung cancer (66). Under normoxia conditions, YTHDF1 depletion restrains non-small cell lung cancer tumor growth *in vitro* and *in vivo*, which resulted from reduced translational efficiency of m^{6}A-marked transcripts such as CDK2, CDK4, and cyclin D1. On the other side, YTHDF1 deficiency renders resistance of cancer cells to cisplatin and indicates poor clinical outcome. Further study revealed that, under chemotherapy stress condition, YTHDF1 depletion leads to decreased translation of m^{6}A-modified Keap1, which upregulates Nrf2 and AKR1C1, the clearance system of reactive oxygen species. The adverse results highlight the importance of achieving a homeostasis of YTHDF1 expression and its targets between normal and stressful conditions.

YTHDF2

In HCC cells, YTHDF2 can be specifically restricted by hypoxia and act as a tumor suppressor with inhibitory effect on tumor growth (67). Mechanistically, YTHDF2 directly binds m^{6}A sites in 3′-UTR and mediates the degradation of *EGFR* mRNA, which is a main upstream regulator of extracellular-signal-regulated kinase/mitogen-activated protein kinase pathway. Hou et al. have also revealed in HCC that YTHDF2 reduction

provokes inflammation and vascular reconstruction, which facilitates the progression of tumor metastasis (68). In detail, the YTHDF2-mediated decay of m^{6}A-containing mRNAs are disrupted, such as interleukin 11 (*IL11*) and serpin family E member 2 (*SERPINE2*), which are account for the inflammation-associated malignancy and vascular abnormalization. What is more, administration of PT2385, a small molecule inhibitor targeting HIF-2α and restoring the expression of YTHDF2, also exhibits favorable effects in treating HCC cells both *in vitro* and *in vivo*.

Moreover, the roles of YTHDF2 in different context mainly depend on the degradation of respective target mRNAs. Paris et al. reported that YTHDF2 shortens half-life of m^{6}A-modified mRNAs of TNF receptor 2 (*TNFR2*), which normally prevents accumulation of leukemic cells and thus facilitates AML propagation (69). Targeting YTHDF2 not only eradicates LSCs but also expands hematopoietic stem cells (HSCs) to enhance myeloid reconstitution. In consequence, YTHDF2 inhibitor is considered as a candidate strategy for AML treatment. A noteworthy phenomenon in biological condition is that YTHDF2 mediates clearance of m^{6}A-modified mRNAs of Wnt-related genes to suppress Wnt signaling at stable state and maintain HSC quiescence (79). Upon hematological stresses, downregulation of YTHDF2 aberrantly upregulates target genes of Wnt signaling as well as survival-associated genes, which elevates not only proliferation but also regeneration capacity of HSCs synergistically, as a protective measure. Thus, we could gain a better understanding of the dual character of YTHDF2 in stem cells under physiological and pathological conditions.

YTHDC2

In colon cancer tissues, expression of YTHDC2 is positively correlated with the tumor stage (70). Further research shows that YTHDC2 unwinds highly structured 5′-UTR of mRNAs encoding transcription factors, HIF-1α and Twist1, and facilitates their translation. Notably, HIF-1α promotes epithelial-to-mesenchymal transition via the key regulator Twist1, initiating tumor metastasis.

IGF2BPs

IGF2BPs, a group of direct m^{6}A-binding proteins, enhance mRNA stability and translation both under normal and stress conditions, which gives rise to accumulation of oncogenic products such as MYC (26). In the absence of IGF2BPs, cell proliferation and invasion are significantly repressed in cervical and liver cancer cells.

IGF2BP1 impairs miRNA-directed degradation of mRNAs and sustains expression of serum response factor in ovarian, liver, and lung cancers, potentially in an m^{6}A dependent manner (71). This process enhances serum response factor-driven transcription and upregulates oncogenic drivers such as PDLIM7 and FOXK1.

Furthermore, IGF2BP2 has recently been proven to mediate colorectal liver metastasis, testified both *in vitro* and *in vivo* with metastasis PDX models (72). Mechanistically, the m^{6}A modification of circNSUN2 is recognized by YTHDC1, which accelerates the cytoplasmic export and further stabilizes *HMGA2* mRNA by forming a circNSUN2/IGF2BP2/*HMGA2* ternary complex in the cytoplasm. This outcome suggests a brand-new role of IGF2BP2 in mRNA stabilization via an m^{6}A-independent way and provides evidence that m^{6}A-modified circRNAs could serve as prognostic markers.

BIOINFORMATICS: AN EMERGING SERIES OF TOOLS FOR m^{6}A EXPLORATION

Meanwhile, with the field of bioinformatics booming in the past several years, researchers have established a number of databases delineating m^{6}A machinery, which provides valuable and comprehensive clues for future study (80–84). For instance, RMBase v2.0 deciphers the landscape of RNA modifications based upon epitranscriptome-sequencing data, while MODOMICS provides information regarding RNA modification pathways (80, 81).

Certainly, there exist multiple databases dedicated to the improvement of the m^{6}A-associated knowledge. To take MeT-DB v2.0 as an example, a powerful platform for methyl-transcriptomic research, identifies m^{6}A peaks as well as single-base sites (82). More importantly, context-specific functions of m^{6}A are elucidated via peak distribution plot and gene expression profiles under different conditions to identify m^{6}A-driven genes and networks. Another database, m6AVar, allows annotation and visualization of functional variants in the vicinity of m^{6}A sites and helps interpret their impact on m^{6}A mark by converting RNA sequences of target sites or key flanking nucleotides (83). This database also incorporates data from genome-wide association studies and ClinVar to identify disease-causing variants and explore their pathogenic molecular mechanisms. Both of the two databases intersect m^{6}A-modified sites with functional data such as binding sites of RNA-binding proteins and splicing factors as well as miRNA target sites to obtain regulatory pairs and speculate their roles in posttranscriptional regulation (82, 83).

In addition, a study has recently reported the molecular feature and clinical relevance of m^{6}A regulators reconstituted across 33 cancer types (84). The authors found widespread genetic alterations (mutations and copy number variations) to m^{6}A enzymes and established the cross-talk between their expression patterns with activity of cancer hallmark-related pathways, putatively helpful in prognostic stratification. Thus, we could see that bioinformatic tools not only complements the experimental results but also expedites the discovery of unrecognized regulatory roles of m^{6}A mark.

CLINICAL RELEVANCE OF m^{6}A-TARGETED STRATEGY

So far, small-molecule inhibitors targeting m^{6}A regulatory enzymes are not available in clinical use. However, due to the tumorigenic role of FTO in various cancers, scientist have developed several FTO inhibitors as promising tools in antileukemia and antiglioblastoma therapies.

As mentioned above, R-2HG exhibits broad antiproliferative effects in high-FTO leukemia via targeting FTO/MYC/CEBPA signaling (60). Meanwhile, R-2HG also has synergistic effect with first-line chemotherapy drugs such as decitabine and daunorubicin, which was validated in mouse models. Later on, Huang et al. utilized structure-guided design and developed two small-molecule FTO inhibitors, FB23 and its derivative FB23-2 (85). In comparison, the latter shows significantly improved antiproliferative activity in AML cells and induces cell differentiation. The authors also observed delayed AML progression and prolonged survival *in vivo*, which enlightens the strategy of targeting FTO demethylase in AML treatment.

Meclofenamic acid (MA) is originally approved by the Food and Drug Administration as a non-steroidal anti-inflammatory drug (86). MA2, which refers to the ethyl ester form of MA, has been identified as a selective FTO inhibitor, increasing m^{6}A levels in mRNAs. Application of MA2 represses GSC-initiated tumor progression and extends lifespan of xenografted mice (42).

In addition, scientist have newly identified entacapone, an inhibitor of catechol-O-methyltransferase applied for treatment of Parkinson's disease, as a chemical FTO inhibitor (87). Entacapone elicits effects on metabolic homeostasis through selectively targeting FTO activity, whereas its function in tumorigenesis remains to be elucidated.

Novel anticancer agents targeting other m^{6}A enzymes could possibly have therapeutic value as well. For example, METTL14 inhibitors are likely to be effective strategies to treat specific AML subtypes with high METTL14 expression, especially in combination with standard agents that induce myeloid differentiation (55). Combinatorial treatment of METTL3 inhibitors plus chemo- or radiotherapy may probably display much better outcome in pancreatic cancer patients (44).

Furthermore, CSCs refer to a group of rare immortal cells that could maintain clones of continuously growing tumors (88). The stem-cell frequency in a cancer is correlated with prognosis and therefore, targeting CSCs through m^{6}A regulation might be beneficial. For instance, competitive antagonists inhibiting ALKBH5 over other AlkB subfamily proteins such as FTO could possibly reduce the enrichment of BCSCs and impair their ability to initiate breast tumor (62). Nevertheless, m^{6}A regulatory enzymes might exert distinct impact on stem cells in physiological and pathological conditions as mentioned above (42, 43, 69, 73, 79). It is plausible to put forward that the m^{6}A-targeted strategy in CSCs must be conducted on the premise of distinguishing the normal stem cells from CSCs.

CONCLUSION

Evidently, m^{6}A modification has tremendous influence on RNA life cycle including RNA processing, nuclear export, and translation or degradation. At the same time, m^{6}A is involved in biological processes such as stem cell maintenance, tissue differentiation, and immune response. It seems that cellular m^{6}A levels need to be kept within an optimal range, whereas aberrant expression of m^{6}A factors will lead to cancer progression. Scientists have explored the impact of m^{6}A modification on gene expression and altered cell phenotypes, in hope of presenting novel approaches to conquer diseases.

However, clinical practice of small-molecular inhibitors targeting enzymes modulating m^{6}A levels has a great prospect but is still in its infancy. Several issues need to be tackled for the realization of its full potential. A major problem is that we need to gain a better understanding of the selectivity in transcripts and methylated sites in various tissues. Methylation patterns on transcripts might be molecular markers, which recruit distinct m^{6}A readers to enter downstream metabolism, respectively. Subsequently, side effects caused by the complex mRNAs targeted by m^{6}A enzymes may prevent the agents from achieving a favorable therapeutic index in the clinic. Moreover, heterogeneity in human cancer gives rise to distinct karyotypic patterns, protein and biomarker levels, and genetic profiles, which also requires consideration (89).

In conclusion, molecular mechanism of m^{6}A regulation in cancer biology still requests further exploration. Future researches could be focused on seeking the general discipline of specific interaction between m^{6}A mark and reader proteins as well as the heterogeneity in distinct tumor origins. Undoubtedly, m^{6}A methylation harbors great potential in exploiting brand-new therapies for human cancers. In the future, combination of small-molecule inhibitors targeting m^{6}A modification, biological agents, and immunotherapies may improve patient outcomes.

AUTHOR CONTRIBUTIONS

SY and XLi wrote the first draft of the manuscript. SL organized the structure of the manuscript. RY, XLiu, and SW contributed conception of the work. All authors contributed to manucript revision, read, and approved the submitted version.

REFERENCES

1. Jia G, Fu Y, He C. Reversible RNA adenosine methylation in biological regulation. *Trends Genet.* (2013) 29:108–15. doi: 10.1016/j.tig.2012.11.003
2. Zhao BS, Roundtree IA, He C. Post-transcriptional gene regulation by mRNA modifications. *Nat Rev Mol Cell Biol.* (2017) 18:31–42. doi: 10.1038/nrm.2016.132
3. Jia G, Fu Y, Zhao X, Dai Q, Zheng G, Yang Y, et al. N6-methyladenosine in nuclear RNA is a major substrate of the obesity-associated FTO. *Nat Chem Biol.* (2011) 7:885–7. doi: 10.1038/nchembio.687
4. Meyer KD, Jaffrey SR. Rethinking m^{6}A readers, writers, and erasers. *Annu Rev Cell Dev Biol.* (2017) 33:319–42. doi: 10.1146/annurev-cellbio-100616-060758
5. Dominissini D, Moshitch-Moshkovitz S, Schwartz S, Salmon-Divon M, Ungar L, Osenberg S, et al. Topology of the human and mouse

m6A RNA methylomes revealed by m6A-seq. *Nature.* (2012) 485:201–6. doi: 10.1038/nature11112
6. Meyer KD, Saletore Y, Zumbo P, Elemento O, Mason CE, Jaffrey SR. Comprehensive analysis of mRNA methylation reveals enrichment in 3′ UTRs and near stop codons. *Cell.* (2012) 149:1635–46. doi: 10.1016/j.cell.2012.05.003
7. Zhou C, Molinie B, Daneshvar K, Pondick JV, Wang J, Van Wittenberghe N, et al. Genome-wide maps of m6A circRNAs identify widespread and cell-type-specific methylation patterns that are distinct from mRNAs. *Cell Rep.* (2017) 20:2262–76. doi: 10.1016/j.celrep.2017.08.027
8. Ping XL, Sun BF, Wang L, Xiao W, Yang X, Wang WJ, et al. Mammalian WTAP is a regulatory subunit of the RNA N6-methyladenosine methyltransferase. *Cell Res.* (2014) 24:177–89. doi: 10.1038/cr.2014.3
9. Maity A, Das B. N6-methyladenosine modification in mRNA: machinery, function and implications for health and diseases. *FEBS J.* (2016) 283:1607–30. doi: 10.1111/febs.13614
10. Liu J, Yue Y, Han D, Wang X, Fu Y, Zhang L, et al. A METTL3-METTL14 complex mediates mammalian nuclear RNA N6-adenosine methylation. *Nat Chem Biol.* (2014) 10:93–5. doi: 10.1038/nchembio.1432
11. Bujnicki JM, Feder M, Radlinska M, Blumenthal RM. Structure prediction and phylogenetic analysis of a functionally diverse family of proteins homologous to the MT-A70 subunit of the human mRNA:m^{6}A methyltransferase. *J Mol Evol.* (2002) 55:431–44. doi: 10.1007/s00239-002-2339-8
12. Sorci M, Ianniello Z, Cruciani S, Larivera S, Ginistrelli LC, Capuano E, et al. METTL3 regulates WTAP protein homeostasis. *Cell Death Dis.* (2018) 9:796. doi: 10.1038/s41419-018-0843-z
13. Pendleton KE, Chen B, Liu K, Hunter OV, Xie Y, Tu BP, et al. The U6 snRNA m^{6}A methyltransferase METTL16 regulates SAM synthetase intron retention. *Cell.* (2017) 169:824–35.e14. doi: 10.1016/j.cell.2017.05.003
14. Shima H, Matsumoto M, Ishigami Y, Ebina M, Muto A, Sato Y, et al. S-adenosylmethionine synthesis is regulated by selective N^6-adenosine methylation and mRNA degradation involving METTL16 and YTHDC1. *Cell Rep.* (2017) 21:3354–63. doi: 10.1016/j.celrep.2017.11.092
15. Warda AS, Kretschmer J, Hackert P, Lenz C, Urlaub H, Höbartner C, et al. Human METTL16 is a N^6-methyladenosine(m^{6}A) (mA) methyltransferase that targets pre-mRNAs and various non-coding RNAs. *EMBO Rep.* (2017) 18:2004–14. doi: 10.15252/embr.201744940
16. Mendel M, Chen KM, Homolka D, Gos P, Pandey RR, McCarthy AA, et al. Methylation of structured RNA by the m^{6}A writer METTL16 is essential for mouse embryonic development. *Mol Cell.* (2018) 71:986–1000.e11. doi: 10.1016/j.molcel.2018.08.004
17. Fischer J, Koch L, Emmerling C, Vierkotten J, Peters T, Brüning JC, et al. Inactivation of the Fto gene protects from obesity. *Nature.* (2009) 458:894–8. doi: 10.1038/nature07848
18. Church C, Moir L, McMurray F, Girard C, Banks GT, Teboul L, et al. Overexpression of Fto leads to increased food intake and results in obesity. *Nat Genet.* (2010) 42:1086–92. doi: 10.1038/ng.713
19. Tsujikawa K, Koike K, Kitae K, Shinkawa A, Arima H, Suzuki T, et al. Expression and sub-cellular localization of human ABH family molecules. *J Cell Mol Med.* (2007) 11:1105–16. doi: 10.1111/j.1582-4934.2007.00094.x
20. Wang X, Zhao BS, Roundtree IA, Lu Z, Han D, Ma H, et al. N(6)-methyladenosine modulates messenger RNA translation efficiency. *Cell.* (2015) 161:1388–99. doi: 10.1016/j.cell.2015.05.014
21. Wang X, Lu Z, Gomez A, Hon GC, Yue Y, Han D, et al. N6-methyladenosine-dependent regulation of messenger RNA stability. *Nature.* (2014) 505:117–20. doi: 10.1038/nature12730
22. Shi H, Wang X, Lu Z, Zhao BS, Ma H, Hsu PJ, et al. YTHDF3 facilitates translation and decay of N-methyladenosine-modified RNA. *Cell Res.* (2017) 27:315–28. doi: 10.1038/cr.2017.15
23. Hsu PJ, Zhu Y, Ma H, Guo Y, Shi X, Liu Y, et al. Ythdc2 is an N-methyladenosine binding protein that regulates mammalian spermatogenesis. *Cell Res.* (2017) 27:1115–27. doi: 10.1038/cr.2017.99
24. Wojtas MN, Pandey RR, Mendel M, Homolka D, Sachidanandam R, Pillai RS. Regulation of mA transcripts by the 3′ → 5′ RNA helicase YTHDC2 is essential for a successful meiotic program in the mammalian germline. *Mol Cell.* (2017) 68:374–87.e12. doi: 10.1016/j.molcel.2017.09.021
25. Kasowitz SD, Ma J, Anderson SJ, Leu NA, Xu Y, Gregory BD, et al. Nuclear m6A reader YTHDC1 regulates alternative polyadenylation and splicing during mouse oocyte development. *PLoS Genet.* (2018) 14:e1007412. doi: 10.1371/journal.pgen.1007412
26. Huang H, Weng H, Sun W, Qin X, Shi H, Wu H, et al. Recognition of RNA N-methyladenosine by IGF2BP proteins enhances mRNA stability and translation. *Nat Cell Biol.* (2018) 20:285–95. doi: 10.1038/s41556-018-0045-z
27. Alarcón CR, Goodarzi H, Lee H, Liu X, Tavazoie S, Tavazoie SF. HNRNPA2B1 is a mediator of m^{6}A-dependent nuclear RNA processing events. *Cell.* (2015) 162:1299–308. doi: 10.1016/j.cell.2015.08.011
28. Meyer KD, Patil DP, Zhou J, Zinoviev A, Skabkin MA, Elemento O, et al. 5′ UTR m^{6}A promotes cap-independent translation. *Cell.* (2015) 163:999–1010. doi: 10.1016/j.cell.2015.10.012
29. Tang C, Klukovich R, Peng H, Wang Z, Yu T, Zhang Y, et al. ALKBH5-dependent m6A demethylation controls splicing and stability of long 3'-UTR mRNAs in male germ cells. *Proc Natl Acad Sci USA.* (2018) 115:E325–33. doi: 10.1073/pnas.1717794115
30. Adhikari S, Xiao W, Zhao YL, Yang YG. m^{6}A: signaling for mRNA splicing. *RNA Biol.* (2016) 13:756–9. doi: 10.1080/15476286.2016.1201628
31. Xiao W, Adhikari S, Dahal U, Chen YS, Hao YJ, Sun BF, et al. Nuclear m^{6}A reader YTHDC1 regulates mRNA splicing. *Mol Cell.* (2016) 61:507–19. doi: 10.1016/j.molcel.2016.01.012
32. Bartel DP. MicroRNAs: target recognition and regulatory functions. *Cell.* (2009) 136:215–33. doi: 10.1016/j.cell.2009.01.002
33. Alarcón CR, Lee H, Goodarzi H, Halberg N, Tavazoie SF. N6-methyladenosine marks primary microRNAs for processing. *Nature.* (2015) 519:482–5. doi: 10.1038/nature14281
34. Roundtree IA, Luo GZ, Zhang Z, Wang X, Zhou T, Cui Y, et al. YTHDC1 mediates nuclear export of N-methyladenosine methylated mRNAs. *eLife.* (2017) 6:e31311. doi: 10.7554/eLife.31311.040
35. Zheng G, Dahl JA, Niu Y, Fedorcsak P, Huang CM, Li CJ, et al. ALKBH5 is a mammalian RNA demethylase that impacts RNA metabolism and mouse fertility. *Mol Cell.* (2013) 49:18–29. doi: 10.1016/j.molcel.2012.10.015
36. Zheng Q, Hou J, Zhou Y, Li Z, Cao X. The RNA helicase DDX46 inhibits innate immunity by entrapping m^{6}A-demethylated antiviral transcripts in the nucleus. *Nat Immunol.* (2017) 18:1094–103. doi: 10.1038/ni.3830
37. Hsu PJ, Shi H, Zhu AC, Lu Z, Miller N, Edens BM, et al. The RNA-binding protein FMRP facilitates the nuclear export of N^6-methyladenosine-containing mRNAs. *J Biol Chem.* (2019). doi: 10.1074/jbc.AC119.010078. [Epub ahead of print].
38. Park OH, Ha H, Lee Y, Boo SH, Kwon DH, Song HK, et al. Endoribonucleolytic cleavage of m^{6}A-containing RNAs by RNase P/MRP complex. *Mol Cell.* (2019) 74:494–507.e8. doi: 10.1016/j.molcel.2019.02.034
39. Gao Y, Pei G, Li D, Li R, Shao Y, Zhang QC, et al. Multivalent m^{6}A motifs promote phase separation of YTHDF proteins. *Cell Res.* (2019). 29:767–9. doi: 10.1038/s41422-019-0210-3
40. Yang Y, Fan X, Mao M, Song X, Wu P, Zhang Y, et al. Extensive translation of circular RNAs driven by N-methyladenosine. *Cell Res.* (2017) 27:626–41. doi: 10.1038/cr.2017.31
41. Baquero-Perez B, Antanaviciute A, Yonchev ID, Carr IM, Wilson SA, Whitehouse A. The Tudor SND1 protein is an m^{6}A RNA reader essential for replication of Kaposi's sarcoma-associated herpesvirus. *eLife.* (2019) 8:e47261. doi: 10.7554/eLife.47261
42. Cui Q, Shi H, Ye P, Li L, Qu Q, Sun G, et al. m^{6}A RNA methylation regulates the self-renewal and tumorigenesis of glioblastoma stem cells. *Cell Rep.* (2017) 18:2622–34. doi: 10.1016/j.celrep.2017.02.059
43. Visvanathan A, Patil V, Arora A, Hegde AS, Arivazhagan A, Santosh V, et al. Essential role of METTL3-mediated m^{6}A modification in glioma stem-like cells maintenance and radioresistance. *Oncogene.* (2018) 37:522–33. doi: 10.1038/onc.2017.351
44. Taketo K, Konno M, Asai A, Koseki J, Toratani M, Satoh T, et al. The epitranscriptome m6A writer METTL3 promotes chemo- and radioresistance in pancreatic cancer cells. *Int J Oncol.* (2018) 52:621–9. doi: 10.3892/ijo.2017.4219
45. Cai X, Wang X, Cao C, Gao Y, Zhang S, Yang Z, et al. HBXIP-elevated methyltransferase METTL3 promotes the progression of breast cancer via inhibiting tumor suppressor let-7g. *Cancer Lett.* (2018) 415:11–9. doi: 10.1016/j.canlet.2017.11.018

46. Han J, Wang JZ, Yang X, Yu H, Zhou R, Lu HC, et al. METTL3 promote tumor proliferation of bladder cancer by accelerating pri-miR221/222 maturation in m^{6}A-dependent manner. *Mol Cancer.* (2019) 18:110. doi: 10.1186/s12943-019-1036-9
47. Yang F, Jin H, Que B, Chao Y, Zhang H, Ying X, et al. Dynamic m^{6}A mRNA methylation reveals the role of METTL3-m^{6}A-CDCP1 signaling axis in chemical carcinogenesis. *Oncogene.* (2019) 38:4755–72. doi: 10.1038/s41388-019-0755-0
48. Lin S, Choe J, Du P, Triboulet R, Gregory RI. The m^{6}A Methyltransferase METTL3 promotes translation in human cancer cells. *Mol Cell.* (2016) 62:335–45. doi: 10.1016/j.molcel.2016.03.021
49. Choe J, Lin S, Zhang W, Liu Q, Wang L, Ramirez-Moya J, et al. mRNA circularization by METTL3-eIF3h enhances translation and promotes oncogenesis. *Nature.* (2018) 561:556–60. doi: 10.1038/s41586-018-0538-8
50. Vu LP, Pickering BF, Cheng Y, Zaccara S, Nguyen D, Minuesa G, et al. The N(6)-methyladenosine (m^{6}A)-forming enzyme METTL3 controls myeloid differentiation of normal hematopoietic and leukemia cells. *Nat Med.* (2017) 23:1369–76. doi: 10.1038/nm.4416
51. Barbieri I, Tzelepis K, Pandolfini L, Shi J, Millan-Zambrano G, Robson SC, et al. Promoter-bound METTL3 maintains myeloid leukaemia by m^{6}A-dependent translation control. *Nature.* (2017) 552:126–31. doi: 10.1038/nature24678
52. Chen M, Wei L, Law CT, Tsang FH, Shen J, Cheng CL, et al. RNA N6-methyladenosine methyltransferase-like 3 promotes liver cancer progression through YTHDF2-dependent posttranscriptional silencing of SOCS2. *Hepatology.* (2018) 67:2254–70. doi: 10.1002/hep.29683
53. Liu J, Eckert MA, Harada BT, Liu SM, Lu Z, Yu K, et al. m^{6}A mRNA methylation regulates AKT activity to promote the proliferation and tumorigenicity of endometrial cancer. *Nat Cell Biol.* (2018) 20:1074–83. doi: 10.1038/s41556-018-0174-4
54. Ma JZ, Fu Y, Chuan-chuan Z, Feng L, Ji-hang Y, Fang W, et al. METTL14 suppresses the metastatic potential of hepatocellular carcinoma by modulating N^6-methyladenosine-dependent primary MicroRNA processing. *Hepatology.* (2017) 65:529–43. doi: 10.1002/hep.28885
55. Weng H, Huang H, Wu H, Qin X, Zhao BS, Dong L, et al. METTL14 inhibits hematopoietic stem/progenitor differentiation and promotes leukemogenesis via mRNA m^{6}A modification. *Cell Stem Cell.* (2018) 22:191–205.e9. doi: 10.1016/j.stem.2017.11.016
56. Tang J, Wang F, Cheng G, Si S, Sun X, Han J, et al. Wilms' tumor 1-associating protein promotes renal cell carcinoma proliferation by regulating CDK2 mRNA stability. *J Exp Clin Cancer Res.* (2018) 37:40. doi: 10.1186/s13046-018-0706-6
57. Li BQ, Liang ZY, Seery S, Liu QF, You L, Zhang TP, et al. WT1 associated protein promotes metastasis and chemo-resistance to gemcitabine by stabilizing Fak mRNA in pancreatic cancer. *Cancer Lett.* (2019) 451:48–57. doi: 10.1016/j.canlet.2019.02.043
58. Niu Y, Lin Z, Wan A, Chen H, Liang H, Sun L, et al. RNA N6-methyladenosine demethylase FTO promotes breast tumor progression through inhibiting BNIP3. *Mol Cancer.* (2019) 18:46. doi: 10.1186/s12943-019-1004-4
59. Li Z, Weng H, Su R, Weng X, Zuo Z, Li C, et al. FTO Plays an oncogenic role in acute myeloid leukemia as a N(6)-methyladenosine RNA demethylase. *Cancer Cell.* (2017) 31:127–41. doi: 10.1016/j.ccell.2016.11.017
60. Su R, Dong L, Li C, Nachtergaele S, Wunderlich M, Qing Y, et al. R-2HG exhibits anti-tumor activity by targeting FTO/m^{6}A/MYC/CEBPA signaling. *Cell.* (2018) 172:90–105.e23. doi: 10.1016/j.cell.2017.11.031
61. Fukumoto T, Zhu H, Nacarelli T, Karakashev S, Fatkhutdinov N, Wu S, et al. N-methylation of adenosine of FZD10 mRNA contributes to PARP inhibitor resistance. *Cancer Res.* (2019) 79:2812–20. doi: 10.1158/0008-5472.CAN-18-3592
62. Zhang C, Samanta D, Lu H, Bullen JW, Zhang H, Chen I, et al. Hypoxia induces the breast cancer stem cell phenotype by HIF-dependent and ALKBH5-mediated m6A-demethylation of NANOG mRNA. *Proc Natl Acad Sci USA.* (2016) 113:E2047–56. doi: 10.1073/pnas.1602883113
63. Zhang S, Zhao BS, Zhou A, Lin K, Zheng S, Lu Z, et al. m^{6}A Demethylase ALKBH5 maintains tumorigenicity of glioblastoma stem-like cells by sustaining FOXM1 expression and cell proliferation program. *Cancer Cell.* (2017) 31:591–606.e6. doi: 10.1016/j.ccell.2017.02.013
64. Nishizawa Y, Konno M, Asai A, Koseki J, Kawamoto K, Miyoshi N, et al. Oncogene c-Myc promotes epitranscriptome m^{6}A reader YTHDF1 expression in colorectal cancer. *Oncotarget.* (2018) 9:7476–86. doi: 10.18632/oncotarget.23554
65. Jia R, Chai P, Wang S, Sun B, Xu Y, Yang Y, et al. m^{6}A modification suppresses ocular melanoma through modulating HINT2 mRNA translation. *Mol Cancer.* (2019) 18(1):161. doi: 10.1186/s12943-019-1088-x
66. Shi Y, Fan S, Wu M, Zuo Z, Li X, Jiang L, et al. YTHDF1 links hypoxia adaptation and non-small cell lung cancer progression. *Nat Commun.* (2019) 10:4892. doi: 10.1038/s41467-019-12801-6
67. Zhong L, Liao D, Zhang M, Zeng C, Li X, Zhang R, et al. YTHDF2 suppresses cell proliferation and growth via destabilizing the EGFR mRNA in hepatocellular carcinoma. *Cancer Lett.* (2019) 442:252–61. doi: 10.1016/j.canlet.2018.11.006
68. Hou J, Zhang H, Liu J, Zhao Z, Wang J, Lu Z, et al. YTHDF2 reduction fuels inflammation and vascular abnormalization in hepatocellular carcinoma. *Mol Cancer.* (2019) 18:163. doi: 10.1186/s12943-019-1082-3
69. Paris J, Morgan M, Campos J, Spencer GJ, Shmakova A, Ivanova I, et al. Targeting the RNA m^{6}A Reader YTHDF2 selectively compromises cancer stem cells in acute myeloid leukemia. *Cell Stem Cell.* (2019) 25:137–148.e6. doi: 10.1016/j.stem.2019.03.021
70. Tanabe A, Tanikawa K, Tsunetomi M, Takai K, Ikeda H, Konno J, et al. RNA helicase YTHDC2 promotes cancer metastasis via the enhancement of the efficiency by which HIF-1α mRNA is translated. *Cancer Lett.* (2016) 376:34–42. doi: 10.1016/j.canlet.2016.02.022
71. Müller S, Glaß M, Singh AK, Haase J, Bley N, Fuchs T, et al. IGF2BP1 promotes SRF-dependent transcription in cancer in a m6A- and miRNA-dependent manner. *Nucleic Acids Res.* (2019) 47:375–90. doi: 10.1093/nar/gky1012
72. Chen RX, Chen X, Xia LP, Zhang JX, Pan ZZ, Ma XD, et al. N-methyladenosine modification of circNSUN2 facilitates cytoplasmic export and stabilizes HMGA2 to promote colorectal liver metastasis. *Nat Commun.* (2019) 10:4695. doi: 10.1038/s41467-019-12651-2
73. Chen J, Zhang YC, Huang C, Shen H, Sun B, Cheng X, et al. m6A regulates neurogenesis and neuronal development by modulating histone methyltransferase Ezh2. *Genomics Proteomics Bioinformatics.* (2019) 17:154–68. doi: 10.1016/j.gpb.2018.12.007
74. Jin DI, Lee SW, Han ME, Kim HJ, Seo SA, Hur GY, et al. Expression and roles of Wilms' tumor 1-associating protein in glioblastoma. *Cancer Sci.* (2012) 103:2102–9. doi: 10.1111/cas.12022
75. Jo HJ, Shim HE, Han ME, Kim HJ, Kim KS, Baek S, et al. WTAP regulates migration and invasion of cholangiocarcinoma cells. *J Gastroenterol.* (2013) 48:1271–82. doi: 10.1007/s00535-013-0748-7
76. Bansal H, Yihua Q, Iyer SP, Ganapathy S, Proia DA, Proia D, et al. WTAP is a novel oncogenic protein in acute myeloid leukemia. *Leukemia.* (2014) 28:1171–4. doi: 10.1038/leu.2014.16
77. Zhang Z, Zhou D, Lai Y, Liu Y, Tao X, Wang Q, et al. Estrogen induces endometrial cancer cell proliferation and invasion by regulating the fat mass and obesity-associated gene via PI3K/AKT and MAPK signaling pathways. *Cancer Lett.* (2012) 319:89–97. doi: 10.1016/j.canlet.2011.12.033
78. Han D, Liu J, Chen C, Dong L, Liu Y, Chang R, et al. Anti-tumour immunity controlled through mRNA m^{6}A methylation and YTHDF1 in dendritic cells. *Nature.* (2019) 566:270–4. doi: 10.1038/s41586-019-0916-x
79. Wang H, Zuo H, Liu J, Wen F, Gao Y, Zhu X, et al. Loss of YTHDF2-mediated m^{6}A-dependent mRNA clearance facilitates hematopoietic stem cell regeneration. *Cell Res.* (2018) 28:1035–8. doi: 10.1038/s41422-018-0082-y
80. Xuan JJ, Sun WJ, Lin PH, Zhou KR, Liu S, Zheng LL, et al. RMBase v2.0: deciphering the map of RNA modifications from epitranscriptome sequencing data. *Nucleic Acids Res.* (2018) 46:D327–34. doi: 10.1093/nar/gkx934
81. Boccaletto P, Machnicka MA, Purta E, Piatkowski P, Baginski B, Wirecki TK, et al. MODOMICS: a database of RNA modification pathways. 2017 update. *Nucleic Acids Res.* (2018) 46:D303–7. doi: 10.1093/nar/gkx1030
82. Liu H, Wang H, Wei Z, Zhang S, Hua G, Zhang SW, et al. MeT-DB V2.0: elucidating context-specific functions of N6-methyl-adenosine methyltranscriptome. *Nucleic Acids Res.* (2018) 46:D281–7. doi: 10.1093/nar/gkx1080
83. Zheng Y, Nie P, Peng D, He Z, Liu M, Xie Y, et al. m6AVar: a database of functional variants involved in m6A modification. *Nucleic Acids Res.* (2018) 46:D139–45. doi: 10.1093/nar/gkx895

84. Li Y, Xiao J, Bai J, Tian Y, Qu Y, Chen X, et al. Molecular characterization and clinical relevance of m6A regulators across 33 cancer types. *Mol Cancer.* (2019) 18:137. doi: 10.1186/s12943-019-1066-3
85. Huang Y, Su R, Sheng Y, Dong L, Dong Z, Xu H, et al. Small-molecule targeting of oncogenic FTO demethylase in acute myeloid leukemia. *Cancer Cell.* (2019) 35:677–91.e10. doi: 10.1016/j.ccell.2019.03.006
86. Huang Y, Yan J, Li Q, Li J, Gong S, Zhou H, et al. Meclofenamic acid selectively inhibits FTO demethylation of m6A over ALKBH5. *Nucleic Acids Res.* (2015) 43:373–84. doi: 10.1093/nar/gku1276
87. Peng S, Xiao W, Ju D, Sun B, Hou N, Liu Q, et al. Identification of entacapone as a chemical inhibitor of FTO mediating metabolic regulation through FOXO1. *Science Transl Med.* (2019) 11:eaau7116. doi: 10.1126/scitranslmed.aau7116
88. Clarke MF. Clinical and therapeutic implications of cancer stem cells. *N Engl J Med.* (2019) 380:2237–45. doi: 10.1056/NEJMra1804280
89. Lawson DA, Kessenbrock K, Davis RT, Pervolarakis N, Werb Z. Tumour heterogeneity and metastasis at single-cell resolution. *Nat Cell Biol.* (2018) 20:1349–60. doi: 10.1038/s41556-018-0236-7

Conflict of Interest: The authors declare that the research was conducted in the absence of any commercial or financial relationships that could be construed as a potential conflict of interest.

frontiers in Cell and Developmental Biology

ORIGINAL RESEARCH
published: 20 December 2019
doi: 10.3389/fcell.2019.00350

Long Non-coding RNA LINC-PINT Suppresses Cell Proliferation and Migration of Melanoma via Recruiting EZH2

Yangfan Xu[1,2†], Huixue Wang[1,2†], Fang Li[1,2†], Ludwig M. Heindl[3], Xiaoyu He[1,2], Jie Yu[1,2], Jie Yang[1,2], Shengfang Ge[1,2], Jing Ruan[1,2], Renbing Jia[1,2*] and Xianqun Fan[1,2*]*

[1] Department of Ophthalmology, Ninth People's Hospital, Shanghai Jiao Tong University School of Medicine, Shanghai, China, [2] Shanghai Key Laboratory of Orbital Diseases and Ocular Oncology, Shanghai, China, [3] Zentrum für Augenheilkunde, Universität zu Köln, Köln, Germany

OPEN ACCESS

Edited by:
Lei Chang,
Soochow University Medical College (SUMC), China

Reviewed by:
Duohui Jing,
Children's Cancer Institute Australia, Australia
Hamid Morjani,
Université de Reims Champagne-Ardenne, France

***Correspondence:**
Jing Ruan
drjruan@163.com
Renbing Jia
renbingjia@sjtu.edu.cn
Xianqun Fan
fanxq@sjtu.edu.cn

[†] These authors have contributed equally to this work

Specialty section:
This article was submitted to Molecular and Cellular Oncology, a section of the journal Frontiers in Cell and Developmental Biology

Received: 23 September 2019
Accepted: 04 December 2019
Published: 20 December 2019

Citation:
Xu Y, Wang H, Li F, Heindl ML, He X, Yu J, Yang J, Ge S, Ruan J, Jia R and Fan X (2019) Long Non-coding RNA LINC-PINT Suppresses Cell Proliferation and Migration of Melanoma via Recruiting EZH2. Front. Cell Dev. Biol. 7:350. doi: 10.3389/fcell.2019.00350

Long non-coding RNAs (lncRNAs) have been identified as crucial regulators in many human cancers. Many lncRNAs show aberrant expression in cancer, and some of them play critical roles in tumor proliferation, invasion, and metastasis. However, the regulatory functions of lncRNAs in melanoma progression remain to be elucidated. We utilized the Real-time PCR methodology to determine the expression of LINC-PINT in melanoma cell lines. To evaluate the effect of LINC-PINT on tumorigenesis of melanoma, we used Cell Counting Kit-8 (CCK8) and colony formation assay. Flow cytometry assay was used to detect the function of LINC-PINT on cell cycle status. PINT-interacting proteins were identified by chromatin isolation using RNA purification (ChIRP). Microarray assay and bioinformatics analysis were used to find the potential target genes of LINC-PINT and the status of LINC-PINT target gene candidate was verified using chromatin immunoprecipitation assay (ChIP). LINC-PINT plays a role in suppressing the tumorigenicity of melanoma, which was further determined by xenograft model assay. LINC-PINT was significantly downregulated in melanoma tissues and cell lines. The overexpression of LINC-PINT in tumor cells resulted in significant tumor growth reduction and migration inhibition in A375, Mum2B and CRMM1 cells. Results based on the *in vivo* xenograft model were further consistent with the *in vitro* findings that LINC-PINT impeded growth and metastasis of melanoma cells. Microarray assay and bioinformatics analysis indicated that CDK1, CCNA2, AURKA, and PCNA were potential targets of LINC-PINT. In conclusion, LINC-PINT inhibits the tumorigenicity of melanoma through recruiting EZH2 to the promoter of its target genes, leading to H3K27 trimethylation and epigenetic silencing of target genes. LINC-PINT may serve as a novel diagnostic and therapeutic target for melanoma.

Keywords: LINC-PINT, melanoma, EZH2, CDK1, CCNA2, AURKA, PCNA

INTRODUCTION

Melanoma is a malignant tumor that initiates from pigment-producing cells called melanocytes and progresses in a step-wise fashion (Bastian, 2014). It occurs in tissue that contains these cells, including the base of the epidermis, the eye, and the epithelia of the respiratory and urogenital tract (Arozarena and Wellbrock, 2019). Melanoma is exceedingly aggressive, which is based on

the high metastatic potential of melanoma cells. Despite recent progresses in melanoma targeted therapies, this malignancy still could not be efficiently managed (Zingg et al., 2015). Although novel therapeutic strategies have been developed over the past few decades (Hersey and Gallagher, 2012; Niezgoda et al., 2015), metastatic melanoma is associated with a poor prognosis (Tsao et al., 2012). Thus, better therapies for melanoma are in urgent need to be established.

Long non-coding RNAs (lncRNAs) are functionally defined as transcripts more than 200 nucleotides in length with no protein coding potential. There're tens of thousands lncRNAs in human cells, many of which are uniquely expressed in differentiated tissues or specific cancer types (Schmitt and Chang, 2016; Arun et al., 2018; Wang et al., 2019). LncRNAs are being increasingly recognized to contribute to many biological processes through diverse mechanisms (Cech and Steitz, 2014; Takahashi et al., 2014). Recently, it is reported that many lncRNAs are affecting gene activity in potent *cis*- and *trans*-regulation pattern and they function as scaffolds for chromatin-modifying complexes (Kim and Sung, 2012), thus regulating the process of RNA degradation and histone modifications (Guttman and Rinn, 2012). LINC-PINT, which is also known as long intergenic non-protein-coding RNA p53-induced transcript, has been reported to exert its functions in some diseases. For example, it directly interacts with the polycomb repressive complex 2 (PRC2) to regulate the expression of its target genes (Marin-Bejar et al., 2013, 2017). In addition, the circular form of LINC-PINT could translate a functional peptide to suppresses the proliferation of glioblastoma cells (Zhang et al., 2018). Although it is reported by a recent study that LINC-PINT is downregulated in melanoma tissues and inhibited cell proliferation through downregulating lncRNA BANCR (Huang et al., 2019), whether LINC-PINT has novel functions with diverse mechanism in human melanoma still remains to be identified.

In this study, it's our aim to identify the potential regulation role of LINC-PINT in melanoma progression. Through gain- and loss-function experiments *in vitro* and *in vivo*, we found that overexpression of LINC-PINT inhibited the progression of human melanoma. Mechanistically, we showed that LINC-PINT recruited the enhancer of zeste homolog 2 (EZH2) protein to the promoters of CDK1, CCNA2, AURKA, and PCNA gene, leading to H3K27 trimethylation and epigenetic silencing of target genes. Our findings elucidated the tumor-suppressive role of LINC-PINT in human melanoma and unveiled its molecular mechanism underlying tumor progression which might thereby suggest a novel therapeutic strategy for melanoma.

MATERIALS AND METHODS

RNA Preparation, Reverse Transcription and Quantitative Real-Time PCR

Total RNA was extracted from malignant melanoma cell lines and normal control cells using TRIzol Reagent (Invitrogen, Carlsbad, CA, United States) and then cDNA was synthesized using PrimeScript RT Master Mix (Takara, Dalian, China) following the manufacturer's protocol. Real-time PCR analyses were performed using Power SYBR Green PCR Master Mix (Applied Biosystems, Irvine, CA, United States) on an ABI 7500 real-time PCR system. The glyceraldehyde-3 phosphate dehydrogenase (GAPDH) gene was selected as a reference control. We performed each experiment in triplicate, and listed the primer sets in **Supplementary Table 3**.

Cell Lines and Cell Culture

The human malignant melanoma cell line A375 and Mum2B were cultured in DMEM (GIBCO, Carlsbad, CA, United States) supplemented with 10% certified heat-inactivated fetal bovine serum (FBS; GIBCO), penicillin (100 U/mL), and streptomycin (100 mg/mL) at 37°C in a humidified 5% CO_2 atmosphere. The human conjunctival melanoma cell line CRMM1 was maintained in Ham's F-12K (Kaighn's) medium (GIBCO), and the human melanocyte cell line PIG1 was cultured in Medium 254 (GIBCO) with 10% FBS and antibiotics under conditions described above.

Plasmid Construction, Lentivirus Packaging and Transfection

The pCDNA3.1 vector (Genechem Technology Co., Shanghai, China) was used in our system. To overexpress LINC-PINT, the LINC-PINT sequence was generated by PCR and cloned into the pcDNA3.1 vector. For lentivirus packaging, the Lipofectamine 2000 reagent (Invitrogen, Carlsbad, CA, United States) was incubated with Opti-MEM I Reduced Serum Medium (GIBCO) and used to transfect 293T cells with 3 μg pCDNA3.1-LINC-PINT or pCDNA3.1-vector plasmids or 3 μg pMD2.D plasmids or 6 μg PsPax plasmids. 48 and 72 h after transfection, the supernatant containing the virus was collected, filtered and concentrated. 24 h prior to the lentiviral transfection, the cells were seeded at 3.0×10^5 cells per well in a 60 mm plate. The next day, an optimal volume of lentivirus was added into the culture medium and supplemented with 8 ng/ml polybrene (Sigma-Aldrich, St. Louis, MO, United States), and the cells were maintained in the virus-containing medium for 48 h. Stable cell lines were selected by incubating with 4 μg/ml puromycin (InvivoGen, San Diego, CA, United States) for 2 weeks.

Western Blot

In brief, cells were harvested, rinsed and lysed with lysis buffer, and the total protein concentration was measured using a BCA protein assay kit (Beyotime Institute of Biotechnology, China). Protein samples were separated using sodium dodecyl sulfate-polyacrylamide gel electrophoresis (SDS-PAGE) in 7.5% (*w*/*v*) polyacrylamide gels and then transferred to polyvinylidene fluoride membranes (PVDF membranes; Millipore, Bedford, MA, United States). After the membranes were blocked with 5% BSA for 1 h at room temperature, they were incubated with the primary antibodies anti-EZH2 (Abcam, Cambridge, MA, United States), anti-CDK1 (Abcam), anti-CCNA2 (CST, Danvers, MA, United States), anti-AURKA (Abcam), anti-PCNA (CST), or anti-β-Actin (Sigma-Aldrich) at 4°C overnight. The horseradish peroxidase-conjugated secondary antibodies (mouse IgG and rabbit IgG, CST) were utilized for 1-h incubation at

room temperature. β-actin served as a reference control. The band signals were visualized and quantified using the ECL-PLUS/Kit (Millipore).

CCK8 Assay

To evaluate cell proliferation capability, the CCK8 (Cell Counting Kit-8) colorimetric assays was utilized. Cells were seeded at 2.0×10^3 cells per well into the flat-bottomed 96-well plates with 100 μl culture medium. Then, 10 μl of CCK8 solution (Dojidon, Kumamoto, Japan) was added to the wells, and the samples were incubated at 37°C in 5% humidified CO_2 atmosphere. A microplate reader (ELX800, BioTec, Winooski, VT, United States) was employed to measure the absorbance of samples at 450 nm for four consecutive days, as previously described. We performed each independent experiment three times and presented the results as the mean ± SD.

Soft Agar Formation Assay

Soft agar formation assay was conducted as described in our previous study. LINC-PINT-oe or Mock cells were harvested, counted and resuspended in 1.0 ml 0.3% agar complete medium and 1.0×10^3 cells were seeded into six-well plates embedded with 1.0 ml 0.6% agar complete medium layer. After 3–4 weeks of incubation, the colonies were stained with 1% crystal violet, sufficiently washed with PBS, then they were counted and photographed. To calculate the colony formation rate, the number of colonies generated in Mock cells group were set to one.

Cell Cycle Analysis

Cells were harvested, washed once with cold PBS and fixed with pre-cold 75% ethanol at −20°C overnight. After incubating with RNase A (Qiagen, Hilden, German) in 37°C for 30 min, the cells were stained with 50 μl/ml PI and treated with 0.5% Triton PBS. Then, the cells were incubated with an anti-H3 antibody (Abcam) at a 1:100 dilution. The stained cells were subjected to analysis by flow cytometry facility (Guava easyCyte HT from Millipore).

Rapid Amplification of cDNA Ends Assay (RACE)

Total RNA was extracted by TRIzol plus RNA Purification Kit (Invitrogen). RACE PCR products were obtained using Platinum PCR Supermix High Fidelity (Invitrogen) and separated using a 1.5% agarose (Sigma) gel. A gel extraction kit was utilized to extract the gel products, which were then cloned into a pGM-T vector and sequenced. The specific 3′ RACE and 5′ RACE primers are listed in **Supplementary Table 3**.

Chromatin Isolation by RNA Purification (ChIRP)

A Magna ChIRP RNA Interactome Kit (Millipore) was used to perform ChIRP experiment according to the manufacturer's protocols. A group of 3′ end Biotin-TEG modified DNA probes targeting LINC-PINT was synthesized and utilized. A total of 5×10^8 cells were cross-linked with 3% formaldehyde and sonicated for the hybridization reaction. The sequences of the probes are available in **Supplementary Table 3**.

RNA-Chromatin Immunoprecipitation (RIP)

The EZ-Magana RIP kit (Millipore) was utilized to perform RIP experiment per the manufacturer's previously reported protocol. A total of 1.0×10^7 cells were lysed with RIP lysis buffer and subjected for co-immunoprecipitation with anti-EZH2 (Active Motif, Carlsbad, CA, United States) or normal mouse IgG antibody (Millipore). Then the retrieved RNA was analyzed by reverse transcription PCR.

Chromatin Immunoprecipitation (ChIP)

For ChIP assay, the EZ-Magna ChIP A/G kit (Millipore) was used following the instructions as previously described by the manufacturer. The anti-EZH2 (Active Motif) and anti-H3K27me3 (Active Motif) were applied. Anti-normal mouse IgG (Millipore) and anti-RNA polymerase-II (Abcam) were used as negative control, or positive control, respectively. Primers for ChIP-qPCR are listed in **Supplementary Table 3**.

DNA Microarray Analysis and Bioinformatics Analysis

For a gene expression study, we purified and hybridized three independent replicates of RNA samples from A375 cells with or without LINC-PINT overexpression to microarray gene chips. In this experiment, the GeneChip PrimeView Human Gene Expression Array (Affymetrix, Santa Clara, CA, United States) was employed. In brief, total RNA samples from A375 Mock cells and A375 LINC-PINT oe cells was extracted using TRIzol reagent (Invitrogen, United States) and quantified by NanoDrop 2000 (Thermo Fisher Scientific, Waltham, MA, United States). 0.5 μg purified RNA was transcribed to cDNA. The Agilent RNA 6000 Nano Kit (Agilent Technologies, Santa Clara, CA, United States) was used to assess the RNA integrity by the Agilent 2100 Bioanalyzer. The GeneChip 3' IVT labeling kit (Affymetrix) was used to synthesize biotin-labeled RNA, which were then hybridized onto the microarrays. After the sample labeling, microarray hybridization and washing steps were conducted following the manufacturer's instructions, the arrays were directly scanned by the Affymetrix Scanner 3000 (Affymetrix). The subsequent microarray data processing was done as previously described (Lu et al., 2017). Differentially expressed genes were identified by a threshold of three-fold change (p-value < 0.05).

Tumor Xenograft Model in Nude Mice

Four-week-old male BALB/c nude mice were maintained in specific pathogen-free (SPF) animal room and used in tumor xenograft assays. A total of 1.0×10^7 A375 cells transfected with or without LINC-PINT lentivirus were subcutaneously injected into the right armpit of the BALB/c nude mice ($n = 5$ for each group). The tumor volume [length (mm) × width $(mm)^2/2$] of each mouse was measured every five days for twenty-five consecutive days. Afterward, the mice were euthanized and the tumors were harvested, evaluated and photographed. For the *in vivo* metastasis assay, the nude mice were deeply anesthetized and total of 2.0×10^6 A375 or Mum2B cells transfected with *Luc*-tag from LINC-PINT overexpression or Mock group were

injected through the caudal vein of each mouse (n = 3 for each group). We utilized live animal BLI system to monitor tumor growth and lung metastases. All the mice were sacrificed after 3 weeks and the lungs were carefully resected, fixed and examined for metastases via haematoxylin and eosine (HE) staining.

The animal experiments were carried out in strict accordance with the guidelines of the Shanghai Jiao Tong University School of Medicine Animal Care and Use Committee, by whom the protocols were also approved (permit number: HKDL [2014]70, 25 February 2014).

Statistical Analyses

For all of the results, the data are presented as the mean ± SD, and a p-value less than 0.05 was considered statistically significant. The differences between two groups were compared by unpaired two-sided Student's t-test or ANOVA. We performed the analyses with IBM SPSS Statistics 20 (Chicago, IL, United States).

RESULTS

LINC-PINT Was Lowly Expressed in Melanoma Tumor Tissues and Cell Lines

We used high-throughput RNA-sequence analysis to identify the lncRNAs that were differentially expressed between melanoma A375 cells and normal control PIG1 cells. We found that LINC-PINT was one of the most downregulated lncRNAs in melanoma cells (**Figure 1A**). Moreover, LINC-PINT expression level was also significantly low in melanoma tissues compared with adjacent normal tissues (**Figure 1B**). Notably, survival analysis showed that low LINC-PINT expression was prominently correlated with poor overall survival (**Figure 1C**) and disease-free survival (**Figure 1D**) for melanoma patients. These data indicated that LINC-PINT might play a key regulatory role in melanoma progression.

Identification and Cellular Distribution of LINC-PINT in Melanoma Cells

Then we aimed to identify the biological characteristics of LINC-PINT in melanoma. We predicted the secondary structure of LINC-PINT in the RNAfold web server (**Figure 2A**). Furthermore, total RNAs extracted from melanoma cells (A375) was used to clone the full-length of LINC-PINT transcripts by 5'- and 3'- RACE technologies (**Figure 2B**). As shown in **Figure 2C**, both 3'-RACE and 5'-RACE results showed that only one band was presented, indicating that there are only one LINC-PINT isoform exists in melanoma cells (**Figure 2C**). According to the National Center for Biotechnology Information (NCBI) database, the transcript of LINC-PINT previously reported was 1173-bp in length with four exons. In our study, however, we identified a novel 1430-bp transcript with five exons through the rapid amplification of cDNA ends (RACE) detection. More precisely, exon one of the novel transcript had an additional 12-bp fragment at the 5-terminus, and exon four was extended by 279-bp. Compared with the predict sequence, this novel transcript also had an additional poly-A tail at the 3-terminus (**Supplementary Figure 1**). We then examined LINC-PINT expression in different tumor cells. The expression levels of LINC-PINT in melanoma cells were significantly low (**Figure 2D**). Thus, we selected melanoma cell lines A375, Mum2B and CRMM1 to test whether LINC-PINT overexpression could alter the tumor behavior. The biological function of lncRNAs is strongly associated with their subcellular localizations. Thus, cellular fractionation assay was conducted and determined that LINC-PINT distributed mainly in the nucleus of melanoma cells (**Figure 2E**). RNA fluorescence *in situ* hybridization (RNA-FISH) further confirmed that LINC-PINT was enriched in the nuclear fraction (**Figure 2F**).

LINC-PINT Inhibited Melanoma Progression *in vitro*

To investigate whether the tumor behavior could be significantly altered by this novel transcript of LINC-PINT, we first overexpressed LINC-PINT by using control cell lines, which was transfected with virus carrying an empty pcDNA3.1 vector. Using EGFP as a tracking marker, we then observed green fluorescence in A375, Mum2B and CRMM1 cells. We detected that LINC-PINT was successfully overexpressed in these melanoma cells by real-time PCR (**Figure 3A**). CCK8 assay showed that cell proliferation was significantly suppressed in LINC-PINT-overexpressed melanoma cells (**Figure 3B**). Consistently, the colony formation of melanoma cells was decreased after overexpressing LINC-PINT. We also observed that the LINC-PINT-overexpressed melanoma cells formed smaller colonies (**Figure 3C**). Moreover, we performed flow cytometry assay to determine whether LINC-PINT was involved in cell cycle regulation and found that LINC-PINT overexpression induced G0/G1 cell cycle arrest in melanoma cells (**Figure 3D**). Furthermore, transwell assay showed that LINC-PINT overexpression also inhibited the migration ability of melanoma cells (**Figure 3E**).

LINC-PINT Inhibited Melanoma Progression *in vivo*

To investigate the ability of LINC-PINT to suppress tumor formation *in vivo*, we established a xenograft model in nude mice using A375 cells. We injected A375 and LINC-PINT-overexpressed A375 cells into nude mice. Then, we evaluated the size of the resultant tumors every 5 days for 25 days. We found that LINC-PINT overexpression notably repressed tumor progression. The tumor volumes in the overexpression group were significantly reduced compared with those of the controls (**Figures 4A,B**). Immunohistochemistry staining showed that compared with those from control group, tumors derived from LINC-PINT-overexpressed group exhibited lower expression of proliferation marker Ki67 (**Figure 4C**). Moreover, the tumor weights from LINC-PINT-overexpressed group were also significantly reduced (**Figure 4D**). In addition, we assessed the impact of LINC-PINT on metastasis ability *in vivo* using a lung metastasis mouse model. The results revealed that LINC-PINT overexpression noticeably inhibited melanoma metastasis (**Figures 4E,F**). Taken together, these data were consistent with *in vitro* results.

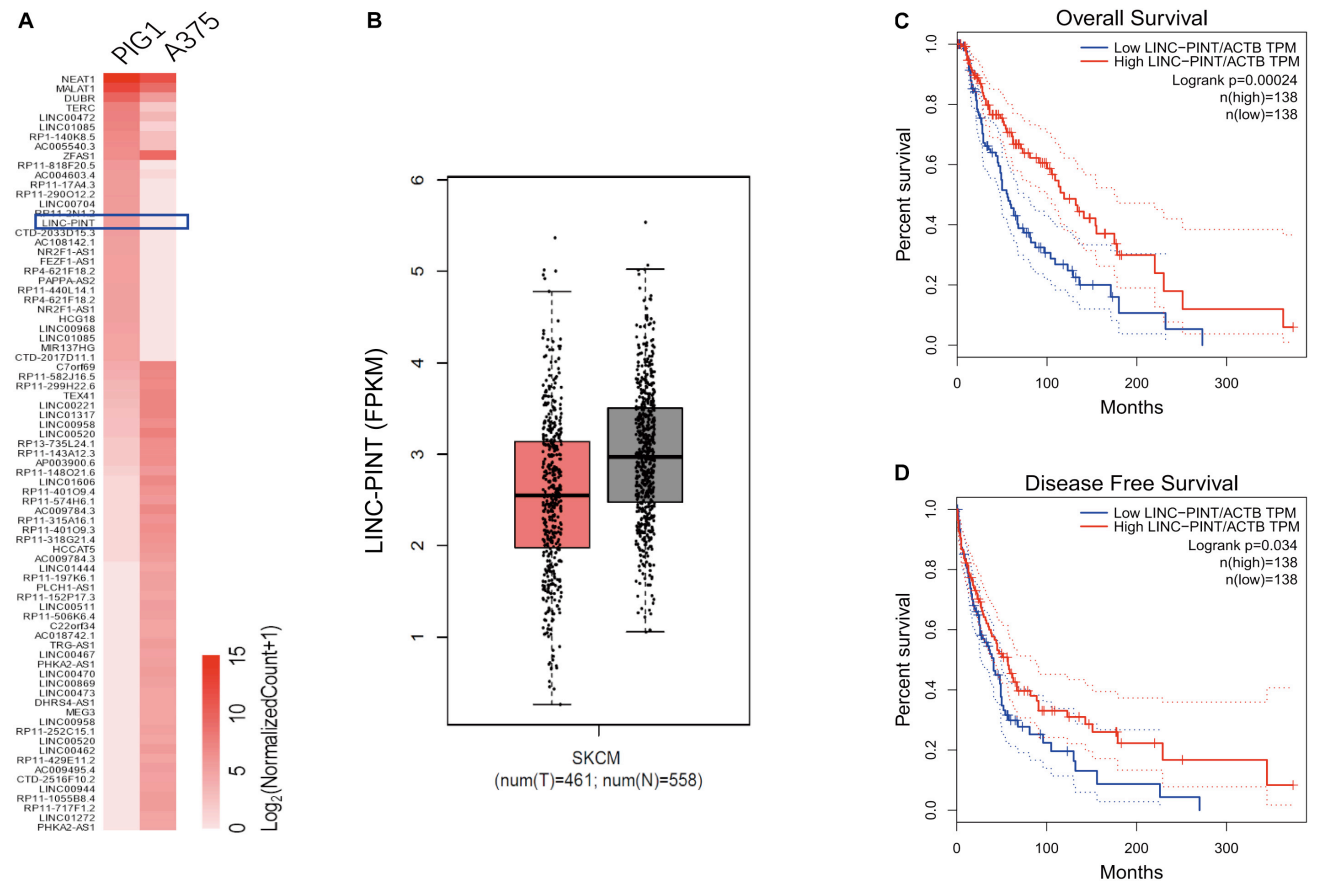

FIGURE 1 | LINC-PINT was lowly expressed in melanoma tumor tissues and cell lines. **(A)** Hierarchical cluster plot showed the top 50 up- and 30 down-regulated lncRNAs (fold change >2, $p < 0.05$). The blue square denotes LINC-PINT **(B)** The expression of LINC-PINT in melanoma tissues ($n = 461$) versus adjacent normal tissues ($n = 558$) from GEPIA database (Gene Expression Profiling Interactive Analysis database; gepia.cancer-pku.cn). The whiskers indicate means ± SD in the plots. **(C–D)** Kaplan–Meier survival analysis of patient overall survival **(C)** and disease-free survival **(D)** according to LINC-PINT levels in melanoma tissues.

Identifying the Target Genes of LINC-PINT in Melanoma Cells

To comprehensively analyze the tumor-suppressive regulatory effect of LINC-PINT on gene expression, we performed a microarray analysis to profile gene expression in melanoma cells with or without LINC-PINT overexpression. The results showed that 2481 transcripts were downregulated while 2072 transcripts were upregulated in LINC-PINT-overexpressed A375 cells (**Figure 5A**). We then performed Kyoto Encyclopedia of Genes and Genomes (KEGG) analysis and found that DNA replication and cell cycle pathways were the highest affected biological processes after LINC-PINT overexpression in A375 cells (**Figure 5B**). Using hierarchical cluster analysis, we found that the expression of several genes (CDK1, CCNA2, AURKA, PCNA) involving in the cell cycle and tumorigenesis were reduced significantly (**Figure 5C**). We then validated the expression of these genes by real-time PCR (**Figures 5D,E**) and western blot (**Figure 5F**). Collectively, these data suggested that LINC-PINT regulated melanoma progression by modulating the expression of a series of cell cycle genes.

LINC-PINT Recruited EZH2 to Inhibit Gene Expression

LncRNAs are reported to fulfill their functions through active interactions with RNA binding proteins (Guttman and Rinn, 2012; Geisler and Coller, 2013). To explore the molecular mechanism by which LINC-PINT affects gene expression, we sought to identify proteins that were interacting with LINC-PINT by chromatin isolation by RNA purification (ChIRP) experiment (**Figure 6A**; **Supplementary Figure 2**). LINC-PINT-binding proteins was then identified by mass spectrometry (**Supplementary Tables 1**, **2**). EZH2 was the only functional protein distributed in the nucleus that was binding to LINC-PINT both in A375 and Mum2B. Tri-methylation of lysine 27 on histone 3 (H3K27me3) by the methyltransferase EZH2, as a part of PRC2, is one of the most important epigenetic mechanism of gene silencing (Hirukawa et al., 2018). The ChIRP-MS results showed that EZH2 protein was enriched by LINC-PINT probes, but not the negative control probes, as further confirmed by western blot (**Figure 6B**). The interaction of LINC-PINT with EZH2 was further validated by RNA immunoprecipitation (RIP) experiment (**Figures 6C,D**). Then we performed a chromatin

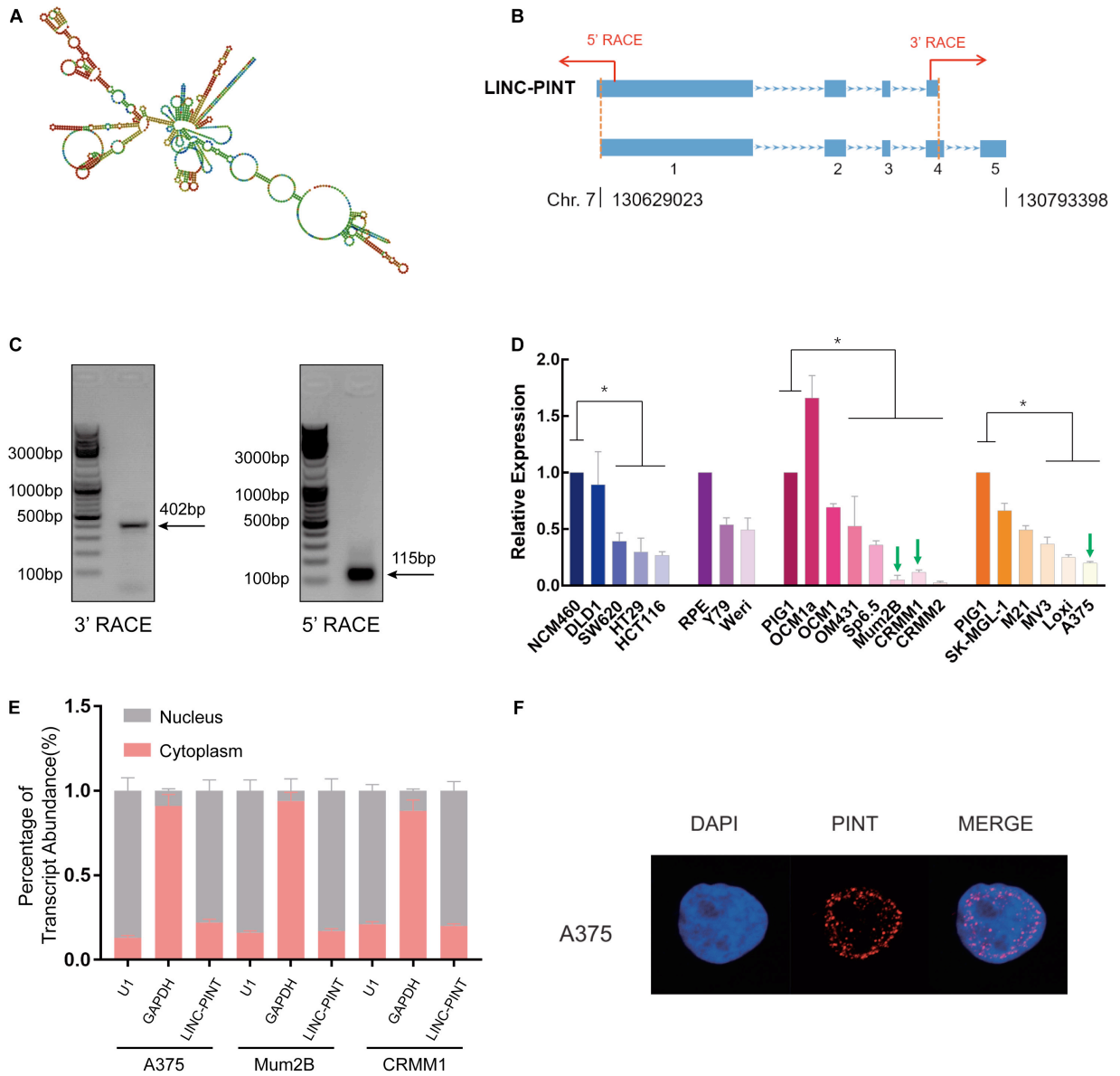

FIGURE 2 | Identification and cellular distribution of LINC-PINT in melanoma cells. **(A)** Secondary structure of LINC-PINT predicted by RNAfold web server (http://rna.tbi.univie.ac.at/cgi-bin/RNAWebSuite/RNAfold.cgi). **(B)** Schematic illustration of the primers for RACE assay. **(C)** Agarose gel electrophoresis of PCR products generated by 3'- (left) and 5'- (right) RACE technologies. **(D)** Real-time PCR analysis of LINC-PINT expression in different cell lines. LINC-PINT presented lower expression in a series of tumor cells than in normal gastrointestinal cells (NCM460), retinal pigment epithelium cells (RPE) and normal skin cells (PIG1) $^*p < 0.05$. **(E)** Cell nuclear/cytoplasmic fraction analysis and real-time PCR confirmed LINC-PINT was expressed mainly in the nucleus; U1 and GAPDH RNA served as positive controls for the nuclear and cytoplasmic fractions, respectively. **(F)** RNA FISH analysis shows that LINC-PINT was located predominantly in the nucleus of A375 cells.

immunoprecipitation (ChIP) assay in Mock and LINC-PINT overexpressed A375 cells to confirm the interactions between epigenetic modifiers and the promoter regions of LINC-PINT target genes. As expected, LINC-PINT overexpression generated decreased location of EZH2, H3K27me3, and RNA polymerase-II levels in the promoter regions of CDK1, CCNA2, AURKA, and PCNA, but not in the negative control and GAPDH, indicating that LINC-PINT overexpression might directly result in downregulation of these genes (**Figures 7A–F**).

DISCUSSION

Although mutation of some genes, such as BRAF, NRAS, and TP53, have been identified as risk factors for melanoma progression (Byron et al., 2012; Posch et al., 2013; Lissanu Deribe et al., 2016; Hayward et al., 2017; Ojha et al., 2019), our knowledge of molecular mechanism underlying the malignant melanoma remains obscure. Recently, numerous lncRNAs have been discovered in diverse types of tumors through high-throughput

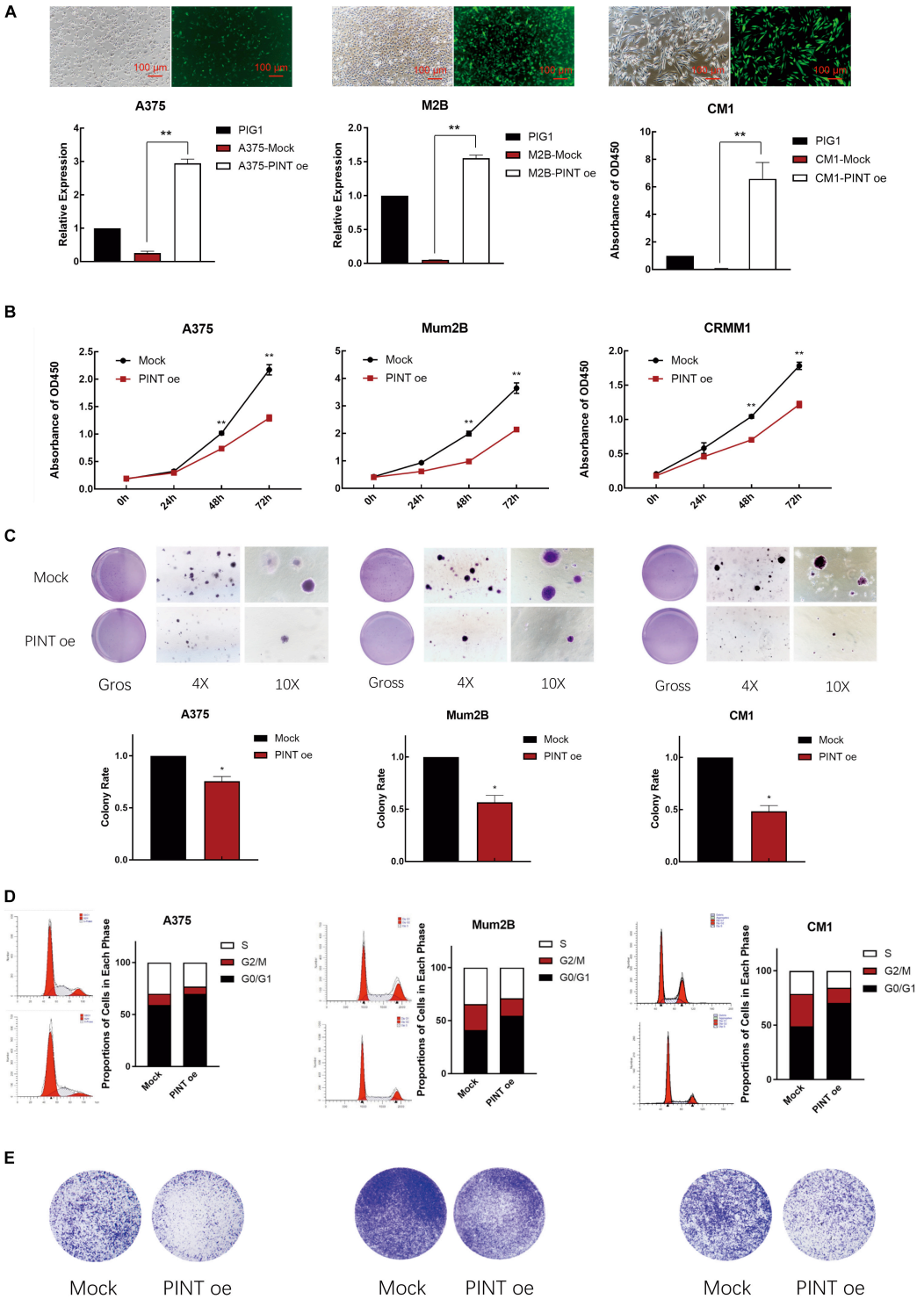

FIGURE 3 | LINC-PINT inhibited melanoma progression *in vitro.* **(A)** The LINC-PINT overexpression plasmid was stably transfected into A375, Mum2B and CRMM1 cells, and the plasmid also contained the EGFP tag. Scale bars: 100 μm. Real-time PCR results showed significantly higher expression of LINC-PINT in A375-PINT oe, M2B-PINT oe and CM1-PINT oe cells. $^{**}P < 0.01$. **(B)** CCK8 assay was performed to assess cell proliferation in the Mock and LINC-PINT overexpression melanoma cells. $^{**}p < 0.01$. **(C)** Colony count statistics demonstrated tumor formation ability. The colony count statistics showed a significant reduction in the numbers of LINC-PINT overexpressed A375, Mum2B and CRMM1 cells. The colony numbers were determined from three independent soft agar plates. $^{**}P < 0.01$. **(D)** Cell cycle analysis by flow cytometry was performed to determine the percentage of cells in different cell cycle phases. The percentage of cells in G0/G1 phase increased after LINC-PINT overexpression in A375, Mum2B and CRMM1 cells. All histograms showed the percentage (%) of cell populations from one independent experimental group. **(E)** The migration and invasion abilities of LINC-PINT overexpressed melanoma cells were detected by transwell assay.

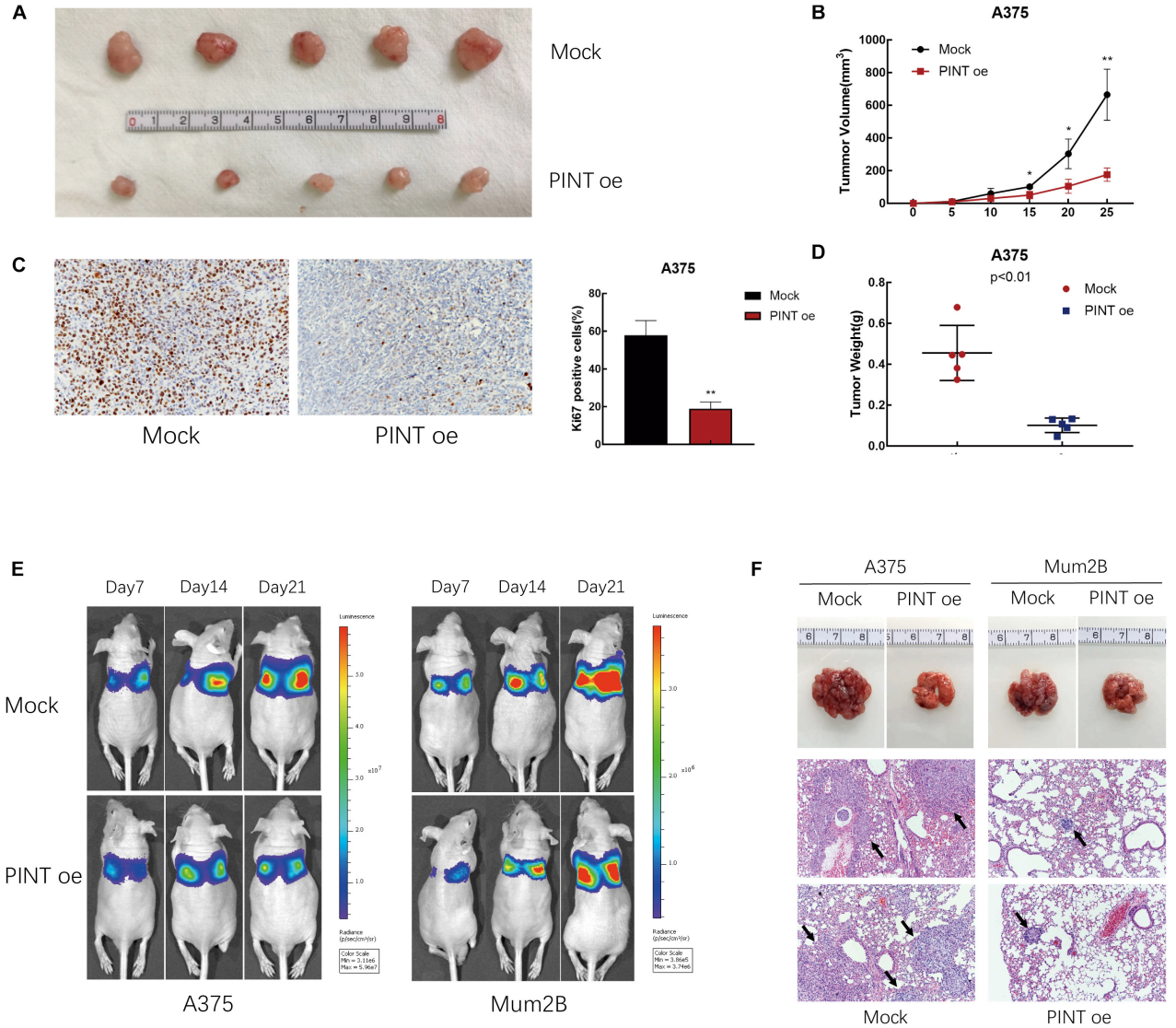

FIGURE 4 | LINC-PINT inhibited melanoma progression *in vivo*. **(A)** Mock and PINT oe A375 cells were injected into the nude mice. Tumors derived from cells with (lower panel) or without (upper panel) LINC-PINT overexpression were removed from the mice. **(B)** Tumor volume was evaluated every 5 days after the injection of Mock ($n = 5$) and PINT oe ($n = 5$) A375 cells for 25 consecutive days. $^*p < 0.05$, $^{**}p < 0.01$. **(C)** Ki-67 staining of Mock and PINT oe tumor tissues. **(D)** The weights of Mock ($n = 5$) and PINT oe ($n = 5$) A375 tumors. **(E)** Effect of LINC-PINT on tumor metastasis in a lung metastasis mouse model. Mock and PINT oe A375 and Mum2B cells were injected into the caudal vein of nude mice ($n = 3$ for each group). **(F)** Representative lung tissues and their HE-stained sections (100× magnification) are shown. The black arrows showed the metastases.

RNA sequencing technologies. Growing evidence suggested that lncRNAs may act as epigenetic modifiers to regulate gene expression in tumor initiation and development (Gupta et al., 2010; Yap et al., 2010; Tseng et al., 2014). In melanoma, lncRNA SAMMSON increases its mitochondrial targeting and pro-oncogenic function by interacting with p32, a master regulator of mitochondrial homeostasis and metabolism (Leucci et al., 2016), lncRNA SLNCR1 mediates melanoma invasion through a highly conserved sequence binding to brain-specific homeobox protein 3a (Brn3a) and the androgen receptor (AR). SLNCR1, AR, and Brn3a are specifically required for transcriptional activation of matrix metalloproteinase 9 (MMP9) and increased melanoma invasion (Schmidt et al., 2016). However, our knowledge of lncRNAs in tumors, especially in melanoma, remains limited. Here, we revealed a novel transcript of LINC-PINT as a tumor suppressor to inhibit melanoma progression via recruiting EZH2 to the promoter of cell cycle related genes.

Polycomb repressive complex 2 (PRC2) is recently reported to play a central role in controlling critical cellular processes including maintaining stem cell pluripotency, promoting cell proliferation and mediating myogenic differentiation (Boyer et al., 2006; Xu et al., 2018). Gene silencing mediated by polycomb is considered to depend mostly on regulation of chromatin structure, in part through post-translational

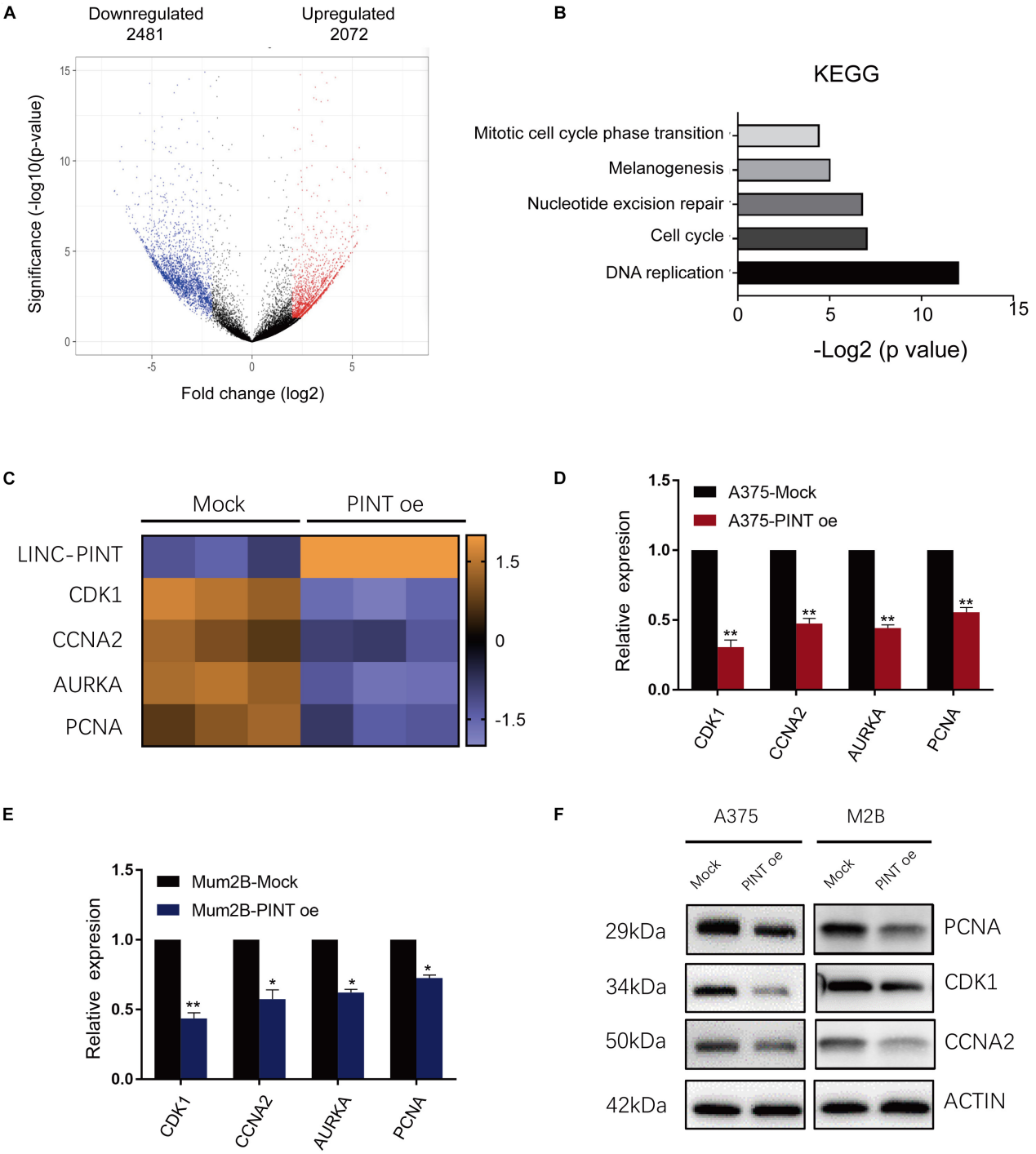

FIGURE 5 | The target genes of LINC-PINT were identified in melanoma cells. **(A)** Volcano plots of differentially expressed gene. The *X* axis represented log fold changes. The *Y* axis represented log *p*-values. The red points denoted the significantly upregulated genes and blue points denoted the significantly downregulated genes. **(B)** KEGG analysis of differentially expressed genes between Mock and PINT oe A375 cells. **(C)** Heat map showed the differentially expressed genes related to cell cycle progression. **(D,E)** The downregulated cell cycle genes in the microarray were verified in A375 and Mum2B cells by real-time PCR. $^{*}p < 0.05$, $^{**}p < 0.01$. **(F)** The expression of LINC-PINT target genes was detected by western blot. Actin were used as internal controls.

modification (PTM) of histones (Margueron and Reinberg, 2011). In the past few years, enhancer of zeste homolog 2 (EZH2), the catalytic subunit of Polycomb repressive complex 2 (PRC2), has aroused broad research interest because of its multiple roles in the development of many types of cancer (Margueron and Reinberg, 2011; Di Croce and Helin, 2013;

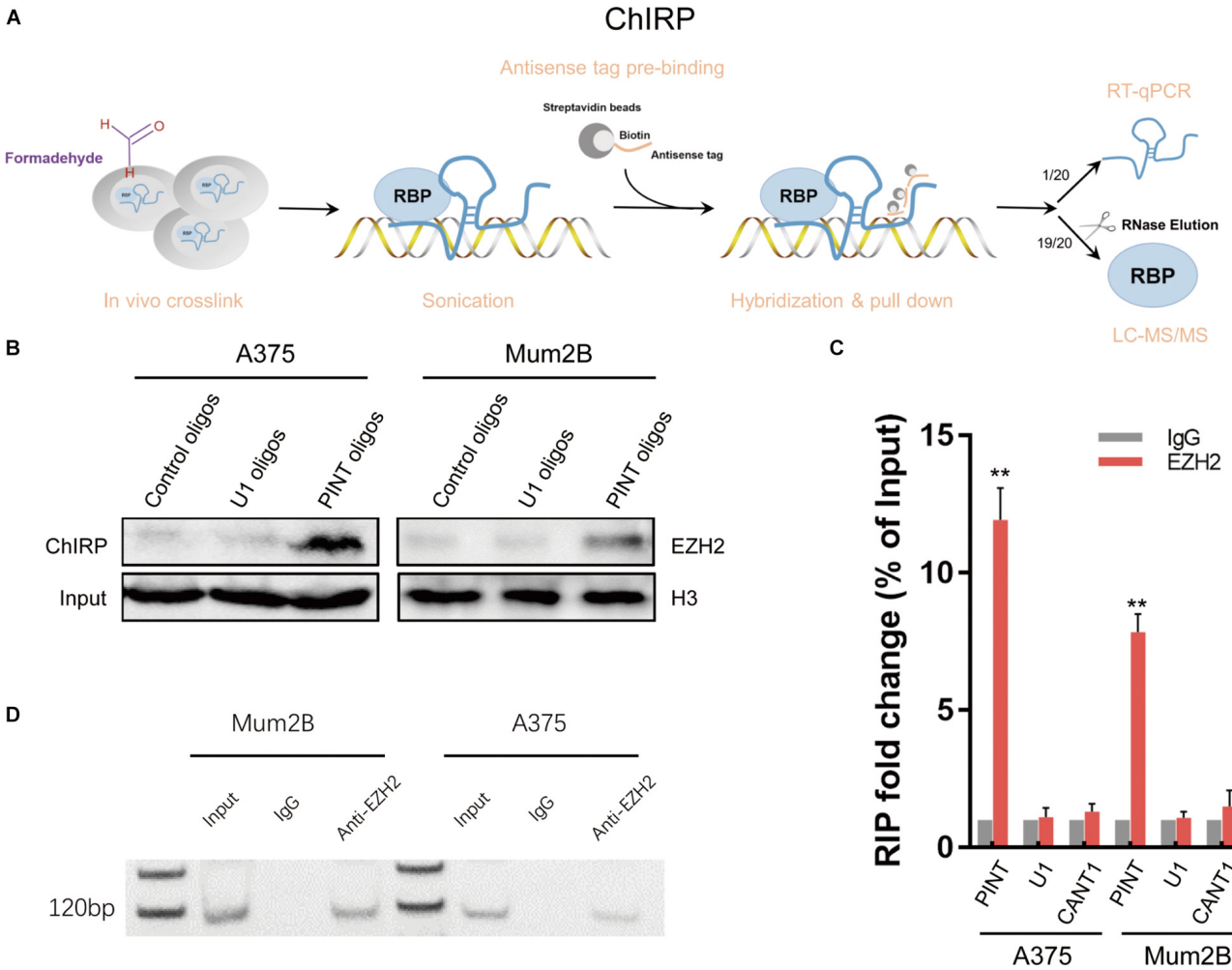

FIGURE 6 | LINC-PINT recruited EZH2 to inhibit gene expression. **(A)** Introduction of the ChIRP method. **(B)** EZH2 was detected from the retrieved ChIRP protein of A375 and Mum2B cells by western blot. PINT oligos indicated the biotinylated antisense oligonucleotides against LINC-PINT. Control oligos indicated the scrambled oligonucleotides, and U1 oligos were selected as a negative control. **(C)** The interaction of LINC-PINT with EZH2 was verified by RIP assay. The values are normalized to input. $^{**}p < 0.01$. LncRNA CANT1 and U1 RNA served as negative controls. **(D)** Agarose gel electrophoresis of RIP products.

Comet et al., 2016; Kim and Roberts, 2016). EZH2 both fulfills its oncogenic and tumor suppressive roles in a variety of cancers. It is demonstrated that EZH2 is mainly upregulated in solid tumors, melanoma included, which indicates a more aggressive tumor growing pattern and poorer prognosis in most cases. In late stage prostate tumors, EZH2 upregulation is related to gene amplification, whereas its expression is profoundly affected by the BRAF (V600E) mutation in melanoma (Volkel et al., 2015). *In vivo* study shows that EZH2 overexpression results in intraductal epithelial hyperplasia through inducing β-catenin nuclear accumulation and activating Wnt/β-catenin signaling in mammary epithelial cells (Li et al., 2009). In addition, expression of $Ezh2^{Y641F}$, the most common somatic EZH2 mutation (Y646F in human, Y641F in the mouse), in mouse melanocytes causes melanoma through a vast reorganization of chromatin structure (Souroullas et al., 2016). Meanwhile, potent molecules selectively targeting EZH2 enzymatic activity have been discovered, including EPZ005687, EPZ-6438, EI1, UNC1999, and GSK126, which also exerts significant anti-tumor effects in distinct melanoma subsets (Volkel et al., 2015; Perotti et al., 2019). Epigenetically, PRC2-mediated gene silencing is mainly dependent on the regulation of EZH2-mediated H3K27me3 (Schuettengruber and Cavalli, 2009; Simon and Kingston, 2009). Recently, a growing body of evidence shows that epigenetic factors, like lncRNAs are involved in the EZH2-mediating tumor regulation. LncRNA exerts its biological function mainly by binding to RNA binding protein (RBP) (Gou et al., 2018). The lncRNAs ANCR, HOTAIR, H19, are involved in the recruitment of EZH2 to the specific regulatory regions of its target genes (Davidovich and Cech, 2015). For instance, the long intergenic non-coding RNA HOTAIR generates the trimethylation of H3K27 and epigenetic silencing of metastasis-suppressor genes via recruiting EZH2 to specific

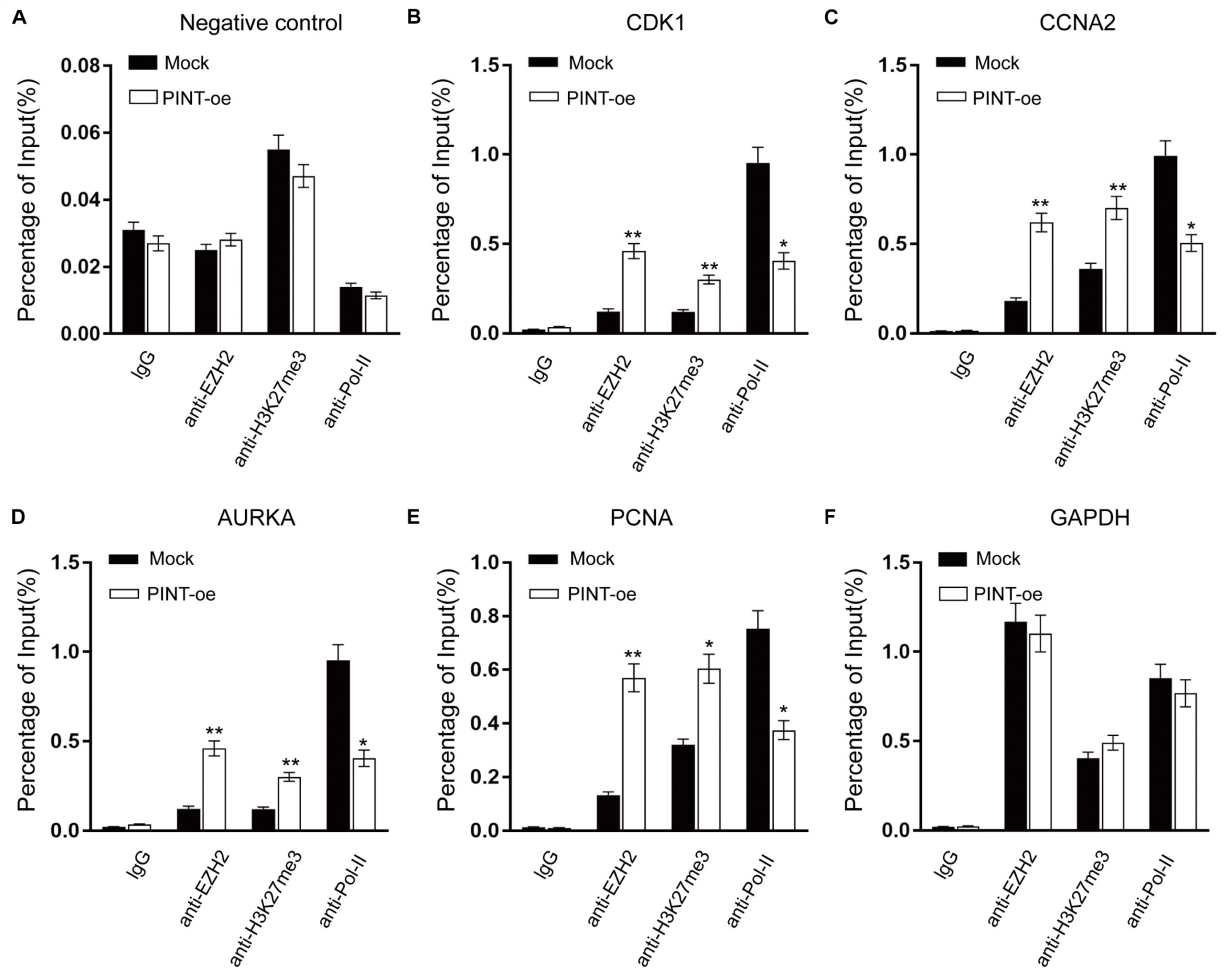

FIGURE 7 | Interactions between epigenetic modifiers and the promoter regions of LINC-PINT target genes. **(A–F)** ChIP analysis of IgG, EZH2, H3K27me3, and RNA polymerase-II showed the status of candidate LINC-PINT target genes in A375 cells with or without LINC-PINT overexpression. The values were normalized to input. *$p < 0.05$; **$p < 0.01$.

target genes (Gupta et al., 2010). LncRNA ANCR interacts with EZH2 to promote its phosphorylation that facilitates EZH2 degradation and suppresses breast cancer progression (Li et al., 2017). In this study, we demonstrated that LINC-PINT was an EZH2-binding lncRNA and play an tumor-suppressive role in melanoma progression. We performed ChIRP assay and mass spectrometry to identify specific association of LINC-PINT with EZH2, which was further confirmed by RIP and Western blot. With more importance, it is confirmed by ChIP assay that LINC-PINT regulated activation of downstream genes by interacting with EZH2, which in turn mediated H3K27me3 at the promoter regions of target genes. Thus, our results demonstrate that LINC-PINT interacts directly with the promoter region of target genes and mediates H3K27me3 to activate transcription via binding to EZH2.

Although the function and structure of LINC-PINT have been studied for more than 4 years, a more comprehensive role of LINC-PINT in regulating the melanoma tumorigenesis still remains to be elucidated. Additionally, recent studies have shown that LINC-PINT plays a vital role in several types of human cancers, melanoma included (Huang et al., 2019). In this manuscript, it is observed that overexpression of LINC-PINT significantly inhibited melanoma proliferation both *in vitro* and *in vivo*. Through further explorations, we identified genes that were mainly suppressed by LINC-PINT, including CDK1, CCNA2, AURKA, and PCNA. These genes have been confirmed as critical regulators in melanoma and might represent therapeutic targets for clinical application. For example, CDK1 was reported to interact with Sox2 and promote tumor initiation in human melanoma (Ravindran Menon et al., 2018), CCNA2 and AURKA inhibitors are now available and has shown encouraging effect for treatment of melanoma (Caputo et al., 2014; George et al., 2019). Taken together, these results suggest LINC-PINT as a multi-potent therapeutic target with great potential.

In summary, we identified an lncRNA, LINC-PINT, and proposed a mechanistic model to elucidate its role in

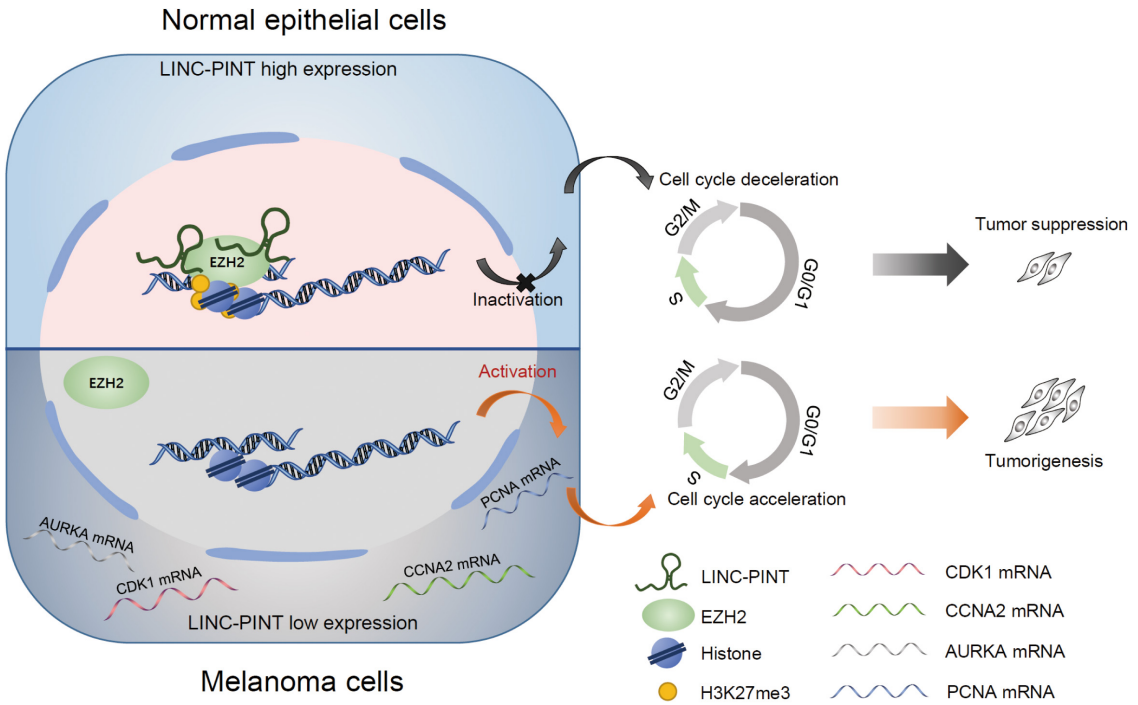

FIGURE 8 | A schematic model of LINC-PINT in epigenetic silencing of target genes in melanoma cells via recruiting EZH2. A novel transcript of LINC-PINT serves as key regulator of melanoma progression. In LINC-PINT highly expressed cells, LINC-PINT inactivated the transcription of CDK1, CCNA2, AURKA, and PCNA genes by the effect of EZH2-mediated H3K27me3, thus leading to the cell cycle deceleration and suppressing the tumorigenesis. However, in LINC-PINT deficient melanoma cells, the epigenetic regulation effect was abolished, subsequently promoting the expression of target genes and contributing to melanoma expansion.

the regulation of melanoma progression through EZH2-mediated epigenetic silencing (**Figure 8**). In the animal xenograft model, LINC-PINT overexpressed melanoma cells represented significant tumor growth inhibition and metastasis reduction effects. Mechanistically, we showed that LINC-PINT recruited EZH2 to the promoter region of its target genes to impede tumor cell proliferation. Therefore, our study elucidates the potential role of LINC-PINT in the development of melanoma and unveils its molecular mechanism underlying tumor progression. Our findings indicate that LINC-PINT could be a potential therapeutic target for human melanoma.

CONCLUSION

In summary, LINC-PINT was expressed at remarkably lower levels in melanoma tissues and cell lines. For melanoma patients, lower expression of LINC-PINT was associated with poorer overall survival and disease-free survival. Strikingly, overexpression of LINC-PINT significantly reduced melanoma cells progression via downregulating the potential target genes CDK1, CCNA2, AURKA, and PCNA through recruiting EZH2 protein, which in turn mediated the trimethylation of H3K27 of promoter regions of target genes. Here, we identified the tumor-suppressive role of LINC-PINT in melanoma and uncovered the underlying epigenetic regulatory mechanism.

DATA AVAILABILITY STATEMENT

The raw data supporting the conclusions of this article will be made available by the authors, without undue reservation, to any qualified researcher.

ETHICS STATEMENT

The animal study was reviewed and approved by the Shanghai Jiao Tong University School of Medicine Animal Care and Use Committee.

AUTHOR CONTRIBUTIONS

YX, XH, and FL designed and performed the experiments and drafted the manuscript. LH, JYu, JYa, and SG was responsible for the data analysis. JR, RJ, and XF wrote and approved the manuscript. All of the authors approved the manuscript.

FUNDING

This work was supported by the National Key Research and Development Plan (2018YFC1106100 and 2017YFE9126300), the National Natural Science Foundation of China (81972530, 81872339, 81772875, and 81802702), the

Science and Technology Commission of Shanghai (17DZ2260100 and 19JC1410200), Shanghai Rising-Star Program (17QA1402000), Shanghai Ninth People's Hospital Training Programs (jyyq09201713), and Shanghai Science and Technology Development Funds (19QA1405100).

SUPPLEMENTARY MATERIAL

The Supplementary Material for this article can be found online at: https://www.frontiersin.org/articles/10.3389/fcell.2019.00350/full#supplementary-material

REFERENCES

Arozarena, I., and Wellbrock, C. (2019). Phenotype plasticity as enabler of melanoma progression and therapy resistance. *Nat. Rev. Cancer* 19, 377–391. doi: 10.1038/s41568-019-0154-4

Arun, G., Diermeier, S. D., and Spector, D. L. (2018). Therapeutic targeting of long non-coding rnas in cancer. *Trends Mol. Med.* 24, 257–277. doi: 10.1016/j.molmed.2018.01.001

Bastian, B. C. (2014). The molecular pathology of melanoma: an integrated taxonomy of melanocytic neoplasia. *Annu. Rev. Pathol.* 9, 239–271. doi: 10.1146/annurev-pathol-012513-104658

Boyer, L. A., Plath, K., Zeitlinger, J., Brambrink, T., Medeiros, L. A., Lee, T. I., et al. (2006). Polycomb complexes repress developmental regulators in murine embryonic stem cells. *Nature* 441, 349–353. doi: 10.1038/nature04733

Byron, S. A., Loch, D. C., Wellens, C. L., Wortmann, A., Wu, J., Wang, J., et al. (2012). Sensitivity to the MEK inhibitor E6201 in melanoma cells is associated with mutant BRAF and wildtype PTEN status. *Mol. Cancer* 11:75. doi: 10.1186/1476-4598-11-75

Caputo, E., Miceli, R., Motti, M. L., Tate, R., Fratangelo, F., Botti, G., et al. (2014). AurkA inhibitors enhance the effects of B-RAF and MEK inhibitors in melanoma treatment. *J. Transl. Med.* 12:216. doi: 10.1186/s12967-014-0216-z

Cech, T. R., and Steitz, J. A. (2014). The noncoding RNA revolution-trashing old rules to forge new ones. *Cell* 157, 77–94. doi: 10.1016/j.cell.2014.03.008

Comet, I., Riising, E. M., Leblanc, B., and Helin, K. (2016). Maintaining cell identity: PRC2-mediated regulation of transcription and cancer. *Nat. Rev. Cancer* 16, 803–810. doi: 10.1038/nrc.2016.83

Davidovich, C., and Cech, T. R. (2015). The recruitment of chromatin modifiers by long noncoding RNAs: lessons from PRC2. *RNA* 21, 2007–2022. doi: 10.1261/rna.053918.115

Di Croce, L., and Helin, K. (2013). Transcriptional regulation by Polycomb group proteins. *Nat. Struct. Mol. Biol.* 20, 1147–1155. doi: 10.1038/nsmb.2669

Geisler, S., and Coller, J. (2013). RNA in unexpected places: long non-coding RNA functions in diverse cellular contexts. *Nat. Rev. Mol. Cell. Biol.* 14, 699–712. doi: 10.1038/nrm3679

George, J., Nihal, M., Singh, C. K., and Ahmad, N. (2019). 4'-Bromo-resveratrol, a dual Sirtuin-1 and Sirtuin-3 inhibitor, inhibits melanoma cell growth through mitochondrial metabolic reprogramming. *Mol. Carcinog.* 58, 1876–1885. doi: 10.1002/mc.23080

Gou, Q., Gao, L., Nie, X., Pu, W., Zhu, J., Wang, Y., et al. (2018). Long noncoding RNA AB074169 inhibits cell proliferation via modulation of KHSRP-mediated CDKN1a expression in papillary thyroid carcinoma. *Cancer Res.* 78, 4163–4174. doi: 10.1158/0008-5472.CAN-17-3766

Gupta, R. A., Shah, N., Wang, K. C., Kim, J., Horlings, H. M., Wong, D. J., et al. (2010). Long non-coding RNA HOTAIR reprograms chromatin state to promote cancer metastasis. *Nature* 464, 1071–1076. doi: 10.1038/nature08975

Guttman, M., and Rinn, J. L. (2012). Modular regulatory principles of large non-coding RNAs. *Nature* 482, 339–346. doi: 10.1038/nature10887

Hayward, N. K., Wilmott, J. S., Waddell, N., Johansson, P. A., Field, M. A., Nones, K., et al. (2017). Whole-genome landscapes of major melanoma subtypes. *Nature* 545, 175–180. doi: 10.1038/nature22071

Hersey, P., and Gallagher, S. (2012). A focus on PD-L1 in human melanoma. *Clin. Cancer Res.* 19, 514–516. doi: 10.1158/1078-0432.ccr-12-3312

Hirukawa, A., Smith, H. W., Zuo, D., Dufour, C. R., Savage, P., Bertos, N., et al. (2018). Targeting EZH2 reactivates a breast cancer subtype-specific anti-metastatic transcriptional program. *Nat. Commun.* 9:2547. doi: 10.1038/s41467-018-04864-8

Huang, Q., Zhang, D., Diao, Q., and Lin, M. (2019). lncRNA LINC-PINT is downregulated in melanoma and regulates cell proliferation by downregulating lncRNA BANCR. *Oncol. Lett.* 18, 2917–2922. doi: 10.3892/ol.2019.10631

Kim, E.D., and Sung, S. (2012). Long noncoding RNA: unveiling hidden layer of gene regulatory networks. *Trends Plant Sci.* 17, 16–21. doi: 10.1016/j.tplants.2011.10.008

Kim, K. H., and Roberts, C. W. (2016). Targeting EZH2 in cancer. *Nat. Med.* 22, 128–134. doi: 10.1038/nm.4036

Leucci, E., Vendramin, R., Spinazzi, M., Laurette, P., Fiers, M., Wouters, J., et al. (2016). Melanoma addiction to the long non-coding RNA SAMMSON. *Nature* 531, 518–522. doi: 10.1038/nature17161

Li, X., Gonzalez, M. E., Toy, K., Filzen, T., Merajver, S. D., and Kleer, C. G. (2009). Targeted overexpression of EZH2 in the mammary gland disrupts ductal morphogenesis and causes epithelial hyperplasia. *Am. J. Pathol.* 175, 1246–1254. doi: 10.2353/ajpath.2009.090042

Li, Z., Hou, P., Fan, D., Dong, M., Ma, M., Li, H., et al. (2017). The degradation of EZH2 mediated by lncRNA ANCR attenuated the invasion and metastasis of breast cancer. *Cell Death Differ.* 24, 59–71. doi: 10.1038/cdd.2016.95

Lu, L., Yu, X., Zhang, L., Ding, X., Pan, H., Wen, X., et al. (2017). The long non-coding RNA RHPN1-AS1 promotes uveal melanoma progression. *Int. J. Mol. Sci.* 18:226. doi: 10.3390/ijms18010226

Margueron, R., and Reinberg, D. (2011). The polycomb complex PRC2 and its mark in life. *Nature* 469, 343–349. doi: 10.1038/nature09784

Marin-Bejar, O., Marchese, F. P., Athie, A., Sanchez, Y., Gonzalez, J., Segura, V., et al. (2013). Pint lincRNA connects the p53 pathway with epigenetic silencing by the Polycomb repressive complex 2. *Genome Biol.* 14:R104.

Marin-Bejar, O., Mas, A. M., Gonzalez, J., Martinez, D., Athie, A., Morales, X., et al. (2017). The human lncRNA LINC-PINT inhibits tumor cell invasion through a highly conserved sequence element. *Genome Biol.* 18:202. doi: 10.1186/s13059-017-1331-y

Niezgoda, A., Niezgoda, P., and Czajkowski, R. (2015). Novel approaches to treatment of advanced melanoma: a review on targeted therapy and immunotherapy. *BioMed. Res. Int.* 2015, 1–16. doi: 10.1155/2015/851387

Ojha, R., Leli, N. M., Onorati, A., Piao, S., Tameire, F., Rebecca, V. W., et al. (2019). ER translocation of the MAPK pathway drives therapy resistance in BRAF-mutant melanoma. *Cancer Discov.* 9, 396–415. doi: 10.1158/2159-8290.CD-18-0348

Perotti, V., Baldassari, P., Molla, A., Nicolini, G., Bersani, I., Grazia, G., et al. (2019). An actionable axis linking NFATc2 to EZH2 controls the EMT-like program of melanoma cells. *Oncogene* 38, 4384–4396. doi: 10.1038/s41388-019-0729-2

Posch, C., Moslehi, H., Feeney, L., Green, G. A., Ebaee, A., Feichtenschlager, V., et al. (2013). Combined targeting of MEK and PI3K/mTOR effector pathways is necessary to effectively inhibit NRAS mutant melanoma in vitro and in vivo. *Proc. Natl. Acad. Sci. U.S.A.* 110, 4015–4020. doi: 10.1073/pnas.1216013110

Ravindran Menon, D., Luo, Y., Arcaroli, J. J., Liu, S., KrishnanKutty, L. N., Osborne, D. G., et al. (2018). CDK1 interacts with Sox2 and promotes tumor initiation in human melanoma. *Cancer Res.* 78, 6561–6574. doi: 10.1158/0008-5472.CAN-18-0330

Schmidt, K., Joyce, C. E., Buquicchio, F., Brown, A., Ritz, J., Distel, R. J., et al. (2016). The lncRNA SLNCR1 mediates melanoma invasion through a conserved SRA1-like region. *Cell Rep.* 15, 2025–2037. doi: 10.1016/j.celrep.2016.04.018

Schmitt, A. M., and Chang, H. Y. (2016). Long noncoding RNAs in cancer pathways. *Cancer Cell* 29, 452–463. doi: 10.1016/j.ccell.2016.03.010

Schuettengruber, B., and Cavalli, G. (2009). Recruitment of polycomb group complexes and their role in the dynamic regulation of cell fate choice. *Development* 136, 3531–3542. doi: 10.1242/dev.033902

Simon, J. A., and Kingston, R. E. (2009). Mechanisms of polycomb gene silencing: knowns and unknowns. *Nat. Rev. Mol. Cell Biol.* 10, 697–708. doi: 10.1038/nrm2763

Souroullas, G. P., Jeck, W. R., Parker, J. S., Simon, J. M., Liu, J. Y., Paulk, J., et al. (2016). An oncogenic Ezh2 mutation induces tumors through global redistribution of histone 3 lysine 27 trimethylation. *Nat. Med.* 22, 632–640. doi: 10.1038/nm.4092

Takahashi, K., Yan, I., Haga, H., and Patel, T. (2014). Long noncoding RNA in liver diseases. *Hepatology* 60, 744–753. doi: 10.1002/hep.27043

Tsao, H., Chin, L., Garraway, L. A., and Fisher, D. E. (2012). Melanoma: from mutations to medicine. *Genes Dev* 26, 1131–1155. doi: 10.1101/gad.191999.112

Tseng, Y. Y., Moriarity, B. S., Gong, W., Akiyama, R., Tiwari, A., Kawakami, H., et al. (2014). PVT1 dependence in cancer with MYC copy-number increase. *Nature* 512, 82–86. doi: 10.1038/nature13311

Volkel, P., Dupret, B., Le Bourhis, X., and Angrand, P. O. (2015). Diverse involvement of EZH2 in cancer epigenetics. *Am. J. Transl. Res.* 7, 175–193.

Wang, X., Yang, J., Guo, G., Feng, R., Chen, K., Liao, Y., et al. (2019). Novel lncRNA-IUR suppresses Bcr-Abl-induced tumorigenesis through regulation of STAT5-CD71 pathway. *Mol. Cancer* 18:84. doi: 10.1186/s12943-019-1013-3

Xu, M., Chen, X., Lin, K., Zeng, K., Liu, X., Pan, B., et al. (2018). The long noncoding RNA SNHG1 regulates colorectal cancer cell growth through interactions with EZH2 and miR-154-5p. *Mol. Cancer* 17:141. doi: 10.1186/s12943-018-0894-x

Lissanu Deribe, Y., Shi, Y., Rai, K., Nezi, L., Amin, S. B., Wu, C. C., et al. (2016). Truncating PREX2 mutations activate its GEF activity and alter gene expression regulation in NRAS-mutant melanoma. *Proc. Natl. Acad. Sci. U.S.A.* 113, E1296–E1305. doi: 10.1073/pnas.1513801113

Yap, K. L., Li, S., Munoz-Cabello, A. M., Raguz, S., Zeng, L., Mujtaba, S., et al. (2010). Molecular interplay of the noncoding RNA ANRIL and methylated histone H3 lysine 27 by polycomb CBX7 in transcriptional silencing of INK4a. *Mol. Cell* 38, 662–674. doi: 10.1016/j.molcel.2010.03.021

Zhang, M., Zhao, K., Xu, X., Yang, Y., Yan, S., Wei, P., et al. (2018). A peptide encoded by circular form of LINC-PINT suppresses oncogenic transcriptional elongation in glioblastoma. *Nat. Commun.* 9:4475. doi: 10.1038/s41467-018-06862-2

Zingg, D., Debbache, J., Schaefer, S. M., Tuncer, E., Frommel, S.C., Cheng, P., et al. (2015). The epigenetic modifier EZH2 controls melanoma growth and metastasis through silencing of distinct tumour suppressors. *Nat. Commun.* 6:6051. doi: 10.1038/ncomms7051

Conflict of Interest: The authors declare that the research was conducted in the absence of any commercial or financial relationships that could be construed as a potential conflict of interest.

frontiers in Oncology

ORIGINAL RESEARCH
published: 21 January 2020
doi: 10.3389/fonc.2019.01565

miR-27a Downregulation Promotes Cutaneous Squamous Cell Carcinoma Progression via Targeting EGFR

Yinghui Wang[1,2†], *Xuyi Deng*[2†], *Yu Dai*[3], *Xinli Niu*[2] *and Meijuan Zhou*[2*]

[1] Jiangmen Central Hospital, Affiliated Jiangmen Hospital of Sun Yat-sen University, Jiangmen, China, [2] Department of Radiation Medicine, Guangdong Provincial Key Laboratory of Tropical Disease Research, School of Public Health, Southern Medical University, Guangzhou, China, [3] Department of Dermatology, Nanfang Hospital, Southern Medical University, Guangzhou, China

Cutaneous squamous cell carcinoma (cSCC) is the second common malignant cancer around the worldwide and is etiologically linked to ultraviolet radiation. miRNAs play an important role in the initiation and progression of cancers. However, the functions of miRNAs in cSCC remain to be elucidated. Here, we screened and identified miR-27a as a consistently downregulated miRNA after UVB irradiation in HaCaT cells. It was found that miR-27a expression was significantly decreased in cSCC cells and tissues. *in vitro* and *in vivo* experiments showed that miR-27a inhibited cell proliferation and invasion of cSCC cells. Mechanistically, EGFR was identified to be directly targeted by miR-27a and miR-27a suppressed the phosphorylation of EGFR and its downstream NF-κB signaling pathway. Overall, these findings suggest that downregulation of miR-27a promotes tumor growth and metastasis via targeting EGFR and its downstream NF-κB signaling pathway, reminding that miR-27a plays a vital role in the progression of cSCC and could be a new therapeutic target.

Keywords: miR-27a, cutaneous squamous cell carcinoma, proliferation, metastasis, EGFR, UVB

OPEN ACCESS

Edited by:
Lei Chang,
Soochow University Medical College (SUMC), China

Reviewed by:
Yukai He,
Augusta University, United States
Min Li,
University of Oklahoma Health Sciences Center, United States

***Correspondence:**
Meijuan Zhou
lkzmj@smu.edu.cn

[†]*These authors share first authorship*

Specialty section:
This article was submitted to Molecular and Cellular Oncology, a section of the journal Frontiers in Oncology

Received: *05 November 2019*
Accepted: *24 December 2019*
Published: *21 January 2020*

Citation:
Wang Y, Deng X, Dai Y, Niu X and Zhou M (2020) miR-27a Downregulation Promotes Cutaneous Squamous Cell Carcinoma Progression via Targeting EGFR. Front. Oncol. 9:1565. doi: 10.3389/fonc.2019.01565

INTRODUCTION

cSCC is the second most common malignant cancer after basal cell carcinoma worldwide (1). The estimated total number of cSCC for 2012 has been increased by 100% as compared with 1992 (2), due to the increase exposure of ultraviolet from solar radiation and artificial sources. Although basal cell carcinoma and cSCC are both derived from epidermis, cSCC is highly invasive and can metastasize to distant organs (3). As the mechanism of cSCC tumorigenesis is very complex and poorly understood, local therapy, including targeting therapy is still deficient. In the majority of cSCC patients, tumors are excised by surgery conduction, which will result in the functional impairments and physical abnormities for skin tissues. Therefore, the mechanism of cSCC tumorigenesis is urgently further exploration and new strategies needed to be developed to reduce relapse and minimize facial defects.

MicroRNAs (miRNA) are a large family of small endogenous non-coding RNAs comprising 18–22 nucleotides, which directly bind to the 3′UTR region of its target genes through complete or incomplete complementary pairing (4). miRNAs participate in many biological processes, which include cell differentiation, cell survival, apoptosis. Extensive studies have demonstrated

that miRNAs play an important role in tumor initiation, progression, and metastasis of various cancers (5, 6) and have emerged as promising therapeutic targets or tools for cancer treatment (7). Recent studies have shown that differential expressed miRNAs in cSCC compared with normal epidermis are associated with tumor initiation and progression (8–10). miR-27a is located on chromosome 19 and aberrant expressed in several types of cancers, including breast cancer (11), osteosarcoma (12), renal cell cancer (13). However, the role of miR-27a in the progression of cSCC has not been elucidated. Here, as ultraviolet radiation is the major risk for cSCC and cumulative sun exposure has a strong dose-response association with cSCC, we selected miR-27a, which is consistently downregulated in response to UVB radiation and aimed to investigate its function in the progression of cSCC, which would be a promising therapeutic target for cSCC treatment.

MATERIALS AND METHODS

Cell Lines and Tissue Samples

cSCC lines HSC-1 and HSC-5 (HonSun Biological Co. Ltd., Shanghai, China) and immortalized human keratinocyte cell line HaCaT (CellCook Biotech Co. Ltd., Guangzhou, China) were cultured in Dulbecco's modified eagle medium (DMEM, Life Technologies) containing 10% fetal bovine serum (Invitrogen) and 100 μg/ml streptomycin and 100 units/ml penicillin in 37°C incubator with 5% CO_2 and a mild atmosphere. CSCC samples were collected from patients who have been diagnosed by expert pathologists from January 2014 to August 2016 in the departments of dermatology, pathology, and oncology at Nanfang Hospital, affiliated to Southern Medical University. This study was approved by the Institutional Review Board of Nanfang Hospital affiliated to Southern Medical University and written informed consent provided from all patients for the use of surgical samples.

UVB Irradiation

UVB exposure to HaCaT cells was performed as described previously (14). In brief, culture medium was removed and PBS was used to wash cells twice. PBS was replaced in a minimal volume and HaCaT cells were exposed to 30 mJ/cm^2 of UVB. After irradiation, PBS was removed and the conditioned cultured medium was added back. HaCaT cells were incubated at 37°C and harvested at different time points. BALB/c mice (female, 4–6 weeks old, $n = 6$ per group) were shaved 24 h before UVB radiation. All animals received UVB exposure every other day at 300 mJ/cm^2 (1/2 MED, minimum erythema dose) and mice skins were collected for further analysis after 4 weeks.

Reverse Transcription and qPCR

Total RNA isolation was performed by using TRIzol (Life technologies) according to the manufacturer's instructions. Reverse transcription was performed by Mir-X miRNA First-Strand Synthesis Kit (Takara) and the expression of miRNA was measured using Taqman Mixture (CWBio, Shanghai, China). The data were normalized to U6 snRNA. PrimeScript RT Reagent Kit (Takara) was used to generate cDNAs and mRNA analysis were performed by UltraSYBR Mixture (CWBio, Beijing, China). GADPH was used as normalization. All qPCR reactions were performed on a LightCycler 96 Detection System (Roche). The primers are listed in **Supplementary Material**.

Western Blot

The total protein of cells was extracted on ice by cell lysis buffer (Beyotime, Shanghai, China) mixed with protease inhibitor cocktail. BCA quantification kit (Beyotime, Shanghai, China) was used to determine protein concentration. Lysates were separated by SDS polyacrylamide gel electrophoresis. Proteins were blotted onto PVDF membranes (Millipore). These membranes were incubated with primer antibodies overnight at 4°C and then secondary HRP-conjugated antibodies at room temperature for 2 h. The following antibodies were used: EGFR (Santa Cruz Biotechnology), β-actin (Santa Cruz Biotechnology), p-p65(Servicebio, Wuhan, China), p-IκB (Servicebio, Wuhan, China), IKK (Servicebio, Wuhan, China), and secondary antibodies anti-mouse IgG-HRP (Millipore), anti-rabbit IgG-HRP (Millipore). Luminata Forte Western HRP substrate (Millipore) was used to visualize the bound antibodies.

Cell Viability

cSCC cells HSC-1 and HSC-5 (4,000 per well) were seeded into 96-well plate and transfected with NC mimic or miR-27a mimic. CCK-8 (Yeasen, Shanghai, China) was added as described in the manual and OD values at 450 nm were detected after 2 h incubation.

Cell Invasion Assay

Matrigel coated chambers (Corning) were used to assess the invasion ability of transfected cells. cSCC cells HSC-1 and HSC-5 (2.0×10^5) transfected with NC mimic or miR-27a mimic were seeded into 8 μm chamber of 24-well plates in serum-free DMEM and the lower chambers were added with culture medium containing 10% FBS. After 16 h cultured at 37°C, the upper chambers were washed and fixed with fresh 3.7% formaldehyde. One hundred percent methanol were used to permeabilize cells, which were stained with 0.1% crystal violet and cell number analyzed by microphotograph.

Luciferase Reporter Assay

The oligos containing the native or mutant binding site were cloned into pMIR-reporter vector (Promega). HEK293T cells were seeded into 12 well plates and co-transfected with pMIR-reporter constructs, renilla luciferase reporter vector, miR-27a mimic or NC mimic. Luciferase activities were measured at 48 h after transfection. The firely luciferase activity was normalized to renilla luciferase activity. The sequences of those oligos are listed in **Supplementary Material**.

Subcutaneous Xenograft Model

BALB/c-nu/nu (male, 4–6 week old) were adopted from Guangdong Medical Laboratory Animal Center. The animal experiments were performed as described previously (15). HSC-5 or HSC-1 cells were transfected with NC mimic or miR-27a mimic. Cells (1.0×10^7) were subcutaneously injected into the two flanks of nude mice. After 9 days of implantation, NC mimic

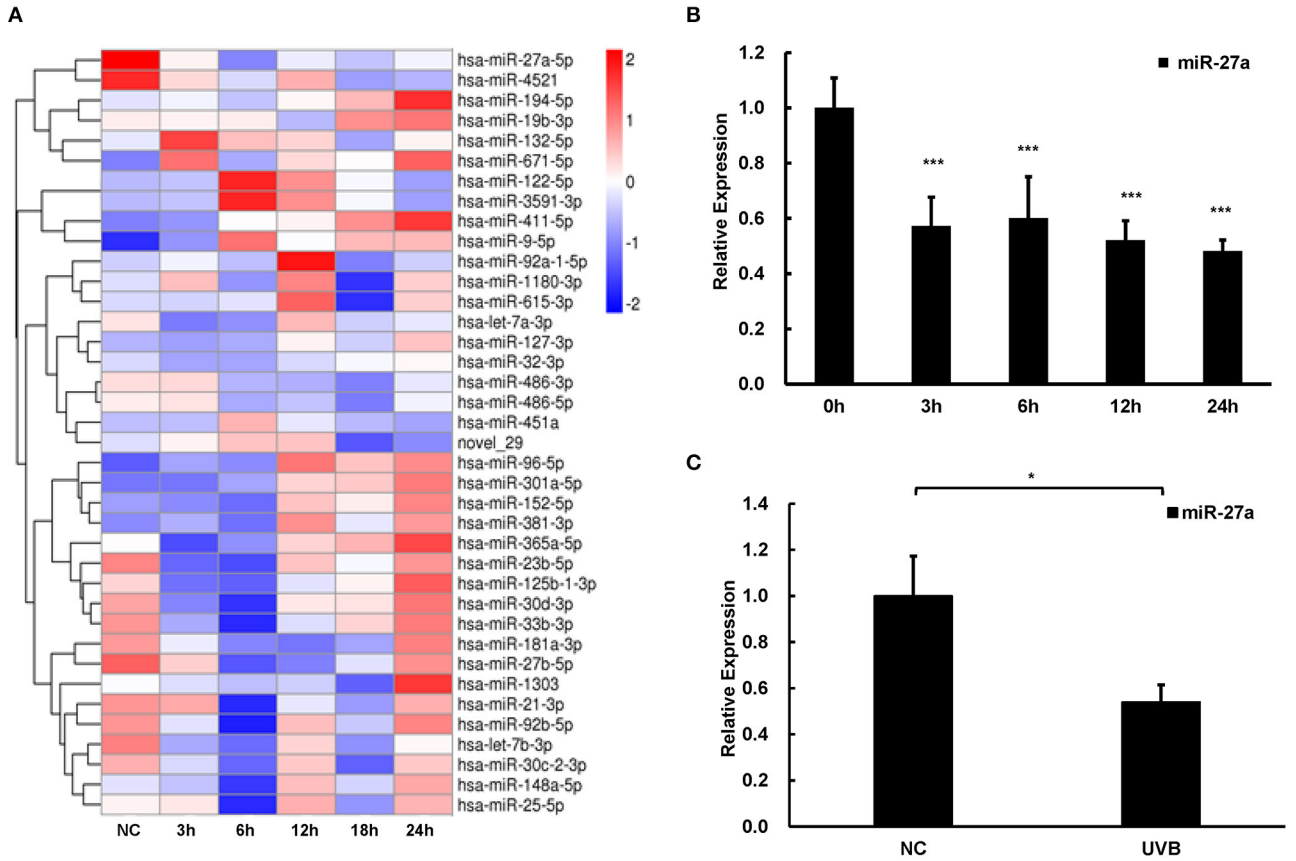

FIGURE 1 | miR-27a was downregulated in respond to UVB radiation. **(A)** Hierarchical clustering analysis of differential expressed miRNAs at 3, 6, 12, 18, and 24 h after UVB radiation in HaCaT cells based on miRNA sequencing. **(B,C)** The expression of miR-27a was identified in HaCaT cells with UVB radiation by qPCR. Each experiment was performed in triplicate and data are presented as mean ± s.d. One-Way ANOVA and Dunnett's Multiple comparison test were used to analyze the data (*$P < 0.05$, ***$P < 0.001$).

or miR-27a mimic were injected into the respective tumors and repeated every 2 days. The tumor diameters were measured and recorded every day to generate a growth curve. The tumors were removed and feezed immediately for experiments followed. All procedures involving the mice were approved by the Southern Medical University Animal Care and Use Committee and in accordance with institutional guidelines.

Statistical Analysis

The experimental results were represented with mean ± S.D. and Student's test or one-way ANOVA was used to analyze statistical difference. It was considered statistically significant when $P < 0.05$.

RESULTS

miR-27a Is Sensitive to UVB Radiation in Epidermis

UVB is the major pathogenic factor for cSCC. To discover miRNAs in response to UVB radiation and explore their functions in the progression of cSCC, we conducted miRNA sequencing to reveal those differentially expressed miRNAs in HaCaT cells at different time points (3, 6, 12, 18, and 24 h) after UVB radiation. Relative expression of miRNAs which were altered at least two-folds change at any time points compared with that in HaCaT cells without UVB radiation were selected and clustered using the hierarchical clustering algorithm (**Figure 1A**). miR-27a was differentially expressed in common at 6, 12, 18, and 24 h time points. The expression of miR-27a in HaCaT cells was significantly downregulated after UVB radiation verified by real-time PCR, which is coincident with RNA-seq (**Figure 1B**). In UVB-irradiated mice skin, miR-27a expression was significantly decreased compared with mice skins without UVB radiation (**Figure 1C**). Those results reminded us that miR-27a may play a vital role in the progression of cSCC.

miR-27a Is Low Expressed in cSCC Cells and Tissues

To explore the function of miR-27a in cSCC progression, we examined miR-27a expression in cSCC cell lines and tissues by qPCR. In contrast with HaCaT cells, miR-27a was dramatically low expressed in cSCC cells, HSC-5 and HSC-1 (**Figure 2A**). In

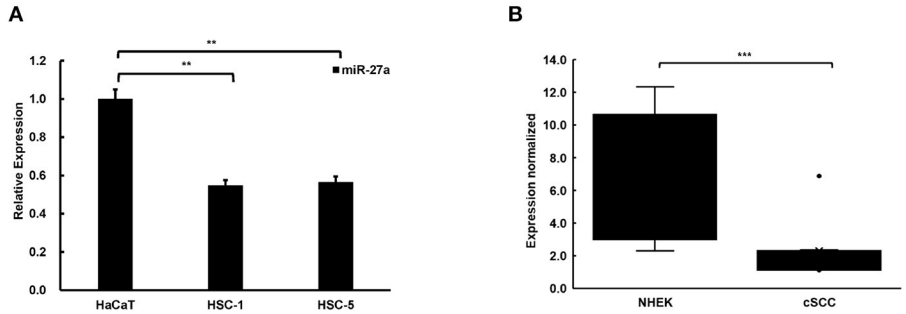

FIGURE 2 | miR-27a was low expressed in cSCC. **(A)** The expression of miR-27a was downregulated in cSCC cells compared with HaCaT. **(B)** miR-27a expression was downregulated in cSCC tissues compared with NHEKs. Each experiment was performed in triplicate and data are presented as mean ± s.d. One-Way ANOVA and Dunnett's Multiple comparison test were used to analyze the data (**P<0.01, ***P < 0.001).

the meantime, miR-27a expression was analyzed in cSCC patient tissues. Compared with normal human epidermal keratinocytes (NHEKs, $n = 4$), miR-27a was significantly reduced in cSCC tissues ($n = 12$) (**Figure 2B**). These results indicate that miR-27a is low expressed in cSCC.

Loss of miR-27a Promotes Proliferation and Invasion of cSCC Cells

To identify the effect of miR-27a in the development of cSCC, we regulated miR-27a expression in HSC-5 or HSC-1 cells by transfected miR-27a mimic or inhibitor. QPCR were performed to determined miR-27a expression. Result showed that miR-27 expression was significantly increased or downregulated in both HSC-5 or HSC-1 cells compared with negative control group (**Figures 3A,B**). Cell proliferation was determined by CCK-8 assays and the data showed proliferation inhibition by exogenous miR-27a (**Figures 3C,D**). Transwell assays were performed to detect the invasion of HSC-5 or HSC-1 cells with miR-27a mimic treatment. The results showed that the invasive ability of cSCC cells were suppressed after miR-27a mimic transfection (**Figure 3E**). Inversely, miR-27a inhibition in HSC-5 or HSC-1 cells were found to promote the invasive ability compared with cells transfected with negative control (**Figure 3F**). The data above demonstrated that miR-27a represses cell proliferation and invasiveness of cSCC cells *in vitro*.

EGFR Is a Direct Target of miR-27a

To explore the downstream of miR-27a, a bioinformatics screen was carried out by using miRTarBase (16). Consideration of the overactivation and crucial role of EGFR in most cancers, it was selected as the underlying downstream genes of miR-27a in cSCC cells. There was a binding site predicted for miR-27a in the 3'UTR region of EGFR mRNA (**Figure 4A**). Wild type or mutant binding site of EGFR were cloned and inserted into luciferase reporter vector. The luciferase reporter assays showed that miR-27a overexpression suppressed the luciferase activity of the wild type vector, while no significant change of the mutant vector (**Figure 4A**). In our previous study, EGFR was identified to be overexpressed in cSCC (14) and upregulated in mice skins receiving UVB radiation (**Figure 4B**), which was opposite to the expression of miR-27a. In HSC-5 or HSC-1 cells which were transfected with miR-27a mimic, EGFR were downregulated in both mRNA and protein level (**Figure 4C**); conversely, upregulated in miR-27a inhibitor treated HSC-5 or HSC-1 cells (**Figure 4D**). These results demonstrated that EGFR is a direct target of miR-27a in cSCC cells and miR-27a knockdown increases the expression of EGFR.

miR-27a Modulates NF-κB Signaling Pathway via Inactivation of EGFR

To investigate the downstream mechanism of miR-27a targeting EGFR in cSCC cells, we detected the changes in the downstream signaling pathway after transfection of cSCC cells with miR-27a mimc or miR-27a inhibitor. Upregulation of miR-27a suppressed the activation of EGFR (**Figure 4E**) and the inhibition of miR-27a expression increased the phosphorylation of EGFR (**Figure 4F**). Therefore, we further investigated whether the downstream pathways of EGFR were modulated by miR-27a. Results showed that miR-27a inhibited the phosphorylation of p65, IKK, and IκB while downregulation of miR-27a increased the phosphorylation of p65, IKK, and IκB, which indicates miR-27a suppresses the activation of NF-κB pathway (**Figures 4E,F**). These results suggested that miR-27a inhibits cSCC development by targeting EGFR and its downstream NF-κB signaling pathway.

miR-27a Inhibits the Growth of cSCC *in vivo*

To evaluate the antitumor function of miR-27a *in vivo*, we established a subcutaneous model. miR-27a mimic or NC mimic was delivered into HSC-5 or HSC-1 cells. The tumor volume was significantly decreased in the group treated with miR-27a mimic compared with that in the negative control group (**Figures 5A,B**). The tumors were removed after implantation for 21 days and miR-27a expression in the xenografts were determined by qPCR. miR-27a was upregulated in the xenografts treated with miR-27a mimic compared the negative control group (**Figures 5C,D**). Furthermore, miR-27a led to the significant downregulation of EGFR and its downstream NF-κB signaling pathway (**Figures 5E,F**), which is consistent with that *in vitro*.

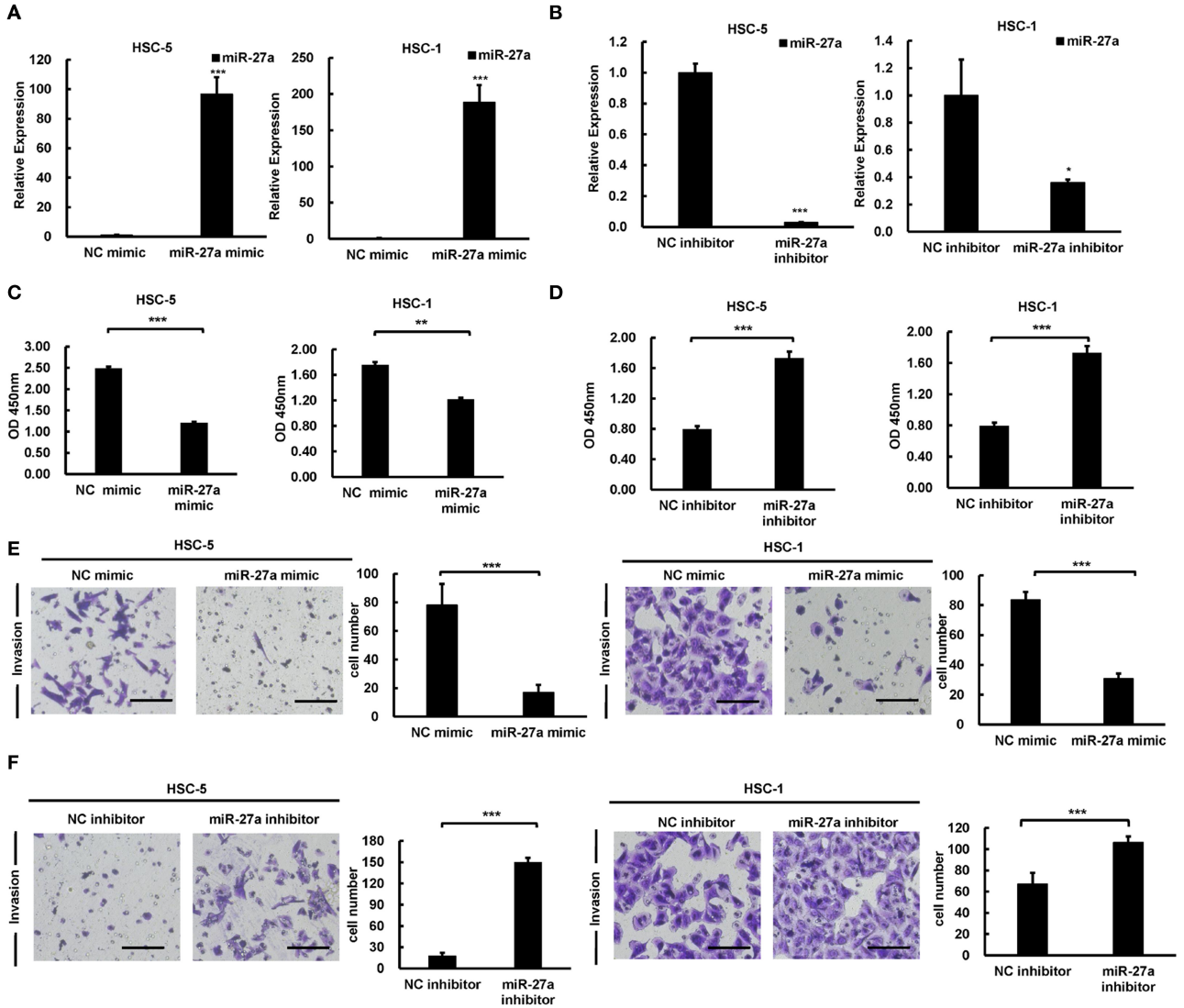

FIGURE 3 | miR-27a acted as a tumor suppressive role in cSCC. Relative expression of miR-27a was detected in HSC-5 or HSC-1 cells treated with miR-27a mimic **(A)** or inhibitor **(B)**. Cell proliferation were determined by CCK-8 assays at 24, 48, and 72 h after transfection **(C,D)**. Cell invasions were detected by transwell assays with matrigels **(E,F)**. Magnification: 200×. Each experiment was performed in triplicate and data are presented as mean ± s.d. One-Way ANOVA and Dunnett's Multiple comparison test were used to analyze the data (*$P < 0.05$, **$P < 0.01$, ***$P < 0.001$).

DISCUSSION

UV is a major environmental carcinogenesis for the initiation and promotion of cSCC. It has been estimated that about 93% of skin cancers could been due to UV exposure. Accumulating data show that miRNAs play a vital role in modulating cell proliferation and invasion by regulating their target genes. In previous studies, we screened and verified miRNAs that are upregulated by UVB radiation in HaCaT cells play an onco-miR role in cSCC (8, 10). However, the role of miR-27a in cSCC remains to be elucidated. It is the first time uncovering the function of UVB-sensitive miR-27a in the development of cSCC. In this study, we revealed that miR-27a inhibits cell proliferation and invasion of cSCC, and suppresses the activation of NF-κB pathway through directly targeting EGFR, indicating that miR-27a plays a tumor suppressive role in cSCC.

miR-27a abnormal expression and mutation has been identified in various malignant tumors, such as breast, renal and colorectal cancer (13, 17, 18). miR-27a decreased the risk of breast cancer in Caucasians (17) and population with the genetic variant of pre-miR-27a had a lower risk of renal cell carcinoma (RCC) (13). Further, low expressed miR-27a was related to high grade in colorectal cancer (18). miR-27a inhibited A549 cell proliferation via MET signaling (19) and in esophageal squamous cell carcinoma functioned as a tumor suppressor through binding to oncogene KRAS (20). Consistent with these

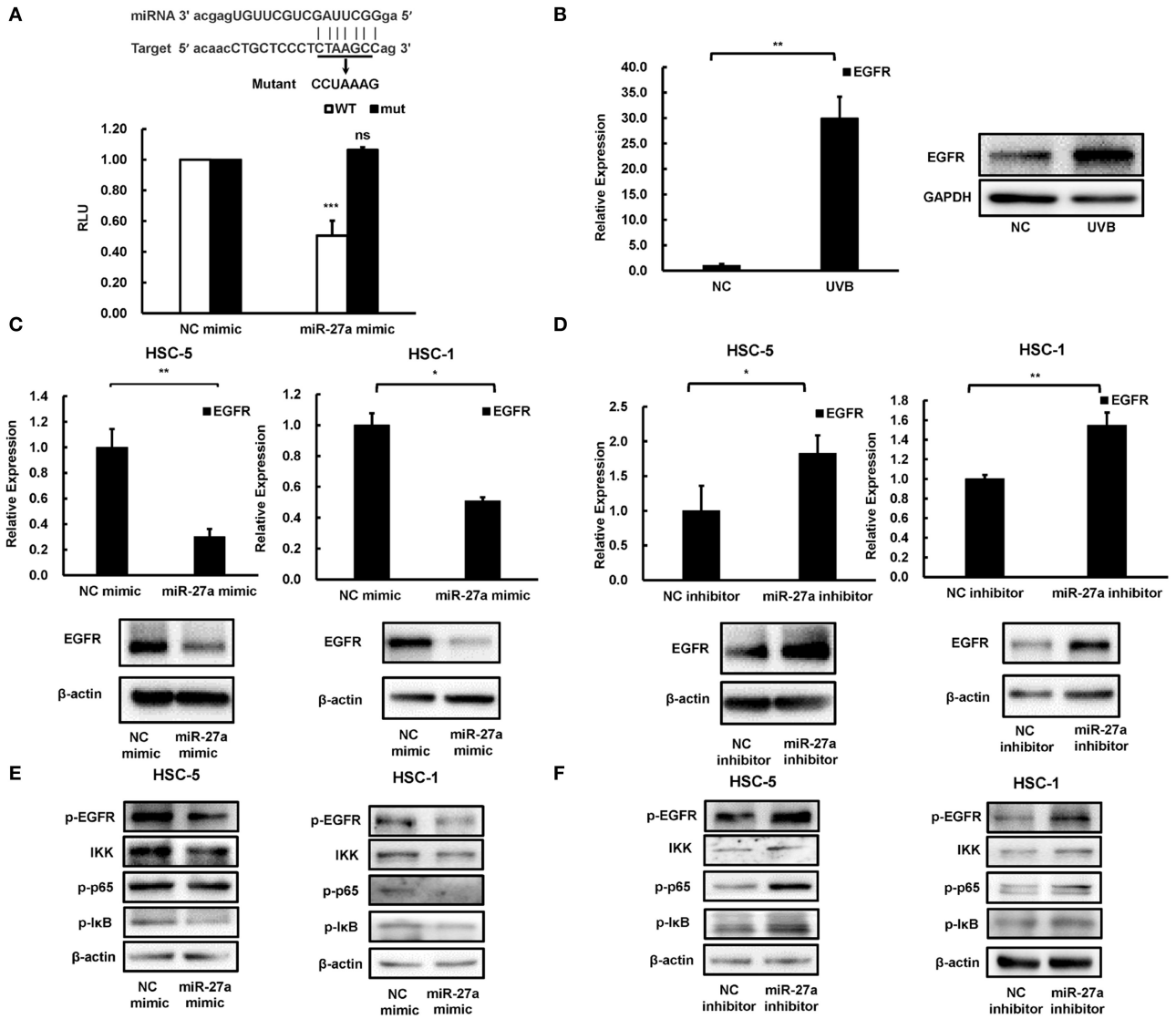

FIGURE 4 | EGFR was a direct target of miR-27a. **(A)** miR-27a inhibits the wild type but not the mutant EGFR 3'UTR luciferase activity. **(B)** EGFR was induced in chronic UVB irradiated mice skins. **(C,D)** the expression of EGFR in cSCC cells transfected with miR-27a mimic or inhibitor were detected by qPCR and western blot. **(E,F)** miR-27a suppresses the phosphorylation of EGFR and regulates its downstream pathways. miR-27a overexpression or inhibition of miR-27a regulated the phosphorylation of EGFR and the phosphorylation of p65, IκB, and IKK. Each experiment was performed in triplicate. Each experiment was performed in triplicate and data are presented as mean ± s.d. One-Way ANOVA and Dunnett's Multiple comparison test were used to analyze the data (*$P < 0.05$, **$P < 0.01$, ***$P < 0.001$).

studies, we found declined levels of miR-27a in cSCC and exogenous miR-27a suppresses cell proliferation and leads to the metastasis inhibition of cSCC significantly *in vivo* and *in vitro*.

EGFR is considered playing a crucial role in regulating cellular processes, including cell proliferation, differentiation and migration during development and homoeostasis (21). In most cancers, especially in most epithelial tumors, EGFR is commonly upregulated and closely associated with poor differentiation or unfavorable prognosis (22–24). Previous studies show that overexpression or constitutive activation of EGFR contributes to cell survival, proliferation, and invasiveness in cSCC (14, 22). In this study, we identified EGFR as a direct target gene of miR-27a by luciferase reporter assay. Exogenous transfected miR-27a led to a decreased level of EGFR and inhibition of miR-27a led to EGFR increased in cSCC cells, indicating that miR-27a suppressed the expression of EGFR by binding to 3′UTR region, which is consistent with the tumor suppressive role of miR-27a in cSCC. As it is getting great attention for EGFR targeted therapies, such as EGFR inhibitors, some clinical trials targeting EGFR have been conducted aiming at cSCC therapy (25, 26). However, it still needs to discover new strategies for cSCC treatment due to the toxicity of EGFR inhibitors and resistance to EGFR (27). NF-κB is highly conserved transcription

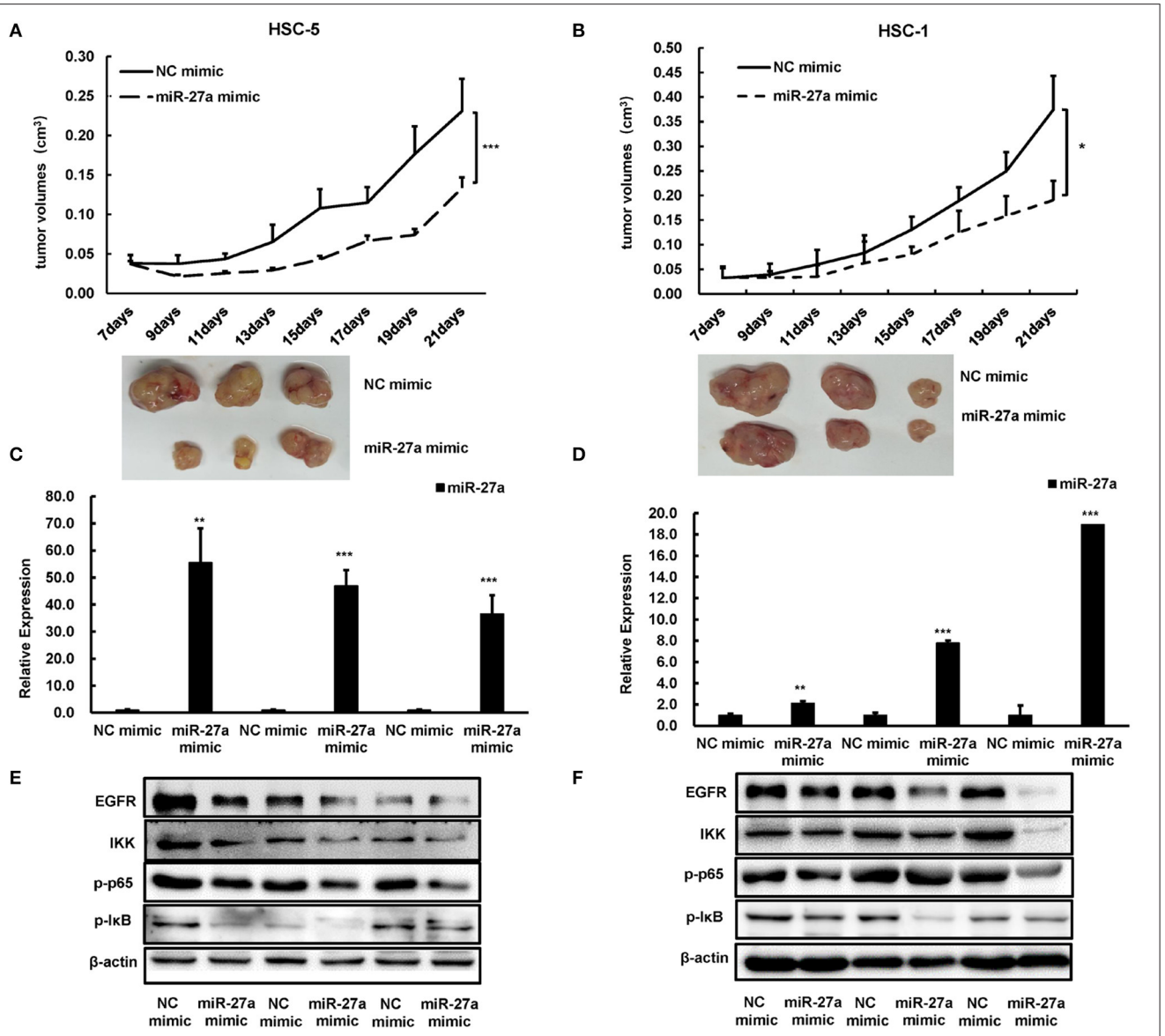

FIGURE 5 | miR-27a inhibited tumor growth of cSCC *in vivo*. **(A,B)** Growth curves of tumor volumes in miR-27a mimic group and NC mimic group were determined every 3 days. Representative photographs of tumors were shown below. **(C,D)** Relative expression of miR-27a in HSC-5 cells treated with miR-27a mimic or negative control. **(E,F)** miR-27a overexpression regulated the phosphorylation of EGFR and the phosphorylation of p65, IκB, and IKK. Each experiment was performed in triplicate and data are presented as mean ± s.d. One-Way ANOVA and Dunnett's Multiple comparison test were used to analyze the data (*$P < 0.05$, **$P<0.01$, ***$P <0.001$).

factor and NF-κB complexes are localized in the cytoplasm in inactivated state (28). In the canonical pathway, IKK is activated and phosphorylates IκB. IκB is subsequently ubiquitinated to release p65, which lead to its nuclear translocation (29). EGFR signals triggers NF-κB activation through IKK complex and the phosphorylation of IκB (30) which is abnormally constitutively activated in cancer cells and driving tumorigenesis by promoting cell proliferation and metastasis (31, 32). In addition, NF-κB activation also promotes the resistance to EGFR inhibitors, which leads to a reduced therapeutic effectiveness of EGFR inhibitors (33). Consistent with these studies, our data showed that miR-27a downregulates EGFR expression by directly binding to the 3′UTR region. Further, miR-27a inhibits the phosphorylation of EGFR and its downstream NF-κB pathway, which repress the phosphorylation of IKK and IκB to inhibit the function of IKK complex and inactivation of NF-κB activation.

Together, our study demonstrated that miR-27a inhibits the progression of cSCC via targeting EGFR and its downstream NF-κB pathway. miR-27a was selected as a sensitivity miRNA in response to UVB radiation and downregulated in cSCC. miR-27a inhibited the proliferation and metastasis of cSCC

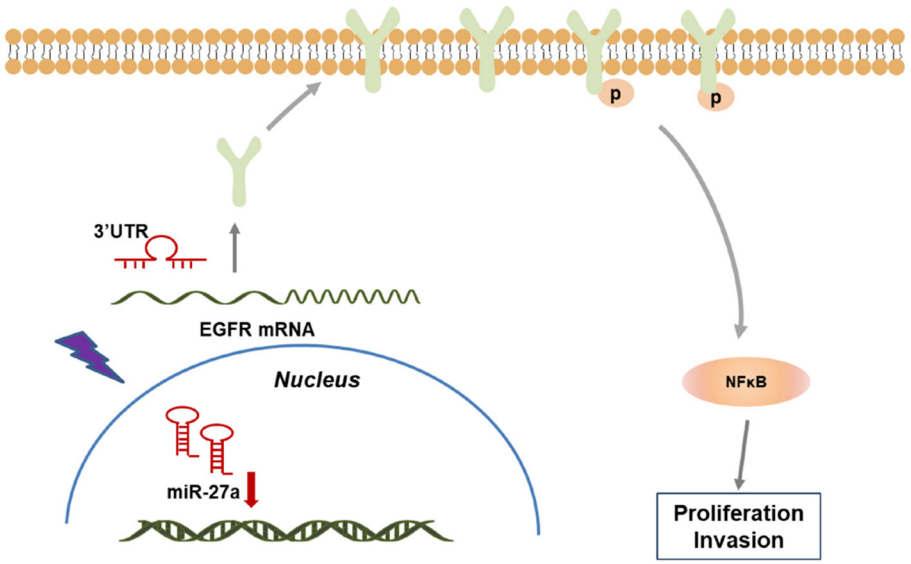

FIGURE 6 | A model of miR-27a-EGFR- NF-κB regulatory axis in cSCC development. In cSCC tumors, loss of miR-27a up-regulates EGFR and the downstream NF-κB pathway, which contributes to the enhancement of proliferation and metastasis, thus promotes cSCC progression.

cells. Furthermore, EGFR was identified to be directly targeted by miR-27a, which restrained the activation of NF-κB via directly targeting EGFR, which indicates that miR-27a may act as a tumor suppressor through NF-κB pathway (**Figure 6**). Our findings reveal a regulatory axis of miR-27a-EGFR-NF-κB that may be a novel putative therapeutic target for cSCC.

DATA AVAILABILITY STATEMENT

The datasets generated for this study are available on request to the corresponding author.

ETHICS STATEMENT

The studies involving human participants were reviewed and approved by Institutional Review Board of Nanfang Hospital affiliated to Southern Medical University. The patients/participants provided their written informed consent to participate in this study. The animal study was reviewed and approved by The Southern Medical University Animal Care and Use Committee. Written informed consent was obtained from the individual(s) for the publication of any potentially identifiable images or data included in this article.

AUTHOR CONTRIBUTIONS

MZ and YW conceived and designed the experiments. YW, XD, XN, and YD performed the experiments. YW and XD analyzed the data. MZ, YW, and XD wrote the paper, reviewed, and edited the manuscript.

FUNDING

The work described in this paper was supported by grants from the National Natural Science Foundation of China (Grant No. 81673105) and China Postdoctoral Science Foundation (Grant No. 2018M640805).

SUPPLEMENTARY MATERIAL

The Supplementary Material for this article can be found online at: https://www.frontiersin.org/articles/10.3389/fonc.2019.01565/full#supplementary-material

REFERENCES

1. Que SKT, Zwald FO, Schmults CD. Cutaneous squamous cell carcinoma: incidence, risk factors, diagnosis, and staging. *J Am Acad Dermatol.* (2018) 78:237–47. doi: 10.1016/j.jaad.2017.08.059
2. Nehal KS, Bichakjian CK. Update on Keratinocyte Carcinomas. *N Engl J Med.* (2018) 379:363–74. doi: 10.1056/NEJMra1708701
3. Bowden GT. Prevention of non-melanoma skin cancer by targeting ultraviolet-B-light signalling. *Nat Rev Cancer.* (2004) 4:23–35. doi: 10.1038/nrc1253
4. Esteller M. Non-coding RNAs in human disease. *Nat Rev Genet.* (2011) 12:861–74. doi: 10.1038/nrg3074
5. Smith B, Agarwal P, Bhowmick NA. MicroRNA applications for prostate, ovarian and breast cancer in the era of precision medicine. *Endocr Relat Cancer.* (2017) 24:R157–72. doi: 10.1530/ERC-16-0525

6. Wu SG, Chang TH, Liu YN, Shih JY. MicroRNA in lung cancer metastasis. *Cancers*. (2019) 11:E265. doi: 10.3390/cancers11020265
7. Shah MY, Ferrajoli A, Sood AK, Lopez-Berestein G, Calin GA. microRNA therapeutics in cancer - an emerging concept. *EBioMedicine*. (2016) 12:34–42. doi: 10.1016/j.ebiom.2016.09.017
8. Konicke K, Lopez-Luna A, Munoz-Carrillo JL, Servin-Gonzalez LS, Flores-de la Torre A, Olasz E, et al. The microRNA landscape of cutaneous squamous cell carcinoma. *Drug Discov Today*. (2018) 23:864–70. doi: 10.1016/j.drudis.2018.01.023
9. Li X, Zhou C, Zhang C, Xie X, Zhou Z, Zhou M, et al. MicroRNA-664 functions as an oncogene in cutaneous squamous cell carcinomas (cSCC) via suppressing interferon regulatory factor 2. *J Dermatol Sci*. (2019) 94:330–8. doi: 10.1016/j.jdermsci.2019.05.004
10. Zhou M, Liu W, Ma S, Cao H, Peng X, Guo L, et al. A novel onco-miR-365 induces cutaneous squamous cell carcinoma. *Carcinogenesis*. (2013) 34:1653–9. doi: 10.1093/carcin/bgt097
11. Vimalraj S, Miranda PJ, Ramyakrishna B, Selvamurugan N. Regulation of breast cancer and bone metastasis by microRNAs. *Dis Markers*. (2013) 35:369–87. doi: 10.1155/2013/451248
12. Ye P, Ke X, Zang X, Sun H, Dong Z, Lin J, et al. Up-regulated miR-27-3p promotes the G1-S phase transition by targeting inhibitor of growth family member 5 in osteosarcoma. *Biomed Pharmacother*. (2018) 101:219–27. doi: 10.1016/j.biopha.2018.02.066
13. Shi D, Li P, Ma L, Zhong D, Chu H, Yan F, et al. A genetic variant in pre-miR-27a is associated with a reduced renal cell cancer risk in a Chinese population. *PLoS ONE*. (2012) 7:e46566. doi: 10.1371/journal.pone.0046566
14. Zhang Y, Gao L, Ma S, Ma J, Wang Y, Li S, et al. MALAT1-KTN1-EGFR regulatory axis promotes the development of cutaneous squamous cell carcinoma. *Cell Death Differ*. (2019) 26:2061–73. doi: 10.1038/s41418-019-0288-7
15. Zhou L, Wang Y, Zhou M, Zhang Y, Wang P, Li X, et al. HOXA9 inhibits HIF-1alpha-mediated glycolysis through interacting with CRIP2 to repress cutaneous squamous cell carcinoma development. *Nat Commun*. (2018) 9:1480. doi: 10.1038/s41467-018-03914-5
16. Chou CH, Shrestha S, Yang CD, Chang NW, Lin YL, Liao KW, et al. miRTarBase update 2018: a resource for experimentally validated microRNA-target interactions. *Nucleic Acids Res*. (2018) 46:D296–302. doi: 10.1093/nar/gkx1067
17. Zhang H, Zhang Y, Zhao X, Ma X, Yan W, Wang W, et al. Association of two microRNA polymorphisms miR-27 rs895819 and miR-423 rs6505162 with the risk of cancer. *Oncotarget*. (2017) 8:46969–80. doi: 10.18632/oncotarget.16443
18. Bao Y, Chen Z, Guo Y, Feng Y, Li Z, Han W, et al. Tumor suppressor microRNA-27a in colorectal carcinogenesis and progression by targeting SGPP1 and Smad2. *PLoS ONE*. (2014) 9:e105991. doi: 10.1371/journal.pone.0105991
19. Yang Y, Zang A, Jia Y, Shang Y, Zhang Z, Ge K, et al. Genistein inhibits A549 human lung cancer cell proliferation via miR-27a and MET signaling. *Oncol Lett*. (2016) 12:2189–93. doi: 10.3892/ol.2016.4817
20. Zhu L, Wang Z, Fan Q, Wang R, Sun Y. microRNA-27a functions as a tumor suppressor in esophageal squamous cell carcinoma by targeting KRAS. *Oncol Rep*. (2014) 31:280–6. doi: 10.3892/or.2013.2807
21. Sigismund S, Avanzato D, Lanzetti L. Emerging functions of the EGFR in cancer. *Mol Oncol*. (2018) 12:3–20. doi: 10.1002/1878-0261.12155
22. Canueto J, Cardenoso E, Garcia JL, Santos-Briz A, Castellanos-Martin A, Fernandez-Lopez E, et al. Epidermal growth factor receptor expression is associated with poor outcome in cutaneous squamous cell carcinoma. *Br J Dermatol*. (2017) 176:1279–87. doi: 10.1111/bjd.14936
23. Wee P, Wang Z. Epidermal growth factor receptor cell proliferation signaling pathways. *Cancers*. (2017) 9: E52. doi: 10.3390/cancers9050052
24. Sabattini S, Marconato L, Zoff A, Morini M, Scarpa F, Capitani O, et al. Epidermal growth factor receptor expression is predictive of poor prognosis in feline cutaneous squamous cell carcinoma. *J Feline Med Surg*. (2010) 12:760–8. doi: 10.1016/j.jfms.2010.04.010
25. William WN Jr, Feng L, Ferrarotto R, Ginsberg L, Kies M, Lippman S, et al. Gefitinib for patients with incurable cutaneous squamous cell carcinoma: A single-arm phase II clinical trial. *J Am Acad Dermatol*. (2017) 77:1110–3.e2. doi: 10.1016/j.jaad.2017.07.048
26. Lewis CM, Glisson BS, Feng L, Wan F, Tang X, Wistuba II, et al. A phase II study of gefitinib for aggressive cutaneous squamous cell carcinoma of the head and neck. *Clin Cancer Res*. (2012) 18:1435–46. doi: 10.1158/1078-0432.CCR-11-1951
27. Shostak K, Chariot A. EGFR and NF-kappaB: partners in cancer. *Trends Mol Med*. (2015) 21:385–93. doi: 10.1016/j.molmed.2015.04.001
28. May MJ, Ghosh S. Rel/NF-kappa B and I kappa B proteins: an overview. *Semin Cancer Biol*. (1997) 8:63–73. doi: 10.1006/scbi.1997.0057
29. Hayden MS, Ghosh S. Shared principles in NF-kappaB signaling. *Cell*. (2008) 132:344–62. doi: 10.1016/j.cell.2008.01.020
30. Le Page C, Koumakpayi IH, Lessard L, Mes-Masson AM, Saad F. EGFR and Her-2 regulate the constitutive activation of NF-kappaB in PC-3 prostate cancer cells. *Prostate*. (2005) 65:130–40. doi: 10.1002/pros.20234
31. Dolcet X, Llobet D, Pallares J, Matias-Guiu X. NF-kB in development and progression of human cancer. *Virchows Arch*. (2005) 446:475–82. doi: 10.1007/s00428-005-1264-9
32. Barkett M, Gilmore TD. Control of apoptosis by Rel/NF-kappaB transcription factors. *Oncogene*. (1999) 18:6910–24. doi: 10.1038/sj.onc.1203238
33. Kobayashi S, Boggon TJ, Dayaram T, Janne PA, Kocher O, Meyerson M, et al. EGFR mutation and resistance of non-small-cell lung cancer to gefitinib. *N Engl J Med*. (2005) 352:786–92. doi: 10.1056/NEJMoa044238

Conflict of Interest: The authors declare that the research was conducted in the absence of any commercial or financial relationships that could be construed as a potential conflict of interest.

frontiers in Oncology

ORIGINAL RESEARCH
published: 14 February 2020
doi: 10.3389/fonc.2020.00037

Genomic Identification of RNA Editing Through Integrating Omics Datasets and the Clinical Relevance in Hepatocellular Carcinoma

Juan Chen[1], *Lu Wang*[1], *Fangbin Wang*[1], *Jian Liu*[1,2]* *and Zhenyu Bai*[3]*

[1] School of Food and Biological Engineering, Hefei University of Technology, Hefei, China, [2] Engineering Research Center of Bio-Process, Ministry of Education, Hefei University of Technology, Hefei, China, [3] Department of Laboratory, General Hospital of Pingmei Shenma Medical Group, Pingdingshan, China

RNA editing is a widespread post-transcriptional mechanism to introduce single nucleotide changes to RNA in human cancers. Here, we characterized the global RNA editing profiles of 373 hepatocellular carcinoma (HCC) and 50 adjacent normal liver samples from The Cancer Genome Atlas (TCGA) and revealed that most editing events tend to occur in minor percentage of samples with moderate editing degrees (20–30%). Moreover, these RNA editing prefer to be A-to-I RNA editing in protein coding genes, especially in 3′UTR regions. Considering the association between DNA mutation and RNA editing, our analysis found that RNA editing maybe a complementary event for DNA mutation of HCC risk genes in HCC patients. We next identified 454 HCC-related editing sites, and many locate on the same genes with the same editing patterns. The functional consequences of editing revealed 2,086 functional editing sites and demonstrated that most editing in coding regions are non-synonymous variations. Furthermore, our results showed that editing in the 3′UTR regions tend to influence miRNA–target binding, and the editing degree seems to be negatively correlated with gene expression. Finally, we found that 46 HCC-related editing sites with consequence are able to distinguish the prognosis differences of HCC patients, suggesting their clinical relevance. Together, our results highlight RNA editing as a valuable molecular resource for investigating HCC mechanisms and clinical treatments.

Keywords: RNA editing, hepatocellular carcinoma, post-transcriptional regulation, bioinformatics, prognosis

OPEN ACCESS

Edited by:
Hailong Pei,
Soochow University, China

Reviewed by:
Yuen Gao,
Michigan State University, United States
Himanshu Tripathi,
National Institute of Biomedical Genomics (NIBMG), India

***Correspondence:**
Jian Liu
liujian509@hfut.edu.cn
Zhenyu Bai
baizhenyu666@outlook.com

Specialty section:
This article was submitted to Molecular and Cellular Oncology, a section of the journal Frontiers in Oncology

Received: *29 October 2019*
Accepted: *09 January 2020*
Published: *14 February 2020*

Citation:
Chen J, Wang L, Wang F, Liu J and Bai Z (2020) Genomic Identification of RNA Editing Through Integrating Omics Datasets and the Clinical Relevance in Hepatocellular Carcinoma. Front. Oncol. 10:37. doi: 10.3389/fonc.2020.00037

INTRODUCTION

Hepatocellular carcinoma (HCC) is a kind of malignant tumor with high mortality. It ranks third among all cancer-related mortality in the world. About 3% of the patients with cirrhosis can result in HCC, which is the most serious complication in chronic liver diseases (1). The high mortality rate of HCC is mainly due to it being asymptomatic in the early stage and the lack of effective treatments for even mid-term patients. This poses a great threat to the patient's life and also brings heavy economic burdens to the society and families. Therefore, it is of great significance to clarify the pathogenesis of HCC as soon as possible, and thus formulate more effective strategies for clinical diagnosis and treatment. Previous studies on the pathogenic mechanisms of cancer suggested that DNA mutations are a driving factor in cancer development; however, many HCC tumor samples

were found to be free of carcinogenic DNA-driven mutations (2), which indicate that other driving events are involved in the occurrence and development of HCC.

RNA editing is an important post-transcriptional modification event, which change genetic information at RNA level and generate results similar to DNA mutations, thus increasing the diversity of transcripts and proteomes (3). The most common type of RNA editing in human cells is the transformation of adenine nucleotides (A) into inosine (I), which was mediated by adenosine deaminase family proteins (ADARs) (4). Because inosine (I) is recognized as guanine (G) nucleotide during translation, it is also called A-to-GRNA editing. In addition to changes in A-to-I (G) RNA editing, human cells also have a small number of other RNA editing types (5). Recent bioinformatics analysis found that RNA editing events are extensive across the human transcriptome (6).

RNA editing in normal cells are associated with adaptive evolution and cell development (7). Conversely, dysfunction in RNA editing systems will have a series of effects on subsequent RNA regulation processes. First, RNA editing in the protein coding region can affect amino acid translation, producing proteins with different structures or functions, and then affecting protein expression activity. For example, the A-to-I hyper-editing in RHOQ transcripts will induce the abnormal elevation of RHOQ protein, and thus promote the invasion and metastasis of cancer cells in colorectal cancer (8). The editing of SLC22A3 transcript can induce the down-expression of SLC22A3 protein, which contributes to the early invasion in familial esophageal squamous cell carcinoma (9). Second, about 95% of multi-exon genes produce different transcripts through alternative splicing (10, 11), which is common in human liver cancer (12). RNA editing occurring in splicing sites or splicing regulatory elements possibly affects the variable splicing processes of RNA. For instance, the hyper-editing on one of the potential branching sites of PTPN6 causes the third intron retention, which is associated with the pathogenesis of acute leukemia (13). Third, genome-wide sequencing analysis revealed that most RNA editing sites were located in the non-coding regions of the genome, including the 3′UTR, intron and intergenic regions, which may influence the regulation of non-coding RNAs, especially miRNA regulation on the 3′UTR regions (14, 15). These studies indicate that RNA editing events will affect a series of downstream RNA regulation processes, which are closely related to the disease processes.

Recently, the incidence and progression of HCC were found associated with RNA editing events and may further help us reveal the pathogenic mechanisms underlying HCC. Chen et al. suggested that the hyper-editing event of AZIN1 results in a serine-to-glycine substitution at residue 367 of the AZIN1 protein, which may be a potential driver in the pathogenesis of HCC (16). Chan et al. identified an average of 20,007 A-to-I RNA editing events in transcripts by utilizing RNA-seq of three paired HCC and their adjacent non-tumor samples, then validated the expression level of ADARs that are related to editing degrees of FLNB and COPA in a large cohort with microarray analysis. They also found that the expression level of ADARs which mediate A-to-I RNA editing is related to the risk of HCC recurrence (17). Similarly, research on two pairs of HCC patients revealed that BLCAP transcript is hyper-edited, which will enhance the phosphorylation of AKT, MTOR, and MDM2 and inhibit the function of TP53, thus promote cell proliferation and tumor development (18). Another study identified HCC-related RNA editing sites by genomic and transcriptomic analysis of nine pairs of HCC and normal samples (19). However, the number of HCC patients used in these studies is relatively small, and their statistical efficacy is limited. Furthermore, the main concern is the limited effect of ADAR enzymes on RNA editing, and the limited analysis of downstream regulation systems, which RNA editing may affect.

Recently, The Cancer Genome Atlas (TCGA) project provides a large number of omics data of malignant tumors. Han et al. and Paz-Yaacov et al. identified RNA editing sites in multiple cancer types from TCGA, including HCC (20, 21). However, they focused on pan-cancer analysis and only used a part of the HCC samples. Han et al. focused on existing RNA editing sites annotated in the RADAR database. Moreover, they removed all mutation sites annotated in the COSMIC database and the ones that were not matched to specific tumor samples. Thus, they may miss a number of HCC-related RNA editing events. Paz-Yaacov et al. focused on the clinical influence of Alu-specific RNA editing and just considered 30 pairs of HCC cancer and normal samples. Most importantly, the specific changes in downstream RNA regulation system caused by RNA editing were not thoroughly analyzed, and the genome-wide distribution pattern of RNA editing in HCC is not described in both studies. In addition, as they focused on the common pathogenic mechanism of multiple cancer types, many HCC-related RNA editing sites were not presented. We suggested that it should be clearly described whether the RNA editing was observed in cases where DNA mutations are absent in HCC-relevant driver genes.

In our study, we intend to *de novo* identification of HCC-related RNA editing sites by integrating multiple omics data with bioinformatics methods, including genomic mutation, transcriptomic variation, and reference single nucleotide polymorphism (SNP) information, using 373 HCC tumor samples and 50 adjacent normals from TCGA. Here, the genomic distribution pattern of RNA editing events was described. We also deeply analyzed the influence of HCC-related RNA editing on downstream regulation system, including the effect on protein translation and miRNA regulation. Based on clinical information of HCC patients, our study further identified new biomarkers for clinical prognosis, which will promote the disclosure of molecular mechanisms of HCC from the perspective view of RNA editing.

MATERIALS AND METHODS

Data Retrieval

Pair-end RNA-seq BAM files originating from 373 HCC cancer samples and 50 adjacent normal liver samples were downloaded from the database of Genotypes and Phenotypes (dbGaP) originally from The Cancer Genome Atlas (TCGA, https://portal.gdc.cancer.gov/) research project (22). Validated RNA-seq FASTQ files of HCC cell lines and normal liver samples were downloaded from ArrayExpress (https://www.ebi.ac.uk/

arrayexpress/, E-MTAB-4052) (23), including three human normal liver samples and two Huh7 RNA-seq FASTQ datasets. DNA mutation, gene expression, and clinical information datasets were also downloaded from TCGA. Single nucleotide polymorphism (SNP) annotations were downloaded from dbSNP version 137 (24) and the 1000 Genomes Project (25).

Gene annotation of the 3′UTR, 5′UTR, CDS, and intron regions were downloaded from the UCSC table browser (http://genome.ucsc.edu/cgi-bin/hgTables) (26). In addition, functional annotation gene sets were downloaded from the MsigDB database (http://software.broadinstitute.org/gsea/msigdb) (27).

We obtained the list of known tumor suppressive genes (TSGs) and oncogenic genes (OGs) from a previous study (28), which integrates mRNA expression, copy number variations (CNV), and DNA mutation information and generated a continuous ranked list for each gene, ranging from more negative (TSGs) to more positive (OGs) with consistent changes across tumors. Here we used a strict score threshold to get OGs (score $\geq$7) and TSGs (score $\leq$−7) for further analysis. The statistical significances for the enrichment of OGs and TSGs were calculated by hypergeometric tests. All of the data resources mentioned above are shown in **Supplementary Table S1**.

De novo Detection of RNA Editing Sites

First, the downloaded BAM files of the TCGA samples were converted to FASTQ using BEDtools (29), the FASTQ files were aligned to the human reference genome (GRCh38) by STAR with default parameters (--outFilterMultimapScoreRange 1 –sjdbScore 2 –outFilterScoreMinOverLread 0.33 --outFilterMultimapNmax 20 --sjdbOverhang 100) (30). Second, putative RNA editing sites were identified by Genome Analysis Toolkit (GATK4) with default parameters (HaplotypeCaller --gcs-max-retries 20 --heterozygosity 0.001 --max-reads-per-alignment-start 50 --min-base-quality-score 10), using uniquely mapped reads after PCR duplicates were removed (31). Third, computational filters for *vcf* files were applied through five steps: (i) removing DNA mutation sites for each HCC sample; (ii) taking out all known SNPs in dbSNP version 137 or the 1000 Genome Project, and also insertion or deletion sites; (iii) further filtering sites to obtain editing sites with high confidence: if Fisher Strand (FS) >20, or Quality by Depth (QD) <2, or editing was supported <2 reads, or total coverage reads <10, these sites were removed, and we required at least 10% difference between the editing degrees of 90% quantile and 10% quantile across all samples; (iv) sites with 100% editing degree were also filtered, as 100% editing efficiency is thought to be unrealistic (6); (v) keeping variants detected in at least 1% of the samples because they are unlikely to be rare variants. Editing degree was defined as the percentage of edited reads among the total mapped reads at a given site (20).

Finally, we restricted editing sites to 46 human chromosomes. To get the exact RNA, which was edited, we used BEDtools to map the editing sites with gene annotation *gtf* files. If the RNA editing sites were simultaneously mapped to two strands, these sites were further removed. At last, we get 19,431 RNA editing sites for further analysis.

The validated RNA-seq FASTQ datasets were aligned to the human reference genome (GRCh38) by *bowtie*, processed by GATK4 with default parameters, with no matched DNA mutation datasets. Other pipelines were similar to the aforementioned method.

Identification of HCC-Related RNA Editing Sites

HCC-related RNA editing sites include HCC gain, HCC loss, and significant dysregulated editing (dys-edit) sites. HCC gain or HCC loss editing sites were defined by Fisher's exact test (Benjamini–Hochberg correction, adjust $p < 0.05$), with HCC gain editing sites restricted to be no more than 5% editing sites in normal samples and HCC loss editing sites restricted to be no more than 5% editing sites in cancer samples. Dys-edit sites were just focused on the editing degree of 50 HCC cancer samples and mapped 50 normal samples, which were determined by two steps: (i) using the paired Student's *t*-test (Benjamini–Hochberg correction, adjust $p < 0.2$ and $p < 0.01$); (ii) restricting editing sites to those having more than 0.25 editing degree change in at least two pairs of normal and cancer samples. The HCC dys-edit sites identified in the above two steps were changed in the same direction (simultaneously hyper-edited or hypo-edited in two steps). Finally, we identified 454 HCC-related RNA editing sites.

Functional Enrichment Analysis for HCC-Related RNA Editing Sites

First, HCC-related RNA editing sites were mapped to gene name by BEDtools. Then, we performed functional enrichment analysis by hypergeometric test (Benjamini–Hochberg correction, adjust $p < 0.05$). We focused on chemical and genetic perturbations (CGP), reactome pathways and biological processes (BP) of gene ontology (GO) originating from MsigDB.

The Functional Consequence Analysis for RNA Editing Sites

Protein Coding and Alternative Splicing Change

To define whether an editing site can change protein translation or alternative splicing, we re-annotated them by ANNOVAR (32).

miRNA–Target Binding Prediction

RNA editing in the 3′UTR regions may influence the binding and regulation of miRNAs, including loss of existing miRNA–target regulation and gain of new regulation, or change the binding strength of existing miRNA–target regulation. Therefore, for each RNA editing site in the 3′UTR regions, we simultaneously calculated and compared the miRNA binding in both edited and reference 3′UTR regions. We computationally predicted whether an miRNA binds to the mRNA regions around editing sites using miRanda (33) as described in Hwang et al. (5), which calculates the binding energy to estimate the thermodynamic properties of a predicted duplex and a complementarity score to estimate the mismatch. Briefly, for mRNA as a target sequence, two types of sequences were prepared with flanking regions of editing sites (50 bp upstream and downstream) in all mRNA transcripts in UCSC: the reference sequence and the editing sequence. The mature miRNA sequences were also prepared, which were

obtained from miRBase (34). The binding energies between miRNA sequence with both a reference and edited mRNA sequences were calculated by miRanda (v3.3a) with default parameters (score > 140, gap-open penalty set to −4 and gap-extend penalty set to −9). We next used delta G <-14 kcal/mol as a threshold for free energy of duplex formation to obtain more confident miRNA–target regulations, which were maintained for the following analysis. The comparison was performed for these two types of mRNA sequence, with all the predicted binding pairs of miRNAs and mRNA targets. If miRNA–target relationships just appeared in reference but not in the edited sequence, these were defined as "edited loss" conversely, defined as "edited gain." As for the relationships that both appeared in the reference and edited sequences, if the binding energies changed more than 14 kcal/mol between the reference and edited sequences, they were defined as "edited change." The "edited gain," "edited loss," and "edited change" constituted the candidate pool of RNA editing sites that may induce miRNA–target regulations to change. Finally, if the editing of an mRNA target induces more than 10 miRNA–target regulation change, this editing site was defined as having an miRNA–target regulation consequence.

Expression-Related RNA Editing Sites

To define whether RNA editing can influence RNA expression, we calculated the Pearson correlation between editing degree and expression level among samples where both expression and editing degree were measured (editing degree is not 0; Benjamini–Hochberg correction; adjust $p < 0.05$). The normalized gene expression levels of raw read counts were calculated using DESeq2 (35).

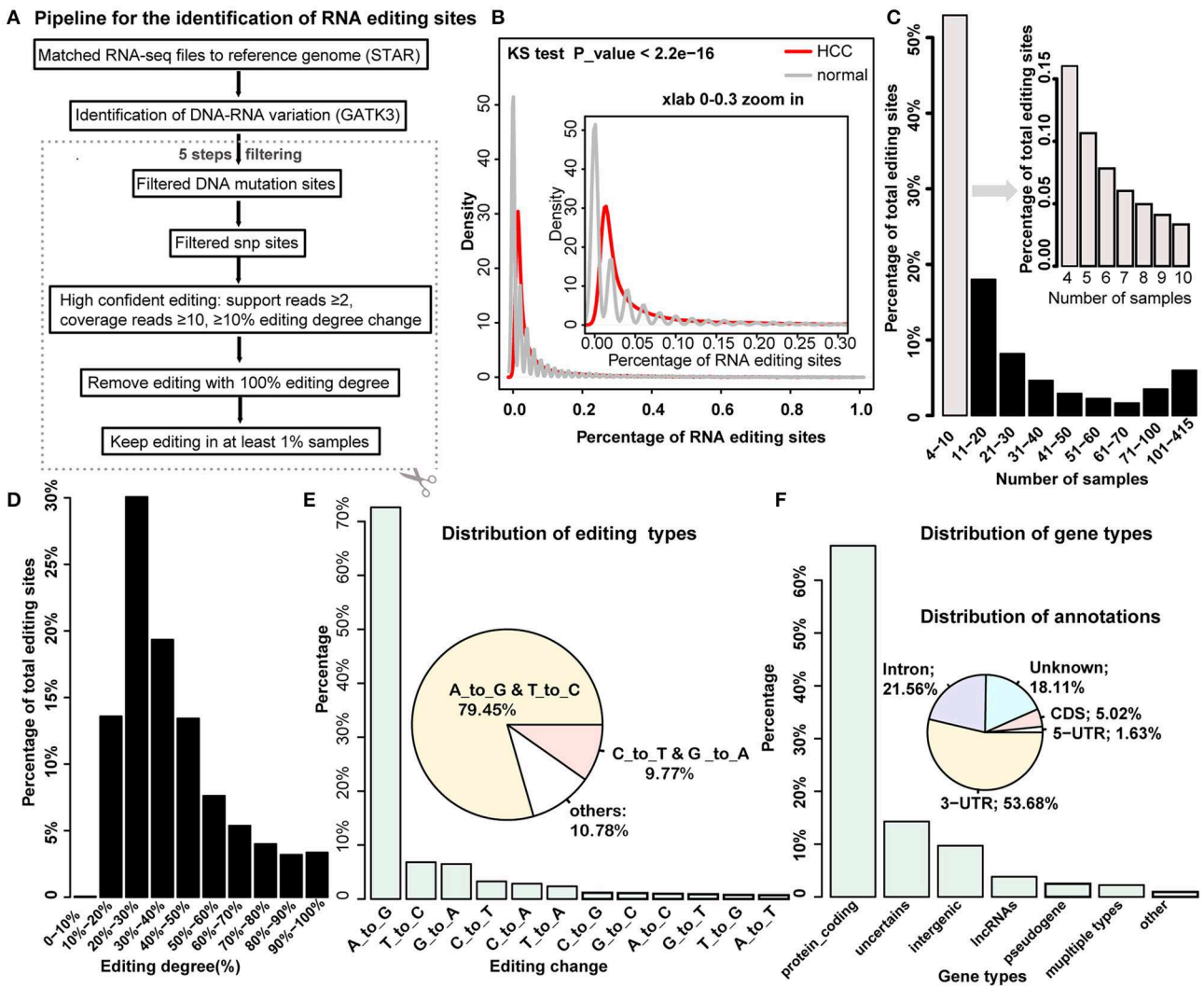

FIGURE 1 | Systemic identification and global properties of RNA editing sites in hepatocellular carcinoma (HCC) and normal samples. **(A)** The pipeline for the identification of RNA editing site in HCC and normal samples. **(B)** The distribution of the percentage of RNA editing sites in HCC cancer and normal sample. **(C)** The distribution of editing percentages across different intervals of samples. **(D)** The percentage of editing sites across different intervals of editing degrees. **(E)** The distribution of editing variation types. **(F)** The distribution of gene types and genomic annotations for identified RNA editing sites.

Correlation Between Editing Risk Score and Survival

First, we defined the editing risk score for each HCC clinical sample. Univariate Cox regression analysis was performed to evaluate the association between survival duration and the editing degree of each editing site. A regression coefficient with a plus sign indicated that increased editing degree is associated with an increased risk of survival (risky editing); conversely, a minus sign indicated that an increased editing degree is associated with a decreased risk of survival (protective editing). More specifically, for editing sites, which are located in a gene region, we assigned a risk score to each HCC patient according to a combination of the product of the editing degree and gene expression, weighted by 1 or −1 according to the regression coefficients from the univariate Cox regression analysis mentioned above. The risk score for each patient was calculated as follows:

$$Risk\_Score = \sum_{i=1}^{n} \beta_i * Exp_{gene(i)} * Edit_i$$

where, β_i is 1 or −1 when the Cox regression coefficient of the editing site i is a positive or negative value, respectively. The n is the number of HCC-related RNA editing sites with consequence that are located in gene regions with an editing degree more than 0 in each sample. $Exp_{gene(i)}$ is the expression level of gene in which the editing site i occurs. $Edit_i$ represents the editing degree of the editing site i.

To investigate whether risk scores are associated with tumor grades and tumor stages, we use the Wilcoxon rank-sum test. As the sample number with a tumor grade 4 or tumor stage 4 is too small, only 12 and 13, respectively, we only considered grade 1, grade 2, and grade 3 plus (including grade 3 and grade 4) for tumor grades and stage 1, stage 2, and stage 3 plus (including stage 3 and stage 4) for tumor stages. All patients were then classified into high-risk and low-risk groups using the median risk score as the cutoff point. The Kaplan–Meier method was further used to estimate the differences in overall survival time for these two patient groups (log-rank test). Patients having higher risk scores were expected to have poor survival outcomes.

We further focused on three prognostic-related editing sites whose editing degrees are significantly correlated with survival ($p < 0.05$). The risk scores were calculated according to the mathematical formula above. For HBV/HCV infected patients or non-alcoholic fatty liver patients, we did a similar analysis mentioned above to obtain a risk score for each sample using three prognostic-related editing sites.

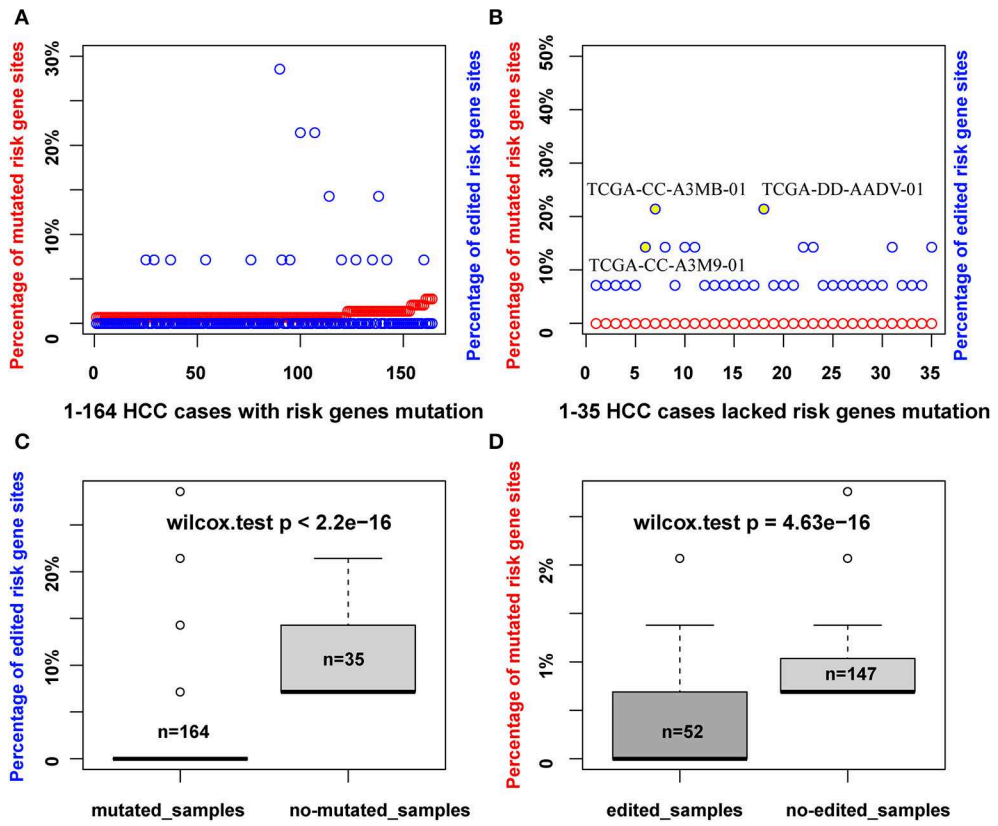

FIGURE 2 | RNA editing maybe a complementary event for DNA mutation of HCC risk genes in HCC patients. **(A)** The percentage of mutated sites or edited sites in 164 HCC samples with DNA mutation of HCC risk genes (red points, number of mutated sites/total mutated HCC risk sites identified; blue points, number of edited sites/total edited HCC risk sites identified). **(B)** The percentage of mutated sites or edited sites in 35 HCC samples without DNA mutation of HCC risk genes. **(C)** The percentage of edited sites account for total edited HCC risk sites identified in mutated and non-mutated HCC samples. **(D)** The percentage of mutated sites account for total mutated HCC risk sites identified in edited and non-edited samples.

To determine whether editing risk scores can provide additional predictive power, we performed a multivariate survival analysis using prognostic factors, including gender, age, body mass index (BMI), grade, and stage of HCC patients, along with editing risk score.

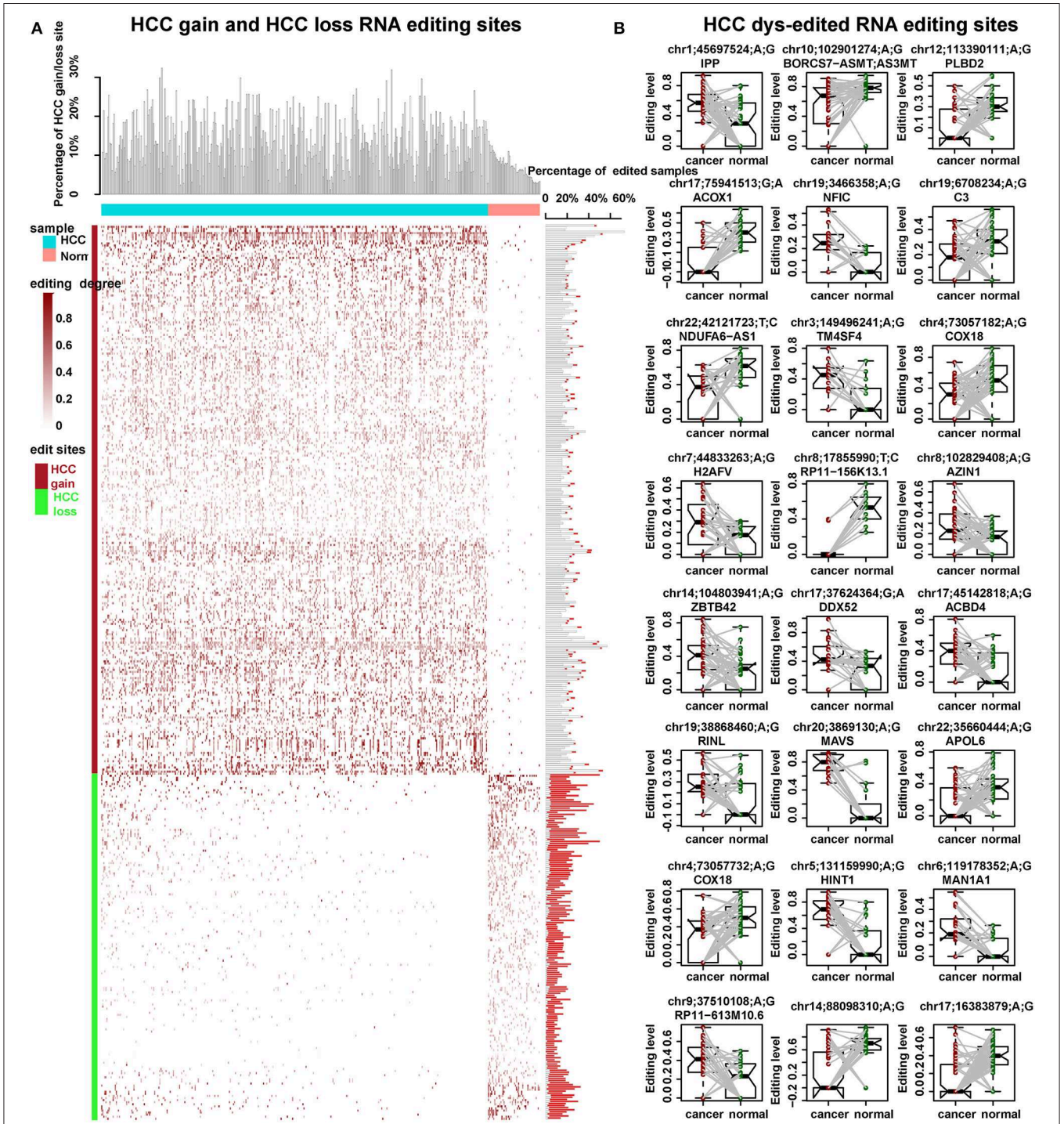

FIGURE 3 | HCC-related RNA editing sites (454) were identified. **(A)** HCC gain and HCC loss RNA editing sites across 373 HCC cancer samples and 50 normal samples. Upper: the percentage of HCC gain and loss site in each HCC or normal samples. Middle: the editing degree in each HCC or normal cases. Right: the percentage of edited samples for each HCC gain or loss editing site. The box filled in red showed the percentage of edited samples in normal samples. Meanwhile, the one filled in white showed the percentage of edited samples in HCC cancer samples. **(B)** The editing degrees of 24 HCC dys-edited RNA editing sites in 50 paired HCC cancer and normal samples. The last two are in the gene interstitial regions.

RESULTS

Global Properties of the Inferred RNA Editing Sites in HCC and Normal Samples

Several *de novo* methods for detecting RNA editing were developed recently (5, 6, 20). Here we combined these methods and proposed a multi-stage method to gradually identify RNA editing sites by integrating DNA mutation and SNP datasets (**Figure 1A**) (see details in the Methods section). Totally, we obtained 19,431 RNA editing sites for further analysis. In general, HCC tumor samples have a higher percentage of RNA editing sites compared to the normal samples (**Figure 1B**). More than half of the editing sites occurred in no more than 10 samples (**Figure 1C**). Most editing sites presented moderate editing degree, where 20–30% editing degree accounted for the largest proportion (**Figure 1D**). We also found that A-to-IRNA editing accounts for most of the RNA variants in the list, and the following enriched variant types were T-to-C, G-to-A, and C-to-T RNA editing, which was consistent with previous research [**Figure 1E**; (5, 6)]. We next annotated these editing sites with gene types and revealed that most of the editing sites are located on protein-coding genes. In addition, a moderate number of RNA editing sites are located in intergenic and lncRNA regions (**Figure 1F**). Consistent with a previous study, more than half of the editing sites are in the 3′UTR regions, accounting for 53.68%, and the following are in the intron regions (**Figure 1F**). Notably, Han et al. reported just a few A-to-I RNA editing in the CDS regions; here we identified about 5% editing events in the CDS regions, which include many other types of RNA editing. After we restricted to A-to-I RNA editing, the percent decreased to be 1.66% in the CDS regions (**Supplementary Figure S1**).

TABLE 1 | HCC-related RNA editing sites.

	Number of editing sites in protein-coding genes	Number of involved protein-coding genes	Total number of RNA editing sites
HCC gain	208	134	264
HCC loss	93	67	166
Dys-edited	19	18	24
Total	320	213	454

RNA Editing May Be a Complementary Event for DNA Mutation of HCC Risk Genes in HCC Patients

As RNA editing and DNA mutation have a similar effect to increase the diversity of transcripts in cells, thus we wonder whether there is a connection between these two events. For a given gene region, if it is identified to be mutated, it would not be identified as editing at the same time in our recognition method. However, we can dissect whether there is a correlation between RNA editing and DNA mutation in HCC risk gene sets.

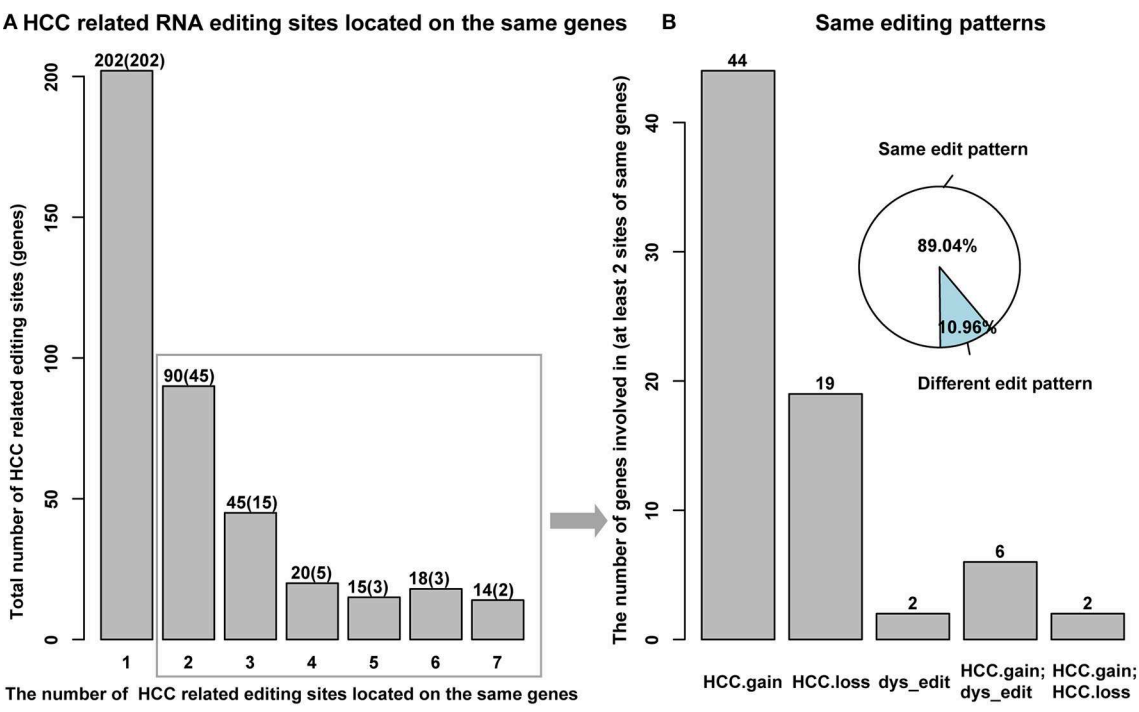

FIGURE 4 | HCC-related RNA editing sites prefer to locate on the same genes with same editing patterns. **(A)** Several HCC-related RNA editing sites located on the same genes. Y axis means the total number of editing sites, and the number of genes involved in were shown in parenthesis. X axis means the number of different editing sites located on the same genes. **(B)** Different HCC-related RNA editing sites, which located on the same genes prefer to have the same editing patterns.

We obtained 33 HCC relevant cancer genes from a previous report (36), which we defined as HCC risk genes, such as TP53, PTEN, and TERT, of which we observed 24 risk genes with DNA mutation (145 mutation sites involved), and six risk genes with RNA editing (14 editing sites involved). HCC patients with DNA mutation (164) and 35 cases lacking DNA mutations in HCC risk genes were observed (**Figures 2A,B**). It is found that all of these 35 patients that lacked DNA mutation had RNA editing in the HCC risk genes. For example, patient TCGA-CC-A3M9-01 had no mutated risk genes, but had RNA editing sites in PTEN (chr10:87967417) and UBE2H (chr7:129830735). In patient TCGA-CC-A3MB-01, three sites of RNA editing occurred in the risk gene, TERT (chr5:1262789, chr5:1262852, chr5:1263350), and the same with patient TCGA-DD-AADV-01 (**Figure 2B**). In addition, we found that the percentage of the edited sites in the HCC risk genes is much higher in patients who lacked DNA mutation compared to patients with DNA mutation in the HCC risk gene regions ($p < 2.2e\text{-}16$, Wilcoxon test) (**Figure 2C**). Meanwhile, the mutation percentage is much lower in edited patients compared with non-edited patients in HCC risk gene regions ($p = 4.63e\text{-}16$, Wilcoxon test) (**Figure 2D**). The observations above implied that RNA editing was a risk factor to HCC as a complementary event for DNA mutation in HCC risk genes.

TABLE 2 | Several HCC-related RNA editing sites located on the same genes with the same editing patterns.

Gene	Frequency	HCC-related sites
MDM4	7	7 HCC gain
DHODH	7	7 HCC loss
JRK	6	6 HCC gain
GINS1	6	6 HCC gain
ALDH2	6	6 HCC loss
SPC24	5	5 HCC gain
SERPINF2	5	5 HCC gain
APC2	5	5 HCC gain
ZNF517	4	4 HCC gain
MOGAT2	4	4 HCC loss
MAVS	4	3 HCC gain; 1 HCC dys-edited
HINT1	4	3 HCC gain; 1 HCC dys-edited
ZNF814	3	3 HCC gain
TTC9C	3	2 HCC gain; 1 HCC dys-edited
TRIM56	3	2 HCC gain; 1 HCC dys-edited
RP5-1061H20.4	3	3 HCC gain
POLR1A	3	3 HCC gain
NPLOC4	3	3 HCC gain
MOGAT3	3	3 HCC gain
METTL7A	3	3 HCC gain
IPP	3	2 HCC gain; 1 HCC dys-edited
HAVCR2	3	3 HCC gain
HAMP	3	3 HCC loss
FADS2	3	3 HCC gain
DCAF16	3	3 HCC gain
ADAMTS13	3	3 HCC loss

This table showed genes related to at least three editing sites.

HCC-Related RNA Editing Prefer to Locate on Liver-Specific Genes

Chen et al. proved that RNA editing of AZIN1 promotes progression of HCC (16). In our study, by genome-wide identification of RNA editing sites across large RNA-seq samples, we aimed to reveal more HCC-related RNA editing sites. Generally, we identified 454 HCC-related RNA editing sites, including 264 HCC gain, 166 HCC loss, and 24 HCC dys-edited sites (**Figures 3A,B**, **Table 1**). Notably, a serine-to-glycine substitution at residue 367 of AZIN1 was also identified by our method, which is reported to be hyper-edited in HCC patients compared to normal samples in previous studies (16). Two editing sites of COX18 were hypo-edited in HCC compared with paired normal samples. The most significantly dys-edited RNA editing sites were editing on the ACOX1 (chr17: 75941513, $p = 1.15e\text{-}05$). Notably, ACOX1 was reported to play important roles in cancer development of HCC by stimulating hepatic fatty acid oxidation and H_2O_2 accumulation (37).

To further investigate the biological function of these HCC-related RNA editing sites, we performed functional enrichment analysis for these genes with the HCC-related RNA editing sites (hypergeometric test, adjust $p < 0.05$; **Supplementary Figure S2**, **Supplementary Table S2**). Our results indicated that HCC-related editing genes prefer to be liver-specific genes, which were involved in nuclear transport, catabolic and cell cycle processes. The enrichment of liver-specific genes and liver cancer-associated genes suggested that RNA editing can be a potential research area to analyze the mechanism, clinical prevention, and treatment of HCC patients.

HCC-Related Editing Sites Prefer to Locate on the Same Genes With the Same Editing Patterns

A large percent of HCC-related RNA editing sites were located on gene regions (88.99%, 404/454) especially for HCC gain and dys-edited sites. Interestingly, 73 genes were shared by at least two HCC-related RNA editing sites and accounted for 50% (202 editing sites of 404) (**Figure 4A**, **Supplementary Table S3**). Notably, we found that different editing sites located on the same genes tend to be with the same HCC editing type, with few exceptions (**Figure 4B**, **Table 2**). For example, there are seven HCC-related RNA editing sites located on MDM4; meanwhile, these seven sites are all HCC gain editing patterns. About 89.04% genes with different editing sites have the same editing patterns, which indicated that these editing sites may have important roles in HCC initiation and development.

The Functional Consequence of RNA Editing Sites

Previous studies have suggested that RNA editing can be functional and involved in carcinoma initiation and progression

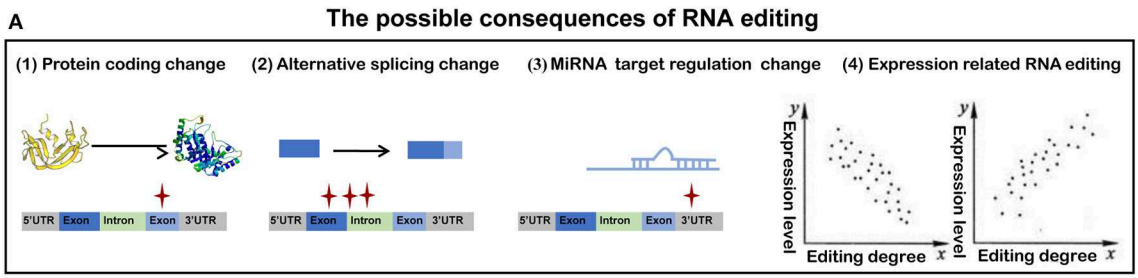

B

The number of RNA Editing sites with possible consequence

	CDS change	Splicing	MiRNA-target	Expression	Total
Total editing	554	30	1356	163	2086
HCC related	11	0	26	10	46

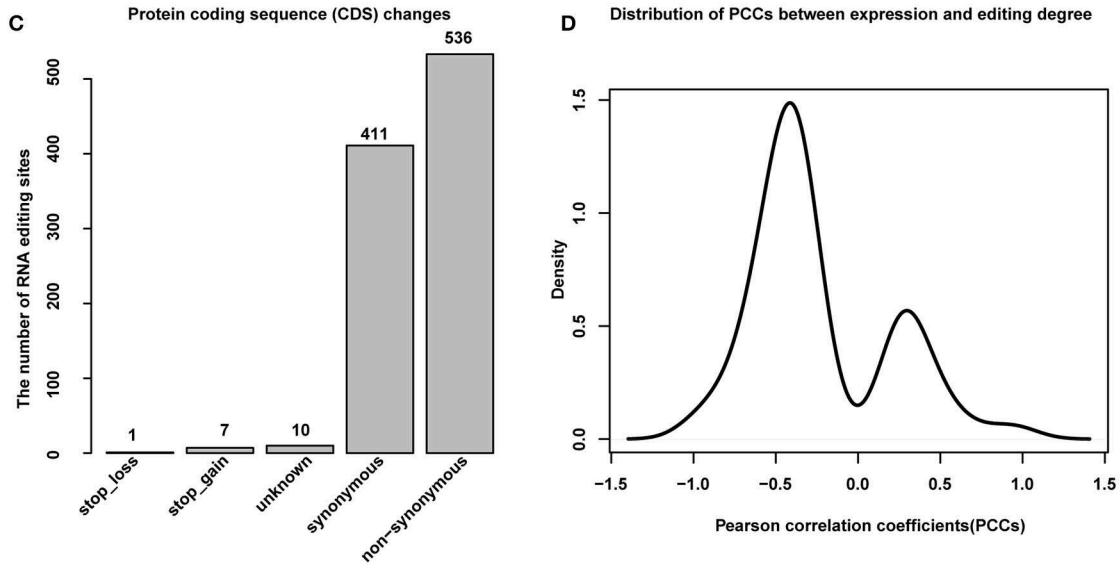

FIGURE 5 | Functional consequence analysis of RNA editing sites. **(A)** The possible functional consequence of RNA editing, including protein-coding sequence change, alternative splicing change, miRNA–target regulation change, and expression level change. **(B)** The number of RNA editing sites with possible consequence. **(C)** The number of RNA editing sites for protein-coding sequence changes. **(D)** The distribution of Pearson correlation coefficients (PCCs) between editing degrees and the expression of corresponding genes.

by influencing amino acid encoding, alternative splicing, miRNA–target regulation, or expression changing of the corresponding gene [(38, 39); **Figure 5A**]. Totally, we identified 2,064 editing sites with functional consequence, of which 46 were HCC-related (**Figure 5B**, **Supplementary Table S4**). For editing in coding sequence (CDS) regions, we identified 554 editing sites with functional change, including one stop loss, seven stop gain, 10 unknown, and 536 non-synonymous (**Figures 5B,C**), of which 11 editing sites were HCC related. Specifically, the serine-to-glycine substitution at residue 367 of AZIN1 was reported in a previous study; the editing may induce a conformational change and a cytoplasmic-to-nuclear translocation, which will result in tumor initiation and aggressive tumor progression (16). Another example is serine-to-threonine substitution at residue 1,768 of MUC6, which located in a proximate repeat region annotated in the Uniprot database (40). Importantly, abnormal expression of MUC6 was reported to be associated with many gastrointestinal cancers, such as HCC and cholangiocarcinoma (41). Hence, we supposed that several RNA editing located in important protein domains, which change the properties of the protein, might play roles in the progression of HCC. In terms of alternative splicing, 30 editing sites identified by ANNOVA can induce splicing change, of which no one was HCC related. As more than half of the RNA editing sites located on the 3′UTR regions, next, we considered miRNA–target regulation change caused by RNA editing in the 3′UTR regions. We use miRanda to calculate the binding energies between miRNA sequence and editing sequence (or reference sequence). We identified 1,356 editing sites that affect miRNA–target regulation, of which 26 were HCC related. Among these 26 HCC-related RNA editing sites, the top three affected miRNAs were miR-17-3p,

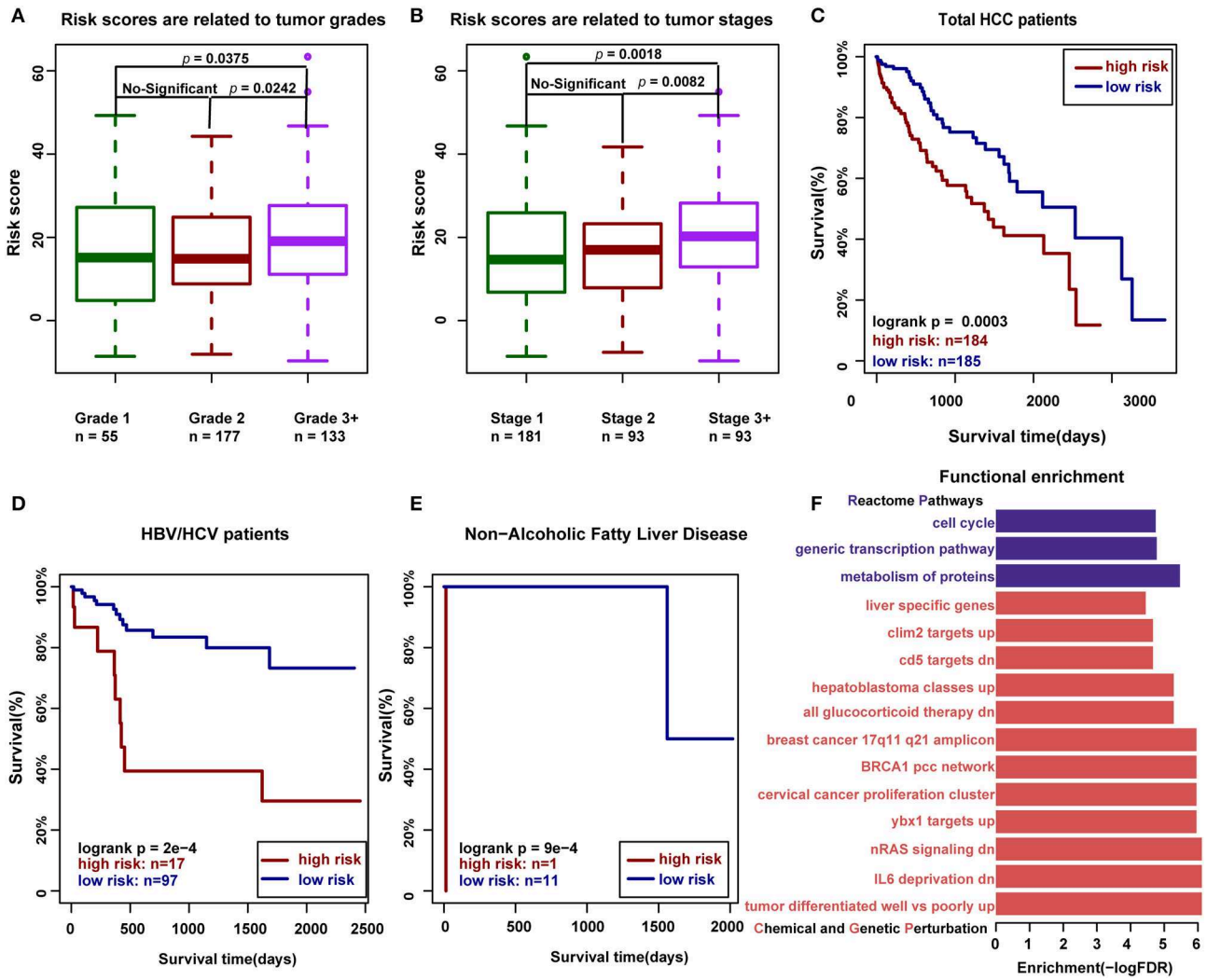

FIGURE 6 | The HCC-related RNA editing sites with functional consequence can predict clinical outcomes of HCC patients. **(A)** Risk scores measured by 46 HCC-related RNA editing sites with functional consequence are related to tumor grades in HCC patients (Wilcoxon rank-sum test). **(B)** Risk scores measured by 46 HCC-related RNA editing sites with functional consequence are related to tumor stages in HCC patients (Wilcoxon rank-sum test). **(C)** Risk scores measured by 46 HCC-related RNA editing sites with functional consequence can predict the prognosis in HCC patients. **(D)** Risk scores measured by three HCC-related prognostic editing sites with functional consequence can predict the prognosis in HBV-/HCV-infected HCC patients. **(E)** Risk scores measured by three HCC-related prognostic editing sites with functional consequence can predict the prognosis in HCC patients with non-alcoholic fatty liver disease. **(F)** Functional enrichment of 46 HCC-related RNA editing sites with consequence. The functional gene sets were downloaded from MsigDB, including Chemical and Genetic Perturbation in red and Reactome pathway in purple.

miR-20b-3p, and miR-593-3p (with 11, 7, and 7 target regulation changes induced by HCC-related editing sites, respectively (**Supplementary Table S5**). Notably, miR-17-3p, miR-20b-3p, and miR-593-3p are widely involved in caner initiation and progression, including HCC (42–46). We observed that the expression levels of 163 RNA editing sites were correlated with the editing degree of corresponding genes, of which 10 were HCC-related editing sites. Moreover, Pearson correlation coefficients (PCCs) tend to be negative values (**Figure 5D**), which indicated that most of the RNA editing sites might cause downexpression of the corresponding genes.

HCC-Related RNA Editing Sites With Functional Consequence Can Predict Clinical Prognosis

To further investigate the relationship between RNA editing and HCC clinical characteristics, we first defined the risk score for each clinical sample by integrating the expression levels and editing degrees of HCC-related RNA editing sites with functional consequence, weighted by 1 or −1 according to the regression coefficients from univariate Cox regression analysis (detailed in the Materials and Methods section). As expected, we found that the risk scores measured by 46 HCC-related RNA

TABLE 3 | The results of multivariate survival analysis of 46 HCC-related RNA editing sites with consequence.

	HR (95% CI)	*p*-Value
Risk score	1.03 (1.01, 1.04)	**0.010****
Gender		
Female	1 (reference)	
Male	0.90(0.55, 1.45)	0.652
Ages	1.00(1.00, 1.00)	**0.025***
BMI	1.03(1.00, 1.06)	0.097
Grades		
Grade G1	1 (reference)	
Grade G2	1.46 (0.65, 3.22)	0.369
Grade G3	1.74(0.75, 4.06)	0.196
Grade G4	4.91(1.47, 16.39)	**0.010***
Stages		
Stage T1	1 (reference)	
Stage T2	1.31 (0.71, 2.43)	0.385
Stage T3	1.70 (0.92, 3.13)	0.089
Stage T4	3.83 (1.45, 10.07)	**0.007****

*Values of p < 0.05 were bolded, of which *p < 0.05 and **p < 0.01.*

TABLE 4 | Three prognostic HCC-related RNA editing sites with functional consequence.

RNA editing	Gene types	Gene name	Editing type	Function
chr12; 111811793;A;G	Protein coding	ALDH2	HCC loss	miRNA–target
chr9;41929326; C;T	Protein coding	CNTNAP3B	HCC gain	CDS change
chr9;65675990; T;G	Protein coding	CBWD5	HCC loss	CDS change

editing sites with functional consequence correlated with tumor grades and stages in HCC patients, where higher risk scores in patients implicated higher tumor malignancy (higher tumor grades or tumor stages, Wilcoxon rank-sum test) (**Figures 6A,B**). We further classified all HCC patients into high-risk and low-risk groups using the median risk score as the cutoff point. Our analysis suggested that patients having higher risk scores were expected to have poor overall survival times (log-rank test, $p = 0.0003$; **Figure 6C**). The risk score was still significantly associated with patient overall survival (hazard ratio $= 1.03$, $p = 0.01$) in the Cox multivariate analysis, after adjusting for patients' gender, age, BMI, tumor grades, and stages (**Table 3**), which indicates that these HCC risk RNA editing sites could be potential biomarkers to predict clinical outcomes of HCC patients.

We next identified three prognostic-related editing sites whose editing degrees are significantly correlated with survival time using univariate Cox regression analysis ($p < 0.05$; **Table 4**). The median risk score using these three prognostic editing sites and matched genes can also significantly classify patients into separate groups with different clinical outcomes (log-rank test, $p = 0.03$, data not shown). After adjusting for patients' gender, age, BMI, tumor grades, and stages, the risk score still has predictive power (hazard ratio $= 1.19$, $p = 0.001$; **Table 5**). As HBV/HCV infection, alcoholic consumption, and non-alcoholic fatty liver diseases are the three main risk factors to HCC patients, we next examined the predictive power of these three editing sites with these risk factors. We found that these three prognostic-related editing sites can be used to predict the clinical outcomes for HBV-/HCV-infected and non-alcoholic fatty liver disease patients (log-rank *p*-values were 2e-4 and 9e-4, respectively) (**Figures 6D,E**), but not alcoholic consumption patients (data not shown).

TABLE 5 | The results of multivariate survival analysis of three prognostic HCC-related RNA editing sites with consequence.

	HR (95% CI)	*p*-Value
Risk score	1.19 (1.07, 1.32)	**0.001****
Gender		
Female	1 (reference)	
Male	0.84 (0.51, 1.38)	0.495
Ages	1.00 (1.00, 1.00)	**0.036***
BMI	1.04 (1.01, 1.07)	**0.009***
Grade		
Grade G1	1 (reference)	
Grade G2	1.42 (0.64, 3.15)	0.390
Grade G3	1.88(0.82, 4.28)	0.135
Grade G4	6.64 (2.03, 21.76)	**0.002****
Stage		
Stage T1	1 (reference)	
Stage T2	1.12 (0.60, 2.09)	0.719
Stage T3	1.59 (0.87, 2.91)	0.132
Stage T4	3.24 (1.20, 8.69)	**0.020***

*Values of p < 0.05 were bolded, of which *p < 0.05 and **p < 0.01.*

Furthermore, we dissected the function of these 46 HCC-related RNA editing sites with functional consequence. It is shown that they were widely involved in three reactome pathways: "metabolism of proteins," "generic transcription pathway," and "cell cycle" (**Figure 6F**, **Supplementary Table S6**). The functional enrichment analysis for chemical and genetic perturbation datasets indicated that they were enriched in tumor differentiation, nRAS signaling pathway, and liver cancer-associated genes.

DISCUSSION

HCC is a complex disease with poor prognosis and affected by multiple genetic alterations. DNA mutations are the most widely investigated driver events in all cancer types, including HCC. However, the mutation events are not presented in all HCC patients. Furthermore, we found that 98.51% mutation sites occurred in only a single HCC patient. Similar to the consequence of DNA mutation, RNA editing can also produce

nucleotide variations at the RNA level. Importantly, the RNA editing seems to be a more sophisticated regulation, as the editing degree can be 0–100%, while DNA mutation should be mutation or not (0 or 1). Here we systematically identified RNA editing sites by integrating DNA mutation and SNP datasets, and found that HCC samples have a significantly high percentage of RNA editing sites compared with normal samples. We also observed RNA editing in 35 cases that lacked DNA mutations in HCC risk genes, and more edited risk genes occurred in mutated patients compared with patients who do not have any DNA mutation in the HCC risk gene. Thus, we proposed that RNA editing may be a risk factor to HCC, as a complementary event for DNA mutation in HCC risk genes.

To further characterize the inferred RNA editing sites in our study, we compared the overlap of A-to-IRNA editing sites in gene regions identified by our study and the editing sites collected in the database of RADAR (**Supplementary Figure S3**). We found that most A-to-IRNA editing sites were in the RADAR database and accounts for 87.11% (9,565/10,981). Furthermore, we re-identified RNA editing sites in three human normal liver tissues and two HCC cell line samples, and found that 38.11% HCC-related RNA editing sites were edited in at least one sample (173/454), and 39.13% HCC-related editing sites with functional consequence were identified (18/46). These results indicated that RNA editing sites identified by our research were authentic, which can be used for further analysis. Next, HCC-related RNA editing sites were identified by comparing editing in HCC cancer samples and normal samples. Functional annotation showed that HCC-related editing sites prefer to be liver-specific genes, which suggested the important roles of RNA editing in the development of HCC.

Previous studies focused on the effect of ADAR enzymes on RNA editing. Here we addressed another important question on whether these editing sites have an effect on the downstream regulation system. By considering the influence of RNA editing on coding sequence change, alternative splicing, miRNA–target regulation, and expression change, we identified 2,064 editing sites with functional consequence, which accounts for 10.62% of the total RNA editing sites (2,064/19,431). This percentage indicates that RNA editing events may play other important roles, such as the alteration of RNA-binding abilities, which were induced by RNA structure change, which was, in turn, induced by editing. Notably, we found a number of editing sites with miRNA–target regulation changes. More were identified when we set lower thresholds (**Supplementary Table S7**). If we defined at least one miRNA relationship change by RNA editing, 90.81% editing sites in the 3′UTR regions can induce miRNA–target regulation change (7,651/8,425). Therefore, we should pay more attention to the effect of miRNA–target regulation change induced by RNA editing. Importantly, in regard to the tumor suppressive genes (TSGs) and the oncogenic genes (OGs) reported (28), we demonstrated that these functional HCC-related editing genes were significantly enriched in OGs, but not TSGs (data not shown), and it remains true when we set lower thresholds to identify editing sites with miRNA–target regulation changes (**Supplementary Table S7**).

Importantly, we found 46 HCC-related RNA editing sites with functional consequence that can be used to predict the clinical outcome in HCC patients. In addition, they have independent predictive power after considering the gender, age, BMI, tumor grades, and stages. We identified three clinical prognostic-related editing sites, which can also provide predictive values in HBV-/HCV-infected patients and non-alcoholic fatty liver disease patients, including editing sites in ALDH2 (chr12:111811793, A-to-I RNA editing), CNTNAP3B (chr9:41929326, C-to-T RNA editing), and CBWD5 (chr9:65675990, T-to-G RNA editing), of which ALDH2 is an HCC-related editing gene with high frequency (six HCC loss editing sites locates on the ALDH2 gene region). Interestingly, multiple studies revealed that ALDH2 is highly correlated with the pathogenic mechanism, risk, and survival of liver cancer patients, including HCC (47–50). Functional annotation suggested that these HCC-related editing sites with functional consequence are widely involved in liver cancer-associated genes, especially tumor suppressive genes, and cancer-associated pathways. Therefore, we assume that some RNA editing events may be "driver events" that promote cancer initiation and progression, as well as play a critical role in clinical survival in cancer patients.

DATA AVAILABILITY STATEMENT

The datasets analyzed in this study can be found in the database of Genotypes and Phenotypes (dbGaP) originated from The Cancer Genome Atlas (TCGA, https://portal.gdc.cancer.gov/) and ArrayExpress (https://www.ebi.ac.uk/arrayexpress/, E-MTAB-4052).

AUTHOR CONTRIBUTIONS

ZB and JL conceived the study. ZB and JC processed the sequencing data. LW and FW analyzed the data. JC wrote the manuscript.

FUNDING

This work was supported by the National Natural Science Foundation of China (Grant Nos. 31801114, 31471320, and 31671485), Natural Science Foundation of Anhui Province (Grant No. 1908085QC98), and the Fundamental Research Funds for the Central Universities (Grant No. PA2018GDQT0015).

SUPPLEMENTARY MATERIAL

The Supplementary Material for this article can be found online at: https://www.frontiersin.org/articles/10.3389/fonc.2020.00037/full#supplementary-material

REFERENCES

1. Torre LA, Bray F, Siegel RL, Ferlay J, Lortet-Tieulent J, Jemal A. Global cancer statistics, 2012. *CA Cancer J Clin*. (2015) 65:87–108. doi: 10.3322/caac.21262
2. Huang J, Deng Q, Wang Q, Li KY, Dai JH, Li N, et al. Exome sequencing of hepatitis B virus-associated hepatocellular carcinoma. *Nat Genet*. (2012) 44:1117–21. doi: 10.1038/ng.2391
3. Peng X, Xu X, Wang Y, Hawke DH, Yu S, Han L, et al. A-to-I RNA editing contributes to proteomic diversity in cancer. *Cancer Cell*. (2018) 33:817–28.e7. doi: 10.1016/j.ccell.2018.03.026
4. Nishikura K. Functions and regulation of RNA editing by ADAR deaminases. *Annu Rev Biochem*. (2010) 79:321–49. doi: 10.1146/annurev-biochem-060208-105251
5. Hwang T, Park CK, Leung AKL, Gao Y, Hyde TM, Kleinman JE, et al. Dynamic regulation of RNA editing in human brain development and disease. *Nat Neurosci*. (2016) 19:1093–9. doi: 10.1038/nn.4337
6. Peng Z, Cheng Y, Tan BCM, Kang L, Tian Z, Zhu Y, et al. Comprehensive analysis of RNA-Seq data reveals extensive RNA editing in a human transcriptome. *Nat Biotechnol*. (2012) 30:253–60. doi: 10.1038/nbt.2122
7. Yu Y, Zhou H, Kong Y, Pan B, Chen L, Wang H, et al. The landscape of A-to-I RNA editome is shaped by both positive and purifying selection. *PLoS Genet*. (2016) 12:e1006191. doi: 10.1371/journal.pgen.1006191
8. Han S-W, Kim H-P, Shin J-Y, Jeong E-G, Lee W-C, Kim KY, et al. RNA editing in RHOQ promotes invasion potential in colorectal cancer. *J Exp Med*. (2014) 211:613–21. doi: 10.1084/jem.20132209
9. Fu L, Qin Y-R, Ming X-Y, Zuo X-B, Diao Y-W, Zhang L-Y, et al. RNA editing of SLC22A3 drives early tumor invasion and metastasis in familial esophageal cancer. *Proc Natl Acad Sci USA*. (2017) 114:E4631–40. doi: 10.1073/pnas.1703178114
10. Pan Q, Shai O, Lee LJ, Frey BJ, Blencowe BJ. Deep surveying of alternative splicing complexity in the human transcriptome by high-throughput sequencing. *Nat Genet*. (2008) 40:1413–5. doi: 10.1038/ng.259
11. Li S, Zhang J, Huang S, He X. Genome-wide analysis reveals that exon methylation facilitates its selective usage in the human transcriptome. *Brief Bioinform*. (2018) 19:754–64. doi: 10.1093/bib/bbx019
12. Li S, Hu Z, Zhao Y, Huang S, He X. Transcriptome-wide analysis reveals the landscape of aberrant alternative splicing events in liver cancer. *Hepatology*. (2019) 69:359–75. doi: 10.1002/hep.30158
13. Beghini A, Ripamonti CB, Peterlongo P, Roversi G, Cairoli R, Morra E, et al. RNA hyperediting and alternative splicing of hematopoietic cell phosphatase (PTPN6) gene in acute myeloid leukemia. *Hum Mol Genet*. (2000) 9:2297–304. doi: 10.1093/oxfordjournals.hmg.a018921
14. Hundley HA, Bass BL. ADAR editing in double-stranded UTRs and other noncoding RNA sequences. *Trends Biochem Sci*. (2010) 35:377–83. doi: 10.1016/j.tibs.2010.02.008
15. Gong J, Wu Y, Zhang X, Liao Y, Sibanda VL, Liu W, et al. Comprehensive analysis of human small RNA sequencing data provides insights into expression profiles and miRNA editing. *RNA Biol*. (2014) 11:1375–85. doi: 10.1080/15476286.2014.996465
16. Chen L, Li Y, Lin CH, Chan THM, Chow RKK, Song Y, et al. Recoding RNA editing of AZIN1 predisposes to hepatocellular carcinoma. *Nat Med*. (2013) 19:209–216. doi: 10.1038/nm.3043
17. Chan THM, Lin CH, Qi L, Fei J, Li Y, Yong KJ, et al. A disrupted RNA editing balance mediated by ADARs (Adenosine DeAminases that act on RNA) in human hepatocellular carcinoma. *Gut*. (2014) 63:832–43. doi: 10.1136/gutjnl-2012-304037
18. Hu X, Wan S, Ou Y, Zhou B, Zhu J, Yi X, et al. RNA over-editing of BLCAP contributes to hepatocarcinogenesis identified by whole-genome and transcriptome sequencing. *Cancer Lett*. (2015) 357:510–9. doi: 10.1016/j.canlet.2014.12.006
19. Kang L, Liu X, Gong Z, Zheng H, Wang J, Li Y, et al. Genome-wide identification of RNA editing in hepatocellular carcinoma. *Genomics*. (2015) 105:76–82. doi: 10.1016/j.ygeno.2014.11.005
20. Han L, Diao L, Yu S, Xu X, Li J, Zhang R, et al. The genomic landscape and clinical relevance of A-to-I RNA editing in human cancers. *Cancer Cell*. (2015) 28:515–28. doi: 10.1016/j.ccell.2015.08.013
21. Paz-Yaacov N, Bazak L, Buchumenski I, Porath HT, Danan-Gotthold M, Knisbacher BA, et al. Elevated RNA editing activity is a major contributor to transcriptomic diversity in tumors. *Cell Rep*. (2015) 13:267–76. doi: 10.1016/j.celrep.2015.08.080
22. Chang K, Creighton C, Davis C, Donehower L, Drummond J, Wheeler D, et al. The Cancer Genome Atlas Pan-Cancer analysis project. *Nat Genet*. (2013) 45:1113–20. doi: 10.1038/ng.2764
23. Rudolph KLM, Schmitt BM, Villar D, White RJ, Marioni JC, Kutter C, et al. Codon-driven translational efficiency is stable across diverse mammalian cell states. *PLoS Genet*. (2016) 12:e1006024. doi: 10.1371/journal.pgen.1006024
24. Sherry ST. dbSNP: the NCBI database of genetic variation. *Nucleic Acids Res*. (2001) 29:308–11. doi: 10.1093/nar/29.1.308
25. Altshuler DM, Durbin RM, Abecasis GR, Bentley DR, Chakravarti A, Clark AG, et al. An integrated map of genetic variation from 1,092 human genomes. *Nature*. (2012) 491:56–65. doi: 10.1038/nature11632
26. Rosenbloom KR, Armstrong J, Barber GP, Casper J, Clawson H, Diekhans M, et al. The UCSC genome browser database: 2015 update. *Nucleic Acids Res*. (2015) 43:D670–81. doi: 10.1093/nar/gku1177
27. Liberzon A. A description of the molecular signatures database (MSigDB) web site. *Methods Mol Biol*. (2014) 1150:153–60. doi: 10.1007/978-1-4939-0512-6
28. Hamilton MP, Rajapakshe K, Hartig SM, Reva B, McLellan MD, Kandoth C, et al. Identification of a pan-cancer oncogenic microRNA superfamily anchored by a central core seed motif. *Nat Commun*. (2013) 4:2730. doi: 10.1038/ncomms3730
29. Quinlan AR, Hall IM. BEDTools: a flexible suite of utilities for comparing genomic features. *Bioinformatics*. (2010) 26:841–2. doi: 10.1093/bioinformatics/btq033
30. Dobin A, Davis CA, Schlesinger F, Drenkow J, Zaleski C, Jha S, et al. STAR: Ultrafast universal RNA-seq aligner. *Bioinformatics*. (2013) 29:15–21. doi: 10.1093/bioinformatics/bts635
31. Van der Auwera GA, Carneiro MO, Hartl C, Poplin R, del Angel G, Levy-Moonshine A, et al. From fastQ data to high-confidence variant calls: the genome analysis toolkit best practices pipeline. *Curr Protoc Bioinformatics*. (2013) 43:11.10.1–11.10.33. doi: 10.1002/0471250953.bi1110s43
32. Wang K, Li M, Hakonarson H. ANNOVAR: Functional annotation of genetic variants from high-throughput sequencing data. *Nucleic Acids Res*. (2010) 38:1–7. doi: 10.1093/nar/gkq603
33. Enright AJ, John B, Gaul U, Tuschl T, Sander C, Marks DS. MicroRNA targets in Drosophila. *Genome Biol*. (2003) 5:R1. doi: 10.1186/gb-2003-5-1-r1
34. Griffiths-Jones S, Saini HK, Van Dongen S, Enright AJ. miRBase: tools for microRNA genomics. *Nucleic Acids Res*. (2008) 36:154–8. doi: 10.1093/nar/gkm952
35. Love MI, Huber W, Anders S. Moderated estimation of fold change and dispersion for RNA-seq data with DESeq2. *Genome Biol*. (2014) 15:550. doi: 10.1186/s13059-014-0550-8
36. Zender L, Villanueva A, Tovar V, Sia D, Chiang DY, Llovet JM. Cancer gene discovery in hepatocellular carcinoma. *J Hepatol*. (2010) 52:921–9. doi: 10.1016/j.jhep.2009.12.034
37. Yeldandi AV, Rao MS, Reddy JK. Hydrogen peroxide generation in peroxisome proliferator-induced oncogenesis. *Mutat Res*. (2000) 448:159–177. doi: 10.1016/S0027-5107(99)00234-1
38. Xu X, Wang Y, Liang H. The role of A-to-I RNA editing in cancer development. *Curr Opin Genet Dev*. (2018) 48:51–6. doi: 10.1016/j.gde.2017.10.009
39. Qi L, Chan THM, Tenen DG, Chen L. RNA editome imbalance in hepatocellular carcinoma. *Cancer Res*. (2014) 74:1301–6. doi: 10.1158/0008-5472.CAN-13-3485
40. Bateman A, Martin MJ, O'Donovan C, Magrane M, Apweiler R, Alpi E, et al. UniProt: a hub for protein information. *Nucleic Acids Res*. (2015) 43:D204–12. doi: 10.1093/nar/gku989
41. Kasprzak A, Adamek A. Mucins: the old, the new and the promising factors in hepatobiliary carcinogenesis. *Int J Mol Sci*. (2019) 20:1288. doi: 10.3390/ijms20061288
42. Awan FM, Naz A, Obaid A, Ikram A, Ali A, Ahmad J, et al. MicroRNA pharmacogenomics based integrated model of miR-17-92 cluster in sorafenib resistant HCC cells reveals a strategy to forestall drug resistance. *Sci Rep*. (2017) 7:11448. doi: 10.1038/s41598-017-11943-1
43. Shan SW, Fang L, Shatseva T, Rutnam ZJ, Yang X, Du WW, et al. Mature miR-17-5p and passenger miR-17-3p induce hepatocellular carcinoma by targeting

PTEN, GalNT7 and vimentin in different signal pathways. *J Cell Sci*. (2013) 126:1517–30. doi: 10.1242/jcs.122895
44. Guo J, Xiao Z, Yu X, Cao R. miR-20b promotes cellular proliferation and migration by directly regulating phosphatase and tensin homolog in prostate cancer. *Oncol Lett*. (2017) 14:6895–900. doi: 10.3892/ol.2017.7041
45. Luo Y, He J, Tao X, Wang H, Fang Q, Guo S, et al. miR-20b negatively regulates VEGF expression by targeting STAT3 in H22 hepatocellular carcinoma cells. *Oncol Rep*. (2018) 40:2806–13. doi: 10.3892/or.2018.6651
46. Dong L, Hong H, Chen X, Huang Z, Wu W, Wu F. LINC02163 regulates growth and epithelial-to-mesenchymal transition phenotype via miR-593-3p/FOXK1 axis in gastric cancer cells. *Artif Cells Nanomed Biotechnol*. (2018) 46:607–15. doi: 10.1080/21691401.2018.1464462
47. Matsumoto A, Thompson DC, Chen Y, Kitagawa K, Vasiliou V. Roles of defective ALDH2 polymorphism on liver protection and cancer development. *Environ Health Prev Med*. (2016) 21:395–402. doi: 10.1007/s12199-016-0579-2
48. Hou G, Chen L, Liu G, Li L, Yang Y, Yan H-X, et al. Aldehyde dehydrogenase-2 (ALDH2) opposes HCC progression by regulating AMPK signaling. *Hepatology*. (2016) 65:1628–44. doi: 10.1002/hep.29006
49. Chen X, Legrand AJ, Cunniffe S, Hume S, Poletto M, Vaz B, et al. Interplay between base excision repair protein XRCC1 and ALDH2 predicts overall survival in lung and liver cancer patients. *Cell Oncol*. (2018) 41:527–39. doi: 10.1007/s13402-018-0390-8
50. Shih S, Huang YT, Yang HI. A multiple mediator analysis approach to quantify the effects of the ADH1B and ALDH2 genes on hepatocellular carcinoma risk. *Genet Epidemiol*. (2018) 42:394–404. doi: 10.1002/gepi.22120

Conflict of Interest: The authors declare that the research was conducted in the absence of any commercial or financial relationships that could be construed as a potential conflict of interest.

frontiers in Oncology

HYPOTHESIS AND THEORY
published: 15 April 2020
doi: 10.3389/fonc.2020.00541

Cell Reversal From a Differentiated to a Stem-Like State at Cancer Initiation

*João Carvalho**

CFisUC, Department of Physics, University of Coimbra, Coimbra, Portugal

Even if the Somatic Mutation Theory of carcinogenesis explains many of the relevant experimental results in tumor origin and development, there are frequent events that are not justified, or are even contradictory to this widely accepted theory. A Cell Reversal Theory is presented, putting forward the hypothesis that cancer is originated by reversal of a differentiated cell into a non-differentiated stem-like state, by a change of its intrinsic epigenetic state, following a perturbation on the cell and/or its microenvironment. In the current proposal a cluster of cancer stem cells can be established, without the strict control mechanisms of a normal stem cell niche, and initiate a tumor. It is proposed that a reversal to a pluripotent state is at tumor origin and not tumor progress that prompts cell dedifferentiation. The uncontrolled proliferation of cancer stem cells causes a microenvironment disorganization, resulting in stressful conditions, like hypoxia and nutrient deprivation, which induces the genetic instability characteristic of a tumor; thus, in most cases, mutations are a consequence and not the direct cause of a tumor. It is also proposed that metastases result from dedifferentiation signaling dispersion instead of cell migration. However, conceivably, once the microenvironment is normalized, the stem cell-like state can differentiate back to a mature cell state and loose its oncogenic capacity. Therefore, this can be a reversible condition, suggesting important therapeutic opportunities.

Keywords: carcinogenesis, epigenetics, cancer stem cells, dedifferentiation, reprogramming, cancer

OPEN ACCESS

Edited by:
Hailong Pei,
Soochow University, China

Reviewed by:
Francesco De Francesco,
Azienda Ospedaliero Universitaria Ospedali Riuniti, Italy
Gabriele Multhoff,
Technical University of Munich, Germany

***Correspondence:**
João Carvalho
jcarlos@uc.pt

Specialty section:
This article was submitted to Molecular and Cellular Oncology, a section of the journal Frontiers in Oncology

Received: *04 February 2020*
Accepted: *25 March 2020*
Published: *15 April 2020*

Citation:
Carvalho J (2020) Cell Reversal From a Differentiated to a Stem-Like State at Cancer Initiation. Front. Oncol. 10:541. doi: 10.3389/fonc.2020.00541

INTRODUCTION

The Somatic Mutation Theory (SMT) of carcinogenesis (1) explains cancer origin by an accumulation of genetic mutations on tumor suppressor genes and on oncogenes that are transmitted to its lineage. It follows that the hallmarks of cancer (2) derive from successive mutations producing advantageous biological capabilities, in a multistep process of tumor development. This widely accepted theory explains many cancer features, from hereditary cancers to successful therapies targeting the product of mutant genes (1). But there are also many important events that are contradictory to its predictions and some *ad-hoc* modifications must be introduced to explain them, leading to serious inconsistencies. There are many reports of zero mutations found in some tumors (3), whereas malignant properties are a result of changes in the DNA methylation pattern and not in its sequence (1). Additionally, there are a few non-genotoxic carcinogens, like chloroform and p-dichlorobenzene (4), which induce cancer without direct modifications to DNA. There are experiments where mutated genes are introduced into animals' cells and lead to cancer onset (5, 6), but this outcome can be due to the procedure burden, causing a transition of the cell from a "normal" to an "abnormal" epigenetic state.

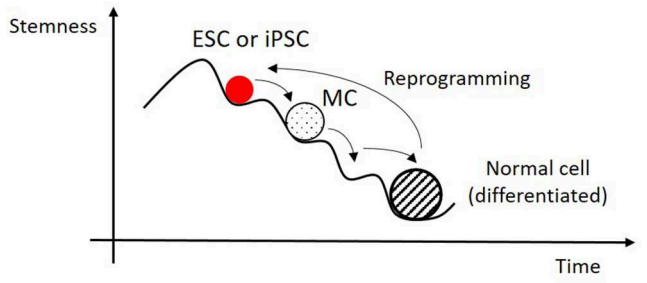

FIGURE 1 | In a highly simplified projection of a very complex epigenetic landscape, an embryonic stem cell (ESC) or an induced pluripotent stem cell (iPSC) can differentiate by successive steps between locally stable states until it reaches a fully differentiated mature state. Time reversal from this state to a pluripotent one is possible, in special conditions, by cell reprogramming. This can take place in a single or a multistep course, which can include Multipotent Cell (MC) states.

Cell genes on DNA can be considered as a large collection of software routines, each one of them with instructions to produce a particular protein. All cells have the same collection of these routines, and they are almost the same in every human being. But, according to its tissue of origin, cells shape, behavior and fate are very different and can change considerably during development. The particular cell epigenetic state (7) is fundamental as it defines the correct course to run the program in that particular circumstances, defining the number and order of calls of different genes, and thus their transcription and protein production rates. This is executed in such a way that the cell survives and performs its duty in the appropriate fashion for the human being continuity and development. Each particular differentiated cell type corresponds to a distinct epigenetic state, specified by, for instance, DNA methylation and histone modification (8, 9), which depends on the tissue where it is placed (its microenvironment) and the development stage of the individual (the particular moment in its maturation history).

A viable cell is then a point of stability on the epigenetic (very large) n-dimensional landscape of possible gene transcription rates and active signaling pathways (see **Figure 1**). It is in one of a multitude of possible phenotypes, where it can be, for instance, a muscle, a bone or an endothelial cell. All of them have the same genetic code, inherited from the same zygote cell, but they have very different gene expression patterns. These epigenetic states are time and location specific, and their modification defines a new state which can be or not stable. If it is not on a viable program the cell will die and not reproduce.

In an adult, stem cells are present in niches, which are regions on a tissue with a very specific microenvironment. These cells interact with each other and with the surrounding more differentiated cells in order to renew cell population, in a highly controlled fashion, by proliferation and differentiation (10).

Cell Reversal Theory: Stem-Like Cells Due to Epigenetic Reversal of Mature Cells at Tumor Origin

A hypothesis for carcinogenesis, the Cell Reversal Theory (CRT), states that due to a perturbation (a potential carcinogenic event) on the cell and/or on its environment, the cell does a transition to a different epigenetic state which, due to the absence of adequate control mechanisms at its current time/place, can lead, in special circumstances, to abnormal proliferation. A cell can enter on the wrong epigenetic program, according to its environment and stage of development, and become what is labeled as a cancer stem cell. It is thus suggested that excessive proliferation rate is due to the absence of the right control mechanisms from the environment that would constrain its behavior and not (only) a result of genetic mutations, as assumed by SMT. Initial under or overexpression of particular genes is then, in many tumors, due to epigenetic factors and not to genetic mutations. Reversal of a differentiated cell into a stem cell-like status, in an environment very different from the stem cell niche, tightly regulated by genetic and epigenetic factors (11), can lead to a chaotic and uncontrolled proliferation. In a multitude of possible cell epigenetic states, only a very small fraction is viable and has survival advantages. So it should be much more probable, and efficient, for a cancer cell to run a program that was evolutionarily selected and optimized, the stem cell or pluripotent program, than by the successive acquisition of all the right characteristics and capacities for enhanced proliferation, cell-death resistance and invasion.

In an earlier stage of organism development (12), as embryonic stem cells (ESC), or later as induced-pluripotent stem cells (iPSC), cells present a higher proliferation rate than at a mature state. In the event of a later cell reversal to one of these states, the cell doesn't receive the right chemical and mechanical signals from the microenvironment in which it is situated to control its development, and this can result in an uncontrollable multiplication. This is one of the risks found on reprogramming techniques being developed for regenerative medicine: iPSC, and also ESC, show a high carcinogenic capacity and must switch to a differentiated state before transplantation into the new tissue (13) (see **Figure 2**). Human embryonic stem (hES) cells conduce to teratoma formation, probably due to expression of survivin upon differentiation (14). However, a cell doesn't need to go all the way to the ESC or iPSC state, can make a transition to an intermediate multipotent state with increased capability of proliferation.

This hypothesis is different from the atavism theory (15), which proposes a cell de-evolution into a more primitive form of life. A cell running the "wrong" epigenetic program for its place/time would, in most of the cases, die, as its state is not adequate for survival in these particular conditions. But, in some special circumstances, could survive and thrive, being at the origin of a tumor. The present proposal is also different from the Tissue Organization Field Theory (TOFT) (16) in the sense that no special morphostat substance is necessary to exist and to be perturbed in order to initiate a tumor. But, as in TOFT, carcinogenesis can also have origin on a perturbation of the tissue environment, leading to a transition between epigenetic states, from normal to pluripotent. The review article by Friedmann-Morvinski and Verma (17) presents a theory with similarities to CRT for the origin of Cancer Stem Cells (CSC) but proposes them as a consequence of tumor progression and not at its origin. They point to the correspondence between the mechanisms of cells reprogramming into a pluripotent state and the dedifferentiation of tumor cells to CSC by epigenetic resetting. There are several

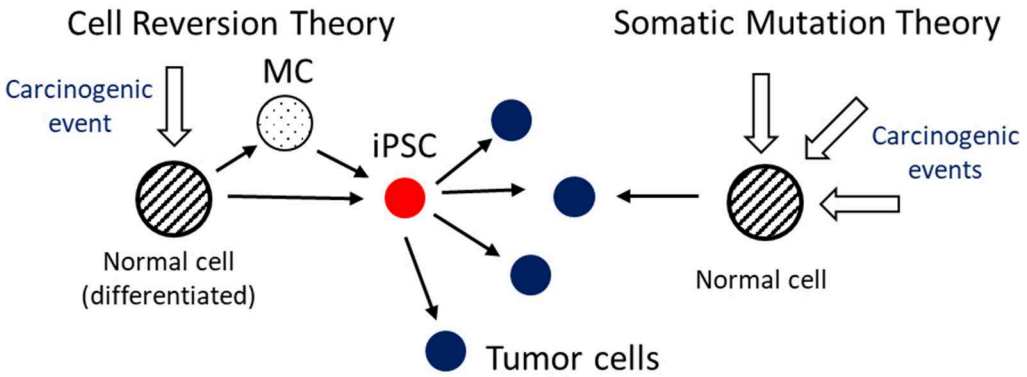

FIGURE 2 | In the Cell Reversion Theory a normal (differentiated) cell can complete a transition to an induced pluripotent stem cell (iPSC) state, of more stem cell like nature, in one or more steps [eventually passing through Multipotent Cell (MC) states], due to a perturbation (e.g., chemical or mechanical) to its conditions and/or its environment equilibrium. The iPSC can proliferate, and differentiate, in an unrestrained way generating a stressful cell environment, like hypoxia, a mutagenic condition. This cell, according to the presented hypothesis, can be at tumor origin. In the Somatic Mutation Theory successive mutations by carcinogenic events lead to the tumor phenotype.

theories about the origin of CSC, reviewed in Nimmakayalaa et al. (18), including cell fusion, horizontal gene transfer, mutations, metabolic reprogramming and dedifferentiation of non-CSC into CSC (in response to stress, wounding or hypoxia, as the hypothesis proposed here). CSC are an intensely researched subject, their existence being gradually accepted for many cancers. Some good reviews on the topic [as (19, 20)] examine and discuss the different hypothesis associated with the acquisition of stemness and tumor heterogeneity, including the effect of epigenetics, microenvironment and mutations.

It was shown that genes used on cells' reprogramming, like the Oct3/4, Sox2, Klf4 and c-Myc (the OSKM cocktail) (21), are also linked to tumors. As shown in Vaux (1), some experiments use oncogenes to activate iPSC; ESC genes and networks, like Oct3/4, SOX2 and Nanog, are activated on cancer initiation and progress (18). This can be interpreted as an association between cells pluripotency, after their regression to a more stem-cell like state, and carcinogenesis (12). Stem and cancer cells' phenotypes share some similarities, the two being in a proliferative state, are invasive and can be considered potentially immortal (22). Also they both show self-renewal capability and block differentiation (22); they are primitive and undifferentiated (1, 23). Our hypothesis is then that carcinogenesis can be due to resurrection of an early stem cell-like behavior, with expression of stem cell transcription factors, in an inappropriate location and time (22).

Probably some cancer cells maintain their stemness competence (24) and these can move into another place and start a new tumoral colony (a metastasis). Or, as a new hypothesis, which seems much simpler and probable, metastases are due to dedifferentiation signaling dispersal and not a result of cell migration. If the epigenetic state changing molecules reach a tissue with susceptibility for cell dedifferentiation, due to stress or some perturbation event on its microenvironment, it is possible to reproduce the transition event to CSC, triggering a tumoral initiation event at a different place.

In the mobilization therapy for bone marrow transplantation (25), stem cell like pluripotent cells are forced into the blood stream from the bone marrow of healthy human donors before being transplanted into a patient. According to the CRT hypothesis this could introduce an increased risk of cancer development, which was not found (26). Possible explanations are the difficulty of stem cells to extravasate the capillary vessels in their relatively short circulation time, or the just proposed hypothesis that dedifferentiation signaling diffusion is involved in metastasis and not cell migration as it is usually considered.

Relevance of the Microenvironment Perturbation for State Transition

The cause of epigenetic program change can be a perturbation to the cell and/or to its environment, a carcinogenic event, which disturbs the equilibrium conditions beyond what the cell can recover from, and eventually moves it toward another stable and viable point on the epigenetic landscape [for instance, by methylation/demethylation processes, (8)]. The stress event (for instance, caused by exposure to a chemical or to radiation) can overwhelm the cell control and feedback systems and make the cell change its epigenetic program as it tries to respond to the disruptive incident. As it endeavors to adapt and survive in new conditions, it can revert its differentiation status. The disorganized microenvironment then becomes a cradle of cells on different differentiation stages and epigenetic states, including pluripotent CSC.

In this scenario, tumoral genetic mutations are, in most cases, a cancer symptom and not its cause, as it was shown in many clinical examples (27). The genetic instability accompanying the excessive cell proliferation and the epigenetic changes (8) can be, at least partially, at the origin of the high mutation rate found in tumors. The uncontrolled cell number expansion results in a hostile microenvironment (hypoxia, nutrient depletion, low pH) that induces mutagenesis, DNA damage and impairment of DNA repair (28, 29). This is shown by the indication that tumors are, in many cases, not a clonal grouping of cells but

polyclonal, due to this genome mutability (8), and, in general, tumor tissue exhibits large heterogeneity on its differentiation status. Even hereditary cancers show some paradoxical behaviors, where, for instance, Xeroderma pigmentosum patients (30), a genetic disease characterized by defects on the DNA repair mechanisms in all cells, show a high rate of skin cancer but not of other cancers, as would be expected. In another example, mutated genes inserted into animals can lead to cancer, but in some cases driver (cancer originator) mutations are not present in the resulting tumor (5, 31). In CRT hereditary cancers can be explained by transmitted variability that make cells more prone to transition to the undifferentiated state at tumor origin. It also explains why cancer is more probable in old age as abnormal cell methylation can be an ordinary result of aging (32), which can make them more susceptible to epigenetic transition (this can be due to an impairment on the activation of genes involved in cell differentiation) (32). There are clear evidences that overweight and obesity are linked to an increased risk of some types of cancer. This outcome can be explained by cellular environment disorganization due to metabolic and inflammatory modifications in adipose tissue, which disrupts homeostasis (33) and promotes epigenetic transition.

In transplantation experiments (34) it was shown that exposure of tissue stroma to a carcinogen (N-nitrosomethylurea) is at the origin of a tumor in the epithelial layer, when placed in contact with the treated stroma, independently of the epithelial cells being or not exposed to the carcinogen. The same procedure applied on the epithelial layer would not lead to a tumor if the stroma was not also treated with the carcinogen. This result can be interpreted by a disturbance of the normal signaling and/or cell state equilibrium from the exposure of stroma to the chemical substance, stimulating the production of an epigenetic state changing molecular cocktail, which induces the transition to pluripotency. It was also found that, in some cases, transplant of tumor cells into a normal tissue leads to their reversion to normal state, which can be explained by their differentiation on the new environment.

The hypothesis that the acquisition of stem-like capabilities by differentiated cell reprogramming, induced by a cell and/or tissue perturbation, can lead to its tumorigenic behavior, including induction of genomic instability and consequent mutations from microenvironment adverse conditions, can then interpret contradictory findings not explained, in a straightforward way, by SMT. Other hypothesis doesn't seem reasonable, where the stem cell like capability is a consequence of tumor progress (17) and CSC origin from cancer cells and not directly from normal mature cells.

Some relevant experimental results discussed in this work favor the CRT model of carcinogenesis, as it justifies many of the results contradictory to SMT predictions while giving a plausible explanation to tumor origin. But, much probably, one or the other tumorigenic events are present in different cancers, and may even cooperate in some circumstances. For instance, this can happen when a cell mutation occurs that leads to a deregulation of its epigenetic control mechanisms and this promotes its transition to a stem-like state. Or the other way around, when the perturbation of the tissue microenvironment created by the uncontrolled stem cell proliferation produces the right conditions for the genetic instability common in tumors. Then, from the initial stem cell properties it can evolve into the mutated and differentiated states present in a tumor.

Proposed Tests of the Carcinogenesis Hypothesis

Several tests can be performed, in different tissues, to assess the current hypothesis, in particular for solid tumors. A particular effort should be placed in the search for stem cell markers in the initial tumor stages, originated by mutagenic and non-mutagenic processes. The evolution of these markers, as the tumor grows in diverse organs and for specific cancer types, would produce relevant evidence for this hypothesis examination. Stress experiments, from hypoxia events to introduction of foreign bodies and cells on a tissue, or addition of external chemical substances, can be used to prove the CRT hypothesis, which doesn't involve mutagenic episodes at the tumor origin. The work by Nakada et al. (35) describes the regeneration of cardiomyocytes by a special procedure involving deep hypoxia. These results can be interpreted as resulting from hypoxia stress inducing a transition of some cardiomyocytes to a stem cell like state, recovering the lost neonatal myocardium regenerating capacity. Similar experiments can be conceived to test for epigenetic transitions by stress events contributing to tumor initiation. It was shown that tumor cells with mutated or down-regulated BRCA1, a multifunctional protein involved in epigenetic control and DNA repair, present an increased expression of CSC-associated markers CD44 and ALDH1A (11). It was found (11) that down-regulation (reconstitution) of BRCA1 resulted in significant increase (decrease) of CSC-like populations in breast cancer. This seems to confirm that genes involved in cancer are also associated with cell reprogramming, and other cancer related genes can be tested for analogous results. Another possible experiment to prove the hypothesis is to test the effect of transplant of stem cells into an adult animal and to check if these cells, when introduced at the wrong time of animal development, can be at the origin of a tumor. This was already proven to occur with iPSC and ESC (13, 36) but the different steps of tumorigenic progress can be more precisely characterized, in particular the transition and/or evolution of the cell epigenetic program. Progression on the level of tumor stemness (37) can also be evaluated to check how the cell differentiation state changes with tumor expansion. Recent stemness measurements (37), applying a machine learning approach to define different indices (involving, for instance, mRNA expression, histone markers and DNA methylation), have shown that stemness is lower in normal cells, larger in primary tumors and highest in metastasis. These results can be related to cell reprogramming into a pluripotent state (with stem cell-like properties), in a dedifferentiation process, as being at the tumor origin, followed by successive divisions and cells gradual differentiation. Stemness is then lower at an earlier primary tumor than at a later onset metastasis.

CONCLUSIONS AND OUTLOOK

If this hypothesis is proved right, a potential therapeutic approach is to pursue the normalization of the tumor environment, according to tissue type, and force cells back to the right epigenetic program. This can be achieved by inducing their differentiation, corresponding to the normal state at that particular development stage and location. There are reported cases of tumors' remission by inhibition of enzymes (5, 38), the ones specifically activated by the mutated genes. This result can also be explained by a transition of cells back to a differentiated state through a change on the biochemical environment and/or on the active signaling pathways. Several examples of spontaneous regression of tumors were reported (5, 39), where tumor cells revert to normal tissue. Tissue normalization implies an adequate supply of oxygen, with the presence of a suitable vasculature network and blood flow, and access to nutrients and the requisite chemical signals. Probably the addition of a specific cocktail of transcription factors will be needed to prompt a state transition to normalcy, or by tuning the level of epigenetic regulating enzymes. A possible approach to cancer remission would then involve differentiation therapies (37). This procedure will not eliminate cells that already suffered mutations but eventually can differentiate the CSC and thus eliminate this particular niche, which is a probable cause of cancer relapse and metastases. This therapy can also be used to prevent cancer and/or to decrease cancer risk. A recent paper (40) reviews possible therapeutic strategies against CSC. Induced differentiation therapies are being considered and a treatment with retinoid acid was proposed (41, 42), which is also under examination to be used in cancer prevention. Another organic molecules are being examined, as vitamin D_3 (43), and they can be used as cancer inhibitors and/or as an adjuvant cancer therapy to reduce or defeat the CSC niche. A different strategy is the search and use of embryonic antigens, as A19, which was demonstrated (44) to be an effective targeted agent for Erbb-2 expressing cancers. Cell surface antigens are widely used to characterize embryonic stem cells, in particular to monitor their differentiation (45), and such antigens, which include both glycolipids and glycoproteins, can also be exploited for cancer diagnosis and therapy. If this carcinogenesis model is correct, in the sense that it explains, at least partially, the events that lead to cancer initiation by dedifferentiation of mature to stem cells, it can also be used in the opposite way. Known carcinogenic events can be used to reprogram cells to a pluripotent state and it can be compared with other techniques in terms of efficiency, simplicity and safety.

From the evolutionary point of view, cancer is greatly deleterious for the individual survival and proliferation, and has been highly suppressed during life evolution. Cells possess many redundant protection mechanisms to avoid cancer, from DNA error check and correction to apoptosis, so it is very hard to get rid of all of them and still be viable and have a competitive advantage with respect to normal cells. But it is not possible to suppress the mechanism of epigenetic reversion to an earlier development (pluripotent) state as this state is a fundamental step on a living being maturation. Then the (potentially dangerous) pluripotent state is so important in embryogenesis and tissue homeostasis that it cannot be eliminated by evolution, even if it can later be at a tumors' origin. Therefore, the reversal of a normal mature cell into a stem-like cell state can explain many tumor initiation and progression observations found to be contradictory with SMT and open new therapeutic avenues. Anyway, one hypothesis can be at the origin of some tumors and the other one for separate cases, but it is also possible that both are present and cooperating in cancer initiation.

AUTHOR CONTRIBUTIONS

The author confirms being the sole contributor of this work and has approved it for publication.

FUNDING

This work was supported by the Portuguese Foundation for Science and Technology (Fundação para a Ciência e a Tecnologia)—FCT—and by the European Regional Development Fund (ERDF/FEDER) through the Operational Program Competitiveness Factors (Programa Operacional Factores de Competitividade)—COMPETE—funding through strategic project UID/FIS/04564/2016.

ACKNOWLEDGMENTS

We would like to thank Mario Graos, Rui Travasso, and Raquel Seruca for valuable discussions.

REFERENCES

1. Vaux DL. In defense of the somatic mutation theory of cancer. *BioEssays.* (2011) 33:341–3. doi: 10.1002/bies.201100022
2. Hanahan D, Weinberg RA. Hallmarks of cancer: the next generation. *Cell.* (2011) 144:646–74. doi: 10.1016/j.cell.2011.02.013
3. Versteeg R. Tumours outside the mutation box. *Nature.* (2014) 506:438–9. doi: 10.1038/nature13061
4. Mally A, Chipman JK. Non-genotoxic carcinogens: early effects on gap junctions, cell proliferation and apoptosis in the rat. *Toxicology.* (2002) 180:233–48. doi: 10.1016/S0300-483X(02)00393-1
5. Baker SG. A cancer theory kerfuffle can lead to new lines of research. *J Natl Cancer Inst.* (2015) 107:2. doi: 10.1093/jnci/dju405
6. Raaijmakers MH, Mukherjee S, Guo S, Zhang S, Kobayashi T, Schoonmaker JA, et al. Bone progenitor dysfunction induces myelodysplasia and secondary leukaemia. *Nature.* (2010) 464:852–7. doi: 10.1038/nature08851
7. Dupont C, Armant DR, Brenner CA. Epigenetics: definition, mechanisms and clinical perspective. *Semin Reprod Med.* (2009) 27:351–7. doi: 10.1055/s-0029-1237423
8. Kanherkar RR, Bhatia-Dey N, Makarev E, Csoka AB. Cellular reprogramming for understanding and treating human disease. *Front Cell Dev Biol.* (2014) 2:67. doi: 10.3389/fcell.2014.00067
9. Godini R, Lafta HY, Fallahi H. Epigenetic modifications in the embryonic and induced pluripotent stem cells. *Gene Exp Patterns.* (2018) 29:1–9. doi: 10.1016/j.gep.2018.04.001

10. Geraerts M, Verfaillie CM. Adult stem and progenitor cells. *Adv Biochem Eng Biot.* (2009) 114:1–21. doi: 10.1007/10_2008_21
11. Kim H, Lin Q, Yun Z. BRCA1 regulates the cancer stem cell fate of breast cancer cells in the context of hypoxia and histone deacetylase inhibitors. *Sci Rep.* (2019) 9:9702. doi: 10.1038/s41598-019-46210-y
12. Cofre J, Abdelhay E. Cancer is to embryology as mutation is to genetics: hypothesis of the cancer as embryological phenomenon. *Sci World J.* (2017) 2017:3578090. doi: 10.1155/2017/3578090
13. Erdö F, Bührle C, Blunk J, Hoehn M, Xia Y, Fleischmann B, et al. Host-dependent tumorigenesis of embryonic stem cell transplantation in experimental stroke. *J Cereb Blood Flow Metab.* (2003) 23:780–5. doi: 10.1097/01.WCB.0000071886.63724.FB
14. Blum B, Bar-Nur O, Golan-Lev T, Benvenisty N. The anti-apoptotic gene survivin contributes to teratoma formation by human embryonic stem cells. *Nat Biotechnol.* (2009) 27:281–7. doi: 10.1038/nbt.1527
15. Davies PCW, Lineweaver CH. Cancer tumors as Metazoa 1.0: tapping genes of ancient ancestors. *Phys Biol.* (2011) 8:015001. doi: 10.1088/1478-3975/8/1/015001
16. Soto AM, Sonnenschein C. The tissue organization field theory of cancer: a testable replacement for the somatic mutation theory. *Bioessays.* (2011) 33:332–40. doi: 10.1002/bies.201100025
17. Friedmann-Morvinski D, Verma IM. Dedifferentiation and reprogramming: origins of cancer stem cells. *EMBO Rep.* (2014) 15:244–53. doi: 10.1002/embr.201338254
18. Nimmakayalaa RK, Batra SK, Ponnusamya MP. Unraveling the journey of cancer stem cells from origin to metastasis. *BBA Rev Cancer.* (2019) 1871:50–63. doi: 10.1016/j.bbcan.2018.10.006
19. Kreso A, Dick JE. Evolution of the cancer stem cell model. *Cell Stem Cell.* (2014) 14:275–91. doi: 10.1016/j.stem.2014.02.006
20. Clarke MF. Clinical and therapeutic implications of cancer stem cells. *N Eng J Med.* (2019) 380:2237–45. doi: 10.1056/NEJMra1804280
21. Takahashi K, Yamanaka S. Induction of pluripotent stem cells from mouse embryonic and adult fibroblast cultures by defined factors. *Cell.* (2006) 126:663–76. doi: 10.1016/j.cell.2006.07.024
22. Kim J, Orkin SH. Embryonic stem cell-specific signatures in cancer: insights into genomic regulatory networks and implications for medicine. *Genome Med.* (2011) 3:75. doi: 10.1186/gm291
23. Monk M, Holding C. Human embryonic genes re-expressed in cancer cells. *Oncogene.* (2001) 20:8085–91. doi: 10.1038/sj.onc.1205088
24. Yu Z, Pestell TG, Lisanti MP, Pestell RG. Cancer stem cells. *Int J Biochem Cell B.* (2012) 44:2144–51. doi: 10.1016/j.biocel.2012.08.022
25. Giralt S, Costa L, Schriber J, DiPersio J, Maziarz R, McCarty J, et al. Optimizing autologous stem cell mobilization strategies to improve patient outcomes: consensus guidelines and recommendations. *Biol Blood Marrow Transplant.* (2014) 20:295–308. doi: 10.1016/j.bbmt.2013.10.013
26. Stroncek D, McCullough J. Safeguarding the long-term health of hematopoietic stem cell donors: a continuous and evolving process to maintain donor safety and trust. *Expert Rev Hematol.* (2012) 5:1–3. doi: 10.1586/ehm.11.78
27. Brucher BLDM, Jamall IS. Somatic mutation theory - why it's wrong for most cancers. *Cell Physiol Biochem.* (2016) 38:1663–80. doi: 10.1159/000443106
28. Bindra RS, Glazer PM. Genetic instability and the tumor microenvironment: towards the concept of microenvironment-induced mutagenesis. *Mutat Res.* (2005) 569:75–85. doi: 10.1016/j.mrfmmm.2004.03.013
29. Papp-Szabó E, Josephy PD, Coomber BL. Microenvironmental influences on mutagenesis in mammary epithelial cells. *Int J Cancer.* (2005) 116:679–85. doi: 10.1002/ijc.21088
30. Leibeling D, Laspe P, Emmert S. Nucleotide excision repair and cancer. *J Mol Histol.* (2006) 37:225–38. doi: 10.1007/s10735-006-9041-x
31. Coulombe L, Kalousek DK, Eaves CJ, Gupta CM, Eaves AC. Long-term marrow culture reveals chromosomally normal hematopoietic progenitor cells in patients with Philadelphia chromosome-positive chronic myelogenous leukemia. *New Engl J Med.* (1983) 308:1493–8. doi: 10.1056/NEJM198306233082502
32. Klutstein M, Nejman D, Greenfield R, Cedar H. DNA Methylation in cancer and aging. *Cancer Res.* (2016) 15:3446–50. doi: 10.1158/0008-5472.CAN-15-3278
33. Quail DF, Dannenberg AJ. The obese adipose tissue microenvironment in cancer development and progression. *Nat Rev Endocrinol.* (2019) 15:139–54. doi: 10.1038/s41574-018-0126-x
34. Maffini MV, Soto AM, Calabro JM, Ucci AA, Sonnenschein C. The stroma as a crucial target in rat mammary gland carcinogenesis. *J Cell Sci.* (2004) 117:1495–502. doi: 10.1242/jcs.01000
35. Nakada Y, Canseco D, Thet S, Abdisalaam S, Asaithamby A, Santos CX, et al. Hypoxia induces heart regeneration in adult mice. *Nature.* (2017) 541:222–7. doi: 10.1038/nature20173
36. Cieslar-Pobuda A, Knoflach V, Ringh MV, Stark J, Likus W, Siemianowicz K, et al. Transdifferentiation and reprogramming: overview of the processes, their similarities and differences. *BBA Mol Cell Res.* (2017) 1864:1359–69. doi: 10.1016/j.bbamcr.2017.04.017
37. Malta TM, Sokolov A, Gentles AJ, Burzykowski T, Poisson L, Weinstein JN, et al. Machine learning identifies stemness features associated with oncogenic dedifferentiation. *Cell.* (2018) 173:338–54. doi: 10.1016/j.cell.2018.03.034
38. Horne SD, Stevens JB, Abdallah BY, Liu G, Bremer SW, Ye CJ, et al. Why imatinib remains an exception of cancer research. *J Cell Physiol.* (2013) 228:665–70. doi: 10.1002/jcp.24233
39. Haas D, Ablin AR, Miller C, Zoger S, Matthay KK. Complete pathologic maturation and regression of stage IVS neuroblastoma without treatment. *Cancer.* (1988) 62:818–25. doi: 10.1002/1097-0142(19880815)62:4<818::AID-CNCR2820620430>3.0.CO;2-K
40. Batlle E, Clevers H. Cancer stem cells revisited. *Nat Med.* (2017) 23:1124–34. doi: 10.1038/nm.4409
41. Sell S. Stem cell origin of cancer and differentiation therapy. *Crit Rev Oncol Hematol.* (2004) 51:1–28. doi: 10.1016/j.critrevonc.2004.04.007
42. Campos B, Wan F, Farhadi M, Ernst A, Zeppernick F, Tagscherer KE, et al. Differentiation therapy exerts antitumor effects on stem-like glioma cells. *Clin Cancer Res.* (2010) 16:2715–28. doi: 10.1158/1078-0432.CCR-09-1800
43. Hughes PJ, Marcinkowska E, Gocek E, Studzinski GP, Brown G. Vitamin D3-driven signals for myeloid cell differentiation-implications for differentiation therapy. *Leuk Res.* (2010) 34:553–65. doi: 10.1016/j.leukres.2009.09.010
44. Tan HL, Yong C, Tan BZ, Fong WJ, Padmanabhan J, Chin A, et al. Conservation of oncofetal antigens on human embryonic stem cells enables discovery of monoclonal antibodies against cancer. *Sci Rep.* (2018) 8:11608. doi: 10.1038/s41598-018-30070-z
45. Wright AJ, Andrews PW. Surface marker antigens in the characterization of human embryonic stem cells. *Stem Cell Res.* (2009) 3:3–11. doi: 10.1016/j.scr.2009.04.001

Conflict of Interest: The author declares that the research was conducted in the absence of any commercial or financial relationships that could be construed as a potential conflict of interest.

frontiers in Cell and Developmental Biology

ORIGINAL RESEARCH
published: 16 April 2020
doi: 10.3389/fcell.2020.00232

ANXA6 Contributes to Radioresistance by Promoting Autophagy via Inhibiting the PI3K/AKT/mTOR Signaling Pathway in Nasopharyngeal Carcinoma

Qianping Chen[1†], Wang Zheng[1†], Lin Zhu[1], Dan Yao[1], Chen Wang[1], Yimeng Song[1], Songling Hu[1], Hongxia Liu[1], Yang Bai[1], Yan Pan[1], Jianghong Zhang[1], Jian Guan[2] and Chunlin Shao[1*]*

[1] *Institute of Radiation Medicine, Shanghai Medical College, Fudan University, Shanghai, China,* [2] *Department of Radiation Oncology, Nanfang Hospital, Southern Medical University, Guangzhou, China*

OPEN ACCESS

Edited by:
Hailong Pei,
Soochow University, China

Reviewed by:
Guoping Zhao,
Hefei Institutes of Physical Science (CAS), China
Lu Cai,
University of Louisville, United States

***Correspondence:**
Jian Guan
guanjian5461@163.com
Chunlin Shao
clshao@shmu.edu.cn

[†]These authors have contributed equally to this work

Specialty section:
This article was submitted to Molecular and Cellular Oncology, a section of the journal Frontiers in Cell and Developmental Biology

Received: *21 February 2020*
Accepted: *19 March 2020*
Published: *16 April 2020*

Citation:
Chen Q, Zheng W, Zhu L, Yao D, Wang C, Song Y, Hu S, Liu H, Bai Y, Pan Y, Zhang J, Guan J and Shao C (2020) ANXA6 Contributes to Radioresistance by Promoting Autophagy via Inhibiting the PI3K/AKT/mTOR Signaling Pathway in Nasopharyngeal Carcinoma. Front. Cell Dev. Biol. 8:232. doi: 10.3389/fcell.2020.00232

Radiotherapy is a conventional and effective treatment method for nasopharyngeal carcinoma (NPC), although it can fail, mainly because radioresistance results in residual or recurrent tumors. However, the mechanisms and predictive markers of NPC radioresistance are still obscure. In this study, we identified Annexin A6 (ANXA6) as a candidate radioresistance marker by using Tandem Mass Tag quantitative proteomic analysis of NPC cells and gene chip analysis of NPC clinical samples with different radiosensitivities. It was observed that a high expression level of ANXA6 was positively correlated with radioresistance of NPC and that inhibition of ANXA6 by siRNA increased the radiosensitivity. The incidence of autophagy was enhanced in the established radioresistant NPC cells in comparison with their parent cells, and silencing autophagy with *LC3* siRNA (siLC3) sensitized NPC cells to irradiation. Furthermore, *ANXA6* siRNA (siANXA6) suppressed cellular autophagy by activating the PI3K/AKT/mTOR pathway, ultimately leading to radiosensitization. The combination of siANXA6 and CAL101 (an inhibitor of PI3K, p-AKT, and mTOR, concurrently) significantly reversed the above siANAX6-reduced autophagy. Suppression of PI3K/AKT/mTOR by CAL101 also increased the expression of ANXA6 in a negative feedback process. In conclusion, this study revealed for the first time that ANXA6 could promote autophagy by inhibiting the PI3K/AKT/mTOR pathway and that it thus contributes to radioresistance of NPC. The significance of this is that ANXA6 could be applied as a new predictive biomarker of NPC prognosis after radiotherapy.

Keywords: ANXA6, radioresistance, autophagy, PI3K/AKT/mTOR, NPC

INTRODUCTION

Nasopharyngeal carcinoma (NPC) is a cancer arising from nasopharynx epithelium. Compared with other types of tumors, NPC has a low incidence rate and a unique geographic distribution pattern. In 2018, there were about 129,000 new cases of NPC in the world, according to the International Agency for Research on Cancer (Chen et al., 2019). Nevertheless, the geographical

distribution of NPC patients across the globe is extremely unbalanced, with more than 70% of new cases located in eastern and southeastern Asia, especially in southern China (Ferlay et al., 2015; Chen et al., 2019). Radiotherapy is the primary and only curative treatment for NPC because of the special anatomical location and high sensitivity to radiation of this cancer. Recently, with the development of intensity-modulated radiotherapy (IMRT), radiotherapy has achieved 5-year overall survivals of 90 and 84% for stage I and stage IIA NPC, respectively (Lee et al., 2005). However, some advanced patients still exhibit radioresistance, leading to the failure of radiotherapy (Li et al., 2006; Liu et al., 2013). At present, few biomarkers have been used in the clinic to predict the radioresistance of NPC (Chen and Hu, 2015).

ANXA6 (Annexin A6) belongs to the highly conserved annexin protein family and has been implicated in mediating the endosome aggregation and vesicle fusion in secreting epithelia during exocytosis (Enrich et al., 2011). Like other annexins, ANXA6 binds to phospholipids and functions in a Ca^{2+}-dependent manner, thus activating cellular membrane in a dynamic, reversible, and regulated way (Grewal et al., 2010). Upon cell activation, ANXA6 is recruited to the plasma membrane, endosomes, and caveolae/membrane rafts to interact with signaling proteins to handle intracellular Ca^{2+} signaling (Enrich et al., 2011) and inhibits the epidermal growth factor receptor (EGFR) and Ras signaling pathway (Grewal et al., 2010; Koese et al., 2013). Overexpression of ANXA6 has been reported to be associated with poor prognosis of tumors (Lomnytska et al., 2011). Moreover, there is evidence that the expression of ANXA6 might represent new Ca^{2+} effectors that regulate converging steps of autophagy in hepatocytes (Enrich et al., 2017). However, its role in radiosensitivity remains unknown.

When exposed to adverse environmental conditions, cells degrade their own content to recycle cellular building blocks through a process of autophagy (Katheder and Rusten, 2017). A large body of literature have connected autophagy to cancer, and some studies have focused on the function of autophagy in radioresistance. Autophagy is also called programed cell death type II, which is different from the apoptotic type I death pathway (Choi et al., 2013). It is a highly conserved catabolic process that maintains cellular homeostasis by targeting damaged proteins or organelles to lysosomal compartments for degradation (Zhang et al., 2019). Autophagy has potential roles in radioresistance of cancer cells such as colorectal cancer, breast cancer, glioma, and pancreatic cancer (Yao et al., 2003; Chaachouay et al., 2011, 2015; Wang et al., 2013; Koukourakis et al., 2016). Inhibition of the PI3K/AKT/mTOR signaling pathway is one of the classical pathways for autophagy induction. There is increasing evidence showing that the activation of autophagy associated with the inhibition of the PI3K/AKT/mTOR pathway regulates many biological processes, including platelet activation, psoriasis regulation, and osteoarthritis attenuation (Varshney and Saini, 2018; Wang et al., 2018; Cai et al., 2019). However, few studies have focused on the role of autophagy induced by PI3K/AKT/mTOR inhibition in the radioresistance of NPC.

This study found that the level of autophagy increased along with the enhancement of radioresistance of NPC cells and that ANXA6 was highly expressed in both radioresistant NPC cells and NPC patients. The relationship among ANXA6, autophagy, and the PI3K/AKT/mTOR pathway in the induction of radioresistance of NPC was further investigated.

MATERIALS AND METHODS

Cell Culture and Irradiation

Nasopharyngeal carcinoma cell lines of CNE1 and HNE2 were purchased from Shanghai Cell Bank in 2016. The cells were used up to a passage number of 15. The cells were cultured with RPMI-1640 medium (Gibco, Hangzhou, China) supplied with 10% fetal bovine serum (Gibco Invitrogen, Grand Island, NY, United States), 100 U/ml penicillin, and 100 mg/ml streptomycin and maintained at 37°C in an atmosphere of 5% CO_2. Testing for mycoplasma was performed on a monthly basis.

To generate a radioresistant cell line, CNE1 cells were irradiated with fractionated doses of 2, 2, 4, 4, 4, 4, 6, 6, 6, 6, 8, and 8 Gy (60 Gy in total) of γ-rays (^{137}Cs, Gammacell-40, MDS Nordion, Canada) at a dose rate of 0.73 Gy/min. Cells were irradiated with 2 Gy once a day, 4 Gy once a week, 6 Gy every 10 days, and 8 Gy every 2 weeks. One day before irradiation, 1.5×10^6 cells were seeded in a 60 mm culture dish. After each irradiation, the cells were passaged two or more times so that they had enough vitality for the next irradiation. After fractionated irradiation of 60 Gy, the surviving cells, named CNE1R cells, became more radioresistant than CNE1 cells.

Colony Formation Assay

The radiosensitivities of CNE1, CNE1R, and HNE2 cells were assessed by cell colony-formation assay. Cells were plated in the six-well plate at a density of 150, 300, 800, and 1600 cells/well. After full attachment, they were exposed to 0, 2, 4, and 6 Gy, respectively. At 8–12 days after radiation, cell colonies were fixed with methanol for 20 min and stained with 0.1% crystal violet for 30 min in order to count them. The cell survival curve was fitted using the single-hit multitarget model.

Western Blot Assay

Total cellular proteins were extracted using SDS lysis buffer (250 nM Tris–HCL, pH 7.4, 2.5% SDS) with 100 mM phenylmethanesulfonyl fluoride (PMSF) (Beyotime, Biotechnology, Haimen, China). After denaturing at 100°C for 10 min, aliquots of protein (20 μg/sample) were electrophoresed on 10 or 12% polyacrylamide gel (according to the molecular weight of goal proteins) using an electrophoresis system (Bio-Rad Laboratories Inc., CA, United States). After electrophoresis, proteins were transferred to a PVDF membrane, blocked with 5% skim milk in Tris-buffered saline/Tween 0.05% (TBST) for 2 h and then incubated overnight at 4°C with a primary antibody of anti-ANXA6 antibody (1:2000, Abclonal), anti-P62 (1:1000, Cell signaling Technology), anti-LC3 (1:1000, Cell signaling Technology) or anti-Actin (1:20000, Abclonal). Then the membrane was triply washed with TBST at room temperature

for 10 min and labeled with a peroxidase-conjugated secondary antibody (1:5000, Beyotime Biotechnology) for 2 h. Proteins in the membrane were detected by the enhanced chemiluminescence system (ECL kit, Millipore, St. Louis, MO, United States), and band images were analyzed with the Bio-Rad ChemiDoc XRS system.

Tandem Mass Tag (TMT) Quantitative Proteomic Analysis

Each protein sample in lysis buffer (8 M urea, 1% Protease Inhibitor Cocktail) was sonicated triply using a high-intensity ultrasonic processor (Scientz, Ningbo, China). The remaining debris was removed by centrifugation at 12,000 g at 4°C for 10 min. Finally, the supernatant was collected, and the protein concentration was determined with a BCA kit according to the manufacturer's instruction. Trypsin was then used for digestion to generate peptide. The peptide was desalted by Strata X C18 SPE column (Phenomenex, CA, United States) and vacuum dried. The tryptic peptides were digested into fractions and separated by high pH reverse-phase HPLC using Agilent 300Extend C18 column (5 μm particles, 4.6 mm ID, 250 mm length) and subjected to a NSI source followed by tandem mass spectrometry (MS/MS) in a Q ExactiveTM Plus (Thermo, MA, United States) coupled online to the UPLC. The MS/MS data were processed with the Maxquant search engine (v.1.5.2.8).

Patients and Clinical Gene Chip

This study was carried out in accordance with the recommendations of international guidelines and ethical standards. All subjects gave written informed consent in accordance with the Declaration of Helsinki. For the experiments using human participants or data, prior approval was obtained from the Nanfang Hospital of Southern Medical University Institutional Board (Guangzhou, China).

A total of 185 NPC patients were recruited in this study, comprising 124 radiosensitive (87 male, 37 female, mean age 46 years) and 61 radioresistant patients (49 male, 12 female, mean age 46 years). All patients accepted a standard regimen of radiotherapy. Three months after therapy was completed, a contrast-enhanced Magnetic Resonance Imaging (MRI) or Computed Tomography (CT) scan and a thorough examination were performed to evaluate short-term efficacy. According to the Response Evaluation Criteria in Solid Tumor (RECIST) guideline, those with complete response (CR) and partial response (PR) were classified into the radiosensitive group, while those with stable disease (SD) and progressive disease (PD) were classified into the radioresistant group. The clinicopathologic characteristics of NPC tissues used in the present study are demonstrated in **Supplementary Table S1**.

Three patients in the radioresistant group were selected to provide paraffin samples for gene chip detection. Paraffin samples were collected before and after treatment and divided into these two groups for differential gene study. Paraffin samples were then extracted using the RNeasy kit (Tiangen, Beijing, China), and gene chips were obtained by hybridization, washing, and staining. We analyzed gene chips by the standardized method provided by the Affymetrix human U133 + 2.0 chip (Bohao Biotechnology Co., Shanghai, China).

RNA Extraction and Quantitative Real-Time PCR Assay

Total RNA was extracted from CNE1, CNE1-R, and HNE2 cells for RT-PCR using total RNA Kit I (Omega, Norcross, GA, United States). Reverse transcription of total RNA to cDNA was carried out in 20 μl reaction reagents of the qRT-PCR Kit (Tiangen, Beijing, China) according to the manufacturer's protocol. For *ANXA6* gene, the forward primer was 5′-ACG GTT GAT TGT GGG CCTG-3′) and the reverse primer was 5′- GTG CAT CTG CTC ATT GGT CC-3′. For β-*actin* gene, the forward primer was 5′-CAT GTA CGT TGC TAT CCA GGC-3′ and the reverse primer was 5′- CTC CTT AAT GTC ACG CAC GAT-3′. The optimal PCR amplification procedure was performed for 40 cycles with pre-denaturation at 95°C for 15 min, denaturation at 95°C for 10 s, and annealing and extension at 60°C for 32 s.

siRNA Transfection

CNE1 and CNE1-R cells were transferred with *ANXA6* siRNA (siANXA6) (target sequence: CGG GCA CTT CTG CCA AGA AAT), *LC3* siRNA (siLC3) (target sequence: GAG UGA GAA AGA UGA AGA UTT), and siRNA negative control of random sequence using riboFECTTM CP Transfection Agent (Ribobio, Guangzhou, China). The transfection efficiency was evaluated by PCR at 24–72 h after transfection, and the survival of siLC3 transfected cells was measured with a colony formation assay.

Autophagy Flux Assay

Cells were plated at a density of 2×10^5 per well and allowed to adhere overnight. Cells in about 70% confluence were transfected with *mRFP-GFP-LC3* double-labeled adenovirus (Ad-*mRFP-GFP-LC3*) to label autophagosome (Hanbio Biotechnology Co., Shanghai, China) according to the manufacturer's instruction. After 2 h of transfection, the cells were cultured in fresh medium for 48 h then washed with pre-cooled PBS twice and stained with DAPI. The intracellular autophagy was observed by a high-content imaging system (ImageXpress Micro 4, Molecular Devices, San Francisco, CA, United States). Double labeling of LC3 (green) and mRFP (red) immunofluorescence corresponds to changes in autophagic flux. When autophagy and lysosome fusion occur, LC3-GFP fluorescence is quenched, and only red fluorescence can be detected. After merging the red and green fluorescence images, yellow spots in the cell image symbolize autophagosomes.

Drug Treatment

CAL-101 is a potent and highly selective inhibitor of PI3K, p-AKT, and m-TOR concurrently and has been approved by the Food and Drug Administration (FDA) for the clinical treatment of certain hematological malignancies in 2014. CAL-101 was dissolved in dimethyl sulfoxide (DMSO) and stored at −20°C as a stock solution (10 mM). CNE1R cells were treated with 5 μM CAL-101 in medium for 12 h, and 1% DMSO was used as a control of CAL-101.

Statistical Analysis

All experiments were repeated at least three times. Data are expressed as mean ± SD and analyzed with the one-way ANOVA method using SPSS17.0 software (SPSS Inc. Chicago, IL, United States). $P < 0.05$ was considered a significant difference between the indicated groups.

RESULTS

High ANXA6 Level Is Closely Associated With the Radioresistance of NPC

Figure 1A illustrates that the two commonly used NPC cell lines, CNE1 and HNE2, had different radiosensitivities and that CNE1 cells were more resistant to radiation. By irradiating CNE1 cells with fractionated doses up to 60 Gy in total, we generated a highly radioresistant cell line named CNE1R. The radioresistance of CNE1R cells was confirmed by the colony-formation assay (**Figure 1A**).

The proteins from CNE1 cells and its radioresistant counterpart CNE1R were collected and subjected to TMT quantitative proteomic analysis in order to determine the differential proteins between radioresistant cells and their parents. These differentially expressed proteins are illustrated on a volcano plot in **Figure 1B**. In total, 1,295 differential proteins were identified, among which 658 proteins were upregulated, while 637 were downregulated (**Supplementary Table S2**, fold change $\geq$ 1.2, p-value < 0.05). Meanwhile, **Figure 1C** illustrates the gene chip assay results regarding the distribution of differentially expressed genes from three NPC radioresistant patients before and after radiotherapy. Following the calculation criteria (fold change ≥ 2, p-value < 0.05), a total of 292 aberrantly expressed genes were obtained, including 155 upregulated and 137 downregulated genes (**Supplementary Table S3**). Thus, a total of 29 genes were identified from NPC cells and clinical specimens and are visualized by heat map in **Figure 1D**, including eight co-upregulated genes and six co-downregulated genes. We speculated that the high expression of ANXA6 among them was probably an important prognostic marker of NPC radioresistance because the elevation of ANXA6 has been previously reported to be an independent risk factor for poor prognosis of many neoplasms, such as cervix carcinogenesis, pancreatic cancer, ovarian carcinoma, and thyroid cancer (Lomnytska et al., 2011; O'Sullivan et al., 2017; Lee et al., 2018; Noreen et al., 2019).

Next, we explored the contribution of ANXA6 to the radioresistance of NPC *in vitro*. It was observed that the expression levels of ANXA6 mRNA and protein in three NPC cell lines (HNE2, CNE1, and CNE1R) were positively related to cell radioresistance (**Figures 1E,F**). To further demonstrate whether *ANXA6* has an essential role in the radioresistance of NPC, the expression of *ANXA6* in CNE1 and CNE1R cells was effectively silenced by siANXA6 (**Figure 1G**). It was found that transfection of cells with siANXA6 significantly sensitized NPC cells to irradiation and reduced cell survival (**Figure 1H**).

Autophagy Contributes to the Radioresistance of NPC Cells

Increasing evidence shows that induction of autophagy contributes to the resistance of anticancer treatments. To determine whether autophagy is involved in the radioresistance of NPC cells, we transfected NPC cells with Ad-*mRFP-GFP-LC3* to label autophagosomes. It was found that the number of LC3 dots increased, in ascending order, in HNE2, CNE1, and CNE1R cells (**Figure 2A**). Consistently, the ratio of LC3II/LC3I (an autophagic marker) increased, and the autophagy substrate protein p62 decreased in HNE2, CNE1, and CNE1R cells step by step (**Figure 2B**). To further assess the regulatory effect of autophagy on NPC cells, we transfected cells with siLC3 to block autophagy and then examined whether autophagy could impact the radioresistance of NPC cells. It was found that, when the expressions of LC3I and LC3II were weakened by siLC3, the survival of CNE1R cells was effectively decreased after irradiation (**Figures 2C,D**). These results suggested that autophagy promoted the radioresistance of NPC cells.

ANXA6 Regulates Autophagy Induction

To determine whether ANXA6 contributes to autophagy-regulated radioresistance of NPC cells, we transfected radioresistant CNE1R cells with siANXA6 and Ad-*mRFP-GFP-LC3*. As shown in **Figure 3A**, the number of autophagic LC3 spots in the siANXA6 group decreased sharply in comparison with siRNA negative control. Meanwhile, suppression of ANXA6 decreased the ratio of LC3II/I and thus, in turn, increased p62 expression (**Figure 3B**). In addition, the expressions of other autophagy-related proteins of Beclin-1 and Autophagy Related 12 (ATG12) also decreased in CNE1R cells after siANXA6 transfection (**Figure 3C**). Therefore, the silence of ANXA6 significantly inhibited the occurrence of intact autophagic flux.

ANXA6 Regulates the PI3K/AKT/mTOR Pathway

To determine the relationship of the PI3K/AKT/mTOR signaling pathway with radioresistance, the expressions of these proteins in NPC cells with different radiosensitivities were measured. **Figure 4A** illustrates that the expression levels of PI3K-α, p-AKT, and p-mTOR decreased along with the radiosensitivity of HNE2, CNE1, and CNE1R cells, in contrast to the LC3II/I ratio in these cells. When the most radioresistant cells of CNE1R were transfected with siANXA6, the levels of PI3K-α, p-AKT, and p-mTOR were obviously increased in comparison with those in the siRNA control cells (**Figure 4B**). Therefore, knockdown of ANXA6 activates the PI3K/AKT/mTOR signaling pathway.

Given our observation of the relationship among ANXA6, PI3K/AKT/mTOR, and autophagy, CNE1R cells transferred with siANXA6 were further treated with CAL101, a specific inhibitor of the PI3K/AKT/mTOR pathway. It was found that CAL101 effectively decreased the expressions of PI3K-α, p-AKT, and p-mTOR. Furthermore, when cells were co-treated with siANXA6 and CAL101, both ANXA6 and LC3II/I ratio were extensively increased in comparison with the siANXA6 alone group, suggesting that the decrease of autophagy

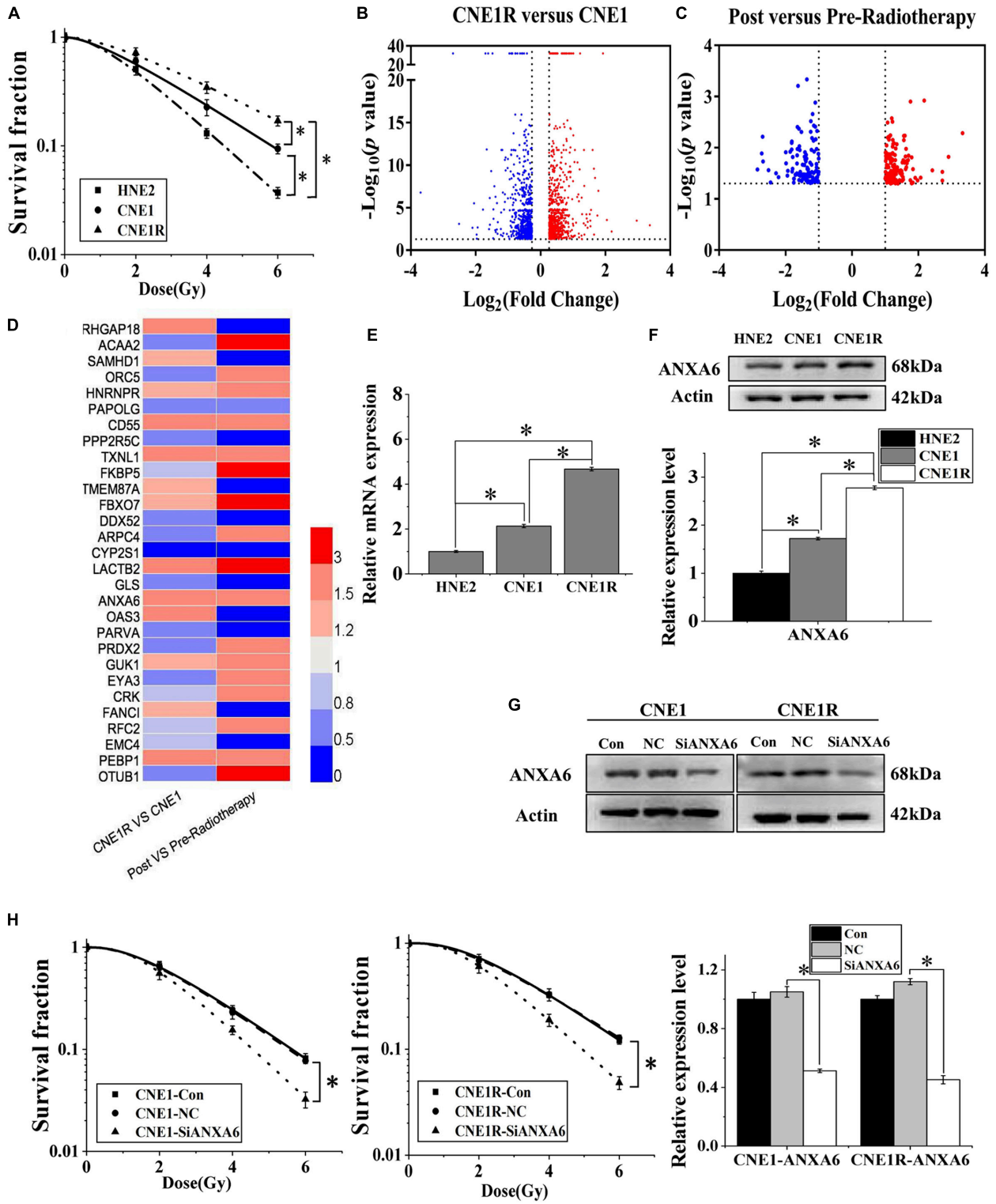

FIGURE 1 | High expression of ANXA6 predicts radioresistance of NPC. **(A)** Survival fractions of HNE2, CNE1, and CNE1R cells after irradiation. **(B)** Volcano plot of differentially expressed genes between CNE1R and CNE1 cells. **(C)** Volcano plot of differentially expressed genes in the tumor tissue of NPC radioresistant patients ($n = 3$) before and after radiotherapy. **(D)** Heat map of the expression levels of 29 differential genes between the above volcano plots, analyzed by Heml (software for drawing volcano maps). **(E)** *ANXA6* mRNA expression levels in HNE2, CNE1, and CNE1R cells. **(F)** Western blot assay of ANXA6 protein in HNE2, CNE1, and CNE1R cells. **(G)** Efficiency of siANXA6 transfection in CNE1 and CNE1R cells. **(H)** Dose responses of survival factions of CNE1 and CNE1R cells after siANXA6 transfection. * $P < 0.05$ between indicated groups.

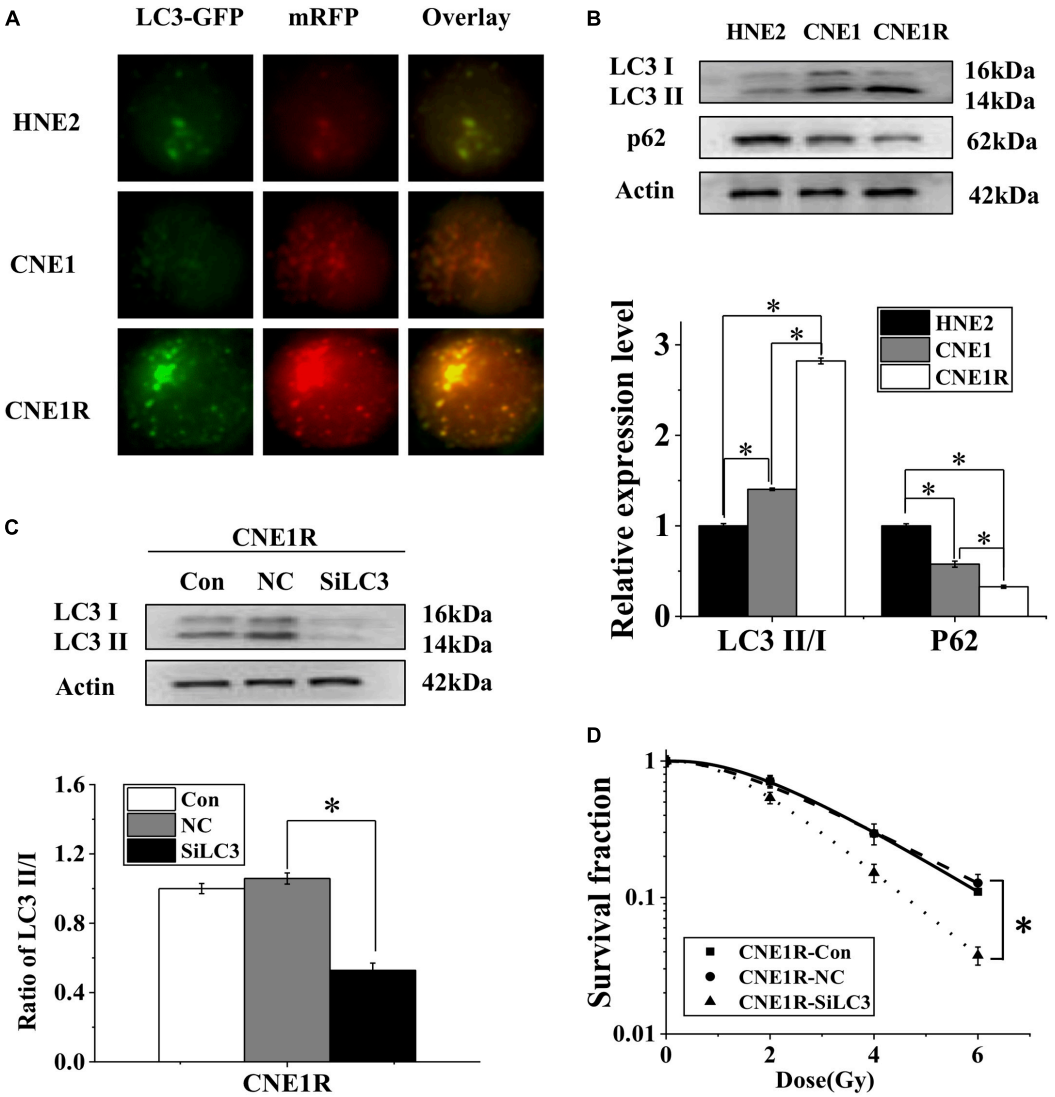

FIGURE 2 | Autophagy contributes to the radioresistance of NPC cells. **(A)** Fluorescence images of HNE2, CNE1, and CNE1R cells transfected with *mRFP-GFP-LC3* (x 40). **(B)** Western blot assay of P62 and LC3 proteins in HNE2, CNE1, and CNE1R cells. **(C)** Efficiency of siLC3 transfection in CNE1R cells. **(D)** Dose responses of survival factions of CNE1R cells before and after siLC3 transfection. *$P < 0.05$ between indicated groups.

induced by siANXA6 could be reversed by blocking the PI3K/AKT/mTOR pathway (**Figure 4C**). Taken together, these results indicate that ANXA6 upregulated the radioresistance of NPC cells by promoting autophagy through the inhibition of the PI3K/AKT/mTOR signaling pathway.

DISCUSSION

Due to the anatomical location and radiosensitivity of NPC, radiotherapy is the primary treatment method of this type of carcinoma, different from most other malignant tumors (Chua et al., 2016; Sun et al., 2016). Current advances in comprehensive population screening and effective drugs have significantly reduced nasopharyngeal cancer mortality, but recurrence and resistance after radiotherapy remain a problem in NPC, and the molecular mechanism of NPC radioresistance is still unresolved.

To further verify the relationship between ANXA6 and radioresistance, we performed a comprehensive analysis of data from the Gene Expression Profiling Interactive Analysis (GEPIA) database and The Cancer Genome Atlas (TCGA) database and found that 10 kinds of tumors overexpress ANXA6 in comparison to their normal tissues (**Supplementary Figure S1**). Besides the four cancers mentioned in the above results section, patients harboring a high expression of ANXA6 also possess a poor prognosis in bladder urothelial carcinoma (BLCA), kidney renal papillary cell carcinoma (KIRP), lung squamous cell carcinoma (LUSC), and mesothelioma (MESO) (**Supplementary Figure S2**), denoting that the overexpression of ANXA6 might serve as a crucial contributor to develop anti-tumor therapy

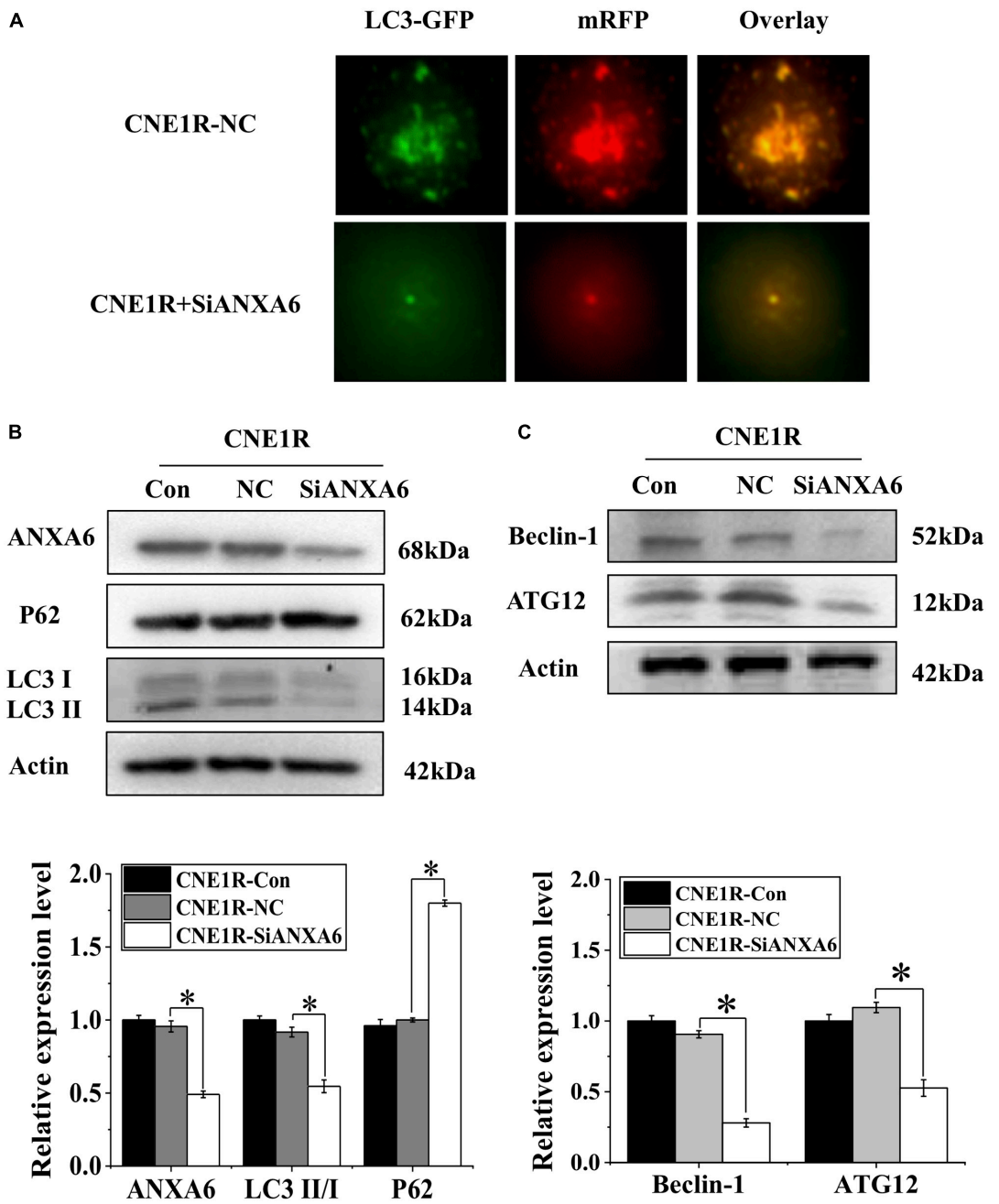

FIGURE 3 | Transfection of siANXA6 inhibits autophagy incidence. **(A)** Fluorescence images of CNE1R cells co-transfected with siANXA6 and mRFP-GFP-LC3 (x40). **(B)** Western blot assay of ANXA6, P62, and LC3 proteins in CNE1R cells. **(C)** Western blot assay of ATG12 and Beclin-1 proteins in CNE1R cells. *$P < 0.05$ between indicated groups.

strategy, especially for radioresistance. Though recent studies have revealed that the expression of ANXA6 is bound up with chemoresistance and poor prognosis of malignant tumors (Lomnytska et al., 2011; Keklikoglou et al., 2019), its role in radioresistance in various kinds of tumors has not yet been reported. In this study, we innovatively observed a positive relationship between ANXA6 expression and the radioresistance of NPC in both cell lines and clinical patients.

It was known that ANXA6 can enhance autophagy in rat liver hepatocytes and trigger endocytic transport and lysosome fusion by inducing re-arrangements of specific lipids and calcium channel transfer (Enrich et al., 2017). But the role of autophagy in radioresistance is still controversial. Wang et al. (2013) hold the view that autophagy promotes radioresistance in pancreatic cancer cells, while Djavid et al. (2017) concluded that the mobilization of autophagy could

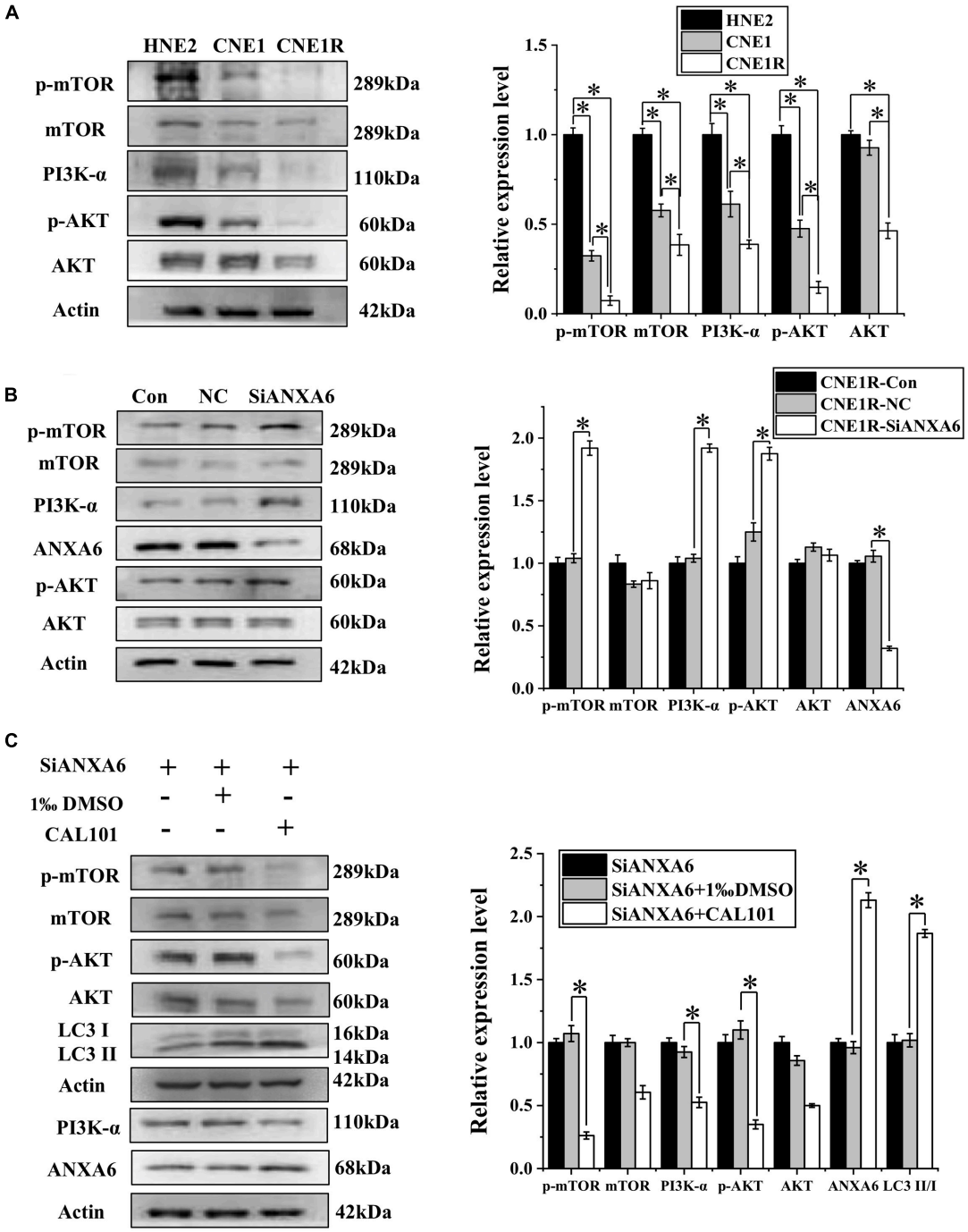

FIGURE 4 | ANXA6 contributes to autophagy incidence via inhibition of the PI3K/AKT/mTOR pathway. **(A)** Western blot assay of PI3K-α, AKT, p-AKT, mTOR, and p-mTOR proteins in HNE2, CNE1, and CNE1R cells. **(B)** Western blot assay of PI3K-α, AKT, p-AKT, mTOR, and p-mTOR proteins in CNE1R cells with or without siANXA6 transfection. **(C)** Western blot assay of PI3K-α, AKT, p-AKT, mTOR, p-mTOR, and ANXA6 proteins in siANXA6-transfected CNE1R cells treated with CAL101 or its control (1‰ DMSO). *$P < 0.05$ between indicated groups.

cause cell death through lysosomal activation, thus causing an enhancement of radiosensitivity in human cervical cancer cells. Our study demonstrated that autophagy inhibition increased the radiosensitivity of NPC cells and that there was a positive correlation between autophagy and radioresistance. Apart from the physiological regulation of calcium channels and re-arrangements of specific lipids, we found that ANXA6 could strengthen autophagy by blocking the PI3K/AKT/mTOR pathway. Meanwhile, siANXA6-suppressed autophagy could be reversed by a PI3K/AKT/mTOR inhibitor of CAL101.

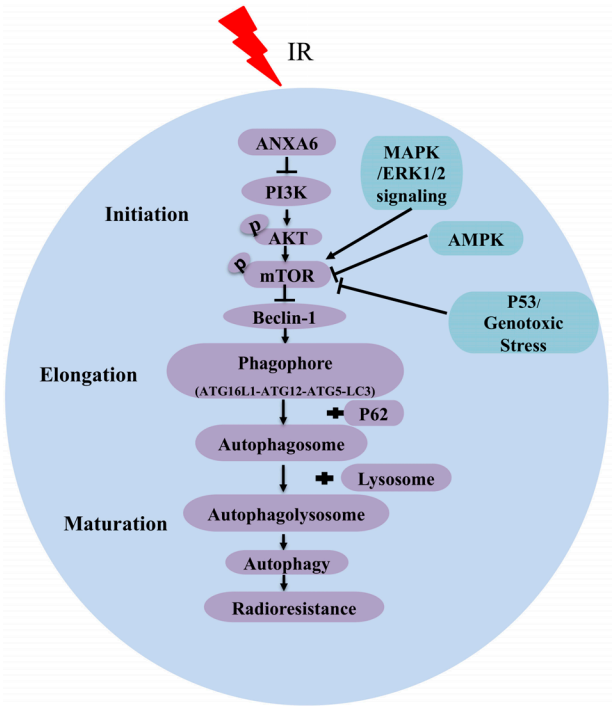

FIGURE 5 | A pattern diagram shows that ANXA6 regulates autophagy via inhibiting the PI3K/AKT/mTOR pathway to induce radioresistance of NPC. Irradiation (IR) increases the expression of ANXA6 in NPC cell lines and patient tumor tissues, which, in turn, directly inhibits the expression of PI3K and further reduces the phosphorylation of AKT and mTOR. The reduced p-mTOR increases the expression of Beclin-1 (a key activator of autophagy) and advances the formation of phagophore consisting of ATG16L1 (autophagy related 16-like 1), ATG12, ATG5 (autophagy related protein 5), and LC3 protein. Additionally, P62 binds to autophagosomal membrane protein LC3 and delivers itself to autophagosome, which ultimately leads to a decline of P62. Finally, autophagolysosome formed by the fusion of autophagosome and lysosome can phagocytize injured organelles to maintain/restore metabolic homeostasis, contributing to the radioresistance of NPC. Arrows represent promotion events, and blunt arrows indicate suppression events.

Taking these results together, we suggest that PI3K/AKT/mTOR complements the mechanism of the incidence of autophagy regulated by ANXA6.

The PI3K/AKT/mTOR pathway is one of the most frequently activated signaling pathways in cancers and is responsible for tumor development, cellular metastasis, and proliferation (Polivka and Janku, 2014; Zhang et al., 2017; Chamcheu et al., 2019). In particular, the PI3K/AKT/mTOR pathway has attracted extensive attention as the modulator of autophagy (Xu et al., 2020). The central checkpoint for the negative regulation of autophagy is mTOR, and anti-tumor drugs stimulate autophagy by attenuating the PI3K/AKT/mTOR pathway (Janku et al., 2011). Recent advances in radiotherapy also indicate that triggering of the PI3K/AKT/mTOR pathway is closely relevant to radioresistance, which is a major challenge for current radiation treatment in prostate cancer (CaP) and other cancers (Heavey et al., 2014; Chang et al., 2015). However, in our study, the PI3K/AKT/mTOR pathway was considered as a negative regulator for tumor progression and radiation resistance. According to many studies, the inhibition of the PI3K/AKT/mTOR pathway may contribute to weakened proliferation (Feng and Qiu, 2018) and prolonged cell cycle (He et al., 2018), which may provide much time for autophagy to phagocytize damaged organelles so as to maintain the stability of the intracellular environment, thus promoting cell survival and radioresistance after irradiation. Besides, it has been reported that targeting PI3K/AKT/mTOR-mediated autophagy strongly enhances the chemosensitivity of tumor cells. The overexpression of miR-142-3p attenuated autophagy by regulating the PI3K/AKT/mTOR pathway and enhanced the chemosensitivity of non-small cell lung cancers (Chen et al., 2017). For hepatocarcinoma, erlotinib induces autophagy through blocking the PI3K/AKT/mTOR pathway to enhance tumor resistance (Li et al., 2019). Another study reported that ZD6474, a small-molecule inhibitor that suppresses the activities of epidermal growth factor receptor, vascular endothelial growth factor receptor, and tyrosine kinases receptor, can activate autophagy depending on attenuation of the PI3K/AKT/mTOR signaling pathway to protect glioblastoma cells (Shen et al., 2013). These studies have demonstrated that the overexpression of the PI3K/AKT/mTOR pathway is beneficial for subduing autophagy and reducing tumor resistance.

Mechanistically, the phosphorylation of EGFR can stimulate several downstream signaling pathways, including MAPK/MEK/ERK and PI3K/AKT, that are involved in a variety of mitogenic, metastatic, and other tumor-promoting cellular activities (Wells, 1999; Roberts and Der, 2007). It was reported that an elevated ANXA6 level could inhibit the phosphorylation of EGFR by promoting protein kinase Cα (PKCα) and restrained EGFR signaling (Koese et al., 2013). Thus, we infer that the negative effect of ANXA6 on the PI3K/AKT/mTOR pathway may result from its inhibition of EGFR phosphorylation, though this needs further verification.

In summary, our results demonstrate that ANXA6-regulated autophagy via the PI3K/AKT/mTOR pathway makes a major contribution to the radioresistance of NPC (**Figure 5**). It is worth mentioning that this study has revealed the connection between ANXA6 and radiosensitivity for the first time and further implies that ANXA6 may be applied as a new biomarker for the diagnosis and prognosis of NPC radiotherapy. In addition, it will be of great benefit to expand the research on ANXA6 to head and neck neoplasms as a potential therapeutic target for radiosensitization in the future.

DATA AVAILABILITY STATEMENT

The raw data supporting the conclusions of this article will be made available by the authors, without undue reservation, to any qualified researcher.

ETHICS STATEMENT

The studies involving human participants were reviewed and approved by the Nanfang Hospital of Southern Medical

University Institutional Board. The patients/participants provided their written informed consent to participate in this study.

AUTHOR CONTRIBUTIONS

CS, QC, WZ, and LZ made contributions to the conception and design of the study. DY, CW, YS, SH, and HL performed acquisition and analysis of data. YB and JZ performed the statistical analysis. QC wrote the first draft of the manuscript. CS, JG, and YP revised the manuscript.

FUNDING

This study was mainly supported by the National Key R&D Program of China (No. 2017YFC0108604), National Natural Science Foundation of China (Nos. 31770910, 11775052, and 81276985), and Health and Medical Collaborative Innovation Project of Guangzhou China (201803040003).

ACKNOWLEDGMENTS

We thank Dr. Yanwu Xu for his excellent technical support with the autophagy flux assay.

SUPPLEMENTARY MATERIAL

The Supplementary Material for this article can be found online at: https://www.frontiersin.org/articles/10.3389/fcell.2020.00232/full#supplementary-material

REFERENCES

Cai, C., Min, S., Yan, B., Liu, W., Yang, X., Li, L., et al. (2019). MiR-27a promotes the autophagy and apoptosis of IL-1beta treated-articular chondrocytes in osteoarthritis through PI3K/AKT/mTOR signaling. *Aging* 11, 6371–6384. doi: 10.18632/aging.102194

Chaachouay, H., Fehrenbacher, B., Toulany, M., Schaller, M., Multhoff, G., and Rodemann, H. P. (2015). AMPK-independent autophagy promotes radioresistance of human tumor cells under clinical relevant hypoxia in vitro. *Radiother. Oncol.* 116, 409–416. doi: 10.1016/j.radonc.2015.08.012

Chaachouay, H., Ohneseit, P., Toulany, M., Kehlbach, R., Multhoff, G., and Rodemann, H. P. (2011). Autophagy contributes to resistance of tumor cells to ionizing radiation. *Radiother. Oncol.* 99, 287–292. doi: 10.1016/j.radonc.2011.06.002

Chamcheu, J. C., Roy, T., Uddin, M. B., Banang-Mbeumi, S., Chamcheu, R. N., Walker, A. L., et al. (2019). Role and therapeutic targeting of the pi3k/akt/mtor signaling pathway in skin cancer: a review of current status and future trends on natural and synthetic agents therapy. *Cells Basel* 8:803. doi: 10.3390/cells8080803

Chang, L., Graham, P. H., Ni, J., Hao, J., Bucci, J., Cozzi, P. J., et al. (2015). Targeting PI3K/Akt/mTOR signaling pathway in the treatment of prostate cancer radioresistance. *Crit. Rev. Oncol. Hematol.* 96, 507–517. doi: 10.1016/j.critrevonc.2015.07.005

Chen, W., and Hu, G. H. (2015). Biomarkers for enhancing the radiosensitivity of nasopharyngeal carcinoma. *Cancer Biol. Med.* 12, 23–32. doi: 10.7497/j.issn.2095-3941.2014.0015

Chen, Y., Zhou, X., Qiao, J., and Bao, A. (2017). MiR-142-3p overexpression increases chemo-sensitivity of NSCLC by Inhibiting HMGB1-mediated autophagy. *Cell Physiol. Biochem.* 41, 1370–1382. doi: 10.1159/000467896

Chen, Y. P., Chan, A. T. C., Le, Q. T., Blanchard, P., Sun, Y., and Ma, J. (2019). Nasopharyngeal carcinoma. *Lancet* 394, 64–80. doi: 10.1016/S0140-6736(19)30956-0

Choi, A. M., Ryter, S. W., and Levine, B. (2013). Autophagy in human health and disease. *N. Engl. J. Med.* 368, 651–662. doi: 10.1056/NEJMra1205406

Chua, M. L. K., Wee, J. T. S., Hui, E. P., and Chan, A. T. C. (2016). Nasopharyngeal carcinoma. *Lancet* 387, 1012–1024. doi: 10.1016/S0140-6736(15)00055-0

Djavid, G. E., Bigdeli, B., Goliaei, B., Nikoofar, A., and Hamblin, M. R. (2017). Photobiomodulation leads to enhanced radiosensitivity through induction of apoptosis and autophagy in human cervical cancer cells. *J. Biophotonics* 10, 1732–1742. doi: 10.1002/jbio.201700004

Enrich, C., Rentero, C., de Muga, S. V., Reverter, M., Mulay, V., Wood, P., et al. (2011). Annexin A6-Linking Ca(2+) signaling with cholesterol transport. *Biochim. Biophys. Acta* 1813, 935–947. doi: 10.1016/j.bbamcr.2010.09.015

Enrich, C., Rentero, C., and Grewal, T. (2017). Annexin A6 in the liver: from the endocytic compartment to cellular physiology. *Biochim. Biophys. Acta Mol. Cell Res.* 1864, 933–946. doi: 10.1016/j.bbamcr.2016.10.017

Feng, F. B., and Qiu, H. Y. (2018). Effects of Artesunate on chondrocyte proliferation, apoptosis and autophagy through the PI3K/AKT/mTOR signaling pathway in rat models with rheumatoid arthritis. *Biomed. Pharmacother.* 102, 1209–1220. doi: 10.1016/j.biopha.2018.03.142

Ferlay, J., Soerjomataram, I., Dikshit, R., Eser, S., Mathers, C., Rebelo, M., et al. (2015). Cancer incidence and mortality worldwide: sources, methods and major patterns in GLOBOCAN 2012. *Int. J. Cancer* 136, E359–E386. doi: 10.1002/ijc.29210

Grewal, T., Koese, M., Rentero, C., and Enrich, C. (2010). Annexin A6-regulator of the EGFR/Ras signalling pathway and cholesterol homeostasis. *Int. J. Biochem. Cell Biol.* 42, 580–584. doi: 10.1016/j.biocel.2009.12.020

He, D., Sun, X., Yang, H., Li, X., and Yang, D. (2018). TOFA induces cell cycle arrest and apoptosis in ACHN and 786-O cells through inhibiting PI3K/Akt/mTOR pathway. *J. Cancer* 9, 2734–2742. doi: 10.7150/jca.26374

Heavey, S., O'Byrne, K. J., and Gately, K. (2014). Strategies for co-targeting the PI3K/AKT/mTOR pathway in NSCLC. *Cancer Treat. Rev.* 40, 445–456. doi: 10.1016/j.ctrv.2013.08.006

Janku, F., McConkey, D. J., Hong, D. S., and Kurzrock, R. (2011). Autophagy as a target for anticancer therapy. *Nat. Rev. Clin. Oncol.* 8, 528–539. doi: 10.1038/nrclinonc.2011.71

Katheder, N. S., and Rusten, T. E. (2017). Microenvironment and tumors-a nurturing relationship. *Autophagy* 13, 1241–1243. doi: 10.1080/15548627.2017.1310361

Keklikoglou, I., Cianciaruso, C., Guc, E., Squadrito, M. L., Spring, L. M., Tazzyman, S., et al. (2019). Chemotherapy elicits pro-metastatic extracellular vesicles in breast cancer models. *Nat. Cell Biol.* 21, 190–202. doi: 10.1038/s41556-018-0256-3

Koese, M., Rentero, C., Kota, B. P., Hoque, M., Cairns, R., Wood, P., et al. (2013). Annexin A6 is a scaffold for PKCalpha to promote EGFR inactivation. *Oncogene* 32, 2858–2872. doi: 10.1038/onc.2012.303

Koukourakis, M. I., Mitrakas, A. G., and Giatromanolaki, A. (2016). Therapeutic interactions of autophagy with radiation and temozolomide in glioblastoma: evidence and issues to resolve. *Br. J. Cancer* 114, 485–496. doi: 10.1038/bjc.2016.19

Lee, A. W., Sze, W. M., Au, J. S., Leung, S. F., Leung, T. W., Chua, D. T., et al. (2005). Treatment results for nasopharyngeal carcinoma in the modern era: the Hong Kong experience. *Int. J. Radiat. Oncol. Biol. Phys.* 61, 1107–1116. doi: 10.1016/j.ijrobp.2004.07.702

Lee, H. S., Kang, Y., Tae, K., Bae, G. U., Park, J. Y., Cho, Y. H., et al. (2018). Proteomic biomarkers for bisphenol a-early exposure and women's thyroid cancer. *Cancer Res. Treat.* 50, 111–117. doi: 10.4143/crt.2017.001

Li, W. Y., Li, Q., Jing, L., Wu, T., Han, L. L., Wang, Y., et al. (2019). P57-mediated autophagy promotes the efficacy of EGFR inhibitors in hepatocellular carcinoma. *Liver Int.* 39, 147–157. doi: 10.1111/liv.13957

Li, Z. Q., Xia, Y. F., Liu, Q., Yi, W., Liu, X. F., Han, F., et al. (2006). Radiotherapy-related typing in 842 patients in canton with nasopharyngeal carcinoma. *Int. J. Radiat. Oncol. Biol. Phys.* 66, 1011–1016. doi: 10.1016/j.ijrobp.2006.06.028

Liu, S. C., Tsang, N. M., Chiang, W. C., Chang, K. P., Hsueh, C., Liang, Y., et al. (2013). Leukemia inhibitory factor promotes nasopharyngeal carcinoma progression and radioresistance. *J. Clin. Invest.* 123, 5269–5283. doi: 10.1172/JCI63428

Lomnytska, M. I., Becker, S., Bodin, I., Olsson, A., Hellman, K., Hellstrom, A. C., et al. (2011). Differential expression of ANXA6, HSP27, PRDX2, NCF2, and TPM4 during uterine cervix carcinogenesis: diagnostic and prognostic value. *Br. J. Cancer* 104, 110–119. doi: 10.1038/sj.bjc.6605992

Noreen, S., Gardner, Q. A., Fatima, I., Sadaf, S., and Akhtar, M. W. (2019). Upregulated expression of calcium-dependent annexin a6: a potential biomarker of ovarian carcinoma. *Proteomics Clin. Appl.* 14:e1900078. doi: 10.1002/prca.201900078

O'Sullivan, D., Dowling, P., Joyce, H., McAuley, E., McCann, A., Henry, M., et al. (2017). A novel inhibitory anti-invasive MAb isolated using phenotypic screening highlights AnxA6 as a functionally relevant target protein in pancreatic cancer. *Br. J. Cancer* 117, 1326–1335. doi: 10.1038/bjc.2017.306

Polivka, J. Jr., and Janku, F. (2014). Molecular targets for cancer therapy in the PI3K/AKT/mTOR pathway. *Pharmacol. Ther.* 142, 164–175. doi: 10.1016/j.pharmthera.2013.12.004

Roberts, P. J., and Der, C. J. (2007). Targeting the Raf-MEK-ERK mitogen-activated protein kinase cascade for the treatment of cancer. *Oncogene* 26, 3291–3310. doi: 10.1038/sj.onc.1210422

Shen, J., Zheng, H., Ruan, J., Fang, W., Li, A., Tian, G., et al. (2013). Autophagy inhibition induces enhanced proapoptotic effects of ZD6474 in glioblastoma. *Br. J. Cancer* 109, 164–171. doi: 10.1038/bjc.2013.306

Sun, Y., Li, W. F., Chen, N. Y., Zhang, N., Hu, G. Q., Xie, F. Y., et al. (2016). Induction chemotherapy plus concurrent chemoradiotherapy versus concurrent chemoradiotherapy alone in locoregionally advanced nasopharyngeal carcinoma: a phase 3, multicentre, randomised controlled trial. *Lancet Oncol.* 17, 1509–1520. doi: 10.1016/S1470-2045(16)30410-7

Varshney, P., and Saini, N. (2018). PI3K/AKT/mTOR activation and autophagy inhibition plays a key role in increased cholesterol during IL-17A mediated inflammatory response in psoriasis. *Biochim. Biophys. Acta Mol. Basis Dis.* 1864, 1795–1803. doi: 10.1016/j.bbadis.2018.02.003

Wang, P., Zhang, J., Zhang, L., Zhu, Z., Fan, J., Chen, L., et al. (2013). MicroRNA 23b regulates autophagy associated with radioresistance of pancreatic cancer cells. *Gastroenterology* 145, e1112. doi: 10.1053/j.gastro.2013.07.048

Wang, X., Fu, Y. F., Liu, X., Feng, G., Xiong, D., Mu, G. F., et al. (2018). ROS promote Ox-LDL-induced platelet activation by up-regulating autophagy through the inhibition of the PI3K/AKT/mTOR pathway. *Cell Physiol. Biochem.* 50, 1779–1793. doi: 10.1159/000494795

Wells, A. (1999). EGF receptor. *Int. J. Biochem. Cell Biol.* 31, 637–643. doi: 10.1016/s1357-2725(99)00015-1

Xu, Z., Han, X., Ou, D., Liu, T., Li, Z., Jiang, G., et al. (2020). Targeting PI3K/AKT/mTOR-mediated autophagy for tumor therapy. *Appl. Microbiol. Biotechnol.* 104, 575–587. doi: 10.1007/s00253-019-10257-8

Yao, K. C., Komata, T., Kondo, Y., Kanzawa, T., Kondo, S., and Germano, I. M. (2003). Molecular response of human glioblastoma multiforme cells to ionizing radiation: cell cycle arrest, modulation of the expression of cyclin-dependent kinase inhibitors, and autophagy. *J. Neurosurg.* 98, 378–384. doi: 10.3171/jns.2003.98.2.0378

Zhang, M., Liu, S., Chua, M. S., Li, H., Luo, D., Wang, S., et al. (2019). SOCS5 inhibition induces autophagy to impair metastasis in hepatocellular carcinoma cells via the PI3K/Akt/mTOR pathway. *Cell Death Dis.* 10, 799 doi: 10.1038/s41419-019-1856-y

Zhang, Y., Kwok-Shing, Ng, P., Kucherlapati, M., Chen, F., Liu, Y., et al. (2017). A pan-cancer proteogenomic atlas of pi3k/akt/mtor pathway alterations. *Cancer Cell* 31, 820.e3–832.e3. doi: 10.1016/j.ccell.2017.04.013

Conflict of Interest: The authors declare that the research was conducted in the absence of any commercial or financial relationships that could be construed as a potential conflict of interest.

frontiers in Cell and Developmental Biology

ORIGINAL RESEARCH
published: 14 May 2020
doi: 10.3389/fcell.2020.00293

ALKBH4 Functions as a Suppressor of Colorectal Cancer Metastasis via Competitively Binding to WDR5

Chaoqin Shen[1,2,3,4,5†], Tingting Yan[1,2,3,4,5†], Tianying Tong[1,2,3,4,5†], Debin Shi[6,7†], Linlin Ren[1,2,3,4,5†], Youwei Zhang[8†], Xinyu Zhang[1,2,3,4,5], Yingying Cao[1,2,3,4,5], Yuqing Yan[1,2,3,4,5], Yanru Ma[1,2,3,4,5], Xiaoqiang Zhu[1,2,3,4,5], Xianglong Tian[1,2,3,4,5], Jing-Yuan Fang[1,2,3,4,5], Haoyan Chen[1,2,3,4,5], Linhua Ji[9], Jie Hong[1,2,3,4,5*] and Baoqin Xuan[1,4*]*

[1] State Key Laboratory of Oncogenes and Related Genes, Ren Ji Hospital, School of Medicine, Shanghai Jiao Tong University, Shanghai, China, [2] Key Laboratory of Gastroenterology & Hepatology, Ministry of Health, Ren Ji Hospital, School of Medicine, Shanghai Jiao Tong University, Shanghai, China, [3] Division of Gastroenterology and Hepatology, Ren Ji Hospital, School of Medicine, Shanghai Jiao Tong University, Shanghai, China, [4] Shanghai Cancer Institute, Ren Ji Hospital, School of Medicine, Shanghai Jiao Tong University, Shanghai, China, [5] Shanghai Institute of Digestive Disease, Ren Ji Hospital, School of Medicine, Shanghai Jiao Tong University, Shanghai, China, [6] Department of Colorectal Surgery, Fudan University Shanghai Cancer Center, Shanghai, China, [7] Department of Oncology, Shanghai Medical College, Fudan University, Shanghai, China, [8] Department of Medical Oncology, Xuzhou Central Hospital, Xuzhou Medical University, Xuzhou, China, [9] Department of Gastrointestinal Surgery, Ren Ji Hospital, School of Medicine, Shanghai Jiao Tong University, Shanghai, China

OPEN ACCESS

Edited by:
Lei Chang,
Soochow University Medical College (SUMC), China

Reviewed by:
Yi Zhou,
Institute of Cancer, Xinqiao Hospital, China
Marco Sciacovelli,
MRC Cancer Unit, University of Cambridge, United Kingdom

***Correspondence:**
Linhua Ji
13564383793@163.com
Jie Hong
jiehong97@sjtu.edu.cn
Baoqin Xuan
bqxuan@126.com

† These authors have contributed equally to this work

Specialty section:
This article was submitted to Molecular and Cellular Oncology, a section of the journal Frontiers in Cell and Developmental Biology

Received: *02 February 2020*
Accepted: *06 April 2020*
Published: *14 May 2020*

Citation:
Shen C, Yan T, Tong T, Shi D, Ren L, Zhang Y, Zhang X, Cao Y, Yan Y, Ma Y, Zhu X, Tian X, Fang J-Y, Chen H, Ji L, Hong J and Xuan B (2020) ALKBH4 Functions as a Suppressor of Colorectal Cancer Metastasis via Competitively Binding to WDR5. Front. Cell Dev. Biol. 8:293. doi: 10.3389/fcell.2020.00293

Background: Epithelial-Mesenchymal Transition (EMT) is a major process in the initiation of tumor metastasis, where cancer cells lose sessile epithelial potential and gain mesenchymal phenotype. Large-scale cell identity shifts are often orchestrated on an epigenetic level and the interplay between epigenetic factors and EMT progression was still largely unknown. In this study, we tried to identify candidate epigenetic factors that involved in EMT progression.

Methods: Colorectal cancer (CRC) cells were transfected with an arrayed shRNA library targeting 384 genes involved in epigenetic modification. Candidate genes were identified by real-time PCR. Western blot, RNA-seq and gene set enrichment analysis were conducted to confirm the suppressive role of ALKBH4 in EMT. The clinical relevance of ALKBH4 in CRC was investigated in two independent Renji Cohorts and a microarray dataset (GSE21510) from GEO database. *In vitro* transwell assay and *in vivo* metastatic tumor model were performed to explore the biological function of ALKBH4 in the metastasis of CRC. Co-IP (Co-Immunoprecipitation) and ChIP (Chromatin Immunoprecipitation) assays were employed to uncover the mechanism.

Results: We screened for candidate epigenetic factors that affected EMT process and identified ALKBH4 as a candidate EMT suppressor gene, which was significantly downregulated in CRC patients. Decreased level of ALKBH4 was associated with metastasis and predicted poor prognosis of CRC patients. Follow-up functional experiments illustrated overexpression of ALKBH4 inhibited the invasion ability of CRC cells *in vitro*, as well as their metastatic capability *in vivo*. Mechanistically, CO-IP and ChIP assays indicated that ALKBH4 competitively bound WDR5 (a key component of

histone methyltransferase complex) and decreased H3K4me3 histone modification on the target genes including *MIR21*.

Conclusions: This study illustrated that ALKBH4 may function as a novel metastasis suppressor of CRC, and inhibits H3K4me3 modification through binding WDR5 during EMT.

Keywords: CRC, EMT, epigenetic modification, metastasis, ALKBH4

INTRODUCTION

Colorectal cancer (CRC) is the second leading cause of cancer-related mortality worldwide (Bray et al., 2018). Despite the advance of treatment strategies involving surgery and medical therapy in CRC over the past decade, metastasis of CRC to distal sites is still the foremost cause of poor patients' prognosis (Nishihara et al., 2013; Fidler and Kripke, 2015; Dekker and Sanduleanu, 2016). Nevertheless, the majority of CRC patients with distant metastasis are not appropriate candidates for conventional therapy and a paucity of effective clinical development exists for agents targeting the biological mechanisms underlying the metastatic process (Brenner et al., 2014). Consequently, identification and characterization of the molecular mechanism are imperative to facilitate the development of effective therapeutic strategies and biomarkers for CRC patients with metastasis.

Epithelial-Mesenchymal Transition (EMT) is a fundamental biological process in the initiation of tumor metastasis, which characterized as reversible loss of epithelial characteristics coupled with gain of mesenchymal properties (Thiery et al., 2009). Diverse lines of studies have revealed interesting links between EMT and epigenetic regulatory mechanisms. For instance, E-cadherin, which plays the essential role as a gatekeeper of the epithelial state in carcinomas (Hay, 1995; Vincent-Salomon and Thiery, 2003), has been discovered to be epigenetically suppressed. Moreover, it is becoming increasingly evident that the EMT is a high dynamic process that large-scale cell identity shifts are often orchestrated on a epigenetic level (Tam and Weinberg, 2013). However, the interplay between the modulation of epigenetic regulatory mechanisms and EMT remains poorly understood. Accordingly, although some molecular pathways explained the function of epigenetic factors in EMT have been partially elucidated, more straightforward targets and partners in the progression of EMT still need further exploration.

In recent years, RNAi technology has been well established as a useful tool for the construction of RNAi libraries and to reveal potential epigenetic markers modulating complex cellular processes at the genome-wide level (Westbrook et al., 2005a,b; Luo et al., 2008; Zender et al., 2008). Using an arrayed short hairpin RNA (shRNA) library targeting 384 genes involved in epigenetic modifications, we identified ALKBH4, a homolog of the *Escherichia coli* DNA demethylase AlkB family, as a suppressive modulator of EMT in CRC cells. In addition, low expression of ALKBH4 was associated with metastasis and poor prognosis in CRC patients and the biological function of ALKBH4 in CRC was also evaluated *in vitro* and *in vivo* models. Mechanically, ALKBH4 competitively bound WDR5 (a key component of histone methyltransferase complex) and decreased H3K4me3 histone modification on the target genes including *MIR21* and eventually prohibited EMT progression in CRC. Taken together, our study suggests that ALKBH4 is an upstream epigenetic inhibitor of EMT and may be a promising biomarker for CRC diagnosis and therapy.

MATERIALS AND METHODS

Clinical Patient Specimen Collection

Tumor tissues and matched corresponding non-cancerous tissues were recruited from patients with CRC who underwent surgical resections at Department of Surgery, Renji Hospital Affiliated to Shanghai Jiao Tong University School of Medicine from December 2011 to March 2016. This study was approved by the Ethics Committee of Renji Hospital, Shanghai Jiao Tong University School of Medicine. Written informed consent was obtained from all participants before enrollment in this study. All the research was carried out in accordance with the provisions of the Declaration of Helsinki of 1975.

Bioinformatics Analysis

CRC microarray datasets GSE21510 (Affymetrix Human Gene 1.0 ST Array) and their corresponding clinical data in this study were directly downloaded from Gene Expression Omnibus (GEO) database[1]. GSE21510 included 123 CRC samples and 25 non-tumor tissue samples.

Cell Culture and Treatment

Human CRC cell lines HCT116, HT29, and SW480 were purchased from American Type Culture Collection (ATCC). All cell lines were cultured as recommended in growth medium supplemented with 10% fetal bovine serum (FBS, Gibco, United States) and incubated at 37°C with a humidified atmosphere of 5% CO_2. ALKBH4 was overexpressed or knocked down by transduced with ALKBH4-overexpressing or ALKBH4 shRNA adenovirus, respectively. The vector was used as controls. Inhibition of miR-21 in cells were treated by miR-21 antagomir, and overexpression of miR-21 in cells were treated by miR-21 mimics (Genepharma, China).

[1]http://www.ncbi.nlm.nih.gov/geo/

Western Blot

Western blot analysis was performed as described previously (Shen et al., 2017). Total protein was extracted from CRC cells using a total protein extraction buffer (Beyotime, China) containing a protease inhibitor mixture (protease inhibitors; phosphatase inhibitors; PMSF; KangChen, Shanghai, China). BCA Protein Assay Kit (Pierce Biotechnology) was used to measure the concentration of protein. Proteins were separated by 10–12% SDS-polyacrylamide gels and transferred to PVDF membranes (Millipore, Bedford, MA, United States). After blocked with 5% BSA at room temperature for 1.5 h, the membranes were incubated overnight with primary rabbit anti-ALKBH4(1:1000 dilution, Sigma, United States), rabbit anti-E-cadherin (1:1000 dilution, CST, United States), rabbit anti-fibronectin (1:1000 dilution, CST, United States), rabbit anti- ZO-1 (1:1000 dilution, CST, United States), rabbit anti-N-cadherin (1:1000 dilution, CST, United States), and GAPDH (1:1000 dilution, KangChen, China) antibodies at 4°C, and then washed with TBST for five times and incubated with species-specific secondary antibodies for 1 h at room temperature the next day. At last, the ECL detection system was used for visualization. Antibodies against GAPDH acted as an internal control.

Immunohistochemical Staining

Human CRC tissue sections were rehydrated and treated with hydrogen peroxide for 15 min. Antigen retrieval was performed by microwave. After blocked with 10% normal goat serum for 30 min, the tissue microarray sections were incubated with ALKBH4 antibodies (1:200 dilution, Abcam, United Kingdom) on a humidified box at 4°C overnight. The next day, the sections were incubated with corresponding peroxidase-labeled secondary antibody for 30 min at room temperature and washed with PBS for three times. At last, Diaminobenzidine tetrahydrochloride (DAB; Maixin Biotech, China) was used for the color-reaction and hematoxylin was use for nucleus counterstaining. The immunohistochemical stained sections were observed under light microscopy.

Protein expression was assessed according to the intensity and extent of staining. The intensity of staining was evaluated on a scale of 0–3: 0, no staining; 1, weak staining; 2, moderate staining; 3, strong staining. The extent of ALKBH4 positive cells was assessed on a scale of 0–4: 0, 0–5%; 1, 6–25%; 2, 26–50%; 3, 51–75%; 4, 76–100%; A final score was obtained by using grades of the intensity staining × grades of extent. The tissues with a final score <6 were sorted into "ALKBH4 low expression" and those with a final score ≥ 6 were classified as "ALKBH4 high expression."

Total RNA Extraction and Quantitative Real-Time PCR

Total RNA was extracted from CRC cells, primary CRC tissues and adjacent non-cancerous tissues using Trizol reagent (Takara, Japan). Total RNA was reverse-transcribed using the PrimeScript RT Reagent Kit (Takara, Japan), and quantitative real-time PCR was performed using ABI reagent (Thermo Fisher Scientific, United States) by the StepOne real-time PCR system according to the manufacturer's instruction. Primer sequences used in this study were listed as follows:

ALKBH4, forward, 5′-GGTCAGCCTCAACCTCCTGT-3′; reverse, 5′-TATCACGCTGTCC ACCAAGG-3′.
GAPDH, forward, 5′-GCATTGCCCTCAACGACCAC-3′; reverse, 5′-CCACCACCCTGTT GCTGTAG-3′.

Transwell Invasion Assay

The transwell invasion assay were assessed using chambers (Millipore, United States). Initially, 2×10^5 cells in serum-free medium were cultured in the upper chamber of a 24-well plate, and the corresponding medium supplemented with 20% FBS was placed in the lower chamber. After 48 h of incubation, the migrated cells were fixed with 4% paraformaldehyde for 20 min, stained with 0.1% crystal violet for 20 min, washed with PBS for five times, air dried and counted under a light microscope. Each experiment was repeated three times.

Tumor Metastasis Model

Four-week-old male BALB/c nude mice were obtained from Experimental Animal Centre of Shanghai Laboratory Animal Center. HCT116 cells (5×10^6 cells) were injected subcutaneously into the right flank of these mice to establish the CRC metastasis model. Seven days after subcutaneous inoculation, mice were randomly divided into different groups and were injected with PBS, control- overexpressing adenovirus or ALKBH4-overexpressing adenovirus by ways of multipoint intratumoral injection twice a week for 13 weeks. The mice were sacrificed at week 13. The numbers of lung metastatic foci were determined in H&E stained lung tissue sections under a binocular microscope (Leica, DM 300). All experimental procedures were approved by the Institutional Animal Care and Use Committee of Renji Hospital, Shanghai Jiao Tong University School of Medicine.

Co-IP Assay

Coimmunoprecipitation was performed as described previously (Uyama et al., 2006). Briefly, HCT116 cells were harvested after indicated treatment. The whole-cell lysates were incubated with 2 μg of antibody or normal rabbit IgG at 4°C overnight, and two additional hours with 20 μl of 50% protein A agarose. Both input and IP samples were analyzed by western blot using various antibodies at the indicated dilutions: anti-WDR5 antibody (1:1000; Abcam), anti-H3K4me3 antibody (1:1000; CST) and anti- ALKBH4 (1:1000; Sigma).

ChIP and High-Throughput Sequencing

Chromatin immunoprecipitation and high-throughput sequencing (ChIP-seq) was performed as follows. ChIP assays were conducted using the ChIP Assay Kit (Millipore, United States) according to the manufacturer's protocols. HCT116 cells were seeded into 10 cm culture dish. Cells were cross-linked with formaldehyde and collected using SDS lysis buffer. The chromatin was sonicated to lengths between 200 and 1000 bp. The DNA-protein complexes were pre-cleared with Protein A Agarose/Salmon DNA and then immunoprecipitated

with anti-WDR5 antibody, anti-H3K4me3 antibody and normal rabbit IgG. The co-precipitated DNAs were purified using phenol/chloroform and subjected to real-time PCR analysis. Library generation was performed using pooled ChIP DNA samples from three independent ChIP preparations using the Illumina protocol. Briefly, ChIP DNA fragment ends were repaired and phosphorylated using Klenow, T4 DNA polymerase and T4 polynucleotide kinase (Illumina kit components, United States). After ligation of Illumina adapters, DNA was size selected by gel purification and then PCR amplified using Illumina primers. Sequencing was performed at Genenergy Inc, Shanghai on an Illumina Hi-Seq 3000 machine. The FASTQ files were aligned to hg19 using Bowtie. Enriched regions were determined by the MACS program[2] (Zhang et al., 2008) with a default setting.

RNA Sequencing

ALKBH4 shRNA adenovirus was transduced into HT29 cells and high-throughput RNA sequencing was performed after knockdown of ALKBH4 in HT29 cells. For RNA sequencing of shRNA-transduced HT29 cells, each sample was cleaned up on a RNeasy Mini Column (Qiagen, Limburg, Netherlands), treated with DNase, and analyzed for quality on an Agilent 2100 Bioanalyzer. Samples were on an Illumina HiSeq 3000 for 2 × 150-bp paired-end sequencing. The RNAseq data analysis was performed according to the TopHat-HTSeq-DeSeq2 frame (Anders et al., 2013). Briefly, reads were mapped to the human genome (hg19) using TopHat v2.0.11[3] (Kim et al., 2013) with the default options with a TopHat transcript index built from Ensembl_GRCh37. Count files of the aligned sequencing reads were generated by the htseq-count script from the Python package HTSeq with union mode, using the GTF annotation file (Anders et al., 2015).The read counts from each sequenced sample were combined into a count file, which was subsequently used for the differential expression analysis. Differential analyses were performed to the count files using DESeq2 packages, following standard normalization procedures (Love et al., 2014). Genes with <5 total counts in both conditions were removed from further analysis.

RNAi Screening

Lentiviral shRNAs were arrayed for testing. Briefly, HT29 cells were transduced at a multiplicity of infection (MOI) of 0.3 in 96-well plate and real-time PCR was performed after 72 h.

Statistical Analysis

All statistical analyses were carried out using R-3.0.2[4]. Correlation between ALKBH4 expression and clinicopathologic parameters in patients with CRC was examined by chi-square test. Overall survival was evaluated by Kaplan–Meier survival curve and analyzed by the log-rank test. Data from at least three independent experiments conducted in triplicates were presented as the mean ± SEM. The correlation of the two variables was examined by Spearman correlation test. Differences were considered to be significant with a value of $p < 0.05$.

[2]https://pypi.org/project/MACS2/

[3]http://tophat.cbcb.umd.edu

[4]http://cran.r-project.org/bin/windows/base/old/3.0.2/

RESULTS

ALKBH4 Suppressed EMT in CRC

For the purpose of identifying candidate epigenetic factors that involved in EMT progression, we performed an *in vitro* screening system using highly sensitive and quantitative lentiviral RNAi library. Briefly, human CRC cell line HT29, which exhibited higher expression of ALKBH4, was transduced with an arrayed lentiviral shRNA library targeting 384 genes involved in epigenetic modifications (**Figure 1A** and **Supplementary Figure S1A**). The expression of E-cadherin (encoded by the *CDH1* gene) was used as a screening criterion to select epigenetic genes involved in the EMT. Among all these candidate epigenetic genes, we discovered that knockdown of ALKBH4 has the most negative correlation with the relative expression of CDH1 in human CRC cells transduced with an arrayed shRNA library (**Figure 1B**). The results indicated that ALKBH4 might negatively regulate the progression of EMT in human CRC cells.

To confirm the suppressive role of ALKBH4 in EMT, Western blot assay was performed to detect the expression of both epithelial and mesenchymal molecular markers in ALKBH4-downregulated or ALKBH4-upregulated CRC cells. Obviously, downregulation of ALKBH4 significantly reduced the expression of epithelial markers, E-cadherin and zonula occludens-1 (ZO-1), and increased the expression of mesenchymal markers, Fibronectin and N-cadherin in HT29 and SW480 cells (**Figures 1C,D**). Conversely, overexpression of ALKBH4 significantly upregulated the expression of E-cadherin and ZO-1, and inhibited the expression of Fibronectin and N-cadherin in HCT116 cells (**Figure 1E**). Next, RNA sequencing (RNA-seq) analysis was performed to compare the gene expression profiles of CRC cells transduced with ALKBH4 shRNA and control shRNA. A total of 1157 downregulated genes and 3396 upregulated genes were detected after knockdown of ALKBH4 in CRC cells (**Supplementary Table S1**). Gene set enrichment analysis (GSEA) illustrated that "CHANDRAN_METASTASIS _UP" pathway was positively correlated with the downregulation of ALKBH4 in CRC cells (**Figure 1F**). These data strongly implicate that ALKBH4 may regulate EMT process in a suppressive way.

Low Expression of ALKBH4 Is Clinically Related to Metastasis and Poor Prognosis in CRC

It is documented that EMT is a critical event involved in the metastasis of CRC (Cao et al., 2015). Accordingly, we further analyzed the clinical significance of ALKBH4 in human samples. Real-time PCR revealed that the mRNA expression of ALKBH4 was significantly decreased in CRC tissues compared with paired adjacent non-tumor tissues from patients in Renji Cohort 1 (**Figure 2A** and **Supplementary Table S2**). Moreover, similar results can be counted in the

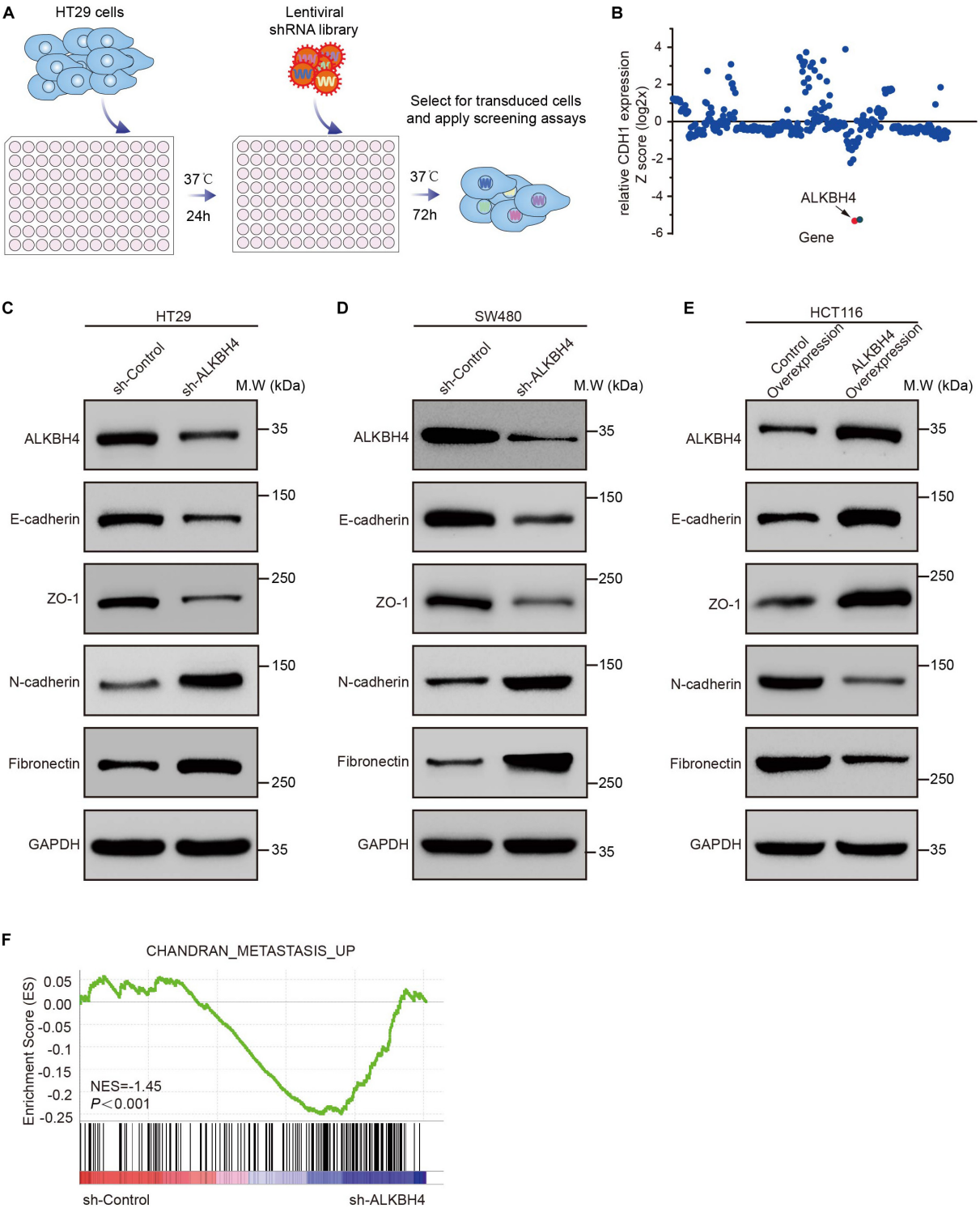

FIGURE 1 | The suppressive role of ALKBH4 during EMT in CRC cells. **(A)** Schematic representation of the experimental workflow. HT29 cells were transduced with an arrayed lentiviral shRNA library targeting 384 genes involved in epigenetic modification. After 72 h transfection, RNA was extracted and real-time PCR was performed. **(B)** Dot plot of the lentiviral shRNA library screening result. The *y*-axis represents the *z*-scores for the relative CDH1 expression for each targeted gene. **(C,D)** Immunoblots of epithelial (E-cadherin and ZO-1) and mesenchymal (Fibronectin and N-cadherin) markers in HT29 and SW480 cells after ALKBH4 shRNA virus transduction, compared with control shRNA virus. GAPDH was used as a loading control. **(E)** Immunoblots of epithelial (E-cadherin and ZO-1) and mesenchymal (Fibronectin and N-cadherin) markers in HCT116 cells after transduced with ALKBH4-overexpressed virus and control- overexpressed virus. GAPDH was used as a loading control. **(F)** GSEA analysis of HT29 cells transduced with ALKBH4 shRNA virus.

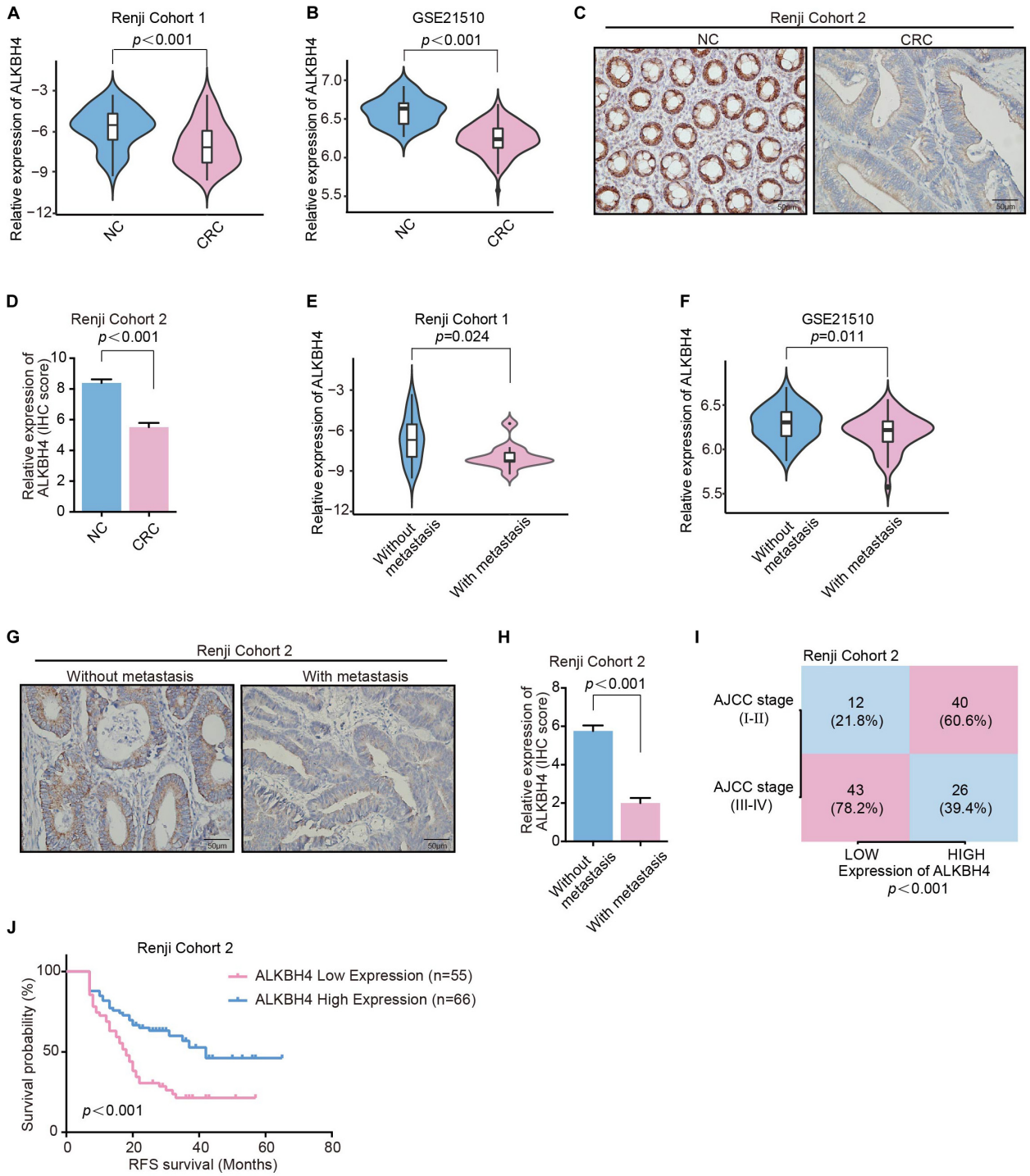

FIGURE 2 | Downregulation of ALKBH4 correlates with metastasis and poor prognosis in CRC patients. **(A,B)** The relative expression of ALKBH4 in CRC tissues and adjacent non-tumor colorectal tissues were detected in Renji Cohort 1 **(A)** and dataset GSE21510 **(B)**, non-parametric Mann–Whitney test. **(C,D)** Representative immunohistochemistry images **(C)** and relative quantitative information **(D)** of CRC tissues and adjacent normal tissues for the protein levels of ALKBH4 in Renji Cohort 2, non-parametric Mann–Whitney test. **(E,F)** The relative expression of ALKBH4 in CRC tissues in patients with or without metastasis were detected in Renji Cohort 1 **(E)** and dataset GSE21510 **(F)**, non-parametric Mann–Whitney test. **(G,H)** Representative immunohistochemistry images **(G)** and relative quantitative information **(H)** of CRC tissues in patients with or without metastasis for the protein levels of ALKBH4 in Renji Cohort 2, non-parametric Mann–Whitney test. **(I)** Percentage of CRC patients with high expression and low expression of ALKBH4 stratified according to AJCC stage in Renji Cohort 2 (n = 121), Chi-square test. **(J)** Survival curves were generated using the Kaplan–Meier method and the log-rank test was used to evaluate the statistical significance of differences between CRC patients in Renji Cohort 2 with High or Low ALKBH4 expression, Log-rank test. Error bars in the scatter plots represent SEM.

microarray dataset (GSE21510) from GEO database that the mRNA expression of ALKBH4 was markedly decreased in human CRC tissues than in normal tissues (**Figure 2B**). Then, to examine endogenous ALKBH4 protein expression, we performed immunohistochemistry staining (IHC) on paraffin-embedded CRC tissues. The results showed a dramatically decreased expression of ALKBH4 in tumor tissues than paired non-tumor tissues from patients in Renji cohort 2 (**Figures 2C,D** and **Supplementary Table S3**).

Furthermore, the association between ALKBH4 expression and clinicopathological characteristics was analyzed. Analysis of the primary tumor tissue showed that patients with distant metastasis exhibited lower mRNA expression of ALKBH4 than those without metastasis both in Renji Cohort1 (**Figure 2E**) and microarray dataset (GSE21510) from GEO database (**Figure 2F**). IHC staining also confirmed that CRC patients with metastasis had a significantly lower expression of ALKBH4 (**Figures 2G,H**). In addition, ALKBH4 expression was negatively correlated with America Joint Committee on Cancer (AJCC) stage (**Figure 2I**). Kaplan–Meier analysis showed that CRC patients with low ALKBH4 expression had significantly shorter recurrence-free survival time than CRC patients with high ALKBH4 expression (**Figure 2J**). Collectively, these results indicate that low expression of ALKBH4 is clinically associated with metastasis and poor prognosis in CRC patients.

ALKBH4 Inhibits Invasion *in vitro* and Metastasis *in vivo* in CRC

To investigate the biological function of ALKBH4 in the metastasis of CRC, *in vitro* and *in vivo* experiments were conducted. As exhibited in the transwell invasion assays, knockdown of ALKBH4 significantly increased the invasion capability of HT29 and SW480 cells (**Figure 3A**). Conversely, the invasive ability was inhibited when ALKBH4 was overexpressed in HCT116 cells (**Figure 3B**). Furthermore, overexpression of ALKBH4 dramatically reduced lung metastasis in metastatic tumor model (**Figures 3C,D**). Notably, mice inoculated with ALKBH4-upregulated CRC cells had a longer overall survival time than the control groups (**Figure 3E**). Collectively, these results suggest that upregulation of ALKBH4 can inhibit the invasive ability of CRC cells *in vitro* and the metastatic capacity *in vivo*.

ALKBH4 Decreases Histone H3K4me3 Modification by Interacting With WDR5

We further explore the mechanism by which ALKBH4 repressed EMT and metastasis in CRC. ALKBH4 belongs to the AlkB family of non-heme Fe (II)/a-ketoglutarate-dependent dioxygenases, whose function has been implicated in the repair of methylation damage in DNA and RNA (Lee et al., 2005). To determine whether the downregulated level of ALKBH4 in CRC cells may promote the alteration in methylation level, Western blot assay was performed to detect the epigenetic modification. The assay demonstrated that overexpression of ALKBH4 resulted in the significant reduction of H3K4me3, but not H3K79me2 (**Figure 4A**). Downregulation of ALKBH4 significantly increased the expression of H3K4me3, but not H3K79me2 (**Figures 4B,C**). Given that WDR5 is a methyltransferase of H3K4me3 (Dou et al., 2006; van Nuland et al., 2013), we speculated the possibility of the interaction between ALKBH4 and WDR5. Co-IP (Co-Immunoprecipitation) assay was then conducted and the results showed that WDR5 and ALKBH4 interacted with each other in HCT116 cells (**Figures 4D,E**). The results indicated that ALKBH4 may regulate histone H3K4me3 modification through interacting with WDR5. To address whether ALKBH4 modulates WDR5 and H3K4me3 genomic binding genome-wide, we performed chromatin immunoprecipitation coupled with high-throughput sequencing (ChIP-seq) for WDR5 and H3K4me3 in ALKBH4-upregulated and control HCT116 cells. ChIP-seq analysis showed that 84 genes exhibited decreased binding to WDR5 after overexpression of ALKBH4 (**Figure 4F**). Furthermore, upregulation of ALKBH4 led to a decrease in H3K4me3 modification of 25,921 gene promoters (**Figure 4F**). Sixty-three genes showed both decreased binding to WDR5 and reduced H3K4me3 modification in ALKBH4-overexpressed cells (**Figure 4F**). Histone H3K4me3 modification is a hallmark for transcription initiation and associated with active gene transcription (Zhang et al., 2016; Batie et al., 2019). The GO analysis showed that WDR5 binding efficiency and H3K4me3 modification level were significantly decreased in the promoter region of those genes, which may regulate EMT and wound healing, after transduction of ALKBH4 overexpression virus in HCT116 cells (**Figure 4G**). The data suggested that ALKBH4 decreased histone H3K4me3 modification by competitively binding to WDR5 and suppressed EMT and metastasis in CRC.

Downregulation of ALKBH4 Promotes EMT Progression in CRC via miR-21

Among the overlapping genes, we discovered miR-21, which has been considered as a representative oncogenic miRNA and also associated with EMT and a poor prognosis in CRC (Yang et al., 2017), might be an essential downstream target. Overexpression of ALKBH4 significantly decreased the expression of miR-21 in HCT116 cells (**Figure 5A**). The ChIP-PCR data further indicated that WDR5 and H3K4me3 directly bound to the promoter region of miR-21 (**Figures 5B,C**). Moreover, overexpression of ALKBH4 resulted in a decrease in the binding efficiency of WDR5 and the modification level of H3K4me3 in miR-21 promoter (**Figures 5D,E**). In addition, real-time PCR data showed there was a significantly negative correlation between ALKBH4 and miR-21 both in microarray dataset (GSE21510) from GEO database and Renji Cohort1 (**Figures 5F,G**). MiR-21 was significantly increased in CRC tissues compared with paired adjacent non-tumor tissues from patients in Renji Cohort 1, especially in patients with metastasis (**Figure 5H**). Furthermore, real-time PCR data showed that down-regulation of WDR5 increased the expression of E-cadherin and ZO-1, and decreased the expression of miR-21, N-cadherin and Fibronection in HCT116 cells (**Supplementary Figures S2A,B**). These data indicated that overexpression of ALKBH4 inhibits the expression of miR-21 by decreasing H3K4me3 modification in the promoter region.

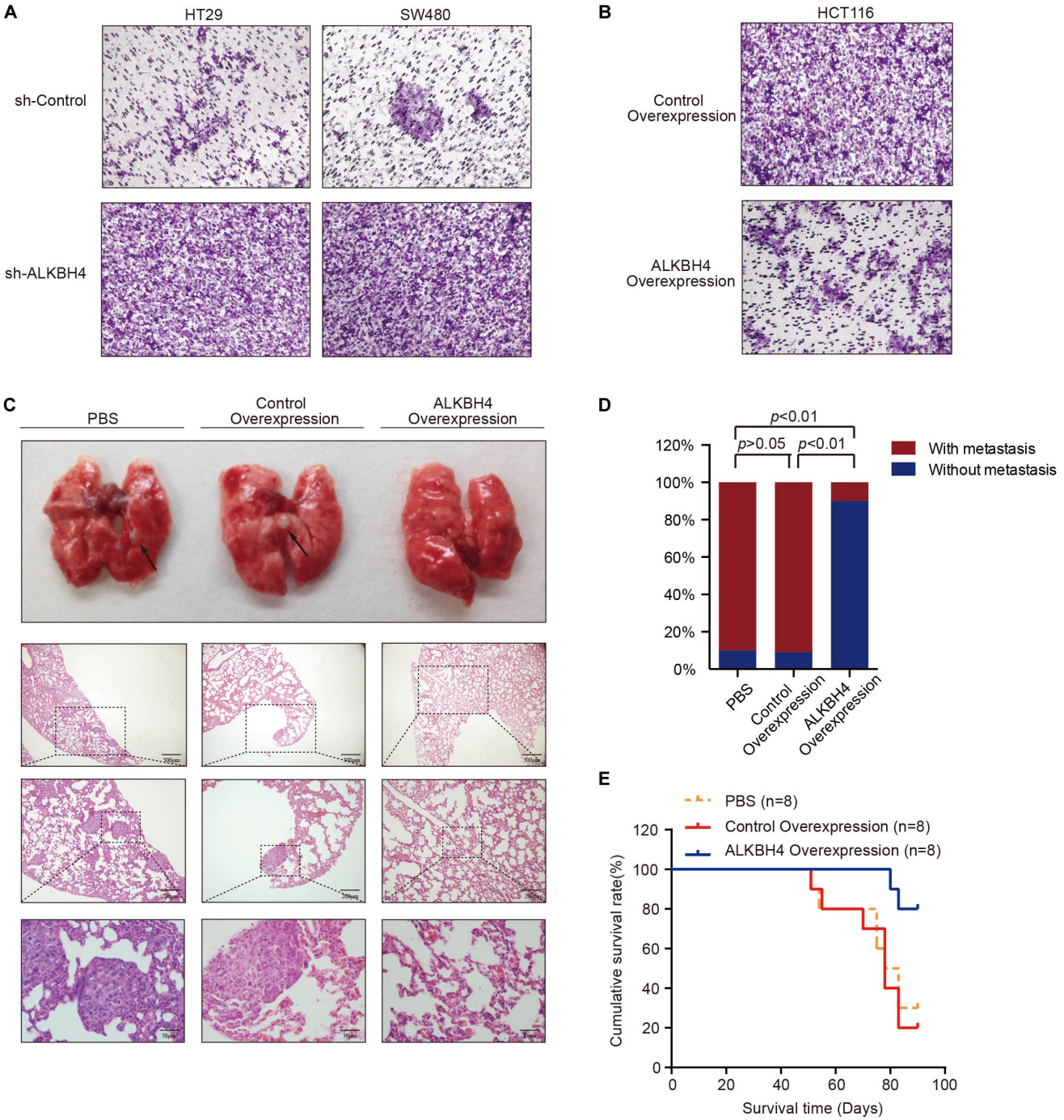

FIGURE 3 | ALKBH4 inhibits cell invasion *in vitro* and metastasis *in vivo*. **(A)** Transwell invasion assay was performed in HT29 **(left)** and SW480 **(right)** cells transduced with ALKBH4 shRNA virus and control shRNA virus; $n = 3$. **(B)** Transwell invasion assay was performed in HCT116 cells transduced with ALKBH4-overexpressed virus and control-overexpressed virus; $n = 3$. **(C)** Pulmonary metastases and representative hematoxylin and eosin staining of nude mice at 13 weeks after intratumorally injected with PBS, control-overexpressed virus or ALKBH4-overexpressed virus; $n = 8$. **(D)** Summarized data on tumor lung foci in nude mice at 13 weeks in PBS, control-overexpression or ALKBH4 overexpression groups; $n = 8$. **(E)** Survival analysis was performed in nude mice bearing colorectal cancer transfected with PBS, control virus or ALKBH4 overexpression virus, respectively; $n = 8$, log-rank test.

Furthermore, to validate whether ALKBH4 inhibits EMT progress via decreasing miR-21, we performed rescue experiments. Real-time PCR data demonstrated that the decreased expression of E-cadherin and ZO-1 and increased expression of N-cadherin and Fibronection caused by downregulation of ALKBH4 could be partially reversed

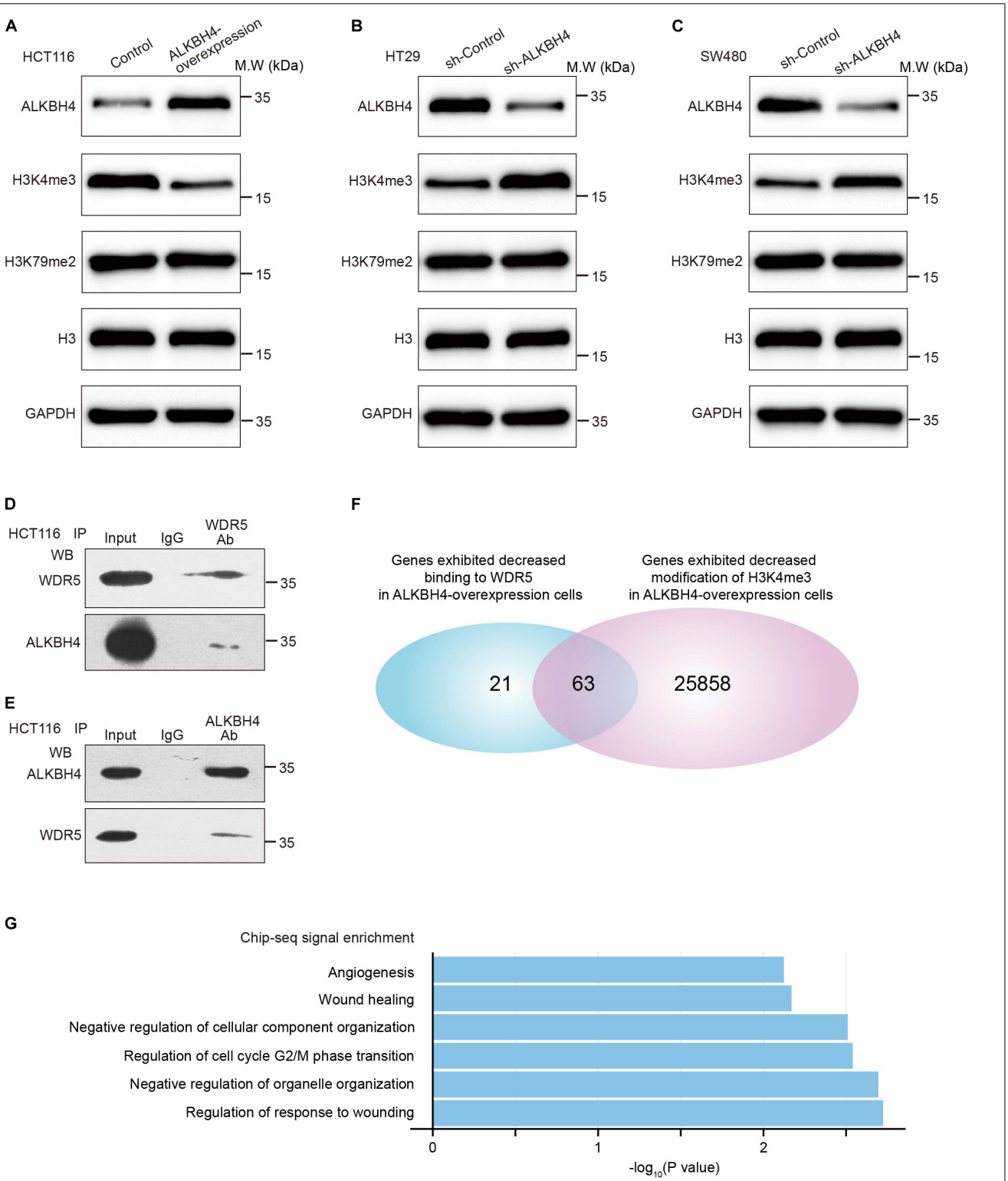

FIGURE 4 | ALKBH4 decreases histone H3K4me3 modification by interacting with WDR5. **(A)** Immunoblot of ALKBH4, H3K4me3, and H3K79me2 in HCT116 cells transduced with ALKBH4-overexpressed virus and control virus. H3 and GAPDH were used as loading controls. **(B,C)** Immunoblot of ALKBH4, H3K4me3, and H3K79me2 in HT29 **(B)** and SW480 **(C)** cells transduced with sh-ALKBH4 and sh-Control virus. H3 and GAPDH were used as loading controls. **(D,E)** coimmunoprecipitation detected the interaction of WDR5 and ALKBH4 in the HCT116 cells. The input and WDR5 **(D)** or ALKBH4 **(E)** immunoprecipitates were separated by SDS-PAGE. The specific immunoprecipitation of WDR5 and ALKBH4 was confirmed by Western blot. **(F)** Venn diagram shows 63 genes with both decreased binding to WDR5 and reduced H3K4me3 modification in ALKBH4 overexpressed cells. **(G)** GO enrichment analysis of 63 overlapping genes.

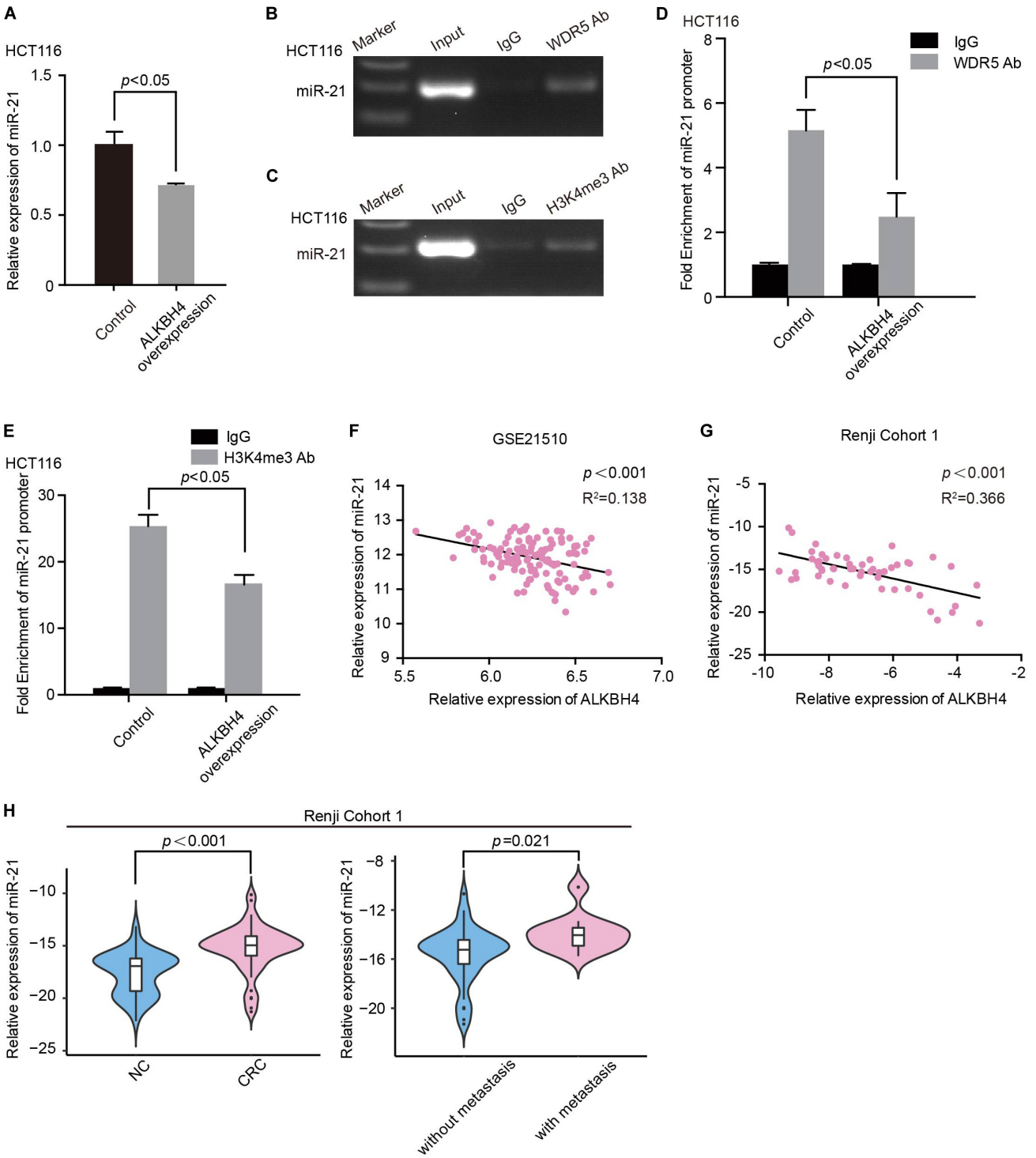

FIGURE 5 | ALKBH4 inhibits miR-21 by decreasing H3K4me3 modification in the promoter region. **(A)** Real-time PCR result of miR-21 expression after transduction of ALKBH4 overexpression adenovirus in HCT116 cells; $n = 3$, non-parametric Mann–Whitney test. **(B,C)** miR-21 was detected in the chromatin sample immunoprecipitated from HCT116 cells using an antibody against WDR5 **(B)** or H3K4me3 **(C)**. **(D,E)** Real-time PCR of the ChIP samples shows the binding efficiency of WDR5 **(D)** or H3K4me3 **(E)** to the miR-21 promoter after transduction of ALKBH4 overexpression adenovirus in HCT116 cells; $n = 3$, non-parametric Mann–Whitney test. **(F,G)** The correlation between the relative expression of ALKBH4 and miR-21 in dataset GSE21510 **(F)** and Renji Cohort 1 **(G)**. **(H)** The relative expression of miR-21 was detected in CRC tissues from patients with or without metastasis and adjacent non-tumor colorectal tissues (Renji Cohort 1), non-parametric Mann–Whitney test. Error bars in the scatter plots represent SEM.

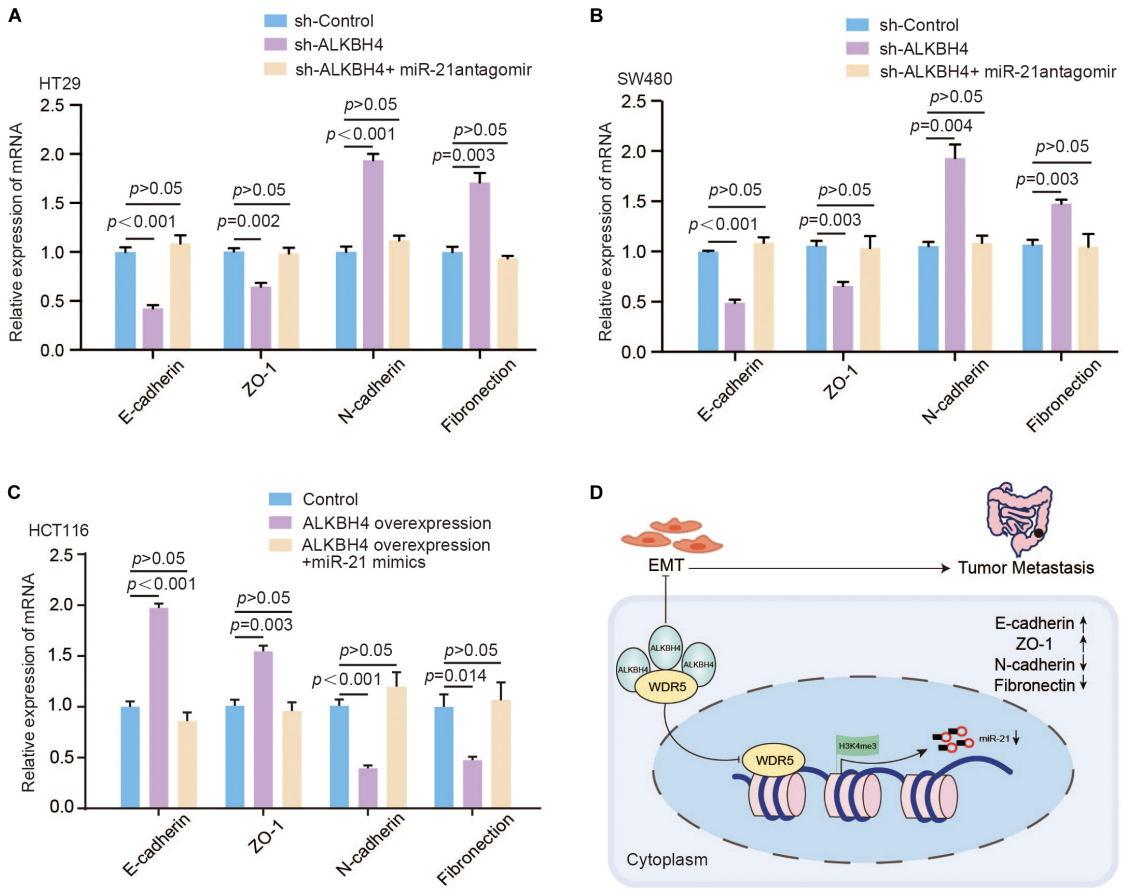

FIGURE 6 | ALKBH4 regulates EMT through modulating the expression of miR-21. **(A,B)** Real-time PCR results of molecular markers of EMT in HT29 **(A)** or SW480 **(B)** cells after sh-ALKBH4 virus and/or miR-21 antagomir treatment; $n = 3$, non-parametric Mann–Whitney test. **(C)** Real-time PCR results of molecular markers of EMT in HCT116 cells after overexpression of ALKBH4 and miR-21; $n = 3$, non-parametric Mann–Whitney test. **(D)** A schematic model of ALKBH4 functions in the metastasis of CRC. ALKBH4 may competitively bound WDR5 and decreased histone H3K4me3 modification on miR-21 promoter and eventually prohibited EMT progression in the metastasis of CRC. Error bars in the scatter plots represent SEM.

by knocking down of miR-21 (**Figures 6A,B**). Meanwhile, upregulation of miR-21 significantly reversed the increased expression of E-cadherin and ZO-1 and decreased expression of N-cadherin and Fibronection in ALKBH4-upregulated cells (**Figure 6C**).

Taken together, ALKBH4 competitively bound WDR5 and decreased histone H3K4me3 modification on miR-21 promoter and eventually prohibited EMT progression in CRC (**Figure 6D**).

DISCUSSION

Metastasis of tumor remains one of the most urgent and poorly addressed challenges in cancer therapy (Fidler and Kripke, 2015). Epithelial-Mesenchymal Transition and its associated cellular changes have been implicated to play a critical role in the metastasis process (Dongre and Weinberg, 2019), yet the interplay between the epigenetic regulatory mechanisms and EMT remains largely unknown. Using a high-content screen with a shRNA library covering 384 genes involved in modulating epigenetic modification, we have identified that ALKBH4 regulates cellular EMT process in a suppressive way. In cultured CRC cells and mouse tumor metastasis models, overexpression of ALKBH4 markedly inhibits cell migration *in vitro* and metastasis *in vivo*. Accordingly, our results consistently point to the notion that ALKBH4 serves as an essential regulator in inhibiting metastasis of CRC.

During the carcinogenesis in CRC, major cellular functions and pathways, including potential to repair DNA damage, are dysregulated (AlDubayan et al., 2018). ALKBH4 belongs to the AlkB family of non-heme Fe (II)/a-ketoglutarate-dependent dioxygenases, whose function have been implicated in the repair of methylation damage in DNA and RNA (Lee et al., 2005). Available evidences also indicate that several members of AlkB family, such as ALKBH3 and ALKBH5, are closely linked to the inhibition of tumorigenesis and progression in various human cancers (Stefansson et al., 2017; Wang et al., 2018; Zhu et al., 2019). ALKBH4 has been previously illustrated in mediating demethylation of a monomethylated site in actin and depletion of ALKBH4 contributes to defects in cytokinesis and cell motility

(Li et al., 2013), however, the underlying molecular mechanisms of ALKBH4 in tumor remain unknown. In our study, ALKBH4 markedly suppressed EMT and CO-IP assay demonstrated that ALKBH4 directly interacted with WDR5 in CRC cells, a key component of histone methyltransferase complex, along with the decreased level of H3K4me3 histone modification (Dou et al., 2006; van Nuland et al., 2013). The previous studies have shown that WDR5 is a major driver of cell progression in various cancer types (Kim et al., 2014; Chen et al., 2015; Dai et al., 2015) and its functional mechanism has been elucidated in CRC by triggering EMT process in response to the PI3K/AKT signaling pathway (Tan et al., 2017). As a consequence, we inferred that ALKBH4 may competitively bind to WDR5, and thus decrease H3K4me3 histone modification on the target genes. It has been documented that aberrant epigenetic signatures are associated with cancer metastasis and deficiency of H3K4 methyltransferase extends the life span in Caenorhabditis elegans (Greer et al., 2010),which are in accordance with our results from a mechanistic perspective.

When we explored the mechanism by which ALKBH4 contributes to the inhibition in metastasis of CRC. We discovered the involvement of miR-21, which is a major player involved in tumor initiation, progression and metastasis of various types of cancers (Frankel et al., 2008; Zhu et al., 2008; Qi et al., 2009; Tian et al., 2019), including CRC (Yang et al., 2017), and considered as a representative oncogenic miRNA. Interestingly, EMT can be inhibited by down-regulating miR-21 expression in breast cancer cell (Du et al., 2019). These observations are consistent with our findings that ALKBH4 suppresses the expression of miR-21 by decreasing H3K4me3 modification in the promoter region and eventually inhibits EMT in CRC cells.

In summary, our study elucidates the mechanism of ALKBH4 in inhibiting the EMT and metastasis of CRC. These findings add diverse roles and mechanistic insight into our understanding of the interplay between epigenetic factors and EMT progression, defining ALKBH4 as a potential prognostic biomarker for the prevention of cancer cell invasion and metastatic spread.

DATA AVAILABILITY STATEMENT

The authors declare that all data supporting the conclusions of this study are presented within the article and the **Supplementary Material** and are available from the authors.

ETHICS STATEMENT

The studies involving human participants were reviewed and approved by the Ethics Committee of Renji Hospital, Shanghai Jiao Tong University School of Medicine. The patients/participants provided their written informed consent to participate in this study. The animal study was reviewed and approved by the Ethics Committee of Renji Hospital, Shanghai Jiao Tong University School of Medicine.

AUTHOR CONTRIBUTIONS

CS, TY, TT, DS, LR, YZ, XZha, YC, YY, YM, XZhu, and XT performed the experiments and analyzed data. J-YF and LJ provided the clinical specimen. HC conducted the data analysis. JH and BX conceived and wrote the manuscript and supervised the study.

FUNDING

This work was supported by grants from the National Natural Science Foundation (81871901, 81790632, 81874159, and 81522008); "Shu Guang" project supported by Shanghai Municipal Education Commission and Shanghai Education Development Foundation (17SG-17); Shuobo fund from the State Key Laboratory of Oncogenes and Related Genes (No. SB1906); Shanghai Municipal Education Commission—Gaofeng Clinical Medicine Grant Support (Nos. 20152512 and 20161309).

ACKNOWLEDGMENTS

We thank the reviewers and editors for their constructive comments.

SUPPLEMENTARY MATERIAL

The Supplementary Material for this article can be found online at: https://www.frontiersin.org/articles/10.3389/fcell.2020.00293/full#supplementary-material

REFERENCES

AlDubayan, S. H., Giannakis, M., Moore, N. D., Han, G. C., Reardon, B., Hamada, T., et al. (2018). Inherited DNA-repair defects in colorectal cancer. *Am. J. Hum. Genet.* 102, 401–414. doi: 10.1016/j.ajhg.2018.01.018

Anders, S., McCarthy, D. J., Chen, Y., Okoniewski, M., Smyth, G. K., Huber, W., et al. (2013). Count-based differential expression analysis of RNA sequencing data using R and bioconductor. *Nat. Protoc.* 8, 1765–1786. doi: 10.1038/nprot.2013.099

Anders, S., Pyl, P. T., and Huber, W. (2015). HTSeq–a Python framework to work with high-throughput sequencing data. *Bioinformatics* 31, 166–169. doi: 10.1093/bioinformatics/btu638

Batie, M., Frost, J., Frost, M., Wilson, J. W., Schofield, P., and Rocha, S. (2019). Hypoxia induces rapid changes to histone methylation and reprograms chromatin. *Science* 363, 1222–1226. doi: 10.1126/science.aau5870

Bray, F., Ferlay, J., Soerjomataram, I., Siegel, R. L., Torre, L. A., and Jemal, A. (2018). Global cancer statistics 2018: GLOBOCAN estimates of incidence and mortality worldwide for 36 cancers in 185 countries. *CA Cancer J. Clin.* 68, 394–424. doi: 10.3322/caac.21492

Brenner, H., Kloor, M., and PoxC, P. (2014). Colorectal cancer. *Lancet* 383, 1490–1502. doi: 10.1016/s0140-6736(13)61649-9

Cao, H., Xu, E., Liu, H., Wan, L., and Lai, M. (2015). Epithelial-mesenchymal transition in colorectal cancer metastasis: a system review. *Pathol. Res. Pract.* 211, 557–569. doi: 10.1016/j.prp.2015.05.010

Chen, X., Gu, P., Li, K., Xie, W., Chen, C., Lin, T., et al. (2015). Gene expression profiling of WDR5 regulated genes in bladder cancer. *Genomics Data* 5, 27–29. doi: 10.1016/j.gdata.2015.05.003

Dai, X., Guo, W., Zhan, C., Liu, X., Bai, Z., and Yang, Y. (2015). WDR5 expression is prognostic of breast cancer outcome. *PLoS One* 10:e0124964. doi: 10.1371/journal.pone.0124964

Dekker, E., and Sanduleanu, S. (2016). Colorectal cancer: strategies to minimize interval CRC in screening programmes. *Nat. Rev. Gastroenterol. Hepatol.* 13, 10–12. doi: 10.1038/nrgastro.2015.216

Dongre, A., and Weinberg, R. A. (2019). New insights into the mechanisms of epithelial-mesenchymal transition and implications for cancer. *Nat. Rev. Mol. Cell. Biol.* 20, 69–84. doi: 10.1038/s41580-018-0080-4

Dou, Y., Milne, T. A., Ruthenburg, A. J., Lee, S., Lee, J. W., Verdine, G. L., et al. (2006). Regulation of MLL1 H3K4 methyltransferase activity by its core components. *Nat. Struct. Biol.* 13, 713–719. doi: 10.1038/nsmb1128

Du, Q., Zhang, X., Zhang, X., Wei, M., Xu, H., and Wang, S. (2019). Propofol inhibits proliferation and epithelial-mesenchymal transition of MCF-7 cells by suppressing miR-21 expression. *Artif. Cells Nanomed. Biotechnol.* 47, 1265–1271. doi: 10.1080/21691401.2019.1594000

Fidler, I. J., and Kripke, M. L. (2015). The challenge of targeting metastasis. *Cancer Metastasis Rev.* 34, 635–641. doi: 10.1007/s10555-015-9586-9

Frankel, L. B., Christoffersen, N. R., Jacobsen, A., Lindow, M., Krogh, A., and Lund, A. H. (2008). Programmed cell death 4 (PDCD4) is an important functional target of the microRNA miR-21 in breast cancer cells. *J. Biol. Chem.* 283, 1026–1033. doi: 10.1074/jbc.m707224200

Greer, E. L., Maures, T. J., Hauswirth, A. G., Green, E. M., Leeman, D. S., Maro, G. S., et al. (2010). Members of the H3K4 trimethylation complex regulate lifespan in a germline-dependent manner in *C. elegans*. *Nature* 466, 383–387. doi: 10.1038/nature09195

Hay. (1995). An overview of epithelio-mesenchymal transformation. *Acta Anatom.* 154, 8–20. doi: 10.1159/000147748

Kim, D., Pertea, G., Trapnell, C., Pimentel, H., Kelley, R., and Salzberg, S. L. (2013). TopHat2: accurate alignment of transcriptomes in the presence of insertions, deletions and gene fusions. *Genome Biol.* 14:R36. doi: 10.1186/gb-2013-14-4-r36

Kim, J. Y., Banerjee, T., Vinckevicius, A., Luo, Q., Parker, J. B., Baker, M. R., et al. (2014). A role for WDR5 in integrating threonine 11 phosphorylation to lysine 4 methylation on histone H3 during androgen signaling and in prostate cancer. *Mol. Cell* 54, 613–625. doi: 10.1016/j.molcel.2014.03.043

Lee, D. H., Jin, S. G., Cai, S., Chen, Y., Pfeifer, G. P., and O'Connor, T. R. (2005). Repair of methylation damage in DNA and RNA by mammalian AlkB homologues. *J. Biol. Chem.* 280, 39448–39459. doi: 10.1074/jbc.m509881200

Li, M. M., Nilsen, A., Shi, Y., Fusser, M., Ding, Y. H., Fu, Y., et al. (2013). ALKBH4-dependent demethylation of actin regulates actomyosin dynamics. *Nat. Commun.* 4:1832. doi: 10.1038/ncomms2863

Love, M. I., Huber, W., and Anders, S. (2014). Moderated estimation of fold change and dispersion for RNA-seq data with DESeq2. *Genome Biol.* 15:550.

Luo, B., Cheung, H. W., Subramanian, A., Sharifnia, T., Okamoto, M., Yang, X., et al. (2008). Highly parallel identification of essential genes in cancer cells. *Proc. Natl. Acad. Sci. U.S.A.* 105, 20380–20385. doi: 10.1073/pnas.0810485105

Nishihara, R., Wu, K., Lochhead, P., Morikawa, T., Liao, X., Qian, Z. R., et al. (2013). Long-term colorectal-cancer incidence and mortality after lower endoscopy. *N. Engl. J. Med.* 369, 1095–1105. doi: 10.1056/nejmoa1301969

Qi, L., Bart, J., Tan, L. P., Platteel, I., Sluis, T. V., Huitema, S., et al. (2009). Expression of miR-21 and its targets (PTEN, PDCD4, TM1) in flat epithelial atypia of the breast in relation to ductal carcinoma in situ and invasive carcinoma. *BMC Cancer* 9:163. doi: 10.1186/1471-2407-9-163

Shen, C. Q., Yan, T. T., Liu, W., Zhu, X. Q., Tian, X. L., Fu, X. L., et al. (2017). High expression of FAM83B predicts poor prognosis in patients with pancreatic ductal adenocarcinoma and correlates with cell cycle and cell proliferation. *J. Cancer* 8, 3154–3165. doi: 10.7150/jca.20086

Stefansson, O. A., Hermanowicz, S., van der Horst, J., Hilmarsdottir, H., Staszczak, Z., Jonasson, J. G., et al. (2017). CpG promoter methylation of the ALKBH3 alkylation repair gene in breast cancer. *BMC Cancer* 17:469. doi: 10.1186/s12885-017-3453-8

Tam, W. L., and Weinberg, R. A. (2013). The epigenetics of epithelial-mesenchymal plasticity in cancer. *Nat. Med.* 19, 1438–1449. doi: 10.1038/nm.3336

Tan, X., Chen, S., Wu, J., Lin, J., Pan, C., Ying, X., et al. (2017). PI3K/AKT-mediated upregulation of WDR5 promotes colorectal cancer metastasis by directly targeting ZNF407. *Cell Death Dis.* 8:e2686. doi: 10.1038/cddis.2017.111

Thiery, J. P., Acloque, H., Huang, R. Y., and Nieto, M. A. (2009). Epithelial-mesenchymal transitions in development and disease. *Cell* 139, 871–890. doi: 10.1016/j.cell.2009.11.007

Tian, X. P., Wang, C. Y., Jin, X. H., Li, M., Wang, F. W., Huang, W. J., et al. (2019). Acidic microenvironment Up-regulates exosomal miR-21 and miR-10b in early-stage hepatocellular carcinoma to promote cancer cell proliferation and metastasis. *Theranostics* 9, 1965–1979. doi: 10.7150/thno.30958

Uyama, N., Zhao, L., Van Rossen, E., Hirako, Y., Reynaert, H., Adams, D. H., et al. (2006). Hepatic stellate cells express synemin, a protein bridging intermediate filaments to focal adhesions. *Gut* 55, 1276–1289. doi: 10.1136/gut.2005.078865

van Nuland, R., Smits, A. H., Pallaki, P., Jansen, P. W., Vermeulen, M., and Timmers, H. T. (2013). Quantitative dissection and stoichiometry determination of the human SET1/MLL histone methyltransferase complexes. *Mol. Cell. Biol.* 33, 2067–2077. doi: 10.1128/mcb.01742-12

Vincent-Salomon, A., and Thiery, J. P. (2003). Host microenvironment in breast cancer development: epithelial-mesenchymal transition in breast cancer development. *Breast Cancer Res.* 5, 101–106.

Wang, Q., Wang, G., Wang, Y., Liu, C., and He, X. (2018). Association of AlkB homolog 3 expression with tumor recurrence and unfavorable prognosis in hepatocellular carcinoma. *J. Gastroenterol. Hepatol.* 33, 1617–1625. doi: 10.1111/jgh.14117

Westbrook, T. F., Martin, E. S., Schlabach, M. R., Leng, Y., Liang, A. C., Feng, B., et al. (2005a). A genetic screen for candidate tumor suppressors identifies REST. *Cell* 121, 837–848. doi: 10.1016/j.cell.2005.03.033

Westbrook, T. F., Stegmeier, F., and Elledge, S. J. (2005b). Dissecting cancer pathways and vulnerabilities with RNAi. *Cold Spring Harb. Symp. Quant. Biol.* 70, 435–444. doi: 10.1101/sqb.2005.70.031

Yang, Y., Weng, W., Peng, J., Hong, L., Yang, L., Toiyama, Y., et al. (2017). *Fusobacterium nucleatum* increases proliferation of colorectal cancer cells and tumor development in mice by activating toll-like receptor 4 signaling to nuclear factor-κB, and up-regulating expression of MicroRNA-21. *Gastroenterology* 152, 851.e24–866.e24. doi: 10.1053/j.gastro.2016.11.018

Zender, L., Xue, W., Zuber, J., Semighini, C. P., Krasnitz, A., Ma, B., et al. (2008). An oncogenomics-based in vivo RNAi screen identifies tumor suppressors in liver cancer. *Cell* 135, 852–864. doi: 10.1016/j.cell.2008.09.061

Zhang, B., Zheng, H., Huang, B., Li, W., Xiang, Y., Peng, X., et al. (2016). Allelic reprogramming of the histone modification H3K4me3 in early mammalian development. *Nature* 537, 553–557. doi: 10.1038/nature19361

Zhang, Y., Liu, T., Meyer, C. A., Eeckhoute, J., Johnson, D. S., Bernstein, B. E., et al. (2008). Model-based analysis of ChIP-Seq (MACS). *Genome Biol.* 9:R137. doi: 10.1186/gb-2008-9-9-r137

Zhu, H., Gan, X., Jiang, X., Diao, S., Wu, H., and Hu, J. (2019). ALKBH5 inhibited autophagy of epithelial ovarian cancer through miR-7 and BCL-2. *J. Exp. Clin. Cancer Res.* 38:163. doi: 10.1186/s13046-019-1159-2

Zhu, S., Wu, H., Wu, F., Nie, D., Sheng, S., and Mo, Y. Y. (2008). MicroRNA-21 targets tumor suppressor genes in invasion and metastasis. *Cell Res.* 18, 350–359. doi: 10.1038/cr.2008.24

Conflict of Interest: The authors declare that the research was conducted in the absence of any commercial or financial relationships that could be construed as a potential conflict of interest.

frontiers in Cell and Developmental Biology

REVIEW
published: 25 May 2020
doi: 10.3389/fcell.2020.00347

Significance of Single-Nucleotide Variants in Long Intergenic Non-protein Coding RNAs

Hecun Zou[1], Lan-Xiang Wu[1], Lihong Tan[2,3], Fei-Fei Shang[1] and Hong-Hao Zhou[1,3]**

[1] *Institute of Life Sciences, Chongqing Medical University, Chongqing, China,* [2] *Chongqing Medical and Pharmaceutical College, Chongqing, China,* [3] *Xiangya Hospital, Central South University, Changsha, China*

Single-nucleotide variants (SNVs) are the most common genetic variants and universally present in the human genome. Genome-wide association studies (GWASs) have identified a great number of disease or trait-associated variants, many of which are located in non-coding regions. Long intergenic non-protein coding RNAs (lincRNAs) are the major subtype of long non-coding RNAs; lincRNAs play crucial roles in various disorders and cellular models *via* multiple mechanisms. With rapid growth in the number of the identified lincRNAs and genetic variants, there is great demand for an investigation of SNVs in lincRNAs. Hence, in this article, we mainly summarize the significant role of SNVs within human lincRNA regions. Some pivotal variants may serve as risk factors for the development of various disorders, especially cancer. They may also act as important regulatory signatures involved in the modulation of lincRNAs in a tissue- or disorder-specific manner. An increasing number of researches indicate that lincRNA variants would potentially provide additional options for genetic testing and disease risk assessment in the personalized medicine era.

Keywords: single-nucleotide variant, long/large intergenic non-protein coding RNA, disease susceptibility, transcription, biological function

OPEN ACCESS

Edited by:
Hongquan Zhang,
Peking University Health Science Center, China

Reviewed by:
Yifeng Zhou,
Soochow University, China
Qinghua Cui,
Peking University, China

****Correspondence:***
Fei-Fei Shang
shangffei@sina.com
Hong-Hao Zhou
hhzhou2005@163.com

Specialty section:
This article was submitted to Molecular and Cellular Oncology, a section of the journal Frontiers in Cell and Developmental Biology

Received: *18 February 2020*
Accepted: *20 April 2020*
Published: *25 May 2020*

Citation:
Zou H, Wu L-X, Tan L, Shang F-F and Zhou H-H (2020) Significance of Single-Nucleotide Variants in Long Intergenic Non-protein Coding RNAs. Front. Cell Dev. Biol. 8:347. doi: 10.3389/fcell.2020.00347

INTRODUCTION

Single-nucleotide variant (SNV), also known as single-nucleotide polymorphism (SNP), is the variant of a single nucleotide that occurs at a specific genomic position. It is the most common type of genetic variants, which has long been confirmed in various loci of the genome (Human Genome Structural Variation Working Group, Eichler et al., 2007). In the past few decades, genetic variants have been typically used to dissect complex human disorders through research on candidate genes, particularly genome-wide association study (GWAS), an observational study of the genome-wide set of genetic variants in different individuals, which is performed to identify whether any variant is associated with the phenotypes. As a representative of a large-scale variant analysis, it has provided an approach to identifying potential genetic variant loci associated with heterogeneous disorders, including cancer susceptibility (Freedman et al., 2011). With the development of emerging technologies, such as microarray-based genotyping and high-throughput next-generation sequencing, it offers a novel avenue for the clinical application of genetic variants (GTEx Consortium et al., 2017). As might be expected, the role of genetic variants in understanding the pathogenesis of diseases,

therapeutic response, and even ultimately personalized medicine will be indispensable in the near future. Based on the implementation of the International HapMap Project and the 1000 Genomes Project, great breakthroughs have been achieved in the research field of genetic variants, particularly focusing on some variants of protein-coding genes (Human Genome Structural Variation Working Group, Eichler et al., 2007; Genomes Project et al., 2015). However, genetic variants, especially SNVs, not only occur to protein-coding sequences, but many of them also fall within non-coding regions or the intergenic regions between two genes. For instance, a considerable genetic component has been confirmed to be involved in the susceptibility of various cancers; the genomic contexts of cancer-associated SNVs (SNPs) have been analyzed within a comprehensive GWAS catalog. Of these risk variants, less than 10% are mapped in protein-coding regions, whereas most of them are located in the intronic or intergenic regions (**Figure 1A**), it brings forward the issue of these non-coding loci and their importance role in cancer research (Hindorff et al., 2009).

The Human Genome Project (HGP) has determined the whole sequence of nucleotide base pairs that compose the human genome and initially provided approximately 20,000 proteins that could serve as therapeutic targets (Venter et al., 2001). Subsequent large-scale annotation efforts, such as the Encyclopedia of DNA Elements (ENCODE) project, surprisingly, have identified hundreds of thousands of non-coding RNAs, which were previously regarded as "junk DNA" (The Encode Project Consortium, 2012). Among them, a great quantity of long non-coding RNAs (lncRNAs) are transcribed in mammalian genomes. Based on their locations and characteristics, lncRNAs can be placed into five broad categories: (1) intergenic, (2) antisense, (3) sense, (4) intronic, and (5) overlapping (Ponting et al., 2009; Derrien et al., 2012). Thereinto, long/large intergenic non-protein coding RNAs (lincRNAs), which are located within the genomic interval between two coding genes, are the major subtypes of lncRNAs accounting for approximately 63% (**Figure 1B**). Compared with other lncRNAs, molecules for which we know next to nothing about, lincRNAs are generally unexplored and have yet to be elucidated. About half of these lincRNAs are transcribed from the vicinity (<10 kb) of protein-coding loci and more likely to be involved in *cis*-regulatory of the expression level of adjacent genes; other transcripts that are well away from an adjacent gene seem to have little chance of *cis*-regulatory within the nearby region. Although they rarely form triplexes within double-stranded DNA owing to their poor complementarity to sequences elsewhere within the genome, these lincRNAs often act as *trans*-regulatory players within some ribonucleoprotein complexes (Ulitsky and Bartel, 2013). LincRNAs may have crucial roles in various disorders and cellular models *via* multiple mechanisms. Alterations in the levels of lincRNA expression have been linked to the occurrence of various disorders, such as cancers; they may act as tumor suppressors or proto-oncogenes (Huarte, 2015). Currently, advances in high-throughput RNA sequencing and computing approaches allow for an unparalleled analysis of transcriptomes. Of the diverse kinds of RNA transcripts, lincRNAs are attractive as they can be found out from the existing RNA-seq datasets through available bioinformatics methods (Cabili et al., 2011).

According to recent reports from the ENCODE project, thousands and thousands of variant loci are present in the non-coding regions of the human genome, and total number continues to increase (Schaub et al., 2012). Generally, genetic variants, such as SNVs, which occur to the non-coding loci, are more frequently than in conservative protein-coding genes regions. A large number of GWAS-identified SNVs loci reside in the regions that encode lincRNAs, indicating that these variants of lincRNAs may play a crucial role in the susceptibility of diseases. More than three quarters of disease-associated genetic variants are remarkably overlapped in promoter or enhancer regions, suggesting that SNVs may serve as an important player in the regulation of transcript levels (Hindorff et al., 2009). Therefore, identification of such variant loci and elucidation of their biological functions would be of profound significance in understanding the etiology of disorders and in promoting novel approaches for the diagnosis, prevention, and treatment of disorder.

LONG INTERGENIC NON-PROTEIN CODING RNA VARIANTS AND DISEASE SUSCEPTIBILITY

As a matter of fact, the occurrence of complex diseases (e.g., cancer) is related to multiple factors, including genetic, environmental, and lifestyle. Among them, genetic factors are of particular interest, just as GWASs and next-generation sequencing studies have greatly broadened the understanding of genetic variants that confer risk of diseases. Numerous genetic variants in lincRNA regions have been determined to be associated with the susceptibility of heterogeneous diseases, especially multiple types of cancer. Herein, we reviewed some lincRNAs that encompass disease or trait-associated variants (**Tables 1**, **2**).

Long Intergenic Non-protein Coding RNA Variants on the chr8q24 Locus

Genome-wide association studies have pointed to the chr8q24 genomic locus as a hotspot for cancer-associated variants owing to the large density, more strength, and high allele frequency of these variants (Yeager et al., 2007; Tuupanen et al., 2009). Even though chromosome 8q24 has been considered as a "gene desert" region owing to the absence of functionally annotated genes, with the only notable exception of the frequently amplified *MYC* (a proto-oncogene involved in tumorigenesis) (Chung et al., 2011). Surprisingly, large-scale studies have revealed that several lincRNAs are transcribed from the chr8q24 locus, such as *CCAT1* (Kim et al., 2014), *CCAT2* (Ling et al., 2013), *PVT1* (Hanson et al., 2007), *PCAT1* (Guo et al., 2016), and *PRNCR1* (Li et al., 2013); all of these encompass multiple cancer-associated variants. For instance, lincRNA *CCAT2* (Colon Cancer-Associated Transcript 2, also termed *LINC00873*), a transcript spanning SNV rs6983267, is associated with an increased risk for prostate, breast,

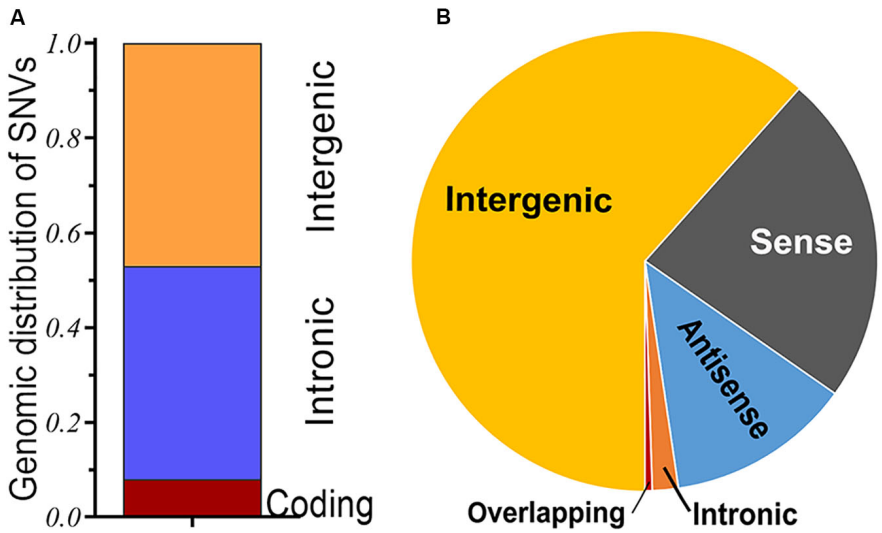

FIGURE 1 | (A) Genomic distribution of single-nucleotide variants in cancers; a majority of cancer-associated single-nucleotide variants (SNVs) [single-nucleotide polymorphisms (SNPs)] are found in the intergenic or intronic regions, and only small numbers are located in protein-coding regions of the human genome. **(B)** Classification of long non-coding RNA (lncRNA) transcripts; long intergenic non-protein coding RNA (lincRNA) is a major subtype of lncRNA.

TABLE 1 | Overviews of trait-associated variants on the chr8q24 locus.

LincRNA	Trait-associated variants	Diseases	Position	References
CASC8	rs378854	Adiposity	Intron	Ng et al., 2017
	rs10505477	Colorectal, gastric, and lung cancers	Intron	Ma et al., 2015; Hu et al., 2016
CASC19	rs138042437	Prostate cancer	Intron	Teerlink et al., 2016
CCAT1	rs6983267	Colorectal cancer, endometrial carcinoma	Enhancer	Kim et al., 2014; Zhao et al., 2016
CCAT2	rs6983267	Prostate, breast, colon, and colorectal cancers; myeloid malignancies	Exon	Yeager et al., 2007; Tuupanen et al., 2009; Ling et al., 2013; Shah et al., 2018
PCAT1	rs7463708	Prostate cancer	Enhancer	Guo et al., 2016
	rs10086908	Prostate cancer	Promoter	Guo et al., 2016
PRNCR1	rs1456315, rs7463708	Prostate cancer	Exon	Chung et al., 2011
	rs13252298, rs1456315	Colorectal cancer	Exon	Li et al., 2013
	rs183373024	Prostate cancer	Exon	Teerlink et al., 2016
PVT1	rs13281615	Breast cancer	Promoter	Zhang et al., 2014
	rs2720709, rs2648875	End-stage renal disease (ESRD)	Intron, intron	Hanson et al., 2007
	rs378854	Prostate cancer	Promoter	Meyer et al., 2011
	rs13255292, rs4733601	Diffuse large B cell lymphoma	Intron, downstream	Cerhan et al., 2014

LincRNA, long intergenic non-protein coding RNA.

colon, and colorectal cancers (Yeager et al., 2007; Tuupanen et al., 2009; Ling et al., 2013). *CCAT2* is overexpressed in various types of cancers and may contribute to tumor growth, metastasis, and chromosomal instability by increasing MYC expression (Ling et al., 2013). LincRNA *PRNCR1* has been reported to be involved in prostate carcinogenesis and may play an oncogene role *via* modulating the androgen receptor (Chung et al., 2011), *PRNCR1* variants, especially rs1456315, are associated with the susceptibility of prostate and colorectal cancers (Li et al., 2013; Teerlink et al., 2016). Through an integrative analysis of the lncRNA transcriptome and GWAS data, Guo et al. (2016) have identified a prostate cancer-associated transcript *PCAT1* and 10 risk loci on the chr8q24.21, including *PCAT1* variants rs10086908 and rs7463708, which are significantly associated with prostate cancer susceptibility. As for *PVT1* (also termed *LINC00079*), a GWAS analysis has identified that its variants rs13255292 and rs4733601 are associated with the susceptibility of diffuse large B cell lymphoma (Cerhan et al., 2014). Other independent SNVs (e.g., rs2720709 and rs2648875), which are mapped on *PVT1*, especially contributes to the development of end-stage renal disease (ESRD) in patients with type 2 diabetes (Hanson et al., 2007). A recent meta-analysis has summarized

TABLE 2 | Overviews of other lincRNAs encompassing trait-associated variants.

LincRNA	Trait-associated variants	Diseases	Position	References
CASC16	rs3803662	Breast cancer, lung cancer	Exon	Orr et al., 2011
CASC15	rs6939340	Neuroblastoma	Intron	Maris et al., 2008
GAS5	rs145204276	Hepatocellular carcinoma (HCC), colorectal, and gastric cancers	Promoter	Tao et al., 2015; Li et al., 2018a
H19	rs217727	Coronary artery disease, type 2 diabetes	Exon	Gao et al., 2015
	rs2067051	Pneumoconiosis, coronary artery disease	Exon	Gao et al., 2015; Wu et al., 2016
	rs2107425	Ovarian and breast cancers, hypertrophic cardiomyopathy	Intron	Chu et al., 2016
	rs2839698	HCC, bladder, colorectal, and gastric cancer	Exon	Verhaegh et al., 2008; Chu et al., 2016; Yang et al., 2018
HULC	rs7763881, rs1041279	HCC	Intron	Wang et al., 2018a
LINC00673	rs11655237	Pancreatic cancer	Exon	Zheng et al., 2016
LINC00951	rs11752942	Esophageal squamous cell carcinoma (ESCC)	Exon	Wu et al., 2013
LOC105378318	rs1875147	Leprosy	Intron	Fava et al., 2017
MALAT1	rs619586	Pulmonary arterial hypertension (PAH), coronary atherosclerotic and congenital heart disease (CAD/CHD), breast cancer	Exon	Zhuo et al., 2017; Li et al., 2018b
	rs1194338	Colorectal cancer	Promoter	Li et al., 2017
	rs4102217	HCC	Promoter	Wang et al., 2018b
MEG3	rs941576, rs34552516	Type 1 diabetes (T1D)	Intron	Wallace et al., 2010; Westra et al., 2018
MIAT	rs2331291	Myocardial infarction	Intron	Ishii et al., 2006
	rs1894720	Paranoid schizophrenia	Exon	Rao et al., 2015
PCGEM1	rs6434568, rs16834898	Prostate cancer	Intron	Xue et al., 2013
PCAT19	rs11672691	Prostate cancer	Promoter	Gao et al., 2018
PTCSC2	rs965513	Papillary thyroid carcinoma (PTC)	Intron	He et al., 2015
PTCSC3	rs944289	PTC, large-vessel ischemic stroke	Promoter	Jendrzejewski et al., 2012; Lee et al., 2016
TDRG1	rs8506	ESCC, gastric cancer	Exon	Han et al., 2017
TINCR	rs2288947, rs8105637	Colorectal cancer, gastric cancer	Exon, intron	Zheng et al., 2017

LincRNA, long intergenic non-protein coding RNA.

the relationship between two common variants (rs10505477 and rs7837328) in the intronic region of *CASC8* (*LINC00860*) at 8q24 locus with the risk of cancers (Cui et al., 2018), including colorectal, gastric, and lung cancers (Ma et al., 2015; Hu et al., 2016). Another intronic loci rs378854 is related to adiposity in the individuals of African ancestry (Ng et al., 2017).

Single-Nucleotide Variants in Long Intergenic Non-protein Coding RNA H19 Locus

The *H19* (also termed *LINC00008*) is located in chromosome 11p15.5, a paternally imprinted onco-fetal gene, which is typically down-regulated in adult tissues but can be overexpressed in multiple types of solid cancer. LincRNA *H19* expression is closely related to tumor growth, metastasis, recurrence, and clinical prognosis (Ge et al., 2018). *H19* variants are involved in the susceptibility of multiple diseases. A meta-analysis study has indicated that variant T allele of rs2107425 is correlated with a decreased risk of developing cancers (e.g., breast, ovarian, lung, and bladder cancers) (Chu et al., 2016; Wu et al., 2017), whereas variant rs2839698 is associated with an increased risk of digestive cancers (colorectal and gastric cancers) *via* up-regulating *H19* expression; of note, there is no significant association observed between rs217727 variant and cancers susceptibility (Chu et al., 2016). However, in other reports, *H19* rs217727 has been linked to the risk of hepatocellular carcinoma (HCC) (Ge et al., 2018), oral squamous cell carcinoma (OSCC), and bladder cancer in the Chinese population (Guo Q. Y. et al., 2017). For coronary artery disease (CAD), the T variant of rs217727 is associated with an increased risk, whereas rs2067051 A variant is linked to a decreased risk (Gao et al., 2015). *H19* rs217727, but not rs2107425 variant, is associated with susceptibility of women with preeclampsia (PE) (Harati-Sadegh et al., 2018). Additionally, maternally transmitted fetal *H19* variants (e.g., rs217727, rs2071094, and rs10732516), along with paternal *IGF2* variants, are independently correlated with the placental DNA methylation levels (Marjonen et al., 2018) and birth weight of newborns (Petry et al., 2011).

Single-Nucleotide Variant in *MALAT1* and *MIAT* Regions

LincRNA *MALAT1* (metastasis-associated lung adenocarcinoma transcript 1, also termed *LINC00047*) has rs619586 A > G variant, which is significantly associated with the susceptibility

of pulmonary arterial hypertension (PAH), and the carriers with variant G genotypes have a decreased PAH risk (Zhuo et al., 2017). Recent study has suggested that rs619586 AG/GG genotypes could reduce the risks of coronary atherosclerotic heart disease and congenital heart disease (CHD) by regulating *MALAT1* expression (Li et al., 2018b). Another report has showed that *MALAT1* is overexpressed in colorectal cancers and that SNV rs1194338 mapping to its promoter region is significantly associated with a decreased risk of colorectal cancer (Li et al., 2017). Moreover, the large-scale case–control association studies have identified a novel myocardial infarction-associated transcript, *MIAT* (also termed *LINC00066*), which encompasses rs2331291, and other variants confer the susceptibility of myocardial infarction (Ishii et al., 2006). As a component of the nuclear matrix, *MIAT* is mainly expressed in neurons, Rao et al. (2015) have reported that SNV rs1894720 is correlated with paranoid schizophrenia susceptibility, and MIAT may contribute to the pathogenesis of schizophrenia.

Other Long Intergenic Non-protein Coding RNA Variants in Human Cancers

In addition to the above lincRNA molecules, recent studies have identified many other cancer-associated variants within lincRNA regions. For example, the tissue differentiation-inducing non-protein coding RNA (*TINCR*), also termed *LINC00036*, is essential for somatic tissue differentiation and tumor progression (Kretz et al., 2013). It has been demonstrated that two variants of *TINCR* (rs2288947 and rs8105637) are significantly correlated with the susceptibility and lymph node metastasis of colorectal cancer (Zheng et al., 2017); the lincRNA *TINCR* rs2288947 G allele and rs8113645 A allele genotypes could reduce the risk of gastric cancer. *HULC*, an HCC up-regulated lncRNA, also termed *LINC00078*, and its variants (rs7763881 and rs1041279) are linked to the susceptibility of HCC (Wang et al., 2018a). In thyroid carcinoma, several papillary thyroid carcinoma susceptibility candidates, such as *PTCSC2*, contain a risk-variant rs965513, and *PTCSC3* encompasses rs944289; two lincRNA expression levels are strongly down-regulated in thyroid carcinoma tissues (Jendrzejewski et al., 2012; He et al., 2015). Additionally, GWAS analyses have identified five tag-SNVs, including rs944289 located in *PTCSC3*, are associated with large-vessel ischemic stroke (Lee et al., 2016). Xue et al. (2013) have reported that a prostate cancer gene expression marker, *PCGEM1* (*LINC00071*), containing two risk-SNVs (rs6434568 C and rs16834898 A alleles) that are associated with a decreased risk of prostate cancer. Another prostate cancer risk-associated allele rs75823044 mapping to promoter of *LINC00676* is almost exclusively found in African ancestry populations (Conti et al., 2017). In a GWAS analysis, five common variants including rs3803662 on the exon of *CASC16* (*LINC00918*) have been identified to contribute to the susceptibility of lung and breast cancers (Orr et al., 2011). Furthermore, the colorectal cancer risk-SNV rs11776042 is located in the promoter of *LNC00964*, in which lincRNA is significantly decreased in colorectal cancer tissues (Chu et al., 2015). For tumor suppressor lncRNA *GAS5*, an insertion/deletion variant of rs145204276 is associated with the susceptibility of HCC (Tao et al., 2015) and colorectal and gastric cancers (Li et al., 2018a).

Other Disease-Associated Variants in Long Intergenic Non-protein Coding RNA Regions

Except for cancer susceptibility, some lincRNA variants are found to be associated with the risk of other heterogeneous diseases. GWAS and expression quantitative trait locus (eQTL) analyses have identified a risk factor for pathological inflammatory responses of leprosy, SNV rs1875147, which is an eQTL variant for lincRNA *LOC105378318* located in chromosome 10p21.2 (Fava et al., 2017). Rautanen et al. have found a variant rs140817150 in the intron of *LOC107986770*, which may be correlated with bacteremia susceptibility in African children (Kenyan Bacteraemia Study Group et al., 2016). A systematic analysis highlights some variant loci in lncRNA regions linked to cardiometabolic disorders; one of them, lincRNA *LOC157273* harboring rs4841132, is linked to the regulation of serum lipid cholesterol (Ghanbari et al., 2018). Shyn et al.'s (2011) GWAS analysis has identified a major depressive disorder (MDD) risk-associated variant rs12526133, which resides in exon of *LINC01108*, in which lincRNA is overexpressed in patients with MDD. Moreover, the maternally expressed imprinted gene, *MEG3* (also termed *LINC00023*), containing variants rs941576 (Wallace et al., 2010) and rs34552516 (Westra et al., 2018), which is found to be associated with susceptibility of type 1 diabetes. Nikpay et al.'s (2015) comprehensive GWAS meta-analyses have reported an association of CAD susceptibility with several SNVs, such as rs1870634, which is located in the downstream of *LINC00841*, and its GG genotype is strongly linked to CAD risk and has a higher frequency in CAD patients.

LONG INTERGENIC NON-PROTEIN CODING RNA VARIANTS AND CLINICOPATHOLOGICAL CHARACTERISTICS, PROGNOSIS, AND TREATMENT RESPONSE

For Clinicopathological Characteristics and Prognosis

In addition to disease susceptibility, trait-associated SNVs are widely used for the indication of clinicopathological characteristics, prognosis, and treatment response (Gong et al., 2017). For example, with regard to a neuroblastoma-associated variant rs6939340, which is mapped on the intronic locus of lincRNA *CASC15* and *NBAT1*, neuroblastoma individuals with the risk alleles are more likely to have clinical aggressive presentation, including metastatic disease, tumor with *MYCN* amplification, and disease relapse (Maris et al., 2008). Two independent cohort studies have observed that risk-SNV rs2608053 of *PVT1* is correlated to the survival outcome of patients with classical Hodgkin lymphoma (Ghesquieres et al., 2018). For multiple sclerosis, several risk loci of *PVT1* may

contribute to the prediction of an optimal response to treatment with glatiramer acetate (Kulakova et al., 2017). LincRNA *H19* variants have been found to increase the risk of ischemic strokes, and the up-regulated *H19* may induce cerebral ischemia reperfusion injury by activating autophagy (Wang et al., 2017). Recent studies have reported that *H19* rs2839698 variant may serve as an indicator for the increased risk and poor prognosis of HCC (Yang et al., 2018). Among individuals with coal workers' pneumoconiosis (CWP), carriers of *H19* rs2067051 CT/TT genotypes are associated with a decreased risk; *H19* rs2067051 may be a possible biomarker for CWP prevention (Wu et al., 2016). A case–control study has shown that lincRNA *MALAT1* variant rs4102217 is related to increased HCC risks; this SNV may be a potential predictor for the risk and prognosis of patients with HCC (Wang et al., 2018b). Another *MALAT1* rs3200401 T allele has been found to confer better survival for patients with advanced lung adenocarcinoma (Wang et al., 2017). Furthermore, *TDRG1* (testis development related 1, also termed *LINC00532*) is overexpressed in esophageal squamous cell carcinoma (ESCC) tissues; the AA genotype of variant rs8506 is linked to an increased risk of ESCC; this risk allele may regulate TDRG1 expression by disrupting the sponge binding of miR-526b; high TDRG1 expression and rs8506 A allele variant may contribute to the advanced tumor–node–metastasis stage and poor survival for ESCC patients (Han et al., 2017). Recent GWAS analyses have demonstrated that variant rs11672691 of *PCAT19* (*LINC01190*) on 19q13 is positively related to aggressive prostate cancer. Further cohort studies have confirmed the association of rs11672691 with clinical characteristics of aggressive disease, including high tumor stage, prostate-specific antigen (PSA) progression, and development of castration-resistant prostate cancer (CRPC). The risk GG genotype of rs11672691 is also associated with a poor prognosis for patients with prostate cancer (Gao et al., 2018). These results highlight the clinical potential of trait-associated SNV, which may serve as risk stratification markers for the management of cancer patients.

Indication of Treatment Response

Recent GWAS analyses have identified two common SNVs (rs4476990 and rs3802201), in which mapping to *MIR2052HG* may affect the recurrence risk of breast cancer patients treated with aromatase inhibitors. Expressions of *MIR2052HG* and estrogen receptor α (ERα, encoded by *ESR1* gene) are induced by aromatase inhibitors and estrogen in a variant-dependent manner. *MIR2052HG* could sustain the levels of ERα *via* promoting AKT/FOXO3-mediated *ESR1* transcription and limiting the ubiquitin-mediated ERα degradation. Its risk variant genotypes could enhance ERα binding to estrogen response elements and result in an alteration of response to aromatase inhibitors treatment for cancer patients (Ingle et al., 2016). In the evaluation of adverse reaction for lung cancer patients receiving platinum-based chemotherapy, the variants *CASC8* rs10505477 (Hu et al., 2016) and *ANRIL* rs1333049 are correlated with overall toxicity, especially severe hematologic and gastrointestinal toxicity; lincRNA *MEG3* rs116907618 is correlated with severe gastrointestinal toxicity; these variants may be considered as biomarkers for the evaluation of platinum-based treatment (Gong et al., 2017). Moreover, the rs10505477 GG genotype of *CASC8* is also associated with tumor size, lymph node metastasis, and tumor–node–metastasis stage and may contribute to the survival for gastric cancers patients (Ma et al., 2015). In nasopharyngeal carcinoma (NPC), lncRNA *GAS5* variant rs2067079 is associated with an increased risk of severe myelosuppression and neutropenia, whereas rs6790 may decrease the incidence rate of toxic reactions induced by chemo-radiotherapy in NPC patients (Guo Z. et al., 2017). Functional genomic studies have revealed that *GAS5* promoter encompassing SNV rs55829688 (T > C), which up-regulates *GAS5* expression *via* interacting with transcription factor TP63, may aggravate myelosuppression and result in a poor prognosis for patients with acute myeloid leukemia (AML) (Yan et al., 2017). Additionally, GWAS analyses have identified that some genetic variants are correlated with the pharmacokinetics of psychotropic drugs, such as variant rs16935279 located in an intron of LINC01592; its C allele carriers have a lower metabolism rate for anti-epileptic drugs (Athanasiu et al., 2015).

LONG INTERGENIC NON-PROTEIN CODING RNA VARIANTS REGULATE GENE TRANSCRIPTION

Genome-wide association studies have identified a lot of trait-associated variants, most of which reside in non-coding regions of the human genome. However, the specific functional mechanism of genetic variants still remains confused, which is one of the major challenges for post-GWAS research (Schaub et al., 2012). The regulatory elements are mainly located within regions of non-coding DNA and play critical roles in the transcription of target genes. Emerging studies have showed that these regulatory elements can affect the expression of lincRNAs and other related genes *via* long-range chromatin interactions in a cell-type- or tissue-specific manner. Many genetic variants reside in the regulatory element regions of lincRNAs and may disrupt the interaction of transcription factors with a region containing SNVs (**Figures 2A,B**). The mapping of SNVs to lincRNA regulatory regions (especially promoters and enhancers) may indicate a potential impact of these variants on the transcription of target genes (GTEx Consortium et al., 2017).

Single-Nucleotide Variants in Super-Enhancer Locus of *MYC* Gene

Many genetic variants are located in the upstream of *MYC*, a gene desert on 8q24, which is related to the susceptibility of multiple cancers. Some observations, such as chromosome conformation capture (3C) assays, histone acetylation, and methylation marks analyses, have demonstrated that these regulatory regions containing SNVs may serve as enhancers for *MYC* gene in a tissue-specific manner. Functional investigations suggest that lincRNA *CCAT2* augments the binding of transcription factor (TCF7L2 or TCF4) to *MYC* promoter region, activates WNT

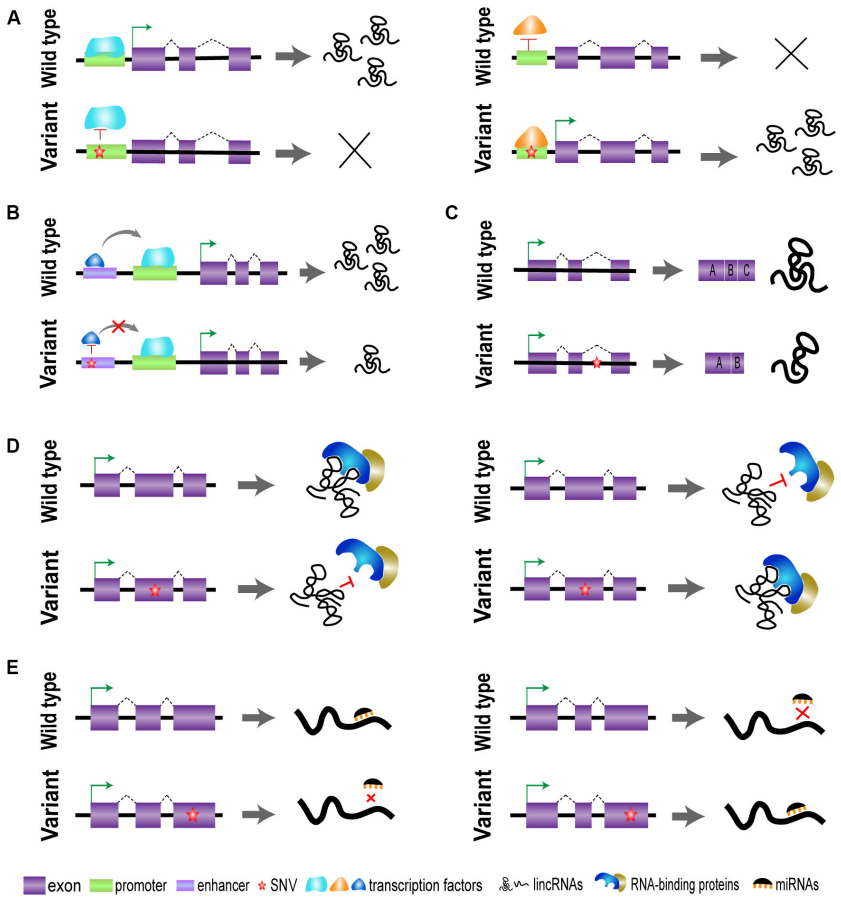

FIGURE 2 | Graphical representations of the driving effect of variants [single-nucleotide variants (SNVs)] on long intergenic non-protein coding RNA (lincRNA) regions. **(A)** Genetic variants located in promoter may affect the binding of transcription factors and regulate the transcription of lincRNAs. **(B)** Genetic variants on enhancer affect the binding of transcription co-regulators and regulate lincRNA expression. **(C)** Genetic variants on intron may affect the process of splicing and stability of lincRNA conformation. **(D)** Genetic variants located in exons affect the lincRNA secondary structure, lincRNA stability, and interactive function. **(E)** Genetic variants on exons may affect the sponging of microRNAs (miRNAs).

signaling, and increases the expression of target genes, especially the *MYC* proto-oncogene (Pomerantz et al., 2009; Ling et al., 2013). Although there is a disputable association between variant rs6983267 and *MYC* expression (Tuupanen et al., 2009), its risk G alleles produce more *CCAT2* transcripts, which are exclusively retained in the nucleus. Interestingly, a risk-SNV rs6983267 also contributes to increased expression of *CCAT1* (Zhao et al., 2016); an adjacent lincRNA of *CCAT2*, through affecting the long-range chromosomal interaction of *MYC* enhancer or *CCAT1* promoter, then results in a cell-cycle regulation and tumor development (Kim et al., 2014). Guo et al. (2016) have reported that a prostate cancer risk-associated T allele of rs7463708 at lincRNA *PCAT1* exhibited enhancer activity, through modulating the binding of novel transcription factor ONECUT2 with a distal enhancer that loops to the *PCAT1* promoter; this process increases *PCAT1* expression upon prolonged androgen treatment and promotes prostate transformation. Moreover, another prostate cancer risk-SNV rs378854 G alleles are also found to increase the expression of *PVT1* oncogene by regulating an interaction of transcription factor YY1 with the promoters of *PVT1* or *MYC* genes (Meyer et al., 2011). Similarly, the GG genotypes of rs13281615 increase *PVT1* transcription and promote cell proliferation in breast cancer (Zhang et al., 2014). Overexpression of *PVT1* may contribute to high levels of MYC mRNA and protein, along with an increased copy number, eventually leading to tumorigenesis (Zou et al., 2017). These results demonstrate the association of genetic variants with lincRNA transcription, although further studies are needed to reveal the relationship of these SNVs and lincRNA*s* on chromosome 8q24 locus.

Single-Nucleotide Variants in Promoter Regions

Some SNVs reside in gene promoter regions and may influence the transcriptional expression of their target genes. Through an eQTL analysis of candidate genes and genetic variants in different tissues, an endometriosis risk-SNV rs3820282 is found to down-regulate *LINC00339* expression by affecting the activity of *LINC00339* promoter (Powell et al., 2016).

Tao et al. (2015) have reported that an indel variant rs145204276 in the promoter region of *GAS5* contributes to the up-regulation of *GAS5 via* affecting the methylation status of *GAS5* promoter and regulating its transcriptional activity, thereby bringing its proto-oncogene role into play. Furthermore, the variant rs944289 of *PTCSC3* is reported to reside in a binding site for CCAAT/enhancer binding proteins (C/EBPα/β); this variant may affect the activity of *PTCSC3* promoter and down-regulate its transcript, then resulting in an abnormal expression of downstream genes and the progression of papillary thyroid carcinoma (Jendrzejewski et al., 2012).

Notably, a gene promoter region is likely to overlap with another super-enhancer locus, suggesting it that may have enhancer-like roles. In these interactions, lincRNA loci may serve as both target genes of its SNVs and the distal regulatory elements of other related genes. Integrative functional genomic and epigenomic analyses have identified that osteoporosis risk-associated SNV rs6426749 may act as a distal variant-specific enhancer and play a pivotal role in bone metabolism. Risk rs6426749 G alleles can affect the enhancer activity by binding to transcription factor TFAP2A; a thin process may increase transcription of *LINC00339* and modulate the expression of downstream gene *via* long-range chromatin loop formation in osteoblast cells (Chen et al., 2018). Recent studies have reported that prostate cancer risk-associated G allele of rs11672691 is associated with an increased expression of lincRNA *PCAT19* and oncogene CEACAM21; SNV rs11672691 is located in an enhancer element and may alter the binding site of its oncogenic transcription factor HOXA2. CRISPR/Cas9-mediated interference and activation assays have demonstrated that rs11672691 variant is involved in the regulation of its eQTL genes *PCAT19* and CEACAM21 expression and affects the cells' aggressive property in prostate cancers (Gao et al., 2018). In another alternative mechanism, risk variant rs11672691 is associated with the decreased levels of a short isoform of *PCAT19* (*PCAT19*-short) and increased levels of a long isoform (*PCAT19*-long). This risk SNV locus is bifunctional with both promoter and enhancer activity, which maps to a promoter of *PCAT19*-short and the third intron of *PCAT19*-long. Risk allele rs11672691 and its linkage disequilibrium SNV rs887391 may alter the binding profiles of transcription factors NKX3.1 and YY1, thereby elevating the abundance of *PCAT19*-long through promoter-enhancer switching. Ultimately, it gives rise to an increased formation of the HNRNPAB-*PCAT19*-long complex to activate a subset of cell-cycle genes and promote prostate cancer aggression (Hua et al., 2018).

Another causative *cis*-regulatory mechanism has been constructed *via* integrative genomic analyses; the breast cancer-associated variant rs4415084 is located in a GATA3-binding motif of *LINC02224*, which refers to the differential GATA3 binding and chromatin accessibility, thereby promoting the transcription of *LINC02224* and *MRPS30* genes (Zhang et al., 2018). It is reasonable to postulate that the interactions of lincRNA, trait-associated variants, and regulatory factor may contribute to the development of specific disorders.

SINGLE-NUCLEOTIDE VARIANTS AFFECT THE BIOLOGICAL FUNCTION OF LONG INTERGENIC NON-PROTEIN CODING RNA

Currently, genetic variants in potential lincRNA regions have attracted increasing interest; it has been established that many SNVs are associated with susceptibility of multiple diseases. It is evident that the expression and function of lincRNAs may be influenced by its SNVs in a cell-type- or tissue-specific manner. A comprehensive analysis has suggested that genetic variants in lincRNA regions also possibly affect the process of splicing and stability of lincRNA conformation, thereby leading to a modification of their interacting partners, as shown in **Figures 2C–E** (Hon et al., 2017).

Effect of Single-Nucleotide Variants on the Role of Long Intergenic Non-protein Coding RNA CCAT2

Several observations, such as eQTL and DNAase peak assays, indicate that genetic variants that occurred in exons of lincRNAs may change the lincRNA secondary structure, thereby affecting its stability, interactive properties, and regulatory functions (Khurana et al., 2016). For example, lincRNA *CCAT2* could act as a scaffold or assembly platform and modulate the alternative splicing of glutaminase (GLS) pre-mRNA *via* directly binding to a Cleavage Factor I (CFIm) complex. However, SNV rs6983267 (G/T) may affect the interaction of CCAT2 with CFIm complex by changing lincRNA secondary structure and initiating a domino effect mechanism; this process leads to allele-specific reprogramming of cellular energy metabolism in colon cancers (Redis et al., 2016). Moreover, by using allele-specific *CCAT2* transgenic mice, recently, Shah et al. (2018) have revealed that overexpression of *CCAT2* may lead to genomic instability and myeloid malignancies; the SNV rs6983267-specific RNA-editing induces the dysregulation of a genome-wide gene expression by down-regulating EZH2, a histone-lysine *N*-methyltransferase, which then results in the impairment of immune processes and development of myelodysplastic neoplasms *in vivo*. In another study, Sur IK and his colleagues have generated mice lacking a *myc* enhancer region spanning risk-SNV rs6983267; the mutant mice have not showed an overt phenotype but confer resistance to intestinal tumorigenesis induced by $APC^{minmutation}$ (Sur et al., 2012). These studies indicate that cancer risk-associated variants identified from the human genome may also exert a functional effect for animals *in vivo*.

Effect of Single-Nucleotide Variants on the Long Intergenic Non-protein Coding RNA Secondary Structure

It is worth noting that lincRNAs have a long average length and that their exon regions contain numerous trait-associated variants; significant alterations of lincRNA secondary structure may be caused by its SNVs on exon loci. Many variants such as *PRNCR1* (prostate cancer-associated non-coding RNA) are

located in exon regions, for example, rs1456315 G/A; it has been predicted to affect the lincRNA secondary structure of *PRNCR1* (Chung et al., 2011) and then alter lincRNA stability and conformation, even giving rise to the modification of its interacting partners. Xue et al. (2015) have also reported that SNV rs7958904 G/C in an exon region does not affect transcription activity of *HOTAIR*; however, in *in silico* analyses, it is shown to alter the RNA secondary structure of *HOTAIR*. These findings indicate that genetic variants, especially SNVs in exon loci, may play a different role *via* affecting the lincRNA structure.

Effect of Single-Nucleotide Variants on MicroRNA Binding

Not surprisingly, it has been documented that some microRNAs (miRNAs) can function in a non-canonical manner to regulate lincRNA expression levels or directly interact with lincRNA molecules. The competing endogenous RNA (ceRNA) is a mechanism that lncRNA could competitively bind or sponge miRNAs, such as ceRNA *MALAT1*; its exon locus contains a variant rs619586 A > G, which can significantly up-regulate the expression of XBP1 (X box-binding protein 1) by sponging miR-214 and then suppressing the proliferation and migration of vascular endothelial cells *in vitro* (Zhuo et al., 2017). In another case, variant rs11752942 of *LINC00951* exon is linked to the susceptibility of ESCC; risk G alleles of rs11752942 may decrease the expression levels of *LINC00951 via* affecting the binding of miR-149-3p, thereby regulating cell proliferation and tumor growth (Wu et al., 2013). Intriguingly, recent studies have demonstrated that pancreatic cancer risk-SNV rs11655237 G > A in the *LINC00673* exon region is likely to create a target site for miR-1231 binding and reduces the function of LINC00673 in an allele-specific manner. Down-regulation of LINC00673 may attenuate the interaction of PTPN11 with an E3 ubiquitin ligase PRPF19 and suppress the ubiquitin-mediated PTPN11 degradation; these processes enhance an oncogenic signaling whereas diminish STAT1-dependent anti-oncogenic signaling in cancer cells (Zheng et al., 2016). These findings highlight the regulatory relationships of miRNAs with lincRNAs in a variant-specific manner and may offer a wider field for future research on lincRNA.

APPROACHES FOR IDENTIFYING DRIVERS

As summarized above, genetic variants play a very significant role in the transcription and biological function of lincRNAs, contributing to various disease susceptibility, progression, prognosis, and treatment response. Genetic variants may act as a driving factor to affect the role of lincRNAs; just like a driver who drives a vehicle, analogously, lincRNA variants may vividly serve as a putative driver to regulate the lincRNA molecules.

Computational Approaches

Driver identification is a challenging task, owing to their complex and diverse modes of action and the inadequate understanding of non-coding regions; the computational prediction of non-coding drivers is even more challenging than that of protein-coding drivers. In addition, non-coding variants are more abundant than protein-coding genes; hence, the key variants with functional significance have to be distinguished from a larger set of passenger events (Khurana et al., 2016). Currently, several online databases have been constructed to describe genomic variants in lncRNA regions, such as lincSNP, lncRNASNP2, and LncVar. More specifically, lincSNP 2.0 is an integrated database to identify and annotate disease-associated SNVs on human lincRNAs and their transcription factor binding sites (Ning et al., 2017). LncRNASNP2 is an updated database of comprehensive information about SNVs or mutations in human and mouse lncRNAs, as well as their impacts on lncRNA structure and potential function on miRNA binding (Miao et al., 2018). LncVar provides genetic variants associated with lncRNAs in multiple species and their effects on biological function of lncRNAs (Chen et al., 2017). Furthermore, a large number of GWAS analyses have successfully identified an array of genetic variants that are associated with various types of human disorders (MacArthur et al., 2017). Numerous public databases have been set out to provide a comprehensive description of genetic variants and GWAS data in the human genome with high impact (Genomes Project et al., 2015). A brief overview of these databases with their key features and corresponding references is presented in **Table 3**.

Functional annotations and linkage disequilibrium analyses of genetic variants can be performed based on public databases and bioinformatic methods. Among tag-SNVs with strong linkage disequilibrium, significant genotype-specific effects on lincRNA expression can be observed by eQTL analysis (GTEx Consortium et al., 2017). Subsequently, according to ChIP-Seq data from the ENCODE database[1], some trait-associated SNVs can be picked out; those variants mapping to *cis*-regulatory motifs may affect the binding activities of many interrelated transcription factors, including EZH2, CHD1, TCF7L2, and CTCF. These transcription factors may be closely related to the occurrence and progression of various human disorders, such as enhancer of zeste homologue 2 (EZH2), which is overexpressed in several human tumors and accounts for the aggressiveness and unfavorable prognoses of various cancers.

Function Verification

Many functional verification studies of genetic variants have focused on protein-coding regions of the human genome. With an expanding appreciation that non-coding variants play a crucial role in the development of disorders, several recent studies have set out to explore approaches to evaluate the function of non-coding variants (Khurana et al., 2016). For example, experimental methods used to understand the effects of *cis*-regulatory variants within a promoter or enhancer region on cellular biological functions is summarized as follows. A main strategy is required to introduce the sequence variants, the mutated DNA fragment can be constructed *via* site-directed mutagenesis, CRISPR–Cas system (Konermann et al., 2015) or oligonucleotide synthesis. Subsequently, the functional output of non-coding variants

[1] http://genome.ucsc.edu/ENCODE/

TABLE 3 | Some databases that may be used for driver identification.

Tools	Functional annotation	Link	References
LincSNP 2.0	Store and annotate disease-associated SNVs in human lncRNAs and their transcription factor binding sites (TFBSs)	http://bioinfo.hrbmu.edu.cn/LincSNP	Ning et al., 2017
lncRNASNP2	Comprehensive information of SNVs and mutations in lncRNAs, as well as their impacts on lncRNA structure and function	http://bioinfo.life.hust.edu.cn/lncRNASNP2	Miao et al., 2018
LncVar	A database of genetic variation associated with long non-coding genes in six species	http://bioinfo.ibp.ac.cn/LncVar	Chen et al., 2017
The 1000 Genomes Project	The largest public catalog of human variation and genotype data	http://www.internationalgenome.org/	Genomes Project et al., 2015
dbSNP	A public-domain archive for a broad collection of simple genetic polymorphisms	https://www.ncbi.nlm.nih.gov/snp	
GWAS Catalog	A catalog that has provided data from published genome-wide association studies	www.ebi.ac.uk/gwas/	MacArthur et al., 2017
GWAS4D	A web server that systematically evaluates GWAS signals and identifies context-specific regulatory variants	http://mulinlab.tmu.edu.cn/gwas4d	Huang et al., 2018

SNVs, single-nucleotide variants; lncRNAs, long non-coding RNAs; GWAS, genome-wide association study.

should be detected through several methods, either luciferase reporter assays or high-throughput sequencing-based assays, such as *cis*-regulatory element analysis by sequencing (CRE-seq) (Kwasnieski et al., 2014) and self-transcribing active regulatory region sequencing (STARR-seq) (Arnold et al., 2013). Furthermore, functional verification is required to determine the direct biological significances, such as the oncogenic properties, which can be manifested though cancer cellular experiments (e.g., cell proliferation, cell cycle, cell death, migration, and invasion tests) along with *in vivo* model assays. In addition, other approaches are needed to be explored to demonstrate the effects of genetic variants within introns, exons, or intergenic regions. For instance, genetic variants mapping to exons of a lincRNA may alter the lincRNA secondary structure, which can be partly predicted using RNAfold web server (Hofacker and Stadler, 2006). The 5′ UTR (un-translated region) variants may affect the process of splicing and stability of RNA conformation, a functional splicing reporter minigene assay should be used to assess the effect of genetic variants on RNA splicing (Giorgi et al., 2015). Through the aforementioned knowable strategies, comprehensive functional verification of non-coding variants is very important to understand their biological consequence; there is an urgent need to explore more practical methods and strategies for functional verification research.

PERSPECTIVES AND DISCUSSION

Single-nucleotide variants are the most common genetic variants and universally present in the human genome, including non-coding regions. One current belief is that heterogeneous disease (e.g., cancers susceptibility) may be caused by the accumulation of multiple driving genetic variations. GWASs have identified a large number of disease or trait-associated SNVs, and many of those are located in non-coding regions of the human genome. The functions of genetic variants are generally unknown and remain to be elucidated. One critical common viewpoint is that the significance of lincRNA variants depends on their genomic position. Certain SNVs are located in regulatory regions of lincRNA genes; it is found to affect the binding efficiency of transcription factor; it is known to possibly regulate the transcription of lincRNAs and other related genes in a cell-type- or tissue-specific manner. The mapping of SNVs to lincRNA transcript itself potentially affects the process of splicing and stability of lincRNA conformation or modulates the lincRNA secondary structure; these effects may lead to an alteration of the interactive properties and regulatory functions of lincRNA (Khurana et al., 2016). Collectively, these findings indicate that genetic variants in lincRNA regions may serve as a regulatory signature for early events, which illustrate the genomic background of lincRNA differential expressions in a tissue- or disorder-specific manner.

Considering their important regulatory role, lincRNAs may serve as the promising biomarkers for the diagnosis, prognosis, and treatment response of various diseases (Zou et al., 2018). With their characteristic of tissue and disease specificity, lincRNAs may be explored as target molecules for personalized medicine in the future (Huarte, 2015). Currently, molecular targets drug approved by the US Food and Drug Administration (FDA) are mainly derived from proteins. However, owing to the finiteness of druggable protein genes in the human genome, the expansion of potentially druggable targets may need to include lncRNA molecules. One lincRNA *PCA3*-based test (the PROGENSA *PCA3* assay approved by the FDA) has been used as a marker for the detection of prostate cancers (Evaluation of Genomic Applications in Practice and Prevention [EGAPP] Working Group, 2014). Moreover, a novel treatment strategy differs from the classical small molecules and antibodies that mainly target proteins. RNA-targeting therapeutics refer to the use of oligonucleotides to target primarily RNA involved in various diseases for therapeutic efforts. Two major approaches are employed to target RNA: double-stranded RNA-mediated interference (RNAi) and antisense oligonucleotides (ASOs) (Kole et al., 2012). Currently, both methods are in clinical trials. Among them, nusinersen (Spinraza), an ASO-targeting drug for spinal muscular atrophy (SMA), has been approved by the FDA (Finkel et al., 2017); patisiran, an RNAi therapeutic strategy for hereditary

transthyretin amyloidosis (hATTR), has also shown promising results (Adams et al., 2018). Hence, we can expect that lincRNA molecules will provide additional options for RNA therapeutics. Importantly, disease-associated variants are found to exhibit a higher frequency in non-coding regions, which encompass enhancers, promoters, and other regulatory elements. It is likely that the role of genetic variants in lincRNA regions should be characterized at the regulatory network level. Genetic variants may offer the possibility to make use of the information from adjacent protein-coding or non-coding regions to link with heterogeneous diseases. Therefore, a combination of SNVs, lincRNAs, and proteins may bring personalized medicine closer to clinical applications in the foreseeable future (Li et al., 2019).

Previous studies may appear to be a slightly biased against the genetic variants that are located in non-coding regions, as their significant roles have not yet been explored to the same extent as those of protein-coding genes. In particular, for the disease-associated variants in lincRNA regions, whether functionally affected or altered in lincRNA expression by risk variants, it may be responsible for the disease development and its pathogenesis. Verification of the mechanisms requires a detailed understanding of the lincRNA structure and function, and a suitable experimental system to distinguish the subtle differences caused by genetic variants. Although it is difficult to describe the consequences of genetic variants in non-coding regions, more emerging technologies and approaches are urgently needed to explore the driving effects of genetic variants on lincRNA regions.

AUTHOR CONTRIBUTIONS

HZ consulted relevant literatures, finished the manuscript, and completed English revision. LT completed the figures and tables. F-FS provided constructive feedback and guidance. L-XW and H-HZ completed critical revisions and proofread the manuscript.

FUNDING

This work was supported by grants from the National Natural Science Foundation of China (Nos. 81603201 and 81473284). This work was also supported by funds from the Joint International Research Laboratory of Reproduction and Development, Institute of life Sciences, Chongqing Medical University.

REFERENCES

Adams, D., Gonzalez-Duarte, A., O'riordan, W. D., Yang, C. C., Ueda, M., Kristen, A. V., et al. (2018). Patisiran, an RNAi therapeutic, for hereditary transthyretin amyloidosis. *N. Engl. J. Med.* 379, 11–21. doi: 10.1056/NEJMoa1716153

Arnold, C. D., Gerlach, D., Stelzer, C., Boryn, L. M., Rath, M., and Stark, A. (2013). Genome-wide quantitative enhancer activity maps identified by STARR-seq. *Science* 339, 1074–1077. doi: 10.1126/science.1232542

Athanasiu, L., Smorr, L. L., Tesli, M., Rossberg, J. I., Sonderby, I. E., Spigset, O., et al. (2015). Genome-wide association study identifies common variants associated with pharmacokinetics of psychotropic drugs. *J. Psychopharmacol.* 29, 884–891. doi: 10.1177/0269881115584469

Cabili, M. N., Trapnell, C., Goff, L., Koziol, M., Tazon-Vega, B., Regev, A., et al. (2011). Integrative annotation of human large intergenic noncoding RNAs reveals global properties and specific subclasses. *Genes Dev.* 25, 1915–1927. doi: 10.1101/gad.17446611

Cerhan, J. R., Berndt, S. I., Vijai, J., Ghesquieres, H., Mckay, J., Wang, S. S., et al. (2014). Genome-wide association study identifies multiple susceptibility loci for diffuse large B cell lymphoma. *Nat. Genet.* 46, 1233–1238. doi: 10.1038/ng.3105

Chen, X., Hao, Y., Cui, Y., Fan, Z., He, S., Luo, J., et al. (2017). LncVar: a database of genetic variation associated with long non-coding genes. *Bioinformatics* 33, 112–118. doi: 10.1093/bioinformatics/btw581

Chen, X. F., Zhu, D. L., Yang, M., Hu, W. X., Duan, Y. Y., Lu, B. J., et al. (2018). An Osteoporosis Risk SNP at 1p36.*12* Acts as an Allele-Specific Enhancer to Modulate LINC00339 Expression via Long-Range Loop Formation. *Am. J. Hum. Genet.* 102, 776–793. doi: 10.1016/j.ajhg.2018.03.001

Chu, H., Xia, L., Qiu, X., Gu, D., Zhu, L., Jin, J., et al. (2015). Genetic variants in noncoding PIWI-interacting RNA and colorectal cancer risk. *Cancer* 121, 2044–2052. doi: 10.1002/cncr.29314

Chu, M., Yuan, W., Wu, S., Wang, Z., Mao, L., Tian, T., et al. (2016). Quantitative assessment of polymorphisms in H19 lncRNA and cancer risk: a meta-analysis of 13,392 cases and 18,893 controls. *Oncotarget* 7, 78631–78639. doi: 10.18632/oncotarget.12530

Chung, S., Nakagawa, H., Uemura, M., Piao, L., Ashikawa, K., Hosono, N., et al. (2011). Association of a novel long non-coding RNA in 8q24 with prostate cancer susceptibility. *Cancer Sci.* 102, 245–252. doi: 10.1111/j.1349-7006.2010.01737.x

Conti, D. V., Wang, K., Sheng, X., Bensen, J. T., Hazelett, D. J., Cook, M. B., et al. (2017). Two novel susceptibility loci for prostate cancer in men of african ancestry. *J. Natl. Cancer Inst.* 109:djx084. doi: 10.1093/jnci/djx084

Cui, Z., Gao, M., Yin, Z., Yan, L., and Cui, L. (2018). Association between lncRNA CASC8 polymorphisms and the risk of cancer: a meta-analysis. *Cancer Manag. Res.* 10, 3141–3148. doi: 10.2147/CMAR.S170783

Derrien, T., Johnson, R., Bussotti, G., Tanzer, A., Djebali, S., Tilgner, H., et al. (2012). The GENCODE v7 catalog of human long noncoding RNAs: analysis of their gene structure, evolution, and expression. *Genome Res.* 22, 1775–1789. doi: 10.1101/gr.132159.111

Evaluation of Genomic Applications in Practice and Prevention [EGAPP] Working Group, (2014). Recommendations from the EGAPP Working Group: does PCA3 testing for the diagnosis and management of prostate cancer improve patient health outcomes?. *Genet. Med.* 16, 338–346. doi: 10.1038/gim.2013.141

Fava, V. M., Manry, J., Cobat, A., Orlova, M., Van Thuc, N., Moraes, M. O., et al. (2017). A genome wide association study identifies a lncRna as risk factor for pathological inflammatory responses in leprosy. *PLoS Genet.* 13:e1006637. doi: 10.1371/journal.pgen.1006637

Finkel, R. S., Mercuri, E., Darras, B. T., Connolly, A. M., Kuntz, N. L., Kirschner, J., et al. (2017). Nusinersen versus sham control in infantile-onset spinal muscular atrophy. *N. Engl. J. Med.* 377, 1723–1732. doi: 10.1056/NEJMoa1702752

Freedman, M. L., Monteiro, A. N., Gayther, S. A., Coetzee, G. A., Risch, A., Plass, C., et al. (2011). Principles for the post-GWAS functional characterization of cancer risk loci. *Nat. Genet.* 43, 513–518. doi: 10.1038/ng.840

Gao, P., Xia, J. H., Sipeky, C., Dong, X. M., Zhang, Q., Yang, Y., et al. (2018). Biology AND CLINICAL IMPLICATIONS OF the 19q13 aggressive prostate cancer susceptibility locus. *Cell* 174, 576.e18–589.e18. doi: 10.1016/j.cell.2018.06.003

Gao, W., Zhu, M., Wang, H., Zhao, S., Zhao, D., Yang, Y., et al. (2015). Association of polymorphisms in long non-coding RNA H19 with coronary artery disease risk in a Chinese population. *Mutat. Res.* 772, 15–22. doi: 10.1016/j.mrfmmm.2014.12.009

Ge, L., Wang, Q., Hu, S., and Yang, X. (2018). Rs217727 polymorphism in H19 promotes cell apoptosis by regulating the expressions of H19 and the activation of its downstream signaling pathway. *J. Cell Physiol.* 234, 7279–7291. doi: 10.1002/jcp.27485

Genomes Project, C., Auton, A., Brooks, L. D., Durbin, R. M., Garrison, E. P., Kang, H. M., et al. (2015). A global reference for human genetic variation. *Nature* 526, 68–74. doi: 10.1038/nature15393

Ghanbari, M., Peters, M. J., De Vries, P. S., Boer, C. G., Van Rooij, J. G. J., Lee, Y. C., et al. (2018). A systematic analysis highlights multiple long non-coding RNAs associated with cardiometabolic disorders. *J. Hum. Genet.* 63, 431–446. doi: 10.1038/s10038-017-0403-x

Ghesquieres, H., Larrabee, B. R., Casasnovas, O., Maurer, M. J., Mckay, J. D., Ansell, S. M., et al. (2018). A susceptibility locus for classical Hodgkin lymphoma at 8q24 near MYC/PVT1 predicts patient outcome in two independent cohorts. *Br. J. Haematol.* 180, 286–290. doi: 10.1111/bjh.14306

Giorgi, G., Casarin, A., Trevisson, E., Dona, M., Cassina, M., Graziano, C., et al. (2015). Validation of CFTR intronic variants identified during cystic fibrosis population screening by a minigene splicing assay. *Clin. Chem. Lab. Med* 53, 1719–1723. doi: 10.1515/cclm-2014-1047

Gong, W. J., Peng, J. B., Yin, J. Y., Li, X. P., Zheng, W., Xiao, L., et al. (2017). Association between well-characterized lung cancer lncRNA polymorphisms and platinum-based chemotherapy toxicity in Chinese patients with lung cancer. *Acta Pharmacol. Sin.* 38, 581–590. doi: 10.1038/aps.2016.164

GTEx Consortium, Data Analysis &Coordinating Center [LDACC], Analysis Working Group, Statistical Methods groups, Analysis Working Group, Enhancing GTEx groups, et al. (2017). Genetic effects on gene expression across human tissues. *Nature* 550, 204–213. doi: 10.1038/nature25160

Guo, H., Ahmed, M., Zhang, F., Yao, C. Q., Li, S., Liang, Y., et al. (2016). Modulation of long noncoding RNAs by risk SNPs underlying genetic predispositions to prostate cancer. *Nat. Genet.* 48, 1142–1150. doi: 10.1038/ng.3637

Guo, Q. Y., Wang, H., and Wang, Y. (2017). LncRNA H19 polymorphisms associated with the risk of OSCC in Chinese population. *Eur. Rev. Med. Pharmacol. Sci.* 21, 3770–3774.

Guo, Z., Wang, Y., Zhao, Y., Jin, Y., An, L., Wu, B., et al. (2017). Genetic polymorphisms of long non-coding RNA GAS5 predict platinum-based concurrent chemoradiotherapy response in nasopharyngeal carcinoma patients. *Oncotarget* 8, 62286–62297. doi: 10.18632/oncotarget.19725

Han, L., Liu, S., Liang, J., Guo, Y., Shen, S., Guo, X., et al. (2017). A genetic polymorphism at miR-526b binding-site in the lincRNA-NR_024015 exon confers risk of esophageal squamous cell carcinoma in a population of North China. *Mol. Carcinog.* 56, 960–971. doi: 10.1002/mc.22549

Hanson, R. L., Craig, D. W., Millis, M. P., Yeatts, K. A., Kobes, S., Pearson, J. V., et al. (2007). Identification of PVT1 as a candidate gene for end-stage renal disease in type 2 diabetes using a pooling-based genome-wide single nucleotide polymorphism association study. *Diabetes Metab. Res. Rev.* 56, 975–983. doi: 10.2337/db06-1072

Harati-Sadegh, M., Kohan, L., Teimoori, B., and Salimi, S. (2018). The long non-coding RNA H19 rs217727 polymorphism is associated with PE susceptibility. *J. Cell. Biochem.* 119, 5473–5480. doi: 10.1002/jcb.26708

He, H., Li, W., Liyanarachchi, S., Srinivas, M., Wang, Y., Akagi, K., et al. (2015). Multiple functional variants in long-range enhancer elements contribute to the risk of SNP rs965513 in thyroid cancer. *Proc. Natl. Acad. Sci. U.S.A.* 112, 6128–6133. doi: 10.1073/pnas.1506255112

Hindorff, L. A., Sethupathy, P., Junkins, H. A., Ramos, E. M., Mehta, J. P., Collins, F. S., et al. (2009). Potential etiologic and functional implications of genome-wide association loci for human diseases and traits. *Proc. Natl. Acad. Sci. U.S.A.* 106, 9362–9367. doi: 10.1073/pnas.0903103106

Hofacker, I. L., and Stadler, P. F. (2006). Memory efficient folding algorithms for circular RNA secondary structures. *Bioinformatics* 22, 1172–1176. doi: 10.1093/bioinformatics/btl023

Hon, C. C., Ramilowski, J. A., Harshbarger, J., Bertin, N., Rackham, O. J., Gough, J., et al. (2017). An atlas of human long non-coding RNAs with accurate 5' ends. *Nature* 543, 199–204. doi: 10.1038/nature21374

Hu, L., Chen, S. H., Lv, Q. L., Sun, B., Qu, Q., Qin, C. Z., et al. (2016). Clinical Significance of Long Non-Coding RNA CASC8 rs10505477 polymorphism in lung cancer susceptibility, platinum-based chemotherapy response, and toxicity. *Int. J. Environ. Res. Public Health* 13:545. doi: 10.3390/ijerph13060545

Hua, J. T., Ahmed, M., Guo, H., Zhang, Y., Chen, S., Soares, F., et al. (2018). Risk SNP-mediated promoter-enhancer switching drives prostate cancer through lncRNA PCAT19. *Cell* 174, 564.e18–575.e18. doi: 10.1016/j.cell.2018.06.014

Huang, D., Yi, X., Zhang, S., Zheng, Z., Wang, P., Xuan, C., et al. (2018). GWAS4D: multidimensional analysis of context-specific regulatory variant for human complex diseases and traits. *Nucleic Acids Res.* 46, W114–W120. doi: 10.1093/nar/gky407

Huarte, M. (2015). The emerging role of lncRNAs in cancer. *Nat. Med.* 21, 1253–1261. doi: 10.1038/nm.3981

Human Genome Structural Variation Working Group, Eichler, E. E., Nickerson, D. A., Altshuler, D., Bowcock, A. M., Brooks, L. D., et al. (2007). Completing the map of human genetic variation. *Nature* 447, 161–165. doi: 10.1038/447161a

Ingle, J. N., Xie, F., Ellis, M. J., Goss, P. E., Shepherd, L. E., Chapman, J. W., et al. (2016). Genetic polymorphisms in the long noncoding RNA MIR2052HG offer a pharmacogenomic basis for the response of breast cancer patients to aromatase inhibitor therapy. *Cancer Res.* 76, 7012–7023. doi: 10.1158/0008-5472.CAN-16-1371

Ishii, N., Ozaki, K., Sato, H., Mizuno, H., Saito, S., Takahashi, A., et al. (2006). Identification of a novel non-coding RNA, MIAT, that confers risk of myocardial infarction. *J. Hum. Genet.* 51, 1087–1099. doi: 10.1007/s10038-006-0070-9

Jendrzejewski, J., He, H., Radomska, H. S., Li, W., Tomsic, J., Liyanarachchi, S., et al. (2012). The polymorphism rs944289 predisposes to papillary thyroid carcinoma through a large intergenic noncoding RNA gene of tumor suppressor type. *Proc. Natl. Acad. Sci. U.S.A.* 109, 8646–8651. doi: 10.1073/pnas.1205654109

Kenyan Bacteraemia Study Group, Wellcome Trust, Case Control, C., Rautanen, A., Pirinen, M., Mills, T. C., et al. (2016). Polymorphism in a lincRNA associates with a doubled risk of pneumococcal bacteremia in kenyan children. *Am. J. Hum. Genet.* 98, 1092–1100. doi: 10.1016/j.ajhg.2016.03.025

Khurana, E., Fu, Y., Chakravarty, D., Demichelis, F., Rubin, M. A., and Gerstein, M. (2016). Role of non-coding sequence variants in cancer. *Nat. Rev. Genet.* 17, 93–108. doi: 10.1038/nrg.2015.17

Kim, T., Cui, R., Jeon, Y. J., Lee, J. H., Lee, J. H., Sim, H., et al. (2014). Long-range interaction and correlation between MYC enhancer and oncogenic long noncoding RNA CARLo-5. *Proc. Natl. Acad. Sci. U.S.A.* 111, 4173–4178. doi: 10.1073/pnas.1400350111

Kole, R., Krainer, A. R., and Altman, S. (2012). RNA therapeutics: beyond RNA interference and antisense oligonucleotides. *Nat. Rev. Drug Discov.* 11, 125–140. doi: 10.1038/nrd3625

Konermann, S., Brigham, M. D., Trevino, A. E., Joung, J., Abudayyeh, O. O., Barcena, C., et al. (2015). Genome-scale transcriptional activation by an engineered CRISPR-Cas9 complex. *Nature* 517, 583–588. doi: 10.1038/nature14136

Kretz, M., Siprashvili, Z., Chu, C., Webster, D. E., Zehnder, A., Qu, K., et al. (2013). Control of somatic tissue differentiation by the long non-coding RNA TINCR. *Nature* 493, 231–235. doi: 10.1038/nature11661

Kulakova, O., Bashinskaya, V., Kiselev, I., Baulina, N., Tsareva, E., Nikolaev, R., et al. (2017). Pharmacogenetics of glatiramer acetate therapy for multiple sclerosis: the impact of genome-wide association studies identified disease risk loci. *Pharmacogenomics* 18, 1563–1574. doi: 10.2217/pgs-2017-0058

Kwasnieski, J. C., Fiore, C., Chaudhari, H. G., and Cohen, B. A. (2014). High-throughput functional testing of ENCODE segmentation predictions. *Genome Res.* 24, 1595–1602. doi: 10.1101/gr.173518.114

Lee, T. H., Ko, T. M., Chen, C. H., Lee, M. T., Chang, Y. J., Chang, C. H., et al. (2016). Identification of PTCSC3 as a novel locus for large-vessel ischemic stroke: a genome-wide association Study. *J. Am. Heart Assoc.* 5:e003003. doi: 10.1161/JAHA.115.003003

Li, C., Rao, T., Chen, X., Zou, Z., Wei, A., Tang, J., et al. (2019). HLA-B*35:01 allele is a potential biomarker for predicting polygonum multiflorum-induced liver injury in humans. *Hepatology* 70, 346–357. doi: 10.1002/hep.30660

Li, L., Sun, R., Liang, Y., Pan, X., Li, Z., Bai, P., et al. (2013). Association between polymorphisms in long non-coding RNA PRNCR1 in 8q24 and risk of colorectal cancer. *J. Exp. Clin. Cancer Res.* 32:104. doi: 10.1186/1756-9966-32-104

Li, Q., Ma, G., Sun, S., Xu, Y., and Wang, B. (2018a). Polymorphism in the promoter region of lncRNA GAS5 is functionally associated with the risk of gastric cancer. *Clin. Res. Hepatol. Gastroenterol.* 42, 478–482. doi: 10.1016/j.clinre.2018.01.006

Li, Q., Zhu, W., Zhang, B., Wu, Y., Yan, S., Yuan, Y., et al. (2018b). The MALAT1 gene polymorphism and its relationship with the onset of congenital heart disease in Chinese. *Biosci. Rep.* 38:BSR20171381. doi: 10.1042/BSR20171381

Li, Y., Bao, C., Gu, S., Ye, D., Jing, F., Fan, C., et al. (2017). Associations between novel genetic variants in the promoter region of MALAT1 and risk of colorectal cancer. *Oncotarget* 8, 92604–92614. doi: 10.18632/oncotarget.21507

Ling, H., Spizzo, R., Atlasi, Y., Nicoloso, M., Shimizu, M., Redis, R. S., et al. (2013). CCAT2, a novel noncoding RNA mapping to 8q24, underlies metastatic progression and chromosomal instability in colon cancer. *Genome Res.* 23, 1446–1461. doi: 10.1101/gr.152942.112

Ma, G., Gu, D., Lv, C., Chu, H., Xu, Z., Tong, N., et al. (2015). Genetic variant in 8q24 is associated with prognosis for gastric cancer in a Chinese population. *J. Gastroenterol. Hepatol.* 30, 689–695. doi: 10.1111/jgh.12801

MacArthur, J., Bowler, E., Cerezo, M., Gil, L., Hall, P., Hastings, E., et al. (2017). The new NHGRI-EBI Catalog of published genome-wide association studies (GWAS Catalog). *Nucleic Acids Res.* 45, D896–D901. doi: 10.1093/nar/gkw1133

Maris, J. M., Mosse, Y. P., Bradfield, J. P., Hou, C., Monni, S., Scott, R. H., et al. (2008). Chromosome 6p22 locus associated with clinically aggressive neuroblastoma. *N. Engl. J. Med.* 358, 2585–2593. doi: 10.1056/NEJMoa0708698

Marjonen, H., Auvinen, P., Kahila, H., Tsuiko, O., Koks, S., Tiirats, A., et al. (2018). rs10732516 polymorphism at the IGF2/H19 locus associates with genotype-specific effects on placental DNA methylation and birth weight of newborns conceived by assisted reproductive technology. *Clin. Epigenetics* 10:80. doi: 10.1186/s13148-018-0511-2

Meyer, K. B., Maia, A. T., O'reilly, M., Ghoussaini, M., Prathalingam, R., Porter-Gill, P., et al. (2011). A functional variant at a prostate cancer predisposition locus at 8q24 is associated with PVT1 expression. *PLoS Genet.* 7:e1002165. doi: 10.1371/journal.pgen.1002165

Miao, Y. R., Liu, W., Zhang, Q., and Guo, A. Y. (2018). lncRNASNP2: an updated database of functional SNPs and mutations in human and mouse lncRNAs. *Nucleic Acids Res.* 46, D276–D280. doi: 10.1093/nar/gkx1004

Ng, M. C. Y., Graff, M., Lu, Y., Justice, A. E., Mudgal, P., Liu, C. T., et al. (2017). Discovery and fine-mapping of adiposity loci using high density imputation of genome-wide association studies in individuals of African ancestry: African ancestry anthropometry genetics Consortium. *PLoS Genet.* 13:e1006719. doi: 10.1371/journal.pgen.1006719

Nikpay, M., Goel, A., Won, H. H., Hall, L. M., Willenborg, C., Kanoni, S., et al. (2015). A comprehensive 1,000 Genomes-based genome-wide association meta-analysis of coronary artery disease. *Nat. Genet.* 47, 1121–1130. doi: 10.1038/ng.3396

Ning, S., Yue, M., Wang, P., Liu, Y., Zhi, H., Zhang, Y., et al. (2017). LincSNP 2.0: an updated database for linking disease-associated SNPs to human long non-coding RNAs and their TFBSs. *Nucleic Acids Res.* 45, D74–D78. doi: 10.1093/nar/gkw945

Orr, N., Cooke, R., Jones, M., Fletcher, O., Dudbridge, F., Chilcott-Burns, S., et al. (2011). Genetic variants at chromosomes 2q35, 5p12, 6q25.1, 10q26.13, and 16q12.1 influence the risk of breast cancer in men. *PLoS Genet.* 7:e1002290. doi: 10.1371/journal.pgen.1002290

Petry, C. J., Seear, R. V., Wingate, D. L., Acerini, C. L., Ong, K. K., Hughes, I. A., et al. (2011). Maternally transmitted foetal H19 variants and associations with birth weight. *Hum. Genet.* 130, 663–670. doi: 10.1007/s00439-011-1005-x

Pomerantz, M. M., Ahmadiyeh, N., Jia, L., Herman, P., Verzi, M. P., Doddapaneni, H., et al. (2009). The 8q24 cancer risk variant rs6983267 shows long-range interaction with MYC in colorectal cancer. *Nat. Genet.* 41, 882–884. doi: 10.1038/ng.403

Ponting, C. P., Oliver, P. L., and Reik, W. (2009). Evolution and functions of long noncoding RNAs. *Cell* 136, 629–641. doi: 10.1016/j.cell.2009.02.006

Powell, J. E., Fung, J. N., Shakhbazov, K., Sapkota, Y., Cloonan, N., Hemani, G., et al. (2016). Endometriosis risk alleles at 1p36.12 act through inverse regulation of CDC42 and LINC00339. *Hum. Mol. Genet.* 25, 5046–5058. doi: 10.1093/hmg/ddw320

Rao, S. Q., Hu, H. L., Ye, N., Shen, Y., and Xu, Q. (2015). Genetic variants in long non-coding RNA MIAT contribute to risk of paranoid schizophrenia in a Chinese Han population. *Schizophr. Res.* 166, 125–130. doi: 10.1016/j.schres.2015.04.032

Redis, R. S., Vela, L. E., Lu, W., Ferreira De Oliveira, J., Ivan, C., Rodriguez-Aguayo, C., et al. (2016). Allele-specific reprogramming of cancer metabolism by the long non-coding RNA CCAT2. *Mol. Cell.* 61:640. doi: 10.1016/j.molcel.2016.02.006

Schaub, M. A., Boyle, A. P., Kundaje, A., Batzoglou, S., and Snyder, M. (2012). Linking disease associations with regulatory information in the human genome. *Genome Res.* 22, 1748–1759. doi: 10.1101/gr.136127.111

Shah, M. Y., Ferracin, M., Pileczki, V., Chen, B., Redis, R., Fabris, L., et al. (2018). Cancer-associated rs6983267 SNP and its accompanying long noncoding RNA CCAT2 induce myeloid malignancies via unique SNP-specific RNA mutations. *Genome Res.* 28, 432–447. doi: 10.1101/gr.225128.117

Shyn, S. I., Shi, J., Kraft, J. B., Potash, J. B., Knowles, J. A., Weissman, M. M., et al. (2011). Novel loci for major depression identified by genome-wide association study of sequenced treatment alternatives to relieve depression and meta-analysis of three studies. *Mol. Psychiatry* 16, 202–215. doi: 10.1038/mp.2009.125

Sur, I. K., Hallikas, O., Vaharautio, A., Yan, J., Turunen, M., Enge, M., et al. (2012). Mice lacking a Myc enhancer that includes human SNP rs6983267 are resistant to intestinal tumors. *Science* 338, 1360–1363. doi: 10.1126/science.1228606

Tao, R., Hu, S., Wang, S., Zhou, X., Zhang, Q., Wang, C., et al. (2015). Association between indel polymorphism in the promoter region of lncRNA GAS5 and the risk of hepatocellular carcinoma. *Carcinogenesis* 36, 1136–1143. doi: 10.1093/carcin/bgv099

Teerlink, C. C., Leongamornlert, D., Dadaev, T., Thomas, A., Farnham, J., Stephenson, R. A., et al. (2016). Genome-wide association of familial prostate cancer cases identifies evidence for a rare segregating haplotype at 8q24.21. *Hum. Genet.* 135, 923–938. doi: 10.1007/s00439-016-1690-6

The Encode Project Consortium, (2012). An integrated encyclopedia of DNA elements in the human genome. *Nature* 489, 57–74. doi: 10.1038/nature11247

Tuupanen, S., Turunen, M., Lehtonen, R., Hallikas, O., Vanharanta, S., Kivioja, T., et al. (2009). The common colorectal cancer predisposition SNP rs6983267 at chromosome 8q24 confers potential to enhanced Wnt signaling. *Nat. Genet.* 41, 885–890. doi: 10.1038/ng.406

Ulitsky, I., and Bartel, D. P. (2013). lincRNAs: genomics, evolution, and mechanisms. *Cell* 154, 26–46.

Venter, J. C., Adams, M. D., Myers, E. W., Li, P. W., Mural, R. J., Sutton, G. G., et al. (2001). The sequence of the human genome. *Science* 291, 1304–1351.

Verhaegh, G. W., Verkleij, L., Vermeulen, S. H., Den Heijer, M., Witjes, J. A., and Kiemeney, L. A. (2008). Polymorphisms in the H19 gene and the risk of bladder cancer. *Eur. Urol.* 54, 1118–1126. doi: 10.1016/j.eururo.2008.01.060

Wallace, C., Smyth, D. J., Maisuria-Armer, M., Walker, N. M., Todd, J. A., and Clayton, D. G. (2010). The imprinted DLK1-MEG3 gene region on chromosome 14q32.2 alters susceptibility to type 1 diabetes. *Nat. Genet.* 42, 68–71. doi: 10.1038/ng.493

Wang, B. G., Lv, Z., Ding, H. X., Fang, X. X., Wen, J., Xu, Q., et al. (2018a). The association of lncRNA-HULC polymorphisms with hepatocellular cancer risk and prognosis. *Gene* 670, 148–154. doi: 10.1016/j.gene.2018.05.096

Wang, B. G., Xu, Q., Lv, Z., Fang, X. X., Ding, H. X., Wen, J., et al. (2018b). Association of twelve polymorphisms in three onco-lncRNA genes with hepatocellular cancer risk and prognosis: a case-control study. *World J. Gastroenterol.* 24, 2482–2490. doi: 10.3748/wjg.v24.i23.2482

Wang, J. Z., Xiang, J. J., Wu, L. G., Bai, Y. S., Chen, Z. W., Yin, X. Q., et al. (2017). A genetic variant in long non-coding RNA MALAT1 associated with survival outcome among patients with advanced lung adenocarcinoma: a survival cohort analysis. *BMC Cancer* 17:167. doi: 10.1186/s12885-017-3151-6

Westra, H. J., Martinez-Bonet, M., Onengut-Gumuscu, S., Lee, A., Luo, Y., Teslovich, N., et al. (2018). Fine-mapping and functional studies highlight potential causal variants for rheumatoid arthritis and type 1 diabetes. *Nat. Genet.* 50, 1366–1374. doi: 10.1038/s41588-018-0216-7

Wu, H., Zheng, J., Deng, J., Hu, M., You, Y., Li, N., et al. (2013). A genetic polymorphism in lincRNA-uc003opf.1 is associated with susceptibility to esophageal squamous cell carcinoma in Chinese populations. *Carcinogenesis* 34, 2908–2917. doi: 10.1093/carcin/bgt252

Wu, N. Y., Huang, H. S., Chao, T. H., Chou, H. M., Fang, C., Qin, C. Z., et al. (2017). Progesterone prevents high-grade serous ovarian cancer by inducing necroptosis of p53-defective fallopian tube epithelial cells. *Cell Rep.* 18, 2557–2565. doi: 10.1016/j.celrep.2017.02.049

Wu, Q., Yan, W., Han, R., Yang, J., Yuan, J., Ji, X., et al. (2016). Polymorphisms in long noncoding RNA H19 contribute to the protective effects of coal workers' pneumoconiosis in a chinese population. *Int. J. Environ. Res. Public Health* 13:903. doi: 10.3390/ijerph13090903

Xue, Y., Gu, D., Ma, G., Zhu, L., Hua, Q., Chu, H., et al. (2015). Genetic variants in lncRNA HOTAIR are associated with risk of colorectal cancer. *Mutagenesis* 30, 303–310. doi: 10.1093/mutage/geu076

Xue, Y., Wang, M., Kang, M., Wang, Q., Wu, B., Chu, H., et al. (2013). Association between lncrna PCGEM1 polymorphisms and prostate cancer risk. *Prostate Cancer Prostatic Dis.* 16, 139–144. doi: 10.1038/pcan.2013.6

Yan, H., Zhang, D. Y., Li, X., Yuan, X. Q., Yang, Y. L., Zhu, K. W., et al. (2017). Long non-coding RNA GAS5 polymorphism predicts a poor prognosis of acute myeloid leukemia in Chinese patients via affecting hematopoietic reconstitution. *Leuk. Lymphoma* 58, 1948–1957. doi: 10.1080/10428194.2016.1266626

Yang, M. L., Huang, Z., Wang, Q., Chen, H. H., Ma, S. N., Wu, R., et al. (2018). The association of polymorphisms in lncRNA-H19 with hepatocellular cancer risk and prognosis. *Biosci. Rep.* 38:BSR20171652. doi: 10.1042/BSR20171652

Yeager, M., Orr, N., Hayes, R. B., Jacobs, K. B., Kraft, P., Wacholder, S., et al. (2007). Genome-wide association study of prostate cancer identifies a second risk locus at 8q24. *Nat. Genet.* 39, 645–649. doi: 10.1016/j.eururo.2007.06.013

Zhang, Y., Manjunath, M., Zhang, S., Chasman, D., Roy, S., and Song, J. S. (2018). Integrative genomic analysis predicts causative Cis-regulatory mechanisms of the breast cancer-associated genetic variant rs4415084. *Cancer Res.* 78, 1579–1591. doi: 10.1158/0008-5472.CAN-17-3486

Zhang, Z., Zhu, Z., Zhang, B., Li, W., Li, X., Wu, X., et al. (2014). Frequent mutation of rs13281615 and its association with PVT1 expression and cell proliferation in breast cancer. *J. Genet. Genomics* 41, 187–195. doi: 10.1016/j.jgg.2014.03.006

Zhao, X., Wei, X., Zhao, L., Shi, L., Cheng, J., Kang, S., et al. (2016). The rs6983267 SNP and long non-coding RNA CARLo-5 are associated with endometrial carcinoma. *Environ. Mol. Mutagen.* 57, 508–515. doi: 10.1002/em.22031

Zheng, J., Huang, X., Tan, W., Yu, D., Du, Z., Chang, J., et al. (2016). Pancreatic cancer risk variant in LINC00673 creates a miR-1231 binding site and interferes with PTPN11 degradation. *Nat. Genet.* 48, 747–757. doi: 10.1038/ng.3568

Zheng, Y., Yang, C., Tong, S., Ding, Y., Deng, W., Song, D., et al. (2017). Genetic variation of long non-coding RNA TINCR contribute to the susceptibility and progression of colorectal cancer. *Oncotarget* 8, 33536–33543. doi: 10.18632/oncotarget.16538

Zhuo, Y., Zeng, Q., Zhang, P., Li, G., Xie, Q., and Cheng, Y. (2017). Functional polymorphism of lncRNA MALAT1 contributes to pulmonary arterial hypertension susceptibility in Chinese people. *Clin. Chem. Lab. Med* 55, 38–46. doi: 10.1515/cclm-2016-0056

Zou, H., Wen, C., Peng, Z., Shao, Y., Hu, L., Li, S., et al. (2018). P4HB and PDIA3 are associated with tumor progression and therapeutic outcome of diffuse gliomas. *Oncol. Rep.* 39, 501–510. doi: 10.3892/or.2017.6134

Zou, H., Wu, L. X., Yang, Y., Li, S., Mei, Y., Liu, Y. B., et al. (2017). lncRNAs PVT1 and HAR1A are prognosis biomarkers and indicate therapy outcome for diffuse glioma patients. *Oncotarget* 8, 78767–78780. doi: 10.18632/oncotarget.20226

Conflict of Interest: The authors declare that the research was conducted in the absence of any commercial or financial relationships that could be construed as a potential conflict of interest.

frontiers in Oncology

ORIGINAL RESEARCH
published: 05 June 2020
doi: 10.3389/fonc.2020.00799

The KDM Inhibitor GSKJ4 Triggers CREB Downregulation via a Protein Kinase A and Proteasome-Dependent Mechanism in Human Acute Myeloid Leukemia Cells

Michela Illiano†, Mariarosaria Conte†, Alessia Salzillo, Angela Ragone, Annamaria Spina, Angela Nebbioso, Lucia Altucci, Luigi Sapio and Silvio Naviglio**

Department of Precision Medicine, University of Campania Luigi Vanvitelli, Naples, Italy

OPEN ACCESS

Edited by:
Paolo Pinton, University of Ferrara, Italy

Reviewed by:
Martina Pigazzi, University of Padova, Italy
Kira Gritsman, Albert Einstein College of Medicine, United States

***Correspondence:**
Luigi Sapio
luigi.sapio@unicampania.it
Silvio Naviglio
silvio.naviglio@unicampania.it

† These authors have contributed equally to this work

Specialty section:
This article was submitted to Molecular and Cellular Oncology, a section of the journal Frontiers in Oncology

Received: *28 November 2019*
Accepted: *23 April 2020*
Published: *05 June 2020*

Citation:
Illiano M, Conte M, Salzillo A, Ragone A, Spina A, Nebbioso A, Altucci L, Sapio L and Naviglio S (2020) The KDM Inhibitor GSKJ4 Triggers CREB Downregulation via a Protein Kinase A and Proteasome-Dependent Mechanism in Human Acute Myeloid Leukemia Cells. Front. Oncol. 10:799. doi: 10.3389/fonc.2020.00799

Acute myeloid leukemia (AML) is a progressive hematopoietic-derived cancer arising from stepwise genetic mutations of the myeloid lineage. cAMP response element-binding protein (CREB) is a nuclear transcription factor, which plays a key role in the multistep process of leukemogenesis, thus emerging as an attractive potential drug target for AML treatment. Since epigenetic dysregulations, such as DNA methylation, histone modifications, as well as chromatin remodeling, are a frequent occurrence in AML, an increasing and selective number of epi-drugs are emerging as encouraging therapeutic agents. Here, we demonstrate that the histone lysine demethylases (KDMs) JMJD3/UTX inhibitor GSKJ4 results in both proliferation decrease and CREB protein downregulation in AML cells. We found that GSKJ4 clearly decreases CREB protein, but not CREB mRNA levels. By cycloheximide assay, we provide evidence that GSKJ4 reduces CREB protein stability; moreover, proteasome inhibition largely counteracts the GSKJ4-induced CREB downregulation. Very interestingly, a rapid CREB phosphorylation at the Ser133 residue precedes CREB protein decrease in response to GSKJ4 treatment. In addition, protein kinase A (PKA) inhibition, but not extracellular signal-regulated kinase (ERK)1/2 inhibition, almost completely prevents both GSKJ4-induced p-Ser133-CREB phosphorylation and CREB protein downregulation. Overall, our study enforces the evidence regarding CREB as a potential druggable target, identifies the small epigenetic molecule GSKJ4 as an "inhibitor" of CREB, and encourages the design of future GSKJ4-based studies for the development of innovative approaches for AML therapy.

Keywords: GSKJ4, acute myeloid leukemia (AML), cAMP response element-binding protein (CREB) downregulation, proteasome-mediated degradation, protein kinase A (PKA)

INTRODUCTION

Acute myeloid leukemia (AML) is a very hostile malignant disease deriving from a rapid clonal expansion of immature granulocyte precursors. As a consequence of multiple transcriptional alterations, due to chromosomal abnormalities, somatic mutations, and epigenetic variations, biological and clinical AML degrees are characterized by heterogeneity and unpredictable treatment

responses (1). With an overall 5-year survival of <40%, AML is considered one of the deadliest leukemia subtypes. Current treatments, which include intensive chemotherapy rounds and bone marrow transplantation, are presumed to be only partially effective due to disease evolution and recurrent drug resistance achievement (2). Moreover, AML therapy is generally associated with a wide variety of side effects, including long-term complications and mortality (3). For this reason, the development of novel and more incisive therapeutic approaches with low toxicity are urgently demanded.

Normal hematopoiesis is mainly dependent on the controlled expression of critical genes by transcription factors. Notably, altered functions, by mutation and/or dysregulated expression, of these transcription factors play a relevant role in leukemogenesis (4). Speaking of which, cAMP response element-binding protein (CREB) is considered one of the most strictly related AML transcription factors (5).

As a member of a structurally related transcription factor family, which also includes activation transcription factor (ATF) and cAMP response element modulator (CREM), CREB proteins specifically recognize and bind DNA to cAMP-responsive element (CRE) promoter sites activating the transcription of specific target genes, including those affecting cell proliferation and survival. In response to various stimuli, such as hormones and growth factors, CREB leucine zipper domains are employed to generate dimeric homodimers and/or heterodimers, when combined with different proteins, complexes that precisely link deoxyribonucleic acid. Homodimer and heterodimer ratio undergoes continuous fluctuations into the cells in order to correlate signals from different pathways and to regulate the CREB transcriptional activity (6). Upon activation by phosphorylation at Ser133 by kinases, such as protein kinase A (PKA) and extracellular signal-regulated kinase (ERK)1/2, the co-activator CREB-binding protein (CBP) is engaged by CREB protein, and the CREB/CBP complex enhances the CREB transcriptional activity, facilitating the expression of the putative CREB-driven genes (7).

Previous studies have described CREB as a key regulator capable of driving both cell growth and survival in AML (8, 9). Specifically, CREB is generally overexpressed in AML cells causing growth rate increase and apoptosis resistance. Consistently, CREB knockdown induces decreased survival and proliferation in different leukemia cell lines (10). Conversely, an increased CREB expression has been associated with a reduced event-free survival in AML patients (11).

Based on the above findings, it is not surprising that CREB is becoming very attractive as a potential drug target for AML (4, 5, 12). Besides, increasing evidence indicates that dysregulation of histone modifications is widely involved in AML (13).

Epigenetic drugs are chemical and well-characterized compounds targeting disordered remodeling enzymes, thus modifying the chromatin cell state and changing the relative expression profile. Recently, several new epigenetic drugs have been developed, and some of them are standing out for their preclinical beneficial effects against cancer, including leukemia (14, 15). In this regard, GSKJ4 compound can be identified as a new inhibitor of the histone lysine demethylases (KDM) JMJD3 and UTX, showing a marked antiproliferative activity in different cancer types and, in particular, in AML cells (16–25). Here, we speculate that GSKJ4 treatment of AML cells could affect CREB pathway *via* a PKA and proteasome-dependent mechanism. The current investigation has been designed with the aim of defining the possible GSKJ4-mediated effects on CREB expression and function and the underlying molecular mechanisms in AML cells.

MATERIALS AND METHODS

Chemical Reagents and Antibodies

Chemical reagents included bovine serum albumin (BSA) (Sigma-Aldrich, B2518), 3-(4,5-dimethylthiazol-2-yl)-2,5-diphenyltetrazolium bromide (MTT) (Sigma-Aldrich, M5655), trypan blue (Sigma-Aldrich, T6146), propidium iodide (PI) (Sigma-Aldrich, P4864), GSKJ4 (Sigma-Aldrich, SML0101), PD98059 (Sigma-Aldrich, P215), PKF118-310 (Sigma-Aldrich, K4394), MG132 (Alexis 133407-82-6), and H89 (Sigma-Aldrich, #B1427). Antibodies obtained from Santa Cruz Biotechnology: anti-nuclear factor kappa-light-chain-enhancer of activated B cells (NF-κB) p65(A) (sc-109), anti-Ub (P4D1) (sc-8017), anti-α-tubulin (B-7) (sc-5286). Antibodies purchased from Cell Signaling Technology: anti-CREB (#9198S), anti-p44/42 mitogen-activated protein kinase (MAPK) (ERK1/2) (#9102), anti-p-CREB (Ser133, #9198), anti-phospho-p44/42 MAPK (ERK1/2) (Thr202/Tyr204) (#9101). Anti-vinculin (ab13007) and anti-H4 (ab10158) were bought from Abcam. Other antibodies used were anti-β-actin AC-74 (Sigma-Aldrich, A2228) and anti-H3K27me3 (Diagenode, C15410195). Conjugate horseradish peroxidase (HRP) goat anti-rabbit (GtxRb-003-DHRPX) and goat anti-mouse (GtxMu-003-EHRPX.0.05) (Immunoreagents Inc.) were employed for immunoblotting detection.

Cell Lines and Treatments

ATCC human U-937 and K-562 cell lines, and DSMZ human NB-4 cells, were kept in standard and unvaried atmosphere conditions (37°C in a 5% CO_2 humidified air) employing phenol red RPMI-1640 (Euroclone) plus 2 mM L-glutamine (Gibco), 10% fetal bovine serum (FBS; Euroclone), and 100 mg/ml penicillin–streptomycin (Gibco) as a medium. A density of 2×10^5/ml cells was seeded and grown in fresh medium with or without GSKJ4 at indicated times and concentrations. GSKJ4, PD98059, H89, and MG132 compounds were dissolved in dimethyl sulfoxide (DMSO), whereas PKF118-310 was prepared in H_2O. In order to obtain the final concentrations required, a single compound was diluted in the medium, and the same amount of solvent(s) (generally less than 0.1% v/v) was employed as internal control.

Dye Exclusion Test for Cell Proliferation Assessment

U-937 and K-562 cells (2×10^5 cells/ml) were plated and treated at different times and concentrations. Afterward, 10 μl of cell suspension was diluted 1:1 in 10 μl of trypan blue (Sigma-Aldrich) and examined by optical microscope. Dead blue-stained cells were discriminated from living unstained cells for

quantitative analysis. Experimental procedures were performed in triplicate, and representative results report both means and standard deviations as shown in figure.

Cell Viability Assay

To assess the relative cell viability in reaction to specific stimuli, a density of 3×10^3 cells/well in 96-well plates were seeded and treated as described in the Results section. Viable cells in each well were estimated by adding 100 μl of 5 mg/ml of 3-[4,5-dimethylthiazol-2-yl]-2,5-diphenyltetrazolium bromide (MTT solution) at the end of each experimental time point. After 3 h of incubation at 37°C, 100 μl/well of isopropanol-HCl 0.04 N (dissolving solution) was added to melt down formazan crystals. Following 30 min of incubation at room temperature on horizontal shaking, absorbance intensity was determined at 570 nm by microplate reader (Infinity 200, TECAN). All procedures were carried out at least three times, and for each data point, six replicates were performed. Representative figures show means and standard deviations.

Cell Cycle Analysis

Cell cycle analysis was assessed as formerly described (26). In detail, cells were plated at a density of 2×10^5 cells/ml, collected after stimulation, centrifuged (5 min at 400 × g) and suspended in 500 μl 1× phosphate buffered saline (PBS), in which NP-40 (0.1%), sodium citrate (0.1%), and PI (50 mg/ml) were previously added. After incubation at room temperature in the dark for 30 min, samples were analyzed for cell cycle distribution using FACS-Calibur (BD Bioscience). At least 50 K events per sample were acquired using CellQuest software (BD Bioscience), whereas ModFit LT V3 software (Verity) was employed to determine the relative percentage number of each cell cycle phase. Biological replicates have been performed in triplicate.

Histone Extraction

U-937 cells were collected at the end of each experimental procedure. Next, cells were resuspended twice in PBS and centrifuged again before adding TEB buffer [PBS with 0.5% Triton X-100 (v/v), 0.02% NaN3 (w/v), and 2 mM phenylmethylsulfonyl fluoride (PMSF)] with a ratio of 10^7 cells/ml. After 10 min on ice, samples were centrifuged, and supernatants were discarded. A similar step, without incubation, was repeated using half TEB volume. Finally, pellet was dissolved in 0.2 N HCl overnight at 4°C, and the supernatant was harvested after additional centrifugation. Bradford assay was employed to define the relative protein content/sample. All spin-down cycles were carried out at 400×g for 10 min at 4°C.

Protein Extraction and Immunodetection

Cells were resuspended in 3–5 volumes of RIPA buffer, containing NP-40 (1%), sodium deoxycholate (0.5%), sodium dodecyl sulfate (SDS) (0.1%), aprotinin (10 μg/ml), leupeptin (1 mM), and PMSF (1 mM) and incubated on ice for 1 h. After centrifugation (18,000×g for 15 min at 4°C), supernatant was collected and protein concentration was determined by Bradford method. Laemmli buffer 4× was added to each sample before boiling at 95°C for 5 min. Typically, a quantity of 20–40 μg of total extracts was applied to polyacrylamide gel (Bio Rad Laboratories); thereafter, proteins were divided by weight in SDS–polyacrylamide gel electrophoresis (PAGE) and moved on nitrocellulose membrane (Sigma-Aldrich) using Mini Trans-Blot BioRad (Bio Rad Laboratories). In order to fill uncovered spots, obtained films were incubated in nonfat milk (5% w/v) and then blotted overnight with primary antibody according to the experimental procedures. The next day, HRP-conjugated goat anti-rabbit or anti-mouse was used to detect protein–antibody complexes. Each incubation was preceded and followed by 5 min wash with TBS Tween-20 (Thermo Fisher Scientific) for three times. Finally, nitrocellulose membranes were detected by standard chemical luminescence method ECL (Euroclone). Immunoblotting signals were captured using Chemi-Doc XRS (Bio-Rad Laboratories) and quantitatively analyzed by ImageJ (NIH, Bethesda).

RNA Extraction, RT-PCR, and Real-Time PCR

With the aim of preventing RNA degradations and contaminations, RNase-free materials and solutions, prepared with diethyl pyrocarbonate (DEPC) water (Sigma-Aldrich), were used for RNA extraction. Total RNA was pulled out by Trizol (Invitrogen-Life Technologies) and successively reverse transcribed using SuperScript VILO kit (Invitrogen). Relative mRNA levels of specific genes of interest were determined by RT-PCR amplification made with iQ SYBR GREEN Supermix (Bio-Rad Laboratories). Glyceraldehyde 3-phosphate dehydrogenase (GAPDH) was used as a housekeeping gene to normalize data through ΔΔCT method. CREB and GAPDH primer sequences are reported as follows: CREB-forward: 5′-CACCTGCCATCACCACTGTAA-3′; CREB-reverse: 5′-GCTGCATTGGTCATGGTTAATGT-3′; GAPDH-forward: 5′-GGAGTCAACGGATTTGGT-3′; GAPDH-reverse: 5′-CTTCCCGTTCTCAGCCTT-3′.

MiRNA Real-Time PCR

Following RNA extraction, the miRNA fraction was converted into cDNA using miScript Reverse Transcription Kit (Qiagen). In detail, 1 μg of RNA was incubated with 1× Buffer, 1× miScript RT, and DEPC-H_2O for 60 min at 37°C and then 5 min at 95°C. Subsequently, miRNA Real-Time PCR was performed with QuantiTect SYBR Green PCR Kit (Qiagen) using 75 ng of cDNA in the presence of 1× QuantiTect SYBR Green PCR Master Mix, miScript Universal Primer, and primer specific for miR-34b (Qiagen); RNU6b (Qiagen) specific primer was used to normalize data. The thermal protocol was as follows: 95°C for 15 min plus 35 cycles at 94°C for 15 s, 55°C for 30 s, and 70°C for 30 s.

Statistical Analysis

Statistical analyses were performed for all biological and technical replicates. In details, Student's *t*-test was applied for the purpose of defining significant differences in the average between two distinct experimental groups, whereas analysis of variance (ANOVA) was used to test differences among more than two clusters. *P*-values of <0.05 were assumed as significant and graphically indicated with asterisks.

RESULTS

GSKJ4 Inhibits Acute Myeloid Leukemia Cell Proliferation

To test the possible GSKJ4-mediated consequences on CREB expression and function in AML, U-937 cell line was used as a widely known representative model of human leukemia cells (27–29). Nevertheless, specific key experiments were also performed in other leukemia cells. In agreement with previous findings, we used GSKJ4 in a range from 1 to 10 μM (16–25).

Over the past few years, GSKJ4 has been reported to exert antiproliferative properties in different tumor cell types but not in normal cells, where no toxicity has been observed (16–23). More recently, Li et al. (25) have highlighted the therapeutic potential of GSKJ4 also for AML. According to the latter findings, we also provided evidence in which GSKJ4 causes growth inhibition in myeloid leukemia cells (30).

In order to confirm our previous experimental setting, we verified the GSKJ4-mediated effects on both H3K27me3 status and leukemia cell viability. Acting as JMJD3/UTX inhibitor, **Figure 1A** shows that GSKJ4 increases H3K27me3. Simultaneously, analysis of cell growth and viability in U-937 and K-562 revealed an antiproliferative outcome in a dose- and time-dependent manner (**Figures 1B–E**).

GSKJ4 Downregulates cAMP Response Element-Binding Protein Level in Acute Myeloid Leukemia Cells

Assuming that CREB has been identified as one of the most relevant transcription factors in AML, driving both growth and survival (5, 9), we supposed that CREB transcription factor might be involved in the antiproliferative action made by GSKJ4 in AML cells. To address our hypothesis, firstly we looked at GSKJ4-mediated effects on CREB expression. To this purpose, U-937 cells were exposed and not to GSKJ4, then CREB protein and RNA levels were evaluated by Western blotting and RT-PCR, respectively. Interestingly, as shown in **Figure 2A**, CREB protein level evidently decreased after 18 and 24 h following GSKJ4 treatment, whereas CREB mRNA level was not influenced (**Figure 2B**).

MicroRNA-34b (miR-34b) regulates CREB protein expression in myeloid cells, where, supporting CREB overexpression, it is generally downregulated and hyper-methylated (31, 32). In order to evaluate whether miR-34b was involved in GSKJ4-induced CREB protein downregulation, we determined the relative expression levels following GSKJ4 stimulation. Intriguingly, **Figure 2C** shows that GSKJ4 further reduced miR-34b levels in U-937 cells, excluding this translational control from GSKJ4-mediated CREB protein regulation.

With the purpose of increasing the consistency of our findings, we also looked at GSKJ4 impact on CREB protein levels in other leukemia cell models, such as K-562 and NB-4. Experimental results revealed that GSKJ4 induces CREB protein downregulation in all cell lines tested (**Figure 2F**). In addition, analyses of other transcription factors in response to GSKJ4, as well as of other histone demethylase inhibitors on CREB protein levels, suggest discrete and not widespread GSKJ4-mediated effects, reinforcing the specificity of our results. Indeed, NF-κB protein levels appeared unchanged upon GSKJ4 treatment (**Figure 2A**), whereas PKF118-310 demethylase inhibitor (33), despite being more effective compared to GSKJ4 in inducing cell cycle and death variations (**Figure 2D**), did not elicit CREB protein downregulation in U-937 cells (**Figure 2E**).

GSKJ4 Affects cAMP Response Element-Binding Protein Stability via Ubiquitin/Proteasome System

To test if GSKJ4 might decrease CREB protein expression levels affecting its stability, we firstly estimated CREB protein half-life in untreated (control) and GSKJ4-treated U-937 cells by the broadly used protein synthesis inhibitor cycloheximide (CHX) (34). Hence, U-937 cells were treated or not with GSKJ4 and cocultured in the presence of CHX for 18 h, afterward, CREB protein levels at different time points were analyzed. Interestingly, **Figure 3A** shows that CREB protein levels were clearly decreased already after 2 h of CHX exposure in GSKJ4-treated group, whereas a significant reduction in the CREB abundance was evident only after 18 h of exposure to CHX in the untreated group, suggesting that GSKJ4 compound effectively influences CREB stability.

To investigate the mechanisms by which GSKJ4 decreases CREB protein stability, we investigated the impact of MG132 proteasome inhibitor on CREB abundance in response to GSKJ4 treatment. Therefore, U-937 cells were kept under proteasome impairment and treated with or without GSKJ4 for 18 h. Subsequently, we aimed to evaluate both CREB and anti-ubiquitin expression levels, the latter for monitoring the effectiveness of MG132 as proteasome inhibitor. **Figure 3B** clearly shows that the presence of MG132 increased the poly-ubiquitin signal and, more interestingly, it largely rescued the GSKJ4-induced CREB downregulation, suggesting the involvement of the ubiquitin/proteasome pathway in CREB protein decrease in response to GSKJ4.

Taken together, these findings indicate that the GSKJ4 treatment causes a decrease of CREB protein in U-937 cells, affecting its stability *via* ubiquitin/proteasome system.

GSKJ4 Rapidly Induces cAMP Response Element-Binding Phosphorylation at Residue Ser133 That Precedes the cAMP Response Element-Binding Protein Downregulation

Activation of transcription factors usually requires posttranslational modifications such as phosphorylation (35, 36). Moreover, in many of them, phosphorylation and dephosphorylation processes regulate stability and degradation, too (37, 38). Regarding CREB transcription factor, it is largely known that phosphorylation at Ser133 residue might modulate both activation and protein stability (39–44). To extend and further investigate the impact of GSKJ4 on CREB function, we investigated Ser133 phosphorylation and CREB protein levels in response to GSKJ4 treatment. To corroborate our study, we treated U-937 cells with GSKJ4 at different times, and then

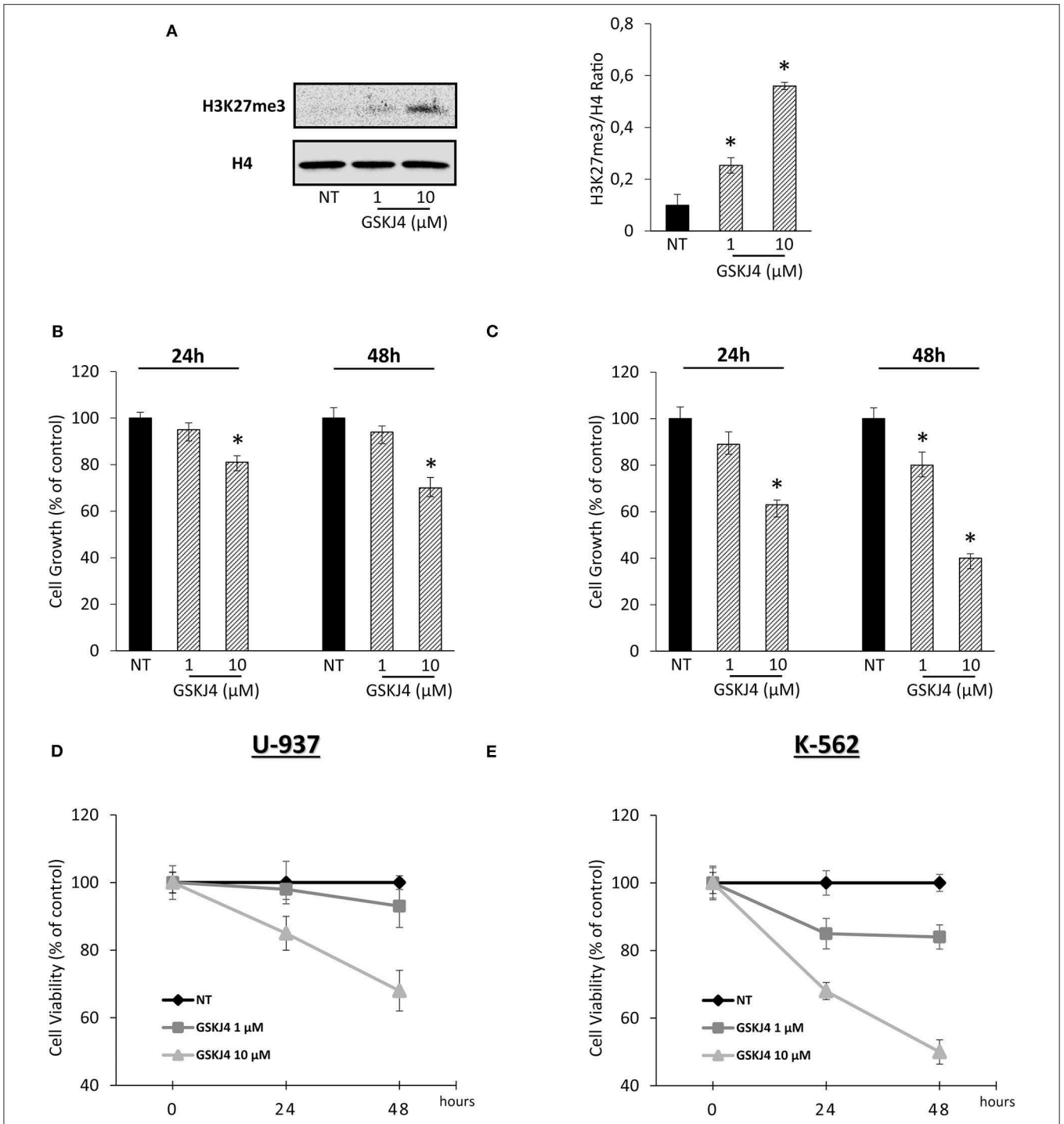

FIGURE 1 | Effects of GSKJ4 on H3K27me3 status in U-937 cells and cell viability/growth in U-937 and K-562. **(A)** H3K27 trimethylation levels were measured in U-937 cells treated or not (NT) with 1 and 10 μM of GSKJ4 for 48 h. U-937 **(B)** and K-562 **(C)** cells were cultured with or without (NT) 1 and 10 μM of GSKJ4 for 24 and 48 h. Later, 3-[4,5-dimethylthiazol-2-yl]-2,5-diphenyltetrazolium bromide (MTT) assays were performed in order to determine the relative cell viability amount. U-937 **(D)** and K-562 **(E)** cell number were recorded after treatment with 1 and 10 μM of GSKJ4 at 24 and 48 h. Cell viability and cell growth data were indicated in % of control. Mean and standard deviation (SD) values of at least three repeated experiments were reported. *$P < 0.05$ by unpaired *t*-test.

we evaluated the p-Ser133-CREB and CREB protein levels. Interestingly, as shown in **Figure 4A** (left panel), we found that CREB phosphorylation strongly increased in response to GSKJ4 already after 1 h, without relevant changes in CREB total levels up to 6 h, suggesting a very early CREB activation that seems to precede CREB protein downregulation.

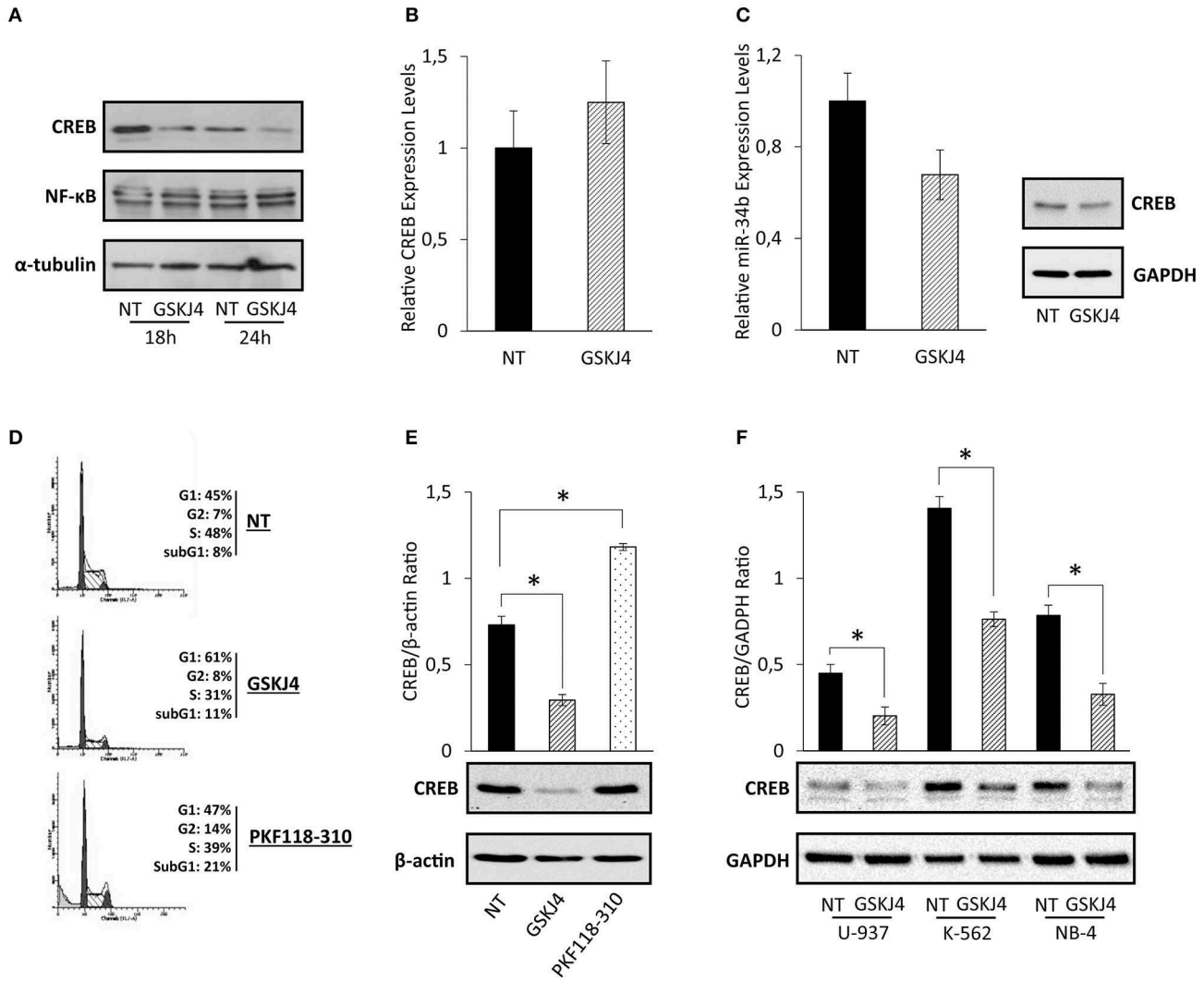

FIGURE 2 | GSKJ4-mediated effects on cAMP response element-binding (CREB) protein, CREB mRNA, and miR-34b: reliability and specificity perspectives. **(A)** CREB and NF-κB protein levels were defined by immunoblotting after 18 and 24 h of treatment with 10 μM GSKJ4. CREB **(B)** and miR-34b **(C)** mRNA expression levels were assessed by RT-PCR after 24 h of 10 μM GSKJ4 treatment. GAPDH was used as a housekeeping gene, whereas differences were calculated by ΔΔCt method. **(D)** Representative cell cycle analysis of propidium iodide (PI)-stained cells achieved after 24 h of 10 μM GSKJ4 and 0.25 μM PKF118-310 treatment were reported. **(E)** CREB protein levels and CREB/β-actin Ratio, obtained in response to the same experimental setting illustrated in **(D)**, were also displayed. **(F)** U-937, K-562, and NB-4 cells were kept under GSKJ4 treatment for 24 h. Later, CREB protein levels were analyzed by Western blotting. Data from three biological replicates were used to calculate average and SD values shown in the densitometric histogram plot. *$P < 0.05$ by ANOVA and unpaired *t*-test.

Overall, the above results indicate that GSKJ4 greatly impacts p-Ser133-CREB protein levels, suggesting that this mechanism might mediate the GSKJ4-induced CREB downregulation.

Protein Kinase A Activity, and Not Extracellular Signal-Regulated Kinase 1/2 Activity, Is Mainly Required in GSKJ4-Induced cAMP Response Element-Binding Protein Downregulation

Among the others kinases, ERK1/2 and PKA play a key role in CREB phosphorylation at Ser133 residue (45–48). To test the possible involvement of ERK1/2 pathway on GSKJ4-mediated Ser133 phosphorylation induction and CREB protein decrease, we treated U-937 cells with GSKJ4 up to 24 h in presence or in absence of the upstream ERK1/2 inhibitor PD98059. Later, we evaluated the p-ERK1/2, p-Ser133-CREB, ERK1/2, and CREB protein expression levels. Notably, as previously described, cell exposure to GSKJ4 provokes a rapid increase of p-Ser133-CREB (**Figure 4A**, left panel) that was partially prevented by pretreatment with PD98059 compound (**Figure 4A**, right panel). Strikingly, the GSKJ4-induced CREB protein downregulation was not counteracted at all by the ERK1/2 inhibitor PD98059 (**Figure 4B**). Indeed, as shown in **Figure 4C**,

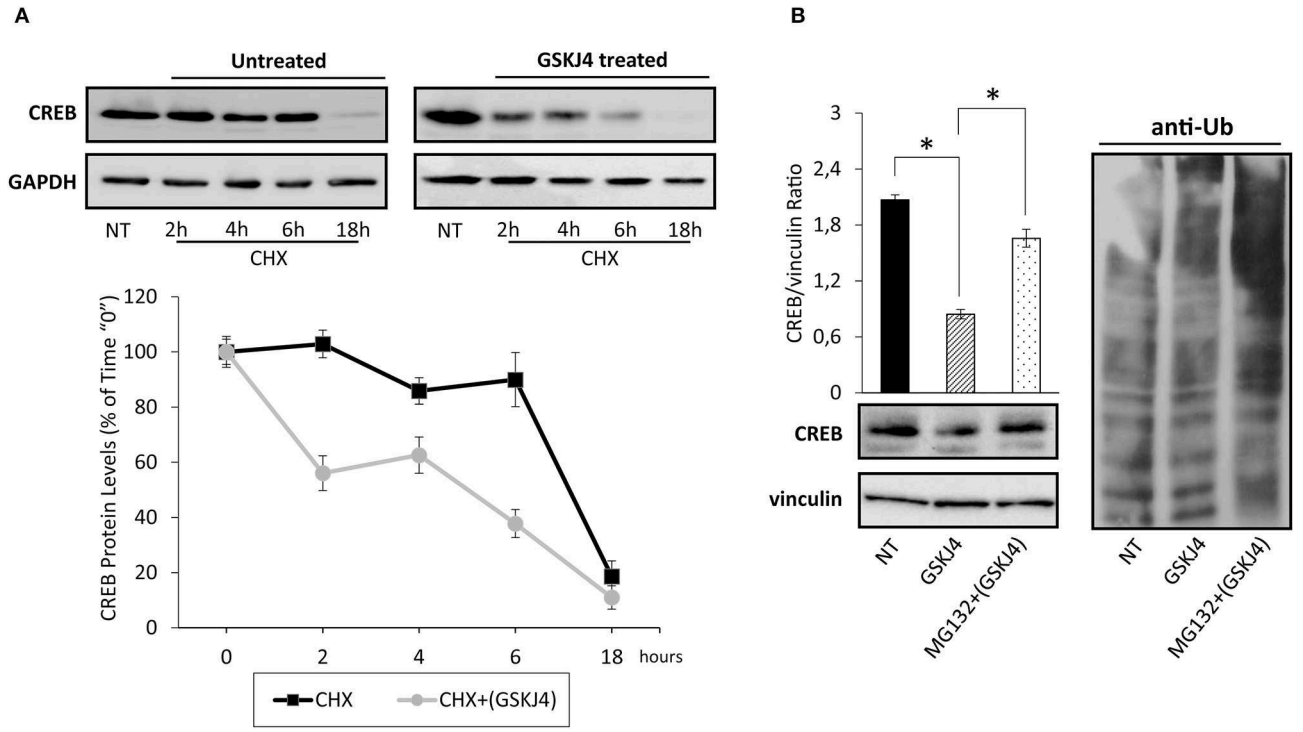

FIGURE 3 | Assessment of cAMP response element-binding (CREB) stability and ubiquitin/proteasome involvement in GSKJ4-mediated CREB downregulation in U-937 cells. **(A)** Cells were treated for up 18 h with or without (NT) 10 μM GSKJ4 and grown in the presence of 20 μg/ml of protein synthesis inhibitor cycloheximide (CHX). Thereafter, CREB protein levels were determined by Western blotting (upper part) after 2, 4, 6, and 18 h of treatment. For each time point, the relative CREB/vinculin Ratio of three unrelated blot images were quantified by ImageJ software and reported in graph as average and SD measure (bottom part). **(B)** Proteasome inhibitor MG132 at 10 μM was administered, or not (NT), for 18 h to U-937 cells kept in the presence of 10 μM GSKJ4. CREB protein levels and the ubiquitin pattern were evaluated through Western blotting analysis in response to the above stimuli. Densitometric analyses of CREB/vinculin Ratio of three independent experiments were shown in chart and represented as average and SD values. *$P < 0.05$ by ANOVA and unpaired *t*-test.

PD98059 was able to totally abrogate ERK1/2 activation in response to GSKJ4 compound (**Figure 4C**). Collectively, the above findings indicate that GSKJ4-mediated phosphorylation on serine 133 residue is partly dependent on ERK1/2 activity, whereas CREB protein downregulation is probably affected by other independent mechanisms.

In order to define the potential PKA implication on both GSKJ4-mediated Ser133 phosphorylation and CREB protein downregulation, GSKJ4-treated U-937 cells were cultured both with or without PKA inhibitor H89, and subsequently, total and phosphorylated CREB protein expression levels were analyzed. Remarkably, **Figures 4D,E** show that pretreatment of U-937 cells with the H89 inhibitor results in both a strong reduction of the p-Ser133-CREB phosphorylation and an almost complete prevention of CREB protein downregulation in response to GSKJ4 compound. Altogether, the above findings indicate that both CREB phosphorylation on Ser133 residue and CREB downregulation are largely dependent on PKA activity.

DISCUSSION

Despite the intensive combination of chemotherapy and stem cell transplantation, AML still remains very difficult to treat (3, 49). It is known that altered functions, such as transcription factors mutation and/or dysregulated expression are deeply involved in leukemogenesis (4). Although therapeutic targeting of transcription factors is still considered challenging, recent evidence is showing that transcription factors can be targeted for cancer care (50–53). Remarkably, targeting the activity of CREB transcription factor appears very promising for the treatment of leukemia in a huge number of preclinical studies (4, 12, 54, 55).

Here, we report that the small epigenetic compound GSKJ4 significantly downregulates CREB protein levels in leukemic cells. Since GSKJ4 treatment causes a strong decrease of CREB protein levels, but not a concurrent reduction of CREB mRNA expression levels, intricate posttranslational mechanisms are supposed to be involved. To further corroborate our hypothesis, the evaluation of GSKJ4-mediated effects on miR-34b, one of the main controllers in CREB translation, reveals no engagement in its downregulation. Contextually, by CHX assay, we provide evidence that CREB protein stability decreases in response to GSKJ4 exposure and that proteasome inhibition largely counteracts the GSKJ4-induced CREB downregulation. In addition, we also describe a rapid CREB phosphorylation at Ser133 residue that seems to precede CREB protein decrease in response to GSKJ4 treatment. From a mechanistic point of view, PKA impairment almost completely prevents both the GSKJ4-induced p-Ser133-CREB and CREB protein downregulation.

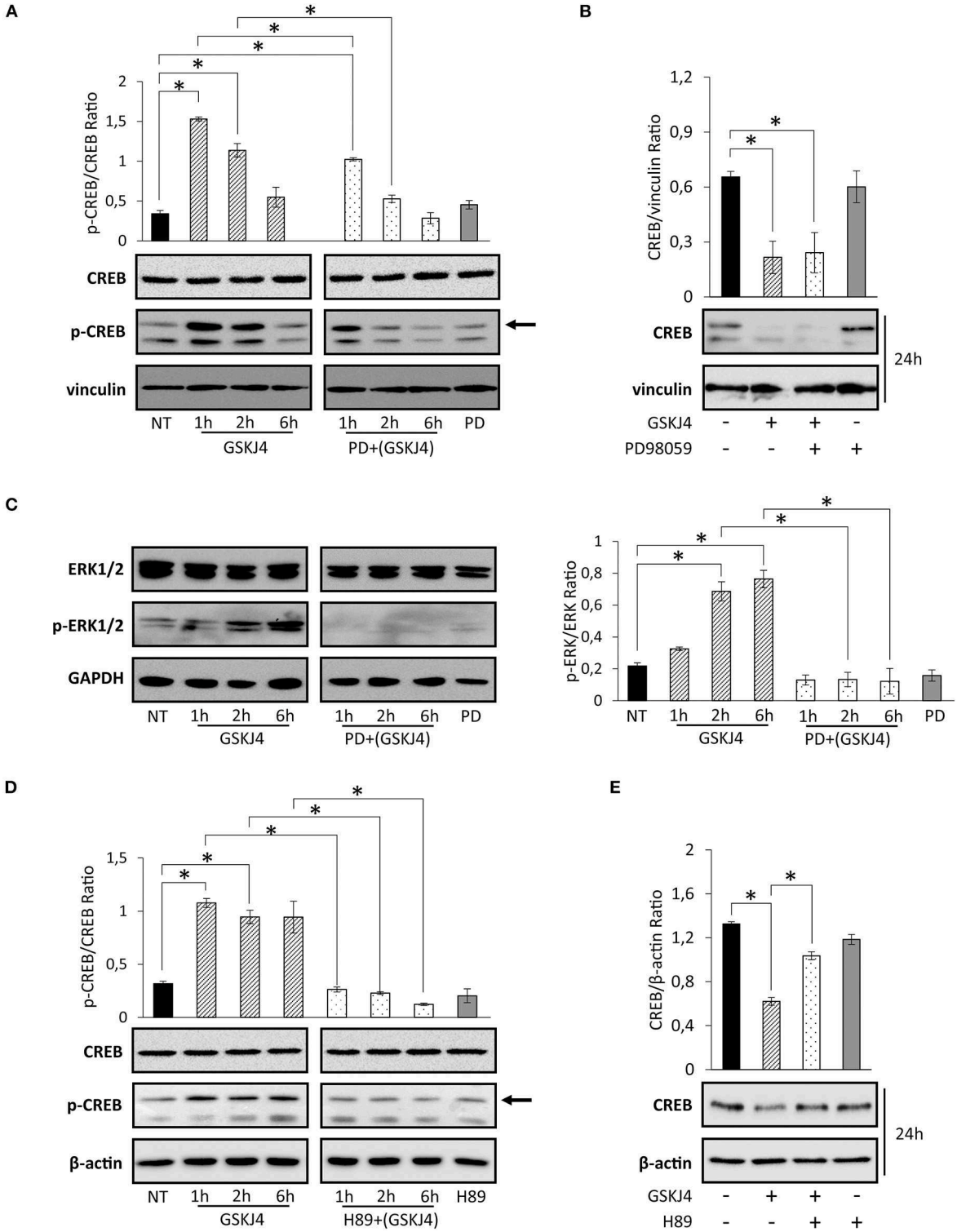

FIGURE 4 | Effects of PD98059 and H89 on GSKJ4-mediated Ser133 phosphorylation induction and cAMP response element-binding (CREB) protein decrease. U-937 cells were treated up to 24 h with 10 μM GSKJ4 in the presence or in the absence of 10 μM PD98059 or 20 μM of H89. Immunoblotting analyses of CREB and phospho-Ser133-CREB were performed after 2, 4, and 6 h of treatment with GSKJ4 alone and in combination with PD98059 **(A)** or H89 **(D)**. Untreated (NT), PD98059 and H89 lines refer to 2 h of treatment. **(C)** ERK1/2 and phospho-ERK1/2 levels were evaluated in the same experimental setting described for **(A)**. CREB protein levels and CREB/housekeeping protein Ratio were determined by Western blotting in response to 24 h of treatment with GSKJ4 alone and in combination with PD98059 **(B)** or H89 **(E)**, respectively. All densitometric analyses shown in this figure were calculated from three distinct experiments. *$P < 0.05$ by ANOVA and unpaired *t*-test.

Notably, targeting CREB has been recently proposed as an effective therapeutic approach in AML. CREB recognized more than thousands of CRE consensus *loci* on the DNA. Upon phosphorylation on Ser133, CREB, together with CBP coactivator, triggers the transcription of CREB-driven genes, which in turn regulate cell proliferation, survival, and signal transduction. Interestingly, Mitton et al. (12) provided evidence that a CBP–CREB interaction blocker disrupts CREB-driven gene expression, causing cell cycle arrest and apoptosis of AML cells. Subsequently, the same group, by structure–activity relationship (SAR) tools, demonstrated that niclosamide, a widely used uncoupled oxidative phosphorylation compound, targets CREB and, preventing its activation, inhibits CREB-driven gene expression and results in cell cycle arrest and apoptosis in AML cells (54, 55).

Our results, showing that the epigenetic compound GSKJ4 causes both CREB protein decrease and inhibition of proliferation in AML cells, are fully in agreement with the above findings. However, we do know that our findings are quite descriptive, thus correlative and more exhaustive experiments are needed to demonstrate the relationship between the antiproliferative effects and CREB decrease in response to GSKJ4 in AML cells. We are going to address this issue as a future scientific focus. By the way, our study clearly demonstrates that GSKJ4 downregulates CREB protein in AML cells, and this is undoubtedly relevant *per sè*.

As JMJD3 and UTX demethylase inhibitor, we have shown that GSKJ4 increases H3K27me3 status in AML cells. Moreover, GSKJ4 has recently been shown to counteract cell proliferation in different tumor types, including AML (16–25, 30).

In the current study, we describe that the GSKJ4 compound, according to previous findings, acts as a small molecule inhibitor against the proliferation of myeloid leukemia cells and elicits a rapid CREB protein downregulation, suggesting that GSKJ4 might exert anticancer properties by inhibiting demethylases JMJD3 and UTX and affecting CREB function. Changes in H3K27me2/3 global level might influence the chromatin configuration and affect the accessibility of CREB transcription factor, making it more susceptible to cellular activities such as kinases, ubiquitin ligases, and proteases. Moreover, possible GSKJ4-mediated effects on other enzymatic functions, maybe involved in CREB activation/stability, cannot be excluded. In addition, methylation of non-histone proteins has recently been demonstrated to impact diverse cellular functions. Notably, many of such non-histone targets include transcription factors, such as CREB (56).

Here we report that upon GSKJ4 treatment, an early phosphorylation of CREB at the Ser133 residue occurs and precedes the proteasome-mediated CREB protein downregulation.

It is largely known that PKA, as well as other kinases such as ERK1/2, can phosphorylate CREB protein at serine 133 residue (45–48). Moreover, phosphorylation at Ser133 is also involved in CREB protein stability (40, 41, 44). Importantly, our findings, indicating that PKA inhibition almost completely prevents both GSKJ4-induced p-Ser133-CREB phosphorylation and CREB protein decrease, are consistent with the above evidence. Based on all these statements, the molecular mechanisms underlying the effects of GSKJ4 on CREB pathway in AML cells are still preliminary and, therefore, they need to be further investigated.

Here we describe that exogenous addition of GSKJ4 epigenetic compound triggers proteasome-mediated CREB protein downregulation *via* a PKA-dependent manner.

CREB is a key regulator of the growth and survival of AML cells that is emerging as a very attractive potential drug target for AML (4, 5, 12).

Collectively, our study identifies the small-molecule GSKJ4 as a valuable potential agent capable of modulating CREB function, encouraging the design of further GSKJ4-based studies for innovative therapeutic approach in AML care.

DATA AVAILABILITY STATEMENT

The datasets generated for this study are available on request to the corresponding author.

AUTHOR CONTRIBUTIONS

MI performed immunoblotting experiments and participated in the development of the current study. MC executed mRNA analyses and contributed to draft the manuscript. ASa and AR carried out MTT and cell counting assays. AN and LA took an active part in the drafting process of this paper. LS made flow cytometry-based data and the statistical analysis. ASp supervised the final text layout. SN conceived and designed the research project, directing both the experimental strategies and the draft of the manuscript. Reading the present article, the authors approve its contents.

FUNDING

This work was supported by VALERE (Vanvitelli per la Ricerca Program), Campania Regional Government (iCURE–CUP B21c17000030007; FASE 2: IDEAL–CUP B63D18000560007; MIUR (proof of concept–CUP:B64I19000290008); the Italian Association for Cancer Research (AIRC-17217).

REFERENCES

1. De Kouchkovsky I, Abdul-Hay M. Acute myeloid leukemia: a comprehensive review and 2016 update. *Blood Cancer J.* (2016) 6:e441. doi: 10.1038/bcj.2016.50
2. Siegel RL, Miller KD, Jemal A. Cancer statistics, 2018. *CA Cancer J Clin.* (2018) 68:7–30. doi: 10.3322/caac.21442
3. Saygin C, Carraway HE. Emerging therapies for acute myeloid leukemia. *J Hematol Oncol.* (2017) 10:93. doi: 10.1186/s13045-017-0463-6
4. Takei H, Kobayashi SS. Targeting transcription factors in acute myeloid leukemia. *Int J Hematol.* (2019) 109:28–34. doi: 10.1007/s12185-018-2488-1
5. Sakamoto KM, Grant S, Saleiro D, Crispino JD, Hijiya N, Giles F, et al. Targeting novel signaling pathways for resistant acute myeloid leukemia. *Mol Genet Metab.* (2015) 114:397–402. doi: 10.1016/j.ymgme.2014.11.017

6. D'Auria F, Di Pietro R. Role of CREB protein family members in human haematological malignancies. In: *Cancer Treatment - Conventional and Innovative Approaches of Letícia Rangel*. London: IntechOpen Limited (2013). p. 556–72. doi: 10.5772/55368
7. Steven A, Seliger B. Control of CREB expression in tumors: from molecular mechanisms and signal transduction pathways to therapeutic target. *Oncotarget*. (2016) 7:35454–65. doi: 10.18632/oncotarget.7721
8. Sandoval S, Pigazzi M, Sakamoto KM. CREB: a key regulator of normal and neoplastic hematopoiesis. *Adv Hematol*. (2009) 2009:634292. doi: 10.1155/2009/634292
9. Cho EC, Mitton B, Sakamoto KM. CREB and leukemogenesis. *Crit Rev Oncog*. (2011) 16:37–46. doi: 10.1615/CritRevOncog.v16.i1-2.50
10. Shabestari RM, Safa M, Alikarami F, Banan M, Kazemi A. CREB knockdown inhibits growth and induces apoptosis in human pre-B acute lymphoblastic leukemia cells through inhibition of prosurvival signals. *Biomed Pharmacother*. (2017) 87:274–9. doi: 10.1016/j.biopha.2016.12.070
11. Tregnago C, Manara E, Zampini M, Bisio V, Borga C, Bresolin S, et al. CREB Engages C/EBPδ to initiate leukemogenesis. *Leukemia*. (2016) 30:1887–96. doi: 10.1038/leu.2016.98
12. Mitton B, Chae HD, Hsu K, Dutta R, Aldana-Masangkay G, Ferrari R, et al. Small molecule inhibition of cAMP response element binding protein in human acute myeloid leukemia cells. *Leukemia*. (2016) 30:2302–11. doi: 10.1038/leu.2016.139
13. Sun Y, Chen BR, Deshpande A. Epigenetic regulators in the development, maintenance, and therapeutic targeting of acute myeloid leukemia. *Front Oncol*. (2018) 8:41. doi: 10.3389/fonc.2018.00041
14. Lu R, Wang GG. Pharmacologic targeting of chromatin modulators as therapeutics of acute myeloid leukemia. *Front Oncol*. (2017) 7:241. doi: 10.3389/fonc.2017.00241
15. Berdasco M, Esteller M. Clinical epigenetics: seizing opportunities for translation. *Nat Rev Genet*. (2019) 20:109–27. doi: 10.1038/s41576-018-0074-2
16. Ntziachristos P, Tsirigos A, Welstead GG, Trimarchi T, Bakogianni S, Xu L, et al. Contrasting roles of histone 3 lysine 27 demethylases in acute lymphoblastic leukaemia. *Nature*. (2014) 514:513–7. doi: 10.1038/nature13605
17. Hashizume R, Andor N, Ihara Y, Lerner R, Gan H, Chen X, et al. Pharmacologic inhibition of histone demethylation as a therapy for pediatric brainstem glioma. *Nat Med*. (2014) 20:1394–6. doi: 10.1038/nm.3716
18. Sakaki H, Okada M, Kuramoto K, Takeda H, Watarai H, Suzuki S, et al. GSKJ4, A selective jumonji H3K27 demethylase inhibitor, effectively targets ovarian cancer stem cells. *Anticancer Res*. (2015) 35:6607–14.
19. Watarai H, Okada M, Kuramoto K, Takeda H, Sakaki H, Suzuki S, et al. Impact of H3K27 demethylase inhibitor GSKJ4 on NSCLC cells alone and in combination with metformin. *Anticancer Res*. (2016) 36:6083–92. doi: 10.21873/anticanres.11198
20. Dalvi MP, Wang L, Zhong R, Kollipara RK, Park H, Bayo J, et al. Taxane-platin-resistant lung cancers co-develop hypersensitivity to JumonjiC demethylase inhibitors. *Cell Rep*. (2017) 19:1669–84. doi: 10.1016/j.celrep.2017.04.077
21. Sui A, Xu Y, Li Y, Hu Q, Wang Z, Zhang H, et al. The pharmacological role of histone demethylase JMJD3 inhibitor GSK-J4 on glioma cells. *Oncotarget*. (2017) 8:68591–8. doi: 10.18632/oncotarget.19793
22. Yan N, Xu L, Wu X, Zhang L, Fei X, Cao Y, et al. GSKJ4, an H3K27me3 demethylase inhibitor, effectively suppresses the breast cancer stem cells. *Exp Cell Res*. (2017) 359:405–14. doi: 10.1016/j.yexcr.2017.08.024
23. Mathur R, Sehgal L, Havranek O, Köhrer S, Khashab T, Jain N, et al. Inhibition of demethylase KDM6B sensitizes diffuse large B-cell lymphoma to chemotherapeutic drugs. *Haematologica*. (2017) 102:373–80. doi: 10.3324/haematol.2016.144964
24. Rejlova K, Musilova A, Kramarzova KS, Zaliova M, Fiser K, Alberich-Jorda M, et al. Low HOX gene expression in PML-RARα-positive leukemia results from suppressed histone demethylation. *Epigenetics*. (2018) 13:73–84. doi: 10.1080/15592294.2017.1413517
25. Li Y, Zhang M, Sheng M, Zhang P, Chen Z, Xing W, et al. Therapeutic potential of GSK-J4, a histone demethylase KDM6B/JMJD3 inhibitor, for acute myeloid leukemia. *J Cancer Res Clin Oncol*. (2018) 144:1065–77. doi: 10.1007/s00432-018-2631-7
26. Catauro M, Tranquillo E, Salzillo A, Capasso L, Illiano M, Sapio L, et al. Silica/polyethylene glycol hybrid materials prepared by a sol-gel method and containing chlorogenic acid. *Molecules*. (2018) 23:2018. doi: 10.3390/molecules23102447
27. Rossetti C, Picardi E, Ye M, Camilli G, D'Erchia AM, Cucina L, et al. RNA editing signature during myeloid leukemia cell differentiation. *Leukemia*. (2017) 31:2824–32. doi: 10.1038/leu.2017.134
28. Hassani S, Ghaffari P, Chahardouli B, Alimoghaddam K, Ghavamzadeh A, Alizadeh S, et al. Disulfiram/copper causes ROS levels alteration, cell cycle inhibition, and apoptosis in acute myeloid leukaemia cell lines with modulation in the expression of related genes. *Biomed Pharmacother*. (2018) 99:561–9. doi: 10.1016/j.biopha.2018.01.109
29. Zhuang MF, Li LJ, Ma JB. LncRNA HOTTIP promotes proliferation and cell cycle progression of acute myeloid leukemia cells. *Eur Rev Med Pharmacol Sci*. (2019) 23:2908–15. doi: 10.26355/eurrev_201904_17569
30. Illiano M, Conte M, Sapio L, Nebbioso A, Spina A, Altucci L, et al. Forskolin sensitizes human acute myeloid leukemia cells to H3K27me2/3 demethylases GSKJ4 inhibitor via protein kinase A. *Front Pharmacol*. (2018) 9:792. doi: 10.3389/fphar.2018.00792
31. Pigazzi M, Manara E, Baron E, Basso G. miR-34b Targets cyclic AMP-responsive element binding protein in acute myeloid leukemia. *Cancer Res*. (2009) 69:2471–8. doi: 10.1158/0008-5472.CAN-08-3404
32. Pigazzi M, Manara E, Bresolin S, Tregnago C, Beghin A, Baron E, et al. MicroRNA-34b promoter hypermethylation induces CREB overexpression and contributes to myeloid transformation. *Haematologica*. (2013) 98:602–10. doi: 10.3324/haematol.2012.070664
33. Franci G, Sarno F, Nebbioso A, Altucci L. Identification and characterization of PKF118-310 as a KDM4A inhibitor. *Epigenetics*. (2017) 12:198–205. doi: 10.1080/15592294.2016.1249089
34. Ko YU, Kim SJ, Lee J, Song MY, Park KS, Park JB, et al. Protein kinase A-induced phosphorylation at the Thr154 affects stability of DJ-1. *Parkinsonism Relat Disord*. (2019) 66:143–50. doi: 10.1016/j.parkreldis.2019.07.029
35. Santos CI, Costa-Pereira AP. Signal transducers and activators of transcription-from cytokine signalling to cancer biology. *Biochim Biophys Acta*. (2011) 1816:38–49. doi: 10.1016/j.bbcan.2011.03.003
36. Yogosawa S, Yoshida K. Tumor suppressive role for kinases phosphorylating p53 in DNA damage-induced apoptosis. *Cancer Sci*. (2018) 109:3376–82. doi: 10.1111/cas.13792
37. Napetschnig J, Wu H. Molecular basis of NF-κB signaling. *Annu Rev Biophys*. (2013) 42:443–68. doi: 10.1146/annurev-biophys-083012-130338
38. Xu R, Won JY, Kim CH, Kim DE, Yim H. Roles of the phosphorylation of transcriptional factors in epithelial-mesenchymal transition. *J Oncol*. (2019) 2019:5810465. doi: 10.1155/2019/5810465
39. Gee K, Angel JB, Ma W, Mishra S, Gajanayaka N, Parato K, et al. Intracellular HIV-Tat expression induces IL-10 synthesis by the CREB-1 transcription factor through Ser133 phosphorylation and its regulation by the ERK1/2 MAPK in human monocytic cells. *J Biol Chem*. (2006) 281:31647–58. doi: 10.1074/jbc.M512109200
40. Mouravlev A, Young D, During MJ. Phosphorylation-dependent degradation of transgenic CREB protein initiated by heterodimerization. *Brain Res*. (2007) 1130:31–7. doi: 10.1016/j.brainres.2006.10.076
41. Costes S, Vandewalle B, Tourrel-Cuzin C, Broca C, Linck N, Bertrand G, et al. Degradation of cAMP-responsive element–binding protein by the ubiquitin-proteasome pathway contributes to glucotoxicity in β-cells and human pancreatic islets. *Diabetes*. (2009) 58:1105–15. doi: 10.2337/db08-0926
42. Wang X, Ren Y, Zhuang H, Meng X, Huang S, Li Y, et al. Decrease of phosphorylated proto-oncogene CREB at Ser 133 site inhibits growth and metastatic activity of renal cell cancer. *Expert Opin Ther Targets*. (2015) 19:985–95. doi: 10.1517/14728222.2015.1053208
43. Wheaton KL, Hansen KF, Aten S, Sullivan KA, Yoon H, Hoyt KR, et al. The phosphorylation of CREB at serine 133 is a key event for circadian clock timing and entrainment in the suprachiasmatic nucleus. *J Biol Rhythms*. (2018) 33:497–514. doi: 10.1177/0748730418791713
44. Du H, Le Y, Sun F, Li K, Xu Y. ILF2 directly binds and stabilizes CREB to stimulate malignant phenotypes of liver cancer cells. *Anal Cell Pathol*. (2019) 2019:1575031. doi: 10.1155/2019/1575031
45. Sands WA, Palmer TM. Regulating gene transcription in response to cyclic AMP elevation. *Cell Signal*. (2008) 20:460–6. doi: 10.1016/j.cellsig.2007.10.005

46. Naqvi S, Martin KJ, Arthur JS. CREB phosphorylation at Ser133 regulates transcription via distinct mechanisms downstream of cAMP and MAPK signalling. *Biochem J*. (2014) 458:469–79. doi: 10.1042/BJ20131115
47. Huante-Mendoza A, Silva-García O, Oviedo-Boyso J, Hancock RE, Baizabal-Aguirre VM. Peptide IDR-1002 inhibits NF-κB nuclear translocation by inhibition of IκBα degradation and activates p38/ERK1/2-MSK1-dependent CREB phosphorylation in macrophages stimulated with lipopolysaccharide. *Front Immunol*. (2016) 7:533. doi: 10.3389/fimmu.2016.00533
48. Koga Y, Tsurumaki H, Aoki-Saito H, Sato M, Yatomi M, Takehara K, et al. Roles of cyclic AMP response element binding activation in the ERK1/2 and p38 MAPK signalling pathway in central nervous system, cardiovascular system, osteoclast differentiation and mucin and cytokine production. *Int J Mol Sci*. (2019) 20:E1346. doi: 10.3390/ijms20061346
49. Döhner H, Estey E, Grimwade D, Amadori S, Appelbaum FR, Büchner T, et al. Diagnosis and management of AML in adults: 2017 ELN recommendations from an international expert panel. *Blood*. (2017) 129:424–47. doi: 10.1182/blood-2016-08-733196
50. Illendula A, Pulikkan JA, Zong H, Grembecka J, Xue L, Sen S, et al. Chemical biology. A small-molecule inhibitor of the aberrant transcription factor CBFbeta-SMMHC delays leukemia in mice. *Science*. (2015) 347:779–84. doi: 10.1126/science.aaa0314
51. Uttarkar S, Dukare S, Bopp B, Goblirsch M, Jose J, Klempnauer KH. Naphthol AS-Ephosphate inhibits the activity of the transcription factor Myb by blocking the interaction with the KIX domain of the coactivator p300. *Mol Cancer Ther*. (2015) 14:1276–85. doi: 10.1158/1535-7163.MCT-14-0662
52. Joerger AC, Fersht AR. The p53 pathway: origins, inactivation in cancer, and emerging therapeutic approaches. *Annu Rev Biochem*. (2016) 85:375–404. doi: 10.1146/annurev-biochem-060815-014710
53. Ramaswamy K, Forbes L, Minuesa G, Gindin T, Brown F, Kharas MG, et al. Peptidomimetic blockade of MYB in acute myeloid leukemia. *Nat Commun*. (2018) 9:110. doi: 10.1038/s41467-017-02618-6
54. Chae HD, Cox N, Dahl GV, Lacayo NJ, Davis KL, Capolicchio S, et al. Niclosamide suppresses acute myeloid leukemia cell proliferation through inhibition of CREB-dependent signaling pathways. *Oncotarget*. (2018) 9:4301–17. doi: 10.18632/oncotarget.23794
55. Chae HD, Cox N, Capolicchio S, Lee JW, Horikoshi N, Kam S, et al. SAR optimization studies on modified salicylamides as a potential treatment for acute myeloid leukemia through inhibition of the CREB pathway. *Bioorg Med Chem Lett*. (2019) 29:2307–15. doi: 10.1016/j.bmcl.2019.06.023
56. Carr SM, Poppy Roworth A, Chan C, La Thangue NB. Post-translational control of transcription factors: methylation ranks highly. *FEBS J*. (2015) 282:4450–65. doi: 10.1111/febs.13524

Conflict of Interest: The authors declare that the research was conducted in the absence of any commercial or financial relationships that could be construed as a potential conflict of interest.

frontiers in Cell and Developmental Biology

ORIGINAL RESEARCH
published: 12 June 2020
doi: 10.3389/fcell.2020.00408

Antagonizing CDK8 Sensitizes Colorectal Cancer to Radiation Through Potentiating the Transcription of e2f1 Target Gene apaf1

*Bin Chen[1,2], Pengbo Wen[1,2], Guanshuo Hu[1,2], Yang Gao[1,2], Xiaojing Qi[1,2], Kaili Zhu[1,2], Shaopeng Chen[1], Lijun Wu[1], An Xu[1] and Guoping Zhao[1]**

[1] Key Laboratory of High Magnetic Field and Ion Beam Physical Biology, Anhui Province Key Laboratory of Environmental Toxicology and Pollution Control Technology, Hefei Institutes of Physical Science, Chinese Academy of Sciences, Hefei, China, [2] University of Science and Technology of China, Hefei, China

Radiotherapy is an essential curative treatment modality for colorectal cancer. Apoptosis is the major mechanism of IR-induced cell death and aberrant apoptotic signaling results in radioresistance, which is a hallmark of most, perhaps all, types of human cancers. Potentiating the induction of apoptosis is an emerging strategy for cancer radiotherapy. Here, we determined that targeting CDK8 selectively radiosensitized colorectal cancer through the mitochondria-dependent intrinsic apoptotic signaling, which was mediated through the induction of the transcription of apaf1 that was e2f1- and not p53-dependent. Importantly, the enhanced transcriptional activity of e2f1 was dependent on the kinase activity of CDK8 itself and not on the assembling of the mediator complex. In addition, clinical inhibitor, and *in vivo* studies confirmed the radiosensitizing effect of CDK8. Our results provide a new targeting strategy to improve the radiotherapy of CRC.

Keywords: CDK8, transcriptional regulation, e2f1, apaf1, radiotherapy, apoptosis

OPEN ACCESS

Edited by:
Lei Chang,
Soochow University Medical College (SUMC), China

Reviewed by:
Kaiyuan Ni,
The University of Chicago, United States
Yanyong Yang,
Second Military Medical University, China

***Correspondence:**
Guoping Zhao
gpz@ipp.ac.cn

Specialty section:
This article was submitted to Molecular and Cellular Oncology, a section of the journal Frontiers in Cell and Developmental Biology

Received: *10 March 2020*
Accepted: *04 May 2020*
Published: *12 June 2020*

Citation:
Chen B, Wen P, Hu G, Gao Y, Qi X, Zhu K, Chen S, Wu L, Xu A and Zhao G (2020) Antagonizing CDK8 Sensitizes Colorectal Cancer to Radiation Through Potentiating the Transcription of e2f1 Target Gene apaf1. Front. Cell Dev. Biol. 8:408. doi: 10.3389/fcell.2020.00408

INTRODUCTION

Colorectal cancer (CRC) is the third most commonly diagnosed cancer and the second most frequent cause of cancer-related deaths (Roberts et al., 2018), over 1.8 million new CRC cases and 880,000 CRC-associated deaths were reported in Bray et al. (2018). Clinically, surgical resection is considered as the main therapeutic modality for CRC, and radiotherapy is considered as an effective treatment option after surgery (Mishra et al., 2013). However, radioresistance is a major cause of treatment failure, which results in incomplete cure, recurrence, and metastasis (Pal et al., 2018; Xiao et al., 2018; Wu et al., 2019). Therefore, appropriate strategies to improve the radiosensitivity of CRC are urgently needed.

Cyclin dependent kinase 8 (CDK8), a nuclear serine threonine kinase, has come under focus owing to its central role in transcription. In association with the mediator complex, it acts as a molecular bridge between transcription factors, chromatin modifiers, promoters, enhancers and RNA Polymerase II (Liu et al., 2004; Kohler et al., 2019; Klatt et al., 2020). Accumulating evidence suggests an underlying role for the CDK8 module in the Wnt, HIF1α, NFκB, e2f1, and p53 pathways, among others (Donner et al., 2007; Galbraith et al., 2013; Birkenheuer et al., 2015; Rzymski et al., 2015; Chen et al., 2017). As most of these CDK8-dependent pathways are altered in cancer, it is not surprising that CDK8 has been proposed to contribute

to tumor development. Notably, CDK8 was first linked to cancer when it was identified as an oncogene that is frequently amplified or overexpressed in CRC (Firestein et al., 2008). Subsequently, CDK8 was found to be amplified in 47% of 123 CRC patient samples in a study and cohort studies revealed a negative correlation between CDK8 expression and the survival of CRC patients (Firestein et al., 2010). In addition, increased level of CDK8 was later found in advanced CRC stages III and IV, suggesting that CDK8 contributes to the progression of colorectal adenoma to carcinoma (Seo et al., 2010). Importantly, it was confirmed that CDK8 has proto-oncogenic effects in CRC as it interacts with the Wnt pathway to enhance the transcriptional activity of β-catenin (Zhao et al., 2013). These observations suggest that CDK8 may play an important role in colorectal carcinogenesis. However, it is not clear whether CDK8 participates in the IR response or affects CRC radiosensitivity.

IR causes DNA damage that activates the p53 and e2f1 pathways in concert or independently to repair the damage or induce apoptosis (Udayakumar et al., 2010). These two pathways induce cell-cycle arrest to repair DNA damage. Depending on the extent of the repair level, the repair process can result in three different cellular outcomes: efficient repair that promotes survival, inefficient repair that leads to survival of gnomically unstable cancer cells, and induction of apoptosis if the damage is severe and irreparable (Sirbu and Cortez, 2013). By altering the functions of p53 and e2f1 through truncation, such that the regions responsible for DNA damage repair are eliminated, efficient killing of tumor cells can be achieved when combined with other therapeutic modalities, such as chemotherapy and IR therapy (Udayakumar et al., 2010). Abrogating the DNA repair function and concomitantly enhancing the proapoptotic functions of p53 and e2f1 represents a novel strategy with clinical potential (Polager and Ginsberg, 2009). Notably, CDK8 has been described as a key regulator that positively or negatively affects the transcription of p53 and e2f1. One study showed that CDK8 was recruited to the p21 promoter in response to specific stress and reported CDK8 to be a stimulus specific positive co-regulator of p53 target genes (Donner et al., 2007). In contrast, another study reported that CDK8 down-regulates the transcriptional activity of e2f1 by phosphorylation, which relieves the repression of e2f1 on β-catenin/TCF pathway, and inhibits e2f1-induced apoptosis in CRC cells (Morris et al., 2008). Given the potent effect of CDK8 in the transcriptional regulation of p53 and e2f1, it is of great interest to target CDK8 in cancer therapy.

In this study, we mainly explored the transcriptional regulation of CDK8 in CRC after IR. We elucidated that targeting CDK8 sensitizes CRC to IR both *in vitro* and *in vivo* through potentiating transcription of e2f1 target gene apaf1. Our study revealed that the IR-induced intrinsic apoptosis in CDK8 knockdown cells was dependent on e2f1 but not p53. Further, the inhibition of e2f1 transcriptional activity by CDK8 was dependent on the kinase activity of CDK8 itself and not on the assembling of the mediator complex. These results provide convincing evidence that CDK8 serves as a promising target to radiosensitize CRC to therapy.

MATERIALS AND METHODS

Reagents and Antibodies

Propidium iodide (PI) were obtained from Invitrogen (Shanghai, China). Primers for quantitative real-time PCR and ChIP analysis were purchased from GENEWIZ (Suzhou, China). Transcriptone-step gDNA removal and cDNA synthesis supermix kit was purchased from Transgen Biotech (Beijing, China). SuperReal PreMix (SYBR GREEN) was purchased from Qiagen (Shanghai, China). The siRNA were purchased from GenePharma (Shanghai, China) and siRNA transfection was carried out using Lipofectamine 2000 (Thermo Fishier, Carlsbad, CA, United States). pLKO.1 plasmid expressing CDK8 shRNA was purchased from GENEWIZ (Suzhou, China). The siRNA sequences and shRNA sequences are listed in **Supplementary Table S1**. ChIP was performed using SimpleChIP Enzymatic Chromatin IP Kit (Agarose Beads) (Cell Signaling Technology, Danvers, MA, United States). Protein G Sepharose beads was purchased from Beyotime (Shanghai, China). Dimethyl sulfoxide (DMSO) and other chemicals were purchased from Sangon (Shanghai, China). Ponatinib and CCT251545 were purchased from Selleckchem and stored following the manufacturer's instruction.

The antibodies against p53, e2f1, p-Rpb1 CTD (S2/5), Rpb1 CTD, cleaved caspase 7, cleaved caspase 8, cleaved caspase 9, γH2AX and CDK8 were purchased from Cell Signaling Technology (Danvers, MA, United States). e2f1 (S375) antibody was obtained from Millipore (Temecula, CA, United States). Cleaved caspase 3 antibody was purchased from R&D Systems (Minneapolis, MN, United States). apaf1 antibody was obtained from Proteintech (Wuhan, China) and housekeeping gene β-actin was purchased from ZSGB-BIO (Beijing, China).

Cell Lines and Human Samples

Human CRC cell lines (HCT116 and LOVO), Human small intestine epithelium cell line (HIEC), Mouse CRC cell line (MC38) and Transformed human embryonic kidney cell line (HEK293T) were purchased from the American Type Culture Collection (ATCC, Manassas, VA, United States). HCT116, HIEC, HEK293T and MC38 cells were maintained in Dulbecco's modified Eagle's medium (HyClone, Logan, UT, United States), LOVO cells were maintained in Dulbecco's modified Eagle's medium with F12 (HyClone, Logan, UT, United States). All cell lines supplemented with 10% fetal bovine serum (Biological Industries, Israel) and 1% penicillin/streptomycin (Beyotime, Shanghai, China) at 37°C with 5% CO_2.

Surgically resected tumor and normal part of human colon from six individual patients were obtained through Anhui Medical University (Hefei, China).

Xenograft Model and Radiation

Stably transfected MC38 cells were inoculated into the subcutaneously in dorsal flank of 4-week-old C57BL/6 wild type mice obtained through Anhui Medical University (Hefei, China). A dosage of 0 Gy and 20 Gy were used to irradiate the mice for 8 days after the injection. Tumor dimensions and

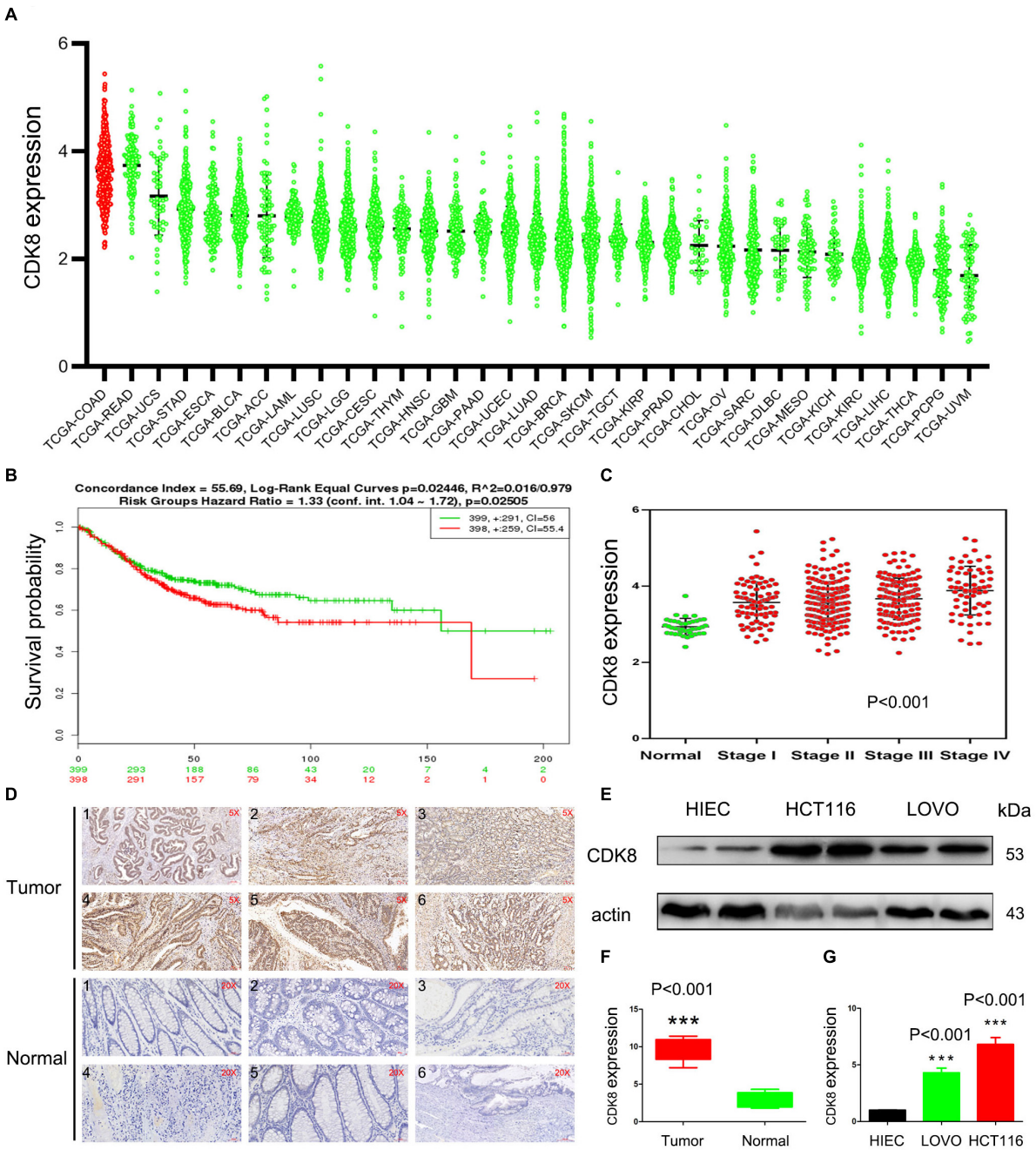

FIGURE 1 | CDK8 Is Overexpressed in CRC. **(A)** Expression of CDK8 in different tumor types in the TCGA database arranged by median. **(B)** Disease free survival of CRC patients with low versus high CDK8 expression. **(C)** Transcriptional expression of CDK8 at different stages of CRC from the TCGA database. **(D)** Immunohistochemical staining for CDK8 expression in representative tissue sections from a large cohort of normal and CRC clinical specimens **(E)** CDK8 protein level was higher in the CRC cell lines, LOVO and HCT116, than in the normal human intestinal epithelial cell line, HIEC, analyzed by western blotting. β-actin served as an internal control. **(F)** Quantitation of the intensity of CDK8 expression in the clinical specimens from panel **(D)** using the IPP software. **(G)** The intensity of CDK8 expression in the CRC cell lines from panel **(E)** were quantified after normalization to β-actin using Image J software. $^{***}p < 0.001$. Typical results from three independent experiments are shown. The difference between two groups were analyzed with the Student's *t* test. One-way analysis of variance (ANOVA) followed by *Post hoc* test was used in multiple groups.

volumes (mm^3) were measured and calculated with calipers every day. In the end, the mice were sacrificed by cervical dislocation on the 18 day after injection and the tumors were harvested. The tumor tissues were fixed in formalin to obtain sections for the TUNEL, H&E and immunohistochemical staining. All animal experiments procedures and uses of clinical samples

were performed according to guidelines approved by Committee review of animal experiments in Anhui Medical University.

For both *in vitro* and *in vivo* experiment, the irradiation was carried out in an X-ray irradiator, X-RAD 320 (Precision X-Ray Inc., United States). The indicated radiation dose was determined by the total radiation time basis on the dose rate 4.987 Gy/min controlled by the compute automatically. The equipment was maintained and calibrated every year by the manufacturer to ensure the precision of radiation dose.

Cell Viability Analysis

The indicated cells were plated in a 35 mm tissue culture plate with 200, 000 cells and cultured for 24 h. After treated or treated with CDK8 shRNA, IR, or CDK8 shRNA plus IR, cells were cultured for 24 h. Then all the cells were harvested in the presence of 2 μg/ml PI. Cell viability was measured by PI exclusion using a flow cytometer (FACScalibur; Beckon Dickinson, San Jose, CA, United States) and normalized as the percentage of the viability of untreated cells.

Colony Formation Analysis

A total of 800 cells were seeded in 60 mm dish. After treatment, the dishes were incubated for 2 weeks at 37°C in a 5% CO2 incubator for 14 days. Then the dishes were washed with PBS, fixed with a solution containing methanol: acetic acid (V/V = 9:1) for 30 min and subsequently stained with crystal violet for 30 min. The colonies containing more than 50 cells per colony was scored and plotted.

Immunoprecipitation Assay

Treated cells were washed with cold PBS twice before the addition of lysis RIPA buffer. After centrifugation, Protein G Sepharose Beads were added to the lysate and incubated on a rotator for 30 min at 4°C. The supernatant was transferred to a new tube, after centrifugation at 460 × *g* for 3 min at 4°C. The primary antibody was added to the supernatant and incubated at 4°C for 12 h while gently stirring. Protein G Sepharose Bead slurry was then added to capture the protein complex. After incubation at 4°C for 3 h with gentle agitation, the samples were centrifuged at 1,000 × *g* for 30 s at 4°C. The supernatant was discarded and the pellet was washed with RIPA buffer. Finally, the immunoprecipitates were resuspended in SDS-PAGE loading buffer for Western blot analysis.

Quantitative Real-Time PCR

The real-time PCR primer sequences for the target genes were summarized in supporting information (**Supplementary Table S4**). The cycling conditions: 2 min, 95°C for PCR initial heat activation; and 5 s, 95°C for denaturation; and 10 s, 60°C for combined annealing/extension; Number of cycles: 40. mRNA expression was assessed by quantitative real-time PCR on an ABI 7500 FAST Real-Time PCR System (Applied Biosystems, Foster City, CA, United States) using SuperReal PreMix (SYBR Green) in a 48-well plate. RNA levels of the genes of interest were normalized to the act-1 level for comparison and gene expression data were analyzed using the comparative $2^{-\Delta\Delta Ct}$ method. Triplicates for each sample were included for one single reaction.

Chromatin Immunoprecipitation Analysis

Chromatin immunoprecipitation analysis was conducted according to the manufacturer's instructions (Cell Signaling Technology, Danvers, MA, United States). Briefly, collected cells were crosslinked with 1% formaldehyde and blocked with glycine. Cells were then washed and digested by micrococcal nuclease. The nuclear pellet was suspended in chromatin immunoprecipitation (ChIP) buffer and sheared by sonication. The sheared chromatin was then incubated with various antibodies, including p53, e2f1, p-Rpb1 CTD (S2/5) and Rpb1 CTD. ChIP-enriched DNA was analyzed by qPCR with ChIP primers (**Supplementary Tables S2, S3**).

RNA-seq Analysis

The sequencing was performed by using Illumina HiSeq 4000 (LianChuan Sciences, Hangzhou, China). For each given gene list, pathway and process enrichment analysis has been carried out with the following ontology sources: KEGG Pathway, GO Biological Processes, Reactome Gene Sets, Canonical Pathways and CORUM. All genes in the genome have been used as the enrichment background. Terms with a p-value < 0.01, a minimum count of 3, and an enrichment factor >1.5 (the enrichment factor was the ratio between the observed counts and the counts expected by chance) were collected and grouped into clusters based on their membership similarities. More specifically, p-values were calculated based on the accumulative hypergeometric distribution, and q-values are calculated using the Banjamini-Hochberg procedure to account for multiple testings. Kappa scores were used as the similarity metric when performing hierachical clustering on the enriched terms, and sub-trees with a similarity of >0.3 were considered a cluster. The most statistically significant term within a cluster was chosen to represent the cluster.

Statistical Analysis

All data are represented as the means plus or minus standard deviations, and all experiments were performed in triplicate at least three times independently. $P < 0.05$ between groups was considered significant. The differences between two groups were analyzed with the Student's t test. One-way analysis of variance (ANOVA) followed by *Post hoc* test was used in multiple groups.

RESULTS

Pan Cancer Transcriptome Profiling of CDK8

TCGA is an invaluable resource to comprehensively analyze the transcriptome profile of CDK8 across a large spectrum of the most common tumor entities from thousands of patients.

In a pan-cancer analysis, the RNA-Seq based expression level of CDK8 across all the 33 tumor entities publicly available at TCGA at the time of analysis for all 10,327 patients was obtained. A scatter plot representation of the mRNA levels showed that majority of CDK8 was expressed in varying degrees across the patient samples at medium to high levels, with the highest levels observed in CRC (**Figure 1A**). This was in line with a previous study that suggested a tumor promoting role for CDK8 in CRC. Moreover, increased CDK8 expression was significantly associated with decreased survival and clinic pathologic parameters of progression (**Figures 1B,C**). To confirm the results of the TCGA data, clinical samples of CRC were analyzed. The results showed that the expression level of CDK8 in the different clinical samples of CRC was higher

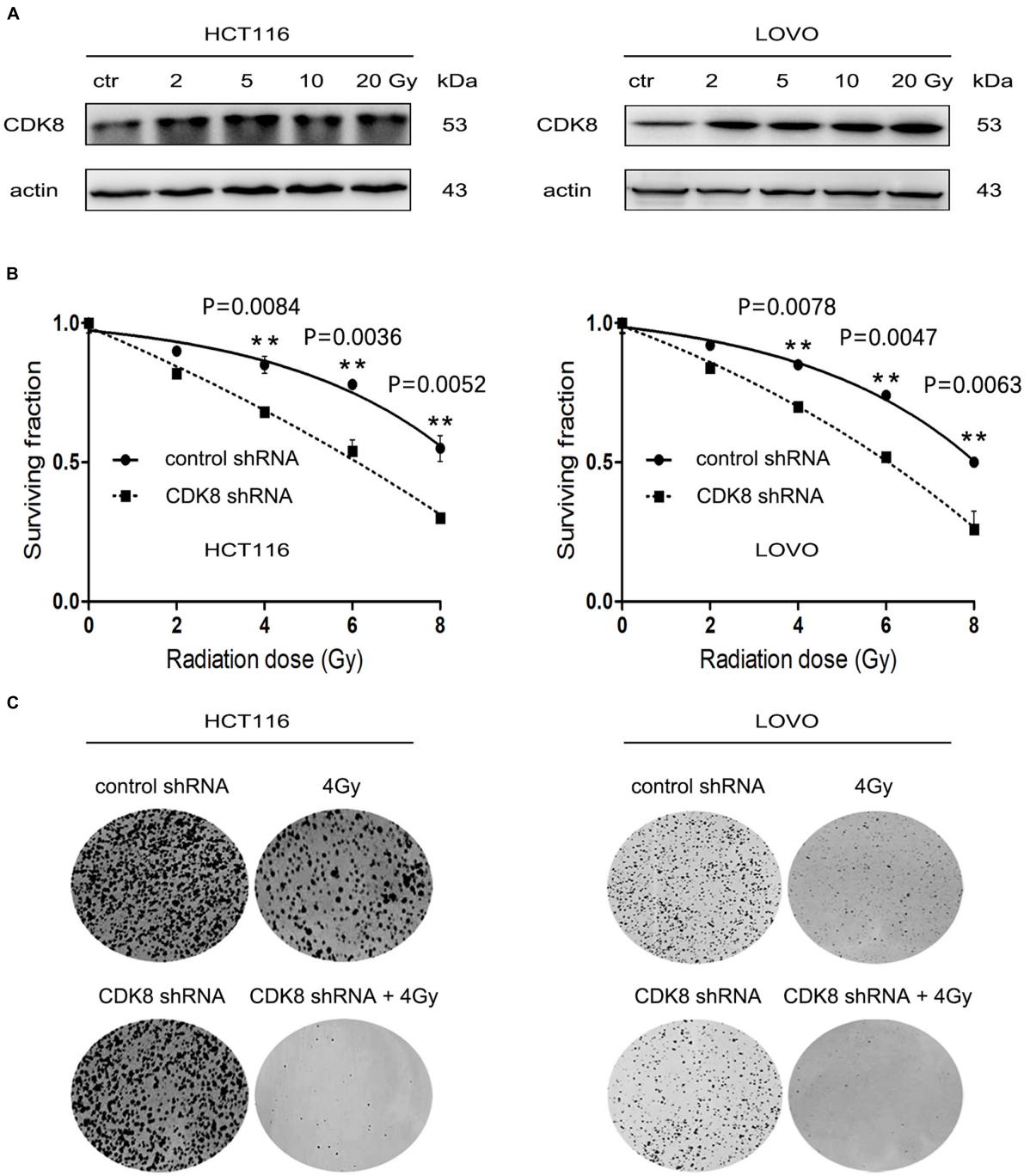

FIGURE 2 | Continued

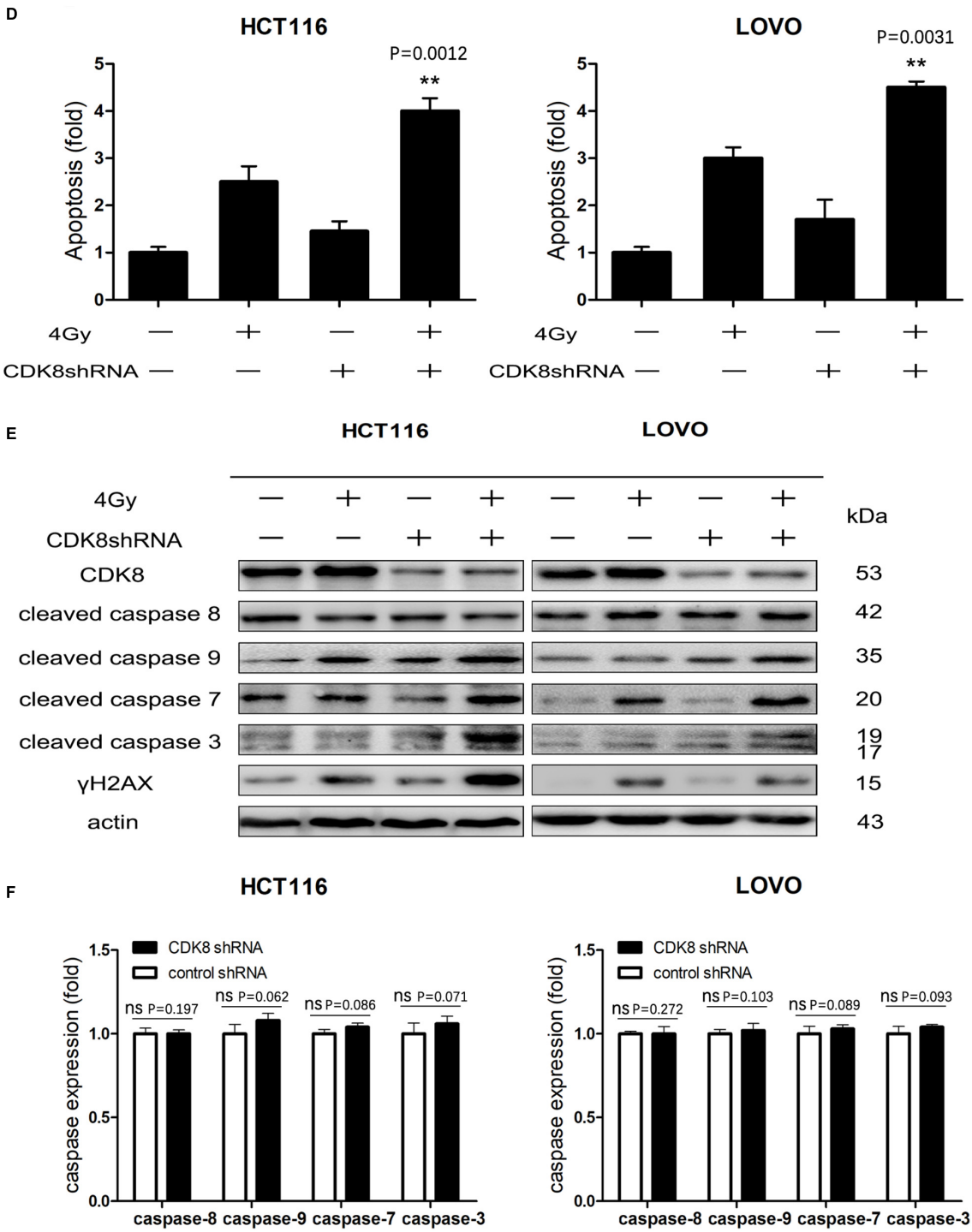

FIGURE 2 | CDK8 Knockdown Increased IR-Induced Intrinsic Apoptotic Signaling in CRC Cells. **(A)** HCT116 (left) and LOVO cells (right) were irradiated with different doses of radiation and CDK8 protein level was analyzed by western blotting 24 h later. **(B)** HCT116 (left) and LOVO cells (right) transfected with CDK8 or control shRNA were exposed to different doses of radiation and cell viability was measured 24 h later. **(C)** Colony formation of HCT116 (left) and LOVO cells (right) transfected with CDK8 or control shRNA was assessed after irradiated with the indicated doses of radiation. **(D)** The apoptosis levels were assessed using Annexin V-FITC/PI double staining in CDK8 kncokdown HCT116 cells (left) and LOVO cells (right) compared with control shRNA cells at 24 h after 4 Gy irradiation. **(E)** The expression level of CDK8, γH2AX, cleaved caspase 9, cleaved caspase 8, cleaved caspase 7, and cleaved caspase 3 were detected by western blotting in CDK8 kncokdown HCT116 cells (left) and LOVO cells (right) compared with control shRNA cells at 24 h after 4 Gy irradiation. **(F)** The intensities of caspase-3,7,8,9 in CDK8 kncokdown HCT116 (left) and LOVO cells (right) were quantified after normalization to β-actin using Image J software. $^{**}p < 0.01$. Typical results from three independent experiments are shown. The difference between two groups were analyzed with the Student's *t* test. One-way analysis of variance (ANOVA) followed by *Post hoc* test was used in multiple groups.

than that in the corresponding normal tissues (**Figures 1D,F**). Furthermore, CDK8 expression in two CRC lines (HCT116 and LOVO) were also analyzed. The expression level of CDK8 was higher in the CRC lines, particularly in the HCT116 cells (**Figures 1E,G**). HIEC is a normal human intestinal epithelial cell line. Although HIEC is derived from intestine, it was widely used as the control for HCT116 and LOVO in a lot of studies (Wu et al., 2018; Hu et al., 2019). Our analysis identified CDK8 to be specifically overexpressed during CRC progression, highlighting its potential as novel therapeutic target in advanced CRC.

Targeting CDK8 Sensitized CRC Cells to IR Through the Intrinsic Apoptotic Pathway

We found that CDK8 was overexpressed and correlated with poor survival and tumor subtypes in CRC. However, it was not clear whether CDK8 participates in the IR response or affects CRC radiosensitivity. Therefore, we investigated the effects of IR on the expression of CDK8 in CRC. As shown in **Figure 2A**, CDK8 expression level was significantly increased in both HCT116 and LOVO cells following treatment with a series of IR doses. Furthermore, we explored whether decreased expression of CDK8 could enhance the radiosensitivity of CRC. We found that shRNA mediated knockdown of CDK8 when combined with IR, decreased cell viability and Colony formation in HCT116 and LOVO cells (**Figures 2B,C**). Analysis of the surviving fractions in HCT116 and LOVO cells showed that the survival fraction values at 4 Gy were reduced from 0.85 and 0.83 to 0.68 and 0.64, respectively.

To further understand the detailed mechanism of induction of radiosensitivity following CDK8 knockdown, we examined the apoptotic level and the expression of the apoptotic proteins. As shown in **Figures 2D,E**, the highest apoptotic level was detected and the apoptotic proteins of cleaved caspase 3, cleaved caspase 7, and cleaved caspase 9 but not cleaved caspase 8 were significantly increased in CDK8 knockdown CRC cells after IR treatment, suggesting that downregulation of CDK8 results in radiosensitivity primarily through the intrinsic apoptotic pathway. In addition, residual γH2AX, a sensitive and robust biomarker of DNA damage (Mah et al., 2010; Zhou et al., 2018), was significantly increased in CDK8 knockdown cells compared with control shRNA cells after IR treatment (**Figure 2F**).

CDK8 Knockdown-Mediated Radiosensitivity of CRC Cells Was Dependent on e2f1 but Not p53

Our data provided compelling evidence that CDK8 regulated the radiosensitivity of CRC cells through the intrinsic apoptotic pathway. However, the potential regulatory mechanism underlying the activation of the intrinsic apoptotic pathway remained unclear. To elucidate the crosstalk between p53, e2f1, and CDK8 in IR-induced apoptotic signaling, the protein level of p53 and e2f1 was examined. As shown in **Figure 3A**, the expression of both p53 and e2f1 proteins were significantly increased in HCT116 and LOVO cells upon IR treatment. However, CDK8 knockdown inhibited the increased expression of p53 induced by IR, while e2f1 remained unaffected. The decreased level of p53 protein could be due either to decreased transcription of p53 gene regulated by CDK8, or to decreased p53 stability induced by CDK8-medaited phosphorylation.

Then, the expression levels of p53 and e2f1 target genes that link the apoptotic signaling pathways (Moroni et al., 2001; Lazzerini Denchi and Helin, 2005; Aubrey et al., 2018), including aen, noxa, p21, puma, bax, bcl2, fas, p73, mcl1, arf, bim, pkr, and apaf1 were analyzed. Our results showed that CDK8 knockdown combined with IR treatment failed to alter the mRNA levels of aen, noxa, p21, puma, bax, bcl2, fas, p73, mcl1, bim, pkr, and arf. By contrast, apaf1 gene expression was the most significantly increased after CDK8 knockdown together with IR treatment compared with IR treatment or CDK8 knockdown alone (**Figure 3B** and **Supplementary Figure S1**), indicating that the intrinsic apoptotic pathway induced by IR treatment in CDK8 knockdown CRC cells was triggered by apaf1.

To further assess the involvement of p53 and e2f1, we carried out a series of ChIP assays using cells that were untreated, or treated with CDK8 siRNA, 4 Gy, or both CDK8 siRNA and 4 Gy. The results of the ChIP analysis for apaf1 and the constitutively expressed housekeeping gene are shown in **Figures 3C,D**. As expected, IR treatment induced binding of p53 and e2f1 to the promoter region of apaf1, but not of the housekeeping gene. Importantly, in the CDK8 knockdown cells, there was a slight increase in the amount of e2f1 but not p53 associated with the apaf1 promoter, indicating that CDK8 served as a negative regulator of e2f1 transcription. Furthermore, e2f1 but not p53 was strongly recruited to the promoter region of apaf1 gene in irradiated CDK8 siRNA cells. Overall, these results demonstrated that the IR-induced intrinsic apoptotic pathway was mediated through potentiating transcription of apaf1 which is e2f1- and not p53-dependent.

CDK8 Interfered With the Transcriptional Activity of e2f1 Independent of Mediator Complex

It has been reported that CDK8 interacts with and phosphorylates e2f1 in cells, and the phosphorylation represses activation of e2f1-dependent genes (Morris et al., 2008; Zhao et al., 2013). In this study, we further demonstrated that CDK8 interacted with e2f1 but not p53 in CRC cells using Co-IP methods (**Figure 4A**). Moreover, CDK8 knockdown decreased the phosphorylation of e2f1 (S375) (**Figure 4B**). In addition, using CCT251545, the most specific CDK8 inhibitor (Dale et al., 2015), we confirmed that the inhibition of CDK8 kinase activity leads to decreased e2f1 phosphorylation (**Figure 4C**), which was reported to be key for the increased transcriptional activity of e2f1. To further demonstrate the effect of CDK8 inhibitor as a radiosensitizer in CRC, cells were treated with 100 nM CCT251545 for 24 h prior to IR treatment. The results showed that CCT251545 sensitized CRC cells to IR treatment (**Figures 4D–F**). Therefore, the

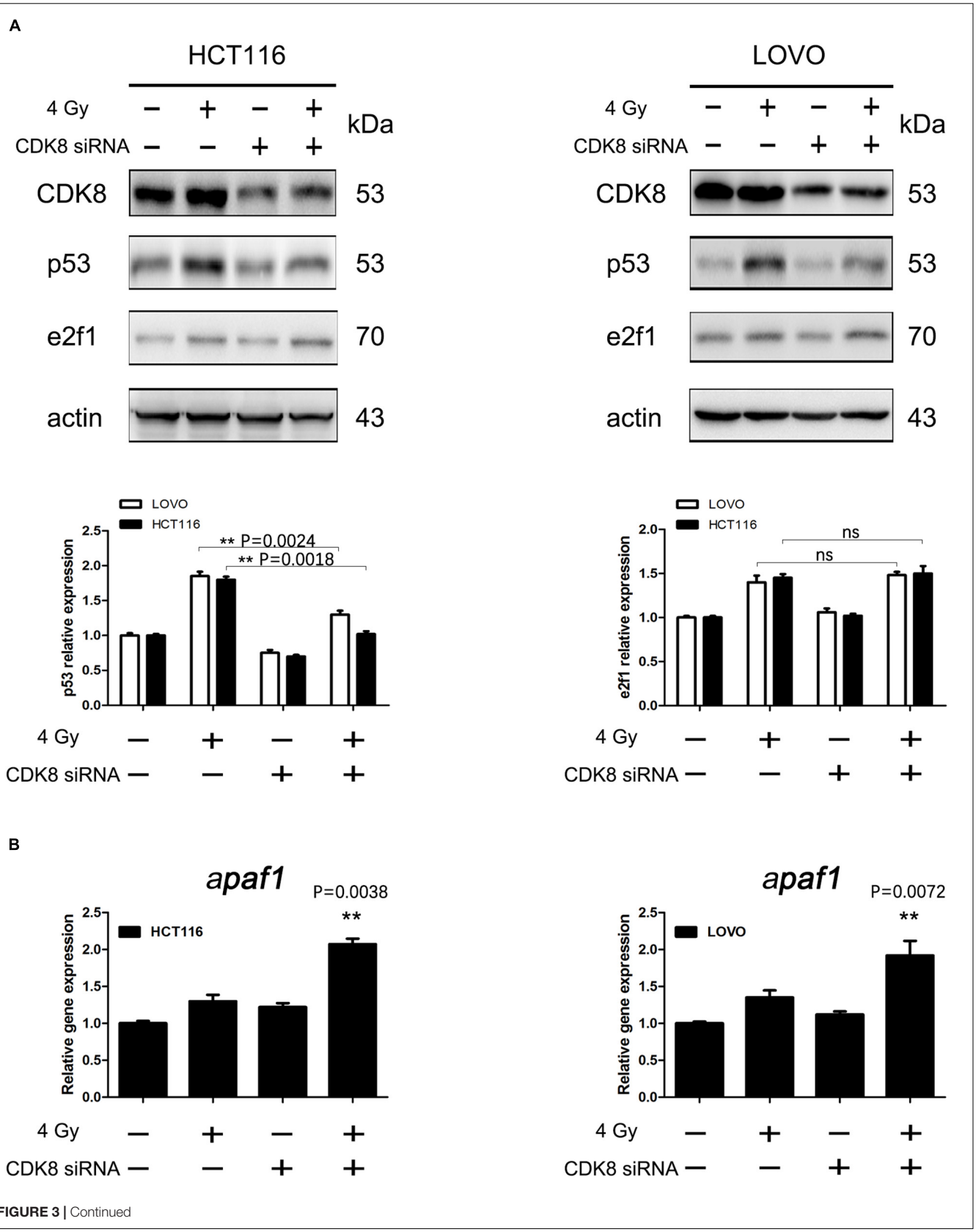

FIGURE 3 | Continued

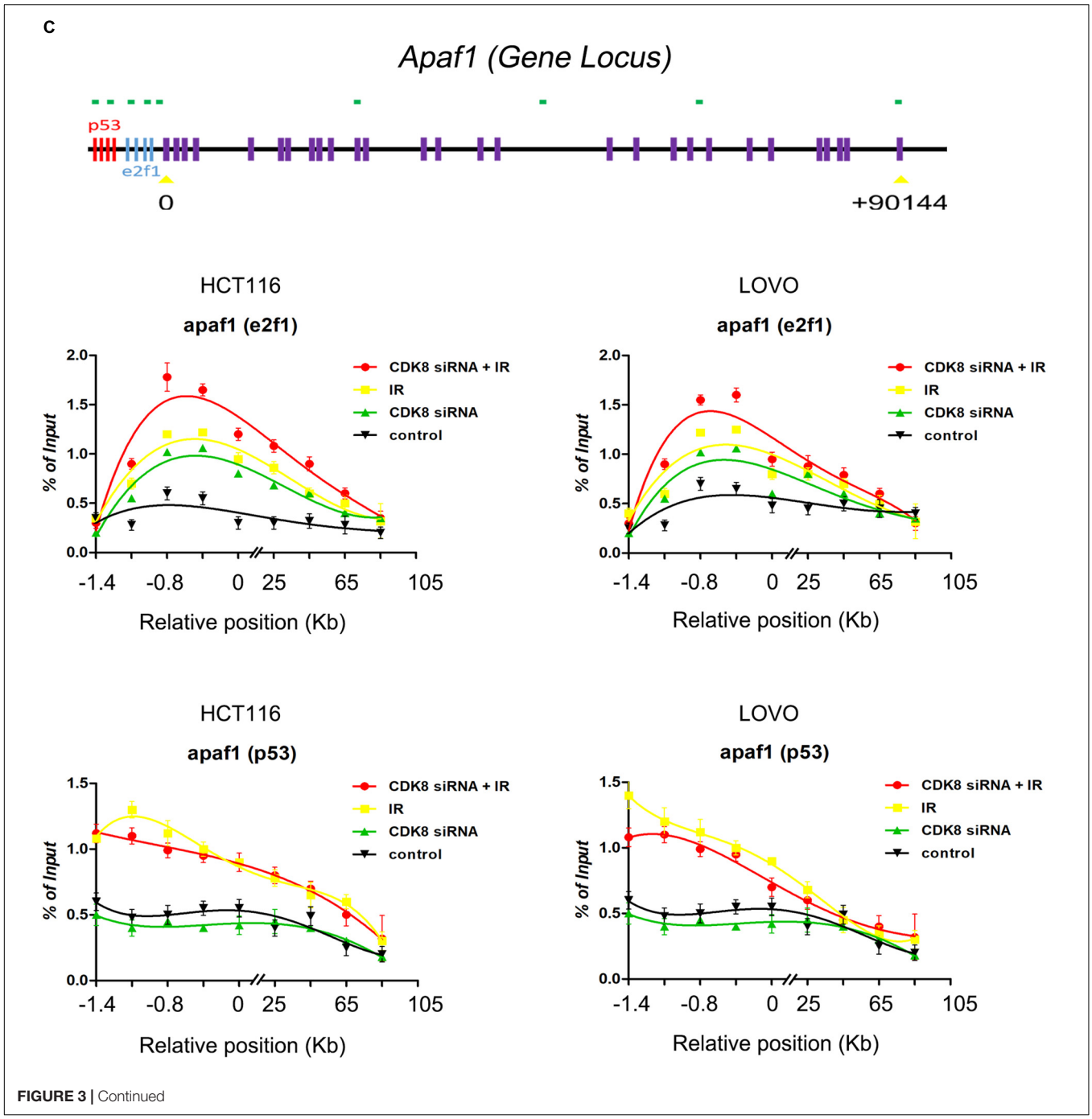

FIGURE 3 | Continued

kinase activity of CDK8 is responsible for the efficacy of IR treatment in CRC.

Subsequently, we detected the role of CDK8 knockdown combined with IR treatment on the binding of RNA Pol II and its CTD phosphorylated forms S2/5P (which promotes Pol II detachment from the promoter and allows for the elongation of transcription). As shown in **Figure 4G**, the effect was less prominent for the binding of S2/5P and total Pol II on the apaf1 promoter, indicating that CDK8 regulated e2f1 transcriptional activity in a form independent of mediator.

Based on the above data, our studies revealed a detailed mechanism of CDK8 down regulating e2f1 transcriptional activity in a CDK8 kinase activity-dependent manner (**Figure 4H**).

Targeting CDK8 Enhanced the Efficacy of Radiotherapy *in vivo*

To determine whether downregulation of CDK8 can sensitize CRC to IR treatment *in vivo*, MC38 with reduced CDK8

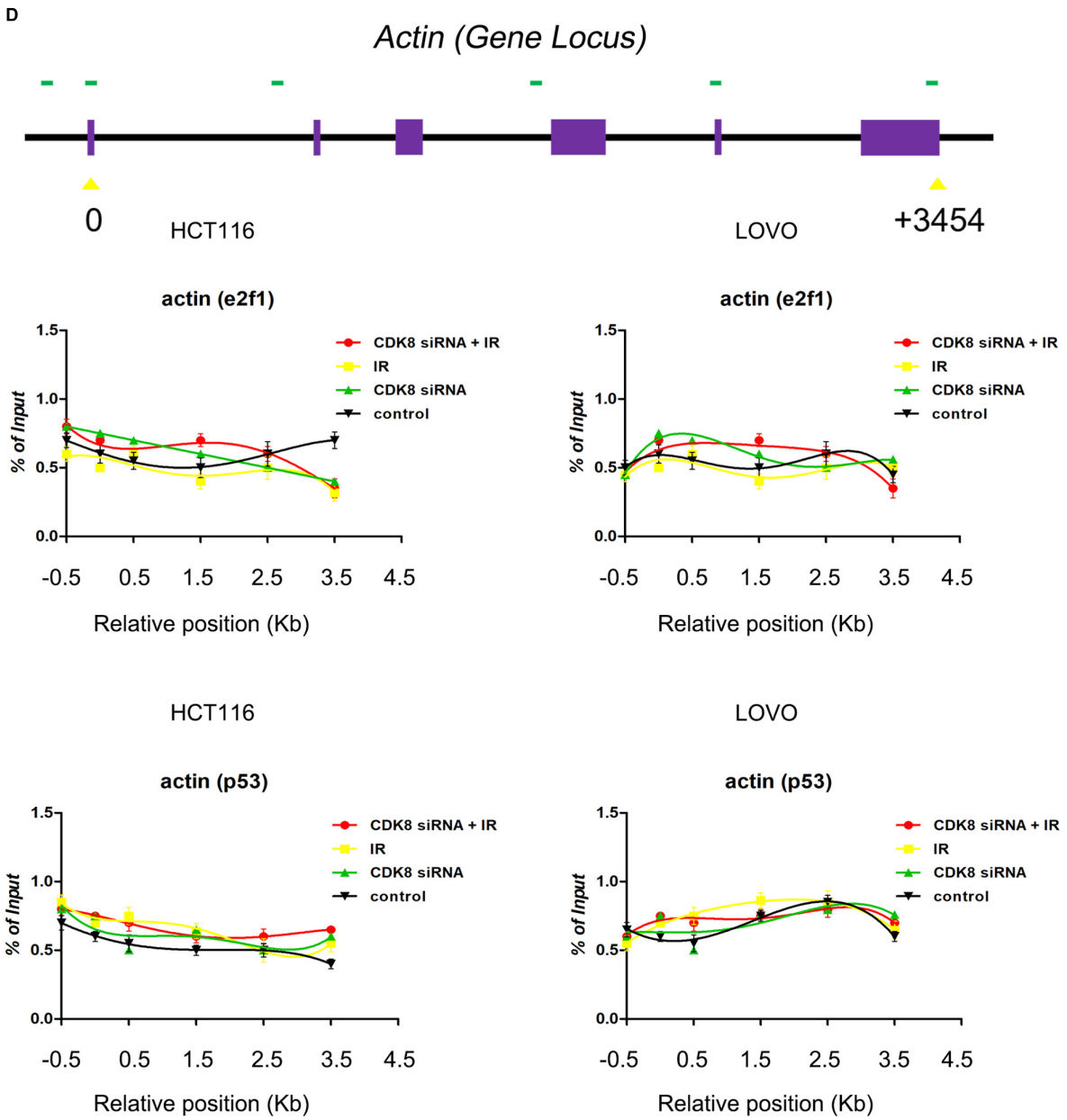

FIGURE 3 | e2f1 But Not p53 Was Involved in IR-Induced Apoptosis in CDK8 Knockdown CRC Cells. **(A)** The expression of p53 and e2f1 were detected by western blotting in CDK8 kncokdown HCT116 cells (left) and LOVO cells (right) compared with control siRNA cells at 24 h after 4 Gy irradiation. The intensities of p53 and e2f1 (lower panels) were quantified after normalization to β-actin using Image J software. **(B)** apaf1 mRNA level in CDK8 knockdown HCT116 (left) and LOVO cells (right) compared with control siRNA cells were detected using qPCR analysis at 24 h after 4 Gy irradiation. **(C,D)** Schemes of the apaf1 **(C, top panel)** and housekeeping β-actin **(D, top panel)** gene loci. The positions of p53 and e2f1 binding sites in the apaf1 gene are shown. ChIP analyses to test for the binding of p53 and e2f1 at the apaf1 loci in the HCT116 **(C,D, left lower panels)** and LOVO **(C,D, right lower panels)** cell lines following the indicated treatments. $^{**}p < 0.01$. Typical results from three independent experiments are shown. The difference between two groups were analyzed with the Student's *t* test. One-way analysis of variance (ANOVA) followed by *Post hoc* test was used in multiple groups.

expression were injected into C57BL/6 wild type mice. As shown in **Figures 5A–D**, reducing CDK8 expression significantly increased the inhibitory effects of 20 Gy on tumor growth. The volumes of tumors from the group with CDK8 shRNA combined with IR treatment were significantly decreased, indicating that knockdown CDK8 increases the radiosensitivity of CRC *in vivo*. In addition, immunohistochemical staining verified the expression of CDK8 protein and positive staining for γH2AX in the combination treatment (**Figure 5E**). To examine whether the radiosensitivity mediated by CDK8 *in vivo* was the result of apoptosis, we performed TUNEL assays. As shown in **Figure 5F**, the apoptotic cell population in CDK8 shRNA combined with

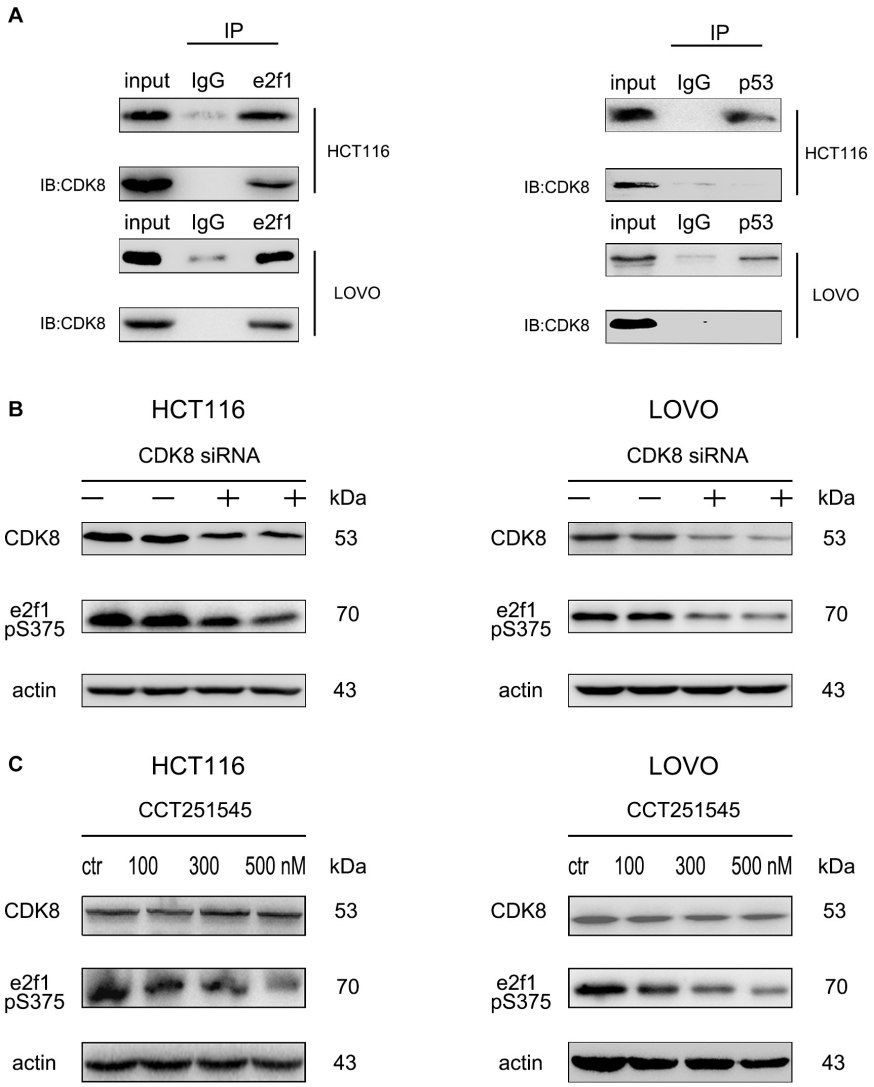

FIGURE 4 | Continued

IR treatment was significantly greater than that in IR treatment alone, indicating that IR synergized with CDK8 shRNA to enhance IR induced apoptosis *in vivo*. These results suggest that CDK8 knockdown improves the radiosensitivity of CRC *in vivo* through the apoptotic pathway, which is consistent with the *in vitro* data described above.

Clinical Drug Ponatinib Increased Sensitivity of CRC Cells to IR

The role of CDK8 in the radiosensitivity of CRC highlights the potential application of CDK8 inhibitors in IR therapy. To explore the potential clinical application of CDK8 inhibitors, biochemical screening of the available clinical and preclinical kinase inhibitors from The IUPHAR/BPS Guide to PHARMACOLOGY[1] revealed potent binding activity for ponatinib (Dale et al., 2015; **Supplementary Figure S2A**). According to our experimental data (**Figure 6A**), the expression level of CDK8 was significantly decreased after treating with different concentrations of ponatinib. Our results also showed that ponatinib combined with IR treatment synergistically decreased cell viability in HCT116 cells (**Supplementary Figure S2B** and **Figure 6B**). Concomitantly, high apoptotic level (**Supplementary Figures S2C,D**), and proteins expression level of cleaved caspase 3, cleaved caspase 7, cleaved caspase 8, cleaved caspase 9, and γH2AX was detected (**Figure 6C**).

To investigate the immediate changes in gene transcription in response to CDK8 inhibition and IR treatment, we conducted RNA-seq analysis. As shown in **Figure 6D** and **Supplementary Figure S2E**, after IR treatment, the majority of the differentially expressed genes associated with low

[1]https://www.guidetopharmacology.org

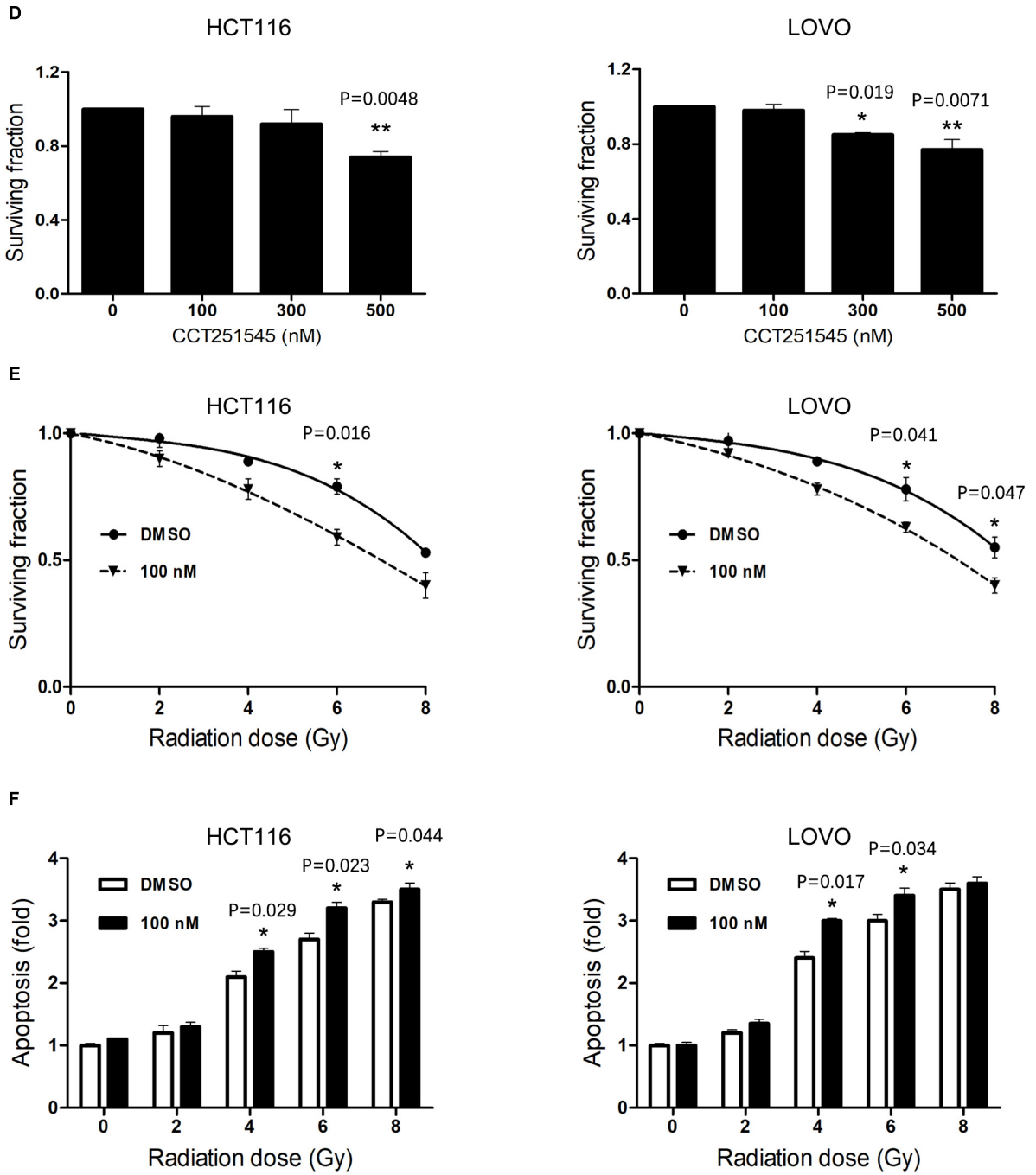

FIGURE 4 | Continued

CDK8 levels are upregulated compared to their expression in the high CDK8 group, and metascape analysis used to evaluate the biological functions of the 94 upregulated genes showed the top 10 clusters of enriched sets. These genes were significantly associated with the pathway interaction database (PID) P53 downstream pathway (**Figure 6E**), which contains e2f1 and apaf1. These results further demonstrate the core role of CDK8 in radiosensitivity of CRC. Overall, our data demonstrate the potential clinical application of the CDK8 inhibitor.

DISCUSSION

The role of CDK8 as an oncogene has been increasingly recognized and widely reported in several human cancers

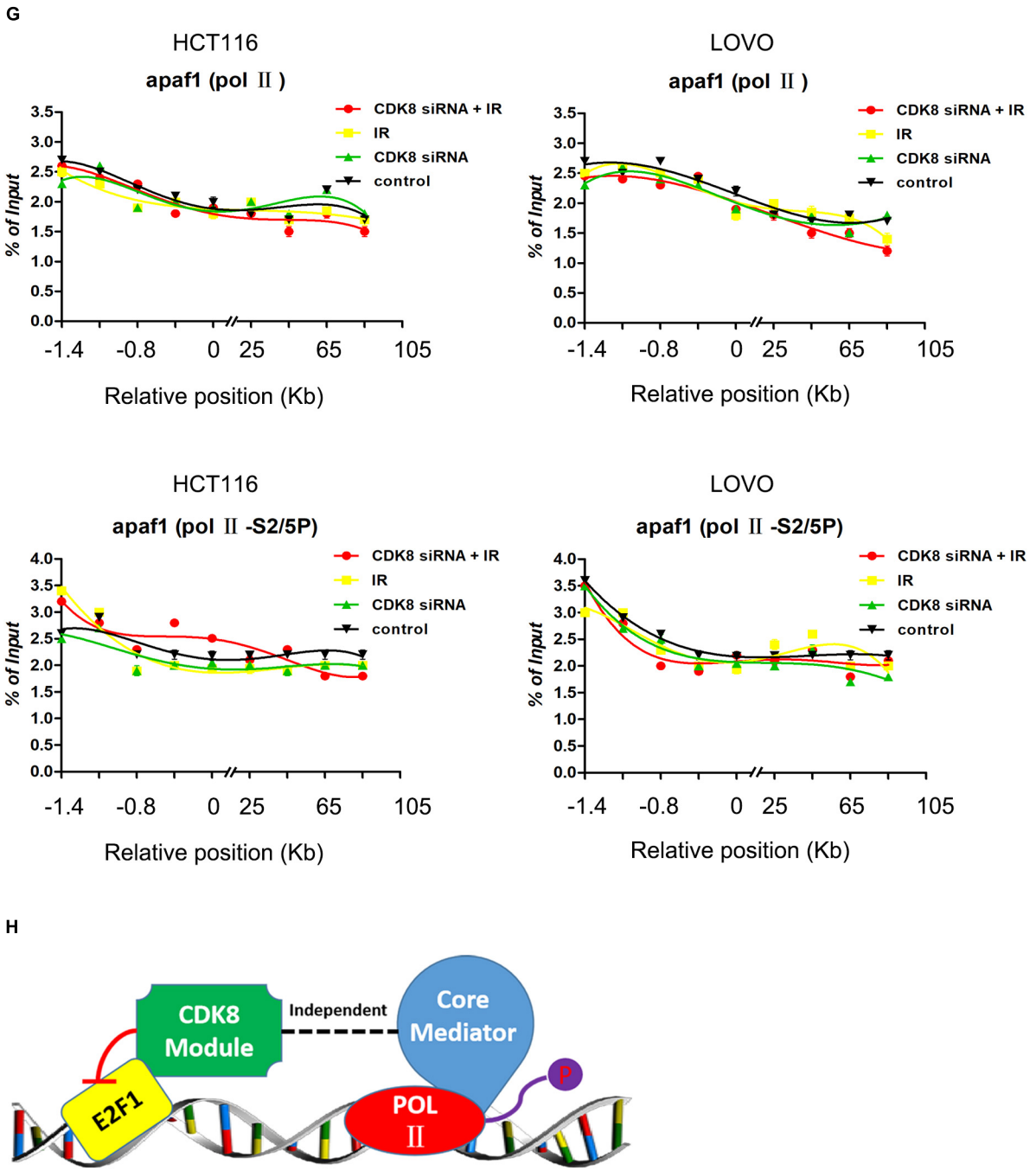

FIGURE 4 | CDK8 Interfered with the Transcriptional Activity of e2f1 Independent of Mediator Complex. **(A)** Co-immunoprecipitation of CDK8 with e2f1 **(left)** or p53 **(right)** was performed with the whole cell extract of HCT116 or LOVO cells. **(B)** HCT116 **(left)** and LOVO cells **(right)** were treated with CDK8 siRNA, and the expression of CDK8, phosphorylated e2f1 (S375), and β-actin were assessed by western blotting. **(C)** HCT116 **(left)** and LOVO cells **(right)** were treated with various concentrations of CCT251545 for 24 h, and the expression of CDK8, phosphorylated e2f1 (S375), and β-actin were assessed by western blotting. **(D)** HCT116 **(left)** and LOVO cells **(right)** were treated with different doses of CCT251545 and the cell viability was measured 24 h later. **(E)** HCT116 **(left)** and LOVO cells **(right)** were pre-treated with 100 nM CCT251545 for 24 h prior to irradiation with different doses of radiation, and cell viability was measured 24 h after irradiation. **(F)** HCT116 **(left)** and LOVO cells **(right)** were pre-treated with 100 nM CCT251545 for 24 h prior to irradiation with different doses of radiation, and the apoptosis level was measured 24 h after irradiation. **(G)** ChIP analyses to test the effects of total Pol II **(top panels)** and Pol II S2/5P (center panels) on binding of apaf1 in HCT116 and LOVO cells. **(H)** Schematic illustration of the mechanism of co-regulation of e2f1 by CDK8. $^{*}p < 0.05$ and $^{**}p < 0.01$. Typical results from three independent experiments are shown. The difference between two groups were analyzed with the Student's *t* test. One-way analysis of variance (ANOVA) followed by *Post hoc* test was used in multiple groups.

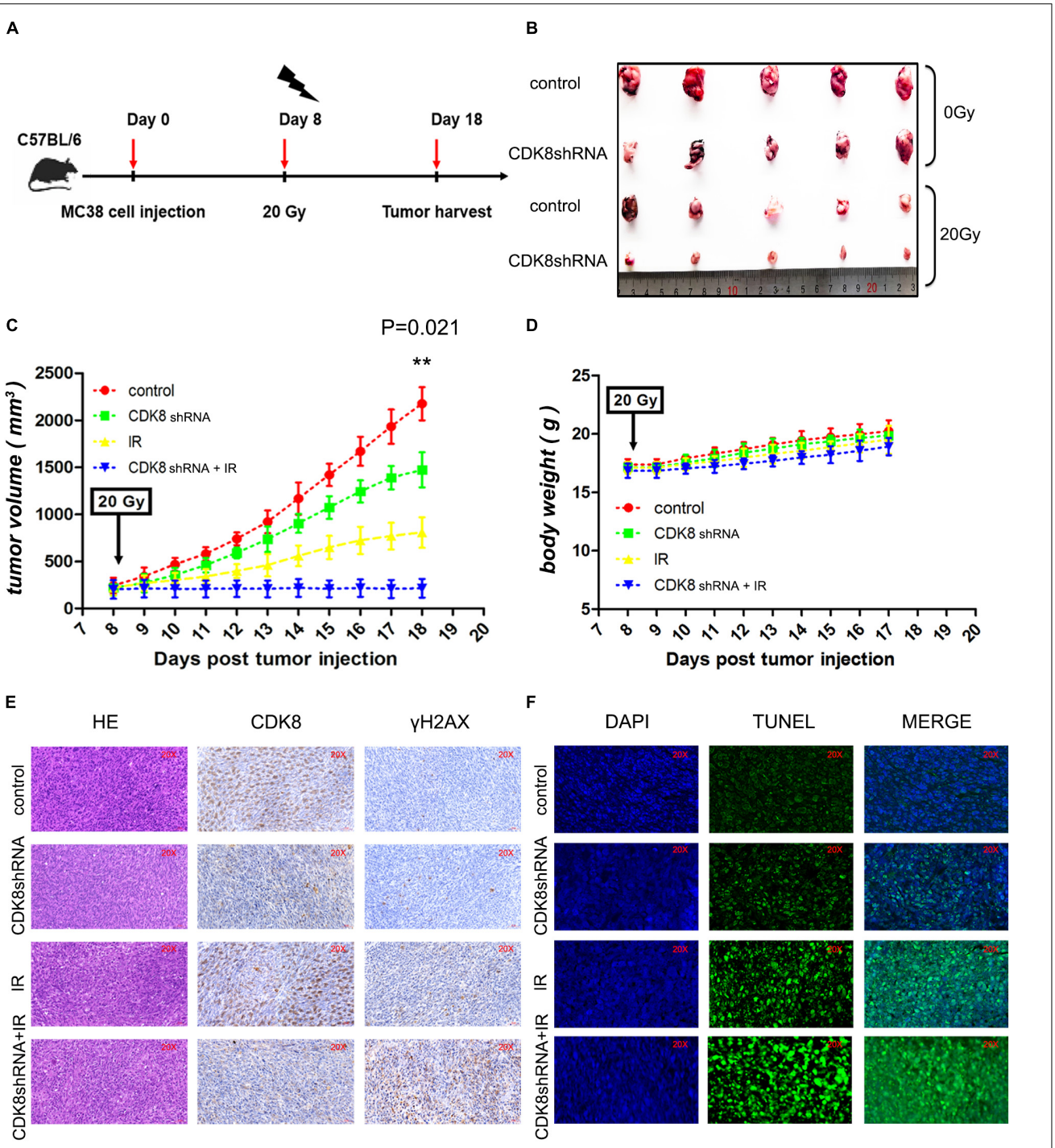

FIGURE 5 | Targeting CDK8 Enhanced the Efficacy of Radiotherapy *in vivo*. **(A)** A schematic of the experimental schedule was shown. **(B)** Each group of mice was composed of five C57BL/6 wild type female mice. Control vector MC38 cells (control, 1×10^7 cells) and CDK8 knockdown MC38 cells (CDK8 shRNA, 1×10^7 cells) were inoculated under the dorsal skin of the mice. After 8 days of injection, the treated mice were irradiated with 0 Gy or 20 Gy X ray. The mice were sacrificed 18 day after injection, and tumors were excised. **(C,D)** The volumes **(C)** and net weights **(D)** of the tumors in each group are shown. **(E)** CDK8 and γH2AX protein expression was verified by IHC staining. Necrotic cells in tumor sections were visualized by H&E staining. **(F)** Apoptotic cells (green) in the tumor sections were identified by TUNEL assay and the nuclei were counterstained with DAPI (blue). $^{**}p < 0.01$. Typical results from three independent experiments are shown. The difference between two groups were analyzed with the Student's *t* test. One-way analysis of variance (ANOVA) followed by *Post hoc* test was used in multiple groups.

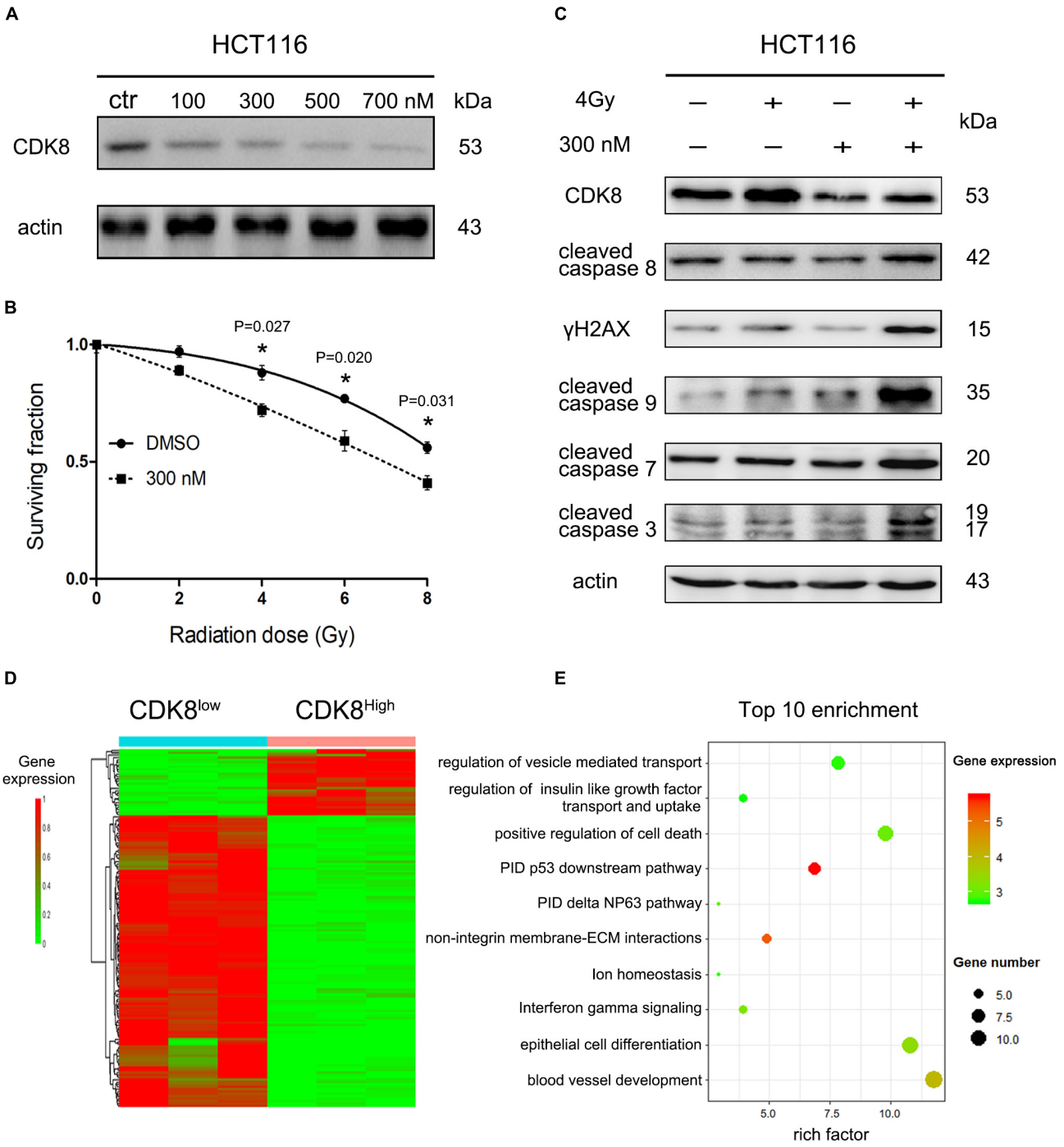

FIGURE 6 | Clinical Drug Ponatinib Increased Radiosensitivity of CRC Cells. **(A)** HCT116 cells were treated with different doses of ponatinib and the protein level of CDK8 was analyzed by western blotting 24 h later. **(B)** HCT116 cells were pre-treated with 300 nM ponatinib for 24 h prior to irradiation with different doses of radiation, and cell viability was measured after 24 h. **(C)** HCT116 cells were pre-treated with 300 nM ponatinib for 24 h before 4 Gy irradiation, and the expression level of CDK8, γH2AX, cleaved caspase 9, cleaved caspase 8, cleaved caspase 7, and cleaved caspase 3 were assessed by western blotting after 24 h. **(D)** Heatmap shows the 122 differentially expressed genes (DEGs) in $CDK8^{Low}$ versus $CDK8^{High}$. Among the 122 genes, 28 were downregulated and 94 were upregulated. **(E)** A bubble plot displays the 10 most significant terms identified by Metascape analysis. Bubble colors represent the corrected *P* values. $^{*}p < 0.05$. Typical results from three independent experiments are shown. The difference between two groups were analyzed with the Student's *t* test. One-way analysis of variance (ANOVA) followed by *Post hoc* test was used in multiple groups.

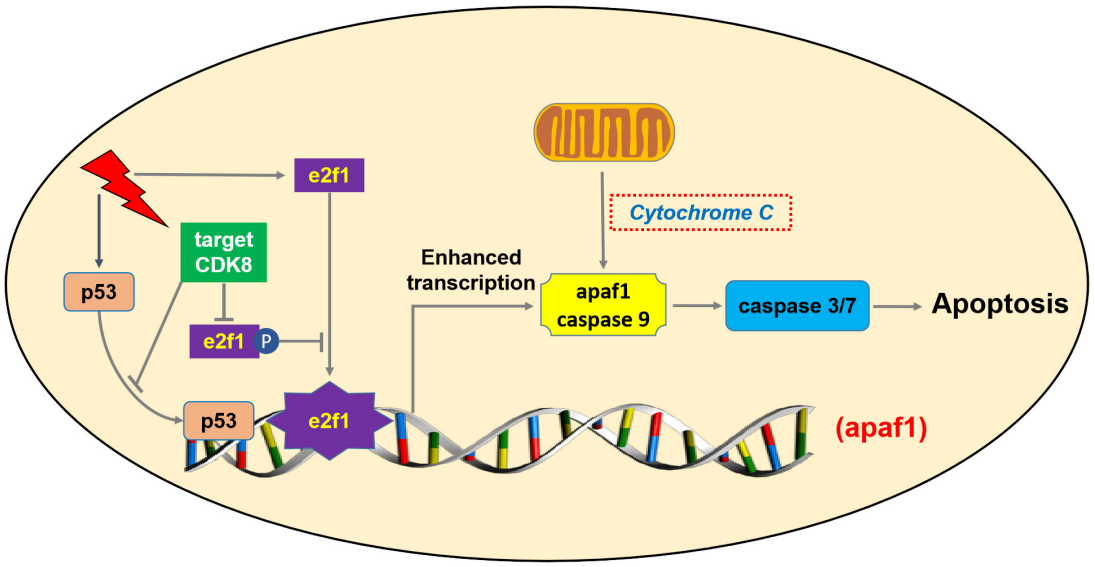

FIGURE 7 | Schematic sepresentation of the mechanism of CDK8 mediated radiosensitization of CRC cells through the mitochondria-dependent intrinsic apoptotic signaling through e2f1-dependent induction of apaf1.

(Bragelmann et al., 2017; Roninson et al., 2019). To determine the expression pattern of CDK8 in human cancers, we performed a pan cancer analysis of CDK8 transcriptome profiles. Analysis of TCGA RNA expression data showed that CDK8 expression was highest in CRC, and associated with significantly decreased disease-free survival (**Figures 1A–C**). The identification of cancer types with frequent amplification of CDK8 and correlation of expression with survival suggests a potential role of CDK8 in the pathogenesis of CRC or its treatment response, but it does not necessarily imply that such cancers will respond to CDK8 inhibitor therapy. Our study provides evidence that inhibiting CDK8 activity genetically or pharmacologically affects CRC growth, and when combined with IR treatment, it significantly augments IR sensitivity of CRC *in vitro* and *in vivo*.

Apoptosis is thought to be the major mechanism of IR-induced cell death and aberrant apoptotic signaling can cause resistance to radiotherapy (Baskar et al., 2012; Cao et al., 2019). It was reported that IR causes DNA damage that activates p53 and e2f1 pathways in concert or independently to repair the damage or induce apoptosis (Udayakumar et al., 2010). In our study, the protein expression of p53 were downregulated by IR treatment when combined with CDK8 knockdown (**Figure 3A**). This may be attributed to the role of CDK8 as a positive regulator of p53-dependent transcription (Donner et al., 2007), and this effect was blocked when CDK8 expression was reduced. Therefore, one possible scenario is that a e2f1-mediated alternative pathway that is p53 independent plays an essential role. As expected, our results showed that both p53 and e2f1 induced an increase in apaf1 level following IR treatment, however, the preferential transcriptional activation of apaf1 in CDK8 knockdown CRC cells prior to IR was regulated by e2f1 and not p53 (**Figure 3C**). This, along with the fact that e2f1 is a more potent inducer of apoptosis in cancer cells, suggests that the increase in apaf1 level is a significant event in e2f1-induced apoptosis in CDK8 knockdown CRC cells.

Transcriptional regulation is considered to be a critical determinant of gene expression, which is a complex process requiring the concerted action of numerous transcription factors and transcriptional co-factors (Lee and Young, 2013; Maeshima et al., 2015). As a nuclear serine threonine kinase, CDK8 has been associated with both positive (Galbraith et al., 2010) and negative (Elmlund et al., 2006) regulatory roles in transcription through mechanisms that include regulation of transcription factor turnover, regulation of CTD phosphorylation, and regulation of activator or repressor function. Previous studies reported that CDK8 physically interacts with e2f1, and is a conserved negative regulator of e2f1-dependent transcription (Morris et al., 2008; Zhao et al., 2013). In our current study, ChIP analysis revealed that CDK8 knockdown enhanced the recruitment of e2f1 to the promoter of the e2f1-responsive gene apaf1 (**Figure 3C**). This effect of CDK8 inhibition is specific to e2f1-induced genes and not with constitutively expressed gene such as actin (**Figure 3D**). Importantly, following CDK8 knockdown, there was already a slight increase in the amount of e2f1 associated with the promoters. Thus, CDK8 inhibition could potentiate the basal transcriptional effects of e2f1, and continuously enhance apaf1 transcriptional activity under external stimulation, such as with IR (**Figure 3B**). A high concentration of apaf1 may increase the probability of physical interaction between procaspase-9 molecules, resulting in oligomerization and subsequent autoactivation of procaspase-9. Then activated caspase-9, in turn, cleaves and activates downstream caspases-3/7, effector proteases that execute the cell death program (**Figure 2E**). In short, we propose that CDK8 knockdown enhanced the transcriptional activity of e2f1 leading to increased apaf1 level which subsequently triggered the downstream apoptosis cascade

and finally induced mitochondria-dependent intrinsic apoptosis to enhance radiosensitizing effect in CRC.

Notably, it has been hypothesized that the negative effect of the CDK8 module on eukaryotic transcription is mediated by CDK8-dependent phosphorylation of CTD (Elmlund et al., 2006). The hyper phosphorylated form of CTD binds less tightly to the mediator, which may result in the dissociation of pol II from the holoenzyme complex (Eick and Geyer, 2013). However, we analyzed the effects of CDK8 knockdown combined with IR on the binding of total RNA Pol II and its CTD phosphorylated forms, S5P and S2P, but did not find any increase in the association of any of the forms of Pol II with the promoter or any other part of the e2f1 responsive gene, apaf1 (**Figure 4G**), indicating that Pol II CTD phosphorylation in the context of activated genes seems to be independent of the mechanism of transcriptional regulation of e2f1 by CDK8. This might be attributed to the fact that although majority of CDK8 sub complex appears to be associated with various forms of mediator in human cells, up to 30% of CDK8 may exist in a form independent of the mediator (Knuesel et al., 2009a,b). It has been reported that the phosphorylation of S375 in e2f1 by CDK8 may be a general mechanism of regulation of e2f1 transcriptional activity (Zhao et al., 2013). This was mirrored by the CDK8 kinase inhibitor, which prevented the phosphorylation of e2f1 and increased the radiosensitivitty in both HCT116 and LOVO cells (**Figures 4D–F**). In general, our studies revealed a detailed mechanism of CDK8 mediated downregulation of e2f1 transcriptional activity in a CDK8 kinase activity -dependent manner independent of the mediator.

γH2AX is a sensitive and robust biomarker of DNA damage (Xiao et al., 2018). Several studies showed that IR enhanced γH2AX also via apoptotic signals (Solier and Pommier, 2014). For example, IR caused the release of mitochondrial cytochrome c into the cytoplasm to activate caspase-3, which triggers the apoptotic cascade to DNA fragmentation including phosphorylation of H2AX (Harada et al., 2014). In addition, DNA repair is curtailed because of caspase-mediated cleavage and inactivation of key DDR (DNA damage response) mediators (such as MDC1) (Dimitrova and de Lange, 2006) and effectors (such as PARP1) (Lazebnik et al., 1994). Along the same lines, caspase-3 also inactivates DNA replication by cleaving CDC6 (Yim et al., 2006). In the present study, we found that targeting CDK8 selectively radiosensitized colorectal cancer through the mitochondria dependent intrinsic apoptotic signaling, which triggered by caspase-3, 7, 9. Besides, the increase of γH2AX was also significant in CDK8 knockdown CRC cells after IR (**Figures 2E**, **5E**). This prompted us to hypothesize that CDK8 knockdown enhanced the transcriptional activity of e2f1 leading to increased apaf1 level, which homo-oligomerizes into a caspase-activating complex that sequentially recruits and activates the initiator caspase-9 and the effector caspases-3/7. Caspases activation in those cells could lead to downstream nuclease activation and DNA fragmentation, which subsequently induced significantly higher levels of γH2AX.

Based on the data presented above, amplification of CDK8 may be a novel way for cells to overcome regulation by e2f1, allowing cells to prevent the expression of e2f1 target genes that are pro-apoptotic. By abrogating e2f1 activity, CDK8 appears to promote cell proliferation at least in CRC. CDK8 mediated regulation of e2f1 appears to be a general mechanism to achieve control over e2f1 mediated activation or repression of transcription. Potentially, targeting CDK8 for inhibition, at least in CDK8 over-expressing tumors, could help restore e2f1 activity in these tumors, promoting inhibition or regression of tumor growth. In summary, our study demonstrated that knockdown or inhibition of CDK8 can inhibit the fractional survival of CRC cells, and targeting CDK8 increased IR-induced apoptosis *in vivo* and *in vitro*. Increased level of apaf1 resulting from enhanced transcriptional activity of e2f1 (not p53) could provide an explanation for the greater sensitivity of CRC cells to IR following CDK8 knockdown (**Figure 7**). Thus, CDK8 is a potent candidate target to enhance cancer radiotherapy.

DATA AVAILABILITY STATEMENT

All datasets generated for this study are included in the article/**Supplementary Material**. Any material described in the article can be requested directly from the corresponding author, without undue reservation, to any qualified researcher.

ETHICS STATEMENT

All animal experiments procedures and uses of clinical samples were performed according to guidelines approved by Committee review of animal experiments in Anhui Medical University. Written informed consent for publication was obtained from all participants.

AUTHOR CONTRIBUTIONS

GZ and BC conceived of the study and wrote the manuscript. BC, GH, YG, PW, KZ, and XQ conducted the experiments. SC, AX, and LW analyzed and interpreted the data. All authors read and approved the final manuscript.

FUNDING

This work was supported by the National Natural Science Foundation of China (31870845, 11835014, and 31601124) and CAS Pioneer Hundred Talents Program.

ACKNOWLEDGMENTS

The authors are grateful to Dr. Ye Zhao (Anhui Medical University, Hefei) for their technical assistance.

SUPPLEMENTARY MATERIAL

The Supplementary Material for this article can be found online at: https://www.frontiersin.org/articles/10.3389/fcell.2020.00408/full#supplementary-material

REFERENCES

Aubrey, B. J., Kelly, G. L., Janic, A., Herold, M. J., and Strasser, A. (2018). How does p53 induce apoptosis and how does this relate to p53-mediated tumour suppression? *Cell Death Differ.* 25, 104–113. doi: 10.1038/cdd.2017.169

Baskar, R., Lee, K. A., Yeo, R., and Yeoh, K. W. (2012). Cancer and radiation therapy: current advances and future directions. *Int. J. Med. Sci.* 9, 193–199. doi: 10.7150/ijms.3635

Birkenheuer, C. H., Brewster, C. D., Quackenbush, S. L., and Rovnak, J. (2015). Retroviral cyclin controls cyclin-dependent kinase 8-mediated transcription elongation and reinitiation. *J. Virol.* 89, 5450–5461. doi: 10.1128/JVI.00464-15

Bragelmann, J., Klumper, N., Offermann, A., von Massenhausen, A., Bohm, D., Deng, M., et al. (2017). Pan-cancer analysis of the mediator complex transcriptome identifies CDK19 and CDK8 as therapeutic targets in advanced prostate cancer. *Clin. Cancer Res.* 23, 1829–1840. doi: 10.1158/1078-0432.CCR-16-0094

Bray, F., Ferlay, J., Soerjomataram, I., Siegel, R. L., Torre, L. A., and Jemal, A. (2018). Global cancer statistics 2018: GLOBOCAN estimates of incidence and mortality worldwide for 36 cancers in 185 countries. *CA Cancer J. Clin.* 68, 394–424. doi: 10.3322/caac.21492

Cao, X., Wen, P., Fu, Y., Gao, Y., Qi, X., Chen, B., et al. (2019). Radiation induces apoptosis primarily through the intrinsic pathway in mammalian cells. *Cell Signal.* 62:109337. doi: 10.1016/j.cellsig.2019.06.002

Chen, M., Liang, J., Ji, H., Yang, Z., Altilia, S., Hu, B., et al. (2017). CDK8/19 Mediator kinases potentiate induction of transcription by NFkappaB. *Proc. Natl. Acad. Sci. U.S.A.* 114, 10208–10213. doi: 10.1073/pnas.1710467114

Dale, T., Clarke, P. A., Esdar, C., Waalboer, D., Adeniji-Popoola, O., Ortiz-Ruiz, M. J., et al. (2015). A selective chemical probe for exploring the role of CDK8 and CDK19 in human disease. *Nat. Chem. Biol.* 11, 973–980. doi: 10.1038/nchembio.1952

Dimitrova, N., and de Lange, T. (2006). MDC1 accelerates nonhomologous end-joining of dysfunctional telomeres. *Genes Dev.* 20, 3238–3243. doi: 10.1101/gad.1496606

Donner, A. J., Szostek, S., Hoover, J. M., and Espinosa, J. M. (2007). CDK8 is a stimulus-specific positive coregulator of p53 target genes. *Mol. Cell.* 27, 121–133. doi: 10.1016/j.molcel.2007.05.026

Eick, D., and Geyer, M. (2013). The RNA polymerase II carboxy-terminal domain (CTD) code. *Chem. Rev.* 113, 8456–8490. doi: 10.1021/cr400071f

Elmlund, H., Baraznenok, V., Lindahl, M., Samuelsen, C. O., Koeck, P. J., Holmberg, S., et al. (2006). The cyclin-dependent kinase 8 module sterically blocks Mediator interactions with RNA polymerase II. *Proc. Natl. Acad. Sci. U.S.A.* 103, 15788–15793. doi: 10.1073/pnas.0607483103

Firestein, R., Bass, A. J., Kim, S. Y., Dunn, I. F., Silver, S. J., Guney, I., et al. (2008). CDK8 is a colorectal cancer oncogene that regulates beta-catenin activity. *Nature* 455, 547–551. doi: 10.1038/nature07179

Firestein, R., Shima, K., Nosho, K., Irahara, N., Baba, Y., Bojarski, E., et al. (2010). CDK8 expression in 470 colorectal cancers in relation to beta-catenin activation, other molecular alterations and patient survival. *Int. J. Cancer* 126, 2863–2873. doi: 10.1002/ijc.24908

Galbraith, M. D., Allen, M. A., Bensard, C. L., Wang, X., Schwinn, M. K., Qin, B., et al. (2013). HIF1A employs CDK8-mediator to stimulate RNAPII elongation in response to hypoxia. *Cell* 153, 1327–1339. doi: 10.1016/j.cell.2013.04.048

Galbraith, M. D., Donner, A. J., and Espinosa, J. M. (2010). CDK8: a positive regulator of transcription. *Transcription* 1, 4–12.

Harada, A., Matsuzaki, K., Takeiri, A., and Mishima, M. (2014). The predominant role of apoptosis in gammaH2AX formation induced by aneugens is useful for distinguishing aneugens from clastogens. *Mutat. Res. Genet. Toxicol. Environ. Mutagen.* 771, 23–29. doi: 10.1016/j.mrgentox.2014.05.010

Hu, F., He, Z., Sun, C., and Rong, D. (2019). Knockdown of GRHL2 inhibited proliferation and induced apoptosis of colorectal cancer by suppressing the PI3K/Akt pathway. *Gene* 700, 96–104. doi: 10.1016/j.gene.2019.03.051

Klatt, F., Leitner, A., Kim, I. V., Ho-Xuan, H., Schneider, E. V., Langhammer, F., et al. (2020). A precisely positioned MED12 activation helix stimulates CDK8 kinase activity. *Proc. Natl. Acad. Sci. U.S.A.* 117, 2894–2905. doi: 10.1073/pnas.1917635117

Knuesel, M. T., Meyer, K. D., Bernecky, C., and Taatjes, D. J. (2009a). The human CDK8 subcomplex is a molecular switch that controls Mediator coactivator function. *Genes Dev.* 23, 439–451. doi: 10.1101/gad.1767009

Knuesel, M. T., Meyer, K. D., Donner, A. J., Espinosa, J. M., and Taatjes, D. J. (2009b). The human CDK8 subcomplex is a histone kinase that requires Med12 for activity and can function independently of mediator. *Mol. Cell Biol.* 29, 650–661. doi: 10.1128/MCB.00993-08

Kohler, K., Sanchez-Pulido, L., Hofer, V., Marko, A., Ponting, C. P., Snijders, A. P., et al. (2019). The Cdk8/19-cyclin C transcription regulator functions in genome replication through metazoan Sld7. *PLoS Biol.* 17:e2006767. doi: 10.1371/journal.pbio.2006767

Lazebnik, Y. A., Kaufmann, S. H., Desnoyers, S., Poirier, G. G., and Earnshaw, W. C. (1994). Cleavage of poly(ADP-ribose) polymerase by a proteinase with properties like ICE. *Nature* 371, 346–347. doi: 10.1038/371346a0

Lazzerini Denchi, E., and Helin, K. (2005). e2f1 is crucial for E2F-dependent apoptosis. *EMBO Rep.* 6, 661–668.

Lee, T. I., and Young, R. A. (2013). Transcriptional regulation and its misregulation in disease. *Cell* 152, 1237–1251.

Liu, Y., Kung, C., Fishburn, J., Ansari, A. Z., Shokat, K. M., and Hahn, S. (2004). Two cyclin-dependent kinases promote RNA polymerase II transcription and formation of the scaffold complex. *Mol. Cell. Biol.* 24, 1721–1735. doi: 10.1128/mcb.24.4.1721-1735.2004

Maeshima, K., Kaizu, K., Tamura, S., Nozaki, T., Kokubo, T., and Takahashi, K. (2015). The physical size of transcription factors is key to transcriptional regulation in chromatin domains. *J. Phys. Condens. Matter.* 27:064116. doi: 10.1088/0953-8984/27/6/064116

Mah, L. J., El-Osta, A., and Karagiannis, T. C. (2010). gammaH2AX: a sensitive molecular marker of DNA damage and repair. *Leukemia* 24, 679–686. doi: 10.1038/leu.2010.6

Mishra, J., Drummond, J., Quazi, S. H., Karanki, S. S., Shaw, J. J., Chen, B., et al. (2013). Prospective of colon cancer treatments and scope for combinatorial approach to enhanced cancer cell apoptosis. *Crit. Rev. Oncol. Hematol.* 86, 232–250. doi: 10.1016/j.critrevonc.2012.09.014

Moroni, M. C., Hickman, E. S., Lazzerini Denchi, E., Caprara, G., Colli, E., Cecconi, F., et al. (2001). Apaf-1 is a transcriptional target for E2F and p53. *Nat. Cell Biol.* 3, 552–558. doi: 10.1038/35078527

Morris, E. J., Ji, J. Y., Yang, F., Di Stefano, L., Herr, A., Moon, N. S., et al. (2008). e2f1 represses beta-catenin transcription and is antagonized by both pRB and CDK8. *Nature* 455, 552–556. doi: 10.1038/nature07310

Pal, S., Kozono, D., Yang, X., Fendler, W., Fitts, W., Ni, J., et al. (2018). Dual HDAC and PI3K inhibition abrogates NFkappaB- and FOXM1-mediated DNA damage response to radiosensitize pediatric high-grade gliomas. *Cancer Res.* 78, 4007–4021. doi: 10.1158/0008-5472.CAN-17-3691

Polager, S., and Ginsberg, D. (2009). p53 and E2f: partners in life and death. *Nat. Rev. Cancer* 9, 738–748. doi: 10.1038/nrc2718

Roberts, B. S., Hardigan, A. A., Moore, D. E., Ramaker, R. C., Jones, A. L., Fitz-Gerald, M. B., et al. (2018). Discovery and validation of circulating biomarkers of colorectal adenoma by high-depth small RNA sequencing. *Clin. Cancer Res.* 24, 2092–2099. doi: 10.1158/1078-0432.CCR-17-1960

Roninson, I. B., Gyorffy, B., Mack, Z. T., Shtil, A. A., Shtutman, M. S., Chen, M., et al. (2019). Identifying cancers impacted by CDK8/19. *Cells* 8:821. doi: 10.3390/cells8080821

Rzymski, T., Mikula, M., Wiklik, K., and Brzozka, K. (2015). CDK8 kinase–An emerging target in targeted cancer therapy. *Biochim. Biophys. Acta* 1854, 1617–1629. doi: 10.1016/j.bbapap.2015.05.011

Seo, J. O., Han, S. I., and Lim, S. C. (2010). Role of CDK8 and beta-catenin in colorectal adenocarcinoma. *Oncol. Rep.* 24, 285–291.

Sirbu, B. M., and Cortez, D. (2013). DNA damage response: three levels of DNA repair regulation. *Cold Spring Harb. Perspect. Biol.* 5:a012724. doi: 10.1101/cshperspect.a012724

Solier, S., and Pommier, Y. (2014). The nuclear gamma-H2AX apoptotic ring: implications for cancers and autoimmune diseases. *Cell. Mol. Life Sci.* 71, 2289–2297. doi: 10.1007/s00018-013-1555-2

Udayakumar, T., Shareef, M. M., Diaz, D. A., Ahmed, M. M., and Pollack, A. (2010). The e2f1/Rb and p53/MDM2 pathways in DNA repair and apoptosis: understanding the crosstalk to develop novel strategies for prostate cancer radiotherapy. *Semin. Radiat. Oncol.* 20, 258–266. doi: 10.1016/j.semradonc.2010.05.007

Wu, L., Tang, Q., Yin, X., Yan, D., Tang, M., Xin, J., et al. (2019). The therapeutic potential of adipose tissue-derived mesenchymal stem cells to

enhance radiotherapy effects on hepatocellular carcinoma. *Front. Cell. Dev. Biol.* 7:267. doi: 10.3389/fcell.2019.00267

Wu, Q., Meng, W. Y., Jie, Y., and Zhao, H. (2018). LncRNA MALAT1 induces colon cancer development by regulating miR-129-5p/HMGB1 axis. *J. Cell. Physiol.* 233, 6750–6757. doi: 10.1002/jcp.26383

Xiao, C., Wang, Y., Zheng, M., Chen, J., Song, G., Zhou, Z., et al. (2018). RBBP6 increases radioresistance and serves as a therapeutic target for preoperative radiotherapy in colorectal cancer. *Cancer Sci.* 109, 1075–1087. doi: 10.1111/cas.13516

Yim, H., Hwang, I. S., Choi, J. S., Chun, K. H., Jin, Y. H., Ham, Y. M., et al. (2006). Cleavage of Cdc6 by caspase-3 promotes ATM/ATR kinase-mediated apoptosis of HeLa cells. *J. Cell. Biol.* 174, 77–88. doi: 10.1083/jcb.200509141

Zhao, J., Ramos, R., and Demma, M. (2013). CDK8 regulates e2f1 transcriptional activity through S375 phosphorylation. *Oncogene* 32, 3520–3530. doi: 10.1038/onc.2012.364

Zhou, Y., Chu, L., Wang, Q., Dai, W., Zhang, X., Chen, J., et al. (2018). CD59 is a potential biomarker of esophageal squamous cell carcinoma radioresistance by affecting DNA repair. *Cell Death Dis.* 9:887. doi: 10.1038/s41419-018-0895-0

Conflict of Interest: The authors declare that the research was conducted in the absence of any commercial or financial relationships that could be construed as a potential conflict of interest.

frontiers in Oncology

REVIEW
published: 24 June 2020
doi: 10.3389/fonc.2020.00992

Understanding the Mechanisms by Which Epigenetic Modifiers Avert Therapy Resistance in Cancer

Anthony Quagliano[1,2], *Anilkumar Gopalakrishnapillai*[1,2] *and Sonali P. Barwe*[1,2*]

[1] Nemours/Alfred I. duPont Hospital for Children, Wilmington, DE, United States, [2] Department of Biological Sciences, University of Delaware, Newark, DE, United States

The development of resistance to anti-cancer therapeutics remains one of the core issues preventing the improvement of survival rates in cancer. Therapy resistance can arise in a multitude of ways, including the accumulation of epigenetic alterations in cancer cells. By remodeling DNA methylation patterns or modifying histone proteins during oncogenesis, cancer cells reorient their epigenomic landscapes in order to aggressively resist anti-cancer therapy. To combat these chemoresistant effects, epigenetic modifiers such as DNA hypomethylating agents, histone deacetylase inhibitors, histone demethylase inhibitors, along with others have been used. While these modifiers have achieved moderate success when used either alone or in combination with one another, the most positive outcomes were achieved when they were used in conjunction with conventional anti-cancer therapies. Epigenome modifying drugs have succeeded in sensitizing cancer cells to anti-cancer therapy via a variety of mechanisms: disrupting pro-survival/anti-apoptotic signaling, restoring cell cycle control and preventing DNA damage repair, suppressing immune system evasion, regulating altered metabolism, disengaging pro-survival microenvironmental interactions and increasing protein expression for targeted therapies. In this review, we explore different mechanisms by which epigenetic modifiers induce sensitivity to anti-cancer therapies and encourage the further identification of the specific genes involved with sensitization to facilitate development of clinical trials.

Keywords: epigenetic aberrations, chemoresistance, mechanism, cancer, epigenetic drugs, epigenetic combination therapies

OPEN ACCESS

Edited by:
Atsushi Fujimura,
Okayama University, Japan

Reviewed by:
Hamid Morjani,
Université de Reims Champagne-Ardenne, France
Antonis Kirmizis,
University of Cyprus, Cyprus

***Correspondence:**
Sonali P. Barwe
sbarwe@nemours.org

Specialty section:
This article was submitted to Molecular and Cellular Oncology, a section of the journal Frontiers in Oncology

Received: *14 March 2020*
Accepted: *19 May 2020*
Published: *24 June 2020*

Citation:
Quagliano A, Gopalakrishnapillai A and Barwe SP (2020) Understanding the Mechanisms by Which Epigenetic Modifiers Avert Therapy Resistance in Cancer. Front. Oncol. 10:992. doi: 10.3389/fonc.2020.00992

EPIGENETICS AND CANCER

The term "epigenetics" refers to the study of heritable phenotypic changes that do not involve mutations in DNA sequence (1). These changes are centered around alterations in gene activity and expression; through a variety of processes including DNA methylation and histone modifications (2). DNA methylation is the covalent addition of a methyl group to the C-5 position of DNA cytosine rings by DNA methyltransferases. Gene promoter hypermethylation often results in transcription depletion leading to decreased gene expression (3). Conversely, hypomethylation of *ABCB1* promoter resulted in upregulation of ABCB1 protein and acquisition of taxane resistance via efficient drug efflux (4). In exceptional cases, promoter methylation of genes, like *TERT* gene encoding telomerase reverse transcriptase, leads to increased transcription and protein expression (5). Methylation in gene bodies also affects transcription; demethylation of gene bodies results in a decrease in gene transcription (6). These patterns of DNA methylation are retained during cell division and can persist across generations.

Histones are modified in multiple ways. These modifications alter chromatin structure and affect gene transcription by regulating the access of transcription machinery to DNA. For an excellent review on the different types of histone modifications, refer to Audia and Campbell (7). Enzymes that modify histone proteins also facilitate post-translational modifications in non-histone proteins, thereby affecting gene expression (8, 9). Acetylation of NFκB and methylation of tumor suppressor protein p53 promotes nuclear localization of these proteins and increases transcriptional activity of respective gene targets (10, 11). Due to the prominent role of these proteins in cancer progression and therapy resistance, targeting their post-translational modifications could have therapeutic benefit (12, 13).

Drastic alterations in the epigenetic landscapes occur in cancer cells (14). Aberrant epigenetic patterns function as key drivers in cancer initiation and progression; often a result of the silencing of tumor suppressor genes or induced overexpression of oncogenes (15). Several tumor suppressors, such as RASSF1A and CASP8, are frequently inactivated in multiple cancer subtypes via epigenetic downregulation rather than by genetic mutation. For an excellent review on this specific function in oncogenesis, see Kazanets et al. (16). On the other hand, certain oncogenes, such as c-Myc and insulin-like growth factor receptor 2 (IGF-2) are upregulated by epigenetic mechanisms (17). These epigenetic changes result in global dysregulation of gene expression; thereby solidifying the development of disease states (18). Anomalous epigenetic alterations can also lead to the acquisition of therapy resistance (19, 20). **Figure 1** outlines how epigenetic-induced gene expression changes can give rise to multiple mechanisms of therapy resistance.

Efforts to revert these epigenetic changes via the use of epigenome modifying drugs have achieved some success, specifically when used in conjunction with other therapies. While these modifiers are "non-specific" in that they affect gene expression on a global level, their action elicits "specific" effects in malignant cells. This is due to the altered epigenome that is acquired during oncogenesis, highlighted by expression changes in tumor suppressor genes (silenced) and oncogenes (augmented) that are responsible for cancer progression or therapy resistance. Thereby, treatment with epigenetic drugs elicits a "specific" effect on cancerous cells by reverting these unique expression changes. Additionally, sensitivity to epigenetic modifiers can be genomic loci specific, possibly due in part to the three-dimensional chromatin structure (21–23). Thus, epigenetic modifiers possess the unique ability to be effective in a broad category of patients; albeit via altering the expression of a set of genes in a patient- specific manner (24).

In order to better understand the uses and indications of epigenetic modifiers in these combinations, it is necessary to uncover mechanisms of epigenetic drug-induced sensitization to anti-cancer therapy. Below, we summarize the gene expression changes induced by specific epigenetic modifiers (listed in **Table 1**), and how they have a variety of intracellular/extracellular consequences to potentiate the effectiveness of subsequent anti-cancer therapies.

EPIGENETIC DRUG-INDUCED SENSITIZATION MECHANISMS

Disruption of Pro-survival Signaling

Epigenetic alterations during oncogenesis can dysregulate the expression of growth factor receptors (25). Increased expression of these receptors drives the development of therapy resistance due to the over-activation of their downstream pathways such as PI3K/Akt and subsequent inhibition of cell death (26). While targeted therapies against growth factor receptors have been used to mitigate their effects, the use of such therapies is limited by the rapid development of resistance. Using epigenetic modifiers to control the expression of growth factor receptors is a promising alternative. In breast cancer, dacinostat (HDACi) disrupted epidermal growth factor (EGF)-mediated signaling, which is associated with increased metastasis and cell survival. This was achieved by reducing HER2 (human EGF receptor-2) protein expression via two independent epigenetic mechanisms: first by decreasing *HER2* mRNA level independent of alterations in promoter activity and secondly by increasing proteasomal degradation due to dissociation from its chaperone protein HSP90 via enhanced acetylation (27). In breast cancer as well, treatment with lapatinib (HER2/EGFR kinase inhibitor) and entinostat (HDACi) synergistically disrupted Akt signaling and promoted apoptosis (28). Though the mechanism of entinostat and lapatinib synergy is unknown, it is suggested that this effect is due to entinostat inhibiting lapatinib-induced expression of HER3; a HER2 heterodimerizing partner responsible for resistance to HER2 targeted therapies (29).

Hormone-dependent cancers such as breast and prostate respond to anti-hormone therapy by induction of apoptosis (30). Resistance to such therapy is acquired by downregulation of estrogen receptor (ER) or androgen receptor (AR) via epigenetic mechanisms. Thus, epigenetic drugs have been used to induce ER and AR expression to mediate sensitization to endocrine therapy in breast and prostate cancer, respectively (31–33).

Activation of pro-death pathways has been utilized as a therapeutic target to promote apoptosis in malignant cells. The binding of tumor necrosis factor-related apoptosis-inducing ligand (TRAIL) to its receptors death domain containing receptor (DR) triggers pro-death signaling and induces apoptosis via the caspase cascade (34). Reduced receptor expression is frequently observed in cancer cells resistant to this pathway. Vorinostat (HDACi) sensitized breast cancer cells to TRAIL-induced apoptosis by increasing expression of DR5 (35, 36). Treatment with epigenetic drugs can also lead to hyperactivation of pro-death pathways such as the unfolded protein response (UPR) pathway. UPR is activated to protect cells from endoplasmic reticulum-stress mediated cell death (37). However, when the pathway becomes hyperactivated, this response actually leads to the activation of apoptotic pathways, making it a target in cancer cells. Treatment with methylstat (inhibitor of KDM4B, a lysine-specific histone demethylase) dissociated the UPR-activating initiation factor eIF2α and synergized with PI3K inhibition to hyperactivate UPR gene transcription, culminating in apoptosis (38).

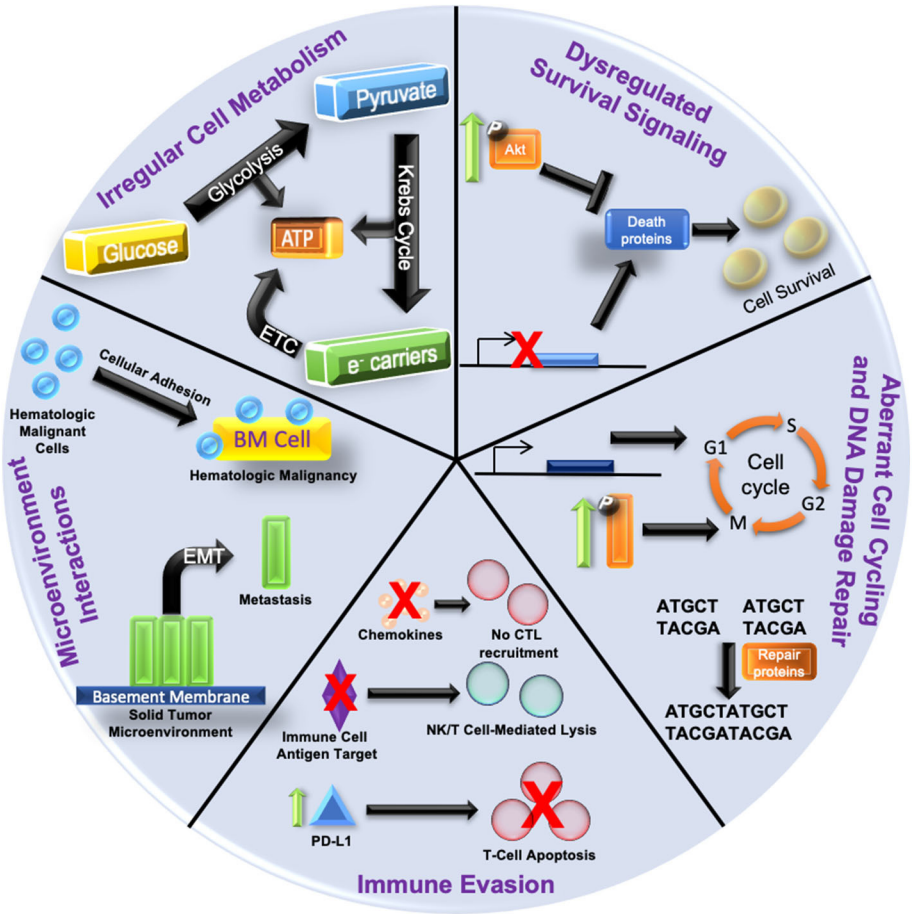

FIGURE 1 | Hallmarks of Epigenetic Alteration-Induced Therapy Resistance Epigenetic dysregulation is a driving force in oncogenesis and the development of therapy resistance. (1) Increased pro-survival signaling (depicted by enhanced phosphorylation and activation of kinases such as Akt) can inhibit the expression of death proteins to promote cancer cell survival. The gene expression of death proteins (shown as transcriptional inhibition at the gene promoter) can also be disrupted, culminating in increased cell survival. (2) Aberrant cell cycling is caused by the over/under-expression of proliferative/checkpoint proteins (blue block with promoter), or increased activation of signaling pathways (shown by increased phosphorylation/activation) related to proliferation. DNA damage repair is augmented by an increased expression of repair proteins and disruption of checkpoint signaling. (3) Aberrant intracellular signaling can also alter cytokine expression and lead to reduced cytotoxic T lymphocyte (CTL) recruitment. Silencing of immune cell antigen targets can also suppress immune targeting of cancer cells (NK, natural killer). Increased expression of PD-L1 (green arrow and blue triangle) on cancer cells can augment the immune checkpoint response, resulting in T cell apoptosis. (4) Increased cellular adhesion within the bone marrow microenvironment (yellow block) in hematologic malignancies activates intracellular signaling pathways that protect malignant cells (blue spheres) from anti-cancer. Epithelial to mesenchymal transition (EMT) dislodges cancer cells (green blocks) from the solid tumor microenvironment and is the first step in metastasis. (5) Irregular cellular metabolism via overactive glucose metabolism leads to the Warburg effect favoring anabolic glycolysis over oxidative phosphorylation, and can render cells resistant to chemotherapeutics or antimetabolites. Resistance mechanisms are not restricted to just one of the categories; often with multiple categories being involved simultaneously.

Through modulation of the expression of growth factor receptors or augmenting apoptosis-inducing pathways, epigenetic modifiers can disrupt pro-survival signaling in cancer cells as an efficient mechanism of sensitization (**Table 2**).

Restoration of Cell Cycle Control and Disruption of DNA Damage Repair

Cancer cells often rely on a dysregulated cell cycle for their continued proliferation (83). Epigenetic modifiers can restore tight control of the cell cycle and proliferation by mediating a reversal of dysregulated gene expression as a mechanism to potentiate therapy. Entinostat (HDACi) downregulated the expression of MYC, E2F, and other G2M cell cycle genes to sensitize breast cancer cells to doxorubicin-induced growth arrest, however, how these genes are downregulated is unknown (84). Previously, Lee et al. showed entinostat treatment in breast cancer inhibited Akt signaling (28). Since Akt signaling controls cell cycle (85), it is likely that Akt is involved in entinostat-mediated doxorubicin sensitization. While entinostat alone inhibited the expression of cell cycle proteins, its combination with decitabine (DNMTi) in pancreatic cancer increased expression of p21 to reinstitute cell cycle control and inhibit tumor growth, likely due to increased acetylation of histone H3 and demethylation of the p21 promoter (86).

TABLE 1 | Epigenetic modifiers discussed in this review.

Type	Inhibitor	Effect
DNMTi	Azacitidine	Traps DNMT and prevents its progression along DNA
	Decitabine	Forms a covalent complex with DNMT1 to deplete its activity
	Guadecitabine	-currently unknown-
	Procaine	Prevents the binding of DNMT1 and 3A to DNA
	Zebularine	Traps DNMT and prevents its progression along DNA
HDACi	4-phenylbutyric acid	Pan HDAC inhibitor
	Belinostat	Pan HDAC inhibitor
	Panobinostat	Pan HDAC inhibitor
	Valproic Acid	Pan inhibitor that binds to catalytic center of HDACs
	Dacinostat	Non-direct pan HDAC inhibitor
	Entinostat	Class 1 HDAC inhibitor
	Givinostat	Class 1 and 2 HDAC inhibitor
	Mocetinostat	Inhibits HDAC 1/2/3/11
	Trichostatin A	Inhibits HDACs 1/3/4/6/10
	Vorinostat	Chelator of zinc ions at active sites of HDACs 1/2/4
	Curcumin	Variable; potent effects of HDAC 1/3/8
	Quercetin	-currently unknown-
HDMi	HCI-2509	Inhibits lysine-specific demethylase 1 (LSD1)
	Iadademstat	Inhibits LSD1
	Pargyline	Inhibits LSD1
	S2101	Inhibits LSD1
	SP2509	Inhibits LSD1
	MC3324	Inhibits LSD1 and lysine-specific demethylase 6A
	DW14800	Inhibits protein arginine N-methyltransferase 5 (PRMT5)
	JIB-04	Pan inhibitor of Jumanji-domain histone demethylases
	Methylstat	Inhibits lysine-specific demethylase 4B
	SGC-0946	Inhibits disruptor of telomeric silencing 1-like (DOT1L)
Other	AZD5153	Inhibits bromodomain-containing protein 4 (BRD4)
	JQ1	Inhibits BRD4
	Cl-Amidine	Inhibits protein-arginine deiminase type-4
	EPZ-6438	Inhibits enhancer of zeste homolog 2
	MI-463	Inhibits menin (MEN1)
	MI-503	Inhibits MEN1

Epigenetic modifiers can potentially mitigate the effects of fusion oncoproteins. Gene fusions formed as a result of chromosomal translocations are often responsible for oncogenesis and therapy resistance (87, 88). In Ewing sarcoma, the EWS/Fli1 fusion gene is a key oncogenic driver. Treatment with JIB-04 (pan inhibitor of Jumanji-domain histone demethylases) simultaneously increased expression of cell-cycle inhibitor genes while suppressing expression of proteins that promote cell cycle, possibly through a disruption of EWS/Fli1 fusion gene program (89).

Hyperactive DNA damage repair pathways in cancer cells promote resistance to DNA damaging chemotherapeutics and radiation (90). In neuroblastoma, treatment with vorinostat (HDACi) diminished the expression of Ku-86, a key protein in non-homologous end joining DNA damage repair, to potentiate the anti-neoplastic effects of DNA damaging radiation (91). How vorinostat affects Ku-86 expression requires further study. Expression of DNA damage repair proteins like 53BP1 and RAD51 was also downregulated following treatment with pevonedistat (NEDD8-activating enzyme inhibitor) and belinostat (HDACi) in acute myeloid leukemia (AML). Downregulation of these proteins occurred in response to pevonedistat-mediated inhibition of belinostat-induced NFκB signaling and belinostat-mediated inhibition of pevonedistat-induced Chk1/Wee1 signaling, identifying a reliance of the two drugs on each other to disrupt DNA damage repair (92).

Restoring control of cell cycle progression and diminishing the activation of DNA damage repair pathways is a promising mechanism to improve responses to treatment. Epigenetic modifiers offer a unique route to achieving this objective (**Table 3**).

Suppress Immune Evasion/Augmenting Immune Responses

The immune system plays a pleiotropic role in cancer progression. Infiltration of immune cells into the tumor microenvironment releases a plethora of cytokines and growth factors that contribute to tumor proliferation, survival, and metastasis. Concurrently, activation of immune cells to target cancer is a promising strategy to utilize the host immune system in the fight against cancer (126). Like other anti-cancer treatments, malignant cells develop a resistance to immunotherapies by evading or suppressing the immune system and its activation via aberrant epigenetics (127, 128). Treatment with epigenetic modifiers has proved successful in augmenting immunotherapy. For a detailed review on this topic, please refer to Gomez et al. (129).

Epigenetic modifiers trigger increased expression of proteins for targeted therapies including immunotherapies. Trichostatin A (HDACi) up-regulated the mRNA and protein levels of both MIC-A and ULBP-2 in glioblastoma, which are recognized by natural killer (NK) cells to increase NK cell-mediated lysis (130). Entinostat (HDACi) blocked regulatory T cells (which negatively regulate the immune system and limit the efficacy of immunotherapy) in renal cell carcinoma via increased STAT3 acetylation, possibly due to increased CBP/p300 expression that acetylates STAT3 (131). In ovarian and colon cancer, azacitidine (DNMTi) increased the expression of multiple cancer cell-specific antigens. Since these antigens can be recognized by the host immune system, they represent prime targets for immunotherapies (132). The increased expression of cancer antigens also provides ample opportunity for the development of anti-cancer vaccines directing the host immune system to target these antigens. Such advances are currently in their infancy but have the potential for exceptional breakthrough in cancer treatment, especially when combined with epigenetic modifiers.

In non-small cell lung cancer, azacitidine (DNMTi) and givinostat (HDACi) induced Type I interferon signaling through transcriptional downregulation of MYC to increase the

TABLE 2 | Epigenetic modifier-induced disruption of pro-survival signaling.

Malignancy	Drug(s)	Gene/Protein	Mechanism	References
Bladder carcinoma	Decitabine	HOXA9	Restores expression	(39)
Glioblastoma	Decitabine	TP53 and CDKN1A	Restores expression	(40)
Glioblastoma	Decitabine	CASP8	Upregulates expression	(41)
Gastric/esophageal adenocarcinoma	Azacitidine	HPP1	Restores expression	(42)
Renal cell carcinoma	Decitabine	RASSF1A	Restores expression	(43)
Renal cell carcinoma	Decitabine or 4-phenylbutyric acid	miR-492	Restores expression	(44)
ALL	Azacitidine	DCK	Restores expression	(45)
ALL	Azacitidine	AhR	Restores expression	(46)
AML	Azacitidine	SHP-1	Increases expression	(47)
Chronic myeloid leukemia	Azacitidine	PRG2	Increases expression	(48)
Cholangiocarcinoma	Guadecitabine	CDKN2A, RASSF1A, SEMA3B	Increases expression	(49)
Hepatocellular carcinoma	Decitabine	SULF1	Restores expression	(50)
Breast cancer	Dacinostat	HER2	Downregulates expression at mRNA and protein level	(27)
Small cell lung carcinoma	Decitabine/Valproic Acid	CASP8	Restores expression	(51)
Small cell lung cancer	Iadademstat	NOTCH1	Restores expression	(52)
Diffuse large B Cell lymphoma	Panobinostat	NOXA	Increases expression	(53)
Prostate	Trichostatin A	ATF3/4	Increases expression	(54)
Prostate	Azacitidine	GST	Restores expression	(55)
Prostate	Azacitidine	miR-34a	Restores expression	(56)
Tongue squamous cell carcinoma	Trichostatin A	miR-375	Increases expression	(57)
Solid tumors	Mocetinostat	miR-203	Restores expression	(58)
Ovarian	Zebularine	RASSF1A, ARHI, BLU	Restores expression	(59)
Bladder	Trichostatin A	CXADR	Increases expression	(60)
Breast	Vorinostat	DR4/DR5	Increases expression	(36)
Breast	Vorinostat	DR5	Increases expression	(35)
T-cell leukemia	HDACi	TRAIL-R2, c-FLIP, and Apaf-1	Increases expression	(61)
Breast	Entinostat	ERα and CYP19A1	Increases expression	(31)
Breast	Vorinostat	ERα	Increases expression	(32)
Prostate	Quercetin/Curcumin	AR	Increases expression	(33)
ALL	Vorinostat	BCR-ABL	Decreases expression	(62)
T-cell ALL	Dacinostat	c-FLIP	Decreases expression along with increasing DR4/5 expression to sensitize to Apo2L/TRAIL-induced apoptosis	(63)
Chronic myeloid leukemia	Dacinostat	BCR-ABL	Decreases expression	(64)
AML	Dacinostat	FLT-3	Decreases expression and activity	(65)
Mixed lineage leukemia	MI-463/MI-503	HOXA9	Decreases expression	(66)
MLL	Azacitidine	TERT	Decreases expression	(67)
Hepatocellular carcinoma	Guadecitabine	WNT/EFG/IGF	Decreases expression of pathway associated genes	(68)
Non-small cell lung carcinoma	Panobinostat	TAZ	Decreases transcription and its targets (EGFR and EGFR ligand)	(69)
Multiple myeloma	EPZ-5676/SGC-0946	IRF4	Decreases expression	(70)
Hematologic	Vorinostat	JAK	Decreases expression	(71)
Breast	Entinostat	Akt	Inhibits phosphorylation	(28)
Breast	Methylstat	eIFα	Increases dissociation from KDM4B leading to increased phosphorylation by ERK and transcription of unfolded protein response genes	(38)
Breast	MC3324	ERα	Inhibits signaling	(72)
Breast	Cl-amidine	Akt/mTOR	Inhibits signaling, leading to increased nuclear accumulation of p53	(73)
Colon	Decitabine	Akt	Inhibits signaling	(74)
Colon	Cl-amidine	p53	Increases transcription of targets, including miR-16	(75)
Retinoblastoma	Vorinostat	NFκB	Inhibits signaling and increases p53 expression	(76)
Gynecologic	Panobinostat	Mutant TP53	Decreases protein expression	(77)
Gynecologic	SP2509	p62	Stabilizes protein expression	(78)
AML	Panobinostat	Akt/NFκB	Inhibits signaling to increase p53-mediated cell death	(79)
Non-small cell lung carcinoma	Panobinostat	EGFR	Inhibits signaling	(80)
Ovarian	S2101	Akt	Inhibits phosphorylation	(81)
Prostate	Azacitidine	Akt	Inhibits activation	(82)

TABLE 3 | Restoration of cell cycle control and disruption of DNA damage repair by epigenetic modifiers.

Malignancy	Drug(s)	Target Gene/Protein	Mechanism	References
Breast	Cl-amidine	CDKN1A and GADD45A	Increases expression to inhibit cell cycle	(93)
Breast	Decitabine/ Trichostatin A	MSH2	Restores expression	(94)
Colorectal	AZD5153	c-Myc/Wee1	Reduces expression	(95)
Gastric	Procaine	CDKN2A and RARβ	Restores expression	(96)
Acute leukemia	Decitabine	CDKN2A	Restores expression	(97)
Non-small cell lung carcinoma	Trichostatin A	CDKN1A	Increases expression to mediate G1 arrest	(98)
Non-small cell lung carcinoma	Azacitidine	MGMT	Restores expression	(99)
Diffuse large B cell lymphoma	Decitabine	SMAD1	Restores expression	(100)
MDS/Chronic myeloid leukemia	Decitabine	CDKN2B	Restores expression	(101)
Multiple myeloma	Azacitidine/EPZ-6438	SMAD3	Restores expression	(102)
Ovarian/Colon	Decitabine	MLH1	Restores expression	(103)
Pancreatic	Decitabine/Vorinostat	CDKN1A	Increases expression to mediate G1 arrest	(86)
Pancreatic	Azacitidine	SST and SSTR2	Restores expression	(104)
Multiple	HDACi	SLFN1	Restores expression	(105)
Solid tumors	Azacitidine/HDACi	Genes related to ionizing radiation	Increases expression for radiosensitivity	(106)
Bladder	Panobinostat	MRE11	Reduces expression to increase radiosensitivity	(107)
Neuroblastoma	Vorinostat	Ku-86	Reduces expression to disrupt DNA damage repair	(91)
Neuroblastoma	Panobinostat	Chk1	Reduces expression and signaling to disrupt DNA damage repair	(108)
Breast	Entinostat	MYC, E2F, and G2M cell cycle genes	Reduces expression to induce G2M cell cycle arrest	(84)
Non-small cell lung carcinoma	Belinostat	ERCC1	Decreases expression to disrupt DNA damage repair	(109)
Lung adenocarcinoma	HCI-2509	PLK1	Decreases expression and target genes	(110)
Non-Hodgkin's Lymphoma	Belinostat	c-Myc	Decreases expression to increase DNA damage	(111)
Ovarian	Panobinostat	RAD51	Decreases expression to increase PARP inhibiton	(112)
Pancreatic	JQ1	c-Myc	Decreases expression	(113)
Testicular	Guadecitabine	p53	Increases activation and target gene expression	(114)
Breast	Valproic Acid	γH2AX and H3S10p	Increases and decreases retention, respectively	(115)
Breast/Ovarian	Guadecitabine	PARP	Increases "trapping" by PARP inhibitors	(116)
Ewing Sarcoma	JIB-04		Disrupts EWS/Fli1 oncogeneic program to increase DNA damage	(89)
AML	Belinostat	Chk1/Wee1	Inhibits signaling to disrupt DNA damage response	(92)
Chronic myeloid leukemia	Decitabine/Vorinostat	p53	Increases cell death through p53-dependent pathway and p21	(117)
AML	Azacitidine/Panobinostat	p53 signaling	Induced remission in patient-derived xenograft models	(118)
AML	Panobinostat	Chk1/Wee1	Decreases signaling to disrupt DNA damage response	(119)
AML	Trichostatin A	γH2A.X	Accumulates to enhance radiosensitivity	(120)
Non-small cell lung carcinoma	Decitabine/Trichostatin A	miRNAs	Enhances DNA damage by dysregulating expression	(121)
Non-small cell lung carcinoma	Panobinostat	p53/p21 and Chk1	Increases expression of p53-dependent pathway and decreased Chk1 signaling	(122)
Ovarian	Guadecitabine	DNA repair genes	Alters expression to disrupt DNA damage repair	(123, 124)
Solid tumors	DNMTi/HDACi		Reduces chromatin condensation to increase DNA damage following chemotherapy	(125)

expression of the T cell chemoattractant CCL5, thereby reversing tumor immune evasion by promoting T cell infiltration. This combination also shifted host T cells from exhausted states (characterized by loss of effector function due to prolonged antigen stimulation) to memory and effector states [capable of durable responses to immune checkpoint blockades) via activation of associated genes (133)].

Cancer cells exploit the "immune checkpoint" function to evade the immune system (134) by expression of programmed cell death-1 (PD-1) or anti–cytotoxic T-lymphocyte-associated antigen-4 (CTLA-4) resulting in increased apoptosis of T cells. Immune checkpoint blockers such as nivolumab (monoclonal antibody blocking PD-1) and ipilimumab (monoclonal antibody blocking CTLA-4) have emerged as an attractive mechanism to

decrease immune system evasion and tumor cell survival. Co-administration of azacitidine (DNMTi) and entinostat (HDACi) alongside immune checkpoint blockers improved treatment outcome in a preclinical metastatic cancer model via their inhibitory action on the myeloid derived suppressor cells within the tumor microenvironment (135).

Exploitation of the immune system to successfully diminish tumor burden is a promising avenue of improving anti-cancer therapy. The use of epigenetic modifiers offers a distinctive method to potentiate these therapies (**Table 4**).

Modulation of Microenvironmental Interactions

Cellular and extracellular matrix interactions within the tumor microenvironment are crucial for cancer development and progression. Epigenetic dysregulation in cancer is known to control adhesion through a variety of mechanisms (141–143). Thus, the use of epigenetic modifiers could provide a way to mollify these alterations. In solid tumors, disengagement from the microenvironment has severe consequences for the patient, as it is the first step in metastasis (144). Therefore, increasing cell adhesion proves beneficial to localize the tumor to the primary site.

In a majority of solid tumors, carcinomas arise from epithelial cells undergoing epithelial to mesenchymal transition (EMT), which causes loss of epithelial polarity/adhesion and increased migratory/invasiveness potential (145). Following EMT, cancer cells acquire stem-cell like properties and a higher rate of metastasis (146). EMT is controlled by multiple epigenetic mechanisms, including DNA methylation and histone modifications (147). The expression of the classical cell adhesion molecule and EMT suppressor E-cadherin is downregulated via promoter hypermethylation in cancer cells (148), or repressed by transcription factor Snail (149) in conjunction with histone modifiers such as lysine-specific histone demethylase 1 (LSD1) recruited by Snail (150). In breast cancer cells, EMT was suppressed by the LSD1 inhibitor pargyline (151). It is important to note, that the same study identified LSD1 to inhibit M1 macrophage infiltration into tumors, which is known to promote tumor progression and therapy resistance (152).

Targeting the SNAIL/LSD1 complex to prevent EMT via depletion of SNAIL expression was accomplished by the BRD4 inhibitor JQ1 in breast cancer. JQ1 repressed the expression of Gli1, an important mediator of *SNAIL* transcription. This prevented SNAIL-mediated repression of epithelial markers such as E-cadherin and prevented EMT (150, 153). Combined, these two studies provide a powerful indication of how the use of epigenetic modifiers can perturb EMT to prevent metastasis and improve treatment efficacy in solid tumors.

In hematologic malignancies, interactions within the bone marrow microenvironment transition malignant cells into chemoresistant states (154). Disruption of these interactions mobilizes cells from the bone marrow into the peripheral blood, thereby sensitizing them to therapy. In acute lymphoblastic leukemia (ALL), azacitidine (DNMTi) and panobinostat (HDACi) combined to disrupt cellular adhesion within the bone marrow microenvironment in ALL by decreasing the surface expression of the tetraspanin protein CD81, resulting in increased chemosensitivity (155, 156).

Hypoxia within the tumor microenvironment can often promote therapy resistance (157). This therapy resistance can be attributed to multiple factors including aberrant micro RNA (miRNA) expression and dysregulated epigenetic machinery (158, 159). Thus, gene expression alterations are accumulated and therapy resistance can occur in a variety of mechanisms such as those described in **Figure 1**. Due to the aberrant epigenetics involved, the use of epigenetic modifiers could sensitize cancer cells by reverting these hypoxic effects. However, further study is required to elucidate their effectiveness.

The role of microenvironmental interactions and their effect on cancer progression has been well-defined, however, the use of epigenetic modifiers to attenuate these effects has not been exploited. More studies across all cancer subtypes are necessary

TABLE 4 | Suppression of immune evasion/augmented immune responses following epigenetic modifier treatment.

Malignancy	Drug(s)	Gene/Protein	Mechanism	References
Osteosarcoma	Entinostat	MIC-A and MIC-B	Increases expression to increase NK cell-mediated cytotoxicity	(136)
Glioblastoma	Trichostatin A	MIC-A and ULBP-2	Increases expression to increase NK cell-mediated death	(130)
Colon	Decitabine/Vorinostat	Fas	Increases expression to sensitize to FasL-induced apoptosis and improve CTL adoptive transfer immunotherapy	(137)
Melanoma	Vorinostat	DR5	Increases expression to overcome immune resistance	(138)
Melanoma	Dacinostat	MHC and tumor antigen	Increases expression to improve functional activity of lymphocytes	(139)
Renal cell carcinoma /Prostate	Entinostat	STAT3	Increases acetylation to improve immunotherapy	(131)
Non-small cell lung carcinoma	Azacitidine/Givinostat	MYC	Inhibits signaling to reverse immune evasion	(133)
Ovarian	Azacitidine	Type I interferon	Activates signaling to reduce immunosuppression	(140)
Colon/Ovarian	Azacitidine	Cancer antigens	Vaccines	(132)
AML	Azacitidine	PD-1, PD-L1, and CTLA-4	Nivolumab and Ipilimumab	NCT02397720

to achieve a greater understanding of how microenvironmental interactions can be modulated by epigenetic therapy.

Reprogramming of Cellular Metabolism

Through a variety of genetic and epigenetic mechanisms, metabolic reprogramming can render cancer cells resistant to chemotherapeutics (160–162). These changes can often result as a compensatory mechanism in response to the exposure of certain chemotherapeutics (162). Therefore, targeting aberrant cellular metabolism is a promising method of circumventing therapy resistance.

Due to the epigenetic regulation involved with aberrant metabolism, epigenetic modifiers could prove highly successful in mitigating the resultant chemoresistant effects. Treatment with entinostat (HDACi) combined with cisplatin upregulated the gene expression of thioredoxin-interacting protein (TXNIP), which inhibited the cellular uptake of glucose and increased DNA damage (163). This occurred via an increase in *TXNIP* promoter activity, however, this increase was only achievable with the two drugs in combination. In AML, treatment with the DNMTi azacitidine combined with the Bcl-2 inhibitor venetoclax disrupted cellular metabolism by decreasing glutathione levels, thereby diminishing electron transport chain complex II activity and oxidative phosphorylation (164).

Epigenetic modifiers can also augment the effectiveness of established antimetabolites like pemetrexed, which targets enzymes like thymidylate synthase (TI) catalyzing purine and pyrimidine synthesis. TI expression can be augmented post treatment with pemetrexed, thus leading to resistance (165). In non-small cell lung cancer, pemetrexed treatment followed by givinostat (HDACi) downregulated the mRNA and protein expression of TI, thereby overcoming therapy resistance and resulting in a synergistic increase in cell death (166).

While there has been strong evidence of the role played by epigenetic-induced metabolic changes in cancer cells in promoting therapy resistance, the study of how epigenetic modifiers can mitigate these effects has yet to be explored in depth. More examination into these effects is required in order to better overcome resistance to therapies.

Opportunities for Development of Rational Combinations With Epigenetic Therapy

The impact of epigenetic modifiers on global gene expression results in modulation of several genes, both promoting and inhibiting therapy resistance, thereby necessitating and offering opportunity to combine with targeted therapies. This is exemplified by a study in ovarian cancer that identified overexpression of CD146, a cell surface marker involved in tumor dissemination, following treatment with vorinostat (HDACi). This increased expression was exploited by combining vorinostat with anti-CD146 monoclonal antibody treatment to synergistically induce cell death via inhibition of CD146-mediated Akt signaling (167). Vorinostat (HDACi) along with decitabine (DNMTi) was also observed to significantly increase the expression of the tyrosine kinase AXL in AML. This led to the identification of a novel triple therapy with the AXL inhibitor BGB324 facilitating synergistic activation of cell death (168). Therefore, mechanistic understanding of epigenetic drug action is essential for developing rational combinations with targeted therapies.

NEED FOR CLINICAL TRIALS

The use of epigenetic modifiers is a robust method for improving treatment efficacy in cancer. Through a variety of mechanisms, epigenetic therapy has the potential to augment the effectiveness of cancer treatments to improve overall survival in patients. In many of the examples presented above, a combination of epigenetic modifiers was used to induce specific changes that potentiate the effects of anti-cancer therapeutics in cancer cells. However, despite a plethora of clinical trials involving the use of epigenetic modifiers, very few have focused on the use of a combination of epigenetic modifiers along with anti-cancer therapy (**Table 5**). The combination therapies identified in this review underline the need and provide the basis for the development of future clinical trials to study their effectiveness.

Additionally, it is worth mentioning that not only the use of epigenetic modifiers (either alone or in combination with one another) in conjunction with chemotherapeutics should

TABLE 5 | List of clinical trials utilizing multiple epigenetic modifiers in combination with traditional therapy.

Malignancy	Epigenetic Modifiers	Other Therapeutics	NCT Identifier
ALL	Decitabine/ Vorinostat	Vincristine/ Dexamethasone/ Mitoxantrone/ Pegasparagase/ Methotrexate	01483690
AML	Azacitidine/ Vorinostat	Gemtuzumab	00895934
AML	Azacitidine/ Valproic Acid	All-trans retinoic acid/ Hydroxyurea	01369368
AML/MDS	Azacitidine/ Valproic Acid	All-trans retinoic acid	00339196
Breast	Decitabine/ Panobinostat	Tamoxifen	01194908
Lymphoma	Azacitidine/ Vorinostat	Gemcitabine/Busulfan/ Melphalan/ Dexamethasone/ Caphosol/Glutamine/ Pyridoxine/Rituximab	01983969
MDS	Azacitidine/ Valproic Acid	All-trans retinoic acid	00326170
MDS	Decitabine/ Vorinostat	CD3-/CD19- NK cell infusion	01593670
MDS	Azacitidine/ Valproic Acid	All-trans retinoic acid	00439673
Melanoma	Decitabine/ Panobinostat	Temozolomide	00925132
Non-small cell lung cancer	Azacitidine/ Entinostat	Docetaxel/ Gemcitabine/Irinotecan	01935947
Non-small cell lung cancer	Azacitidine/ Entinostat	Nivolumab	01928576

be studied, but the protocols in which they are administered should be considered as well. Simultaneous exposures have been shown to have an inhibitory effect on cell viability compared to sequential treatment (169). Additionally, a study of the use of azacitidine and panobinostat in B-ALL identified that following treatment in mice; leukemic cells were mobilized from the bone marrow into the peripheral blood. This mobilization was responsible for the improved efficacy of subsequent chemotherapy treatment, thus suggesting that staggering the treatments had a significant effect (170). More study on this effect as well as its potential in other cancer subtypes must be performed to exploit the efficacy of epigenetic treatments.

CONCLUSIONS

Aberrant epigenetics is responsible for the development and progression of several cancers. These alterations can be the driving forces of therapy resistance and survival. Treatment with epigenetic modifiers offers a unique route to diminishing these effects and re-sensitizing cancer cells to traditional therapies. While there have been some clinical trials studying the efficacy of epigenetic modifiers in cancer, more studies focusing on identifying specific gene targets are required, particularly with a combination of epigenetic modifiers in conjunction with other therapies. By precisely identifying sensitization biomarkers, epigenetic/chemotherapeutic/immunotherapeutic combination therapies can achieve greater translational success (171). Follow-up studies using comprehensive analyses like RNAseq, global methylation, and chromatin immunoprecipitation-Seq are required to identify pathways of sensitization.

It is also imperative to include analyses of non-coding regions of the DNA, such as miRNA. While epigenetic alterations during oncogenesis directly affect the transcription of coding genes, these variations can have an effect on the expression of miRNAs (172, 173), which are non-coding RNAs that function in RNA silencing and post-transcriptional regulation of gene expression. miRNAs can mediate either tumor suppressive or oncogenic effects depending on their gene target (174). Examination of alterations in miRNA expression following treatment with epigenetic modifiers could identify additional sensitization mechanisms and therapeutic markers.

Studies investigating the development of inhibitors of atypical histone modifications, such as citrullination, phosphorylation, sumoylation, ubiquitylation, and ribosylation; are needed because these modifications are also known to regulate gene transcription and contribute to cancer progression (175–178). The mechanisms outlined in this review offer not only a rationale for successful combinations and mechanisms, but also identify indications for their use in specific patients based on the markers being modulated, in line with the advancements in personalized medicine. Further studies on the mechanisms of epigenetic modifier action in cancer are needed to identify markers that can detect and predict clinical response.

AUTHOR CONTRIBUTIONS

AQ wrote the draft manuscript and generated figures and tables. AG and SB edited the manuscript. All authors approved the final version of the manuscript.

FUNDING

This work was supported by Andrew McDonough B+ Foundation.

REFERENCES

1. Dupont C, Armant DR, Brenner CA. Epigenetics: definition, mechanisms and clinical perspective. *Semin Reprod Med.* (2009) 27:351–7. doi: 10.1055/s-0029-1237423
2. Berger SL, Kouzarides T, Shiekhattar R, Shilatifard A. An operational definition of epigenetics. *Genes Dev.* (2009) 23:781–3. doi: 10.1101/gad.1787609
3. Jin B, Li Y, Robertson KD. DNA methylation: superior or subordinate in the epigenetic hierarchy? *Genes Cancer.* (2011) 2:607–17. doi: 10.1177/1947601910393957
4. Sumarpo A, Ito K, Saiki Y, Ishizawa K, Wang R, Chen N, et al. Genetic and epigenetic aberrations of ABCB1 synergistically boost the acquisition of taxane resistance in esophageal squamous cancer cells. *Biochem Biophys Res Commun.* (2020) 526:586–91. doi: 10.1016/j.bbrc.2020.03.114
5. Lee DD, Leao R, Komosa M, Gallo M, Zhang CH, Lipman T, et al. DNA hypermethylation within TERT promoter upregulates TERT expression in cancer. *J Clin Invest.* (2019) 129:1801. doi: 10.1172/JCI128527
6. Yang X, Han H, De Carvalho DD, Lay FD, Jones PA, Liang G. Gene body methylation can alter gene expression and is a therapeutic target in cancer. *Cancer Cell.* (2014) 26:577–90. doi: 10.1016/j.ccr.2014.07.028
7. Audia JE, Campbell RM. Histone modifications and cancer. *Cold Spring Harb Perspect Biol.* (2016) 8:a019521. doi: 10.1101/cshperspect.a019521
8. Das C, Kundu TK. Transcriptional regulation by the acetylation of nonhistone proteins in humans – a new target for therapeutics. *IUBMB Life.* (2005) 57:137–49. doi: 10.1080/15216540500090629
9. Narita T, Weinert BT, Choudhary C. Functions and mechanisms of non-histone protein acetylation. *Nat Rev Mol Cell Biol.* (2019) 20:156–74. doi: 10.1038/s41580-018-0081-3
10. Huang J, Sengupta R, Espejo AB, Lee MG, Dorsey JA, Richter M, et al. p53 is regulated by the lysine demethylase LSD1. *Nature.* (2007) 449:105–8. doi: 10.1038/nature06092
11. Park J, Lee JH, La M, Jang MJ, Chae GW, Kim SB, et al. Inhibition of NF-kappaB acetylation and its transcriptional activity by Daxx. *J Mol Biol.* (2007) 368:388–97. doi: 10.1016/j.jmb.2007.02.047
12. Scoumanne A, Chen X. Protein methylation: a new mechanism of p53 tumor suppressor regulation. *Histol Histopathol.* (2008) 23:1143–9. doi: 10.14670/HH-23.1143
13. Sung B, Pandey MK, Ahn KS, Yi T, Chaturvedi MM, Liu M, et al. Anacardic acid (6-nonadecyl salicylic acid), an inhibitor of histone acetyltransferase, suppresses expression of nuclear factor-kappaB-regulated gene products involved in cell survival, proliferation, invasion, and inflammation through inhibition of the inhibitory subunit of nuclear factor-kappaBalpha kinase, leading to potentiation of apoptosis. *Blood.* (2008) 111:4880–91. doi: 10.1182/blood-2007-10-117994
14. You JS, Jones PA. Cancer genetics and epigenetics: two sides of the same coin? *Cancer Cell.* (2012) 22:9–20. doi: 10.1016/j.ccr.2012.06.008

15. Baylin SB, Jones PA. A decade of exploring the cancer epigenome - biological and translational implications. *Nat Rev Cancer.* (2011) 11:726–34. doi: 10.1038/nrc3130
16. Kazanets A, Shorstova T, Hilmi K, Marques M, Witcher M. Epigenetic silencing of tumor suppressor genes: paradigms, puzzles, and potential. *Biochim Biophys Acta.* (2016) 1865:275–88. doi: 10.1016/j.bbcan.2016.04.001
17. Kanwal R, Gupta S. Epigenetic modifications in cancer. *Clin Genet.* (2012) 81:303–11. doi: 10.1111/j.1399-0004.2011.01809.x
18. Hassler MR, Egger G. Epigenomics of cancer - emerging new concepts. *Biochimie.* (2012) 94:2219–30. doi: 10.1016/j.biochi.2012.05.007
19. Crea F, Danesi R, Farrar WL. Cancer stem cell epigenetics and chemoresistance. *Epigenomics.* (2009) 1:63–79. doi: 10.2217/epi.09.4
20. Zeller C, Brown R. Therapeutic modulation of epigenetic drivers of drug resistance in ovarian cancer. *Ther Adv Med Oncol.* (2010) 2:319–29. doi: 10.1177/1758834010375759
21. Farhy C, Hariharan S, Ylanko J, Orozco L, Zeng FY, Pass I, et al. Improving drug discovery using image-based multiparametric analysis of the epigenetic landscape. *Elife.* (2019) 8:e49683. doi: 10.7554/eLife.49683.sa2
22. Achinger-Kawecka J, Valdes-Mora F, Luu PL, Giles KA, Caldon CE, Qu W, et al. Epigenetic reprogramming at estrogen-receptor binding sites alters 3D chromatin landscape in endocrine-resistant breast cancer. *Nat Commun.* (2020) 11:320. doi: 10.1038/s41467-019-14098-x
23. Zhang T, Pilko A, Wollman R. Loci specific epigenetic drug sensitivity. *Nucleic Acids Res.* (2020) 48:4797–810. doi: 10.1093/nar/gkaa210
24. Jones PA, Issa JP, Baylin S. Targeting the cancer epigenome for therapy. *Nat Rev Genet.* (2016) 17:630–41. doi: 10.1038/nrg.2016.93
25. Tiash S, Chowdhury E. Growth factor receptors: promising drug targets in cancer. *J Cancer Metast Treat.* (2015) 1:190. doi: 10.4103/2394-4722.163151
26. Yang J, Nie J, Ma X, Wei Y, Peng Y, Wei X. Targeting PI3K in cancer: mechanisms and advances in clinical trials. *Mol Cancer.* (2019) 18:26. doi: 10.1186/s12943-019-0954-x
27. Fuino L, Bali P, Wittmann S, Donapaty S, Guo F, Yamaguchi H, et al. Histone deacetylase inhibitor LAQ824 down-regulates Her-2 and sensitizes human breast cancer cells to trastuzumab, taxotere, gemcitabine, and epothilone B. *Mol Cancer Ther.* (2003) 2:971–84.
28. Lee J, Bartholomeusz C, Mansour O, Humphries J, Hortobagyi GN, Ordentlich P, et al. A class I histone deacetylase inhibitor, entinostat, enhances lapatinib efficacy in HER2-overexpressing breast cancer cells through FOXO3-mediated Bim1 expression. *Breast Cancer Res Treat.* (2014) 146:259–72. doi: 10.1007/s10549-014-3014-7
29. Novotny CJ, Pollari S, Park JH, Lemmon MA, Shen W, Shokat KM. Overcoming resistance to HER2 inhibitors through state-specific kinase binding. *Nat Chem Biol.* (2016) 12:923–30. doi: 10.1038/nchembio.2171
30. Maximov PY, Abderrahman B, Curpan RF, Hawsawi YM, Fan P, Jordan VC. A unifying biology of sex steroid-induced apoptosis in prostate and breast cancers. *Endocr Relat Cancer.* (2018) 25:R83–113. doi: 10.1530/ERC-17-0416
31. Sabnis GJ, Goloubeva O, Chumsri S, Nguyen N, Sukumar S, Brodie AM. Functional activation of the estrogen receptor-alpha and aromatase by the HDAC inhibitor entinostat sensitizes ER-negative tumors to letrozole. *Cancer Res.* (2011) 71:1893–903. doi: 10.1158/0008-5472.CAN-10-2458
32. Stark K, Burger A, Wu J, Shelton P, Polin L, Li J. Reactivation of estrogen receptor alpha by vorinostat sensitizes mesenchymal-like triple-negative breast cancer to aminoflavone, a ligand of the aryl hydrocarbon receptor. *PLoS ONE.* (2013) 8:e74525. doi: 10.1371/journal.pone.0074525
33. Sharma V, Kumar L, Mohanty SK, Maikhuri JP, Rajender S, Gupta G. Sensitization of androgen refractory prostate cancer cells to anti-androgens through re-expression of epigenetically repressed androgen receptor - synergistic action of quercetin and curcumin. *Mol Cell Endocrinol.* (2016) 431:12–23. doi: 10.1016/j.mce.2016.04.024
34. von Karstedt S, Montinaro A, Walczak H. Exploring the TRAILs less travelled: TRAIL in cancer biology and therapy. *Nat Rev Cancer.* (2017) 17:352–66. doi: 10.1038/nrc.2017.28
35. Butler LM, Liapis V, Bouralexis S, Welldon K, Hay S, Thai le M, et al. The histone deacetylase inhibitor, suberoylanilide hydroxamic acid, overcomes resistance of human breast cancer cells to Apo2L/TRAIL. *Int JCancer.* (2006) 119:944–54. doi: 10.1002/ijc.21939
36. Frew AJ, Lindemann RK, Martin BP, Clarke CJ, Sharkey J, Anthony DA, et al. Combination therapy of established cancer using a histone deacetylase inhibitor and a TRAIL receptor agonist. *Proc Natl Acad Sci USA.* (2008) 105:11317–22. doi: 10.1073/pnas.0801868105
37. Madden E, Logue SE, Healy SJ, Manie S, Samali A. The role of the unfolded protein response in cancer progression: From oncogenesis to chemoresistance. *Biol Cell.* (2019) 111:1–17. doi: 10.1111/boc.201800050
38. Wang W, Oguz G, Lee PL, Bao Y, Wang P, Terp MG, et al. KDM4B-regulated unfolded protein response as a therapeutic vulnerability in PTEN-deficient breast cancer. *J Exp Med.* (2018) 215:2833–49. doi: 10.1084/jem.20180439
39. Xylinas E, Hassler MR, Zhuang D, Krzywinski M, Erdem Z, Robinson BD, et al. An epigenomic approach to improving response to neoadjuvant cisplatin chemotherapy in bladder cancer. *Biomolecules.* (2016) 6:37. doi: 10.3390/biom6030037
40. Cui Y, Naz A, Thompson DH, Irudayaraj J. Decitabine nanoconjugate sensitizes human glioblastoma cells to temozolomide. *Mol Pharm.* (2015) 12:1279–88. doi: 10.1021/mp500815b
41. Eramo A, Pallini R, Lotti F, Sette G, Ricci-Vitiani L, Bartucci M, et al. Effective treatment of glioblastoma tumors by combined administration of decitabine and TRAIL. *Cancer Res.* (2005) 65:425–425. doi: 10.1158/0008-5472.CAN-05-1724
42. Schneider BJ, Shah MA, Klute K, Ocean A, Popa E, Altorki N, et al. Phase I study of epigenetic priming with azacitidine prior to standard neoadjuvant chemotherapy for patients with resectable gastric and esophageal adenocarcinoma: evidence of tumor hypomethylation as an indicator of major histopathologic response. *Clin Cancer Res.* (2017) 23:2673–80. doi: 10.1158/1078-0432.CCR-16-1896
43. Reu FJ, Leaman DW, Maitra RR, Bae SI, Cherkassky L, Fox MW, et al. Expression of RASSF1A, an epigenetically silenced tumor suppressor, overcomes resistance to apoptosis induction by interferons. *Cancer Res.* (2006) 66:2785–93. doi: 10.1158/0008-5472.CAN-05-2303
44. Wu A, Wu K, Li M, Bao L, Shen X, Li S, et al. Upregulation of microRNA-492 induced by epigenetic drug treatment inhibits the malignant phenotype of clear cell renal cell carcinoma *in vitro*. *Mol Med Rep.* (2015) 12:1413–20. doi: 10.3892/mmr.2015.3550
45. Avramis VI, Mecum RA, Nyce J, Steele DA, Holcenberg JS. Pharmacodynamic and DNA methylation studies of high-dose 1-beta-D-arabinofuranosyl cytosine before and after *in vivo* 5-azacytidine treatment in pediatric patients with refractory acute lymphocytic leukemia. *Cancer Chemother Pharmacol.* (1989) 24:203–10. doi: 10.1007/BF00257619
46. Andrade AF, Borges KS, Castro-Gamero AM, Silveira VS, Suazo VK, Oliveira JC, et al. Zebularine induces chemosensitization to methotrexate and efficiently decreases AhR gene methylation in childhood acute lymphoblastic leukemia cells. *Anticancer Drugs.* (2014) 25:72–81. doi: 10.1097/CAD.0000000000000028
47. Al-Jamal HA, Mat Jusoh SA, Hassan R, Johan MF. Enhancing SHP-1 expression with 5-azacytidine may inhibit STAT3 activation and confer sensitivity in lestaurtinib (CEP-701)-resistant FLT3-ITD positive acute myeloid leukemia. *BMC Cancer.* (2015) 15:869. doi: 10.1186/s12885-015-1695-x
48. Al-Jamal HAN, Johan MF, Mat Jusoh SA, Ismail I, Wan Taib WR. Re-expression of bone marrow proteoglycan-2 by 5-azacytidine is associated with STAT3 inactivation and sensitivity response to imatinib in resistant CML cells. *Asian Pac J Cancer Prev.* (2018) 19:1585–90. doi: 10.22034/APJCP.2018.19.6.1585
49. Surriga O, Schwartz GK. Abstract 2940: chemosensitization of cholangiocarcinoma by guadecitabine. *Cancer Res.* (2018) 78:2940. doi: 10.1158/1538-7445.AM2018-2940
50. Shire A, Lomberk G, Lai JP, Zou H, Tsuchiya N, Aderca I, et al. Restoration of epigenetically silenced SULF1 expression by 5-aza-2-deoxycytidine sensitizes hepatocellular carcinoma cells to chemotherapy-induced apoptosis. *Med Epigenet.* (2015) 3:1–18. doi: 10.1159/000375461
51. Kaminskyy VO, Surova OV, Vaculova A, Zhivotovsky B. Combined inhibition of DNA methyltransferase and histone deacetylase restores caspase-8 expression and sensitizes SCLC cells to TRAIL. *Carcinogenesis.* (2011) 32:1450–8. doi: 10.1093/carcin/bgr135
52. Augert A, Eastwood E, Ibrahim AH, Wu N, Grunblatt E, Basom R, et al. Targeting NOTCH activation in small cell lung cancer through LSD1 inhibition. *Sci Signal.* (2019) 12:eaau2922. doi: 10.1126/scisignal.aau2922

53. Liu Y, Mondello P, Erazo T, Tannan NB, Asgari Z, de Stanchina E, et al. NOXA genetic amplification or pharmacologic induction primes lymphoma cells to BCL2 inhibitor-induced cell death. *Proc Natl Acad Sci USA.* (2018) 115:12034–9. doi: 10.1073/pnas.1806928115
54. Xu Q, Liu X, Zhu S, Hu X, Niu H, Zhang X, et al. Hyper-acetylation contributes to the sensitivity of chemo-resistant prostate cancer cells to histone deacetylase inhibitor Trichostatin A. *J Cell Mol Med.* (2018) 22:1909–22. doi: 10.1111/jcmm.13475
55. Sabatino MA, Geroni C, Ganzinelli M, Ceruti R, Broggini M. Zebularine partially reverses GST methylation in prostate cancer cells and restores sensitivity to the DNA minor groove binder brostallicin. *Epigenetics.* (2013) 8:656–65. doi: 10.4161/epi.24916
56. Liao H, Xiao Y, Hu Y, Xiao Y, Yin Z, Liu L, et al. Methylation-induced silencing of miR-34a enhances chemoresistance by directly upregulating ATG4B-induced autophagy through AMPK/mTOR pathway in prostate cancer. *Oncol Rep.* (2016) 35:64–72. doi: 10.3892/or.2015.4331
57. Jia L, Zhang S, Huang Y, Zheng Y, Gan Y. Trichostatin A increases radiosensitization of tongue squamous cell carcinoma via miR375. *Oncol Rep.* (2017) 37:305–12. doi: 10.3892/or.2016.5261
58. Meidhof S, Brabletz S, Lehmann W, Preca BT, Mock K, Ruh M, et al. ZEB1-associated drug resistance in cancer cells is reversed by the class I HDAC inhibitor mocetinostat. *EMBO Mol Med.* (2015) 7:831–47. doi: 10.15252/emmm.201404396
59. Balch C, Yan P, Craft T, Young S, Skalnik DG, Huang TH, et al. Antimitogenic and chemosensitizing effects of the methylation inhibitor zebularine in ovarian cancer. *Mol Cancer Ther.* (2005) 4:1505–14. doi: 10.1158/1535-7163.MCT-05-0216
60. El-Zawahry A, Lu P, White SJ, Voelkel-Johnson C. *In vitro* efficacy of AdTRAIL gene therapy of bladder cancer is enhanced by trichostatin A-mediated restoration of CAR expression and downregulation of cFLIP and Bcl-XL. *Cancer Gene Ther.* (2006) 13:281–9. doi: 10.1038/sj.cgt.7700905
61. Morales JC, Ruiz-Magana MJ, Carranza D, Ortiz-Ferron G, Ruiz-Ruiz C. HDAC inhibitors with different gene regulation activities depend on the mitochondrial pathway for the sensitization of leukemic T cells to TRAIL-induced apoptosis. *Cancer Lett.* (2010) 297:91–100. doi: 10.1016/j.canlet.2010.04.029
62. Okabe S, Tauchi T, Kimura S, Maekawa T, Ohyashiki K. The analysis of HDAC inhibitor, vorinostat efficacy against wild type and BCR-ABL mutant positive leukemia cells in monotherapy and in combination with a pan-aurora kinase inhibitor, MK-0457. *Blood.* (2008) 112:5025. doi: 10.1182/blood.V112.11.5025.5025
63. Guo F, Sigua C, Tao J, Bali P, George P, Li Y, et al. Cotreatment with histone deacetylase inhibitor LAQ824 enhances Apo-2L/tumor necrosis factor-related apoptosis inducing ligand-induced death inducing signaling complex activity and apoptosis of human acute leukemia cells. *Cancer Res.* (2004) 64:2580–9. doi: 10.1158/0008-5472.CAN-03-2629
64. Nimmanapalli R, Fuino L, Bali P, Gasparetto M, Glozak M, Tao J, et al. Histone deacetylase inhibitor LAQ824 both lowers expression and promotes proteasomal degradation of Bcr-Abl and induces apoptosis of imatinib mesylate-sensitive or -refractory chronic myelogenous leukemia-blast crisis cells. *Cancer Res.* (2003) 63:5126–35.
65. Bali P, George P, Cohen P, Tao J, Guo F, Sigua C, et al. Superior activity of the combination of histone deacetylase inhibitor LAQ824 and the FLT-3 kinase inhibitor PKC412 against human acute myelogenous leukemia cells with mutant FLT-3. *Clin Cancer Res.* (2004) 10:4991–7. doi: 10.1158/1078-0432.CCR-04-0210
66. Wu Y, Doepner M, Hojnacki T, Feng Z, Katona BW, He X, et al. Disruption of the menin-MLL interaction triggers menin protein degradation via ubiquitin-proteasome pathway. *Am J Cancer Res.* (2019) 9:1682–94.
67. Zhang X, Li B, de Jonge N, Bjorkholm M, Xu D. The DNA methylation inhibitor induces telomere dysfunction and apoptosis of leukemia cells that is attenuated by telomerase over-expression. *Oncotarget.* (2015) 6:4888–900. doi: 10.18632/oncotarget.2917
68. Kuang Y, El-Khoueiry A, Taverna P, Ljungman M, Neamati N. Guadecitabine (SGI-110) priming sensitizes hepatocellular carcinoma cells to oxaliplatin. *Mol Oncol.* (2015) 9:1799–814. doi: 10.1016/j.molonc.2015.06.002
69. Lee WY, Chen PC, Wu WS, Wu HC, Lan CH, Huang YH, et al. Panobinostat sensitizes KRAS-mutant non-small-cell lung cancer to gefitinib by targeting TAZ. *Int J Cancer.* (2017) 141:1921–31. doi: 10.1002/ijc.30888
70. Ishiguro K, Kitajima H, Niinuma T, Ishida T, Maruyama R, Ikeda H, et al. DOT1L inhibition blocks multiple myeloma cell proliferation by suppressing IRF4-MYC signaling. *Haematologica.* (2019) 104:155–65. doi: 10.3324/haematol.2018.191262
71. Civallero M, Cosenza M, Pozzi S, Sacchi S. Ruxolitinib combined with vorinostat suppresses tumor growth and alters metabolic phenotype in hematological diseases. *Oncotarget.* (2017) 8:103797–814. doi: 10.18632/oncotarget.21951
72. Benedetti R, Dell'Aversana C, De Marchi T, Rotili D, Liu NQ, Novakovic B, et al. Inhibition of histone demethylases LSD1 and UTX regulates ERalpha signaling in breast cancer. *Cancers.* (2019) 11:2027. doi: 10.3390/cancers11122027
73. Li F, Miao L, Xue T, Qin H, Mondal S, Thompson PR, et al. Inhibiting PAD2 enhances the anti-tumor effect of docetaxel in tamoxifen-resistant breast cancer cells. *J Exp Clin Cancer Res.* (2019) 38:414. doi: 10.1186/s13046-019-1404-8
74. Lou YF, Zou ZZ, Chen PJ, Huang GB, Li B, Zheng DQ, et al. Combination of gefitinib and DNA methylation inhibitor decitabine exerts synergistic anti-cancer activity in colon cancer cells. *PLoS ONE.* (2014) 9:e97719. doi: 10.1371/journal.pone.0097719
75. Cui X, Witalison EE, Chumanevich AP, Chumanevich AA, Poudyal D, Subramanian V, et al. The induction of microRNA-16 in colon cancer cells by protein arginine deiminase inhibition causes a p53-dependent cell cycle arrest. *PLoS ONE.* (2013) 8:e53791. doi: 10.1371/journal.pone.0053791
76. Poulaki V, Mitsiades CS, Kotoula V, Negri J, McMullan C, Miller JW, et al. Molecular sequelae of histone deacetylase inhibition in human retinoblastoma cell lines: clinical implications. *Invest Ophthalmol Vis Sci.* (2009) 50:4072–9. doi: 10.1167/iovs.09-3517
77. Meng X, Yang S, Li Y, Li Y, Devor EJ, Bi J, et al. Combination of proteasome and histone deacetylase inhibitors overcomes the impact of gain-of-function p53 mutations. *Dis Mark.* (2018) 2018:3810108. doi: 10.1155/2018/3810108
78. Chao A, Lin CY, Chao AN, Tsai CL, Chen MY, Lee LY, et al. Lysine-specific demethylase 1 (LSD1) destabilizes p62 and inhibits autophagy in gynecologic malignancies. *Oncotarget.* (2017) 8:74434–50. doi: 10.18632/oncotarget.20158
79. Jiang XJ, Huang KK, Yang M, Qiao L, Wang Q, Ye JY, et al. Synergistic effect of panobinostat and bortezomib on chemoresistant acute myelogenous leukemia cells via AKT and NF-kappaB pathways. *Cancer Lett.* (2012) 326:135–42. doi: 10.1016/j.canlet.2012.07.030
80. Wang L, Syn NL, Subhash VV, Any Y, Thuya WL, Cheow ESH, et al. Pan-HDAC inhibition by panobinostat mediates chemosensitization to carboplatin in non-small cell lung cancer via attenuation of EGFR signaling. *Cancer Lett.* (2018) 417:152–60. doi: 10.1016/j.canlet.2017.12.030
81. Feng S, Jin Y, Cui M, Zheng J. Lysine-Specific Demethylase 1 (LSD1) Inhibitor S2101 induces autophagy via the AKT/mTOR pathway in SKOV3 ovarian cancer cells. *Med Sci Monit.* (2016) 22:4742–8. doi: 10.12659/MSM.898825
82. Festuccia C, Gravina GL, D'Alessandro AM, Muzi P, Millimaggi D, Dolo V, et al. Azacitidine improves antitumor effects of docetaxel and cisplatin in aggressive prostate cancer models. *Endocr Relat Cancer.* (2009) 16:401–13. doi: 10.1677/ERC-08-0130
83. Stewart ZA, Westfall MD, Pietenpol JA. Cell-cycle dysregulation and anticancer therapy. *Trends Pharmacol Sci.* (2003) 24:139–45. doi: 10.1016/S0165-6147(03)00026-9
84. Merino VF, Cho S, Nguyen N, Sadik H, Narayan A, Talbot C Jr, et al. Induction of cell cycle arrest and inflammatory genes by combined treatment with epigenetic, differentiating, and chemotherapeutic agents in triple-negative breast cancer. *Breast Cancer Res.* (2018) 20:145. doi: 10.1186/s13058-018-1068-x
85. Chang F, Lee JT, Navolanic PM, Steelman LS, Shelton JG, Blalock WL, et al. Involvement of PI3K/Akt pathway in cell cycle progression, apoptosis, and neoplastic transformation: a target for cancer chemotherapy. *Leukemia.* (2003) 17:590–603. doi: 10.1038/sj.leu.2402824
86. Susanto JM, Colvin EK, Pinese M, Chang DK, Pajic M, Mawson A, et al. The epigenetic agents suberoylanilide hydroxamic acid and 5AZA2' deoxycytidine decrease cell proliferation, induce cell death and delay the

growth of MiaPaCa2 pancreatic cancer cells *in vivo*. *Int J Oncol.* (2015) 46:2223–30. doi: 10.3892/ijo.2015.2894
87. Robin TP, Smith A, McKinsey E, Reaves L, Jedlicka P, Ford HL. EWS/FLI1 regulates EYA3 in Ewing sarcoma via modulation of miRNA-708, resulting in increased cell survival and chemoresistance. *Mol Cancer Res.* (2012) 10:1098–108. doi: 10.1158/1541-7786.MCR-12-0086
88. Knott MML, Holting TLB, Ohmura S, Kirchner T, Cidre-Aranaz F, Grunewald TGP. Targeting the undruggable: exploiting neomorphic features of fusion oncoproteins in childhood sarcomas for innovative therapies. *Cancer Metastasis Rev.* (2019) 38:625–42. doi: 10.1007/s10555-019-09839-9
89. Parrish JK, McCann TS, Sechler M, Sobral LM, Ren W, Jones KL, et al. The Jumonji-domain histone demethylase inhibitor JIB-04 deregulates oncogenic programs and increases DNA damage in Ewing Sarcoma, resulting in impaired cell proliferation and survival, and reduced tumor growth. *Oncotarget.* (2018) 9:33110–23. doi: 10.18632/oncotarget.26011
90. Turgeon MO, Perry NJS, Poulogiannis G. DNA damage, repair, and cancer metabolism. *Front Oncol.* (2018) 8:15. doi: 10.3389/fonc.2018.00015
91. Mueller S, Yang X, Sottero TL, Gragg A, Prasad G, Polley MY, et al. Cooperation of the HDAC inhibitor vorinostat and radiation in metastatic neuroblastoma: efficacy and underlying mechanisms. *Cancer Lett.* (2011) 306:223–9. doi: 10.1016/j.canlet.2011.03.010
92. Zhou L, Chen S, Zhang Y, Kmieciak M, Leng Y, Li L, et al. The NAE inhibitor pevonedistat interacts with the HDAC inhibitor belinostat to target AML cells by disrupting the DDR. *Blood.* (2016) 127:2219–30. doi: 10.1182/blood-2015-06-653717
93. McElwee JL, Mohanan S, Griffith OL, Breuer HC, Anguish LJ, Cherrington BD, et al. Identification of PADI2 as a potential breast cancer biomarker and therapeutic target. *BMC Cancer.* (2012) 12:500. doi: 10.1186/1471-2407-12-500
94. Ponnusamy L, Mahalingaiah PKS, Chang YW, Singh KP. Reversal of epigenetic aberrations associated with the acquisition of doxorubicin resistance restores drug sensitivity in breast cancer cells. *Eur J Pharm Sci.* (2018) 123:56–69. doi: 10.1016/j.ejps.2018.07.028
95. Zhang P, Li R, Xiao H, Liu W, Zeng X, Xie G, et al. BRD4 Inhibitor AZD5153 suppresses the proliferation of colorectal cancer cells and sensitizes the anticancer effect of PARP Inhibitor. *Int J Biol Sci.* (2019) 15:1942–54. doi: 10.7150/ijbs.34162
96. Li YC, Wang Y, Li DD, Zhang Y, Zhao TC, Li CF. Procaine is a specific DNA methylation inhibitor with anti-tumor effect for human gastric cancer. *J Cell Biochem.* (2018) 119:2440–9. doi: 10.1002/jcb.26407
97. Niitsu N, Hayashi Y, Sugita K, Honma Y. Sensitization by 5-aza-2'-deoxycytidine of leukaemia cells with MLL abnormalities to induction of differentiation by all-trans retinoic acid and 1alpha,25-dihydroxyvitamin D3. *Br J Haematol.* (2001) 112:315–26. doi: 10.1046/j.1365-2141.2001.02523.x
98. Mukhopadhyay NK, Weisberg E, Gilchrist D, Bueno R, Sugarbaker DJ, Jaklitsch MT. Effectiveness of trichostatin A as a potential candidate for anticancer therapy in non-small-cell lung cancer. *Ann Thorac Surg.* (2006) 81:1034–42. doi: 10.1016/j.athoracsur.2005.06.059
99. Fuller M, Klein M, Schmidt E, Rohde C, Gollner S, Schulze I, et al. 5-azacytidine enhances efficacy of multiple chemotherapy drugs in AML and lung cancer with modulation of CpG methylation. *Int J Oncol.* (2015) 46:1192–204. doi: 10.3892/ijo.2014.2792
100. Clozel T, Yang S, Elstrom RL, Tam W, Martin P, Kormaksson M, et al. Mechanism-based epigenetic chemosensitization therapy of diffuse large B-cell lymphoma. *Cancer Discov.* (2013) 3:1002–19. doi: 10.1158/2159-8290.CD-13-0117
101. Kantarjian H, Oki Y, Garcia-Manero G, Huang X, O'Brien S, Cortes J, et al. Results of a randomized study of 3 schedules of low-dose decitabine in higher-risk myelodysplastic syndrome and chronic myelomonocytic leukemia. *Blood.* (2007) 109:52–7. doi: 10.1182/blood-2006-05-021162
102. Dimopoulos K, Sogaard Helbo A, Fibiger Munch-Petersen H, Sjo L, Christensen J, Sommer Kristensen L, et al. Dual inhibition of DNMTs and EZH2 can overcome both intrinsic and acquired resistance of myeloma cells to IMiDs in a cereblon-independent manner. *Mol Oncol.* (2018) 12:180–95. doi: 10.1002/1878-0261.12157
103. Plumb JA, Strathdee G, Sludden J, Kaye SB, Brown R. Reversal of drug resistance in human tumor xenografts by 2'-deoxy-5-azacytidine-induced demethylation of the hMLH1 gene promoter. *Cancer Res.* (2000) 60:6039–44.
104. Gailhouste L, Liew LC, Hatada I, Nakagama H, Ochiya T. Epigenetic reprogramming using 5-azacytidine promotes an anti-cancer response in pancreatic adenocarcinoma cells. *Cell Death Dis.* (2018) 9:468. doi: 10.1038/s41419-018-0487-z
105. Tang SW, Thomas A, Murai J, Trepel JB, Bates SE, Rajapakse VN, et al. Overcoming resistance to DNA-targeted agents by epigenetic activation of Schlafen 11 (SLFN11) expression with class i histone deacetylase inhibitors. *Clin Cancer Res.* (2018) 24:1944–53. doi: 10.1158/1078-0432.CCR-17-0443
106. Ren J, Chu Y, Ma H, Zhang Y, Zhang X, Zhao D, et al. Epigenetic interventions increase the radiation sensitivity of cancer cells. *Curr Pharm Des.* (2014) 20:1857–65. doi: 10.2174/13816128113199990529
107. Groselj B, Ruan JL, Scott H, Gorrill J, Nicholson J, Kelly J, et al. Radiosensitization *In vivo* by histone deacetylase inhibition with no increase in early normal tissue radiation toxicity. *Mol Cancer Ther.* (2018) 17:381–92. doi: 10.1158/1535-7163.MCT-17-0011
108. Wang G, Edwards H, Caldwell JT, Buck SA, Qing WY, Taub JW, et al. Panobinostat synergistically enhances the cytotoxic effects of cisplatin, doxorubicin or etoposide on high-risk neuroblastoma cells. *PLoS ONE.* (2013) 8:e76662. doi: 10.1371/journal.pone.0076662
109. To KK, Tong WS, Fu LW. Reversal of platinum drug resistance by the histone deacetylase inhibitor belinostat. *Lung Cancer.* (2017) 103:58–65. doi: 10.1016/j.lungcan.2016.11.019
110. Dalvi PS, Macheleidt IF, Lim SY, Meemboor S, Muller M, Eischeid-Scholz H, et al. LSD1 Inhibition attenuates tumor growth by disrupting PLK1 mitotic pathway. *Mol Cancer Res.* (2019) 17:1326–37. doi: 10.1158/1541-7786.MCR-18-0971
111. Nguyen T, Parker R, Hawkins E, Holkova B, Yazbeck V, Kolluri A, et al. Synergistic interactions between PLK1 and HDAC inhibitors in non-Hodgkin's lymphoma cells occur *in vitro* and *in vivo* and proceed through multiple mechanisms. *Oncotarget.* (2017) 8:31478–93. doi: 10.18632/oncotarget.15649
112. Wilson AJ, Sarfo-Kantanka K, Barrack T, Steck A, Saskowski J, Crispens MA, et al. Panobinostat sensitizes cyclin E high, homologous recombination-proficient ovarian cancer to olaparib. *Gynecol Oncol.* (2016) 143:143–51. doi: 10.1016/j.ygyno.2016.07.088
113. Sahai V, Kumar K, Knab LM, Chow CR, Raza SS, Bentrem DJ, et al. BET bromodomain inhibitors block growth of pancreatic cancer cells in three-dimensional collagen. *Mol Cancer Ther.* (2014) 13:1907–17. doi: 10.1158/1535-7163.MCT-13-0925
114. Albany C, Hever-Jardine MP, von Herrmann KM, Yim CY, Tam J, Warzecha JM, et al. Refractory testicular germ cell tumors are highly sensitive to the second generation DNA methylation inhibitor guadecitabine. *Oncotarget.* (2017) 8:2949–59. doi: 10.18632/oncotarget.13811
115. Sharda A, Rashid M, Shah SG, Sharma AK, Singh SR, Gera P, et al. Elevated HDAC activity and altered histone phospho-acetylation confer acquired radio-resistant phenotype to breast cancer cells. *Clin Epigenet.* (2020) 12:4. doi: 10.1186/s13148-019-0800-4
116. Pulliam N, Fang F, Ozes AR, Tang J, Adewuyi A, Keer H, et al. An effective epigenetic-PARP inhibitor combination therapy for breast and ovarian cancers independent of BRCA mutations. *Clin Cancer Res.* (2018) 24:3163–75. doi: 10.1158/1078-0432.CCR-18-0204
117. Brodska B, Holoubek A, Otevrelova P, Kuzelova K. Combined treatment with low concentrations of decitabine and SAHA causes cell death in leukemic cell lines but not in normal peripheral blood lymphocytes. *Biomed Res Int.* (2013) 2013:659254. doi: 10.1155/2013/659254
118. Gopalakrishnapillai A, Kolb EA, McCahan SM, Barwe SP. Epigenetic drug combination induces remission in mouse xenograft models of pediatric acute myeloid leukemia. *Leuk Res.* (2017) 58:91–7. doi: 10.1016/j.leukres.2017.05.004
119. Qi W, Zhang W, Edwards H, Chu R, Madlambayan GJ, Taub JW, et al. Synergistic anti-leukemic interactions between panobinostat and MK-1775 in acute myeloid leukemia *ex vivo*. *Cancer Biol Ther.* (2015) 16:1784–93. doi: 10.1080/15384047.2015.1095406
120. Karagiannis TC, Harikrishnan KN, El-Osta A. The histone deacetylase inhibitor, Trichostatin A, enhances radiation sensitivity and accumulation of gammaH2A.X. *Cancer Biol Ther.* (2005) 4:787–93. doi: 10.4161/cbt.4.7.1922
121. El-Awady RA, Hersi F, Al-Tunaiji H, Saleh EM, Abdel-Wahab AH, Al Homssi A, et al. Epigenetics and miRNA as predictive markers and

targets for lung cancer chemotherapy. *Cancer Biol Ther.* (2015) 16:1056–70. doi: 10.1080/15384047.2015.1046023
122. Greve G, Schiffmann I, Pfeifer D, Pantic M, Schuler J, Lubbert M. The pan-HDAC inhibitor panobinostat acts as a sensitizer for erlotinib activity in EGFR-mutated and -wildtype non-small cell lung cancer cells. *BMC Cancer.* (2015) 15:947. doi: 10.1186/s12885-015-1967-5
123. Fang F, Cardenas H, Huang H, Jiang G, Perkins SM, Zhang C, et al. Genomic and Epigenomic signatures in ovarian cancer associated with resensitization to platinum drugs. *Cancer Res.* (2018) 78:631–44. doi: 10.1158/0008-5472.CAN-17-1492
124. Oza AM, Matulonis UA, Alvarez Secord A, Nemunaitis J, Roman LD, Blagden SP, et al. A Randomized phase II trial of epigenetic priming with guadecitabine and carboplatin in platinum-resistant, recurrent ovarian cancer. *Clin Cancer Res.* (2020) 26:1009–16. doi: 10.1158/1078-0432.CCR-19-1638
125. Li J, Hao D, Wang L, Wang H, Wang Y, Zhao Z, et al. Epigenetic targeting drugs potentiate chemotherapeutic effects in solid tumor therapy. *Sci Rep.* (2017) 7:4035. doi: 10.1038/s41598-017-04406-0
126. Gonzalez H, Hagerling C, Werb Z. Roles of the immune system in cancer: from tumor initiation to metastatic progression. *Genes Dev.* (2018) 32:1267–84. doi: 10.1101/gad.314617.118
127. Sylvestre M, Tarte K, Roulois D. Epigenetic mechanisms driving tumor supportive microenvironment differentiation and function: a role in cancer therapy? *Epigenomics.* (2020) 12:157–69. doi: 10.2217/epi-2019-0165
128. Xiao Q, Nobre A, Pineiro P, Berciano-Guerrero MA, Alba E, Cobo M, et al. Genetic and epigenetic biomarkers of immune checkpoint blockade response. *J Clin Med.* (2020) 9:286. doi: 10.3390/jcm9010286
129. Gomez S, Tabernacki T, Kobyra J, Roberts P, Chiappinelli KB. Combining epigenetic and immune therapy to overcome cancer resistance. *Semin. Cancer Biol.* (2019). doi: 10.1016/j.semcancer.2019.12.019. [Epub ahead of print].
130. Horing E, Podlech O, Silkenstedt B, Rota IA, Adamopoulou E, Naumann U. The histone deacetylase inhibitor trichostatin a promotes apoptosis and antitumor immunity in glioblastoma cells. *Anticancer Res.* (2013) 33:1351–60.
131. Shen L, Ciesielski M, Ramakrishnan S, Miles KM, Ellis L, Sotomayor P, et al. Class I histone deacetylase inhibitor entinostat suppresses regulatory T cells and enhances immunotherapies in renal and prostate cancer models. *PLoS ONE.* (2012) 7:e30815. doi: 10.1371/journal.pone.0030815
132. Siebenkas C, Chiappinelli KB, Guzzetta AA, Sharma A, Jeschke J, Vatapalli R, et al. Inhibiting DNA methylation activates cancer testis antigens and expression of the antigen processing and presentation machinery in colon and ovarian cancer cells. *PLoS ONE.* (2017) 12:e0179501. doi: 10.1371/journal.pone.0179501
133. Topper MJ, Vaz M, Chiappinelli KB, DeStefano Shields CE, Niknafs N, Yen RC, et al. Epigenetic therapy ties MYC depletion to reversing immune evasion and treating lung cancer. *Cell.* (2017) 171:1284–300 e1221. doi: 10.1016/j.cell.2017.10.022
134. Jiang X, Wang J, Deng X, Xiong F, Ge J, Xiang B, et al. Role of the tumor microenvironment in PD-L1/PD-1-mediated tumor immune escape. *Mol Cancer.* (2019) 18:10. doi: 10.1186/s12943-018-0928-4
135. Kim K, Skora AD, Li Z, Liu Q, Tam AJ, Blosser RL, et al. Eradication of metastatic mouse cancers resistant to immune checkpoint blockade by suppression of myeloid-derived cells. *Proc Natl Acad Sci USA.* (2014) 111:11774–9. doi: 10.1073/pnas.1410626111
136. Kiany S, Huang G, Kleinerman ES. Effect of entinostat on NK cell-mediated cytotoxicity against osteosarcoma cells and osteosarcoma lung metastasis. *Oncoimmunology.* (2017) 6:e1333214. doi: 10.1080/2162402X.2017.1333214
137. Yang D, Torres CM, Bardhan K, Zimmerman M, McGaha TL, Liu K. Decitabine and vorinostat cooperate to sensitize colon carcinoma cells to Fas ligand-induced apoptosis *in vitro* and tumor suppression *in vivo*. *J Immunol.* (2012) 188:4441–9. doi: 10.4049/jimmunol.1103035
138. Jazirehi AR, Kurdistani SK, Economou JS. Histone deacetylase inhibitor sensitizes apoptosis-resistant melanomas to cytotoxic human T lymphocytes through regulation of TRAIL/DR5 pathway. *J Immunol.* (2014) 192:3981–9. doi: 10.4049/jimmunol.1302532
139. Vo DD, Prins RM, Begley JL, Donahue TR, Morris LF, Bruhn KW, et al. Enhanced antitumor activity induced by adoptive T-cell transfer and adjunctive use of the histone deacetylase inhibitor LAQ824. *Cancer Res.* (2009) 69:8693–9. doi: 10.1158/0008-5472.CAN-09-1456
140. Stone ML, Chiappinelli KB, Li H, Murphy LM, Travers ME, Topper MJ, et al. Epigenetic therapy activates type I interferon signaling in murine ovarian cancer to reduce immunosuppression and tumor burden. *Proc Natl Acad Sci USA.* (2017) 114:E10981–990. doi: 10.1073/pnas.1712514114
141. Katto J, Mahlknecht U. Epigenetic regulation of cellular adhesion in cancer. *Carcinogenesis.* (2011) 32:1414–8. doi: 10.1093/carcin/bgr120
142. Dreger H, Ludwig A, Weller A, Stangl V, Baumann G, Meiners S, et al. Epigenetic regulation of cell adhesion and communication by enhancer of zeste homolog 2 in human endothelial cells. *Hypertension.* (2012) 60:1176–83. doi: 10.1161/HYPERTENSIONAHA.112.191098
143. Furukawa Y, Kikuchi J. Epigenetic regulation of cell adhesion-mediated drug resistance acquisition in multiple myeloma. *Rinsho Ketsueki.* (2016) 57:546–55.
144. Emon B, Bauer J, Jain Y, Jung B, Saif T. Biophysics of tumor microenvironment and cancer metastasis - a mini review. *Comput Struct Biotechnol J.* (2018) 16:279–87. doi: 10.1016/j.csbj.2018.07.003
145. Kalluri R, Weinberg RA. The basics of epithelial-mesenchymal transition. *J Clin Invest.* (2009) 119:1420–8. doi: 10.1172/JCI39104
146. Pal M, Chen H, Lee BH, Lee JYH, Yip YS, Tan NS, et al. Epithelial-mesenchymal transition of cancer cells using bioengineered hybrid scaffold composed of hydrogel/3D-fibrous framework. *Sci Rep.* (2019) 9:8997. doi: 10.1038/s41598-019-45384-9
147. O'Leary K, Shia A, Schmid P. Epigenetic regulation of EMT in non-small cell lung cancer. *Curr Cancer Drug Targets.* (2018) 18:89–96. doi: 10.2174/1568009617666170203162556
148. Shargh SA, Sakizli M, Khalaj V, Movafagh A, Yazdi H, Hagigatjou E, et al. Downregulation of E-cadherin expression in breast cancer by promoter hypermethylation and its relation with progression and prognosis of tumor. *Med Oncol.* (2014) 31:250. doi: 10.1007/s12032-014-0250-y
149. Batlle E, Sancho E, Franci C, Dominguez D, Monfar M, Baulida J, et al. The transcription factor snail is a repressor of E-cadherin gene expression in epithelial tumour cells. *Nat Cell Biol.* (2000) 2:84–9. doi: 10.1038/35000034
150. Lin T, Ponn A, Hu X, Law BK, Lu J. Requirement of the histone demethylase LSD1 in Snai1-mediated transcriptional repression during epithelial-mesenchymal transition. *Oncogene.* (2010) 29:4896–904. doi: 10.1038/onc.2010.234
151. Boulding T, McCuaig RD, Tan A, Hardy K, Wu F, Dunn J, et al. LSD1 activation promotes inducible EMT programs and modulates the tumour microenvironment in breast cancer. *Sci Rep.* (2018) 8:73. doi: 10.1038/s41598-017-17913-x
152. Lee C, Jeong H, Bae Y, Shin K, Kang S, Kim H, et al. Targeting of M2-like tumor-associated macrophages with a melittin-based pro-apoptotic peptide. *J Immunother Cancer.* (2019) 7:147. doi: 10.1186/s40425-019-0610-4
153. Lu L, Chen Z, Lin X, Tian L, Su Q, An P, et al. Inhibition of BRD4 suppresses the malignancy of breast cancer cells via regulation of Snail. *Cell Death Differ.* (2020) 27:255–68. doi: 10.1038/s41418-019-0353-2
154. Barwe SP, Quagliano A, Gopalakrishnapillai A. Eviction from the sanctuary: development of targeted therapy against cell adhesion molecules in acute lymphoblastic leukemia. *Semin Oncol.* (2017) 44:101–12. doi: 10.1053/j.seminoncol.2017.06.005
155. Quagliano A, Gopalakrishnapillai A, Barwe SP. Epigenetic drug combination overcomes osteoblast-induced chemoprotection in pediatric acute lymphoid leukemia. *Leuk Res.* (2017) 56:36–43. doi: 10.1016/j.leukres.2017.01.030
156. Quagliano A, Gopalakrisnapillai A, Kolb EA, Barwe S. Epigenetic drug combination overcomes bone marrow microenvironment-induced chemoprotection in pediatric acute lymphoblastic leukemia via modulation of CD81. *Blood.* (2018) 132:3957. doi: 10.1182/blood-2018-99-120275
157. Jing X, Yang F, Shao C, Wei K, Xie M, Shen H, et al. Role of hypoxia in cancer therapy by regulating the tumor microenvironment. *Mol Cancer.* (2019) 18:157. doi: 10.1186/s12943-019-1089-9
158. Liao WLS, Sun HS, Tsai SJ. Hypoxia-induced tumor malignancy and drug resistance: role of microRNAs. *Biomark Genom Med.* (2014) 6:1–11. doi: 10.1016/j.bgm.2014.01.003
159. Macedo-Silva C, Miranda-Goncalves V, Henrique R, Jeronimo C, Bravo I. The critical role of hypoxic microenvironment and epigenetic

deregulation in esophageal cancer radioresistance. *Genes.* (2019) 10:927. doi: 10.3390/genes10110927
160. Miranda-Goncalves V, Lameirinhas A, Henrique R, Jeronimo C. Metabolism and epigenetic interplay in cancer: regulation and putative therapeutic targets. *Front Genet.* (2018) 9:427. doi: 10.3389/fgene.2018.00427
161. Marengo B, Garbarino O, Speciale A, Monteleone L, Traverso N, Domenicotti C. MYC expression and metabolic redox changes in cancer cells: a synergy able to induce chemoresistance. *Oxid Med Cell Longev.* (2019) 2019:7346492. doi: 10.1155/2019/7346492
162. Desbats MA, Giacomini I, Prayer-Galetti T, Montopoli M. Metabolic plasticity in chemotherapy resistance. *Front Oncol.* (2020) 10:281. doi: 10.3389/fonc.2020.00281
163. Feingold PL, Surman DR, Brown K, Xu Y, McDuffie LA, Shukla V, et al. Induction of thioredoxin-interacting protein by a histone deacetylase inhibitor, entinostat, is associated with DNA damage and apoptosis in esophageal adenocarcinoma. *Mol Cancer Ther.* (2018) 17:2013–23. doi: 10.1158/1535-7163.MCT-17-1240
164. Pollyea DA, Stevens BM, Jones CL, Winters A, Pei S, Minhajuddin M, et al. Venetoclax with azacitidine disrupts energy metabolism and targets leukemia stem cells in patients with acute myeloid leukemia. *Nat Med.* (2018) 24:1859–66. doi: 10.1038/s41591-018-0233-1
165. Takezawa K, Okamoto I, Okamoto W, Takeda M, Sakai K, Tsukioka S, et al. Thymidylate synthase as a determinant of pemetrexed sensitivity in non-small cell lung cancer. *Br J Cancer.* (2011) 104:1594–601. doi: 10.1038/bjc.2011.129
166. Del Bufalo D, Desideri M, De Luca T, Di Martile M, Gabellini C, Monica V, et al. Histone deacetylase inhibition synergistically enhances pemetrexed cytotoxicity through induction of apoptosis and autophagy in non-small cell lung cancer. *Mol Cancer.* (2014) 13:230. doi: 10.1186/1476-4598-13-230
167. Ma X, Wang J, Liu J, Mo Q, Yan X, Ma D, et al. Targeting CD146 in combination with vorinostat for the treatment of ovarian cancer cells. *Oncol Lett.* (2017) 13:1681–7. doi: 10.3892/ol.2017.5630
168. Young CS, Clarke KM, Kettyle LM, Thompson A, Mills KI. Decitabine-Vorinostat combination treatment in acute myeloid leukemia activates pathways with potential for novel triple therapy. *Oncotarget.* (2017) 8:51429–46. doi: 10.18632/oncotarget.18009
169. Leonard SM, Perry T, Woodman CB, Kearns P. Sequential treatment with cytarabine and decitabine has an increased anti-leukemia effect compared to cytarabine alone in xenograft models of childhood acute myeloid leukemia. *PLoS ONE.* (2014) 9:e87475. doi: 10.1371/journal.pone.0087475
170. Quagliano A, Gopalakrishnapillai A, Kolb EA, Barwe S. Modulation of CD81 by epigenetic drug combination sensitizes acute lymphoblastic leukemia via decreased BTK signaling. *Blood.* (2019) 134:2628. doi: 10.1182/blood-2019-129198
171. Berdasco M, Esteller M. Clinical epigenetics: seizing opportunities for translation. *Nat Rev Genet.* (2019) 20:109–27. doi: 10.1038/s41576-018-0074-2
172. Chuang JC, Jones PA. Epigenetics and microRNAs. *Pediatr Res.* (2007) 61:24–9R. doi: 10.1203/pdr.0b013e3180457684
173. Tomasetti M, Gaetani S, Monaco F, Neuzil J, Santarelli L. Epigenetic regulation of miRNA expression in malignant mesothelioma: miRNAs as biomarkers of early diagnosis and therapy. *Front Oncol.* (2019) 9:1293. doi: 10.3389/fonc.2019.01293
174. Bartel DP. MicroRNAs: target recognition and regulatory functions. *Cell.* (2009) 136:215–33. doi: 10.1016/j.cell.2009.01.002
175. Shiio Y, Eisenman RN. Histone sumoylation is associated with transcriptional repression. *Proc Natl Acad Sci USA.* (2003) 100:13225–30. doi: 10.1073/pnas.1735528100
176. Martinez-Zamudio R, Ha HC. Histone ADP-ribosylation facilitates gene transcription by directly remodeling nucleosomes. *Mol Cell Biol.* (2012) 32:2490–502. doi: 10.1128/MCB.06667-11
177. Rossetto D, Avvakumov N, Cote J. Histone phosphorylation: a chromatin modification involved in diverse nuclear events. *Epigenetics.* (2012) 7:1098–108. doi: 10.4161/epi.21975
178. Jeusset LM, McManus KJ. Developing targeted therapies that exploit aberrant histone ubiquitination in cancer. *Cells.* (2019) 8:165. doi: 10.3390/cells8020165

Conflict of Interest: The authors declare that the research was conducted in the absence of any commercial or financial relationships that could be construed as a potential conflict of interest.

frontiers in Oncology

REVIEW
published: 30 June 2020
doi: 10.3389/fonc.2020.00961

The Roles of Embryonic Transcription Factor BRACHYURY in Tumorigenesis and Progression

Ming Chen[1,2], *Yinghui Wu*[1,3], *Hong Zhang*[1,3], *Suoyuan Li*[1,3], *Jundong Zhou*[4] and *Jun Shen*[1,3]*

[1] Department of Orthopeadic Surgery, The Affiliated Suzhou Hospital of Nanjing Medical University, Suzhou, China, [2] Department of Orthopeadic Surgery, Wuxi No. 2 People's Hospital, Nanjing Medical University, Wuxi, China, [3] Suzhou Municipal Hospital, Suzhou, China, [4] Suzhou Cancer Center Core Laboratory, The Affiliated Suzhou Hospital of Nanjing Medical University, Suzhou, China

Transcription factor brachyury, with a DNA-binding T-domain, regulates posterior mesoderm formation and notochord development through binding with highly conserved palindromic consensus sequence in a variety of organisms. The absence of brachyury expression in majority of adult normal tissues and exclusive tumor-specific expression provides the potential to be developed into a novel and promising diagnostic and therapeutic target in cancer. As a sensitive and specific marker in the diagnosis of chordoma, brachyury protein has been verified to involve in the process of carcinogenesis and progression of chordoma and several epithelial carcinomas in various studies, but the mechanism by which brachyury promotes tumor cells migrate, invade and metastasis still remains less clear. To this end, we attempt to summarize the literature on the upstream regulatory pathway of brachyury transcription and downstream controlling network by brachyury activation, all of which involve in both the embryonic development and tumor progression. We present the respective correlation of brachyury expression with tumor progression, distant metastasis, survival rate and prognosis in several types of tumor samples (including chordoma, lung cancer, breast carcinoma, and prostate cancer), and various brachyury gain-of-function and loss-of-function experiments are summarized to explore its specific role in respective tumor cell line *in vitro*. In addition, we also discuss another two programs relating to brachyury function: epithelial-to-mesenchymal transition (EMT) and cell cycle control, both of which implicate in the regulation of brachyury on biological behavior of tumor cells. This review will provide an overview of the function of master transcriptional factor brachyury, compare the similarities and differences of its role between embryonic development and carcinogenesis, and list the evidence on which brachyury-target therapies have the potential to help control advanced cancer populations.

Keywords: BRACHYURY, notochord, chordoma, tumorigenesis, transcriptional factor, EMT

OPEN ACCESS

Edited by:
Hailong Pei,
Soochow University, China

Reviewed by:
Fiona Wardle,
King's College London, United Kingdom
Nan Ding,
Institute of Modern Physics (CAS), China

***Correspondence:**
Jun Shen
18112603158@163.com

Specialty section:
This article was submitted to Molecular and Cellular Oncology, a section of the journal Frontiers in Oncology

Received: *03 March 2020*
Accepted: *15 May 2020*
Published: *30 June 2020*

Citation:
Chen M, Wu Y, Zhang H, Li S, Zhou J and Shen J (2020) The Roles of Embryonic Transcription Factor BRACHYURY in Tumorigenesis and Progression. Front. Oncol. 10:961. doi: 10.3389/fonc.2020.00961

INTRODUCTION

The T-box genes encode a family of transcription factors, characterized by a highly conserved DNA-binding domain of about 180 amino acid residues, which is designated as T-domain (1, 2), and are essential in controlling many aspects of embryogenesis in a wide variety of organisms (3). Eighteen different mammalian T-box genes have been identified so far. T-box transcription factors preferentially bind to 24-nucleotide palindromic consensus sequence: AATTTCACACCT AGGTGTGAAATT (2).

The first of the T-Box family molecularly characterized is BRACHYURY (3, 4). *Brachyury* ("short tail" from Greek) origins from the phenotype of this gene mutant mice, most striking defect with a truncated tail, which was first described by Dobrovolskaia-Zavadskaia in 1927 (3). Orthologs of *Brachyury* have been identified in a large amount of multicellular organisms, such as ascidians, zebrafish, *Xenopus*, mouse, human, and others (4–6), which are required for posterior mesoderm formation and notochord differentiation, normal cell movements during gastrulation and tail outgrowth, and establishment of left–right asymmetry (4, 7). *BRACHYURY* encodes a protein of 435 amino acids, which functions as a transcription factor to bind with half site of abovementioned consensus sequence: TCACACCT.

Miettinen et al. (8) performed an immunohistochemical study of 5,229 cases, demonstrating nuclear BRACHYURY expression to be a sensitive and fairly specific marker for chordoma. Beyond that, BRACHYURY has been reported to express in various types of tumors (9–14), especially highly expressed in several tumors of epithelial origin. BRACHYURY expression is negative among most normal tissues, with the exception of testis and thyroid (15–17). The cause why BRACHYURY is absent in majority of adult non-neoplastic tissue and exclusively expressed in tumor-specific manner (18) drives researchers to discover the underlying role played by BRACHYURY on tumorigenesis.

THE FUNCTION OF BRACHYURY IN MESODERM AND NOTOCHORD DEVELOPMENT

The *BRACHYURY (T)* gene is required for the formation of posterior mesoderm and axial development. In all vertebrates, the gene is initially expressed throughout the presumptive mesoderm, and during later stage, the expression is gradually restricted to the developing notochord and tail bud (3, 19, 20). Mutant embryos lacking *Brachyury* gene function demonstrate deficiency in notochord differentiation and the formation of posterior mesoderm but develop normal anterior mesoderm (3, 21). BRACHYURY expression is lost with maturation of the notochord, which disappears largely before birth. But some residual notochordal cells may persist in the intervertebral disks of the spine until early childhood and possibly throughout life in some people (15, 22).

Mice homozygous with *Brachyury* mutations will die shortly after gastrulation and display several mesodermal abnormalities (3, 4). *BRACHYURY* encodes sequence-specific activator that contains a T DNA-binding domain, through which BRACHYUYR exerts its mesoderm-inducing effects by directly activating downstream mesoderm-specific genes (4, 23). In addition, the role of *BRACHYURY* gene in developing mesoderm, morphogenesis, and cell fate is evolutionarily conserved (3).

THE REGULATORY NETWORK BY BRACHYURY IN EMBRYONIC DEVELOPMENT AND TUMORIGENESIS

Upstream Regulatory Pathway of *BRACHYURY* Transcription

Fibroblast growth factor (FGF) and fibroblast growth factor receptor (FGFR) signaling has been implicated in the patterning of mesoderm and activated *Brachyury* expression (24–28). In *Xenopus* embryos, the expression of *Xbra*, the *Xenopus* homolog of *Brachyury,* requires an intact FGF signaling pathway. Formation of mesoderm tissue requires a regulatory loop in which Xbra activates the expression of a member of the FGF family and FGF maintains the expression of Xbra (27, 29).

Another study in embryos of the ascidian found that *Brachyury* is expressed in a manner dependent on the FGF-mitogen-activated protein kinase kinase (MEK)-mitogen-activated protein kinase (MAPK)-Ets signaling pathway and on the intrinsic factors Zic and FoxA. Binding of Ets and ZicN at the 5′ upstream of *Brachyury* promoter region is required for FGF-responsive *Brachyury* gene activation in notochord precursor cells (30). In the chordoma cells, FGFR/MEK/extracellular signal-regulated kinase (ERK)/*BRACHYURY* pathway represents a novel therapeutic target (31). FGF2 induces MEK/ERK phosphorylation and upregulates *BRACHYURY* expression, *BRACHYURY* knockdown blocks the effects of FGF signaling, suggesting a positive feedback loop between FGF/FGFR and BRACHYURY could be required for chordoma cells' growth and survival.

The study by Hu et al. (32) suggests that FGFR1/MAPK signaling is also important for *BRACHYURY* activation in lung cancer cells. FGF1/FGFR1 signaling promotes ERK phosphorylation in the nucleus followed by transcriptional activation of *BRACHYURY*, which is further verified to be important for facilitating epithelial-to-mesenchymal transition (EMT), tumor cell growth, and invasion.

In addition, basic fibroblast growth factor (bFGF) has been reported to induce notochord formation and *Brachyury* expression in ascidian embryogenesis (26). Activin, BMP-4, Δp63, WNT3, WNT8A, BMP/Nodal pathway (33–37) have also been shown to regulate transcriptional activation of *Brachyury* in mouse, *Xenopus*, and zebrafish embryo and in tumor cells, human embryonic cardiomyocyte, etc.

Downstream Regulatory Network by BRACHYURY Activation

BRACHYURY exerts its regulatory role by controlling transcription of a large number of target genes (23). Using ascidian *Ciona,* an invertebrate chordate, which is a commonly

used model to study BRACHYURY function, over 50 validated genes have been identified to be controlled by BRACHYURY (38) In the embryo of *Ciona intestinalis*, Hotta et al. (20) showed that 20 of the putative BRACHYURY target genes encoded components for regulation of the cytoskeletal architecture, the extracellular matrix (ECM), proteins implicated in signal transduction and cell cycle control, etc. Morley et al. (7) investigated targets and gene regulatory network of No tail (Ntl), a zebrafish BRACHYURY ortholog, in mesoderm formation, discovering an *in vivo* binding site for Ntl, which accords with the conserved T-box binding site: TCACACCT. Ntl acts in combination with other factors, including other T-box factors and several signaling pathways, to mediate its activities in mesoderm development (7).

Further study by Katikala et al. (39) in 2012 revealed that transcriptional regulator BRACHYURY can establish multitiered transcriptional output and temporal readouts of target gene expression in ascidian Ciona. This molecule regulates most of its targets by directly activating early- and middle-onset genes, respectively, while indirectly controlling late-onset genes *via* transcriptional intermediaries.

The chief transcriptional targets of BRACHYURY in humans were firstly identified by Nelson et al. (40), integrating transcriptome data from chordoma U-CH1 cell line in which *BRACHYURY* was silenced with ChIP-seq data generated from the same cell line. Enriched gene sets controlled by BRACHYURY are mainly involved in the regulation of cell cycle and the production of ECM, multiple growth factors, and cytokines.

Yes-associated protein (YAP), an effector of the Hippo pathway and a master regulator of organ development (41), was recently found to be directly transactivated by BRACHYURY in chordoma cells through binding to the proximal region of the YAP promoter. Interestingly, BRACHYURY regulates YAP signaling through a non-transcriptional mechanism in lung carcinoma (18). Both BRACHYURY and YAP expressions were found to be elevated in glioblastoma and brain metastases originating from lung carcinomas, and *BRACHYURY* knockdown resulted in a significant decrease in YAP protein and mRNA expression in primary glioblastoma cells. BRACHYURY was identified as a positive regulator of YAP in various types of cancers (18).

THE CORRELATION OF BRACHYURY WITH CLINICAL TUMORS

Chordoma

Although it is still unclear what role *BRACHYURY* could be in the tumorigenesis of chordoma, gene duplication mutation and overexpression in samples verified by previous various studies suggest that BRACHYURY might be a crucial molecular driver in the initiation and propagation of chordoma (42).

BRACHYURY/BRACHYURY expression in chordoma

Henderson et al. (43) performed a comprehensive study of the gene expression profile from 96 tumor samples with representatives of all mesenchymal tissues, *BRACHYURY* gene was found to be uniquely expressed in chordomas. By screening 53 chordomas, over 300 other neoplasms, and 33 normal tissues, BRACHYURY was found to be expressed in the embryonic notochord and all chordomas, labeling both chondroid and chordoid areas, and absent in all other neoplasms and non-neoplastic tissues (44). BRACHYURY is the first identified molecule to link notochord formation and chordoma pathogenesis (21). Miettinen et al. (8) immunohistochemically evaluated 5,229 different tumors for nuclear BRACHYURY expression, and all chordomas (75/76) were positive except a sarcomatous one. Another report (45) revealed that BRACHYURY was positively expressed in about 90% of all pathologically confirmed chordomas. As for exceptionally rare extra-axial skeletal chordomas and soft tissue chordomas, BRACHYURY was also reported to be a useful diagnostic tool (15, 46). All the above mentioned studies demonstrated that BRACHYURY expression (especial nuclear positivity) is a sensitive and fairly specific marker for the diagnosis and differential diagnosis of chordoma.

Our previous study on chordoma specimens inadvertently found two types of pathological components coexisting in the same one specimen, chordoma tumor elements with strong BRACHYURY expression and notochordal cell rests with rarely and no expression (47, 48). BRACHYURY was shown to be a sensitive (100%) and specific (100%) marker in distinguishing coexisting notochordal cell rests from chordoma tumor components (48).

The Role of *BRACHYURY*/BRACHYURY in Chordoma

JHC7 is the first chordoma cell line established with stable *BRACHYURY* expression. Silencing of *BRACHYURY* expression by using shRNA led to complete growth arrest and inability to be passaged serially *in vitro* (49). Similarly, U-CH1 cell line, which shows polysomy of chromosome 6 involving 6q27, was validated as representing chordoma by the generation of xenografts in the mouse model, demonstrating typical chordoma morphology and immunohistochemistry characteristics. Silencing of *BRACHYURY* in this cell line led to cell growth arrest and acquisition of a senescence-like phenotype (50).

The Genetic Basis of *BRACHYURY* Expression in Chordoma

Using combined genetic linkage and comparative genomic hybridization analyses, germline *BRACHYURY* duplication was identified to associate with the familial risk of developing chordoma (51), which is the first report of *BRACHYURY* copy number gain (CNG) in any disease type. Nevertheless, *BRACHYURY* duplication is extremely rare in sporadic chordoma (52).

Presneau et al. (50) and Dei Tos (53) demonstrated that close to half of the investigated chordoma cases showed a gain of chromosome band 6q27 (the locus wherein *BRACHYURY* locates) either through polysomy of the entire chromosome 6 or structural rearrangements, which indicates that cCNGs of *BRACHYURY* are pathogenetically relevant in sporadic chordoma. Cho et al. (35) and Pillay et al. (54) demonstrated that a common single-nucleotide polymorphism (SNP) located in the

BRACHYURY gene, rs2305089, has strong association with the risk of sporadic chordoma.

In the following case-control comparison study (52), the risk estimated for rs2305089 was similar in familial and sporadic chordoma. Another common variant, rs1056048, was identified to strongly associate with familial chordoma with *BRACHYURY* duplication, and rs3816300 was significantly correlated with earlier age onset, which further corroborates the importance of genetic variations of *BRACHYURY* gene in the pathogenesis of both familial and sporadic chordoma. Recently, Sharifnia et al. (55) revealed that regulation of *BRACHYURY* by super-enhancers is a dominant feature of the chordoma gene-regulatory landscape. Chordoma JHC7 cells had a focal amplification at *BRACHYUYR* locus that encompassed proximal super-enhancers and a 1.5 Mb upstream region with broad H3K27ac occupancy, and patient-derived chordoma tumors were also found to have this hyper-acetylated region.

Lung Carcinoma

Various studies have demonstrated that BRACHYURY is positively associated with the motility and invasiveness ability of lung tumor cell *in vitro* and highly expressed in late-stage lung tumor tissue, which supports *BRACHYURY* could be developed into a potential therapeutic target (12, 17, 56).

In addition, 37.5–62.5% of human lung cancer tissues are positive for *BRACHYURY* mRNA expression, which has a significantly higher percentage than normal lung tissue with 12.5% (10, 17). Moreover, BRACHYURY expression is significantly positively correlated with tumor stage (10) and no obvious relationship with histological type (12). High *BRACHYURY* mRNA expression significantly correlates with poor prognosis in both 5 year disease-free survival (DFS) and overall survival rate in primary lung carcinoma samples (12).

BRACHYURY protein expression was detected in ∼41–60% of primary lung carcinoma tissues (17, 57) and 40% of non-small-cell lung carcinomas (NSCLCs) (16, 17), all of which demonstrated intense nuclear staining and weak, more diffuse cytoplasmic staining. BRACHYURY protein expression in the nuclei is significantly related to its mRNA level expression in lung cancer tissues (12). High expression of BRACHYURY protein is significantly associated with poor prognosis in overall survival (58) and high tumor stages, as well as lymph node metastases (59) in NSCLC samples.

BRACHYURY/BRACHYURY has been proved to play an important role in promoting lung tumor cell progression and metastasis *in vitro* (56). Seventy percent of lung cancer cell lines are positive for *BRACHYURY* mRNA expression (16, 17). *BRACHYURY*-inhibited lung H460 (10) and A549 cells (59) showed significantly reduced migratory and invasive capability. In addition, inhibition of *BRACHYURY* in H460 cells resulted in diminished capability to invade ECM and reduced expression of genes encoding for matrix metalloproteinase (MMP)2 and MMP24 (10), both of which participate in the ECM degradation. *BRACHYURY* expression did not influence primary tumor growth, whereas inhibition of *BRACHYURY* expression significantly diminished the ability of lung H460 cells developing experimental lung metastasis *in vivo*, whether by subcutaneous injection or by intravenous injection (10). All the above results suggest BRACHYURY is involved in several key steps of metastatic process in lung cancer cells: invasion, migration, adhesion, and colonization in the target organ.

BRACHYURY confers survival advantage to the lung cancer cells in response to treatment with various doses of the epidermal growth factor receptor (EGFR) inhibitor (17). Silencing of *BRACHYURY* in A549 cells increases cell sensitivity to cisplatin (59).

Breast Carcinoma

BRACHYURY/BRACHYURY expression has been reported to positively associate with the invasive and metastatic capability of breast carcinoma cells *in vitro* and with the risk of recurrence and distal metastasis in breast patients (9, 60). Different studies have demonstrated the potential of *BRACHYURY* as a target for the treatment of breast carcinoma using cancer vaccines or immunotherapy approaches (61, 62).

BRACHYURY/BRACHYURY is obviously highly expressed at the mRNA and protein levels in breast cancer tissues and cell lines compared to negativity in normal breast cancer tissues and cells (9, 60, 63–66). Hormone receptor status of breast cancer is an important and recognized prognostic factor and can reflect different stages (67), including estrogen receptor (ER) and progesterone receptor (PR). *BRACHYURY* mRNA level expression in breast carcinomas with negativity for ER and/or PR is statistically significantly higher than those with positivity for ER and/or PR (9, 61), and triple-negative breast cancer (TNBC) is significantly higher than triple-positive and non-TNBC (61). Immunohistochemistry detection showed 90% of primary infiltrating ductal carcinomas were positive for BRACHYURY expression, comparing with almost absence of BRACHYURY in benign breast lesions. No significant differences were found between BRACHYURY protein level and various clinical parameters (grade, lymph node status, et al.) (9). Primary and metastatic TNBC samples showed 92–100% positive BRACHYURY protein expression, contrasting with <1% positive expression in adjacent normal breast tissue (61). Nuclear BRACHYURY protein expression is significantly higher in tumors of advanced stages III–IV than that of stages I–II (61) and an independent prognostic factor for DFS, while BRACHYURY cytoplasmic expression has no correlation with prognosis (68).

BRACHYURY gain-of-function and loss-of-function experiments were performed in various studies to investigate its role in breast carcinoma tumorigenesis, progression, and resistance to therapeutic intervention *in vitro*. Silencing of *BRACHYURY* in breast MDA-MB-436 cells statistically significantly reduced the ability to invade the ECM and form mammospheres in primary and secondary cultures (9). Our study (60) demonstrated that *BRACHYURY* promoted breast cancer cell invasion, migration, adhesion, and colonization in bone microenvironment *in vitro*, and *BRACHYURY* knockdown in MDA-MB-231 cells decreased the colonization and survival capability in bone tissue *in vivo*. BRACHYURY-high breast tumor cells were more resistant to the cytotoxic effects of docetaxel *in vitro* (9). *BRACHYURY* has also been confirmed

to enhance breast cancer cell survival capability in response to tamoxifen therapy, and *BRACHYURY* silencing demonstrated more sensitive and higher apoptosis than control group upon tamoxifen treatment (63). Collectively, all the results of *in vitro* assays indicate that *BRACHYURY*-targeting therapeutic approaches under clinical trials and laboratory could have the potential to help control advanced breast carcinomas and improve prognosis.

Prostate Cancer

BRACHYURY was shown to express in prostate cancer tissues, which increased with tumor malignancy and aggressiveness and was positively associated with Gleason score and TNM stage (69). Besides, *BRACHYURY*/BRACHYURY was also associated with tumor chemotherapy resistance (70). Targeting *BRACHYURY* is becoming a promising therapeutic option for advanced and metastatic prostate cancer patients.

Pinto et al. (14) demonstrated BRACHYURY nuclear staining was present in a comparable positive rate in prostatic intraepithelial neoplasia (PIN) lesions and prostate cancer tissue, contrasting with 100% positivity for metastatic prostate cancer. BRACHYURY nuclear expression is highly associated with the occurrence of metastasis (14, 69). There is a strong correlation between BRACHYURY expression and well-established markers of prostate cancer progression, such as Bcl2, ETS-related gene (ERG), and phosphatase and tensin homolog (PTEN) loss (70). A high level of BRACHYURY is verified to associate with poor prognosis (4, 69, 71). In addition, prostate cell lines with endogenous *BRACHYURY*/BRACHYURY expression were demonstrated to be more resistant to docetaxel and cabazitaxel treatment than that with negative expression (70).

Androgen receptor (AR) is the mediator of androgen activity in normal and malignant prostate cells. The BRACHYURY protein level in the nucleus of primary prostate cancer cells is statistically associated with the presence of AR (70), and the enhanced AR expression in the nucleus may be activated by BRACHYURY protein (70). Moreover, a genome-wide analysis on AR in prostate cancer cells revealed that BRACHYURY binding motif is highly enriched in AR-bound promoter region (72), suggesting that BRACHYURY is involved in AR regulation on target.

Although androgen-targeted therapy demonstrates recognized a therapeutic benefit in advanced prostate cancer, following castration-resistant prostate cancer (CRPC) develops and tumor progression occurs due to the induced epithelial-to-mesenchymal plasticity (EMP) and neuroendocrine transdifferentiation (NEtD) programs by androgen deprivation (71, 72), the mechanism through which has yet to be elucidated. Overexpression of BRACHYURY is strongly associated with NEtD markers, including chromogranin A (CHGA) and synaptophysin (SYP) (70), and targeting *BRACHYURY*/BRACHYURY has become a potential promising option in such a tricky scenario. A phase I/II trial (NCT03493945) testing a BRACHYURY-targeted antitumor vaccine has been performed in metastatic CRPC recently (73).

Although the specific role of *BRACHYURY*/BRACHYURY on the tumorigenesis and progression of prostate cancer has been recognized, more details need to be further investigated and unveiled, for instance, the mechanism of *BRACHYURY* involved in NEtD, the biological significance of BRACHYURY binding with the regulatory elements of the marker genes (*AMACR, AR*) of prostate cancer.

Colorectal Cancer

BRACHYURY mRNA expression was found to elevate in tumors of the small intestine and in the majority of cell lines derived from the colon (16). Nearly 90% of the colorectal adenocarcinomas were immunohistochemically positive for BRACHYURY expression (74), which is demonstrated as distinct nucleus staining or widespread cytoplasmic staining (74, 75). The heterogeneity of BRACHYURY distribution suggests that it may have region-specific functions (75). High BRACHYURY expression correlates significantly with higher tumor stage, grade, and lymph node metastasis. Early-stage colorectal cancer samples (Dukes A) with BRACHYURY expression showed a significantly decreased survival and poor prognosis, while no correlation was observed in later tumor stages (74).

Oral Cancer

Immunohistochemical studies demonstrated that BRACHYURY was positively expressed in 71.0% of oral squamous cell carcinoma (OSCC), including cytoplasmic and nuclear staining (76). BRACHYURY expression in OSCC tissue is significantly associated with lymph node metastasis (76), distant metastasis, and Anneroth scores (77). High BRACHYURY expression is also significantly associated with decreased disease-specific survival and DFS in OSCC patients, which may represent a valuable prognostic marker of OSCC (76, 77).

THE MECHANISM OF BRACHYURY TO PROMOTE TUMOR PROGRESSION

Epithelial-to-Mesenchymal Transition

The process of EMT, converting immotile epithelial cells to migratory mesenchymal cells, is associated with enhancement of invasive and metastatic potential of tumor cells, as well as resistance to therapeutic interventions (78, 79). BRACHYURY has been identified as a driver of EMT in a wide variety of tumors, including lung cancer (59), breast cancer (66), prostate cancer (14), hepatocellular carcinoma (80), oral squamous cell carcinoma (76), adenoid cystic carcinoma (81), among others, which is responsible for the acquisition of mesenchymal-like phenotype and positively correlates with aggressive characteristics of tumor cells (9, 10, 14, 16, 81–83).

Some other mediators have been reported to be involved in tumor EMT process, such as Slug, Snail, MMPs, fibronectin, interleukin (IL)8, and transforming growth factor (TGF)-β1, among others. Various studies have attempted to investigate the correlation between the expressions of these genes and *BRACHYURY* (12, 84, 85). As mesenchymal markers, Snail and Slug have been shown to act as transcriptional repressors of E-cadherin expression during the EMT process (86, 87). Fernando et al. (10) reported BRACHYURY could directly bind to the T-box half-site consensus sequence (TCACACCT) located at the

promoter of E-cadherin, resulting in silencing of E-cadherin expression. BRACHYURY can directly enhance the Snail and Slug expression, through which can indirectly repress E-cadherin expression in several types of lung carcinoma cell lines (10, 82). In chordoma cells, loss of *BRACHYURY* resulted in a significant decrease of Snail and Slug (31, 49), and the upregulation of Snail and Slug by FGF2 was blocked by *BRACHYURY* knockdown, suggesting that BRACHYURY plays a critical role in the direct regulation of Snail and Slug expressions and EMT process of chordoma (31). BRACHYURY can directly bind with the T-Box binding sites at the promoter of Snail and fibronectin in prostate cancer cells (70).

Wan et al. (11) firstly revealed that BRACHYURY upregulated MMP12 expression in lung NSCLC cells to promote tumor cell migration and invasion, and a potential T-box binding site was found in the promoter of MMP12. In addition, Slug and IL-8 expressions were positively correlated with *BRACHYURY* expression at mRNA and protein levels in primary and metastatic lung tumor tissues and associated with poor prognosis (12, 58). In TNBC MDA-MB-436 cell line, silencing of *BRACHYURY* resulted in diminished vimentin and fibronectin expression and increased epithelial ZO1 expression (61). In prostate cancer cells, *BRACHYURY* expression was associated with a decrease of the epithelial marker and increased expression of mesenchymal signature genes, as well as upregulation of the MMP14, MMP24 (14, 70).

The Effect of BRACHYURY on Tumor Cell Proliferation and Cell Cycle

Regulating of cell cycle progression is another paramount mechanism to modulate tumor cell biological behavior (88). Various studies have reported divergent effects of BRACHYURY on cell proliferation. Some demonstrated BRACHYURY promoted tumor cell growth and proliferation *in vitro*, including chordoma, prostate cancer, colorectal cancer, adenoid cystic carcinoma, and breast carcinoma cells (14, 31, 40, 42, 49, 50, 60, 75, 81). Whereas, others showed that BRACHYURY inhibited tumor cell growth and proliferation, including breast carcinoma, lung, and colorectal cells (9, 10, 82). The lower proliferation rate may protect tumor cells from stressful conditions, such as nutrient deprivation and genotoxic injuries induced by radiation or chemotherapy (79), accordingly, attain a certain survival advantage. The reported divergent roles of BRACHYURY on cell proliferation in specific cell line, for instance, breast carcinoma cell lines, need to be further elucidated, whether it is cell type-dependent or context-dependent or other causes.

In regard to the mechanism by which BRACHYURY inhibits cell proliferation in lung carcinoma cells, Fernando et al. (10) has revealed BRACHYURY blocks the cell cycle progression likely at the G1-S transition through suppressing cyclin D1 expression and activity of cyclin/CDK complexes. Huang et al. (82) have reported BRACHYURY impairs cell cycle progression and reduces tumor cell proliferation by transcriptional silencing of P21, through directly binding with the T-box half-site binding sequence located at position −14 relative to the transcription initiation site in the promoter of P21.

THE TUMOR SUPPRESSOR ROLE OF BRACHYURY

Unlike the established oncogenic function in some types of solid tumors, BRACHYURY has been reported to play a tumor suppressor role in lung cancer (89) and glioma (90). Pinto et al. (90) recently reported that glioma patients with absence or low level of BRACHYURY were associated with tumor aggressiveness and poor survival. BRACHYURY could have different functions in tumorigenesis and progression depending on the cofactors and specific context.

CONCLUSION

The T-box transcription factor BRACHYURY, which is required for mesoderm formation and notochord development, has been recognized as a sensitive and fairly specific marker for chordoma and reported to be expressed in various types of tumors, especially in tumors of epithelial origin (lung, breast, prostate, colorectal, oral, et al.). BRACHYURY promotes tumor metastasis through modulating the EMT process and regulating cell cycle and closely correlates with patient poor prognosis. *BRACHYURY*/BRACHYURY has become an attractive target in the study of tumorigenesis and therapy not only because multiple signaling pathways converge to activate its expression (10) but also it regulates a complex downstream network. With the development of several clinical trials of therapeutic cancer vaccine (62, 91, 92), *BRACHYURY*/BRACHYURY will become a potential paramount target to help control advanced cancer populations.

AUTHOR CONTRIBUTIONS

All authors listed have made a substantial, direct, and intellectual contribution to the work and approved it for publication.

FUNDING

This work was supported by 333 talent project of Jiangsu province (BRA2017057) to JS and Foundation of Social Development in Jiangsu-Clinical Frontier Technology (Grant No. BE2017661) to JS.

REFERENCES

1. Papaioannou VE, Silver LM. The T-box gene family. *Bioessays.* (1998) 20:9–19.
2. Müller CW, Herrmann BG. Crystallographic structure of the T domain-DNA complex of the brachyury transcription factor. *Nature.* (1997) 389:884–8. doi: 10.1038/39929

3. Showell C, Binder O, Conlon FL. T-box genes in early embryogenesis. *Dev Dyn.* (2004) 229:201–18. doi: 10.1002/dvdy.10480
4. Herrmann BG, Labeit S, Poustka A, King TR, Lehrach H. Cloning of the T gene required in mesoderm formation in the mouse. *Nature.* (1990) 343:617–22. doi: 10.1038/343617a0
5. Kispert A, Herrmann BG, Leptin M, Reuter R. Homologs of the mouse brachyury gene are involved in the specification of posterior terminal structures in *Drosophila*, *Tribolium*, and *Locusta*. *Genes Dev.* (1994) 8:2137–50. doi: 10.1101/gad.8.18.2137
6. Di Gregorio A. T-Box genes and developmental gene regulatory networks in ascidians. *Curr Top Dev Biol.* (2017) 122:55–91. doi: 10.1016/bs.ctdb.2016.08.007
7. Morley RH, Lachani K, Keefe D, Gilchrist MJ, Flicek P, Smith JC, et al. A gene regulatory network directed by zebrafish no tail accounts for its roles in mesoderm formation. *Proc Natl Acad Sci USA.* (2009) 106:3829–34. doi: 10.1073/pnas.0808382106
8. Miettinen M, Wang Z, Lasota J, Heery C, Schlom J, Palena C. Nuclear brachyury expression is consistent in chordoma, common in germ cell tumors and small cell carcinomas, and rare in other carcinomas and sarcomas: an immunohistochemical study of 5229 cases. *Am J Surg Pathol.* (2015) 39:1305–12. doi: 10.1097/PAS.0000000000000462
9. Palena C, Roselli M, Litzinger MT, Ferroni P, Costarelli L, Spila A, et al. Overexpression of the EMT driver brachyury in breast carcinomas: association with poor prognosis. *J Natl Cancer Inst.* (2014) 106:dju054. doi: 10.1093/jnci/dju054
10. Fernando RI, Litzinger M, Trono P, Hamilton DH, Schlom J, Palena C. The T-box transcription factor brachyury promotes epithelial-mesenchymal transition in human tumor cells. *J Clin Invest.* (2010) 120:533–44. doi: 10.1172/JCI38379
11. Wan Z, Jiang D, Chen S, Jiao J, Ji L, Shah AS, et al. T-box transcription factor brachyury promotes tumor cell invasion and metastasis in non-small cell lung cancer via upregulation of matrix metalloproteinase 12. *Oncol Rep.* (2016) 36:306–14. doi: 10.3892/or.2016.4792
12. Haro A, Yano T, Kohno M, Yoshida T, Koga T, Okamoto T, et al. Expression of brachyury gene is a significant prognostic factor for primary lung carcinoma. *Ann Surg Oncol.* (2013) 20(Suppl. 3) S509–16. doi: 10.1245/s10434-013-2914-9
13. Sarkar D, Shields B, Davies ML, Müller J, Wakeman JA. Brachyury confers cancer stem cell characteristics on colorectal cancer cells. *Int J Cancer.* (2012) 130:328–37. doi: 10.1002/ijc.26029
14. Pinto F, Pertega-Gomes N, Pereira MS, Vizcaino JR, Monteiro P, Henrique RM, et al. T-box transcription factor brachyury is associated with prostate cancer progression and aggressiveness. *Clin Cancer Res.* (2014) 20:4949–61. doi: 10.1158/1078-0432.CCR-14-0421
15. Tirabosco R, Mangham DC, Rosenberg AE, Vujovic S, Bousdras K, Pizzolitto S, et al. Brachyury expression in extra-axial skeletal and soft tissue chordomas: a marker that distinguishes chordoma from mixed tumor/myoepithelioma/parachordoma in soft tissue. *Am J Surg Pathol.* (2008) 32:572–80. doi: 10.1097/PAS.0b013e31815b693a
16. Palena C, Polev DE, Tsang KY, Fernando RI, Litzinger M, Krukovskaya LL, et al. The human T-box mesodermal transcription factor brachyury is a candidate target for T-cell-mediated cancer immunotherapy. *Clin Cancer Res.* (2007) 13:2471–8. doi: 10.1158/1078-0432.CCR-06-2353
17. Roselli M, Fernando RI, Guadagni F, Spila A, Alessandroni J, Palmirotta R, et al. Brachyury, a driver of the epithelial-mesenchymal transition, is overexpressed in human lung tumors: an opportunity for novel interventions against lung cancer. *Clin Cancer Res.* (2012) 18:3868–79. doi: 10.1158/1078-0432.CCR-11-3211
18. Shah SR, David JM, Tippens ND, Mohyeldin A, Martinez-Gutierrez JC, Ganaha S, et al. Brachyury-YAP regulatory axis drives stemness and growth in cancer. *Cell Rep.* (2017) 21 495–507. doi: 10.1016/j.celrep.2017.09.057
19. Schulte-Merker S, Ho RK, Herrmann BG, Nüsslein-Volhard C. The protein product of the zebrafish homologue of the mouse T gene is expressed in nuclei of the germ ring and the notochord of the early embryo. *Development.* (1992) 116:1021–32.
20. Hotta K, Takahashi H, Asakura T, Saitoh B, Takatori N, Satou Y, et al. Characterization of brachyury-downstream notochord genes in the *Ciona* intestinalis embryo. *Dev Biol.* (2000) 224:69–80. doi: 10.1006/dbio.2000.9765
21. Romeo S, Hogendoorn PC. Brachyury and chordoma: the chondroid-chordoid dilemma resolved. *J Pathol.* (2006) 209:143–6. doi: 10.1002/path.1987
22. Salisbury JR. The pathology of the human notochord. *J Pathol.* (1993) 171:253–5. doi: 10.1002/path.1711710404
23. Kispert A, Hermann BG. The Brachyury gene encodes a novel DNA binding protein. *EMBO J.* (1993) 12:4898–9.
24. Ciruna BG, Schwartz L, Harpal K, Yamaguchi TP, Rossant J. Chimeric analysis of fibroblast growth factor receptor-1 (Fgfr1) function: a role for FGFR1 in morphogenetic movement through the primitive streak. *Development.* (1997) 124:2829–41.
25. Umbhauer M, Marshall CJ, Mason CS, Old RW, Smith JC. Mesoderm induction in *Xenopus* caused by activation of MAP kinase. *Nature.* (1995) 376:58–62. doi: 10.1038/376058a0
26. Nakatani Y, Yasuo H, Satoh N, Nishida H. Basic fibroblast growth factor induces notochord formation and the expression of As-T, a brachyury homolog, during ascidian embryogenesis. *Development.* (1996) 122:2023–31.
27. Schulte-Merker S, Smith JC. Mesoderm formation in response to brachyury requires FGF signalling. *Curr Biol.* (1995) 5:62–7. doi: 10.1016/S0960-9822(95)00017-0
28. Latinkić BV, Umbhauer M, Neal KA, Lerchner W, Smith JC, Cunliffe V. The *Xenopus* brachyury promoter is activated by FGF and low concentrations of activin and suppressed by high concentrations of activin and by paired-type homeodomain proteins. *Genes Dev.* (1997) 11:3265–76.
29. Isaacs HV, Pownall ME, Slack JM. eFGF regulates Xbra expression during *Xenopus* gastrulation. *EMBO J.* (1994) 13:4469–81.
30. Matsumoto J, Kumano G, Nishida H. Direct activation by Ets and Zic is required for initial expression of the brachyury gene in the ascidian notochord. *Dev Biol.* (2007) 306:870–82. doi: 10.1016/j.ydbio.2007.03.034
31. Hu Y, Mintz A, Shah SR, Quinones-Hinojosa A, Hsu W. The FGFR/MEK/ERK/brachyury pathway is critical for chordoma cell growth and survival. *Carcinogenesis.* (2014) 35:1491–9. doi: 10.1093/carcin/bgu014
32. Hu Y, Feng X, Mintz A, Petty WJ, Hsu W. Regulation of brachyury by fibroblast growth factor receptor 1 in lung cancer. *Oncotarget.* (2016) 7:87124–35. doi: 10.18632/oncotarget.13547
33. Vidricaire G, Jardine K, McBurney MW. Expression of the brachyury gene during mesoderm development in differentiating embryonal carcinoma cell cultures. *Development.* (1994)120:115–22.
34. Arnold SJ, Robertson EJ. Making a commitment: cell lineage allocation and axis patterning in the early mouse embryo. *Nat Rev Mol Cell Biol.* (2009) 10:91–103. doi: 10.1038/nrm2618
35. Cho MS, Chan IL, Flores ER. ΔNp63 transcriptionally regulates brachyury, a gene with diverse roles in limb development, tumorigenesis and metastasis. *Cell Cycle.* (2010) 9:2434–41. doi: 10.4161/cc.9.12.12051
36. Mazzotta S, Neves C, Bonner RJ, Bernardo AS, Docherty K, Hoppler S. Distinctive roles of canonical and noncanonical Wnt signaling in human embryonic cardiomyocyte development. *Stem Cell Rep.* (2016) 7:764–76. doi: 10.1016/j.stemcr.2016.08.008
37. Satoh N, Tagawa K, Takahashi H. How was the notochord born. *Evol Dev.* (2012) 14:56–75. doi: 10.1111/j.1525-142X.2011.00522.x
38. Takahashi H, Hotta K, Erives A, Gregorio AD, Zeller RW, Levine M, et al. Brachyury downstream notochord differentiation in the ascidian embryo. *Genes Dev.* (1999) 13:1519–23. doi: 10.1101/gad.13.12.1519
39. Katikala L, Aihara H, Passamaneck YJ, Gazdoiu S, José-Edwards DS, Kugler JE, et al. Functional brachyury binding sites establish a temporal read-out of gene expression in the Ciona notochord. *PLoS Biol.* (2013) 11:e1001697. doi: 10.1371/journal.pbio.1001697
40. Nelson AC, Pillay N, Henderson S, Presneau N, Tirabosco R, Halai D, et al. An integrated functional genomics approach identifies the regulatory network directed by brachyury (T) in chordoma. *J Pathol.* (2012) 228:274–85. doi: 10.1002/path.4082
41. Dong J, Feldmann G, Huang J, Wu S, Zhang N, Comerford SA, et al. Elucidation of a universal size-control mechanism in *Drosophila* and mammals. *Cell.* (2007) 130:1120–33. doi: 10.1016/j.cell.2007.07.019
42. Walcott BP, Nahed BV, Mohyeldin A, Coumans JV, Kahle KT, Ferreira MJ. Chordoma: current concepts, management, and future directions. *Lancet Oncol.* (2012) 13:e69–76. doi: 10.1016/S1470-2045(11)70337-0

43. Henderson SR, Guiliano D, Presneau N, McLean S, Frow R, Vujovic S, et al. A molecular map of mesenchymal tumors. *Genome Biol.* (2005) 6:R76. doi: 10.1186/gb-2005-6-9-r76
44. Vujovic S, Henderson S, Presneau N, Odell E, Jacques TS, Tirabosco R, et al. Brachyury, a crucial regulator of notochordal development, is a novel biomarker for chordomas. *J Pathol.* (2006) 209:157–65. doi: 10.1002/path.1969
45. Oakley GJ, Fuhrer K, Seethala RR. Brachyury, SOX-9, and podoplanin, new markers in the skull base chordoma vs chondrosarcoma differential: a tissue microarray-based comparative analysis. *Mod Pathol.* (2008) 21:1461–9. doi: 10.1038/modpathol.2008.144
46. O'donnell P, Tirabosco R, Vujovic S, Bartlett W, Briggs TWR, Henderson S, et al. Diagnosing an extra-axial chordoma of the proximal tibia with the help of brachyury, a molecule required for notochordal differentiation. *Skelet Radiol.* (2007) 36:59–65. doi: 10.1007/s00256-006-0167-4
47. Shen J, Li CD, Yang HL, Lu J, Zou TM, Wang DL, et al. Classic chordoma coexisting with benign notochordal cell rest demonstrating different immunohistological expression patterns of brachyury and galectin-3. *J Clin Neurosci.* (2011) 18:96–9. doi: 10.1016/j.jocn.2010.03.066
48. Shen J, Shi Q, Lu J, Wang DL, Zou TM, Yang HL, et al. Histological study of chordoma origin from fetal notochordal cell rests. *Spine*. (2013) 38:2165–70. doi: 10.1097/BRS.0000000000000010
49. Hsu W, Mohyeldin A, Shah SR, Rhys CM, Johnson LF, Sedora-Roman NI, et al. Generation of chordoma cell line JHC7 and the identification of brachyury as a novel molecular target. *J Neurosurg.* (2011) 115:760–9. doi: 10.3171/2011.5.JNS11185
50. Presneau N, Shalaby A, Ye H, Pillay N, Halai D, Idowu B, et al. Role of the transcription factor T (brachyury) in the pathogenesis of sporadic chordoma: a genetic and functional-based study. *J Pathol.* (2011) 223:327–35. doi: 10.1002/path.2816
51. Yang XR, Ng D, Alcorta DA, Liebsch NJ, Sheridan E, Li S, et al. T (brachyury) gene duplication confers major susceptibility to familial chordoma. *Nat Genet*. (2009) 41:1176–8. doi: 10.1038/ng.454
52. Kelley MJ, Shi J, Ballew B, Hyland PL, Li WQ, Rotunno M, et al. Characterization of T gene sequence variants and germline duplications in familial and sporadic chordoma. *Hum Genet*. (2014) 133:1289–97. doi: 10.1007/s00439-014-1463-z
53. Dei Tos AP. Unveiling the molecular pathogenesis of chordoma: a new paradigm for molecular targeting of rare cancers. *J Pathol.* (2011) 223:565–6. doi: 10.1002/path.2847
54. Pillay N, Plagnol V, Tarpey PS, Lobo SB, Presneau N, Szuhai K, et al. A common single-nucleotide variant in T is strongly associated with chordoma. *Nat Genet.* (2012) 44:1185–7. doi: 10.1038/ng.2419
55. Sharifnia T, Wawer MJ, Chen T, Huang QY, Weir BA, Sizemore A, et al. Small-molecule targeting of brachyury transcription factor addiction in chordoma. *Nat Med.* (2019) 25:292–300. doi: 10.1038/s41591-018-0312-3
56. Chen S, Jiao J, Jiang D, Wan Z, Li L, Li K, et al. T-box transcription factor Brachyury in lung cancer cells inhibits macrophage infiltration by suppressing CCL2 and CCL4 chemokines. *Tumour Biol.* (2015) 36:5881–90. doi: 10.1007/s13277-015-3260-2
57. Hamilton DH, Fernando RI, Schlom J, Palena C. Aberrant expression of the embryonic transcription factor brachyury in human tumors detected with a novel rabbit monoclonal antibody. *Oncotarget*. (2015) 6:4853–62. doi: 10.18632/oncotarget.3086
58. Shimamatsu S, Okamoto T, Haro A, Kitahara H, Kohno M, Morodomi Y, et al. Prognostic significance of expression of the epithelial-mesenchymal transition-related factor brachyury in intrathoracic lymphatic spread of non-small cell lung cancer. *Ann Surg Oncol.* (2016) 23(Suppl. 5):1012–20. doi: 10.1245/s10434-016-5530-7
59. Xu K, Liu B, Liu Y. Impact of brachyury on epithelial-mesenchymal transitions and chemosensitivity in non-small cell lung cancer. *Mol Med Rep.* (2015) 12:995–1001. doi: 10.3892/mmr.2015.3348
60. Chen M, Zou S, He C, Zhou J, Li S, Shen M, et al. Transactivation of SOX5 by Brachyury promotes breast cancer bone metastasis. *Carcinogenesis.* (2019). doi: 10.1093/carcin/bgz142. [Epub ahead of print].
61. Hamilton DH, Roselli M, Ferroni P, Costarelli L, Cavaliere F, Taffuri M, et al. Brachyury, a vaccine target, is overexpressed in triple-negative breast cancer. *Endocr Relat Cancer.* (2016) 23:783–96. doi: 10.1530/ERC-16-0037
62. Heery CR, Singh BH, Rauckhorst M, Marté JL, Donahue RN, Grenga I, et al. Phase I trial of a yeast-based therapeutic cancer vaccine (GI-6301) Targeting the transcription factor brachyury. *Cancer Immunol Res.* (2015)3:1248–56. doi: 10.1158/2326-6066.CIR-15-0119
63. Li K, Ying M, Feng D, Du J, Chen S, Dan B, et al. Brachyury promotes tamoxifen resistance in breast cancer by targeting SIRT1. *Biomed Pharmacother.* (2016) 84:28–33. doi: 10.1016/j.biopha.2016.09.011
64. Li K, Ying M, Feng D, Chen Y, Wang J, Wang Y. SMC1 promotes epithelial-mesenchymal transition in triple-negative breast cancer through upregulating brachyury. *Oncol Rep.* (2016) 35:2405–12. doi: 10.3892/or.2016.4564
65. Pires MM, Aaronson SA. Brachyury: a new player in promoting breast cancer aggressiveness. *J Natl Cancer Inst.* (2014) 106:dju094. doi: 10.1093/jnci/dju094
66. Shao C, Zhang J, Fu J, Ling F. The potential role of Brachyury in inducing epithelial-to-mesenchymal transition (EMT) and HIF-1α expression in breast cancer cells. *Biochem Biophys Res Commun.* (2015) 467:1083–9. doi: 10.1016/j.bbrc.2015.09.076
67. Anderson WF, Chu KC, Chatterjee N, Brawley O, Brinton LA. Tumor variants by hormone receptor expression in white patients with node-negative breast cancer from the surveillance, epidemiology, and end results database. *J Clin Oncol.* (2001) 19:18–27. doi: 10.1200/JCO.2001.19.1.18
68. Lee KH, Kim EY, Yun JS, Park YL, Do SI, Chae SW, et al. Prognostic significance of expression of epithelial-mesenchymal transition driver brachyury in breast cancer and its association with subtype and characteristics. *Oncol Lett.* (2018) 15:1037–45. doi: 10.3892/ol.2017.7402
69. Thoma C. Prostate cancer: brachyury–a biomarker for progression and prognosis. *Nat Rev Urol.* (2014) 11:485. doi: 10.1038/nrurol.2014.184
70. Pinto F, Pértega-Gomes N, Vizcaíno JR, Andrade RP, Cárcano FM, Reis RM. Brachyury as a potential modulator of androgen receptor activity and a key player in therapy resistance in prostate cancer. *Oncotarget.* (2016) 7:28891–902. doi: 10.18632/oncotarget.8499
71. Nouri M, Ratther E, Stylianou N, Nelson CC, Hollier BG, Williams ED. Androgen-targeted therapy-induced epithelial mesenchymal plasticity and neuroendocrine transdifferentiation in prostate cancer: an opportunity for intervention. *Front Oncol.* (2014) 4:370. doi: 10.3389/fonc.2014.00370
72. Perets R, Kaplan T, Stein I, Hidas G, Tayeb S, Avraham E, et al. Genome-wide analysis of androgen receptor targets reveals COUP-TF1 as a novel player in human prostate cancer. *PLoS ONE.* (2012) 7:e46467. doi: 10.1371/journal.pone.0046467
73. Redman JM, Steinberg SM, Gulley JL. Quick efficacy seeking trial (QuEST1): a novel combination immunotherapy study designed for rapid clinical signal assessment metastatic castration-resistant prostate cancer. *J Immunother Cancer.* (2018) 6:91. doi: 10.1186/s40425-018-0409-8
74. Kilic N, Feldhaus S, Kilic E, Tennstedt P, Wicklein D, Rv W, et al. Brachyury expression predicts poor prognosis at early stages of colorectal cancer. *Eur J Cancer.* (2011) 47:1080–5. doi: 10.1016/j.ejca.2010.11.015
75. Jezkova J, Williams JS, Jones-Hutchins F, Sammut SJ, Gollins S, Cree I, et al. Brachyury regulates proliferation of cancer cells via a p27Kip1-dependent pathway. *Oncotarget.* (2014) 5:3813–22. doi: 10.18632/oncotarget.1999
76. Imajyo I, Sugiura T, Kobayashi Y, Shimoda M, Ishii K, Akimoto N, et al. T-box transcription factor brachyury expression is correlated with epithelial-mesenchymal transition and lymph node metastasis in oral squamous cell carcinoma. *Int J Oncol.* (2012) 41:1985–95. doi: 10.3892/ijo.2012.1673
77. Yoshihama R, Yamaguchi K, Imajyo I, Mine M, Hiyake N, Akimoto N, et al. Expression levels of SOX2, KLF4 and brachyury transcription factors are associated with metastasis and poor prognosis in oral squamous cell carcinoma. *Oncol Lett.* (2016) 11:1435–46. doi: 10.3892/ol.2015.4047
78. Das V, Bhattacharya S, Chikkaputtaiah C, Hazra S, Pal M. The basics of epithelial-mesenchymal transition (EMT): a study from a structure, dynamics, and functional perspective. *J Cell Physiol.* (2019) 243:14535–55. doi: 10.1002/jcp.28160
79. Palena C, Fernando RI, Litzinger MT, Hamilton DH, Huang B, Schlom J. Strategies to target molecules that control the acquisition of a mesenchymal-like phenotype by carcinoma cells. *Exp Biol Med*. (2011) 236:537–45. doi: 10.1258/ebm.2011.010367
80. Du R, Wu S, Lv X, Fang H, Wu S, Kang J. Overexpression of brachyury contributes to tumor metastasis by inducing epithelial-mesenchymal transition in hepatocellular carcinoma. *J Exp Clin Cancer Res.* (2014) 33:105. doi: 10.1186/s13046-014-0105-6

81. Shimoda M, Sugiura T, Imajyo I, Ishii K, Chigita S, Seki K, et al. The T-box transcription factor brachyury regulates epithelial-mesenchymal transition in association with cancer stem-like cells in adenoid cystic carcinoma cells. *BMC Cancer.* (2012) 12:377. doi: 10.1186/1471-2407-12-377
82. Huang B, Cohen JR, Fernando RI, Hamilton DH, Litzinger MT, Hodge JW, et al. The embryonic transcription factor brachyury blocks cell cycle progression and mediates tumor resistance to conventional antitumor therapies. *Cell Death Dis.* (2013) 4:e682. doi: 10.1038/cddis.2013.208
83. Zhu J, Kwan KM, Mackem S. Putative oncogene Brachyury (T) is essential to specify cell fate but dispensable for notochord progenitor proliferation and EMT. *Proc Natl Acad Sci USA.* (2016) 113:3820–5. doi: 10.1073/pnas.1601252113
84. Larocca C, Cohen JR, Fernando RI, Huang B, Hamilton DH, Palena C. An autocrine loop between TGF-β1 and the transcription factor brachyury controls the transition of human carcinoma cells into a mesenchymal phenotype. *Mol Cancer Ther.* (2013) 12:1805–15. doi: 10.1158/1535-7163.MCT-12-1007
85. Fernando RI, Castillo MD, Litzinger M, Hamilton DH, Palena C. IL-8 signaling plays a critical role in the epithelial-mesenchymal transition of human carcinoma cells. *Cancer Res.* (2011) 71:5296–306. doi: 10.1158/0008-5472.CAN-11-0156
86. Cano A, Pérez-Moreno MA, Rodrigo I, Locascio A, Blanco MJ, del Barrio MG, et al. The transcription factor snail controls epithelial-mesenchymal transitions by repressing E-cadherin expression. *Nat Cell Biol.* (2000) 2:76–83. doi: 10.1038/35000025
87. Huber MA, Kraut N, Beug H. Molecular requirements for epithelial-mesenchymal transition during tumor progression. *Curr Opin Cell Biol.* (2005) 17:548–58. doi: 10.1016/j.ceb.2005.08.001
88. Pei H, Hu W, Guo Z, Chen H, Ma J, Mao W, et al. Long Noncoding RNA CRYBG3 Blocks cytokinesis by directly binding G-actin. *Cancer Res.* (2018) 78:4563–72. doi: 10.1158/0008-5472.CAN-18-0988
89. Park JC, Chae YK, Son CH, Kim MS, Lee J, Ostrow K, et al. Epigenetic silencing of human T (brachyury homologue) gene in non-small-cell lung cancer. *Biochem Biophys Res Commun.* (2008) 365:221–6. doi: 10.1016/j.bbrc.2007.10.144
90. Pinto F, Costa ÂM, Santos GC, Matsushita MM, Costa S, Silva VA, et al. The T-box transcription factor brachyury behaves as a tumor suppressor in gliomas. *J Pathol.* (2020) 251:87–99. doi: 10.1002/path.5419
91. Hamilton DH, Litzinger MT, Jales A, Huang B, Fernando RI, Hodge JW, et al. Immunological targeting of tumor cells undergoing an epithelial-mesenchymal transition via a recombinant brachyury-yeast vaccine. *Oncotarget.* (2013) 4:1777–90. doi: 10.18632/oncotarget.1295
92. Heery CR, Palena C, McMahon S, Donahue RN, Lepone LM, Grenga I, et al. Phase I study of a poxviral TRICOM-based vaccine directed against the transcription factor brachyury. *Clin Cancer Res.* (2017) 23:6833–45. doi: 10.1158/1078-0432.CCR-17-1087

Conflict of Interest: The authors declare that the research was conducted in the absence of any commercial or financial relationships that could be construed as a potential conflict of interest.

frontiers in Oncology

ORIGINAL RESEARCH
published: 03 July 2020
doi: 10.3389/fonc.2020.01078

The Role of Transcriptional Factor Brachyury on Cell Cycle Regulation in Non-small Cell Lung Cancer

Jingyi Xu[1†], Ming Chen[2†], Yinghui Wu[1†], Hong Zhang[1], Jundong Zhou[3], Donglai Wang[1], Tianming Zou[1] and Jun Shen[1]*

[1] Department of Orthopeadic Surgery, The Affiliated Suzhou Hospital of Nanjing Medical University, Suzhou Municipal Hospital, Suzhou, China, [2] Department of Orthopeadic Surgery, The Affiliated Wuxi No. 2 People's Hospital of Nanjing Medical University, Wuxi, China, [3] Suzhou Cancer Center Core Laboratory, The Affiliated Suzhou Hospital of Nanjing Medical University, Suzhou Municipal Hospital, Suzhou, China

OPEN ACCESS

Edited by:
Hailong Pei,
Soochow University, China

Reviewed by:
Dong Pan,
Duke University, United States
Meijuan Zhou,
Southern Medical University, China

***Correspondence:**
Jun Shen
18112603158@163.com

[†]These authors have contributed equally to this work

Specialty section:
This article was submitted to Molecular and Cellular Oncology, a section of the journal Frontiers in Oncology

Received: 28 February 2020
Accepted: 29 May 2020
Published: 03 July 2020

Citation:
Xu J, Chen M, Wu Y, Zhang H, Zhou J, Wang D, Zou T and Shen J (2020) The Role of Transcriptional Factor Brachyury on Cell Cycle Regulation in Non-small Cell Lung Cancer. Front. Oncol. 10:1078. doi: 10.3389/fonc.2020.01078

Lung cancer is the leading cause of cancer-related death, and non-small cell lung cancer (NSCLC) accounts for almost 80–85% of all lung cancer cases. The transcriptional factor brachyury has been verified to promote tumor cells migrate, invade, and metastasis in various types of tumors, whereas divergent roles of brachyury on cell proliferation have been reported in several types of tumor cells. In this study, we attempted to explore the effect of brachyury on the cell cycle progression and proliferation capability of NSCLC cells. Firstly, we performed RNA-sequence and ChIP-sequence to explore underlying downstream pathways regulated by brachyury. Cell proliferation and colony formation assays were utilized to detect the effect of brachyury on the proliferation ability of two types of lung NSCLC cells: H460 and Calu-1, which represent different brachyury expression levels. Following cell cycle and cell apoptosis assays were used to investigate the mechanism by which brachyury promotes NSCLC grow and progression. RNA-sequence and ChIP-sequence (ChIP-seq) showed that one of the vital downstream pathways regulated by brachyury involves in cell cycle progression. Through cell proliferation assays and colony formation assays, we found that inhibition of brachyury could decrease the capability of proliferation in H460 cells. We also found that brachyury overexpression could prevent the transition from G0/G1 to S phase in Calu-1 cells, and brachyury knockdown could decrease the transition of G2/M phase in H460 cells. The cell apoptosis assays showed that inhibition of brachyury could promote apoptosis in H460 cells. In this study we demonstrate that brachyury and downstream target genes together involve in tumor cell cycle regulation by inducing accelerated transition through G2/M, promote tumor cell proliferation and inhibit apoptosis in lung NSCLC H460 cells. Targeting brachyury expression could be developed into a promising avenue for the prevention of lung cancer progression.

Keywords: brachyury, lung cancer, NSCLC, transcriptional factor, tumorigenesis

INTRODUCTION

Lung cancer is the leading cause of cancer-related death in both men and women, non-small cell lung cancer (NSCLC) accounts for almost 80–85% of all lung cancer cases (1). Histologically, NSCLC is mainly divided into adenocarcinoma, squamous cell carcinoma and large cell carcinoma. Different subtype has specific molecular and genomic signature that drives the progression and metastasis of tumor cells.

The human brachyury protein (Bry), the transcriptional factor regulating posterior mesoderm formation and notochord differentiation, has been reported as a specific and sensitive marker (2–5) and a master regulator of the oncogenic transcriptional network of chordoma (6). Further studies demonstrated up-regulation of *brachyury* gene occurs in various human tumors of epithelial origin, including lung, breast, colorectal, prostate cancer and others, but not in the majority of normal adult tissues (7–9). In primary lung carcinoma samples, brachyury mRNA expression was identified as a significant predictor in 5 year disease free survival and overall survival rate (10) and positively correlated with tumor stage and poor prognosis (8, 10, 11). Silencing of brachyury expression significantly diminished migratory, invasive and metastatic ability in endogenously positive lung cancer cells *in vitro* (8, 11), which suggests brachyury can be developed into a potential therapeutic target in anti-tumor treatment of lung cancer.

Several previous studies have demonstrated that brachyury drives epithelial-mesenchymal transition (EMT) in various types of human tumor cells, including lung carcinoma, breast carcinoma, among others, to promote progression and metastasis (8, 9, 12). In addition, as a master regulator, brachyury governs an elaborate oncogenic transcriptional network involving diverse signaling pathways (12), by one of which brachyury implicates in controlling cell cycle and regulating proliferation and apoptosis (8, 13, 14). Brachyury expression levels vary a lot among different subtypes of NSCLC tissue and cell lines, ranging from strong to almost no expression (15). Therefore, the role of brachyury in specific NSCLC subtype could be different and context-dependent.

Our previous study on the breast cancer cells (9) uncovered that brachyury promote tumor cell proliferate *in vitro* and *in vivo*. Whereas, another study by Palena et al. (16) demonstrated that silencing of brachyury in MDA-MB-436 cells significantly enhanced the proliferation ability of tumor cells, which means brachyury play an opposite role of what we reported. In regard to lung cancer cells, some studies demonstrated brachyury inhibits tumor cells grow and proliferate (8, 13). But recently Hu et al. (17) showed upregulated brachyury increases lung cancer cell growth and invasion. The cause of the divergent role played by brachyury on lung cancer cell proliferation still remains unclear. In this study, we attempted to explore the potential mechanism from the perspective of cell cycle regulation, which is one of the paramount downstream pathways regulated by brachyury.

MATERIALS AND METHODS

Cell Lines and Cell Culture

Human large cell lung cancer cell line H460, Human lung cancer cell line Calu-1 were purchased from the State Key Laboratory of radiation medicine and radiation protection (Suzhou, China). H460 cells and Calu-1 cells were cultured in RPMI-1640 medium. The media (Gibco, Suzhou, China) were supplemented with 10% fetal bovine serum (FBS, Gibco, Australia) and 1% antibiotics (Penicillin-Streptomycin). Cells were incubated in a humidified atmosphere at 37°C and 5% CO_2.

RNA-Seq Transcriptome Analysis

Total RNA from MDA-MB-231 shNC/shBry was prepared and kept at 80°C. The RNA quality was determined using a Bioanalyzer 2200 (Agilent, Santa Clara, CA, USA). RNA with RIN (RNA integrity number)>8.0 was considered acceptable for cDNA library construction. Sequencing and bioinformatic analysis were performed by Shanghai Novelbio. Genes were considered to be significantly differentially expressed between groups when the $P < 0.05$ and the fold change of expression was more than 1.5.

Chromatin Immunoprecipitation and Sequencing

To explore the underlying mechanisms of brachyury in lung cancer cells, Chromatin immunoprecipitation and sequencing (ChIP-seq) using wildtype MDA-MB-231 cells was performed. The ChIP assay kit (Millipore) was used to perform the ChIP assay. The anti-Bry antibodies used in this assay were purchased from R&D Systems (Bio-Techne, Minneapolis, MN). The Qubit® Fluorometer was used to determine the purity and concentration of DNA samples. TruSeq Nano DNA Sample Prep Kit (#FC-121–4002, Illumina, San Diego, CA) was used to end repair, tail and adaptor ligate DNA samples. AMPure XP beads were used to select the fragments of ∼200–1,500 bp. The samples were diluted to a final concentration of 8 pM and cluster generation was then performed on the Illumina cBot using a HiSeq 3000/4000 PE Cluster Kit (#PE-410–1001, Illumina). Last, HiSeq 3000/4000 SBS Kit (300 cycles; #FC-410–1003, Illumina) was used to perform the sequencing on an Illumina HiSeq 4000. The data were then collected and analyzed.

Construction of Cell Lines

To construct brachyury overexpression/knockdown cell lines, viral particles containing a small interfering RNA (siRNA-1 and siRNA-2) targeting brachyury or the human brachyury coding region purchased from GenePharma (Suzhou, China) were utilized in H460 cells and Calu-1 cells. The cell lines were constructed as described (9, 18) previously and validated using western blotting (siRNA-1: CGAATCCACATAGTGA GAGTT; siRNA-2: GAGGATGTTTCCGGTGCTGAA; siRNA-Control: TTCTCCGAACGTGTCACGT).

Protein Extraction and Western Blotting

Total protein from lung cancer cells was extracted using a mammalian protein extraction reagent (MPER, Thermo

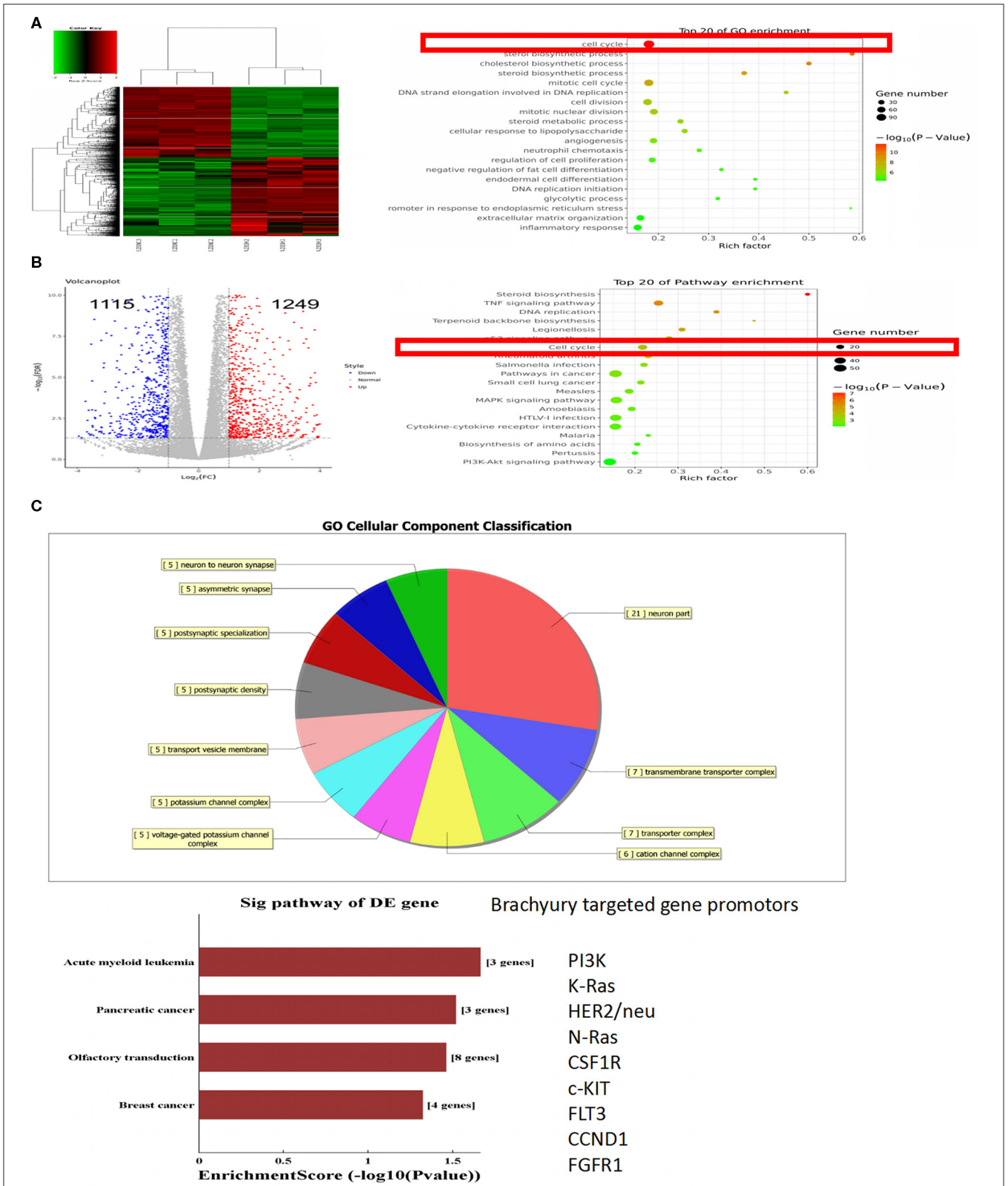

FIGURE 1 | RNA-sequence and ChIP-sequence analyses of MDA-MB-231 cells. **(A)** Heat map of differentially expressed transcripts, Gene ontology (GO) analysis, and **(B)** pathway analysis, based on all identified transcripts. **(C)** Cellular component classification analysis and targeted genes of ChIP-seq. *P*-value of GO analysis and enrichment of pathway analysis are listed for each category. *P*-value of pathway is colored in red ($P < 0.05$).

Fisher Scientific, Waltham, MA, USA) containing a protease inhibitor cocktail (Thermo Fisher Scientific). An equivalent amount of protein was electrophoresed using 10% SDS gel electrophoresis and then transferred to the polyvinylidene fluoride (PVDF) membrane (Millipore, Billerica, MA, USA). The membranes were blocked with 5% skimmed milk for 1 h, and then incubated overnight with primary antibodies. The membranes were washed 3 times and incubated with secondary antibodies (Anti-Brachyury ab20680, Multi-sciences Biotechnology, Zhejiang, China). The membranes were then visualized using a chemiluminescence (ECL) (Multi-sciences Biotechnology) detection system. The primary antibodies used included anti-Brachyury (Abcam) and anti-GAPDH-HRP (MultiSciences, Zhejiang, China).

Cell Proliferation Assay

Cell counting plates were used to detect cell proliferation after transfection. 3×10^3 Calu-1 and H460 cells were seeded in 24-well plates and allowed to adhere. Cell viability was measured every day for 4 days using Cell Counting Kit-8 (Dojindo Laboratories, Kumamoto, Japan) according to the manufacturer's instructions. All results were recorded and the cell proliferation curves were drawn.

Colony Formation Assay

1×10^2 Calu-1 (Calu-1 Bry cells and NC cells) and H460 cells (H460 siBry-1 cells, siBry-2 cells and siNC cells) were used to perform the colony formation assay. Cells were cultured in the RPMI-1640 medium containing 10% fetal bovine serum and 1% antibiotics for 10 days. The remaining colonies were stained with crystal violet and then recorded.

Cell Cycle Assay

Cells (2×10^5) were harvested at 24 h after siRNA transfection, and fixed with cold 70% alcohol at-20°C overnight. Alcohol was removed and cells were washed twice with cold phosphate buffer saline (PBS). Cells were stained with propidium iodide solution containing 20 μg/ml RNase and incubated at room temperature for 30 min. After filtering by a nylon mesh filter, cell cycle was performed on a fluorescence-activated cell sorting (FACS, FACSVerse) analysis. Data were analyzed using the Flowjo software (Version 7.6.1, Tree Star Software, San Carlos, CA, USA).

Cell Apoptosis Assay

Sub-G1 Method

Calu-1 and H460 cells were first seeded in 6-well plates. 2×10^5 cells cultured for 24 h were harvested from each well and fixed with 70% alcohol in refrigerator. The alcohol were washed off with PBS, and the cells were resuspended in 1 ml DNA staining solution at room temperature for 30 min in the dark. Flow cytometry was used to select blue excitation light with a wavelength of 488 nm, and simultaneously measure red fluorescence and forward-angle scattered light.

Annexin V/PI Method

Cells were harvested at 24 h after transfection, and stained with Annexin V-FITC and propidium iodide (Annexin V-FITC apoptosis detection kit, B.D. Biosciences Pharmingen, San Jose, CA, USA). Then cells were put in the dark for 15 min at room temperature. The apoptosis rate was detected by BD FACS Calibur (Beckman Coulter, CA, U.S.A.).

Statistical Analysis

Values as shown were mean ± S.E.M. of at least three independent repeats. Statistical analysis was performed using SPSS17.0 software (IBM Corp, Armonk, NY). Student's *t*-test was used to compare the differences between two groups. The difference between more than two groups was analyzed by single factor analysis of variance (ANOVA). $P < 0.05$ was defined as statistically significant.

RESULTS

Differentially Expressed Genes in Brachyury-Knocking Down MDA-MB-231 Cells and Control Cells

Brachyury was constitutively overexpressed in breast cancer MDA-MB-231 cells. To explore the potential downstream targets and pathways regulated by brachyury in tumor cells, RNA-Sequence was performed to profile the transcriptome in brachyury-knockdown MDA-MB-231 cells (MDA-MB-231 shBry) vs. control MDA-MB-231 cells. A total of 2,364 genes were identified to be differentially expressed, which were further analyzed to characterize potential pathways or biological processes. Involving pathways mainly includes: Steroid biosynthesis, TNF signaling pathway, and DNA replication, etc. The gene ontology analysis revealed some biological processes are involved: cell cycle, sterol biosynthetic process and the cholesterol biosynthetic process, etc. (**Figures 1A,B**). For ChIP-seq assays, the results showed that the cellular components were classified into 11 types, including neuron, asymmetric synapse, postsynaptic specialization, etc. Furthermore, ChIP-seq results in this study showed that several downstream genes were significantly associated with brachyury-binding events, including PIK3, K-RAS, HER2, N-Ras, CSF1R, etc. PIK3 and K-RAS are potential target genes of brachyury according to *P*-value (**Figure 1C**), both of which are involved in cell cycle regulation pathway. Combining and integrating RNA-seq and ChIP-seq results, we speculated that brachyury promotes tumor cell grow and progress through regulation of cell cycle. The predictive target genes above in breast cancer cells were further verified to be expressed highly in endogenous brachyury-expressing lung cancer cells using PCR assays.

Brachyury Knockdown Decreased Lung Cancer Cell Proliferation *in vitro*

To identify the role of brachyury on the proliferation capability of lung NSCLC cells *in vitro*, Calu-1 cell line (absence of brachyury expression) and H460 cell line (endogenously high expression of brachyury) were utilized for further study. Inhibition of brachyury in H460 cells (H460 siBry cells) and brachyury overexpression in Calu-1(Calu-1 Bry cells) were used to investigate whether brachyury could enhance the proliferation

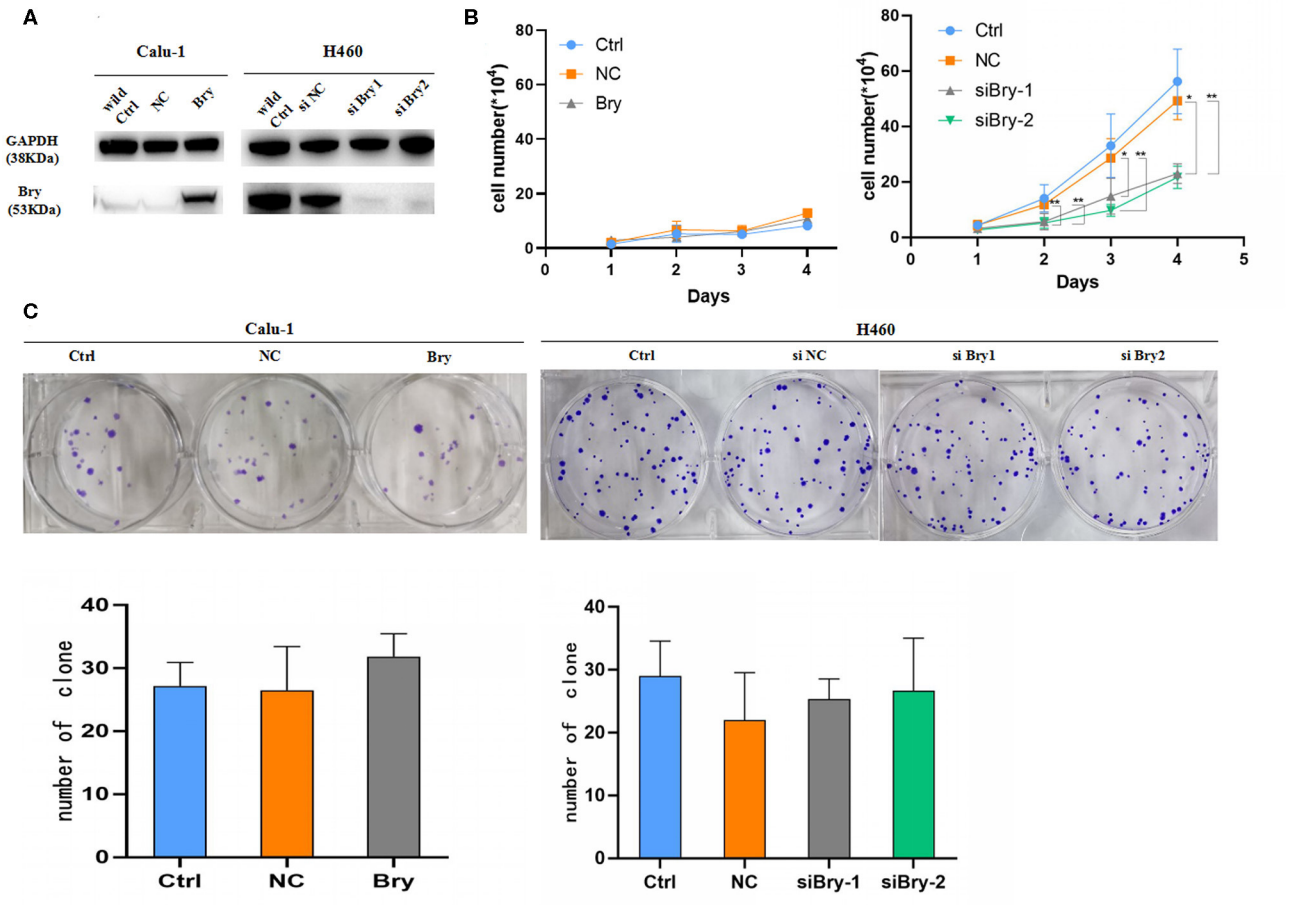

FIGURE 2 | Proliferation assays and colony formation assays to assess the effect of Bry in lung cancer cells. **(A)** The protein levels of Bry in Bry-overexpression Calu-1 cells or Bry-knockdown H460 cells compared with their respective control cells. **(B)** Cell proliferation assays to assess the proliferation capacity of Bry-overexpression Calu-1 cells and Bry-knockdown H460 cells. **(C)** Colony formation assays to assess the proliferation capacity of Bry-overexpression Calu-1 cells and Bry-knockdown H460 cells (*$P < 0.05$, **$P < 0.01$).

capability of lung cancer cells (**Figure 2A**). The results showed that brachyury overexpression in Calu-1 cells had no significant effect on the proliferation, while brachyury knockdown in H460 cells reduced the proliferation ability compared to the control cells (**Figure 2B**). Brachyury overexpression or knockdown had no effect on the ability of colony formation in Calu-1 and H460 cells (**Figure 2C**). In summary, brachyury knockdown could decrease the proliferation capability in H460 cells.

The Effect of Brachyury Expression on Cell Cycle

The impact of brachyury on cell cycle progression was also investigated. The cell cycle experiment was performed and analyzed by flow cytometry. Calu-1 Bry cells demonstrated significant lower G0/G1 fraction (48.37%, **Figure 3A**) than control cells (61.32%), and the percentage of S phase in Calu-1 Bry cells (32.53%, **Figure 3A**) was markedly higher than control cells (23.94%, **Figure 3A**). However, the percentage of G2/M phase did not have significant difference (**Figure 3A**). Hence, overexpression of brachyury in Calu-1 cells could inhibit the transition from G0/G1 to S phase.

For H460 cells, the percentage of G0/G1 and S phase did not have significant difference between the brachyury knockdown group and the control group (**Figure 3B**). However, the percentages of G2/M in the H460 siBry-1 and H460 siBry-2 (26.10% and 27.81%, respective, **Figure 3B**) were significantly higher than the control cells (15.89%, **Figure 3B**). We concluded that inhibition of brachyury expression in H460 cells could prevent G2/M transition of cell cycle progression.

Brachyury Knockdown Promotes Apoptosis in H460 Cells

Next, we investigated the effect of brachyury on cell apoptosis in H460 cell line and Calu-1 cell line. After overexpression of brachyury in Calu-1 cells, the percentage of apoptotic cells was assessed using sub-G1 and Annexin V/ PI method, followed by flow cytometry (**Figures 4A,C**). The results showed that the percentage of apoptotic Calu-1 Bry cells (2.37%) was not

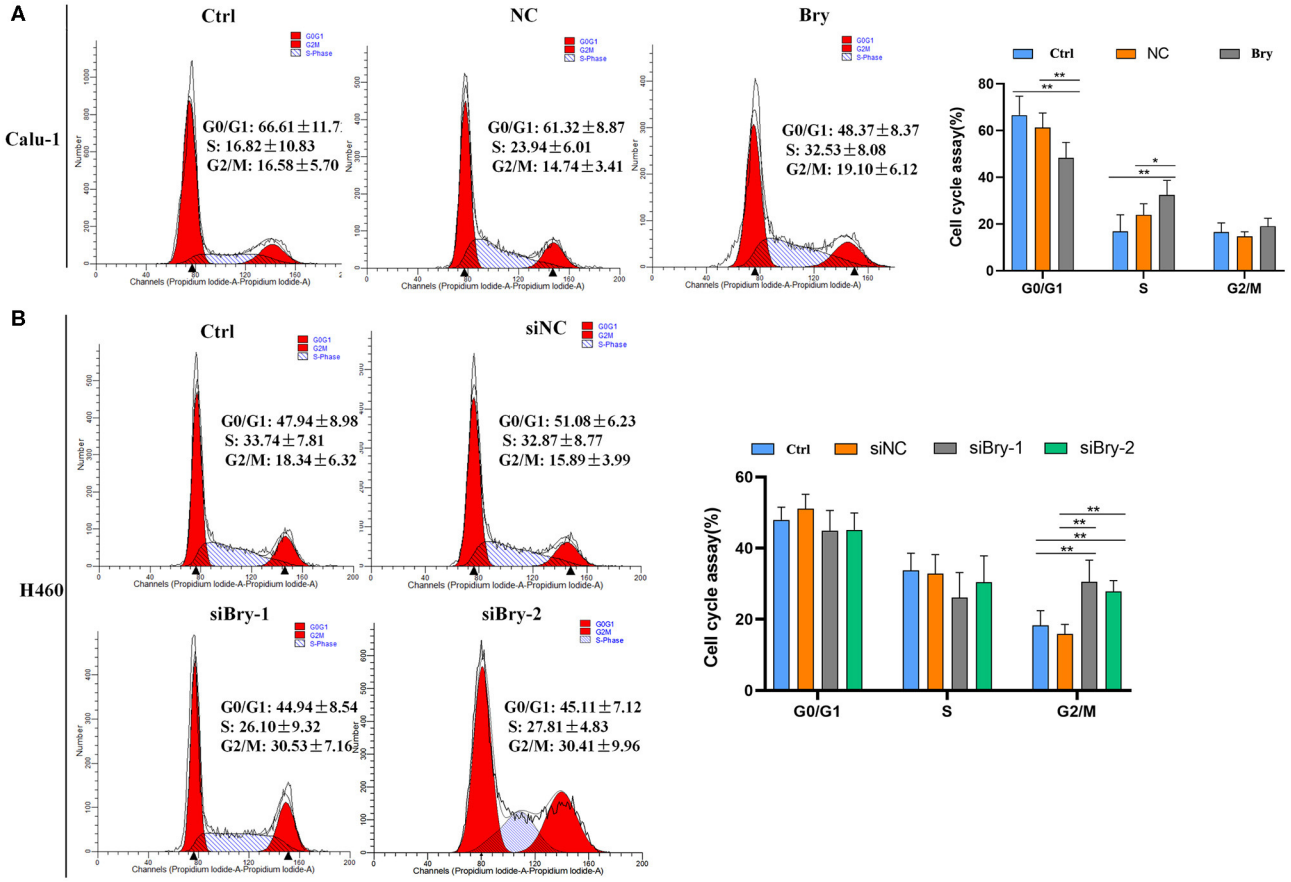

FIGURE 3 | The effect of Bry on cell cycle. **(A)** Cell cycle analysis of Bry-overexpression Calu-1 cells. Overexpression of brachyury in Calu-1 cells could promote the transition from G0/G1 to S phase. **(B)** Cell cycle analysis of Bry-knockdown H460 cells. Inhibition of brachyury expression in H460 cells could increase the percentage of G2/M phase (*$P < 0.05$, **$P < 0.01$).

significant lower than control cells (5.23%), and a dot-plot of Annexin V-FITC fluorescence vs. PI fluorescence indicated a non-significant increase in the percentage of apoptotic cells after overexpression of brachyury (**Figure 4C**). Similarly, we evaluated the apoptosis of H460 cells after knockdown with siRNA-1 and siRNA-2. The results showed that the percentage of apoptotic H460 siBry-1 cells (19.50%) and apoptotic H460 siBry-2 cells (14.61%) was significant higher than the control cells (1.13%) (**Figure 4B**). **Figure 4D** was consistent with **Figure 4B**. In conclusion, brachyury knockdown could expedite apoptosis of H460 cells.

DISCUSSION

A comparable range of brachyury mRNA expression levels has been observed in the lung tumor tissue samples and the various lung carcinoma cell lines, which suggests available cell line models can be used as useful tools to ravel the individual mechanism associated with tumorigenesis and progression (15). Elevated expression of brachyury in H460 cells has been validated to associate with invasive and metastasis capability of tumor cells along with survival benefit (8, 13). However, human squamous cell carcinoma cell line Calu-1 was reported and characterized by negative brachyury expression (15). It is because that these two types of cell lines represent different subtype of NSCLC. So we utilized Calu-1cells as the control to reveal the specific role of brachyury in endogenously brachyury-expressing lung tumor cell. Compared with control cells, inhibition of brachyury expression in H460 cells demonstrated significantly diminished proliferation capability. However, overexpression of brachyury did not result in significantly enhanced proliferation of Calu-1 cells. In the present study, we found that brachyury plays a role of promoting cell proliferation in lung H460 cells, which is consistent with our previous study of brachyury on breast cancer cells (9) and other reports on chordoma (3, 6, 19, 20), prostate cancer (21), colorectal cancer (22),adenoid cystic carcinoma (13), among others (20, 21).

H460 cells with silencing of brachyury (H460 siBry-1, H460 siBry-2) demonstrated significantly higher G2/M fraction, and insignificantly decreased G1/G0 and S fraction than control with highly endogenous expression of brachyury. In addition, brachyury-silenced H460 cells demonstrated significantly

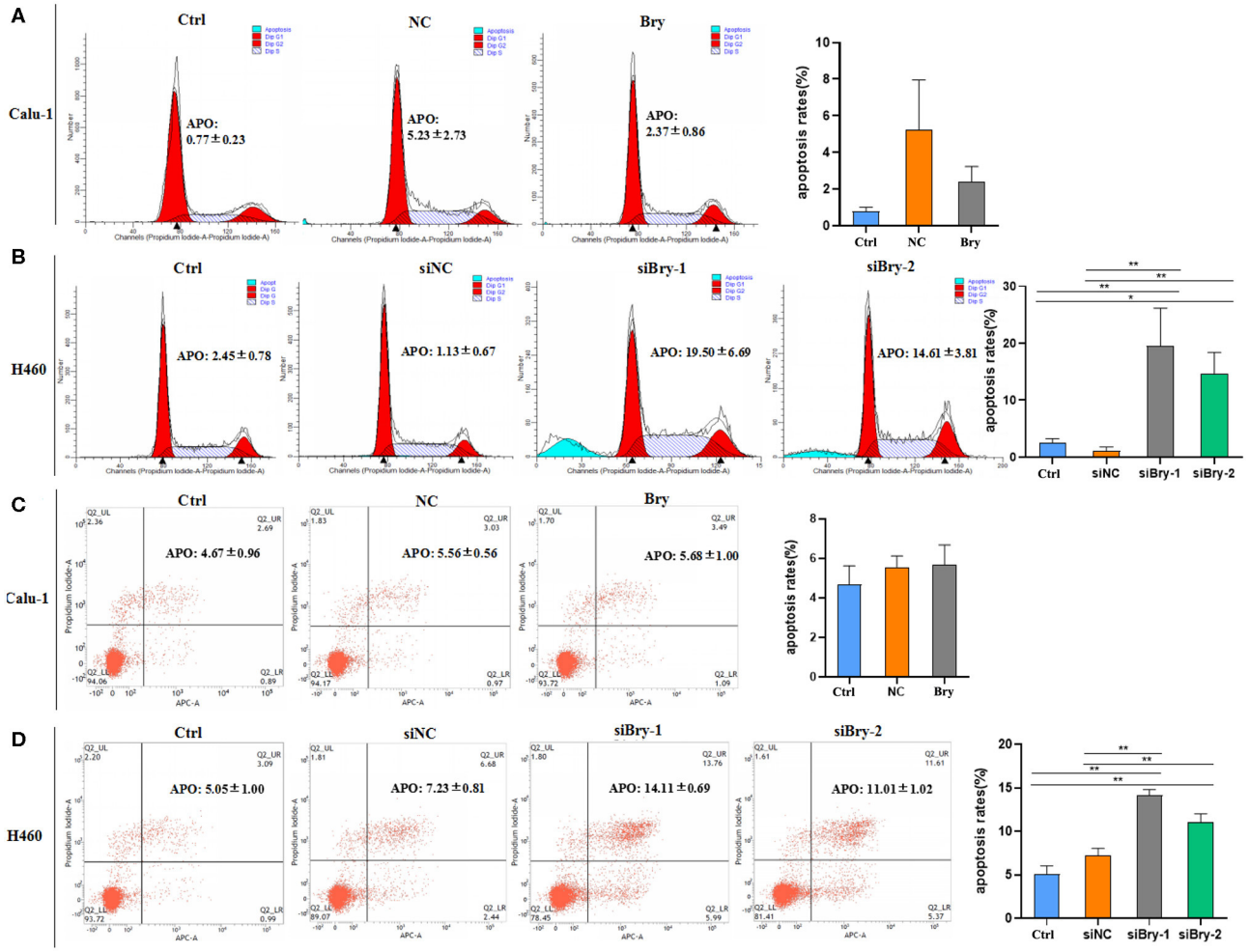

FIGURE 4 | The effect of Bry on cell apoptosis. **(A)** The effect of Bry on apoptosis of Bry-overexpression Calu-1 cells. There was no significant difference between the experimental group and the control group. **(B)** The effect of Bry on apoptosis of Bry-knockdown H460 cells. **(C)** Annexin V/PI method to analyze the effect of Bry on apoptosis of Bry-overexpression Calu-1 cells. There was no significant difference between the experimental group and the control group. **(D)** Annexin V/PI method to analyze of the effect of Bry on apoptosis of Bry-knockdown H460 cells (*$P < 0.05$, **$P < 0.01$).

increased apoptosis. Altogether, these results indicate that brachyury inhibits apoptosis in H460 cells, although overexpression of brachyury did not demonstrate the similar anti-apoptosis effect in Calu-1 cells. The reason we speculate is that the downstream brachyury-responsive elements are in the state of inactivation or silencing due to the absence of endogenous brachyury stimulation in Calu-1 cells. The exogenously forced brachyury expression cannot find and bind with corresponding functioning targets.

Based on the gene expression microarray data and ChIP-seq data, gene ontology (GO) functional enrichment analysis of differentially expressed genes (DEGs) between wild brachyury-expressing and absence of expression breast cancer cells was performed to uncover the downstream target genes of brachyury. The up-regulated DEGs are listed in **Figure 1C**. Further GO annotation indicates that the top two PI3K and K-Ras are mainly involved in the regulation of cell cycle and proliferation. Following verified experiments were performed to confirm that these top DEGs were expressed samely in endogenously brachyury-expressing lung cancer cells.

K-Ras is one member of the *ras* gene family, which encodes small GTP-binding proteins. Five- to 50-fold amplification of the wild-type gene or mutation can make it convert into oncogene (23). Activated Ras oncogenes have been found in a variety of human tumors (24), and K-Ras has been considered as the most commonly altered oncogene in NSCLC, especially in adenocarcinoma (25, 26). PI3K is one of three major downstream effectors of K-Ras, and its activation initiates a signal transduction cascade that promotes cancer cell growth, survival and metabolism (27). In addition, RAS–PI3K pathway has been also reported to mediate the anti-apoptotic function of

oncogenic RAS (28) and regulate the expression or activity of apoptotic-relating molecules or proteins (29).

In this study we demonstrate that brachyury and downstream target genes together involve in tumor cell cycle regulation by inducing accelerated transition through G2/M, promote tumor cell proliferation and inhibit apoptosis in lung NSCLC H460 cells. Targeting brachyury and downstream effectors pathway has the potential to be developed into a promising treatment strategy, which has far reaching significance for the therapy of NSCLC.

DATA AVAILABILITY STATEMENT

The datasets presented in this study can be found in online repositories. The names of the repository/repositories and accession number(s) can be found below: NCBI Gene Expression Omnibus (GSE151170, GSE151171, GSE151172).

AUTHOR CONTRIBUTIONS

JX carried out cell culture-based assays. MC carried out RNA-Seq transcriptome analysis and ChIP-sequence assay. YW performed data statistical analysis and wrote the manuscript. HZ, JZ, DW, and TZ carried out data statistical analysis. JS designed, supervised the study, and wrote the manuscript. All authors contributed to the article and approved the submitted version.

FUNDING

This work was supported by 333 Talent Project of Jiangsu Province (BRA2017057) to JS and Foundation of Social Development in Jiangsu—Clinical Frontier Technology (Grant No. BE2017661) to JS.

REFERENCES

1. Rao G, Pierobon M, Kim IK, Hsu WH, Deng J, Moon YW, et al. Inhibition of AKT1 signaling promotes invasion and metastasis of non-small cell lung cancer cells with K-RAS or EGFR mutations. *Sci Rep.* (2017) 7:7066. doi: 10.1038/s41598-017-06128-9
2. Vujovic S, Henderson S, Presneau N, McLean S, Frow R, Vujovic S, et al. Brachyury, a crucial regulator of notochordal development, is a novel biomarker for chordomas. *J Pathol.* (2006) 209:157–65. doi: 10.1002/path.1969
3. Hsu W, Mohyeldin A, Shah SR, Rhys CM, Johnson LF, Sedora-Roman NI, et al. Generation of chordoma cell line JHC7 and the identification of brachyury as a novel molecular target. *J Neurosurg.* (2011) 115:760–9. doi: 10.3171/2011.5.JNS11185
4. Shen J, Shi Q, Lu J, Wang DL, Zou TM, Yang HL, et al. Histological study of chordoma origin from fetal notochordal cell rests. *Spine.* (2013) 38:2165–70. doi: 10.1097/BRS.0000000000000010
5. Shen J, Li CD, Yang HL, Lu J, Zou TM, Wang DL, et al. Classic chordoma coexisting with benign notochordal cell rest demonstrating different immunohistological expression patterns of brachyury and galectin-3. *J Clin Neurosci.* (2011) 18:96–9. doi: 10.1016/j.jocn.2010.03.066
6. Nelson AC, Pillay N, Henderson S, Presneau N, Tirabosco R, Halai D, et al. An integrated functional genomics approach identifies the regulatory network directed by brachyury (T) in chordoma. *J Pathol.* (2012) 228:274–85. doi: 10.1002/path.4082
7. Palena C, Polev DE, Tsang KY, Fernando RI, Litzinger M, Krukovskaya LL, et al. The human T-box mesodermal transcription factor brachyury is a candidate target for T-cell-mediated cancer immunotherapy. *Clin Cancer Res.* (2007) 13:2471–8. doi: 10.1158/1078-0432.CCR-06-2353
8. Fernando RI, Litzinger M, Trono P, Hamilton DH, Schlom J, Palena C. The T-box transcription factor brachyury promotes epithelial-mesenchymal transition in human tumor cells. *J Clin Invest.* (2010) 120:533–44. doi: 10.1172/JCI38379
9. Chen M, Zou S, He C, Zhou J, Li S, Shen M, et al. Transactivation of SOX5 by brachyury promotes breast cancer bone metastasis. *Carcinogenesis.* (2019) bgz142. doi: 10.1093/carcin/bgz142. [Epub ahead of print].
10. Haro A, Yano T, Kohno M, Yoshida T, Koga T, Okamoto T, et al. Expression of brachyury gene is a significant prognostic factor for primary lung carcinoma. *Ann Surg Oncol.* (2013) 20(Suppl. 3):S509–16. doi: 10.1245/s10434-013-2914-9
11. Palena C, Fernando RI, Litzinger MT, Hamilton DH, Huang B, Schlom J. Strategies to target molecules that control the acquisition of a mesenchymal-like phenotype by carcinoma cells. *Exp Biol Med.* (2011) 236:537–45. doi: 10.1258/ebm.2011.010367
12. Akimoto N, Nakamura K, Hijioka H, Kume K, Matsumura Y, Sugiura T. Transfection of T-Box transcription factor *BRACHYURY* and *SOX2* synergistically promote self-renewal and invasive phenotype in oral cancer cells. *Int J Mol Sci.* (2018) 19:3620. doi: 10.3390/ijms19113620
13. Huang B, Cohen JR, Fernando RI, Hamilton DH, Litzinger MT, Hodge JW, et al. The embryonic transcription factor brachyury blocks cell cycle progression and mediates tumor resistance to conventional antitumor therapies. *Cell Death Dis.* (2013) 4:e682. doi: 10.1038/cddis.2013.208
14. Sarkar D, Shields B, Davies ML, Müller J, Wakeman JA. BRACHYURY confers cancer stem cell characteristics on colorectal cancer cells. *Int J Cancer.* (2012) 130:328–37. doi: 10.1002/ijc.26029
15. Roselli M, Fernando RI, Guadagni F, Spila A, Alessandroni J, Palmirotta R, Human lung tumors: an opportunity for novel interventions against lung cancer. *Clin Cancer Res.* (2012) 18:3868–79. doi: 10.1158/1078-0432.CCR-11-3211
16. Palena C, Roselli M, Litzinger MT, Ferroni P, Costarelli L, Spila A, et al. Overexpression of the EMT driver brachyury in breast carcinomas: association with poor prognosis. *J Natl Cancer Inst.* (2014) 106:dju054. doi: 10.1093/jnci/dju054
17. Hu Y, Feng X, Mintz A, Petty WJ, Hsu W. Regulation of brachyury by fibroblast growth factor receptor 1 in lung cancer. *Oncotarget.* (2016) 7:87124–35. doi: 10.18632/oncotarget.13547
18. Pei H, Hu W, Guo Z, Chen H, Ma J, Mao W, et al. Long noncoding RNA CRYBG3 blocks cytokinesis by directly binding G-Actin. *Cancer Res.* (2018) 78:4563–72. doi: 10.1158/0008-5472.CAN-18-0988
19. Hu Y, Mintz A, Shah SR, Quinones-Hinojosa A, Hsu W. The FGFR/MEK/ERK/brachyury pathway is critical for chordoma cell growth and survival. *Carcinogenesis.* (2014) 35:1491–9. doi: 10.1093/carcin/bgu014
20. Presneau N, Shalaby A, Ye H, Pillay N, Halai D, Idowu B, et al. Role of the transcription factor T (brachyury) in the pathogenesis of sporadic chordoma: a genetic and functional-based study. *J Pathol.* (2011) 223:327–35. doi: 10.1002/path.2816
21. Pinto F, Pertega-Gomes N, Pereira MS, Vizcaíno JR, Monteiro P, Henrique RM, et al. T-box transcription factor brachyury is associated with prostate cancer progression and aggressiveness. *Clin Cancer Res.* (2014) 20:4949–61. doi: 10.1158/1078-0432.CCR-14-0421
22. Jezkova J, Williams JS, Jones-Hutchins F, Sammut SJ, Gollins S, Cree I, et al. Brachyury regulates proliferation of cancer cells via a p27Kip1-dependent pathway. *Oncotarget.* (2014) 5:3813–22. doi: 10.18632/oncotarget.1999
23. Bos JL. The *ras* gene family and human carcinogenesis. *Mutat Res.* (1988) 195:255–71. doi: 10.1016/0165-11108890004-8
24. Serrano M, Lin AW, McCurrach ME, Beach D, Lowe SW. Oncogenic RAS provokes premature cell senescence associated with accumulation of p53 and p16INK4a. *Cell.* (1997) 88:593–602. doi: 10.1016/S0092-86740081902-9
25. Román M, Baraibar I, López I, Nadal E, Rolfo C, Vicent S, et al. KRAS oncogene in non-small cell lung cancer: clinical perspectives on the treatment of an old target. *Mol Cancer.* (2018) 17:33. doi: 10.1186/s12943-018-0789-x

26. Pylayeva-Gupta Y, Grabocka E, Bar-Sagi D. RAS oncogenes: weaving a tumorigenic web. *Nat Rev Cancer.* (2011) 11:761–74. doi: 10.1038/nrc3106
27. Engelman JA. Targeting PI3K signalling in cancer: opportunities, challenges and limitations. *Nat Rev Cancer.* (2009) 9:550–62. doi: 10.1038/nrc2664
28. Cox AD, Der CJ. The dark side of RAS: regulation of apoptosis. *Oncogene.* (2003) 22:8999–9006. doi: 10.1038/sj.onc.1207111
29. Rosen K, Rak J, Jin J, Kerbel RS, Newman MJ, Filmus J. Downregulation of the pro-apoptotic protein Bak is required for the RAS-induced transformation of intestinal epithelial cells. *Curr Biol.* (1998) 8:1331–4. doi: 10.1016/S0960-98220700564-7

Conflict of Interest: The authors declare that the research was conducted in the absence of any commercial or financial relationships that could be construed as a potential conflict of interest.

frontiers in Oncology

REVIEW
published: 07 July 2020
doi: 10.3389/fonc.2020.01105

Mechanisms of RNA N^6-Methyladenosine in Hepatocellular Carcinoma: From the Perspectives of Etiology

Jiahua Lu[1,2,3,4], *Junjie Qian*[1,2,3,4], *Shengyong Yin*[1,2,3,4], *Lin Zhou*[1,2,3,4], *Shusen Zheng*[1,2,3,4]* *and Wu Zhang*[5,6]*

[1] Division of Hepatobiliary and Pancreatic Surgery, Department of Surgery, First Affiliated Hospital, School of Medicine, Zhejiang University, Hangzhou, China, [2] Key Laboratory of Combined Multi-Organ Transplantation, Ministry of Public Health, Hangzhou, China, [3] Key Laboratory of the Diagnosis and Treatment of Organ Transplantation, CAMS, Hangzhou, China, [4] Collaborative Innovation Center for Diagnosis Treatment of Infectious Diseases, Zhejiang University, Hangzhou, China, [5] Shulan (Hangzhou) Hospital Affiliated to Zhejiang Shuren University Shulan International Medical College, Hangzhou, China, [6] Institution of Organ Transplantation, Zhejiang University, Hangzhou, China

N6-Methyladenosine (m^{6}A) is the most common RNA internal modification in eukaryotic cells. Its regulatory effects at the post-transcriptional level on both messenger RNAs (mRNAs) and noncoding RNAs have been widely studied; these include alternative splicing, stability, translation efficiency, nucleus export, and degradation. m^{6}A modification is implicated in a series of physiological and pathological activities, such as embryonic stem cell differentiation, immunoregulation, adipogenesis, and cancer development. Recently, the significance of m^{6}A methylation has been identified in both viral hepatitis and non-alcohol fatty liver disease (NAFLD), which are major risk factors in the development of hepatocellular carcinoma (HCC). Given the high incidence and mortality rate of HCC worldwide, it is of great importance to elucidate the mechanisms underlying HCC initiation and progression. m^{6}A as an emerging research focus has great potential to facilitate the understanding of HCC, particularly from an etiological perspective. Thus, in this review, we summarize recent progress in understanding m^{6}A modification related to viral hepatitis, NAFLD, and HCC, including their mechanisms and clinical applications.

Keywords: m^{6}A methylation, hepatocellular carcinoma, molecular mechanism, cancer etiology, viral hepatitis, non-alcohol fatty liver disease

OPEN ACCESS

Edited by:
Hailong Pei,
Soochow University, China

Reviewed by:
Dali Han,
Beijing Institute of Genomics (CAS), China
Xing Huang,
Zhejiang University, China

***Correspondence:**
Shusen Zheng
shusenzheng@zju.edu.cn
Wu Zhang
zhangwu516@zju.edu.cn

Specialty section:
This article was submitted to Molecular and Cellular Oncology, a section of the journal Frontiers in Oncology

Received: *23 February 2020*
Accepted: *02 June 2020*
Published: *07 July 2020*

Citation:
Lu J, Qian J, Yin S, Zhou L, Zheng S and Zhang W (2020) Mechanisms of RNA N^6-Methyladenosine in Hepatocellular Carcinoma: From the Perspectives of Etiology. Front. Oncol. 10:1105. doi: 10.3389/fonc.2020.01105

INTRODUCTION

Hepatocellular carcinoma (HCC) is the fourth leading cause of cancer-related death worldwide and accounts for more than 80% of primary liver cancers (1). Viral hepatitis and non-alcoholic fatty liver disease (NAFLD) are two significant risk factors for HCC development (2–4). The infection rates of hepatitis B virus (HBV) and hepatitis C virus (HCV) remain significant in high-risk areas, although vaccines and effective medicines have been designed for the prevention and treatment of viral hepatitis (5, 6). With the global epidemic of obesity, NAFLD has emerged as another nonnegligible force in HCC etiology (7). Due to asymptomatic disease progression, most patients have already advanced into liver cirrhosis or even HCC at the first diagnosis (3). Hence, these patients are

not eligible for curative treatments such as surgical resection or liver transplantation, and instead are left with the exclusive choice of palliative therapies. Worse still, first-line-medicines such as sorafenib can only extend the overall survival of patients for another 3 months, and the response rate of the emerging programmed cell death ligand-1 (PD-L1) immune checkpoint inhibitor is lower than 20% in HCC patients (8, 9). Thus, it is of great urgency to develop novel therapies for the effective prevention, early diagnosis and precision treatment of HCC.

N^6-methyladenosine (m^{6}A) is a ubiquitous RNA internal modification at the posttranscriptional level; it was first identified in eukaryotic cells, and later found in prokaryotic cells and viruses (10–15). In 2012, the landscape of m^{6}A modification was for the first time identified at the whole-transcriptome level (16, 17). Most m^{6}A sites are enriched within a consensus motif of RRACH (R = G or A, A = m^{6}A and H = A, C, or U), and are preferentially located around stop codons and within long internal exons. Regulators of m^{6}A modification include "writers," which are methyltransferases responsible for transferring the methyl group to the N6 position; "readers," which are RNA-binding proteins that recognize specific m^{6}A-modified positions to regulate RNA functions; and "erasers," which are demethylases that mediate this reversible biological process (18–20).

m^{6}A modification regulates the metabolic processes of both messenger RNAs (mRNAs) and noncoding RNAs (ncRNAs), which include structural stability, alternative splicing, translation efficacy, export, and decay (21–24). The reciprocal effects of m^{6}A methylation with mRNAs or ncRNAs are associated with a series of physiological and pathological biological behaviors such as stem cell differentiation, immunoregulation and carcinogenesis (25–27). There is mounting evidence that m^{6}A dysregulation is critically involved in HCC occurrence and development. For example, elevated m^{6}A levels in HCC fuel inflammation and neovascularization in tumors by inhibiting m^{6}A readers (28). In addition, a reduction of m^{6}A modification promotes HCC metastasis in an m^{6}A-dependent manner by modulating microRNA (miRNA) processing (29). Furthermore, some m^{6}A regulators have shown clinical value as biomarkers or therapeutic targets in HCC (30). Therefore, in this review, we mainly summarize the potential mechanisms of m^{6}A modification in HCC development from an etiological perspective, as well as its possible clinical applications, including as biomarkers and therapeutic targets.

Regulators of m^{6}A Modification

The m^{6}A regulators, including "writers," "erasers," and "readers," cooperatively maintain the dynamic and reversible balance of m^{6}A methylation (31) (**Figure 1**). "Writers" including methyltransferase-like 3 (METTL3), METTL14, and Wilm's tumor 1-associated protein (WTAP) comprise the major components of the methyltransferase complex within the nucleus, which is responsible for the m^{6}A methylation process (20). METTL3 is the core catalytic enzyme for transferring methyl groups to N^6 positions, while METTL14 is vital for recognizing and stabilizing the METTL3-METTL14 complex (32). WTAP binds the methyltransferase complex and recruits it toward mRNA targets (33). Other identified "writers" include METTL16, KIAA1429, zinc finger CCCH domain-containing protein 13 (ZC3H13), and RNA-binding motif protein 15 (RBM15) (20). It was not until 2011 that scientists discovered that m^{6}A modification could be reverted by demethylase, which drew the attention of the broader academic community (34). Then it was discovered that the dynamic demethylation process could be achieved by "erasers" including AlkB homolog 5 (ALKBH5), and fat mass and obesity-associated protein (FTO). *FTO* was the first identified gene contributing to human obesity, and its polymorphisms are closely related to insulin resistance and metabolic diseases (35, 36). Two studies reported the identical increase in intracellular m^{6}A methylation after knocking out two different "erasers" (34, 37). Moreover, the demethylation of FTO and ALKBH5 mainly affects m^{6}A residues within the nucleus.

The most studied m^{6}A "readers" are YTH domain-containing proteins, including YTHDF1-3 (located in the cytoplasm), YTHDC1 (in the nucleus), and YTHDC2 (in both) (19). YTHDF1 and YTHDF3 have coordinated functions that promote the translation of m^{6}A-modified mRNAs, while YTHDF2 expedites mRNA degradation, and YTHDC1 takes part in mRNA alternative splicing and nuclear export (38–40). YTHDC2 acts paradoxically in either promoting translation or accelerating mRNA degradation (41). Recently, a novel cellular biological process called liquid-liquid phase separation (LLPS) was discovered, through which degradation, translation and

Abbreviations: HCC, Hepatocellular carcinoma; NAFLD, Non-alcohol fatty liver disease; HBV, Hepatitis B virus; HCV, Hepatitis C virus; PD-L1, Programmed cell death ligand-1; m6A, N6-methyladenosine; mRNAs, Messenger RNAs; ncRNAs, Noncoding RNAs; METTL3, Methyltransferase-like 3; METTL14, Methyltransferase-like 14; WTAP, Wilm's tumor 1-associated protein; ZC3H13, Zinc finger CCCH domain-containing protein 13; ALKBH5, AlkB homolog 5; FTO, Fat mass and obesity-associated protein; YTHDC1, YTH domain-containing 1; YTHDF2, YTH N6-methyladenosine RNA-binding protein; RBM15, RNA-binding motif protein 15; HNRNPC, Heterogeneous nuclear ribonucleoprotein C; RBM15, RNA-binding motif protein 15; siRNA, Small interfering RNA; RIOK3, ROI kinase 3; CIRBP, Cold inducible RNA binding protein; dsDNA, Double-stranded DNA; IFNs, Interferons; ISGs, IFN-stimulated genes; DAA, 3-deazaadenosine; SAC, S-adenosylhomocysteine; SAM, S-adenosylmethionine; PQSs, Putative quadruplex-forming sequences; G4s, Guanine-quadruplexes; SNP, Single nucleotide polymorphism; NASH, Non-alcoholic steatohepatitis; SRSF2, Serine and arginine rich splicing factor 2; RUNX1T1, Runt-related transcription factor 1; CCNA2, Cellular cycle regulators cyclin A2; CDK2, Cyclin-dependent kinase 2; Fasn, Fatty acid synthase; BCAA, Branched-chain amino acids; AMPKα1, AMP-activated protein kinase α1 subunit; LPS, Lipopolysaccharide; ZCCHC4, Zinc finger CCHC-type containing 4; IL11, interleukin 11; SERPINE2, Serpin family E member 2; HIF-2α, Hypoxia-inducible factor 2α; SOCS2, Suppressor of cytokine signaling 2; ETS1, ETS proto-oncogene 1; HuR, Hu-antigen R; IGF2BP1, Insulin-like growth factor 2 mRNA-binding proteins; SRF, Serum response factor; ID2, DNA binding 2; PKM2, Pyruvate kinase M1/2; Me-RIP-PCR, Methylated- RNA immunoprecipitation- polymerase chain reaction; lincRNAs, Long noncoding RNAs; miRNAs, MicroRNAs; CircRNAs, circular RNAs; pri-miRNA, primary miRNA; DGCR8, DiGeorge syndrome chromosomal region 8; GATA3, GATA binding protein 3; pre-mRNA, Precursor mRNA; YAP, Yes-associated protein; CeRNA, Competitive endogenous RNA; PDX, Patient derived xenograft; PLGA-PEG NP, PEGylated PLGA nanoplatform; rRNAs, Ribosomal RNAs; CSAD, Cysteine sulfinic acid decarboxylase; GOT2, Glutamic-oxaloacetic transaminase 2; LLPS, Liquid-liquid phase separation; H3K36me3, H3 trimethylation at Lys36; carRNA, Chromosome-associated regulatory RNA; EMT, Epithelial mesenchymal transition; GC, Gastric cancer; ZMYM1, Zinc finger MYM-type containing 1; CRC, Colorectal cancer; NSCLC, Non-small cell lung cancer; AML, Acute myeloid leukemia.

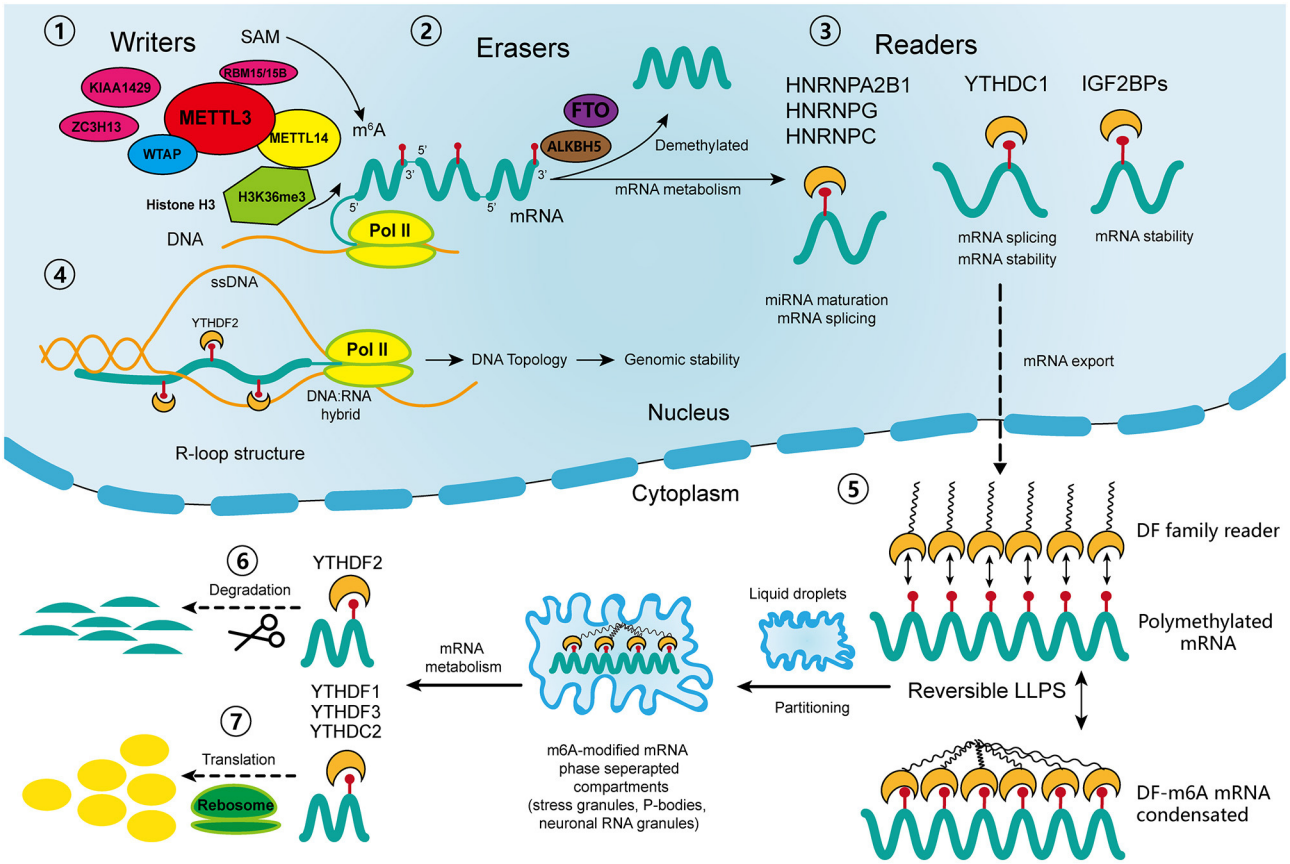

FIGURE 1 | Schematic diagram of the process and biological function of RNA m^{6}A methylation. The methyltransferase complex composed of METTL3, METTL14 and WTAP co-transcriptionally catalyzes the transfer of the methyl group from adenosylmethionine (SAM) onto the N6 position of adenosine; other "writers" include RBM15/15B, KIAA1429, and ZC3H13. With the guidance of histone H3K36me, the m6A sites are preferentially located near the 3′ terminus of the transcripts. Demethylases FTO and ALKBH5 reverse the m^{6}A process. In nucleus, the "readers" of YTHDC1, IGF2BPs, HNRNPs participate in diverse RNA biological processes, including mRNA alternative splicing, stability, export, and miRNA maturation. The m^{6}A-modified R-loop structures are implicated in the regulation of genomic stability. In cytoplasm, the m6A-modified mRNAs are targeted for regulation through a process called liquid-liquid phase separation (LLPS), which is mediated by YTHDFs. Then, other "readers" regulate the degradation and translation of mRNAs in the cytoplasm. ssDNA, single strand DNA; pol II: RNA polymerase II.

splicing of m^{6}A-modified mRNAs are regulated (42). Some low-complexity domains belonging to YTHDFs have the ability to interact with each other and to partition into liquid droplets within the cytoplasm (43). This process can be greatly enhanced by mRNA transcripts containing multiple m^{6}A residues, which recruit and juxtapose YTHDF proteins, initiating the phase separation process. Subsequently, the mRNA-YTHDF complexes partition into endogenous phase-separated liquid droplets, such as stress granules, P-bodies, or neuronal RNA granules, thereby transforming into membraneless compartments, where their degradation, splicing, and transportation are regulated (42). In addition to the YTH reader proteins, there are some binding proteins regulated by m^{6}A-induced structural changes called m^{6}A "switches," which include heterogeneous nuclear ribonucleoprotein C (HNRNPC), HNRNPG, HNRNPA2B1, and insulin-like growth factor 2 mRNA binding protein 1-3 (IGF2BP1-3) (44). HNRNPC and HNRNPG are involved in mRNA splicing, and HNRNPA2B1 participates in miRNA maturation (18). IGF2BPs function through the recruitment of RNA stabilizers, such as Hu antigen R (HuR), an RNA stabilizer, to maintain mRNA stability (45–47). However, the detailed mechanisms of their interactions with m^{6}A-modified sites require further exploration.

In addition to the well-studied functions of m^{6}A regulators, there are some newly identified mechanisms that participate in the regulation of m^{6}A modification. Huang et al. discovered that histone H3 trimethylation at Lys36 (H3K36me3), one of the transcriptional markers, interacts with METTL14 to guide the methyltransferase complex to nascent RNA and to specific regions of mRNA transcripts (48). In that study, silence of either METTL14 or H3K36me greatly reduced the m^{6}A levels throughout the transcriptome. Moreover, the overlapped sites of histone modification and m^{6}A modification are preferentially located near the coding sequence (CDS) and 3′ terminus of the transcripts. This finding partially explained the site specificity of m^{6}A modification in mRNA transcripts, and revealed another

layer of regulatory mechanism involving crosstalk between m^{6}A methylation and histone modification. Other recent studies have shown that m^{6}A modification regulates not only the stability of mRNAs but also DNA structures. R-loops are nucleic acid structures consisting of three strands: an RNA: DNA hybrid and a single strand of unpaired DNA (49). They actively regulate genome dynamics and functions, including immunoglobulin class switching, transcription initiation and termination as well as genomic stability (49). Two independent studies have confirmed the existence of m^{6}A modified-RNAs within R-loops. Abakir et al. found that YTHDF2 recognized m^{6}A-modified R-loops and promoted their degradation (50). By contrast, Yang et al. observed a decreased R-loop levels upon METTL3 silencing, which suggests that m^{6}A may promote R-loop formation (51). Although there are discrepancies between these two studies, they both indicate that m^{6}A plays an important role in maintaining genomic integrity by modulating the accumulation of R-loops. Further, this modulation prevented the occurrence of a variety of diseases such as cancers, Kaposi's sarcoma and neurological disorders. In addition, Liu et al. identified METTL3-catalyzed m^{6}A on chromosome-associated regulatory RNAs (carRNAs), such as enhancer RNAs, repeats RNAs and promoter-associated RNAs, and YTHDC1 promotes the degradation of these RNAs (52). Moreover, a reduction of m^{6}A modification increases carRNA levels and promotes the open chromatin state and transcription. This finding suggests a regulatory effect of m^{6}A on carRNAs, which in turn affects the chromatin state and transcription.

Role of m^{6}A Modification in Hepatocellular Carcinoma

The regulators of m^{6}A play a pleiotropic role in the modulation of HCC, and both mRNA and ncRNA participate in m^{6}A-mediated biological processes in HCC (**Figure 2**). The m^{6}A regulators reviewed in this article include the "writers" METTL3, METTL14, WTAP, and KIAA1429; the "eraser" FTO and the "readers" YTHDF1, YTHDF2 and IGF2BP1; their regulatory effects in HCC are summarized in **Table 1**.

m^{6}A in Hepatocellular Carcinoma and Other Cancers

Dysregulation of m^{6}A methylation and abnormal expression of regulators are involved in various cancer functions, such as distant metastasis, cancer immunoregulation, tumor angiogenesis and cancer stem cell formation, by modulating the degradation, processing or translation of the downstream targeted RNAs. The epithelial mesenchymal transition (EMT), a critical process for cancer cell metastasis, is regulated by the m^{6}A writer METTL3, not only in HCC but across diverse cancers. Lin et al. discovered that METTL3 is upregulated in HCC, promoting EMT by enhancing the m^{6}A modification of Snail mRNA (53). Moreover, YTHDF1 mediates the m^{6}A-increased translation of Snail mRNA, which promotes the HCC metastasis. Notably, METTL3 also participates in EMT in gastric cancer (GC), ovarian cancer and prostatic cancer (27, 54). Yue et al. found that m^{6}A modification of zinc finger MYM-type containing 1 (ZMYM1), a downstream target of METTL3, enhanced its stability through the regulation of HuR, and that ZMYM1 represses E-cadherin promoter by recruiting the CtBP/LSD1/CoREST complex, thereby facilitating the EMT process and metastasis of GC (55). Intriguingly, Ma et al. reported that METTL14 suppresses HCC metastasis by regulating miRNA in an m^{6}A-dependent manner (29). METTL14 also inhibits the progression and metastasis of colorectal cancer (CRC) by downregulating oncogenic lncRNA (56). Moreover, it can inhibit CRC cell growth via miR-375 /Yes-associated protein 1 (*YAP1*) pathway (57). These findings confirm the significant roles of m^{6}A writers in regulating tumor metastasis and progression across diverse cancers.

It is noteworthy that, because m^{6}A modification and the expression of m^{6}A regulators are highly heterogeneous across various cancer types, the effects of m^{6}A methylation may differ even in the same context. For instance, hypoxia in breast cancer stimulates hypoxia-inducible factor (HIF)-1α and HIF-2α- dependent expression of ALKBH5, which leads to the demethylation of NANOG mRNA and the induction of cancer stem cell phenotype (58). In non-small cell lung cancer (NSCLC), YTHDF1 is identified as a hypoxia adaptor, whose depletion inhibits tumor progression by regulating translation efficacy (59). However, in HCC, hypoxia induces the reduction of YTHDF2, which promoted tumor inflammation and angiogenesis (28). Additionally, YTHDF2 is recognized as an oncogene that is upregulated in lung cancer and acute myeloid leukemia (AML) to promote tumor initiation and growth, exhibiting a completely opposite function as in HCC (60, 61).

The functional implications of m^{6}A in tumor immunology are drawing increasing attention. Yang et al. reported overexpression of FTO in melanoma, and that its knockdown increased the m^{6}A level of critical tumorigenic genes such as *PD-1, CXCR4,* and *SOX10*, leading to increased mRNA degradation mediated by YTHDF2 (62). Moreover, silencing of FTO sensitized melanoma to anti-PD-1 treatment. Li et al. found that overexpression of WTAP is associated with poor prognosis in GC patients, which might be correlated with T lymphocyte infiltration (63). However, to date, no studies have explored the relationship between m^{6}A and immunoregulation in HCC. Due to the low response rate of advanced HCC patients to anti-PD-L1 treatment, m^{6}A might be a promising new target for the study of drug insensitivity and resistance in immunotherapies.

Overall, the above evidence indicates that dysregulated m^{6}A modification plays an important role in cancer biology, and this epigenetic alteration is highly heterogeneous.

m^{6}A and mRNA in Hepatocellular Carcinoma

Two recent studies have revealed m^{6}A mechanisms underlying the negative correlation between YTHDF2 and HCC under hypoxic conditions (28, 64). Hou et al. reported that reduced expression of YTHDF2 in HCC tumor tissues was accompanied by increases in m^{6}A methylation and mRNA expression, and was associated with unfavorable survival outcomes and poor clinical classification (28). The study revealed that YTHDF2 inhibits HCC progression through m^{6}A modification by decreasing the stability of interleukin 11 (*IL11*) and serpin family E member 2 (*SERPINE2*) mRNA, which are involved in tumor angiogenesis and inflammation activation respectively (**Figure 2A**). Moreover, repression of HCC by YTHDF2 was reversed by HIF-2α

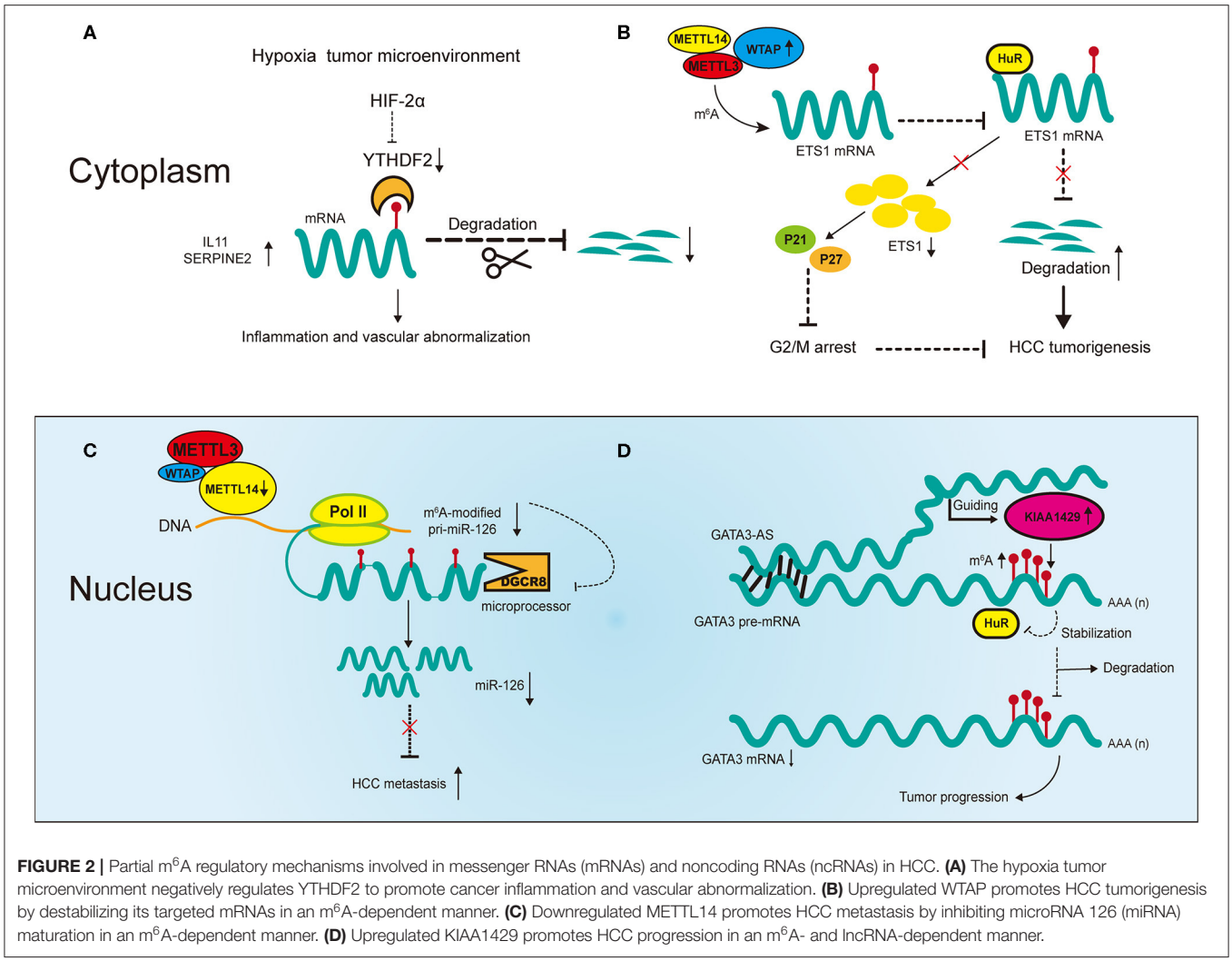

FIGURE 2 | Partial m^{6}A regulatory mechanisms involved in messenger RNAs (mRNAs) and noncoding RNAs (ncRNAs) in HCC. **(A)** The hypoxia tumor microenvironment negatively regulates YTHDF2 to promote cancer inflammation and vascular abnormalization. **(B)** Upregulated WTAP promotes HCC tumorigenesis by destabilizing its targeted mRNAs in an m^{6}A-dependent manner. **(C)** Downregulated METTL14 promotes HCC metastasis by inhibiting microRNA 126 (miRNA) maturation in an m^{6}A-dependent manner. **(D)** Upregulated KIAA1429 promotes HCC progression in an m^{6}A- and lncRNA-dependent manner.

under hypoxic conditions. These findings reveal molecular mechanisms through which targeted HCC treatment may be utilized. Interestingly, Zhong et al. showed different mechanisms in HCC in terms of YTHDF2 reduction induced by hypoxia (64). YTHDF2 directly bound with the 3′ terminus of the EGFR m^{6}A site to accelerate its decay, which impeded the MEK/ERK signaling and thereby suppressed HCC. In addition, the expression of YTHDF2 was repressed under hypoxic conditions in HCC. Although the study demonstrated the significant role of YTHDF2 in inhibiting HCC, whether it involves m^{6}A modification requires validation in more experiments.

In addition to the direct regulatory effect of YTHDF2, there is evidence suggesting the cooperative function of m^{6}A regulators in HCC. Chen et al. showed that METTL3 promotes HCC progression in a YTHDF2- and m^{6}A-dependent manner (65). In that study, overexpression of METTL3 promoted tumor growth in *CRISPR/dCas9-VP64* models *in vivo* and *in vitro*, indicating its positive correlation with HCC. Suppressor of cytokine signaling 2 (*SOCS2*), a direct downstream target of METTL3, inhibited tumor progression. The expression of *SOCS2* was downregulated by METTL3 through m^{6}A modification, in which YTHDF2 bound to the 3′ terminus of *SOCS2* to facilitate its decay. Therefore, the m^{6}A regulators METTL3 and YTHDF2 cooperatively promoted the development of HCC in an m^{6}A-dependent manner. Another regulator of m^{6}A, WTAP, has also been found to promote HCC progression through m^{6}A modification (**Figure 2B**) (66). WTAP is significantly upregulated in HCC and this is associated with unfavorable survival outcomes (66). ETS proto-oncogene 1 (*ETS1*), a tumor suppressor in HCC, is negatively regulated by WTAP via m^{6}A modification. Moreover, m^{6}A modification of ETS1 simultaneously inhibits its binding with HuR, the RNA stabilizer, which promotes its degradation. In addition, WTAP promotes the G2/M phase transition via ETS1-p21/p27 signaling pathway to regulate the HCC cell cycle. Overall, these results confirm the significance of cooperative effects between m^{6}A regulators themselves and RNA stabilizers in HCC progression.

As m^{6}A research advances, new regulators are being identified that take part in the biological processes of tumors. IGF2BPs (including IGF2BP1/2/3) are newly identified m^{6}A reader

TABLE 1 | Role of m6A regulators in HCC occurrence and development.

Diseases	Regulators	Specific function	Mechanisms	References
HBV	METTL3	Promoting viral replication and inhibiting viral proteins expression	Promoting reverse transcription and reducing HBV RNA stability	(81)
	METTL14			
	YTHDF2			
	YTHDF3			
HCV	YTHDF	Inhibiting viral infection	Inhibiting infectious virions production by relocating them to lipid droplets where virions assemble	(79)
	METTL3			
	METTL14			
NAFLD	FTO	Promoting adipogenesis and enhancing adipocyte differentiation	Promoting alternative splicing of RUNX1T1 by inhibiting RNA-binding of SRSF2	(87)
	FTO	Promoting adipogenesis	Inhibiting YTHDF2-mediated degradation of CCNA2 and CDK2	(108)
	FTO, METTL3		FTO promoting lipid accumulation while METTL3 inhibiting adipogenesis	(109)
	METTL3	Facilitating insulin resistance and accelerating fatty acid metabolism *in vitro*	Promoting Fasn expression	(84)
	METTL14	Promoting insulin resistance, lipogenesis and lipolysis *in vivo*	Activating the AKT signaling	(83)
HCC	METTL3	Promoting proliferation, migration and colony formation *in vitro*, promoting tumorigenesis and metastasis *in vivo*	Inhibiting SOCS2 expression by facilitating YTHDF2-mediated SOCS2 degradation	(65)
		METTL3-mediated upregulation of LINC00958 promoting proliferation, migration and lipogenesis in HCC cells	Upregulating LINC00958 by enhancing its stability	(72)
		Promoting EMT phenotypes *in vitro* and *in vivo*	Promoting YTHDF1-mediated translation of Snail mRNA	(53)
	WTAP	Promoting proliferation and tumor growth *in vitro* and *in vivo*	Inhibiting ETS1 expression by destabilizing its binding with HuR	(66)
	METTL14	Inhibiting HCC metastasis	Promoting pri-miR-126 processing by binding to DGCR8	(29)
	KIAA1429	Inhibiting proliferation and metastasis *in vitro* and *in vivo*	Promoting GATA3 pre-mRNA decay by inhibiting HuR	(73)
		Promoting HCC cells migration and invasion	Inhibiting ID2	(68)
	YTHDF2	Inhibiting hypoxia-induced inflammation, angiogenesis and metastasis in HCC	Inhibiting IL11 and SERPINE2 by promoting their degradation	(28)
		Suppressing proliferation and tumor growth	Promoting the decay of EGFR mRNA by binding to its 3′ terminus	(64)
		Positively associated with HCC malignancy	Inhibited by miR-145 binding to its 3′ terminus	(71)
	IGF2BP1	Promoting cancer cell growth and invasion	Inhibiting miRNA-mediated degradation of SRF transcripts	(67)
	ZCCHC4	Promoting proliferation *in vitro* and tumor growth *in vivo*	Promoting 28S ribosomal RNA methylation	(75)
	FTO	Promoting proliferation and *in vivo* tumor growth	Increasing PKM2 expression	(69)
	METTL3, YTHDF1	Predicts worse survival	Overexpressed in HCC tissues	(76, 77)
	METTL14	Predicts worse survival	Regulating CSAD, GOT2 and SOCS2	(30)

proteins that promote the stability and storage of targeted transcripts by recognizing the consensus motif GGAC (A = m^{6}A) (45). In HCC cells, IGF2BP1 upregulates serum response factor (*SRF*) by binding with its 3′ terminus and promoting its m^{6}A modification (67). It also inhibits the miRNA-mediated degradation of *SRF* transcripts. The dual regulations enhance the expression of *SRF*-targeted genes thereby facilitating HCC tumorigenesis. Strikingly, there are 35 genes regulated by *SRF* or IGF2BP1 in total, which in combination construct an oncogenic cellular network in HCC, making themselves valuable

therapeutic targets. Recently, KIAA1429 and FTO were both found to be overexpressed in HCC, which predicted unfavorable prognoses in HCC patients (68, 69). KIAA1429 inhibits the expression of inhibitor of DNA binding 2 (*ID2*) by promoting its m^{6}A methylation while FTO downregulates pyruvate kinase M1/2 (*PKM2*) by triggering its demethylation. Consequently, KIAA1429 and FTO together promote the tumorigenesis of HCC. However, these results need higher levels of evidence for validation.

Overall, these findings suggest that mRNA stability and degradation are the most common m^{6}A regulatory function in HCC. We believe that with more in-depth research on m^{6}A regulators, new mechanisms will soon be revealed.

m^{6}A and Noncoding RNAs in Hepatocellular Carcinoma

The regulatory effects of ncRNAs including long noncoding RNAs (lncRNAs), microRNAs and circular RNAs (circRNAs) on m^{6}A are nonnegligible in HCC. Recently, several studies revealed how the interplay between m^{6}A modification and ncRNAs influences the biological behaviors of HCC.

METTL14 inhibits HCC metastasis by regulating primary miR-126 (*pri-miR-126*) processing in an m^{6}A-dependent manner (**Figure 2C**) (29). The processing of pri-miRNAs is usually performed by microprocessor proteins such as DiGeorge syndrome chromosomal region 8 (*DGCR8*) (70). In this study, overexpression of METTL14 upregulated the expression of miR-126 by promoting pri-miR-126 binding with DGCR8, which facilitated its processing. The same study found that in metastatic HCC, decreased METTL14 led to the accumulation of unprocessed pri-miR-126. Moreover, the inhibition of metastasis was reversed by miR-126 inhibitor in METTL14-overexpressing HCC cells, indicating the significance of miR-126 as a downstream target of METTL14 to inhibit metastatic HCC. In another study, miR-145 regulated m^{6}A levels in HCC cells through the modulation of reader protein YTHDF2 (71). Overexpression of miR-145 increased m^{6}A methylation in HCC cells and this regulation was reversed by overexpression of YTHDF2. Moreover, the luciferase activities confirmed that miR-145 directly targeted the 3′ terminus of YTHDF2 mRNA, and *in vitro* experiments proved its inhibition of HCC cell proliferation. This is the first report in HCC that ncRNAs regulate m^{6}A regulators to influence cancer development. However, it should be noted that the effects of YTHDF2 in that study contradict earlier reports, which we suspected could be due to tumor heterogeneity in HCC (28, 64).

More recently, m^{6}A modification has been reported to be correlated with the upregulation of LINC00958 in HCC, which may promote proliferation, invasion, migration and lipogenesis of HCC cells *in vitro* (72). Moreover, the upregulation of LINC00958 may be regulated by METTL3 via the modulation of the stability of RNA in HCC cells, and high expression of both genes may predict poor prognosis in HCC. However, this only shows that METTL3 is positively related with LINC0958, and thus more specific experimental methods are needed for validation. KIAA1429 can also promote HCC development via the m^{6}A-dependent modification of GATA binding protein 3 (*GATA3*), in which its antisense transcript-derived lncRNA called GATA3-AS plays an important role (**Figure 2D**) (73). KIAA1429 is significantly upregulated in HCC and predicts worse survival outcomes in HCC patients. Knockdown of KIAA1429 is negatively related with hepatoma growth both *in vitro* and *in vivo*. KIAA1429 promotes the decay of *GATA3* precursor mRNA (pre-mRNA) through m^{6}A modification, thereby promoting HCC progression. The RNA binding protein HuR increases the stability of *GATA3* pre-mRNA by binding with the 3′ terminus of pre-mRNA. However, this binding is negatively regulated by KIAA1429 through m^{6}A modification. On the other hand, the lncRNA GATA3-AS acts as a cis-acting element for KIAA1429 to guide m^{6}A methylation on GATA3 pre-mRNA 3′ terminus. This KIAA1429/GATA3 regulatory axis in HCC development reflects the breakdown of m6A dynamic balance under pathological conditions.

In recent research, circRNA has been found to facilitate HCC progression indirectly through m^{6}A modification. CircRNA_104075 promotes *YAP*-related HCC progression via hepatocyte nuclear factor 4 α (*HNF4a*) in HCC (74). It also acts as a competitive endogenous RNA (ceRNA) to increase *YAP* expression by absorbing miR-583-3p. Intriguingly, an m^{6}A motif, AGACU, has been identified within the 3′ terminus of *YAP*, which may be critical for the interplay between *YAP* and miR-582-3p. Furthermore, the critical effects of m^{6}A was confirmed by luciferase activities and RNA immunoprecipitation quantitative polymerase chain reaction (RIP-qPCR) analyses. However, the mechanisms underlying this m^{6}A modification should be further validated.

Overall, in HCC, m^{6}A modification regulates ncRNAs in diverse ways, such as through splicing, preprocessing, stability and decay, and in turn ncRNAs affect and participate in the m^{6}A process. Therefore, the interactions between m^{6}A and ncRNAs play an important role in HCC progression, and we believe that more regulatory mechanisms will be identified in the future.

Future Prospects and Clinical Applications of m^{6}A in Hepatocellular Carcinoma

Considering the diverse biological effects mediated by m^{6}A modification in HCC, there may ample opportunity to devise effective treatments and targeted therapies for HCC patients.

Recently, progress has been made on experimental therapies targeting m^{6}A-specific mechanisms. Not only novel medicines but also new m^{6}A regulators are being identified. Hou et al. demonstrated that PT2385 has excellent efficacy in the treatment of HCC, and significantly reduces tumor volume in subcutaneous HCC tumor models (28). It can reverse the reduction of YTHDF2 regulated by *HIF-2α*, which attenuates tumorous inflammation and angiogenesis thereby suppressing HCC growth. Although the administration of PT2385 does not affect the localization of YTHDF2 and cannot take effect with YTHDF2 deficiency, it does provide an opportunity to inhibit hypoxia-induced HCC development. Zuo et al. invented a novel PEGylated PLGA nanoplatform (PLGA-PEG NP) encapsulating si-LINC00958 targeting LINC00958 for the treatment of HCC (72). In the study, it exhibited controllable release, excellent cellular drug

uptake and precise tumor-targeting capacity. Moreover, tumor size was effectively reduced in PLGA-PEG (si-LINC00958) NPs-treated HCC-patient-derived xenograft (PDX) model, and the pathological results and blood examination exhibited no significant treatment-related toxicity in the mouse model. A new m^{6}A methyltransferase, zinc finger CCHC-type containing 4 (*ZCCHC4*), which mainly takes part in the methylation of 28S ribosomal RNAs (rRNAs), has been identified both *in vitro* and *in vivo* in HCC (75). Silence of ZCCHC4 decreases m^{6}A methylation in 28S rRNA and inhibits proliferation of CRISPR/cas9-edited HepG2 cells. In addition, it is overexpressed in HCC tumor tissues and its silence significantly inhibits tumor growth in a xenograft animal model, confirming its significant role in promoting HCC progression through m^{6}A methylation. Although its detailed biological functions in HCC require more validation, it might be a potential novel target for HCC treatment.

The application of m^{6}A in HCC is not limited to clinical treatment; it may also be applied to cancer diagnosis and prognostic prediction. Recent studies have shown that m^{6}A regulators have significant potential to serve as biomarkers. METTL3 and YTHDF1 are both overexpressed in HCC in several studies, and thus may be useful biomarkers for survival prediction and clinical classification (76, 77). Another study identified three METTL14-related downstream genes including cysteine sulfinic acid decarboxylase (*CSAD*), glutamic-oxaloacetic transaminase 2 (*GOT2*), and *SOCS2* using bioinformatics methods (30). They were included in a nomogram for the prediction of overall survival. Other overexpressed m^{6}A regulators in HCC include WTAP, KIAA1429 and FTO, while downregulated enzymes include METTL14 and YTHDF2 (28, 66, 68, 69, 73).

Relationship Between Hepatocellular Carcinoma and Viral Hepatitis and Non-alcoholic Fatty Liver Disease

Infection with hepatitis virus is the leading cause of HCC worldwide (3). There is a high rate of HBV infection in eastern Asia while HCV infection is more prevalent in developed countries (2, 5). The etiological connection between viral hepatitis and HCC enable us to intervene with the progression of disease for early prevention of HCC. HBV or HCV infection underlies the context of chronic liver inflammation, which would lead to liver cirrhosis and eventually HCC (3, 78). During the process of carcinogenesis, dysregulation of m^{6}A may facilitate virus activity and disturb host immunity, causing persistent virus infection, shaping inflammatory microenvironment and consequently leading to HCC occurrence (**Figure 2**). For instance, depletion of certain m^{6}A regulators in HCV can enhance viral activity, which increases virus titers without disturbing viral replication (79). Moreover, HCV infection affects host immunity in an m^{6}A-dependent manner (80). m^{6}A modification has also been observed in HBV, and is associated with virus reverse transcription (81). Thus, dysregulation of m^{6}A in viral host cells is closely associated with the development of viral hepatitis, and may contribute to the occurrence of HCC.

NAFLD or non-alcohol steatohepatitis (NASH) is gaining increasing attention for its prevalence around the world and has become one of the leading etiologies in HCC (7). NAFLD is in fact a wide-range of chronic liver diseases, characterized by excessive accumulation of triglycerides in hepatocytes. It tends to progress from isolated hepatocyte triglyceride accumulation and steatosis (NAFL), to hepatic triglyceride accumulation with inflammation and hepatic injury (NASH), and eventually to liver fibrosis and HCC (82). NAFLD is strongly correlated with metabolic syndromes such as diabetes and obesity, and these risk factors interact to increase the risk for HCC occurrence in NAFLD patients. The pathogenesis of HCC in NAFLD patients is a complex process involving multiple mechanisms including lipogenesis, fat accumulation, insulin resistance, oxidative, and endoplasmic reticulum (ER) stress, inflammatory response and DNA damage (83–86) (**Figure 2**). Recent studies have indicated that m^{6}A modification actively participates in these processes. The m^{6}A demethylase FTO has been widely studied due to its established relationship with obesity, and it has been found to promote adipogenesis through multiple signaling pathways (87). Additionally, other m^{6}A regulators such as METTL3 and METTL14 have been reported to participate in the regulation of insulin resistance (83, 84). These studies prove the significance of m^{6}A modification in NAFLD progression, opening up an opportunity to prevent HCC in the future.

Role of m^{6}A Modification in Viral Hepatitis

Gokhale et al. outlined the mechanisms of m^{6}A methylation in regulating the cellular activity of HCV in host cells (79). Knockdown of METTL3 and METTL14 with small interfering RNA (siRNA) increases the production of infectious virions of HCV, which has also been observed in YTHDF reader proteins (79). This may suggest that HCV replication can be inhibited by m^{6}A modification. In addition, m^{6}A can directly modulate the generation of HVC virions as revealed by immunofluorescent staining that YTHDF reader proteins are directly localized to the lipid droplets on which HCV virions assemble (**Figure 3A**) (79). Gokhale et al. discovered new signaling pathways affected by m^{6}A modification after HCV infection, and reported that the infection alters m^{6}A modification of cellular mRNA (80); for example, increased m^{6}A levels of ROI kinase 3 (*RIOK3)* promotes its translation while decreased m^{6}A levels of cold inducible RNA binding protein (*CIRBP*) promotes its alternative splicing (80). *RIOK3* may be translated into serine/threonine kinase, which may modulate antiviral pathways, and *CIRBR* encoding protein might bond RNA in the cellular stress response (88–90). Moreover, the innate immune response and endoplasmic reticulum (ER) stress can trigger this m^{6}A methylation. However, it remains unclear whether the specific cellular changes involving those two mRNAs result from the innate immune response of the host to defend against infection or is normal cellular response to ensure robust replication of the HCV. Still, study of new m^{6}A-modified transcripts could help better elucidate the dynamic changes that occur during viral infection and such materials may be potential antiviral-targets.

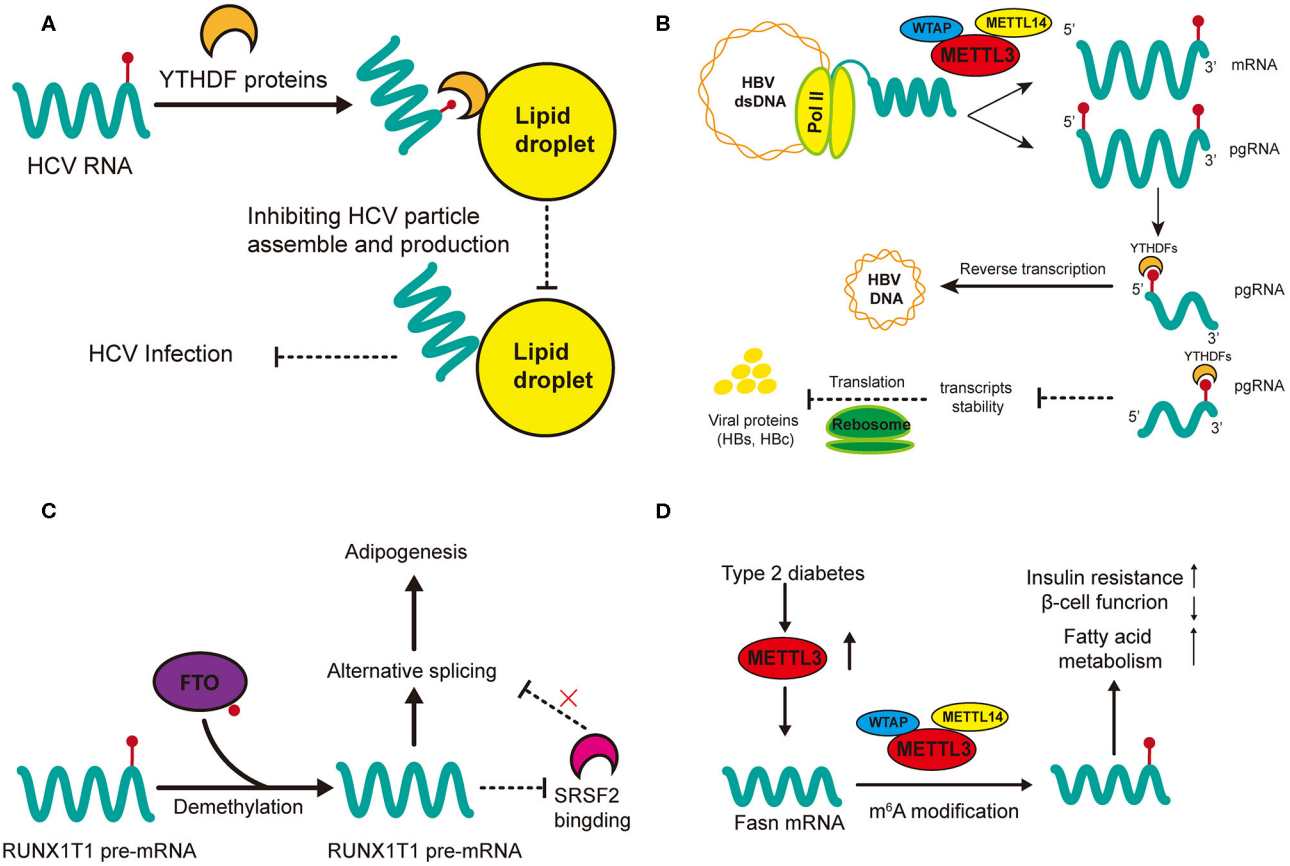

FIGURE 3 | Regulatory functions of m^{6}A in HCC-related hepatic diseases. m^{6}A regulation in HCV **(A)** and HBV **(B)** affect viral activities (infection and replication) while m^{6}A modification in non-alcohol fatty liver disease (NAFLD) promotes adipogenesis **(C)** and insulin resistance **(D)**. **(A)** m^{6}A-modified HCV RNAs are recruited by YTHDF proteins onto lipid droplets to impede the assembly of unmodified RNAs, thus inhibiting the production of HCV infectious particles. **(B)** m^{6}A modification at the 5′ terminus of the pregenomic RNA (pgRNA) is required for HBV reverse transcription while m^{6}A at the 3′ terminus of pgRNA lead to destabilization of HBV transcripts. **(C)** FTO promotes the demethylation of *RUNX1T1* pre-mRNA; this inhibits *SRSF2* binding and alters the alternative splicing of pre-mRNA, therefore promoting adipogenesis. **(D)** The expression of METTL3 is upregulated in type 2 diabetes. Upregulated METTL3 inhibits hepatic insulin sensitivity through m^{6}A modification of Fasn mRNA and facilitates fatty acid metabolism.

m^{6}A modification is vital in the regulation of HBV activity (81). Although HBV is a double-stranded DNA (dsDNA) virus, the extension of its life (replication) is fulfilled by RNA transcripts (91). Imam et al. was the first time to identify m^{6}A in HBV-infected cell lines and liver tissues of chronic HBV patients (**Figure 3B**) (81). They also reported the determinant m^{6}A motif DRACH (D = A, G, or U and H = A, C, or U) within the epsilon loop near the 3′ terminus of HBV mRNA, and that the m^{6}A site is located at A1907 (1905-1909, GGACA) (81). Knockdown of the m^{6}A regulatory enzymes (YTHDF2, YTHDF3, METTL3, and METTL14) may increase the expression of HBV proteins (HBc and HBs), by reducing the stability of HBV RNA. However, m^{6}A at the 5′ stem loop increases reverse transcription and silencing of MTEEL3 as well as METTL14 reduces reverse transcription (81). Thus, it is obvious that the effects of m^{6}A in regulating HBV replication or infection is two-sided, which suggests that m^{6}A modification in viral metabolism is more of a temporal and transient modulation to adapt to the environment of host cells.

Potential Antiviral Therapies Targeting m^{6}A and Future Prospects

Antiviral treatment is indispensable in HCC patients with viral hepatitis, not only for the inhibition of viral replication but also for the prevention of tumor progression (92, 93). The universal presence of m^{6}A in various viruses makes it a potential target for a wide range of viral infection including HBV and HCV.

Interferons (IFNs) have been used in HCC patients with chronic viral hepatitis to impede virus infection and replication, which can effectively prevent the occurrence, recurrence and metastasis of HCC (94–96). Recent studies have shown that, one IFN-stimulated genes (ISG), ISG20, selectively recognize and promotes degradation of m^{6}A-modified HBV transcripts (97). In that study, ISG20-mediated decay of specific HBV RNAs was inhibited by the knockdown of YTHDF2 reader proteins or methyltransferases. Moreover, this ISG20-mediated RNA decay occurred only at m^{6}A sites of A1907 and combined with YTHDF2 reader protein to form a complex (97). These

results lead to the assumption that any degradation process of virus transcripts can be regulated by the combination of YTHDF2 protein and its recognition at the epsilon stem loop (A1907), therefore opening a new gate for the treatment of HCC patients infected with hepatitis virus. There is evidence that 3-deazaadenosine (DAA), the S-adenosylhomocysteine (SAC) hydrolase inhibitor, could serve as a broad-spectrum antiviral (98). The inhibition of SAC hydrolase results in the accumulation of SAC, therefore impairing the generation of S-adenosylmethionine (SAM), from which METTL3 acquire methyl groups for m^{6}A methylation (98). In several studies, DAA has been found to inhibit the replication of diverse viruses by indirectly targeting m^{6}A modification, and the compound has demonstrated no detectable toxicity (99–102). After more *in vivo* validation, DAA could be a promising medicine for the treatment of viral hepatitis and the prevention of HCC.

In addition to currently available medicines that inhibit viral activity through m^{6}A mechanisms, there may be a relationship between specific structural overlaps of viral genome and consensus sequences of m^{6}A modification (103). The guanine-based putative-quadruplex-forming sequences (PQSs) is a conserved secondary structure in viral RNA, which can fold into guanine-quadruplexes (G4s) to regulate viral replication and inhibit protein translation in flaviviruses (79, 104, 105). If viruses can transform PQSs into G4s to counteract surveillance by host cells, G4s could be a potential antiviral target (106, 107). In one study, during the matching of viral PQS and m^{6}A sequencing data, it was found that some sites of m^{6}A occur within the loops of PQSs (103). In addition, mutation data have confirmed some overlapped m^{6}A site are vital for HBV replication. Therefore, it is reasonable to propose that the colocalization of m^{6}A and PQSs in HBV RNA might result from the topological control of m^{6}A methylation, which could generate synergistic effects if it becomes a therapeutic target. However, more sequencing data of m^{6}A is needed for further validation.

Role of m^{6}A Modification in Non-alcohol Fatty Liver Disease

m^{6}A may play an important role in the metabolism of adipose tissues (85). Significant differences in m^{6}A methylation landscape have been observed between NAFLD mice induced through a high-fat diet and normal mice (85). In addition, differential m^{6}A genes are highly expressed in pathways associated with lipid metabolism (85). FTO has been widely studied since its relationship with obesity was discovered (35). Zhao et al. first demonstrated that demethylase FTO promotes the process of adipogenesis by reversing m^{6}A modification (87). Silence of FTO can promote m^{6}A modification, which strengthens the binding capacity of serine and arginine rich splicing factor 2 (*SRSF2*) with targeted exon Runt-related transcription factor 1 (*RUNX1T1*) (**Figure 3C**). This alters the alternative splicing of adipogenesis regulatory factor *RUNX1T1*, thereby slowing the differentiation of preadipocytes and adipogenesis (87). This positive regulation of FTO in lipogenesis has also been confirmed in other cellular networks (108, 109). FTO knockdown lowers the expression of cellular cycle regulators cyclin A2 (*CCNA2*) and cyclin-dependent kinase 2 (*CDK2*) but increases their m^{6}A modification (108). In the meantime, their m^{6}A-modified mRNAs are recognized and degraded by YTHDF2, resulting in suppressed adipogenesis. In addition, both FTO knockdown and METTL3 overexpression can decrease the accumulation of lipids by increasing mRNA m^{6}A methylation (109). There are many other studies on the potential role of FTO in NAFLD, which we do not describe in detail here, because their mechanisms may not involve m^{6}A modification or the methods used for m^{6}A examination are not specific (110–112). In general, FTO and its related signaling could be a prospective research target in the treatment of NAFLD, and the prevention of NAFLD-related HCC.

Another major mechanism of NAFLD progression is insulin resistance (**Figure 3D**) (86). Intracellular METTL3 and m^{6}A methylation in type 2 diabetes patients are positively related with insulin resistance (HOMA-β) and negatively related with β-cell function (84). METTL3 knockout in the liver of mice inhibits m^{6}A modification and decreases the intracellular level of fatty acid synthase (*Fasn*). However, the depletion of METTL3 improves insulin sensitivity and inhibits fatty acid synthesis (84). These results indicate that insulin resistance is mediated by METTL3 through m^{6}A modification of *Fasn* mRNA and it may accelerate the metabolism of fatty acids. Interestingly, another study reported that depletion of METTL14 in β cells in mice fed a high-fat diet led to seemingly paradoxical effects: insulin sensitivity increased while insulin secretion decreased (83). In that study, knockout of METTL14 lowered insulin secretion, increased insulin sensitivity, inhibited lipogenesis and enhanced lipolysis. Insulin sensitivity was enhanced due to the activation of AKT signaling and decreased gluconeogenesis; we speculate that the decrease in lipid accumulation might have resulted from the enhanced insulin signaling in the liver (83). All in all, METTL14 in β cells is positively correlated with lipogenesis and insulin secretion but negatively related with insulin sensitivity. Its function in insulin resistance and lipo-metabolism needs further validation in hepatocytes. However, METTL14 has great potential in the treatment of NAFLD, especially regarding to its multiple effects on insulin and lipid metabolism.

Potential Therapies in Non-alcohol Fatty Liver Disease and Future Prospects

Although the number of people diagnosed with NAFLD is large, only a minority will fall into progressive liver disease or liver cancers (113). Thus, it is important to identify patients who are more likely to progress to HCC and conduct timely interventions.

The regulators of m^{6}A methylation including METTL3, METTL14, YTHDF2, and FTO are potential targets based on their significant roles in the pathogenesis of NAFLD. For instance, dietary branched-chain amino acids (BCAA) can effectively regulate lipid metabolism in weanling piglets via m^{6}A modification (114). In one study, high- and low-dose feeding of BCAA was associated with significantly lower levels of fatty acid synthesis compared to normal-dose feeding, due to the upregulation of lipolysis genes and downregulation of lipogenic genes. Moreover, a lower level of m^{6}A methylation was identified

with downregulation of METTL3 and FTO in the livers of the high-BCAA group (114). The results indicated that a dietary with high BCAAs can decrease lipid accumulation through the regulation of m^{6}A modification.

The protective effects of betaine (trimethylglycine) on liver, including alleviation of impaired liver function and decreased lipid accumulation, have long been recognized (115, 116). Recently, it was confirmed that these protective effects are mediated by FTO through m^{6}A modification (117). Betaine promotes lipolysis and lipid oxidative by reversing the hypomethylated-mRNA and overexpressed FTO in adipocytes of mice fed with high fat diet (118). In addition, this reversion requires the existence of AMP-activated protein kinase α1 subunit (*AMPK*α1) (118). Another study reported that lipopolysaccharide (LPS)-induced liver function and lipid metabolism disorder can be alleviated by curcumin through the upregulation of m^{6}A (119). Furthermore, curcumin supplementation affected the expression of major m^{6}A regulators, indicating its powerful hepatoprotective effect (119). There are plenty of other compounds such as exenatide and entacapone that directly target m^{6}A regulator, that worth more researching in the future (120, 121).

CONCLUSION

In summary, m^{6}A modification plays an important role in the occurrence and development of HCC. Viral hepatitis and NAFLD are major risk factors for HCC, which shows a significant relationship with m^{6}A methylation. In HCV and HBV, m^{6}A regulates the infection and replication of virus. In NAFLD, it participates in insulin resistance and the accumulation of lipids. Therapeutic experiments regarding m^{6}A have been conducted on two diseases, which will greatly promote the prevention of HCC. However, the chronic inflammation that accompanies these ailments will lead to liver fibrosis and/or cirrhosis, whose pathogeneses regarding m^{6}A warrant further study. In HCC, m^{6}A regulators specifically regulate mRNA splicing, translation, and degradation, while ncRNAs interact with m^{6}A, leading to changes in gene expression; consequently, mRNAs and ncRNAs both regulate the progression of HCC. Therefore, in terms of the diversity of m^{6}A in HCC, m^{6}A-related molecules are potential biomarkers for early diagnosis and prospective therapeutic targets for clinical treatment. Furthermore, in the age of precision medicine, m^{6}A-related therapies could be tailored based on the etiology and pathogenesis of HCC patients, which will optimize treatments and their benefits.

AUTHOR CONTRIBUTIONS

JL wrote the first draft of the manuscript. JQ conceived the idea of the manuscript. LZ and SY designed the structure of the manuscript. SZ and WZ revised, read, and approved the submitted version. All authors contributed to the article and approved the submitted version.

FUNDING

This work was supported by the National S&T Large Project (No. 2018ZX10301201) and the National Science Foundation of China (Nos. 81721091 and 2017ZX10203205).

REFERENCES

1. Bray F, Ferlay J, Soerjomataram I, Siegel RL, Torre LA, Jemal A. Global cancer statistics 2018: gLOBOCAN estimates of incidence and mortality worldwide for 36 cancers in 185 countries. *CA Cancer J Clin.* (2018) 68:394–424. doi: 10.3322/caac.21492
2. Yang JD, Hainaut P, Gores GJ, Amadou A, Plymoth A, Roberts LR. A global view of hepatocellular carcinoma: trends, risk, prevention and management. *Nat Rev Gastroenterol Hepatol.* (2019) 16:589–604. doi: 10.1038/s41575-019-0186-y
3. Villanueva A. Hepatocellular carcinoma. *N Engl J Med.* (2019) 380:1450–62. doi: 10.1056/NEJMra1713263
4. Forner A, Reig M, Bruix J. Hepatocellular carcinoma. *Lancet.* (2018) 391:1301–14. doi: 10.1016/S0140-6736(18)30010-2
5. El-Serag HB. Epidemiology of viral hepatitis and hepatocellular carcinoma. *Gastroenterology.* (2012) 142:1264–73 e1. doi: 10.1053/j.gastro.2011.12.061
6. Global Burden of Disease Cancer C, Fitzmaurice C, Akinyemiju TF, Al Lami FH, Alam T, Alizadeh-Navaei R, et al. Global, regional, and national cancer incidence, mortality, years of life lost, years lived with disability, and disability-Adjusted life-Years for 29 cancer groups, 1990 to 2016: a Systematic analysis for the global burden of disease study. *JAMA Oncol.* (2018) 4:1553–68. doi: 10.1001/jamaoncol.2018.2706
7. Anstee QM, Reeves HL, Kotsiliti E, Govaere O, Heikenwalder M. From nASH to hCC: current concepts and future challenges. *Nat Rev Gastroenterol Hepatol.* (2019) 16:411–28. doi: 10.1038/s41575-019-0145-7
8. El-Khoueiry AB, Sangro B, Yau T, Crocenzi TS, Kudo M, Hsu C, et al. Nivolumab in patients with advanced hepatocellular carcinoma (CheckMate 040): an open-label, non-comparative, phase 1/2 dose escalation and expansion trial. *Lancet.* (2017) 389:2492–502. doi: 10.1016/S0140-6736(17)31046-2
9. Kudo M, Finn RS, Qin S, Han KH, Ikeda K, Piscaglia F, et al. Lenvatinib versus sorafenib in first-line treatment of patients with unresectable hepatocellular carcinoma: a randomised phase 3 non-inferiority trial. *Lancet.* (2018) 391:1163–73. doi: 10.1016/S0140-6736(18)30207-1
10. Fu Y, Dominissini D, Rechavi G, He C. Gene expression regulation mediated through reversible m(6)A rNA methylation. *Nat Rev Genet.* (2014) 15:293–306. doi: 10.1038/nrg3724
11. Jia G, Fu Y, He C. Reversible rNA adenosine methylation in biological regulation. *Trends Genet.* (2013) 29:108–15. doi: 10.1016/j.tig.2012.11.003
12. Deng X, Chen K, Luo GZ, Weng X, Ji Q, Zhou T, et al. Widespread occurrence of n6-methyladenosine in bacterial mRNA. *Nucleic Acids Res.* (2015) 43:6557–67. doi: 10.1093/nar/gkv596
13. Sommer S, Salditt-Georgieff M, Bachenheimer S, Darnell JE, Furuichi Y, Morgan M, et al. The methylation of adenovirus-specific nuclear and cytoplasmic rNA. *Nucleic Acids Res.* (1976) 3:749–65. doi: 10.1093/nar/3.3.749
14. Kennedy EM, Courtney DG, Tsai K, Cullen BR. Viral epitranscriptomics. *J Virol.* (2017) 91. doi: 10.1128/JVI.02263-16
15. Yadav PK, Rajasekharan R. The m(6)A methyltransferase ime4 epitranscriptionally regulates triacylglycerol metabolism and vacuolar morphology in haploid yeast cells. *J Biol Chem.* (2017) 292:13727–44. doi: 10.1074/jbc.M117.783761
16. Dominissini D, Moshitch-Moshkovitz S, Schwartz S, Salmon-Divon M, Ungar L, Osenberg S, et al. Topology of the human and mouse m6A rNA methylomes revealed by m6A-seq. *Nature.* (2012) 485:201–6. doi: 10.1038/nature11112

17. Meyer KD, Saletore Y, Zumbo P, Elemento O, Mason CE, Jaffrey SR. Comprehensive analysis of mRNA methylation reveals enrichment in 3' uTRs and near stop codons. *Cell.* (2012) 149:1635–46. doi: 10.1016/j.cell.2012.05.003
18. Liu N, Dai Q, Zheng G, He C, Parisien M, Pan T. N(6)-methyladenosine-dependent rNA structural switches regulate rNA-protein interactions. *Nature.* (2015) 518:560–4. doi: 10.1038/nature14234
19. Patil DP, Pickering BF, Jaffrey SR. Reading m(6)A in the transcriptome: m(6)A-Binding proteins. *Trends Cell Biol.* (2018) 28:113–27. doi: 10.1016/j.tcb.2017.10.001
20. Meyer KD, Jaffrey SR. Rethinking m(6)A readers, writers, and erasers. *Annu Rev Cell Dev Biol.* (2017) 33:319–42. doi: 10.1146/annurev-cellbio-100616-060758
21. Yang D, Qiao J, Wang G, Lan Y, Li G, Guo X, et al. N6-Methyladenosine modification of lincRNA 1281 is critically required for mESC differentiation potential. *Nucleic Acids Res.* (2018) 46:3906–20. doi: 10.1093/nar/gky130
22. Liu Z, Zhang J. Human c-to-U coding rNA editing is largely nonadaptive. *Mol Biol Evol.* (2018) 35:963–9. doi: 10.1093/molbev/msy011
23. Zhou C, Molinie B, Daneshvar K, Pondick JV, Wang J, Van Wittenberghe N, et al. Genome-Wide maps of m6A circRNAs identify widespread and cell-Type-Specific methylation patterns that are distinct from mRNAs. *Cell Rep.* (2017) 20:2262–76. doi: 10.1016/j.celrep.2017.08.027
24. Lin S, Choe J, Du P, Triboulet R, Gregory RI. The m(6)A methyltransferase mETTL3 promotes translation in human cancer cells. *Mol Cell.* (2016) 62:335–45. doi: 10.1016/j.molcel.2016.03.021
25. Lin S, Gregory RI. Methyltransferases modulate rNA stability in embryonic stem cells. *Nat Cell Biol.* (2014) 16:129–31. doi: 10.1038/ncb2914
26. Shulman Z, Stern-Ginossar N. The rNA modification n(6)-methyladenosine as a novel regulator of the immune system. *Nat Immunol.* (2020) doi: 10.1038/s41590-020-0650-4
27. Hua W, Zhao Y, Jin X, Yu D, He J, Xie D, et al. METTL3 promotes ovarian carcinoma growth and invasion through the regulation of aXL translation and epithelial to mesenchymal transition. *Gynecol Oncol.* (2018) 151:356–65. doi: 10.1016/j.ygyno.2018.09.015
28. Hou J, Zhang H, Liu J, Zhao Z, Wang J, Lu Z, et al. YTHDF2 reduction fuels inflammation and vascular abnormalization in hepatocellular carcinoma. *Mol Cancer.* (2019) 18:163. doi: 10.1186/s12943-019-1082-3
29. Ma JZ, Yang F, Zhou CC, Liu F, Yuan JH, Wang F, et al. METTL14 suppresses the metastatic potential of hepatocellular carcinoma by modulating n(6) -methyladenosine-dependent primary microRNA processing. *Hepatology.* (2017) 65:529–43. doi: 10.1002/hep.28885
30. Li Z, Li F, Peng Y, Fang J, Zhou J. Identification of three m6A-related mRNAs signature and risk score for the prognostication of hepatocellular carcinoma. *Cancer Medicine.* (2020) doi: 10.1002/cam4.2833
31. Pan Y, Ma P, Liu Y, Li W, Shu Y. Multiple functions of m(6)A rNA methylation in cancer. *J Hematol Oncol.* (2018) 11:48. doi: 10.1186/s13045-018-0590-8
32. Wang X, Feng J, Xue Y, Guan Z, Zhang D, Liu Z, et al. Structural basis of n(6)-adenosine methylation by the mETTL3-METTL14 complex. *Nature.* (2016) 534:575–8. doi: 10.1038/nature18298
33. Ping XL, Sun BF, Wang L, Xiao W, Yang X, Wang WJ, et al. Mammalian wTAP is a regulatory subunit of the rNA n6-methyladenosine methyltransferase. *Cell Res.* (2014) 24:177–89. doi: 10.1038/cr.2014.3
34. Jia G, Fu Y, Zhao X, Dai Q, Zheng G, Yang Y, et al. N6-methyladenosine in nuclear rNA is a major substrate of the obesity-associated fTO. *Nat Chem Biol.* (2011) 7:885–7. doi: 10.1038/nchembio.687
35. Frayling TM, Timpson NJ, Weedon MN, Zeggini E, Freathy RM, Lindgren CM, et al. A common variant in the fTO gene is associated with body mass index and predisposes to childhood and adult obesity. *Science.* (2007) 316:889–94. doi: 10.1126/science.1141634
36. Wahlen K, Sjolin E, Hoffstedt J. The common rs9939609 gene variant of the fat mass- and obesity-associated gene fTO is related to fat cell lipolysis. *J Lipid Res.* (2008) 49:607–11. doi: 10.1194/jlr.M700448-JLR200
37. Zheng G, Dahl JA, Niu Y, Fedorcsak P, Huang CM, Li CJ, et al. ALKBH5 is a mammalian rNA demethylase that impacts rNA metabolism and mouse fertility. *Mol Cell.* (2013) 49:18–29. doi: 10.1016/j.molcel.2012.10.015
38. Xiao W, Adhikari S, Dahal U, Chen YS, Hao YJ, Sun BF, et al. Nuclear m(6)A reader yTHDC1 regulates mRNA splicing. *Mol Cell.* (2016) 61:507–19. doi: 10.1016/j.molcel.2016.01.012
39. Roundtree IA, Luo GZ, Zhang Z, Wang X, Zhou T, Cui Y, et al. YTHDC1 mediates nuclear export of n(6)-methyladenosine methylated mRNAs. *Elife.* (2017) 6. doi: 10.7554/eLife.31311
40. Liao S, Sun H, Xu C. YTH domain: a Family of n(6)-methyladenosine (m(6)A) readers. *Genomics Proteomics Bioinformatics.* (2018) 16:99–107. doi: 10.1016/j.gpb.2018.04.002
41. Hsu PJ, Zhu Y, Ma H, Guo Y, Shi X, Liu Y, et al. Ythdc2 is an n(6)-methyladenosine binding protein that regulates mammalian spermatogenesis. *Cell Res.* (2017) 27:1115–27. doi: 10.1038/cr.2017.99
42. Ries RJ, Zaccara S, Klein P, Olarerin-George A, Namkoong S, Pickering BF, et al. m(6)A enhances the phase separation potential of mRNA. *Nature.* (2019) 571:424–8. doi: 10.1038/s41586-019-1374-1
43. Gao Y, Pei G, Li D, Li R, Shao Y, Zhang QC, et al. Multivalent m(6)A motifs promote phase separation of yTHDF proteins. *Cell Res.* (2019) 29:767–9. doi: 10.1038/s41422-019-0210-3
44. Zhao Y, Shi Y, Shen H, Xie W. m(6)A-binding proteins: the emerging crucial performers in epigenetics. *J Hematol Oncol.* (2020) 13:35. doi: 10.1186/s13045-020-00872-8
45. Huang H, Weng H, Sun W, Qin X, Shi H, Wu H, et al. Recognition of rNA n(6)-methyladenosine by iGF2BP proteins enhances mRNA stability and translation. *Nat Cell Biol.* (2018) 20:285–95. doi: 10.1038/s41556-018-0045-z
46. Zhou KI, Shi H, Lyu R, Wylder AC, Matuszek Z, Pan JN, et al. Regulation of co-transcriptional pre-mRNA splicing by m(6)A through the low-Complexity protein hnRNPG. *Mol Cell.* (2019) 76:70–81 e9. doi: 10.1016/j.molcel.2019.07.005
47. Alarcon CR, Goodarzi H, Lee H, Liu X, Tavazoie S, Tavazoie SF. HNRNPA2B1 is a mediator of m(6)A-Dependent nuclear rNA processing events. *Cell.* (2015) 162:1299–308. doi: 10.1016/j.cell.2015.08.011
48. Huang H, Weng H, Zhou K, Wu T, Zhao BS, Sun M, et al. Histone h3 trimethylation at lysine 36 guides m(6)A rNA modification co-transcriptionally. *Nature.* (2019) 567:414–9. doi: 10.1038/s41586-019-1016-7
49. Santos-Pereira JM, Aguilera A. R loops: new modulators of genome dynamics and function. *Nat Rev Genet.* (2015) 16:583–97. doi: 10.1038/nrg3961
50. Abakir A, Giles TC, Cristini A, Foster JM, Dai N, Starczak M, et al. N(6)-methyladenosine regulates the stability of rNA:DNA hybrids in human cells. *Nat Genet.* (2020) 52:48–55. doi: 10.1038/s41588-019-0549-x
51. Yang X, Liu QL, Xu W, Zhang YC, Yang Y, Ju LF, et al. m(6)A promotes r-loop formation to facilitate transcription termination. *Cell Res.* (2019) 29:1035–8. doi: 10.1038/s41422-019-0235-7
52. Liu J, Dou X, Chen C, Chen C, Liu C, Xu MM, et al. N (6)-methyladenosine of chromosome-associated regulatory rNA regulates chromatin state and transcription. *Science.* (2020) 367:580–6. doi: 10.1126/science.aay6018
53. Lin X, Chai G, Wu Y, Li J, Chen F, Liu J, et al. RNA m(6)A methylation regulates the epithelial mesenchymal transition of cancer cells and translation of snail. *Nat Commun.* (2019) 10:2065. doi: 10.1038/s41467-019-09865-9
54. Li E, Wei B, Wang X, Kang R. METTL3 enhances cell adhesion through stabilizing integrin beta1 mRNA via an m6A-HuR-dependent mechanism in prostatic carcinoma. *Am J Cancer Res.* (2020) 10:1012–25.
55. Yue B, Song C, Yang L, Cui R, Cheng X, Zhang Z, et al. METTL3-mediated n6-methyladenosine modification is critical for epithelial-mesenchymal transition and metastasis of gastric cancer. *Mol Cancer.* (2019) 18:142. doi: 10.1186/s12943-019-1065-4
56. Yang X, Zhang S, He C, Xue P, Zhang L, He Z, et al. METTL14 suppresses proliferation and metastasis of colorectal cancer by down-regulating oncogenic long non-coding rNA xIST. *Mol Cancer.* (2020) 19:46. doi: 10.1186/s12943-020-1146-4
57. Chen X, Xu M, Xu X, Zeng K, Liu X, Sun L, et al. METTL14 suppresses cRC progression via regulating n6-Methyladenosine-Dependent primary miR-375 processing. *Mol Ther.* (2020) 28:599–612. doi: 10.1016/j.ymthe.2019.11.016
58. Zhang C, Samanta D, Lu H, Bullen JW, Zhang H, Chen I, et al. Hypoxia induces the breast cancer stem cell phenotype by hIF-dependent and

aLKBH5-mediated m(6)A-demethylation of nANOG mRNA. *Proc Natl Acad Sci U S A*. (2016) 113:E2047–56. doi: 10.1073/pnas.1602883113
59. Shi Y, Fan S, Wu M, Zuo Z, Li X, Jiang L, et al. YTHDF1 links hypoxia adaptation and non-small cell lung cancer progression. *Nat Commun.* (2019) 10:4892. doi: 10.1038/s41467-019-12801-6
60. Sheng H, Li Z, Su S, Sun W, Zhang X, Li L, et al. YTH domain family 2 promotes lung cancer cell growth by facilitating 6-phosphogluconate dehydrogenase mRNA translation. *Carcinogenesis.* (2019) doi: 10.1093/carcin/bgz152. [Epub ahead of print].
61. Paris J, Morgan M, Campos J, Spencer GJ, Shmakova A, Ivanova I, et al. Targeting the rNA m(6)A reader yTHDF2 selectively compromises cancer stem cells in acute myeloid leukemia. *Cell Stem Cell.* (2019) 25:137–48 e6. doi: 10.1016/j.stem.2019.03.021
62. Yang S, Wei J, Cui YH, Park G, Shah P, Deng Y, et al. m(6)A mRNA demethylase fTO regulates melanoma tumorigenicity and response to anti-PD-1 blockade. *Nat Commun.* (2019) 10:2782. doi: 10.1038/s41467-019-10669-0
63. Li H, Su Q, Li B, Lan L, Wang C, Li W, et al. High expression of wTAP leads to poor prognosis of gastric cancer by influencing tumour-associated t lymphocyte infiltration. *J Cell Mol Med.* (2020) 24:4452–65. doi: 10.1111/jcmm.15104
64. Zhong L, Liao D, Zhang M, Zeng C, Li X, Zhang R, et al. YTHDF2 suppresses cell proliferation and growth via destabilizing the eGFR mRNA in hepatocellular carcinoma. *Cancer Lett.* (2019) 442:252–61. doi: 10.1016/j.canlet.2018.11.006
65. Chen M, Wei L, Law CT, Tsang FH, Shen J, Cheng CL, et al. RNA n6-methyladenosine methyltransferase-like 3 promotes liver cancer progression through yTHDF2-dependent posttranscriptional silencing of sOCS2. *Hepatology.* (2018) 67:2254–70. doi: 10.1002/hep.29683
66. Chen Y, Peng C, Chen J, Chen D, Yang B, He B, et al. WTAP facilitates progression of hepatocellular carcinoma via m6A-HuR-dependent epigenetic silencing of eTS1. *Mol Cancer.* (2019) 18:127. doi: 10.1186/s12943-019-1053-8
67. Muller S, Glass M, Singh AK, Haase J, Bley N, Fuchs T, et al. IGF2BP1 promotes sRF-dependent transcription in cancer in a m6A- and miRNA-dependent manner. *Nucleic Acids Res.* (2019) 47:375–90. doi: 10.1093/nar/gky1012
68. Cheng X, Li M, Rao X, Zhang W, Li X, Wang L, et al. KIAA1429 regulates the migration and invasion of hepatocellular carcinoma by altering m6A modification of iD2 mRNA. *Onco Targets Ther.* (2019) 12:3421–8. doi: 10.2147/OTT.S180954
69. Li J, Zhu L, Shi Y, Liu J, Lin L, Chen X. m6A demethylase fTO promotes hepatocellular carcinoma tumorigenesis via mediating pKM2 demethylation. *Am J Transl Res.* (2019) 11:6084–92.
70. Han J, Lee Y, Yeom KH, Kim YK, Jin H, Kim VN. The drosha-DGCR8 complex in primary microRNA processing. *Genes Dev.* (2004) 18:3016–27. doi: 10.1101/gad.1262504
71. Yang Z, Li J, Feng G, Gao S, Wang Y, Zhang S, et al. MicroRNA-145 modulates n(6)-Methyladenosine levels by targeting the 3'-Untranslated mRNA region of the n(6)-Methyladenosine binding yTH domain family 2 protein. *J Biol Chem.* (2017) 292:3614–23. doi: 10.1074/jbc.M116.749689
72. Zuo X, Chen Z, Gao W, Zhang Y, Wang J, Wang J, et al. M6A-mediated upregulation of lINC00958 increases lipogenesis and acts as a nanotherapeutic target in hepatocellular carcinoma. *J Hematol Oncol.* (2020) 13:5. doi: 10.1186/s13045-019-0839-x
73. Lan T, Li H, Zhang D, Xu L, Liu H, Hao X, et al. KIAA1429 contributes to liver cancer progression through n6-methyladenosine-dependent post-transcriptional modification of gATA3. *Mol Cancer.* (2019) 18:186. doi: 10.1186/s12943-019-1106-z
74. Zhang X, Xu Y, Qian Z, Zheng W, Wu Q, Chen Y, et al. circRNA_104075 stimulates yAP-dependent tumorigenesis through the regulation of hNF4a and may serve as a diagnostic marker in hepatocellular carcinoma. *Cell Death Dis.* (2018) 9:1091. doi: 10.1038/s41419-018-1132-6
75. Ma H, Wang X, Cai J, Dai Q, Natchiar SK, Lv R, et al. N(6-)Methyladenosine methyltransferase zCCHC4 mediates ribosomal rNA methylation. *Nat Chem Biol.* (2019) 15:88–94. doi: 10.1038/s41589-018-0184-3
76. Zhao X, Chen Y, Mao Q, Jiang X, Jiang W, Chen J, et al. Overexpression of yTHDF1 is associated with poor prognosis in patients with hepatocellular carcinoma. *Cancer Biomark.* (2018) 21:859–68. doi: 10.3233/CBM-170791
77. Zhou Y, Yin Z, Hou B, Yu M, Chen R, Jin H, et al. Expression profiles and prognostic significance of rNA n6-methyladenosine-related genes in patients with hepatocellular carcinoma: evidence from independent datasets. *Cancer Manag Res.* (2019) 11:3921–31. doi: 10.2147/CMAR.S191565
78. Barnett R. Liver cirrhosis. *Lancet.* (2018) 392:275. doi: 10.1016/S0140-6736(18)31659-3
79. Gokhale NS, McIntyre ABR, McFadden MJ, Roder AE, Kennedy EM, Gandara JA, et al. N6-Methyladenosine in flaviviridae viral rNA genomes regulates infection. *Cell Host Microbe.* (2016) 20:654–65. doi: 10.1016/j.chom.2016.09.015
80. Gokhale NS, McIntyre ABR, Mattocks MD, Holley CL, Lazear HM, Mason CE, et al. Altered m(6)A modification of specific cellular transcripts affects flaviviridae infection. *Mol Cell.* (2020) 77:542–55 e8. doi: 10.1016/j.molcel.2019.11.007
81. Imam H, Khan M, Gokhale NS, McIntyre ABR, Kim GW, Jang JY, et al. N6-methyladenosine modification of hepatitis b virus rNA differentially regulates the viral life cycle. *Proc Natl Acad Sci USA.* (2018) 115:8829–34. doi: 10.1073/pnas.1808319115
82. Younes R, Bugianesi E. Should we undertake surveillance for hCC in patients with nAFLD? *J Hepatol.* (2018) 68:326–34. doi: 10.1016/j.jhep.2017.10.006
83. Liu J, Luo G, Sun J, Men L, Ye H, He C, et al. METTL14 is essential for beta-cell survival and insulin secretion. *Biochim Biophys Acta Mol Basis Dis.* (2019) 1865:2138–48. doi: 10.1016/j.bbadis.2019.04.011
84. Xie W, Ma LL, Xu YQ, Wang BH, Li SM. METTL3 inhibits hepatic insulin sensitivity via n6-methyladenosine modification of fasn mRNA and promoting fatty acid metabolism. *Biochem Biophys Res Commun.* (2019) 518:120–6. doi: 10.1016/j.bbrc.2019.08.018
85. Luo Z, Zhang Z, Tai L, Zhang L, Sun Z, Zhou L. Comprehensive analysis of differences of n(6)-methyladenosine rNA methylomes between high-fat-fed and normal mouse livers. *Epigenomics.* (2019) 11:1267–82. doi: 10.2217/epi-2019-0009
86. Friedman SL, Neuschwander-Tetri BA, Rinella M, Sanyal AJ. Mechanisms of nAFLD development and therapeutic strategies. *Nat Med.* (2018) 24:908–22. doi: 10.1038/s41591-018-0104-9
87. Zhao X, Yang Y, Sun BF, Shi Y, Yang X, Xiao W, et al. FTO-dependent demethylation of n6-methyladenosine regulates mRNA splicing and is required for adipogenesis. *Cell Res.* (2014) 24:1403–19. doi: 10.1038/cr.2014.151
88. Takashima K, Oshiumi H, Takaki H, Matsumoto M, Seya T. RIOK3-mediated phosphorylation of mDA5 interferes with its assembly and attenuates the innate immune response. *Cell Rep.* (2015) 11:192–200. doi: 10.1016/j.celrep.2015.03.027
89. Feng J, De Jesus PD, Su V, Han S, Gong D, Wu NC, et al. RIOK3 is an adaptor protein required for iRF3-mediated antiviral type i interferon production. *J Virol.* (2014) 88:7987–97. doi: 10.1128/JVI.00643-14
90. Liao Y, Tong L, Tang L, Wu S. The role of cold-inducible rNA binding protein in cell stress response. *Int J Cancer.* (2017) 141:2164–73. doi: 10.1002/ijc.30833
91. Seeger C, Mason WS. Hepatitis b virus biology. *Microbiol Mol Biol Rev.* (2000) 64:51–68. doi: 10.1128/mmbr.64.1.51-68.2000
92. Kanwal F, Kramer J, Asch SM, Chayanupatkul M, Cao Y, El-Serag HB. Risk of hepatocellular cancer in hCV patients treated with direct-Acting antiviral agents. *Gastroenterology.* (2017) 153:996–1005 e1. doi: 10.1053/j.gastro.2017.06.012
93. Papatheodoridis GV, Chan HL, Hansen BE, Janssen HL, Lampertico P. Risk of hepatocellular carcinoma in chronic hepatitis b: assessment and modification with current antiviral therapy. *J Hepatol.* (2015) 62:956–67. doi: 10.1016/j.jhep.2015.01.002
94. Ren H, Huang Y. Effects of pegylated interferon-alpha based therapies on functional cure and the risk of hepatocellular carcinoma development in patients with chronic hepatitis b. *J Viral Hepat.* (2019) 26 Suppl 1:5–31. doi: 10.1111/jvh.13150
95. Teng W, Jeng WJ, Yang HI, Chen WT, Hsieh YC, Huang CH, et al. Interferon is superior to direct acting antiviral therapy in tertiary prevention

of early recurrence of hepatocellular carcinoma. *Cancers (Basel).* (2019) 12:23. doi: 10.3390/cancers12010023
96. Miyake Y, Takaki A, Iwasaki Y, Yamamoto K. Meta-analysis: interferon-alpha prevents the recurrence after curative treatment of hepatitis c virus-related hepatocellular carcinoma. *J Viral Hepat.* (2010) 17:287–92. doi: 10.1111/j.1365-2893.2009.01181.x
97. Imam H, Kim GW, Mir SA, Khan M, Siddiqui A. Interferon-stimulated gene 20 (ISG20) selectively degrades n6-methyladenosine modified hepatitis b Virus transcripts. *PLoS Pathog.* (2020) 16:e1008338. doi: 10.1371/journal.ppat.1008338
98. Bader JP, Brown NR, Chiang PK, Cantoni GL. 3-Deazaadenosine, an inhibitor of adenosylhomocysteine hydrolase, inhibits reproduction of Rous sarcoma virus and transformation of chick embryo cells. *Virology.* (1978) 89:494–505. doi: 10.1016/0042-6822(78)90191-5
99. Wyde PR, Ambrose MW, Meyer HL, Zolinski CL, Gilbert BE. Evaluation of the toxicity and antiviral activity of carbocyclic 3-deazaadenosine against respiratory syncytial and parainfluenza type 3 viruses in tissue culture and in cotton rats. *Antiviral Res.* (1990) 14:215–25. doi: 10.1016/0166-3542(90)90003-p
100. Bray M, Driscoll J, Huggins JW. Treatment of lethal ebola virus infection in mice with a single dose of an s-adenosyl-L-homocysteine hydrolase inhibitor. *Antiviral Res.* (2000) 45:135–47. doi: 10.1016/s0166-3542(00)00066-8
101. Mayers DL, Mikovits JA, Joshi B, Hewlett IK, Estrada JS, Wolfe AD, et al. Anti-human immunodeficiency virus 1 (HIV-1) activities of 3-deazaadenosine analogs: increased potency against 3'-azido-3'-deoxythymidine-resistant hIV-1 strains. *Proc Natl Acad Sci USA.* (1995) 92:215–9. doi: 10.1073/pnas.92.1.215
102. de Clercq E, Montgomery JA. Broad-spectrum antiviral activity of the carbocyclic analog of 3-deazaadenosine. *Antiviral Res.* (1983) 3:17–24. doi: 10.1016/0166-3542(83)90011-6
103. Fleming AM, Nguyen NLB, Burrows CJ. Colocalization of m6A and g-Quadruplex-Forming sequences in viral rNA (HIV, zika, hepatitis b, and sV40) suggests topological control of adenosine n6-Methylation. *ACS Central Science.* (2019) 5:218–28. doi: 10.1021/acscentsci.8b00963
104. Wang SR, Min YQ, Wang JQ, Liu CX, Fu BS, Wu F, et al. A highly conserved g-rich consensus sequence in hepatitis c virus core gene represents a new anti-hepatitis c target. *Sci Adv.* (2016) 2:e1501535. doi: 10.1126/sciadv.1501535
105. Jaubert C, Bedrat A, Bartolucci L, Di Primo C, Ventura M, Mergny JL, et al. RNA synthesis is modulated by g-quadruplex formation in hepatitis c virus negative rNA strand. *Sci Rep.* (2018) 8:8120. doi: 10.1038/s41598-018-26582-3
106. Saranathan N, Vivekanandan P. G-Quadruplexes: more than just a kink in microbial genomes. *Trends Microbiol.* (2019) 27:148–63. doi: 10.1016/j.tim.2018.08.011
107. Cammas A, Millevoi S. RNA g-quadruplexes: emerging mechanisms in disease. *Nucleic Acids Res.* (2017) 45:1584–95. doi: 10.1093/nar/gkw1280
108. Wu R, Liu Y, Yao Y, Zhao Y, Bi Z, Jiang Q, et al. FTO regulates adipogenesis by controlling cell cycle progression via m(6)A-YTHDF2 dependent mechanism. *Biochim Biophys Acta Mol Cell Biol Lipids.* (2018) 1863:1323–30. doi: 10.1016/j.bbalip.2018.08.008
109. Wang X, Zhu L, Chen J, Wang Y. mRNA m(6)A methylation downregulates adipogenesis in porcine adipocytes. *Biochem Biophys Res Commun.* (2015) 459:201–7. doi: 10.1016/j.bbrc.2015.02.048
110. Chen X, Luo Y, Jia G, Liu G, Zhao H, Huang Z. FTO promotes adipogenesis through inhibition of the wnt/beta-catenin signaling pathway in porcine intramuscular preadipocytes. *Anim Biotechnol.* (2017) 28:268–74. doi: 10.1080/10495398.2016.1273835
111. Merkestein M, Laber S, McMurray F, Andrew D, Sachse G, Sanderson J, et al. FTO influences adipogenesis by regulating mitotic clonal expansion. *Nat Commun.* (2015) 6:6792. doi: 10.1038/ncomms7792
112. Guo J, Ren W, Li A, Ding Y, Guo W, Su D, et al. Fat mass and obesity-associated gene enhances oxidative stress and lipogenesis in nonalcoholic fatty liver disease. *Dig Dis Sci.* (2013) 58:1004–9. doi: 10.1007/s10620-012-2516-6
113. White DL, Kanwal F, El-Serag HB. Association between nonalcoholic fatty liver disease and risk for hepatocellular cancer, based on systematic review. *Clin Gastroenterol Hepatol.* (2012) 10:1342–59 e2. doi: 10.1016/j.cgh.2012.10.001
114. Heng J, Wu Z, Tian M, Chen J, Song H, Chen F, et al. Excessive bCAA regulates fat metabolism partially through the modification of m(6)A rNA methylation in weanling piglets. *Nutr Metab (Lond).* (2020) 17:10. doi: 10.1186/s12986-019-0424-x
115. Ji C, Kaplowitz N. Betaine decreases hyperhomocysteinemia, endoplasmic reticulum stress, and liver injury in alcohol-fed mice. *Gastroenterology.* (2003) 124:1488–99. doi: 10.1016/s0016-5085(03)00276-2
116. Zhang L, Qi Y, Z AL, Liu S, Zhang Z, Zhou L. Betaine increases mitochondrial content and improves hepatic lipid metabolism. *Food Funct.* (2019) 10:216–23. doi: 10.1039/c8fo02004c
117. Chen J, Zhou X, Wu W, Wang X, Wang Y. FTO-dependent function of n6-methyladenosine is involved in the hepatoprotective effects of betaine on adolescent mice. *J Physiol Biochem.* (2015) 71:405–13. doi: 10.1007/s13105-015-0420-1
118. Zhou X, Chen J, Chen J, Wu W, Wang X, Wang Y. The beneficial effects of betaine on dysfunctional adipose tissue and n6-methyladenosine mRNA methylation requires the aMP-activated protein kinase alpha1 subunit. *J Nutr Biochem.* (2015) 26:1678–84. doi: 10.1016/j.jnutbio.2015.08.014
119. Lu N, Li X, Yu J, Li Y, Wang C, Zhang L, et al. Curcumin attenuates lipopolysaccharide-Induced hepatic lipid metabolism disorder by modification of m(6) a RNA methylation in piglets. *Lipids.* (2018) 53:53–63. doi: 10.1002/lipd.12023
120. Li S, Wang X, Zhang J, Li J, Liu X, Ma Y, et al. Exenatide ameliorates hepatic steatosis and attenuates fat mass and fTO gene expression through pI3K signaling pathway in nonalcoholic fatty liver disease. *Braz J Med Biol Res.* (2018) 51:e7299. doi: 10.1590/1414-431x20187299
121. Peng S, Xiao W, Ju D, Sun B, Hou N, Liu Q, et al. Identification of entacapone as a chemical inhibitor of fTO mediating metabolic regulation through fOXO1. *Sci Transl Med.* (2019) 11:7116. doi: 10.1126/scitranslmed.aau7116

Conflict of Interest: The authors declare that the research was conducted in the absence of any commercial or financial relationships that could be construed as a potential conflict of interest.

The reviewer XH declared a shared affiliation, with no collaboration, with the authors to the handling editor at the time of review.

frontiers in Oncology

REVIEW
published: 07 August 2020
doi: 10.3389/fonc.2020.01152

Role of DNA Methylation in the Resistance to Therapy in Solid Tumors

*Susana Romero-Garcia, Heriberto Prado-Garcia and Angeles Carlos-Reyes**

Department of Chronic-Degenerative Diseases, National Institute of Respiratory Diseases "Ismael Cosío Villegas", Mexico City, Mexico

Despite the recent advances in chemotherapeutic treatments against cancer, some types of highly aggressive and invasive cancer develop drug resistance against conventional therapies, which continues to be a major problem in the fight against cancer. In recent years, studies of alterations of DNA methylome have given us a better understanding of the role of DNA methylation in the development of tumors. DNA methylation (DNAm) is an epigenetic change that promotes the covalent transfer of methyl groups to DNA. This process suppresses gene expression through the modulation of the transcription machinery access to the chromatin or through the recruitment of methyl binding proteins. DNAm is regulated mainly by DNA methyltransferases. Aberrant DNAm contributes to tumor progression, metastasis, and resistance to current anti-tumoral therapies. Aberrant DNAm may occur through hypermethylation in the promoter regions of tumor suppressor genes, which leads to their silencing, while hypomethylation in the promoter regions of oncogenes can activate them. In this review, we discuss the impact of dysregulated methylation in certain genes, which impact signaling pathways associated with apoptosis avoidance, metastasis, and resistance to therapy. The analysis of methylome has revealed patterns of global methylation, which regulate important signaling pathways involved in therapy resistance in different cancer types, such as breast, colon, and lung cancer, among other solid tumors. This analysis has provided gene-expression signatures of methylated region-specific DNA that can be used to predict the treatment outcome in response to anti-cancer therapy. Additionally, changes in cancer methylome have been associated with the acquisition of drug resistance. We also review treatments with demethylating agents that, in combination with standard therapies, seem to be encouraging, as tumors that are in early stages can be successfully treated. On the other hand, tumors that are in advanced stages can be treated with these combination schemes, which could sensitize tumor cells that are resistant to the therapy. We propose that rational strategies, which combine specific demethylating agents with conventional treatment, may improve overall survival in cancer patients.

Keywords: DNA methylation, tumor suppressor genes, oncogenes, DNMTs, therapeutic targets, biomarkers, solid tumors, chemotherapy

OPEN ACCESS

Edited by:
Atsushi Fujimura, Okayama University, Japan

Reviewed by:
Prasanna Ekambaram, University of Pittsburgh, United States
Patrizia Zavattari, University of Cagliari, Italy

****Correspondence:***
Angeles Carlos-Reyes
reyes_cardoso@yahoo.com

Specialty section:
This article was submitted to Molecular and Cellular Oncology, a section of the journal Frontiers in Oncology

Received: *15 March 2020*
Accepted: *08 June 2020*
Published: *07 August 2020*

Citation:
Romero-Garcia S, Prado-Garcia H and Carlos-Reyes A (2020) Role of DNA Methylation in the Resistance to Therapy in Solid Tumors. Front. Oncol. 10:1152. doi: 10.3389/fonc.2020.01152

INTRODUCTION

During carcinogenesis, genetic and epigenetic alterations lead to dysregulated expression of genes associated with cellular pathways that regulate processes such as cell proliferation, cell differentiation, cell death, and cell cycle, among others. Epigenetic alterations that include DNA methylation (DNAm), histone modifications, aberrant expression of microRNAs (miRNAs), and long non-coding RNA (lncRNA) are common in several types of cancer. These epigenetic changes are hereditary, transient, and reversible and do not cause modification in the DNA sequence (1). Cancer can be treated by resection, chemotherapeutic agents, radiation, and immunotherapy, among others, as well as any combination of the aforementioned therapies. However, the 5-year survival rate remains low in many solid tumors due to tumor intrinsic or acquired resistance (2).

DNAm is a pivotal mechanism in normal cell development, which plays an important role in the regulation of gene expression, as well as chromatin stability, genetic imprinting, X-chromosome inactivation, the suppression of repetitive element transcription, and transposition. In mammals, DNAm involves the covalent transfer of methyl groups ($-CH_3$) from S-adenosyl-1-methionine (SAM) to cytosine in the CpG islands (2). CpG islands are characterized by a length longer than 200 bp. They possess a GC content >50% and present a ratio of observed to expected CpG dinucleotides >0.6. Moreover, CpG islands have been located in or near ∼50% of human promoters (3). DNAm is catalyzed by three DNA methyltransferases (DNMTs), which have been identified in mammals: DNMT1, DNMT3A, and DNMT3B. DNMT1 maintains hemimethylated DNA patterns during DNA replication, while DNMT3A and DNMT3B establish new patterns of methylation in early embryonic development (4).

Here, we review several DNAm alterations in cancer that have been associated with carcinogenesis, apoptosis avoidance, migration, invasion, and metastasis. Several studies have found that some of these DNAm alterations may be associated with tumor clinical features such as disease risk, TNM (tumor, node and metastasis)-stage, prognosis, diagnosis, survival, and response to treatment. We also discuss several DNAm alterations in genes and some pathways that have been reported to promote tumor resistance to therapeutic agents. Additionally, we argue that the promotion or inhibition of DNAm in a non-specific way should be carefully revised because of their side effects. In contrast, more extensive studies should be further developed by considering the targeting specific alterations in DNAm or editing the epigenome by CRISPR-Cas9 technology.

DNA METHYLATION REGULATES GENE EXPRESSION

Genetic mechanisms and epigenetic modifications such as DNAm, histone modifications, and non-coding RNAs (including microRNAs) regulate gene expression, which is a fundamental process that maintains cellular homeostasis. Each cell type possesses its own gene expression pattern, driven by a specific epigenetic signature, which may also produce cell heritable characteristics (5).

DNAm is a covalent modification in which a methyl group is linked to the cytosine in the dinucleotides cytosine-guanine (CpG), which is often located in "CpG islands" in the gene promoters; as a consequence, DNAm can modify gene expression. The CpG island is a short sequence of DNA in which the frequency of the CpG sequence is higher than that in other regions. Hypomethylation of promoter regions allows gene expression machinery to access the promoters of target genes. Hypermethylation, on the other hand, can suppress gene expression through the modulation of the transcription machinery access to the chromatin or through the recruitment of methyl binding proteins (5). In addition to promoters, other upstream DNA regions are rich in CpG sequences, up to 2 Kb distant to CpG islands, which are named "CpG island shores." These CpG island shores have been observed in colon and breast cancers (6, 7), or up to 700 bp in prostate cancer (8). Methylation of these CpG island shores also regulates gene expression. This epigenetic regulation was confirmed with the reactivation of downregulated genes in colon cancer, by demethylation of hypermethylated CpG island shores, using 5-aza2′-deoxycytidine (a DNA methyltransferase inhibitor) and DNA methyltransferase knockout (6).

Throughout the human lifespan, epigenetic patterns may change and constitute an important component of the aging process. Studies of human DNA methylome have revealed that one-third of 476,366 DNAm sites are affected by age. When age increases from 14 to 94 years, 60.5% of these affected DNAm sites become hypomethylated, and 39.5% become hypermethylated (9).

DNAm is a dynamic process that can also be affected by environmental factors, diet, and exercise habits, which can induce particular gene-expression signatures. For instance, the presence of short-chain fatty acids, such as butyric acid, can induce changes in DNAm patterns in normal and cancer cells; diets deficient in methyl-donor folic acid also promote dynamic changes in DNAm (5). Exercise favors hypomethylation of peroxisome proliferator-activated receptor gamma coactivator 1-alfa and delta (PGC-1α, PPAR-δ), pyruvate dehydrogenase kinase-4 (PDK4), which regulate mitochondrial function and fuel usage. mRNA upregulation of these genes during acute exercise is correlated with a transient but marked hypomethylation on each respective promoter (5). Interestingly, the change in the DNAm patterns associated with exercise is stronger among older people. The decreased DNAm associated with exercise habits among older people has been associated with cancer prevention, rewinding the "epigenetic clock" as people age (10).

CANCER MODIFIES GENE EXPRESSION THROUGH DNA METHYLATION

Studies of global DNA methylation have found methylation patterns or signatures that have been associated with different cancer hallmarks, such as cell proliferation, migration, invasion, and metastasis, and also with clinical features such as disease

stage, prognosis, survival, and response to treatment (2). Many regulatory regions of tumor suppressor genes and oncogenes present an altered methylation pattern (6). Aberrant DNAm, mediated by the overexpression of DNMTs, affects tumor suppressor genes through their hypermethylation, leading to transcriptional silencing of these genes. On the other hand, transcriptional activation by hypomethylation is observed in proto-oncogenes. Hypomethylation may be detected in early and late stages of the tumorigenesis in several cancer types, such as lung cancer, breast cancer, prostate cancer, gastric cancer (GC), and hepatocellular cancer, among others (6).

Neoplastic transformation, carcinogenesis, and cancer progression may be led by DNAm disruption, given that epigenetic changes have been demonstrated in multiple cancers (11). Most DNAm changes in cancer occur in both CpG islands and CpG island shores, affecting the expression of tumor suppressors and oncogenes (6). For instance, it has been found that ∼7,000 CpG islands are altered in the genome of human bladder cancer (12).

Analysis of methylation patterns in genomes of normal breast tissue indicates that the 5' end of highly expressed genes presents enriched sites of hypomethylation. This 5' end region includes the promoter, first intron, and first exon. In contrast, the methylome's analysis of genomes of the breast tumor cell lines (MDA-MB-231 and MCF-7) shows extensive hypomethylation in the intergenic and intragenic regions. These tumor cell lines present megabase-sized hypomethylated zones, which are associated with gene-poor regions containing tissue-specific gene clusters, fragile sites, chromosomal rearrangement breakpoints, and large genes. This suggests that hypomethylation is involved in genome instability. Interestingly, the extensively hypomethylated genes are all silenced. Also, primary breast tumors exhibit a methylation pattern that is between those of the cell lines and the normal tissue (13). It is well-documented that inactivation of tumor-suppressor genes can also be caused by deletions, point mutations, or allelic loss. Marsit et al. speculated that there might be a mutual relationship between the predisposition to promoter hypermethylation and genetic deletion in non-small cell lung carcinomas (NSCLCs). Interestingly, tumors that exhibit a high loss of heterozygosity show a reduced propensity for hypermethylation. The authors conclude that tumor suppressor gene silencing might be caused by allele loss events or epigenetic silencing events, occurring in a roughly dichotomous fashion, which would promote different molecular phenotypes in lung cancer (14).

Table 1 (15–85) summarizes genes with decreased expression in cancer as a consequence of hypermethylation of their promoter regions. The absence or reduction of the protein function associated with these genes has been implicated in the development, progression, invasion, and metastasis of many cancer types. Moreover, many hypermethylated genes included in **Table 1** participate in pathways involved with cell death processes. On the other hand, **Table 2** (86–120) summarizes epigenetically regulated genes by hypomethylation of their promoter regions, which have been found to be highly expressed in cancer. The expression or increased protein function associated with some of these genes has been shown to support cell proliferation, migration, and invasion of many cancer types. Many hypomethylated genes are highly expressed and participate in pathways involved in proliferation and evasion of the immune system (see **Table 2**). Both the hypermethylation and hypomethylation status of the regulatory regions of tumor suppressor genes and oncogenes have been tested as possible biomarkers for evaluating several parameters, such as cancer risk, diagnosis, and prognosis. Furthermore, analysis of the methylation status of certain genes may be useful for chemotherapy selection for cancer patients, and even for immunotherapy or target therapy (see **Tables 1**, **2**).

CANCER CELLS PRESENT THERAPY RESISTANCE BY CHANGING THEIR DNA PATTERNS

One of the major reasons for the failure of cancer chemotherapy is multidrug resistance (MDR). MDR is divided into the categories of primary drug resistance, which already existed prior to chemotherapy treatment (intrinsic resistance), and acquired drug resistance, which develops during the administration of chemotherapy. This MDR is associated with the regulation and function of apoptotic pathways, intracellular pH, drug pumps, DNA damage repair ability, and drug detoxification. All of these mechanisms reduce the concentration of chemotherapeutic drugs inside the cell, and hyper- and hypomethylation of certain genes appear to play a role (121).

Multiple changes in the methylation of CpG islands and CpG island shores have been found following the acquisition of drug resistance in different cancers. Studies of global DNA methylation profiling have identified different proportions of hypermethylated genes against hypomethylated ones. Baharudin et al. performed DNAm profiling on five recurrent and 43 non-recurrent patients with colorectal cancer (CRC) with 5-fluorouracil (5-FU) treatment (122). The researchers identified 4,787 significantly differentially methylated genes in the recurrent group of CRC compared to the non-recurrent group; 3,112 genes were hypermethylated, and 1,675 genes were hypomethylated. Interestingly, many hypermethylated genes were associated with the MAPK signaling pathway, which is implicated in apoptosis regulation. Conversely, many hypomethylated genes were associated with the PI3K-AKT signaling pathway and the promotion of proliferation (122). In another study, Guo et al. compared the methylation of promoters in a genome-wide study of human lung adenocarcinoma A549 cells resistant to cisplatin (A549/CDDP) with its progenitor A549 cells. The study identified 3,617 genes with differentially methylated promoters; 2,036 were hypomethylated, and 1,581 were hypermethylated. The promoters of RAS association domain family gene 1 (RASSF1), metallothionein 1G (MT1G), and G protein-coupled receptor 56 isoform 3 (GPR56) showed significantly higher hypermethylation in A549/CDDP cells compared to the progenitor A549 cells (123). Thus, increasing evidence supports the notion that epigenetic changes are a driving force behind the acquisition of drug resistance.

TABLE 1 | Hypermethylated promoters of genes associated with tumor suppression, prognosis, response to treatment, or as potential biomarkers.

Cancer type	Hypermethylated promoter	Biological function associated with hypermethylation
Breast (BC)	BRCA1, DAPK1, and RASSF1A	Associated with disease progression and poor overall survival of breast cancer patients (15)
	DACT2	Contributes to the progression of breast cancer through activation of WNT signaling pathway (16)
	ATM	Useful as a potential new biomarker for relatively young patients with breast cancer (17)
	FOXA1	Impacts parity and breastfeeding because FOXA1regulates a luminal gene expression signature in progenitor cells and represses the basal phenotype (18)
Cervical (CC)	RASSF2	Associated with shorter survival in squamous CC (19)
	RASSF1A	Increases the risk of CC (20)
	TFPI2	Important role in carcinogenesis, it correlates with cancer incidence in China (21)
	SIM1	Potential diagnostic biomarker (22)
	MEG3	Associated with worse recurrence-free and overall survival, potential plasma-based biomarker (23)
	P16INK4a	Associated with smoking habit and increased risk of cervical carcinogenesis (24)
	SALL3	HPV infection correlates with SALL3 hypermethylation and contribution to carcinogenesis (25)
	IFN-γ	Associated with tumorigenesis (26)
	KLF4	Inactivates its tumor suppressor function in cervical carcinogenesis (27)
	RAD51L3 and XRCC2	Predict late toxicity in chemoradiotherapy-treated CC patients (28)
Colorectal (CRC)	RASGRF1	Is a putative biomarker of overall survival in CRC patients (29)
	HADHB	Impacts in metastasis because HADHB reduces cancer cell migration and invasiveness (30)
	EYA4	Potential candidate screening marker in Iranian population and may improve early detection of CRC (31)
	STK33	Promising biomarker for the diagnosis, prognosis, and suitable treatment of CRC (32)
	BEND5	Promotes to cell proliferation and is a prognostic marker (33)
	FAM134B	Associated with aggressiveness and poor prognosis of colorectal adenocarcinomas (34)
	CHFR	Associated with worse overall survival in CRC patients, its loss contributes to tumorigenesis of epithelial cancers (35)
	APC 1A	Implicated in smoking-associated colorectal carcinogenesis (36)
	NDN	Promotes cell proliferation by activating the Wnt signaling pathway (37)
	hMLH1	Associated with microsatellite instability and CRC risk (38)
Gastric (GC)	EIF4E	Associated with early onset, and it is a prognostic marker for GC (39)
	GPX7	Important role in gastric tumorigenesis and progression (40)
	IGF2/DMR	Hypermethylation of IGF2/DMR in leukocyte are associated with prognosis (41)
	RAR-β	Association with histological type and clinical outcomes (42)
	TERT	A potential stool biomarker in non-invasive gastrointestinal cancer screening (43)
	MGMT	Associated with an increased risk of GC, correlation with TNM-stage (44)
	CHRDL1	Induces proliferation and metastasis by activating Akt and Erk (45)
	p16	Considered an potential early marker (46)
	miR-335	Associated with poor clinical features and prognosis (47)
	SFRP2 and DKK2	Associated with poor prognosis via the activation of Wnt/ β-catenin pathway (48)
	NDRG4	Contributes to GC risk, associated with poor prognosis (49)
	RUNX3	Associated with poor prognosis, valuable diagnostic and prognostic biomarker (50)
	ADAMTS8	Important role in the invasion and metastasis (51)
	DAL-1	Associated with GC aggressiveness, potential diagnosis biomarker (52)
Hepato-cellular (HCC)	NKAPL	Predicts poor outcome in HCC patients prognostic biomarker (53)
	HOXD10	Activates ERK signaling supporting human HCC (54)
	FHIT	Associated with live cancer risk, low FHIT expression correlates with TNM-stage, tumor size, and merging of cirrhosis of liver cancer in the Chinese population (55)
	RASSF1A	Hypermethylated RASSF1A in serum as a screen method for risk and diagnostic biomarker (56)
	HCCS1	Potential biomarker for diagnosis and prognosis of HCC patients (57)
	SOCS3	Its hypermethylation stimulates HCC development in patients with HBV (58)

(Continued)

TABLE 1 | Continued

Cancer type	Hypermethylated promoter	Biological function associated with hypermethylation
	miR-142	Promotes TGF-β-mediated tumor growth and metastasis (59)
Lung (LC)	MLH1	Associated with increased risk of NSCLC (60)
	PGCP	Associated with human bronchial epithelial cells immortalization (61)
	AGTR1	Biomarker to assist the detection and diagnosis of lung squamous cell carcinoma (62)
	RASSF1A and p16INK4a	The evaluation of methylation status of both genes is a promising diagnostic method in lung cancer (63)
	RARβ	Contributes to the NSCLC tumorigenesis and may serve as a potential risk factor, diagnostic marker, and drug target of NSCLC (20)
	WIF-1	Correlates with smoking behavior, promising non-invasive biomarker using blood or pleural effusion (64)
	CDKN2A	Correlates with tobacco smoking, detected in early stages of LC carcinogenesis (14)
Ovarian (OC)	RASSF1A	Decreased RASSF1A levels in serum is a sensitive tool for diagnosis and monitoring OC (65)
	BTG1	Involved in ovarian carcinogenesis (66)
	APC	Associated with increased risk of OC, biomarker value using blood samples (67)
	miR-34a	Prognostic relevance, inverse association with grading, p53 mutation status (68)
	FANCF	Associated with the susceptibility and clinicopathologic features of epithelial OC (69)
	RUNX3 and CAMK2N1	Associated with poor clinical outcome in type II of epithelial OC after complete resection (70)
	ABCA1	Associated with poor prognosis (71)
	MEG3	Contribute to the development of epithelial OC by inability to activate p53 (72)
Pancreatic (PC)	TERT	Diagnostic value in early state I of PC, recurrence, and survival prediction (73)
	SAV1	Promotes invasion and migration, represses pancreatic cancer cell apoptosis (74)
	HOPX	Prognostic indicator of pancreatic neuroendocrine tumor (75)
	CDKN2A	Critical role in pancreatic carcinogenesis and prognostic marker value (76)
Prostate (PCa)	ST6GALNAC3 and ZNF660	Potential diagnostic and prognostic biomarkers for PCa in liquid biopsies (77)
	SOX11	Correlates with adverse clinicopathological characteristics of PCa, including higher PSA level and perineural invasion (78)
	IGF2	Relevant during early stages of tumor development, during chemotherapy or androgen deprivation (79)
	SPARC	Correlation with poorer prognosis based on specific hypermethylated CpG sites (80)
	PAQR3	Associated with perineural invasion, biomarker for detection and monitoring PCa (81)
	PCDH8	Methylation status is associated with tumor size, shape, stage, and grade, hypermethylation associated with poorer prognosis (82)
	RHCG-TCAF1	Predictive of biochemical recurrence, pathological tumor stage and pre-operative PSA (83)
	TERT	Predicts biochemical relapse (84)
	GSTP1	Marker of high risk of PCa in rebiopsy on an initially negative prostate biopsy (85)

HYPERMETHYLATION OF KEY GENES ASSOCIATED WITH THERAPY RESISTANCE IN CANCER

Downregulation of specific genes by hypermethylation of their promoters may lead to MDR. **Table 3** (124–153) shows genes whose promoters may suffer hypermethylation and have been associated with resistance to antitumoral therapy in several types of cancer. The products of some of these genes are associated with signaling pathways, such as JAK-STAT, Wnt/β-catenin, MAPK/mTOR, and FAK/Ekt. The promoter hypermethylation pattern or the downregulated gene expression are promising biomarkers for early detection of intrinsic or acquired MRD (**Table 3**).

The transcriptional silencing mediated by hypermethylation can be used as a therapeutic strategy to diminish the expression of genes associated with drug resistance. For instance, it has been shown that the transmembrane ectoenzyme CD13 endows GC patients with insensitivity to CDDP and that expression of this molecule predicts a poor prognosis in CDDP-treated GC patients. CD13 functions upstream of the epithelial membrane protein 3 (EMP3) to induce its expression. The optimal phosphorylation of PI3K is facilitated by EMP3 upregulation. Phosphorylated PI3K activates the PI3K/AKT/NF-κB pathway suppressing autophagy and epithelial-mesenchymal transition (EMT) and overcoming CDDP resistance in GC cells. Ubenimex, a CD13 inhibitor, induces transcriptional silencing of EMP3 that is mediated by hypermethylation. Therefore, to overcome CDDP

TABLE 2 | Hypomethylated promoters of genes involved in tumor progression, prognosis, or potential therapeutic targets.

Cancer type	Hypomethylated promoter	Biological function associated with hypomethylation
Breast (BC)	NSUN2	Associated with metastatic progression in BC, promoting cell proliferation, migration and invasion (86)
	MMP7	Distinguishes the basal-like breast cancer subtype from other triple-negative tumors (87)
	IL-10	Involved in the process of breast carcinogenesis (88)
Cervical (CC)	STK31	It could be a novel cellular target gene for the HPV16 oncogeneE7, hypomethylation biomarker for CC (89)
Colorectal (CRC)	HES1	Critical role in the progression and prognosis of CRC, associated with poor prognosis (90)
	RORA1	Correlation with stages III and IV, but not with stages I and II, biomarker for chemotherapy selection in highly advanced CRC (91)
	MUC5AC	Marker of high microsatellite instability in CRC, detects microvesicular hyperplastic polyps and sessile serrated adenoma (92, 93)
	TCF3	Prognostic value indicating recurrence in stage II and III of CRC (94)
Gastric (GC)	COX2	Associated with the intestinal type of gastric cancer (95)
	IGF2	Surrogate marker of gastric cancer risk, through IGF2 hypomethylation in blood leukocyte DNA (96)
Hepato-cellular	BORIS	Promising prognostic biomarker for the prognosis of HCC (97)
(HCC)	RNA5SP38, IL21, and SDC4P macroH2A1	Prognostic and diagnostic value associated with HCC patient survival (98)
	hsa-miR-191	Associated with poor prognosis via activation of c-MET in hepatocellular carcinoma (99)
	miR-106a miR-106a	Promotes the epithelial-to-mesenchymal transition in HCC (100) Associated with stronger invasiveness, faster cell cycle progression, increased apoptosis resistance (101)
Lung (LC)	NSD1	A tumor cell-intrinsic driver of an immune cold phenotype, associated with reduced T cell infiltration into the tumor microenvironment in LC (102)
	NY-ESO-1	Associated with poor prognosis in patients not treated with chemotherapy, prognostic marker in stage 3 NSCLCs (103)
	MUC-4	TET1 regulates MUC-4 hypomethylation, which plays crucial role in carcinogenesis and tumor invasion (104)
	AHRR and F2RL3	Reflects long-term effect of smoking on the LC risk, biomarkers for smoking exposure (105)
	ARL4C	Involved in tumorigenesis of lung squamous cell carcinoma (SqCC) (106)
	TMPRSS4	Associated with poor prognosis in SqCC, a potential therapeutic target (107)
	EYA2	Promoter factor of lung adenocarcinoma oncogenesis, altering proliferation and cell cycle distribution (108)
Ovarian (OC)	SLC6A12	Associated with poor overall survival, it is a metastasis-promoting gene in OC (109)
	CT45	Possible prognostic biomarker, immunological or therapeutic target (110)
	CA9	Correlated with a more aggressive phenotype in ovarian cancer cells (111)
	AGR2	Modulator of more aggressive cancer phenotypes (112)
	ATG4A and HIST1H2BN	Associated with poor progression-free survival and overall survival (113)
Pancreatic (PC)	SERPINB5	Diagnostic marker for pancreatic ductal adenocarcinoma from pancreatitis (114)
	MUC4	Involved in carcinogenesis, prognostic marker for pancreatic cancer (115)
	S100A4	Associated with poor differentiation, promising diagnostic marker for early detection (116)
	MET and ITGA2	Associated with poor survival, having a role in pancreatic carcinogenesis (117)
Prostate (PCa)	TFF3	Potential diagnostic biomarker for PCa (118)
	CD147	Promotes aggressive tumor progression in human PC (119)
	TFF1 and TFF3	Their overexpression in PC may serve as biomarkers (120)

resistance in GC cells, ubenimex epigenetically inhibits the activation of the CD13/EMP3/PI3K/AKT/NF-κB pathway (154). Additionally, the NFκB pathway participates in the acquisition of resistance to tyrosine kinase inhibitor (TKI) treatment in lung cancer. Although it is a rare event, methylated cytosine may be converted to thymine by deamination. As a result, the methylated CG sequence could be converted into the TG sequence. Treatment with EGFR TKIs leads to activation of the NFκB pathway and also induces the activation-induced cytidine deaminase (AICDA) expression. AICDA deaminates

TABLE 3 | Hypermethylation associated with chemotherapy resistance in cancer.

Cancer type	Hypermethylated promoter	Mechanism associated with hypermethylation and diminished expression	Associated resistance
Breast (BC)	TGBI	Associated with trastuzumab resistance in HER2+ BC patients	Trastuzumab (124)
	ER-α	The formation of the ZEB1/DNA methyltransferase (DNMT)3B/histone deacetylase (HDAC)1 complex on the ER-α promoter leads to DNA hypermethylation and the silencing of ER-α. Thus, ZEB1 represses ER-α transcription.	Antiestrogen (125)
	MSH2	Biomarker for early detection of resistance, target for epigenetic therapy	Doxorubicin (126)
	MGP	Associated with chemoresistant phenotype in ER+ breast cancer cells	Doxorubicin (127)
	PSAT1	Associated with cytokine and JAK-STAT signaling, and poor clinical outcome to tamoxifen in ER positive primary tumors	Tamoxifen (128)
Cervical (CC)	SOCS	Ectopic expression of SOCS1 and SOCS3 confer radio-resistance to HeLa cells	Radiation (129)
	ZNF582	Associated with resistance to radiation and chemotherapy in HeLa cells	Radiation (130)
Colorectal (CRC)	NKX6.1	Metastasis suppressor by regulating epithelial-mesenchymal transition/outcome predictor of stage II CR patients, associated with poor prognosis	5-FU (131)
	DCR1	Silencing of DCR1 in cancer cells may promote pro-survival and pro-growth signals, predictive biomarker when a combination of irinotecan and capecitabine is used	Irinotecan (132)
	MEIS2	Possibly involved in the Wnt/β-catenin pathway to maintain CRC stemness, which leads to L-OHP resistance	Oxaliplatin (133)
	miR-26b	Tumor suppressive role of miR-26b is mediated by negatively regulating P-glycoprotein protein expression	5-FU (134)
	CCNEI, CCNDBP1, PON3, DDX43, and CHL1	Associated with the recurrence of CRC and 5-azadC-mediated restoration of 5-FU sensitivity is mediated at least in part by MAPK signaling pathway.	5-FU (122)
Gastric (GC)	TFAP2E	High expression of miR 106a 5p and miR 421 regulate the chemoresistance induced by TFAP2E methylation	5-FU (135)
	TFAP2E	The lack of response to fluorouracil-based chemotherapy is associated with TFAP2E hypermethylation, indicating that it might be a potential predictor of treatment response in patients with GC	5-FU (136)
Hepato-cellular (HCC)	CSF3R	Associated with poor prognosis, higher recurrence rates, indicative of non-CDDP regimens in hepatoblastoma patients	Cisplatin (137)
	KCNQ1	Remarkable inhibitory roles on tumor metastasis *in vitro* and *in vivo*	Cisplatin (138)
Lung (LC)	PDE3A	Inhibitor of DNA synthesis and cell viability in cancer cells/PD3A re-expression improves overall survival in adenocarcinoma patients.	Cisplatin (139)
	LRP12	Associated with shorter survival, marker for carboplatin resistance	Carboplatin (140)
	miR-483-3p	Because miR-483-3p directly targets integrin β3, and represses downstream FAK/Erk signaling pathway, its absence promotes acquired EGFR TKI resistance in EGFR-mutant NSCLC	Gefitinib (141)
	GPR56, MT1G, and RASSF1	Potential methylation markers associated with acquired methylation in multidrug resistance of lung adenocarcinoma	Cisplatin (123)
Ovarian (OC)	UCHL1	Knockdown of UCHL1 reduces cell apoptosis contributing to cisplatin resistance in OC cells	Cisplatin (142)
	OXCT1	Silencing of OXCT1 is associated with cisplatin resistance	Cisplatin (143)
	BRCA1	Loss of promoter hypermethylation restore BRCA1 function in recurrent disease	Cisplatin (144)
	miR-199a-3p	Favors migratory, invasive and tumorigenic capabilities, and cisplatin resistance	Cisplatin (145)
	hMSH2	Associated with platinum resistance, poor prognosis value	Platinum (146)
	RASSF1A	Associated with multidrug resistance	Platinum and Placlitaxel (121)
	NAGA	NAGA acts as a cisplatin sensitizer	Cisplatin (147)
	TRIB2	Downregulation of TRIB2 contributes to platin-resistance, promising prognostic and predictive marker	Cisplatin (148)
	miR-490-3p	miR-490-3p enhances CDDP sensitivity of OC cells through downregulating ABCC2 expression.	Cisplatin (149)
Pancreatic (PC)	BNIP3	Associated with chemoresistance in pancreatic ductal adenocarcinoma cell lines	Gemcitabine (150)
	miR-132	Promotes TGF-β-driven progression of pancreatic cancer	Dexamethasone (151)
Prostate (PCa)	miR-34a	Diminished miR-34a expression enhances chemoresistance, allowing upregulation of ATG4B-induced autophagy through AMPK/mTOR pathway	Dox, Topo (152)
	miR-205 and miR-31	Associated with apoptosis resistance in advanced PCa, the antiapoptotic genes BCL2L2 (encoding Bcl-w) and E2F6 have been identified as the targets of miR-205 and miR-31, respectively.	Docetaxel and Cisplatin (153)

the 5-methylcytosine, resulting in thymine to generate a T790M mutation. Hence, this is also a methylation-associated mechanism behind the acquisition of a mutation that provides resistance to TKI treatment in lung cancer (155).

DNAm-induced silencing of tumor suppressors is common in cancer. The hypermethylation can be reverted using the FDA-approved DNMT inhibitor 5-aza-2'-deoxycytidine, also named 5-azacytidine or decitabine. 5-Azacytidine has proven to be effective in the treatment of hematological neoplasms. However, its antitumor effect varies in solid tumors (156). The inhibition of methylation has presented good results in GC; Zhang et al. reported that growth arrest-specific transcript 5 (GAS5), which is a tumor suppressor lncRNA, is downregulated in GC. Adriamycin (ADM)-resistant cells (SGC-7901/ADM) have significantly higher levels of hypermethylation in the GAS5 promoter than GC SGC-7901 cells. The authors enforced GAS5 expression, provoking a significant reduction in tumor growth rate and apoptosis after Adriamycin treatment (157). Additionally, Wu et al. have shown that hypermethylation of miR-129-5p CpG island promotes miR-129-5p downregulation, favoring chemoresistance in GC cells. In the GC MDR cell line (SGC7901/VCR), the expression of miR-129-5p was restored through the use of 5-azacytidine, which reduced the chemo-resistance to 5-FU, vincristine, and cisplatin in this cell line. When the authors downregulated miR-129-5p, the chemoresistance was recovered. Furthermore, three members of ABC transporters (ABCG1, ABCC5, and ABCB1), which are associated with MDR, are direct targets of miR-129-5p regulation (158). In contrast, the demethylation of regulatory regions can induce chemoresistance in cervical cancer. Sensitivity to DNA topoisomerase I inhibitors in cancer therapy can be affected by DNA hypermethylation of the Werner (WRN) gene that reduces WRN expression. The WRN gene codes for a DNA helicase that contributes to genomic stability. Masuda et al. reported that cervical cancer-derived cell lines and primary cervical cancer that presented decreased WRN expression due to DNA hypermethylation showed high sensitivity to the topoisomerase I inhibitor (CPT-11). After treatment with 5-azacytidine, the tumor cells became resistant to CPT-11. To confirm this result, they transfected with a siRNA against WRN in tumor cells. These cells increased the sensitivity to CPT-11 (159). Therefore, treatment with demethylating drugs may have unforeseen and opposing results in cancer patients.

Silencing mechanisms to prevent the expression of tumor suppressor genes may also be induced by hypermethylation in cancer. For instance, potassium (K+) channels are dysregulated in different tumors and contribute significantly to the malignant phenotypes, such as chemoresistance, proliferation, and migration. KCNQ1 (potassium channel) can interact with β-catenin to affect its subcellular distribution. The interaction of KCNQ1 with β-catenin reduces Wnt/β-catenin signaling, which consequently blocks the expression of its downstream targets, such as MMP7, CCND1, and c-Myc. As a result, proliferation and cell migration are inhibited. DNA hypermethylation of KCNQ1 promoter has been shown to downregulate KCNQ1 expression in hepatocellular carcinoma (HCC). Downregulation of KCNQ1 is found in HCC cell lines and tissues and is associated with a poor prognosis (138). Additionally, the KCNQ1 Opposite Strand/Antisense Transcript 1 (KCNQ1OT1) gene is a lncRNA, which has been reported to be highly expressed in colorectal and lung cancers. High KCNQ1OT1 expression is correlated with malignant phenotypes in lung cancer. The transfection of si-KCNQ1OT1 can effectively knock down the expression of KCNQ1OT1, increasing KCNQ1 levels and, thus, inhibiting the malignancy and chemoresistance of lung cancer cells to paclitaxel (160). Accordingly, treatments that focus on recovering KCNQ1 expression must consider both the hypermethylation of regulatory regions and the expression of lncRNA. Another example of multiple mechanisms for silencing gene expression is the downregulation of BCL2 interacting protein 3 (BNIP3), which is a proapoptotic member of the BCL-2 family that induces necrotic-like cell death. Loss of BNIP3 expression in pancreatic cancer is correlated with methylation of the BNIP3 promoter. Mahon et al. showed an association between the decreased expression of BNIP3 and chemoresistance to gemcitabine in pancreatic ductal adenocarcinoma (PDAC) cell lines. Besides promoter hypermethylation, S100A4 overexpression, which belongs to the S100 calcium-binding protein family, represents an alternative mechanism for inhibiting BNIP3 function in PDAC. S100A4 knockdown, mediated by RNA interference, upregulated the expression of BNIP3 in PDAC cell lines that have an unmethylated BNIP3 promoter, which led to an increased sensitivity to gemcitabine in PDAC cell lines (150). Consequently, it is important to keep in mind that hypermethylation is one of several mechanisms that inhibits tumor suppressor genes, and anti-cancer treatments must consider this fact.

HYPOMETHYLATION OF KEY GENES IS ASSOCIATED WITH THERAPY RESISTANCE IN CANCER

Hypomethylation of promoters for a certain type of gene may also function as tumor mechanisms for acquiring resistance to drug therapy. **Table 4** (161–181) shows some genes whose promoters are hypomethylated in several types of cancer. Hypomethylation of the promoters of these genes leads to their upregulation. The product of some of these genes supports mechanisms involved in MDR, proliferation, the repression of apoptotic signaling, mitochondrial function, and DNA repair. For instance, Luzhna et al. found that diminished radiation responsiveness was correlated with significant global DNA hypomethylation in radiation-resistant cells (MCF-7/DOX). This radiation resistance can be reversed by an epigenetic treatment, which is the use of SAM, a methyl donor. The radiation sensitivity in MCF-7/DOX cells was promoted through use of the SAM-mediated reversal of DNA methylation. However, the researchers found that SAM should be carefully used because the SAM application decreased responsiveness to radiation on MCF-7 cells that were originally radiation-sensitive and highly methylated. Remarkably, the authors concluded that a fine balance of DNA

TABLE 4 | Hypomethylation associated with chemotherapy resistance in cancer.

Cancer type	Hypomethylated promoter	Mechanism associated with hypomethylation and increased expression	Associated resistance
Breast (BC)	ID4	Potential biomarker in distinguishing acquired tamoxifen-refractory BC	Tamoxifen (161)
	ERp29/ MGMT	ERp29 expression in the triple negative MDA-MB-231 breast cancer cells significantly increases cell survival against ionizing radiation, by downregulating DNA methyltransferase 1, ERp29 promotes promoter's hypomethylation of the DNA repair gene (MGMT)	Radiation (162)
	ETS-1	Inhibitor of miR-320a expression, downregulation of miR-320a triggers TRPC5 and NFATC3 overexpression, which are essential for BC chemoresistance	Adriamycin and paclitaxel (163)
	miR-663	Overexpression of hypomethylated miR-663 induces chemoresistance in breast cancer cells by down-regulating HSPG2.	Cyclophosphamide and docetaxel (164)
	MDR1, GSTpi, MGMT, and Upa	Hypomethylation of the promoter regions of the MDR1, GSTpi, MGMT, and Upa genes is associated with acquirement of doxorubicin resistance of MCF-7 cells	Doxorubicin (165)
Colorectal (CRC)	NME2	Enhancer of growth abilities and reduced apoptosis in HCT-8 cells	5-FU (166)
	CDO1	CDO1 hypomethylation in stage III colon cancer with postoperative chemotherapy exhibits worst prognosis than CDO1 hypermethylation. In some CRC cell lines, forced expression of CDO1 gene increases mitochondrial membrane potential accompanied by chemoresistance and/or tolerance under hypoxia.	Adjuvant (167)
	Nrf2	TET-dependent demethylation of the Nrf2 promoter upregulates Nrf2 and HO-1 expression, which induces cellular protection mechanisms, leading to 5-FU resistance in CRC cells	5-FU (168)
Gastric (GC)	ASCL2	Enhanced ASCL2 expression increases cell growth and promotes resistance to 5-FU in GC cells, a useful prognostic marker for GC patients	5-FU (169)
	MDR1	Overexpression of DCTPP1 decreases the concentration of intracellular 5-methyl-dCTP, which results in promoter hypomethylation and hyper-expression of MDR1	5-FU (170)
	GTSE1	GTSE1 expression represses apoptotic signaling and confers cisplatin resistance in gastric cancer cells.	Cisplatin (171)
Hepato-cellular (HCC)	PD-L1/DNMT1 axis	Highly DNMT1 upregulation positively correlates with PD-L1 overexpression in sorafenib-resistant HCC cells, where PD-L1 induced DNMT1-dependent DNA hypomethylation	Sorafenib (172)
	MDR1	MDR1 promoter hypomethylation might be regulated by the riboregulatory H19, inducing the P-glycoprotein expression through the upregulation of its gene MDR1 in liver cancer cells	Doxorubicin (173)
Lung (LC)	TDRD9	Associated with aberrant mitosis and abnormal-shaped nuclei, protects from replicative stress increasing drug resistance	Aphydicolin (174)
Ovarian (OC)	SERPINE1	Associated with EMT process and carboplatin resistance in A2780cp cells	Carboplatin (175)
	TMEM88	Functions as an inhibitor of Wnt signaling contributing to the platinum resistance	Platinum (176)
	BRCA1/SIRT1/EGFR axis	Cisplatin-resistant ovarian cancers increase BRCA1, SIRT1, and EGFR levels compared with those in cisplatin-sensitive ovarian cancers. Decreased nicotinamide adenine dinucleotide (NAD)-mediated SIRT1 activity, decreased EGFR levels, significantly elevated SIRT1 levels, and BRCA1 activation are associated with hypomethylation in the BRCA1 promoter	Cisplatin (177)
	HERV	HERV-K hypomethylation is associated with a poor prognosis and platinum resistance in ovarian clear cell carcinoma (OCCC), promising biomarker for predicting OCCC treatment response and prognosis.	Platinum (178)
	MAL	Highly expressed MAL gene in serous ovarian cancers from short-term survivors (<3 years) and treated with platinum-based therapy. MAL methylation status is a potential target for enhancing sensitivity to platinum-based drugs in epithelial ovarian cancer	Platinum (179)
Prostate (PCa)	miR-27a-5p	miR-27a-5p promoter becomes hypomethylated during PCa progression, miR-27a-5p upregulation decreases EGFR/Akt1/mTOR signaling	Castration (180)
	CD117 and ABCG2	Prostate cancer cell line 22RV1 expresses high surface levels of both CD117 and ABCG2 (CD117+ABCG2+ cells). This subpopulation shows hypomethylation in ABCG2 promoter and also overexpresses stem cells markers such as Nanog, Oct4, Sox2, Nestin, and CD133	Cisplatin, paclitaxel, adriamycin, and methotrexate (181)

methylation is needed to ensure proper drug and radiation responsiveness (182).

Activation of drug-resistance-associated genes, besides the hypomethylation of their promoters, can be caused by *de novo* gene fusions. In the case of breast cancer, BRCA1-deficient tumors are extremely sensitive to DNA-damaging drugs and poly(ADP-ribose) polymerase (PARP) inhibitors. However, BRCA1 protein was detected in 31 of 42 drug-resistant cases, despite presenting a hypermethylated promoter. BRCA1-intragenic deletions and the loss of BRCA1 promoter hypermethylation have been shown to occur, and *de novo* gene fusions take place, where BRCA1 expression can be under the transcriptional control of a heterologous promoter (183).

Therefore, targeting methylation should be carefully evaluated because most compounds that promote or inhibit this process are not gene-specific, which may lead to undesirable effects.

REGULATION OF WNT CANONICAL AND NON-CANONICAL PATHWAYS BY DNA METHYLATION THAT SUPPORTS CANCER DEVELOPMENT AND THERAPY RESISTANCE

In this section, we include potential mechanisms by which differentially methylated genes take part in the development of cancer, by integrating protein interactions and pathways regulated by methylation (11). Tumors present a dysregulated pattern of methylation in genes that impact in pathways like the Wnt canonical pathway and PI3K/AKT/mTOR (e.g., DKK, SFRPs, WIF1, DVL, APC, PTEN, SALL2, and IGFBP-3), which support resistance to specific inhibitors as well as conventional chemotherapeutic agents.

The Wnt/beta-catenin signaling pathway plays important roles in carcinogenesis and therapy resistance. Wnt is a large family of secreted lipoproteins that can join to receptors and co-receptors at the cell surface and activate a complex signaling network. This pathway participates in a wide range of physiological cellular processes like embryonic development, tissue homeostasis, tissue regeneration, cell polarity, cell proliferation, cell migration, and apoptosis (184, 185). The Wnt signaling pathway may be activated by the Wnt/ß-catenin pathway (also known as the canonical pathway (**Figure 1**) (185, 186) or non-canonical Wnt signaling. Non-canonical Wnt signaling, which is independent of β-catenin, is activated by the pathways Wnt/planar cell polarity and Wnt/Ca^{2+} (187, 188).

Methylation of genes involved in the Wnt pathway plays a crucial role in regulating the development and progression of tumors, as well as metastasis, diagnosis, and treatment. Several tumors, such as lung, breast, prostate, colon, gastric, and ovarian cancers, among others, exhibit a pattern of deregulated methylation in this pathway (184, 189, 190). For instance, Dickkopf-related protein (DKK3), secreted frizzled-related protein 1 (SFRP1), SFRP2, and Wnt inhibitory factor-1 (WIF1), which are tumor suppressor genes, prevent LRP5/6 receptors from interacting with their ligands, consequently inhibiting the signaling of the Wnt pathway (191, 192). In the context of methylation, it has been said that several tumors show the downregulation of DKK3, SFRP1, SFRP2, and WIF1 by hypermethylation in their promoters (193). The hypermethylation of DKK3 has been associated with docetaxel (DTX) resistance in the lung cancer H1299/DTX cell line. Moreover, treatment with 5-azacytidine on the H1299/DTX cell line upregulates DKK3 expression at both the mRNA and protein levels, which inhibits colony formation and induces apoptosis due to recovered sensitivity to DTX. Additionally, P-glycoprotein is a drug efflux pump associated with MDR, encoded by the MDR-1 gene (MDR-1). MDR-1 overexpression is associated with DTX resistance in lung cancer. Restored expression of DKK3 leads to the downregulation of MDR-1 and P-glycoprotein, thus increasing sensitivity to DTX. This is a mechanism of regulation in lung cancer therapy. Therefore, DKK3 may be a therapeutic target that may help tumor cells recover sensitivity to DTX (194). Another study found that the decreased expression of DKK3 is associated with hypermethylation in pancreatic cancer biopsies in comparison to non-tumor tissue. In this study, DKK3 expression was not detected in three pancreatic cancer cell lines (Aspc-1, Bxpc-3, and CFPAC-1). DKK3 overexpression by DKK3 transfection in the Bxpc-3 pancreatic cell line promotes the inhibition of β-catenin translocation to the nucleus, as well as its transcriptional role under conditions of hypoxia or normoxia. Furthermore, DKK3 repressed the EMT and migration of Bxpc-3 cells, mediated by the inhibition of β-catenin. These effects improved the response to gemcitabine in Bxpc-3 tumor cells, suggesting that DKK3 may be a potential target for therapy (195).

In advanced stages of lung cancer, treatment based on taxanes is one treatment option, such as paclitaxel and DTX; however, resistance to therapy is presented in some patients (196). Ren et al. showed that hypermethylated SFRP1 regulates the chemotherapy resistance of taxanes and DTX in A-549 and SPC-A1 lung adenocarcinomas cell lines. The resistance was mediated by Wnt pathway activation because SFRP1 reduces β-catenin stability, leading to cell death, whereas SFRP2 promotes β-catenin accumulation, inducing resistance to apoptosis. Moreover, 5-azacytidine treatment restored the SFRP1 expression level, inducing the inhibition of the Wnt pathway and promoting drug sensitivity in resistant cell lines. Thus, the overexpression of SFRP1 can improve patients' responses to taxanes and DTX therapies (196). Zhu et al. also found that SFRP1 and SFRP5 were hypermethylated in NSCLC. Furthermore, the hypermethylation of SFRP5 predicted a poor response to TKI therapy; hence, SFRP5 methylation could be associated with TKI resistance (197). Additionally, higher levels of the hypermethylation of SFRP1, SFRP2, and WIF1 genes were found in colon cancer compared to non-tumoral tissues. Thus, the hypermethylation of one or both SFRP1and SFRP2 genes is a promising prognostic marker for predicting survival in patients who receive post-operative chemotherapy (198–200). Su et al. found that SFRP5 was hypermethylated in 44.4% of ovarian cancer tissues, as well as in SKOV3 and A2780 tumor cell lines. The SFRP5 low expression promotes EMT, tumor growth, invasion, tumor progression, and cisplatin resistance. Restored expression of SFRP5 reduces Wnt non-canonical signaling, promoting sensitivity to cisplatin in a mouse model of ovarian cancer (201).

Several genes whose protein products participate in the Wnt transduction signaling cascade are regulated by hypermethylation. Hence, the deregulation of this process during carcinogenesis may contribute to drug resistance. For instance, hypermethylation of DVL in prostate cancer has been suggested to favor resistance to cabazitaxel in DU145 cells. Reactivation of DVL by 5-azacytidine treatment in DU145 10DRCR cells restores sensitivity to cabazitaxel in this prostate tumor cell line (202). Hypermethylation of adenoma polyposis coli (APC), a tumor suppressor gene, inhibits the Wnt pathway, promoting tumorigenesis and tumor progression

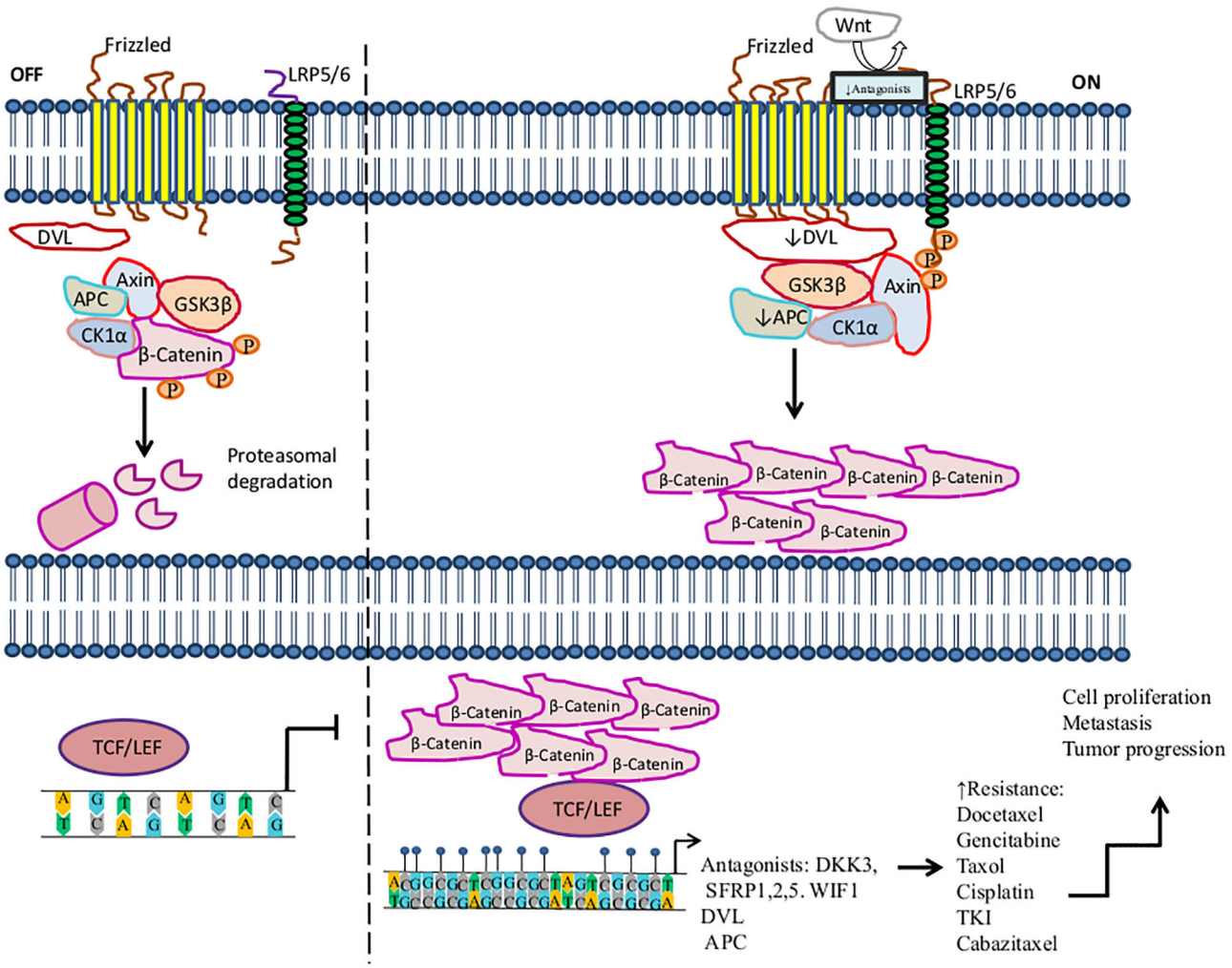

FIGURE 1 | Activation of the Wnt/β-catenin signaling pathway in the resistance to therapy in cancer by methylation. The canonical Wnt/β-catenin pathway is activated by the binding of Wnt to the Frizzled receptor (Fzd). Then LRP is phosphorylated by casein kinase 1 (CK1α) and glycogen synthase kinase 3 beta (GSK3β) associated with tumor suppressor adenomatous polyposis coli (APC). LRP phosphorylation promotes the recruitment of disheveled proteins (DVL) to the plasma membrane, where they are polymerized and activated. DVL complex interacts with Axin, which inhibits the degradation of β-catenin and leads to its accumulation in the cytoplasm and translocation into the nucleus, where β-catenin promotes the activation of LEF/TCF transcription factors inducing the transcription of several genes. In the absence of Wnt, β-catenin is a target of the destruction complex conformed by Axin, CK1α, APC, and GSK-3β. CK1α and GSK-3β phosphorylate β-catenin, promoting its ubiquitination by the β-TrCP ubiquitin ligase and degradation through the proteasome. On the other hand, this figure shows some aberrantly methylated key genes that increase resistance to therapeutic agents and the dysregulation of the Wnt/β-catenin signaling pathway. These genes play an antagonist role in the Wnt pathway, for instance, Dickkopf-related protein (DKK3), secreted frizzled-related proteins (SFRP1, SFRP2), and WNT inhibitory factor-1 (WIF1), which are tumor suppressor genes and inhibit the signaling of Wnt to bind LRP5/6 receptors. P, phosphorylation; ↑, increase; ↓, decrease, , methylation.

in CRC (203, 204). In breast cancer, Matuschek et al. reported that hypermethylated APC promotes tumor aggressiveness in circulating tumor cells. Additionally, 70% of breast cancer tissues presented hypermethylation in the APC gene (205). By the same token, loss of APC inactivates the repair of double-stranded breaks mediated by ATM, Chk1, and Chk2, which induces doxorubicin resistance (205, 206). Thus, we suggest that the methylation status of several key genes involved in the Wnt/canonical signaling pathway may be used as predictive markers of tumor progression and therapy response.

REGULATION OF THE PI3K/PTEN/AKT/MTOR SIGNALING PATHWAY BY DNA METHYLATION SUPPORTS CANCER DEVELOPMENT AND THERAPY RESISTANCE

AKT is also recognized as protein kinase B (Serine/Threonine Kinase 1, or Protein Kinase B), which participates in several processes such as cell metabolism, cell proliferation, angiogenesis,

apoptosis, motility, and cell survival (207). Aberrant DNAm of key genes in PI3K/PTEN/AKT/mTOR signaling pathway promotes therapy resistance in solid tumors (**Figure 2**).

Tamoxifen (TAM) is the first line of therapy for the treatment of estrogen-receptor-positive breast cancer. This type of breast cancer develops TAM resistance, promoting tumor relapse (208). Phuong et al. found that the MCF-7 breast cancer cell line showed TAM resistance (TAMR/MCF-7). This resistance is mediated by a high expression of DNMT1. DNMT1 along with SAM induce the hypermethylation of PTEN in amplicon A and amplicon B sites, leading to its downregulation and the constitutive activation and phosphorylation of PI3K/AKT. 5-Azacytidine treatment inhibits DNMT1 in TAMR/MCF-7 cells, restoring PTEN expression, suppressing cell proliferation, and promoting cell death by apoptosis (209). Spalt-like transcription factor 2 (SALL2) functions as a tumor suppressor, which regulates the AKT/mTOR pathway (**Figure 2**). Hypermethylated SALL2 is found in the TAM-resistant ER+ TAMR/MCF-7 breast cancer cell line, which leads to SALL2 downregulation. SALL2 decreased expression promotes decreased expression

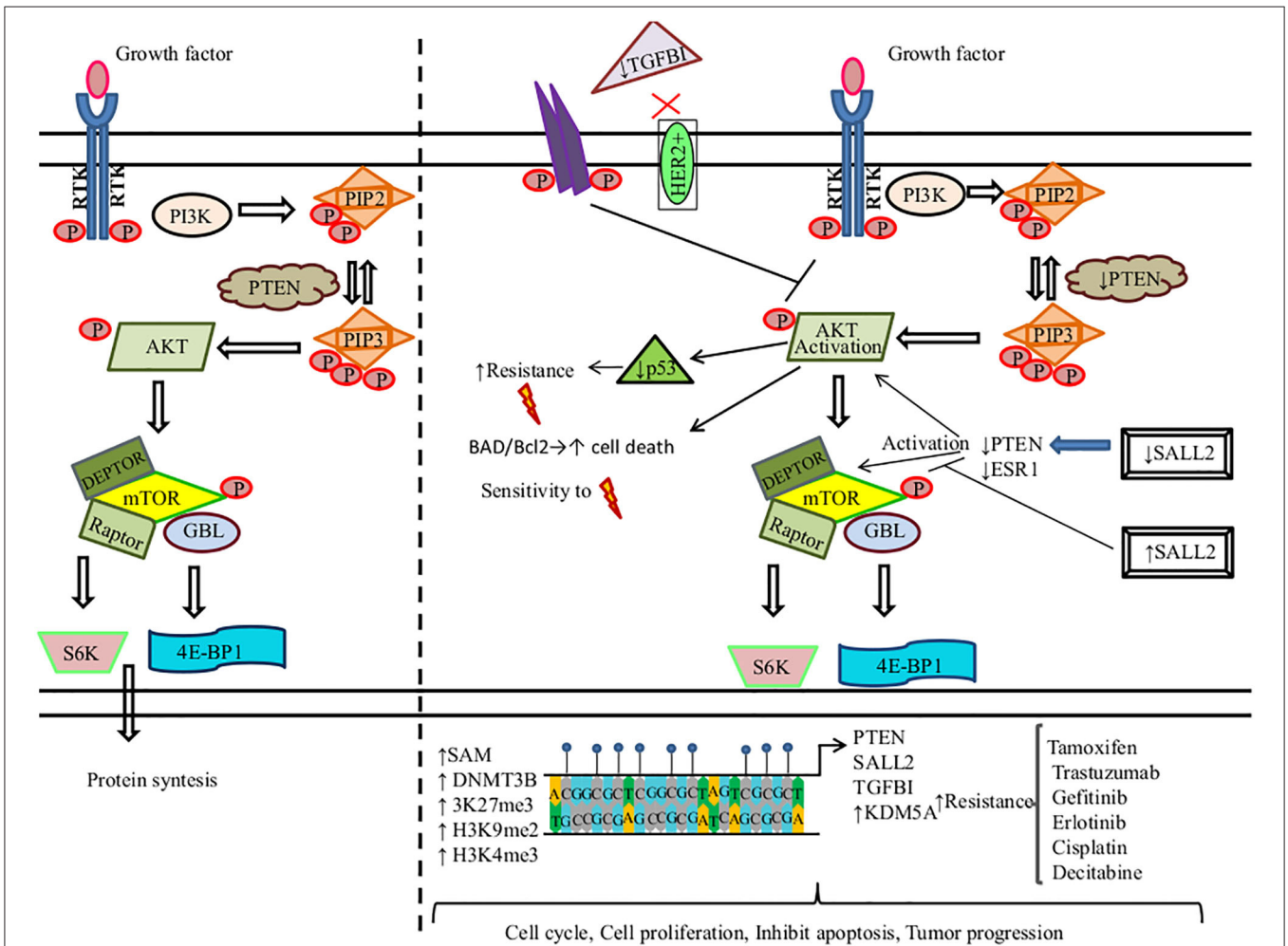

FIGURE 2 | DNA methylation regulates the PI3K/PTEN/AKT/mTOR signaling pathway in the resistance to therapy in cancer. **(Left)** PI3K induces the phosphorylation and activation of AKT/mTOR. This transduction signal begins with the activation of the membrane tyrosine kinase receptors (RTKs) or G-protein-coupled receptors, which promotes the change of phosphatidylinositol (4,5)-bisphosphate (PIP2) in phosphatidylinositol (3-5)-trisphosphate (PIP3). The activation of PI3K (phosphoinositide-3-kinase) is regulated by the phosphatase and tensin homolog (PTEN) by dephosphorylating PIP3 into PIP2. **(Right)** We show the aberrant methylation of the PTEN, Spalt-like transcription factor 2 (SALL2), transforming growth factor beta-induced protein (TGFB1), and Lysine (K)-specific demethylase 5A (KDM5A) genes through the high expression of methyltransferase (DNMT3B), s-adenosylmethionine (SAM), H3K27me3, H3K9me2, and H3K4me3, promoting a continued activation of the PI3K/AKT/mTOR signaling pathway associated with resistance therapy in solid tumors. P, phosphorylation; ↑, increase; ↓, decrease; |, methylation, ⚡, radiotherapy.

levels of estrogen receptor-alpha (ERα) and PTEN, which causes the continued activation of AKT/mTOR. In addition, hypomethylation of SALL2 increases its expression, leading to the upregulation of ER and PTEN and the further inhibition of the AKT/mTOR signaling pathway, which consequently leads to TAM sensitivity (210).

Among breast cancers, 15–20% are human epidermal growth factor receptor 2 positive (HER2+) and may develop resistance to trastuzumab. Palomeras et al. reported that primary breast tumors that developed trastuzumab resistance present a loss of expression of transforming growth factor beta-induced protein (TGFBI) by hypermethylation. TGFBI inhibits the HER2 receptor and AKT (124). Abnormal activation of PI3K/AKT is common in breast cancer. Among the most frequent causes is constitutive signaling through mutational activation of phosphatidylinositol-4,5-bisphosphate 3-kinase catalytic subunit alpha (PIK3CA), which is mutated in 45% of luminal breast cancers. Thus, a promising therapeutic strategy is to develop PI3K/AKT inhibitors. KDM5A lysine demethylase can remove tri- and dimethyl marks on histone H3 (H3K4me3), leading to tumor progression and drug tolerance. KDM5A is a target of AKT and, together, they regulate certain cell-cycle genes. AKT phosphorylates KDM5A, thus promoting the subcellular localization of KDM5A from the chromatin-bound regions and nucleus to the cytoplasm. As a result, KDM5A is rendered unable to demethylate H3K4me2/3. PI3K/AKT inhibition decreases KDM5A phosphorylation, promoting the low expression of cell-cycle promoting genes. Additionally, KDM5A regulates resistance to PI3K/AKT inhibitors (211).

On the other hand, some mutated EGFR lung cancers induce resistance to EGFR-TKIs (gefitinib and erlotinib). Two gefitinib-resistant cell lines (GEF1-1 and GEF2-1) derived from the PC-9 cell line were treated with 5-azacytidine. This treatment restored PTEN expression and promoted sensitivity to gefitinib and erlotinib in GEF1-1 and GEF2-1 cell lines. Nonetheless, the parental cell line (PC-9 cells) did not show this sensitivity due to the hypermethylation of PTEN and hyperactivation of AKT (212). Furthermore, the hypermethylation of insulin-like growth factor-binding protein-3 (IGFBP-3) promotes cisplatin resistance in lung cancer. Downregulation of IGFBP-3 induces PI3K/AKT activation by specific de-repression of insulin-like growth factor-I receptor (IGFIR) signaling (213).

Methylation of PTEN promoter is an alternative mechanism to PTEN downregulation that induces drug resistance. For instance, lung cancer cells develop radioresistance due to hypermethylated PTEN that induces low expression of pAKT and downregulates p53 expression (214). In similar research, Pappas et al. showed that restoring PTEN expression in the human lung cancer cell line H1299 by the use of the adenovirus expression vector (Ad-PTEN) increases sensitivity to ionizing therapy. Of note, PTEN promoter is methylated in H1299 cells. The phosphorylation of BAD, a proapoptotic molecule regulated by AKT, inhibits its binding to Bcl-2, leading to apoptosis. Thus, restoring PTEN induces lower levels of phosphorylated AKT and BAD, which sensitizes to apoptosis. Also, Ad-PTEN regulates the DNA repair of double-strand breaks, mediated by the activation of H2AX (215).

Differential DNA methylation profiles are found in prostate cancer samples. These tumors show hypermethylated PTEN and hemi- and homozygous PTEN loss. The latter has been associated with poor prognosis, recurrence, and tumor progression (216).

Qian et al. found that DNMTs were highly expressed in nasopharyngeal carcinoma resistant cells; consequently, PTEN and PPP2R2B promoter hypermethylation is induced. DNMT upregulation activates two important signaling pathways, PI3K/mTOR and PDK1/MYC, favoring survival, proliferation, and resistance to the BEZ235 inhibitor (217). Treatment with BEZ235 and the inhibition of DNMT expression with 5-azacytidine induces drug sensitivity in resistant tumor cells. Furthermore, 5-azacytidine dephosphorylates the AKT, GSK3β, MYC, P70, and 4EBP-1 proteins involved in the AKT/mTOR and PDK1/MYC pathways. The combination of decitabine and BEZ235 upregulates PTEN protein expression, inhibiting cell growth. Hence, new combinations of chemotherapeutic agents with inhibitors against components of the PI3K/AKT/mTOR signaling pathway should be tested to increase tumor chemotherapy sensitivity.

CONCLUSIONS AND FUTURE DIRECTIONS

Several studies have shown that modifications in DNAm patterns may support cancer development, invasion, and metastasis. Global methylation analyses suggest that CpG islands tend to be a highly altered methylation status that depends on the cancer type (122, 123). Importantly, several studies have reported that DNAm patterns of drug-treated tumor cells can change and support the acquisition of resistance to treatments, such as radiotherapy and chemotherapy. Some of these DNAm changes have been proposed as promising biomarkers whose presence would be indicative that therapy must be replaced (**Tables 3**, **4**).

Additionally, the study of the DNAm patterns and their involvement in the regulation of several signaling pathways in cancer has provided significant insight into the molecular mechanisms underlying the development of cancer. For instance, dysregulation of Wnt canonical and PI3K/AKT/mTOR signaling pathways, caused by an altered methylation status in a variety of genes, has been associated with resistance to current treatments (taxanes, DTX, cisplatin, TKI, etc.) in many types of cancer.

Some studies have tried to change drug-resistance-associated DNAm patterns using SAM and DNMTs to increase the methylation grade or TET-dependent demethylation to diminish DNAm. Although they have changed the DNAm pattern of the target gene, these treatments also modify the DNAm patterns of other genes, causing undesirable secondary effects. For this reason, a fine balance of DNAm is needed to ensure proper drug responsiveness.

Recent advances in applied genetic engineering and genome editing may provide new tools for targeting methylation status in

cancer patients. In particular, the clustered regularly interspaced short palindromic repeats/associated protein 9 (CRISPR/Cas9) system allows for the addition or removal of DNA from the genome in a specific manner. Genetic engineering has produced a new version of Cas9 (dCas9), in which the activity of endonuclease has been removed but in which the DNA binding activity is maintained. dCas9 can also be linked to DNMT3A or ten-eleven translocation-1 (TET1) enzymes, generating the systems dCas9-DNMT3A or dCas9-TET1, respectively (218, 219). These systems can induce the methylation and demethylation of target genes in a specific-sequence manner, which makes them promising tools in the fight against cancer or the acquisition of therapy resistance.

AUTHOR CONTRIBUTIONS

SR-G and AC-R designed the study. SR-G, HP-G, and AC-R wrote the manuscript and integrated the tables. AC-R designed and elaborated the figures. All authors contributed to the critical revision of the manuscript, read, and approved the submitted version.

ACKNOWLEDGMENTS

The authors acknowledge to Instituto Nacional de Enfermedades Respiratorias Ismael Cosio Villegas for supporting the publication of this manuscript.

REFERENCES

1. Ilango S, Paital B, Jayachandran P, Padma PR, Nirmaladevi R. Epigenetic alterations in cancer. *Front Biosci.* (2020) 25:4847. doi: 10.2741/4847
2. Fouad MA, Salem SE, Hussein MM, Zekri ARN, Hafez HF, El Desouky ED, et al. Impact of global DNA methylation in treatment outcome of colorectal cancer patients. *Front Pharmacol.* (2018) 9:1173. doi: 10.3389/fphar.2018.01173
3. Janitz KJM. Assessing epigenetic information. In: *Handbook of Epigenetics,* 1st ed. Amsterdam: Elsevier (2011). p. 173–81. doi: 10.1016/B978-0-12-375709-8.00012-5
4. Damelin M, Bestor TH. Biological functions of DNA methyltransferase 1 require its methyltransferase activity. *Mol Cell Biol.* (2007) 27:3891–9. doi: 10.1128/MCB.00036-07
5. Barres R, Yan J, Egan B, Treebak JT, Rasmussen M, Fritz T, et al. Acute exercise remodels promoter methylation in human skeletal muscle. *Cell Metab.* (2012) 15:405–11. doi: 10.1016/j.cmet.2012.01.001
6. Irizarry RA, Ladd-Acosta C, Wen B, Wu Z, Montano C, Onyango P, et al. The human colon cancer methylome shows similar hypo- and hypermethylation at conserved tissue-specific CpG island shores. *Nat Genet.* (2009) 41:178–86. doi: 10.1038/ng.298
7. Tsuboi K, Nagatomo T, Gohno T, Higuchi T, Sasaki S, Fujiki N, et al. Single CpG site methylation controls estrogen receptor gene transcription and correlates with hormone therapy resistance. *J Steroid Biochem Mol Biol.* (2017) 171:209–17. doi: 10.1016/j.jsbmb.2017.04.001
8. Ramachandran K, Gopisetty G, Gordian E, Navarro L, Hader C, Reis IM, et al. Methylation-mediated repression of GADD45alpha in prostate cancer and its role as a potential therapeutic target. *Cancer Res.* (2009) 69:1527–35. doi: 10.1158/0008-5472.CAN-08-3609
9. Johansson A, Enroth S, Gyllensten U. Continuous aging of the human DNA methylome throughout the human lifespan. *PLoS ONE.* (2013) 8:e67378. doi: 10.1371/journal.pone.0067378
10. Brown WM. Exercise-associated DNA methylation change in skeletal muscle and the importance of imprinted genes: a bioinformatics meta-analysis. *Br J Sports Med.* (2015) 49:1567–78. doi: 10.1136/bjsports-2014-094073
11. Aref-Eshghi E, Schenkel LC, Ainsworth P, Lin H, Rodenhiser DI, Cutz JC, et al. Genomic DNA methylation-derived algorithm enables accurate detection of malignant prostate tissues. *Front Oncol.* (2018) 8:100. doi: 10.3389/fonc.2018.00100
12. Markl ID, Cheng J, Liang G, Shibata D, Laird PW, Jones PA. Global and gene-specific epigenetic patterns in human bladder cancer genomes are relatively stable *in vivo* and *in vitro* over time. *Cancer Res.* (2001) 61:5875–84.
13. Shann YJ, Cheng C, Chiao CH, Chen DT, Li PH, Hsu MT. Genome-wide mapping and characterization of hypomethylated sites in human tissues and breast cancer cell lines. *Genome Res.* (2008) 18:791–801. doi: 10.1101/gr.070961.107
14. Marsit CJ, Houseman EA, Nelson HH, Kelsey KT. Genetic and epigenetic tumor suppressor gene silencing are distinct molecular phenotypes driven by growth promoting mutations in nonsmall cell lung cancer. *J Cancer Epidemiol.* (2008) 2008:215809. doi: 10.1155/2008/215809
15. Yadav P, Masroor M, Nandi K, Kaza RCM, Jain SK, Khurana N, et al. Promoter methylation of BRCA1, DAPK1 and RASSF1A is associated with increased mortality among indian women with breast cancer. *Asian Pac J Cancer Prev.* (2018) 19:443–8. doi: 10.22034/APJCP.2018.19.2.443
16. Guo L, Wang X, Yang Y, Xu H, Zhang Z, Yin L, et al. Methylation of DACT2 contributes to the progression of breast cancer through activating WNT signaling pathway. *Oncol Lett.* (2018) 15:3287–94. doi: 10.3892/ol.2017.7633
17. Begam N, Jamil K, Raju SG. Promoter hypermethylation of the ATM gene as a novel biomarker for breast cancer. *Asian Pac J Cancer Prev.* (2017) 18:3003–9. doi: 10.22034/APJCP.2017.18.11.3003
18. Espinal AC, Buas MF, Wang D, Cheng DT, Sucheston-Campbell L, Hu Q, et al. FOXA1 hypermethylation: link between parity and ER-negative breast cancer in African American women? *Breast Cancer Res Treat.* (2017) 166:559–68. doi: 10.1007/s10549-017-4418-y
19. Guerrero-Setas D, Perez-Janices N, Blanco-Fernandez L, Ojer A, Cambra K, Berdasco M, et al. RASSF2 hypermethylation is present and related to shorter survival in squamous cervical cancer. *Mod Pathol.* (2013) 26:1111–22. doi: 10.1038/modpathol.2013.32
20. Li JY, Huang T, Zhang C, Jiang DJ, Hong QX, Ji HH, et al. Association between RASSF1A promoter hypermethylation and oncogenic HPV infection status in invasive cervical cancer: a meta-analysis. *Asian Pac J Cancer Prev.* (2015) 16:5749–54. doi: 10.7314/APJCP.2015.16.14.5749
21. Dong Y, Tan Q, Tao L, Pan X, Pang L, Liang W, et al. Hypermethylation of TFPI2 correlates with cervical cancer incidence in the uygur and han populations of Xinjiang, China. *Int J Clin Exp Pathol.* (2015) 8:1844–54.
22. Kim HJ, Kim CY, Jin J, Bae MK, Kim YH, Ju W, et al. Aberrant single-minded homolog 1 methylation as a potential biomarker for cervical cancer. *Diagn Cytopathol.* (2018) 46:15–21. doi: 10.1002/dc.23838
23. Zhang J, Yao T, Lin Z, Gao Y. Aberrant methylation of MEG3 functions as a potential plasma-based biomarker for cervical cancer. *Sci Rep.* (2017) 7:6271. doi: 10.1038/s41598-017-06502-7
24. Han YD, Wang XB, Cui NH, Zhang S, Wang C, Zheng F. Associations of P16INK4a promoter hypermethylation with squamous intra-epithelial lesion, cervical cancer and their clinicopathological features: a meta-analysis. *Oncotarget.* (2017) 8:1871–83. doi: 10.18632/oncotarget.12202
25. Wei X, Zhang S, Cao D, Zhao M, Zhang Q, Zhao J, et al. Aberrant hypermethylation of SALL3 with HPV involvement contributes to the carcinogenesis of cervical cancer. *PLoS ONE.* (2015) 10:e0145700. doi: 10.1371/journal.pone.0145700
26. Ma D, Jiang C, Hu X, Liu H, Li Q, Li T, et al. Methylation patterns of the IFN-gamma gene in cervical cancer tissues. *Sci Rep.* (2014) 4:6331. doi: 10.1038/srep06331
27. Yang WT, Zheng PS. Promoter hypermethylation of KLF4 inactivates its tumor suppressor function in cervical carcinogenesis. *PLoS ONE.* (2014) 9:e88827. doi: 10.1371/journal.pone.0088827

28. Paulikova S, Chmelarova M, Petera J, Palicka V, Paulik A. Hypermethylation of RAD51L3 and XRCC2 genes to predict late toxicity in chemoradiotherapy-treated cervical cancer patients. *Folia Biol.* (2013) 59:240–5.
29. Chen H, Xu Z, Yang B, Zhou X, Kong H. RASGRF1 hypermethylation, a putative biomarker of colorectal cancer. *Ann Clin Lab Sci.* (2018) 48:3–10.
30. Zhu Y, Lu H, Zhang D, Li M, Sun X, Wan L, et al. Integrated analyses of multi-omics reveal global patterns of methylation and hydroxymethylation and screen the tumor suppressive roles of HADHB in colorectal cancer. *Clin Epigenetics.* (2018) 10:30. doi: 10.1186/s13148-018-0458-3
31. Barati Bagerabad M, Tavakolian S, Abbaszadegan MR, Kerachian MA. Promoter hypermethylation of the eyes absent 4 gene is a tumor-specific epigenetic biomarker in iranian colorectal cancer patients. *Acta Med Iran.* (2018) 56:21–7. doi: 10.18502/acta.v57i5.1874
32. Yin MD, Ma SP, Liu F, Chen YZ. Role of serine/threonine kinase 33 methylation in colorectal cancer and its clinical significance. *Oncol Lett.* (2018) 15:2153–60. doi: 10.3892/ol.2017.7614
33. Lin RK, Hung WY, Huang YF, Chang YJ, Lin CH, Chen WY, et al. Hypermethylation of BEND5 contributes to cell proliferation and is a prognostic marker of colorectal cancer. *Oncotarget.* (2017) 8:113431–43. doi: 10.18632/oncotarget.22266
34. Islam F, Gopalan V, Pillai S, Lu CT, Kasem K, Lam AK. Promoter hypermethylation inactivate tumor suppressor FAM134B and is associated with poor prognosis in colorectal cancer. *Genes Chromosomes Cancer.* (2018) 57:240–51. doi: 10.1002/gcc.22525
35. Sun Z, Liu J, Jing H, Dong SX, Wu J. The diagnostic and prognostic value of CHFR hypermethylation in colorectal cancer, a meta-analysis and literature review. *Oncotarget.* (2017) 8:89142–8. doi: 10.18632/oncotarget.19408
36. Barrow TM, Klett H, Toth R, Bohm J, Gigic B, Habermann N, et al. Smoking is associated with hypermethylation of the APC 1A promoter in colorectal cancer: the colocare study. *J Pathol.* (2017) 243:366–75. doi: 10.1002/path.4955
37. Hu YH, Chen Q, Lu YX, Zhang JM, Lin C, Zhang F, et al. Hypermethylation of NDN promotes cell proliferation by activating the Wnt signaling pathway in colorectal cancer. *Oncotarget.* (2017) 8:46191–203. doi: 10.18632/oncotarget.17580
38. Zhang HF, Lu YW, Xie ZR, Wang KH. Relationship between human mutL homolog 1 (hMLH1) hypermethylation and colorectal cancer: a meta-analysis. *Med Sci Monit.* (2017) 23:3026–38. doi: 10.12659/MSM.895643
39. Ge Y, Wu Q, Ma G, Shao W, Liu H, Zhang Q, et al. Hypermethylation of EIF4E promoter is associated with early onset of gastric cancer. *Carcinogenesis.* (2018) 39:66–71. doi: 10.1093/carcin/bgx110
40. Chen Z, Hu T, Zhu S, Mukaisho K, El-Rifai W, Peng DF. Glutathione peroxidase 7 suppresses cancer cell growth and is hypermethylated in gastric cancer. *Oncotarget.* (2017) 8:54345–56. doi: 10.18632/oncotarget.17527
41. Tahara T, Tahara S, Horiguchi N, Kawamura T, Okubo M, Yamada H, et al. Methylation status of IGF2 DMR and LINE1 in leukocyte DNA provides distinct clinicopathological features of gastric cancer patients. *Clin Exp Med.* (2018) 18:215–20. doi: 10.1007/s10238-017-0471-4
42. Mohsenzadeh M, Sadeghi RN, Vahedi M, Kamani F, Hashemi M, Asadzadeh H, et al. Promoter hypermethylation of RAR-beta tumor suppressor gene in gastric carcinoma: association with histological type and clinical outcomes. *Cancer Biomark.* (2017) 20:7–15. doi: 10.3233/CBM-160331
43. Liu L, Liu C, Fotouhi O, Fan Y, Wang K, Xia C, et al. TERT promoter hypermethylation in gastrointestinal cancer: a potential stool biomarker. *Oncologist.* (2017) 22:1178–88. doi: 10.1634/theoncologist.2017-0064
44. Zhang Z, Xin S, Gao M, Cai Y. Promoter hypermethylation of MGMT gene may contribute to the pathogenesis of gastric cancer: a PRISMA-compliant meta-analysis. *Medicine.* (2017) 96:e6708. doi: 10.1097/MD.0000000000006708
45. Pei YF, Zhang YJ, Lei Y, Wu WD, Ma TH, Liu XQ. Hypermethylation of the CHRDL1 promoter induces proliferation and metastasis by activating Akt and Erk in gastric cancer. *Oncotarget.* (2017) 8:23155–66. doi: 10.18632/oncotarget.15513
46. Guo L, Huang C, Ji QJ. Aberrant promoter hypermethylation of p16, survivin, and retinoblastoma in gastric cancer. *Bratisl Lek Listy.* (2017) 118:164–8. doi: 10.4149/BLL_2017_033
47. Zhang JK, Li YS, Zhang CD, Dai DQ. Up-regulation of CRKL by microRNA-335 methylation is associated with poor prognosis in gastric cancer. *Cancer Cell Int.* (2017) 17:28. doi: 10.1186/s12935-017-0387-9
48. Wang H, Duan XL, Qi XL, Meng L, Xu YS, Wu T, et al. Concurrent hypermethylation of SFRP2 and DKK2 activates the Wnt/beta-catenin pathway and is associated with poor prognosis in patients with gastric cancer. *Mol Cells.* (2017) 40:45–53. doi: 10.14348/molcells.2017.2245
49. Chen X, Yang Y, Liu J, Li B, Xu Y, Li C, et al. NDRG4 hypermethylation is a potential biomarker for diagnosis and prognosis of gastric cancer in Chinese population. *Oncotarget.* (2017) 8:8105–19. doi: 10.18632/oncotarget.14099
50. Wang N, Sui F, Ma J, Su X, Liu J, Yao D, et al. Site-specific hypermethylation of RUNX3 predicts poor prognosis in gastric cancer. *Arch Med Res.* (2016) 47:285–92. doi: 10.1016/j.arcmed.2016.07.011
51. Chen J, Zhang J, Li X, Zhang C, Zhang H, Jin J, et al. Downregulation of ADAMTS8 by DNA hypermethylation in gastric cancer and its clinical significance. *Biomed Res Int.* (2016) 2016:5083841. doi: 10.1155/2016/5083841
52. Wang H, Xu M, Cui X, Liu Y, Zhang Y, Sui Y, et al. Aberrant expression of the candidate tumor suppressor gene DAL-1 due to hypermethylation in gastric cancer. *Sci Rep.* (2016) 6:21755. doi: 10.1038/srep21755
53. Ng PKS, Lau CPY, Lam EKY, Li SSK, Lui VWY, Yeo W, et al. Hypermethylation of NF-kappaB-activating protein-like (NKAPL) promoter in hepatocellular carcinoma suppresses its expression and predicts a poor prognosis. *Dig Dis Sci.* (2018) 63:676–86. doi: 10.1007/s10620-018-4929-3
54. Guo Y, Peng Y, Gao D, Zhang M, Yang W, Linghu E, et al. Silencing HOXD10 by promoter region hypermethylation activates ERK signaling in hepatocellular carcinoma. *Clin Epigenetics.* (2017) 9:116. doi: 10.1186/s13148-017-0412-9
55. Zhang Y, Xu X, Chen Z, Zhao Z. Association of FHIT expression and FHIT gene hypermethylation with liver cancer risk: a PRISMA-compliant meta-analysis. *Onco Targets Ther.* (2017) 10:3083–93. doi: 10.2147/OTT.S138036
56. Mansour LA, El Raziky M, Mohamed AA, Mahmoud EH, Hamdy S, El Sayed EH. Circulating hypermethylated RASSF1A as a molecular biomarker for diagnosis of hepatocellular carcinoma. *Asian Pac J Cancer Prev.* (2017) 18:1637–43. doi: 10.22034/APJCP.2017.18.6.1637
57. Tian MM, Fan YC, Zhao J, Gao S, Zhao ZH, Chen LY, et al. Hepatocellular carcinoma suppressor 1 promoter hypermethylation in serum. A diagnostic and prognostic study in hepatitis B. *Clin Res Hepatol Gastroenterol.* (2017) 41:171–80. doi: 10.1016/j.clinre.2016.10.003
58. Hoan NX, Van Tong H, Giang DP, Cuong BK, Toan NL, Wedemeyer H, et al. SOCS3 genetic variants and promoter hypermethylation in patients with chronic hepatitis B. *Oncotarget.* (2017) 8:17127–39. doi: 10.18632/oncotarget.15083
59. Yu Q, Xiang L, Yin L, Liu X, Yang D, Zhou J. Loss-of-function of miR-142 by hypermethylation promotes TGF-beta-mediated tumour growth and metastasis in hepatocellular carcinoma. *Cell Prolif.* (2017) 50:e12384. doi: 10.1111/cpr.12384
60. Hu H, Chen X, Zhou C, Li B, Yang Y, Ying X, et al. Aberrant methylation of mutL homolog 1 is associated with increased risk of non-small cell lung cancer. *J Clin Lab Anal.* (2018) 32:e22370. doi: 10.1002/jcla.22370
61. Gao C, Xing X, He Z, Chen S, Wang S, Li Q, et al. Hypermethylation of PGCP gene is associated with human bronchial epithelial cells immortalization. *Gene.* (2018) 642:505–12. doi: 10.1016/j.gene.2017.11.063
62. Chen R, Hong Q, Jiang J, Chen X, Jiang Z, Wang J, et al. AGTR1 promoter hypermethylation in lung squamous cell carcinoma but not in lung adenocarcinoma. *Oncol Lett.* (2017) 14:4989–94. doi: 10.3892/ol.2017.6824
63. El-Sherif WT, Sayed SK, Galal SH, Makhlouf HA, Hassan AT, Yousef HA. Diagnostic role of RASSF1A and p16INK4a promoter gene hypermethylation in serum DNA of lung cancer patients: clinicopathological significance. *Egypt J Immunol.* (2016) 23:1–16.
64. Zheng Y, Li X, Jiang Y, Xu Y, Song B, Zhou Q, et al. Promoter hypermethylation of Wnt inhibitory factor-1 in patients with lung cancer: a systematic meta-analysis. *Medicine.* (2016) 95:e5433. doi: 10.1097/MD.0000000000005433
65. Rezk NA, Mohamed RH, Alnemr AA, Harira M. Promoter methylation of RASSF1A gene in egyptian patients with ovarian cancer. *Appl Biochem Biotechnol.* (2018) 185:153–62. doi: 10.1007/s12010-017-2648-4

66. Kim JY, Do SI, Bae GE, Kim HS. B-cell translocation gene 1 is downregulated by promoter methylation in ovarian carcinoma. *J Cancer.* (2017) 8:2669–75. doi: 10.7150/jca.21037
67. Shen C, Sheng Q, Zhang X, Fu Y, Zhu K. Hypermethylated APC in serous carcinoma based on a meta-analysis of ovarian cancer. *J Ovarian Res.* (2016) 9:60. doi: 10.1186/s13048-016-0271-6
68. Schmid G, Notaro S, Reimer D, Abdel-Azim S, Duggan-Peer M, Holly J, et al. Expression and promotor hypermethylation of miR-34a in the various histological subtypes of ovarian cancer. *BMC Cancer.* (2016) 16:102. doi: 10.1186/s12885-016-2135-2
69. Ding JJ, Wang G, Shi WX, Zhou HH, Zhao EF. Promoter hypermethylation of FANCF and susceptibility and prognosis of epithelial ovarian cancer. *Reprod Sci.* (2016) 23:24–30. doi: 10.1177/1933719115612136
70. Hafner N, Steinbach D, Jansen L, Diebolder H, Durst M, Runnebaum IB. RUNX3 and CAMK2N1 hypermethylation as prognostic marker for epithelial ovarian cancer. *Int J Cancer.* (2016) 138:217–28. doi: 10.1002/ijc.29690
71. Chou JL, Huang RL, Shay J, Chen LY, Lin SJ, Yan PS, et al. Hypermethylation of the TGF-beta target, ABCA1 is associated with poor prognosis in ovarian cancer patients. *Clin Epigenetics.* (2015) 7:1. doi: 10.1186/s13148-014-0036-2
72. Sheng X, Li J, Yang L, Chen Z, Zhao Q, Tan L, et al. Promoter hypermethylation influences the suppressive role of maternally expressed 3, a long non-coding RNA, in the development of epithelial ovarian cancer. *Oncol Rep.* (2014) 32:277–85. doi: 10.3892/or.2014.3208
73. Faleiro I, Apolonio JD, Price AJ, De Mello RA, Roberto VP, Tabori U, et al. The TERT hypermethylated oncologic region predicts recurrence and survival in pancreatic cancer. *Future Oncol.* (2017) 13:2045–51. doi: 10.2217/fon-2017-0167
74. Wang L, Wang M, Hu C, Li P, Qiao Y, Xia Y, et al. Protein salvador homolog 1 acts as a tumor suppressor and is modulated by hypermethylation in pancreatic ductal adenocarcinoma. *Oncotarget.* (2017) 8:62953–61. doi: 10.18632/oncotarget.17972
75. Ushiku H, Yamashita K, Kawamata H, Waraya M, Katoh H, Yokoi K, et al. Homeobox-only protein expression is a critical prognostic indicator of pancreatic neuroendocrine tumor and is regulated by promoter DNA hypermethylation. *Pancreas.* (2016) 45:1255–62. doi: 10.1097/MPA.0000000000000646
76. Tang B, Li Y, Qi G, Yuan S, Wang Z, Yu S, et al. Clinicopathological significance of CDKN2A promoter hypermethylation frequency with pancreatic cancer. *Sci Rep.* (2015) 5:13563. doi: 10.1038/srep13563
77. Haldrup C, Pedersen AL, Ogaard N, Strand SH, Hoyer S, Borre M, et al. Biomarker potential of ST6GALNAC3 and ZNF660 promoter hypermethylation in prostate cancer tissue and liquid biopsies. *Mol Oncol.* (2018) 12:545–60. doi: 10.1002/1878-0261.12183
78. Pugongchai A, Bychkov A, Sampatanukul P. Promoter hypermethylation of SOX11 correlates with adverse clinicopathological features of human prostate cancer. *Int J Exp Pathol.* (2017) 98:341–6. doi: 10.1111/iep.12257
79. Kuffer S, Gutting T, Belharazem D, Sauer C, Michel MS, Marx A, et al. Insulin-like growth factor 2 expression in prostate cancer is regulated by promoter-specific methylation. *Mol Oncol.* (2018) 12:256–66. doi: 10.1002/1878-0261.12164
80. Liu T, Qiu X, Zhao X, Yang R, Lian H, Qu F, et al. Hypermethylation of the SPARC promoter and its prognostic value for prostate cancer. *Oncol Rep.* (2018) 39:659–66. doi: 10.3892/or.2017.6121
81. Lounglaithong K, Bychkov A, Sampatanukul P. Aberrant promoter methylation of the PAQR3 gene is associated with prostate cancer. *Pathol Res Pract.* (2018) 214:126–9. doi: 10.1016/j.prp.2017.10.010
82. Zhang P, Wang H, Wang J, Liu Q, Wang Y, Feng F, et al. Association between protocadherin 8 promoter hypermethylation and the pathological status of prostate cancer. *Oncol Lett.* (2017) 14:1657–64. doi: 10.3892/ol.2017.6282
83. Strand SH, Switnicki M, Moller M, Haldrup C, Storebjerg TM, Hedegaard J, et al. RHCG and TCAF1 promoter hypermethylation predicts biochemical recurrence in prostate cancer patients treated by radical prostatectomy. *Oncotarget.* (2017) 8:5774–88. doi: 10.18632/oncotarget.14391
84. Castelo-Branco P, Leao R, Lipman T, Campbell B, Lee D, Price A, et al. A cancer specific hypermethylation signature of the TERT promoter predicts biochemical relapse in prostate cancer: a retrospective cohort study. *Oncotarget.* (2016) 7:57726–36. doi: 10.18632/oncotarget.10639
85. Zelic R, Fiano V, Zugna D, Grasso C, Delsedime L, Daniele L, et al. Global hypomethylation (LINE-1) and gene-specific hypermethylation (GSTP1) on initial negative prostate biopsy as markers of prostate cancer on a rebiopsy. *Clin Cancer Res.* (2016) 22:984–92. doi: 10.1158/1078-0432.CCR-15-0606
86. Yi J, Gao R, Chen Y, Yang Z, Han P, Zhang H, et al. Overexpression of NSUN2 by DNA hypomethylation is associated with metastatic progression in human breast cancer. *Oncotarget.* (2017) 8:20751–65. doi: 10.18632/oncotarget.10612
87. Sizemore ST, Sizemore GM, Booth CN, Thompson CL, Silverman P, Bebek G, et al. Hypomethylation of the MMP7 promoter and increased expression of MMP7 distinguishes the basal-like breast cancer subtype from other triple-negative tumors. *Breast Cancer Res Treat.* (2014) 146:25–40. doi: 10.1007/s10549-014-2989-4
88. Son KS, Kang HS, Kim SJ, Jung SY, Min SY, Lee SY, et al. Hypomethylation of the interleukin-10 gene in breast cancer tissues. *Breast.* (2010) 19:484–8. doi: 10.1016/j.breast.2010.05.011
89. Yin FF, Wang N, Bi XN, Yu X, Xu XH, Wang YL, et al. Serine/threonine kinases 31(STK31) may be a novel cellular target gene for the HPV16 oncogene E7 with potential as a DNA hypomethylation biomarker in cervical cancer. *Virol J.* (2016) 13:60. doi: 10.1186/s12985-016-0515-5
90. Wu Y, Gong L, Xu J, Mou Y, Xu X, Qian Z. The clinicopathological significance of HES1 promoter hypomethylation in patients with colorectal cancer. *Onco Targets Ther.* (2017) 10:5827–34. doi: 10.2147/OTT.S151857
91. Kano H, Takayama T, Midorikawa Y, Nagase H. Promoter hypomethylation of RAR-related orphan receptor alpha 1 is correlated with unfavorable clinicopathological features in patients with colorectal cancer. *Biosci Trends.* (2016) 10:202–9. doi: 10.5582/bst.2016.01097
92. Renaud F, Mariette C, Vincent A, Wacrenier A, Maunoury V, Leclerc J, et al. The serrated neoplasia pathway of colorectal tumors: identification of MUC5AC hypomethylation as an early marker of polyps with malignant potential. *Int J Cancer.* (2016) 138:1472–81. doi: 10.1002/ijc.29891
93. Renaud F, Vincent A, Mariette C, Crepin M, Stechly L, Truant S, et al. MUC5AC hypomethylation is a predictor of microsatellite instability independently of clinical factors associated with colorectal cancer. *Int J Cancer.* (2015) 136:2811–21. doi: 10.1002/ijc.29342
94. Li C, Cai S, Wang X, Jiang Z. Hypomethylation-associated up-regulation of TCF3 expression and recurrence in stage II and III colorectal cancer. *PLoS ONE.* (2014) 9:e112005. doi: 10.1371/journal.pone.0112005
95. de Melo CF, Gigek CO, da Silva JN, Cardoso Smith Mde A, de Araujo RM, Burbano RR, et al. Association of COX2 gene hypomethylation with intestinal type gastric cancer in samples of patients from northern Brazil. *Tumour Biol.* (2014) 35:1107–11. doi: 10.1007/s13277-013-1148-6
96. Yuasa Y, Nagasaki H, Oze I, Akiyama Y, Yoshida S, Shitara K, et al. Insulin-like growth factor 2 hypomethylation of blood leukocyte DNA is associated with gastric cancer risk. *Int J Cancer.* (2012) 131:2596–603. doi: 10.1002/ijc.27554
97. He J, Huang Y, Liu Z, Zhao R, Liu Q, Wei L, et al. Hypomethylation of BORIS is a promising prognostic biomarker in hepatocellular carcinoma. *Gene.* (2017) 629:29–34. doi: 10.1016/j.gene.2017.07.077
98. Zhong D, Cen H. Aberrant promoter methylation profiles and association with survival in patients with hepatocellular carcinoma. *Onco Targets Ther.* (2017) 10:2501–9. doi: 10.2147/OTT.S128058
99. Zhu C, Utsunomiya T, Ikemoto T, Yamada S, Morine Y, Imura S, et al. Hypomethylation of long interspersed nuclear element-1 (LINE-1) is associated with poor prognosis via activation of c-MET in hepatocellular carcinoma. *Ann Surg Oncol.* (2014) 21(Suppl 4):S729–35. doi: 10.1245/s10434-014-3874-4
100. He Y, Cui Y, Wang W, Gu J, Guo S, Ma K, et al. Hypomethylation of the hsa-miR-191 locus causes high expression of hsa-mir-191 and promotes the epithelial-to-mesenchymal transition in hepatocellular carcinoma. *Neoplasia.* (2011) 13:841–53. doi: 10.1593/neo.11698
101. Yuan R, Zhi Q, Zhao H, Han Y, Gao L, Wang B, et al. Upregulated expression of miR-106a by DNA hypomethylation plays an oncogenic role in hepatocellular carcinoma. *Tumour Biol.* (2015) 36:3093–100. doi: 10.1007/s13277-014-2945-2

102. Brennan K, Shin JH, Tay JK, Prunello M, Gentles AJ, Sunwoo JB, et al. NSD1 inactivation defines an immune cold, DNA hypomethylated subtype in squamous cell carcinoma. *Sci Rep.* (2017) 7:17064. doi: 10.1038/s41598-017-17298-x
103. Chueh AC, Liew MS, Russell PA, Walkiewicz M, Jayachandran A, Starmans MHW, et al. Promoter hypomethylation of NY-ESO-1, association with clinicopathological features and PD-L1 expression in non-small cell lung cancer. *Oncotarget.* (2017) 8:74036–48. doi: 10.18632/oncotarget.18198
104. Yokoyama S, Higashi M, Tsutsumida H, Wakimoto J, Hamada T, Wiest E, et al. TET1-mediated DNA hypomethylation regulates the expression of MUC4 in lung cancer. *Genes Cancer.* (2017) 8:517–27. doi: 10.18632/genesandcancer.139
105. Lee DH, Hwang SH, Lim MK, Oh JK, Song DY, Yun EH, et al. Performance of urine cotinine and hypomethylation of AHRR and F2RL3 as biomarkers for smoking exposure in a population-based cohort. *PLoS ONE.* (2017) 12:e0176783. doi: 10.1371/journal.pone.0176783
106. Fujii S, Shinjo K, Matsumoto S, Harada T, Nojima S, Sato S, et al. Epigenetic upregulation of ARL4C, due to DNA hypomethylation in the 3'-untranslated region, promotes tumorigenesis of lung squamous cell carcinoma. *Oncotarget.* (2016) 7:81571–87. doi: 10.18632/oncotarget.13147
107. Villalba M, Diaz-Lagares A, Redrado M, de Aberasturi AL, Segura V, Bodegas ME, et al. Epigenetic alterations leading to TMPRSS4 promoter hypomethylation and protein overexpression predict poor prognosis in squamous lung cancer patients. *Oncotarget.* (2016) 7:22752–69. doi: 10.18632/oncotarget.8045
108. Gao T, Zheng S, Li Q, Ran P, Sun L, Yuan Y, et al. Aberrant hypomethylation and overexpression of the eyes absent homologue 2 suppresses tumor cell growth of human lung adenocarcinoma cells. *Oncol Rep.* (2015) 34:2333–42. doi: 10.3892/or.2015.4245
109. Sung HY, Yang SD, Park AK, Ju W, Ahn JH. Aberrant hypomethylation of solute carrier family 6 member 12 promoter induces metastasis of ovarian cancer. *Yonsei Med J.* (2017) 58:27–34. doi: 10.3349/ymj.2017.58.1.27
110. Zhang W, Barger CJ, Link PA, Mhawech-Fauceglia P, Miller A, Akers SN, et al. DNA hypomethylation-mediated activation of cancer/testis antigen 45 (CT45) genes is associated with disease progression and reduced survival in epithelial ovarian cancer. *Epigenetics.* (2015) 10:736–48. doi: 10.1080/15592294.2015.1062206
111. Sung HY, Ju W, Ahn JH. DNA hypomethylation-mediated overexpression of carbonic anhydrase 9 induces an aggressive phenotype in ovarian cancer cells. *Yonsei Med J.* (2014) 55:1656–63. doi: 10.3349/ymj.2014.55.6.1656
112. Sung HY, Choi EN, Lyu D, Park AK, Ju W, Ahn JH. Aberrant hypomethylation-mediated AGR2 overexpression induces an aggressive phenotype in ovarian cancer cells. *Oncol Rep.* (2014) 32:815–20. doi: 10.3892/or.2014.3243
113. Liao YP, Chen LY, Huang RL, Su PH, Chan MW, Chang CC, et al. Hypomethylation signature of tumor-initiating cells predicts poor prognosis of ovarian cancer patients. *Hum Mol Genet.* (2014) 23:1894–906. doi: 10.1093/hmg/ddt583
114. Mardin WA, Ntalos D, Mees ST, Spieker T, Senninger N, Haier J, et al. SERPINB5 promoter hypomethylation differentiates pancreatic ductal adenocarcinoma from pancreatitis. *Pancreas.* (2016) 45:743–7. doi: 10.1097/MPA.0000000000000526
115. Zhu Y, Zhang JJ, Zhu R, Zhu Y, Liang WB, Gao WT, et al. The increase in the expression and hypomethylation of MUC4 gene with the progression of pancreatic ductal adenocarcinoma. *Med Oncol.* (2011) 28(Suppl. 1):S175–84. doi: 10.1007/s12032-010-9683-0
116. Rosty C, Ueki T, Argani P, Jansen M, Yeo CJ, Cameron JL, et al. Overexpression of S100A4 in pancreatic ductal adenocarcinomas is associated with poor differentiation and DNA hypomethylation. *Am J Pathol.* (2002) 160:45–50. doi: 10.1016/S0002-9440(10)64347-7
117. Nones K, Waddell N, Song S, Patch AM, Miller D, Johns A, et al. Genome-wide DNA methylation patterns in pancreatic ductal adenocarcinoma reveal epigenetic deregulation of SLIT-ROBO, ITGA2 and MET signaling. *Int J Cancer.* (2014) 135:1110–8. doi: 10.1002/ijc.28765
118. Norgaard M, Haldrup C, Storebjerg TM, Vestergaard EM, Wild PJ, Hoyer S, et al. Comprehensive evaluation of TFF3 promoter hypomethylation and molecular biomarker potential for prostate cancer diagnosis and prognosis. *Int J Mol Sci.* (2017) 18:2017. doi: 10.3390/ijms18092017
119. Liang YX, Mo RJ, He HC, Chen JH, Zou J, Han ZD, et al. Aberrant hypomethylation-mediated CD147 overexpression promotes aggressive tumor progression in human prostate cancer. *Oncol Rep.* (2015) 33:2648–54. doi: 10.3892/or.2015.3870
120. Vestergaard EM, Nexo E, Torring N, Borre M, Orntoft TF, Sorensen KD. Promoter hypomethylation and upregulation of trefoil factors in prostate cancer. *Int J Cancer.* (2010) 127:1857–65. doi: 10.1002/ijc.25209
121. Gao B, Yang F, Chen W, Li R, Hu X, Liang Y, et al. Multidrug resistance affects the prognosis of primary epithelial ovarian cancer. *Oncol Lett.* (2019) 18:4262–9. doi: 10.3892/ol.2019.10745
122. Baharudin R, Ab Mutalib NS, Othman SN, Sagap I, Rose IM, Mohd Mokhtar N, et al. Identification of predictive DNA methylation biomarkers for chemotherapy response in colorectal cancer. *Front Pharmacol.* (2017) 8:47. doi: 10.3389/fphar.2017.00047
123. Guo R, Wu G, Li H, Qian P, Han J, Pan F, et al. Promoter methylation profiles between human lung adenocarcinoma multidrug resistant A549/cisplatin (A549/DDP) cells and its progenitor A549 cells. *Biol Pharm Bull.* (2013) 36:1310–6. doi: 10.1248/bpb.b13-00153
124. Palomeras S, Diaz-Lagares A, Vinas G, Setien F, Ferreira HJ, Oliveras G, et al. Epigenetic silencing of TGFBI confers resistance to trastuzumab in human breast cancer. *Breast Cancer Res.* (2019) 21:79. doi: 10.1186/s13058-019-1160-x
125. Zhang J, Zhou C, Jiang H, Liang L, Shi W, Zhang Q, et al. ZEB1 induces ER-alpha promoter hypermethylation and confers antiestrogen resistance in breast cancer. *Cell Death Dis.* (2017) 8:e2732. doi: 10.1038/cddis.2017.154
126. Ponnusamy L, Mahalingaiah PKS, Chang YW, Singh KP. Reversal of epigenetic aberrations associated with the acquisition of doxorubicin resistance restores drug sensitivity in breast cancer cells. *Eur J Pharm Sci.* (2018) 123:56–69. doi: 10.1016/j.ejps.2018.07.028
127. Tuo YL, Ye YF. MGP is downregulated due to promoter methylation in chemoresistant ER+ breast cancer and high MGP expression predicts better survival outcomes. *Eur Rev Med Pharmacol Sci.* (2017) 21:3871–8.
128. De Marchi T, Timmermans MA, Sieuwerts AM, Smid M, Look MP, Grebenchtchikov N, et al. Phosphoserine aminotransferase 1 is associated to poor outcome on tamoxifen therapy in recurrent breast cancer. *Sci Rep.* (2017) 7:2099. doi: 10.1038/s41598-017-02296-w
129. Kim MH, Kim MS, Kim W, Kang MA, Cacalano NA, Kang SB, et al. Suppressor of cytokine signaling (SOCS) genes are silenced by DNA hypermethylation and histone deacetylation and regulate response to radiotherapy in cervical cancer cells. *PLoS ONE.* (2015) 10:e0123133. doi: 10.1371/journal.pone.0123133
130. Wu NY, Zhang X, Chu T, Zhu S, Deng Y, Zhou Y, et al. High methylation of ZNF582 in cervical adenocarcinoma affects radiosensitivity and prognosis. *Ann Transl Med.* (2019) 7:328. doi: 10.21037/atm.2019.06.15
131. Chang SY, Kuo CC, Wu CC, Hsiao CW, Hu JM, Hsu CH, et al. NKX6.1 hypermethylation predicts the outcome of stage II colorectal cancer patients undergoing chemotherapy. *Genes Chromosomes Cancer.* (2018) 57:268–77. doi: 10.1002/gcc.22529
132. Bosch LJW, Trooskens G, Snaebjornsson P, Coupe VMH, Mongera S, Haan JC, et al. Decoy receptor 1 (DCR1) promoter hypermethylation and response to irinotecan in metastatic colorectal cancer. *Oncotarget.* (2017) 8:63140–54. doi: 10.18632/oncotarget.18702
133. Wang X, Ghareeb WM, Zhang Y, Yu Q, Lu X, Huang Y, et al. Hypermethylated and downregulated MEIS2 are involved in stemness properties and oxaliplatin-based chemotherapy resistance of colorectal cancer. *J Cell Physiol.* (2019) 234:18180–91. doi: 10.1002/jcp.28451
134. Wang B, Lu FY, Shi RH, Feng YD, Zhao XD, Lu ZP, et al. MiR-26b regulates 5-FU-resistance in human colorectal cancer via down-regulation of Pgp. *Am J Cancer Res.* (2018) 8:2518–27.
135. Jingyue S, Xiao W, Juanmin Z, Wei L, Daoming L, Hong X. TFAP2E methylation promotes 5fluorouracil resistance via exosomal miR106a5p and miR421 in gastric cancer MGC803 cells. *Mol Med Rep.* (2019) 20:323–31. doi: 10.3892/mmr.2019.10237
136. Sun J, Du N, Li J, Zhou J, Tao G, Sun S, et al. Transcription factor AP2epsilon: a potential predictor of chemoresistance in patients with gastric cancer. *Technol Cancer Res Treat.* (2016) 15:285–95. doi: 10.1177/1533034615577028

137. Fujiyoshi S, Honda S, Minato M, Ara M, Suzuki H, Hiyama E, et al. Hypermethylation of CSF3R is a novel cisplatin resistance marker and predictor of response to postoperative chemotherapy in hepatoblastoma. *Hepatol Res.* (2020) 50:598–606. doi: 10.1111/hepr.13479
138. Fan H, Zhang M, Liu W. Hypermethylated KCNQ1 acts as a tumor suppressor in hepatocellular carcinoma. *Biochem Biophys Res Commun.* (2018) 503:3100–7. doi: 10.1016/j.bbrc.2018.08.099
139. Tian FM, Zhong CY, Wang XN, Meng Y. PDE3A is hypermethylated in cisplatin resistant non-small cell lung cancer cells and is a modulator of chemotherapy response. *Eur Rev Med Pharmacol Sci.* (2017) 21:2635–41.
140. Grasse S, Lienhard M, Frese S, Kerick M, Steinbach A, Grimm C, et al. Epigenomic profiling of non-small cell lung cancer xenografts uncover LRP12 DNA methylation as predictive biomarker for carboplatin resistance. *Genome Med.* (2018) 10:55. doi: 10.1186/s13073-018-0562-1
141. Yue J, Lv D, Wang C, Li L, Zhao Q, Chen H, et al. Epigenetic silencing of miR-483-3p promotes acquired gefitinib resistance and EMT in EGFR-mutant NSCLC by targeting integrin beta3. *Oncogene.* (2018) 37:4300–12. doi: 10.1038/s41388-018-0276-2
142. Jin C, Yu W, Lou X, Zhou F, Han X, Zhao N, et al. UCHL1 is a putative tumor suppressor in ovarian cancer cells and contributes to cisplatin resistance. *J Cancer.* (2013) 4:662–70. doi: 10.7150/jca.6641
143. Yang SD, Ahn SH, Kim JI. 3-Oxoacid CoA transferase 1 as a therapeutic target gene for cisplatin-resistant ovarian cancer. *Oncol Lett.* (2018) 15:2611–8. doi: 10.3892/ol.2017.7560
144. Prieske K, Prieske S, Joosse SA, Trillsch F, Grimm D, Burandt E, et al. Loss of BRCA1 promotor hypermethylation in recurrent high-grade ovarian cancer. *Oncotarget.* (2017) 8:83063–74. doi: 10.18632/oncotarget.20945
145. Deng Y, Zhao F, Hui L, Li X, Zhang D, Lin W, et al. Suppressing miR-199a-3p by promoter methylation contributes to tumor aggressiveness and cisplatin resistance of ovarian cancer through promoting DDR1 expression. *J Ovarian Res.* (2017) 10:50. doi: 10.1186/s13048-017-0333-4
146. Tian H, Yan L, Xiao-Fei L, Hai-Yan S, Juan C, Shan K. Hypermethylation of mismatch repair gene hMSH2 associates with platinum-resistant disease in epithelial ovarian cancer. *Clin Epigenetics.* (2019) 11:153. doi: 10.1186/s13148-019-0748-4
147. Ha YN, Sung HY, Yang SD, Chae YJ, Ju W, Ahn JH. Epigenetic modification of alpha-N-acetylgalactosaminidase enhances cisplatin resistance in ovarian cancer. *Korean J Physiol Pharmacol.* (2018) 22:43–51. doi: 10.4196/kjpp.2018.22.1.43
148. Kritsch D, Hoffmann F, Steinbach D, Jansen L, Mary Photini S, Gajda M, et al. Tribbles 2 mediates cisplatin sensitivity and DNA damage response in epithelial ovarian cancer. *Int J Cancer.* (2017) 141:1600–14. doi: 10.1002/ijc.30860
149. Tian J, Xu YY, Li L, Hao Q. MiR-490-3p sensitizes ovarian cancer cells to cisplatin by directly targeting ABCC2. *Am J Transl Res.* (2017) 9:1127–38.
150. Mahon PC, Baril P, Bhakta V, Chelala C, Caulee K, Harada T, et al. S100A4 contributes to the suppression of BNIP3 expression, chemoresistance, and inhibition of apoptosis in pancreatic cancer. *Cancer Res.* (2007) 67:6786–95. doi: 10.1158/0008-5472.CAN-07-0440
151. Abukiwan A, Nwaeburu CC, Bauer N, Zhao Z, Liu L, Gladkich J, et al. Dexamethasone-induced inhibition of miR-132 via methylation promotes TGF-beta-driven progression of pancreatic cancer. *Int J Oncol.* (2019) 54:53–64. doi: 10.3892/ijo.2018.4616
152. Liao H, Xiao Y, Hu Y, Xiao Y, Yin Z, Liu L, et al. Methylation-induced silencing of miR-34a enhances chemoresistance by directly upregulating ATG4B-induced autophagy through AMPK/mTOR pathway in prostate cancer. *Oncol Rep.* (2016) 35:64–72. doi: 10.3892/or.2015.4331
153. Bhatnagar N, Li X, Padi SK, Zhang Q, Tang MS, Guo B. Downregulation of miR-205 and miR-31 confers resistance to chemotherapy-induced apoptosis in prostate cancer cells. *Cell Death Dis.* (2010) 1:e105. doi: 10.1038/cddis.2010.85
154. Guo Q, Jing FJ, Xu W, Li X, Li X, Sun JL, et al. Ubenimex induces autophagy inhibition and EMT suppression to overcome cisplatin resistance in GC cells by perturbing the CD13/EMP3/PI3K/AKT/NF-kappaB axis. *Aging.* (2019) 12:80–105. doi: 10.18632/aging.102598
155. El Kadi N, Wang L, Davis A, Korkaya H, Cooke A, Vadnala V, et al. The EGFR T790M mutation is acquired through AICDA-mediated deamination of 5-methylcytosine following TKI treatment in lung cancer. *Cancer Res.* (2018) 78:6728–35. doi: 10.1158/0008-5472.CAN-17-3370
156. Yu J, Qin B, Moyer AM, Nowsheen S, Liu T, Qin S, et al. DNA methyltransferase expression in triple-negative breast cancer predicts sensitivity to decitabine. *J Clin Invest.* (2018) 128:2376–88. doi: 10.1172/JCI97924
157. Zhang N, Wang AY, Wang XK, Sun XM, Xue HZ. GAS5 is downregulated in gastric cancer cells by promoter hypermethylation and regulates adriamycin sensitivity. *Eur Rev Med Pharmacol Sci.* (2016) 20:3199–205.
158. Wu Q, Yang Z, Xia L, Nie Y, Wu K, Shi Y, et al. Methylation of miR-129-5p CpG island modulates multi-drug resistance in gastric cancer by targeting ABC transporters. *Oncotarget.* (2014) 5:11552–63. doi: 10.18632/oncotarget.2594
159. Masuda K, Banno K, Yanokura M, Tsuji K, Kobayashi Y, Kisu I, et al. Association of epigenetic inactivation of the WRN gene with anticancer drug sensitivity in cervical cancer cells. *Oncol Rep.* (2012) 28:1146–52. doi: 10.3892/or.2012.1912
160. Ren K, Xu R, Huang J, Zhao J, Shi W. Knockdown of long non-coding RNA KCNQ1OT1 depressed chemoresistance to paclitaxel in lung adenocarcinoma. *Cancer Chemother Pharmacol.* (2017) 80:243–50. doi: 10.1007/s00280-017-3356-z
161. Zhang Y, Zhang B, Fang J, Cao X. Hypomethylation of DNA-binding inhibitor 4 serves as a potential biomarker in distinguishing acquired tamoxifen-refractory breast cancer. *Int J Clin Exp Pathol.* (2015) 8:9500–5.
162. Chen S, Zhang Y, Zhang D. Endoplasmic reticulum protein 29 (ERp29) confers radioresistance through the DNA repair gene, O(6)-methylguanine DNA-methyltransferase, in breast cancer cells. *Sci Rep.* (2015) 5:14723. doi: 10.1038/srep14723
163. He DX, Gu XT, Jiang L, Jin J, Ma X. A methylation-based regulatory network for microRNA 320a in chemoresistant breast cancer. *Mol Pharmacol.* (2014) 86:536–47. doi: 10.1124/mol.114.092759
164. Hu H, Li S, Cui X, Lv X, Jiao Y, Yu F, et al. The overexpression of hypomethylated miR-663 induces chemotherapy resistance in human breast cancer cells by targeting heparin sulfate proteoglycan 2 (HSPG2). *J Biol Chem.* (2013) 288:10973–85. doi: 10.1074/jbc.M112.434340
165. Chekhun VF, Kulik GI, Yurchenko OV, Tryndyak VP, Todor IN, Luniv LS, et al. Role of DNA hypomethylation in the development of the resistance to doxorubicin in human MCF-7 breast adenocarcinoma cells. *Cancer Lett.* (2006) 231:87–93. doi: 10.1016/j.canlet.2005.01.038
166. Wen S, Wang X, Wang Y, Shen J, Pu J, Liang H, et al. Nucleoside diphosphate kinase 2 confers acquired 5-fluorouracil resistance in colorectal cancer cells. *Artif Cells Nanomed Biotechnol.* (2018) 46:896–905. doi: 10.1080/21691401.2018.1439835
167. Yokoi K, Harada H, Yokota K, Ishii S, Tanaka T, Nishizawa N, et al. Epigenetic status of CDO1 gene may reflect chemosensitivity in colon cancer with postoperative adjuvant chemotherapy. *Ann Surg Oncol.* (2019) 26:406–14. doi: 10.1245/s10434-018-6865-z
168. Zhao XQ, Zhang YF, Xia YF, Zhou ZM, Cao YQ. Promoter demethylation of nuclear factor-erythroid 2-related factor 2 gene in drug-resistant colon cancer cells. *Oncol Lett.* (2015) 10:1287–92. doi: 10.3892/ol.2015.3468
169. Kwon OH, Park JL, Baek SJ, Noh SM, Song KS, Kim SY, et al. Aberrant upregulation of ASCL2 by promoter demethylation promotes the growth and resistance to 5-fluorouracil of gastric cancer cells. *Cancer Sci.* (2013) 104:391–7. doi: 10.1111/cas.12076
170. Xia LL, Tang YB, Song FF, Xu L, Ji P, Wang SJ, et al. DCTPP1 attenuates the sensitivity of human gastric cancer cells to 5-fluorouracil by up-regulating MDR1 expression epigenetically. *Oncotarget.* (2016) 7:68623–37. doi: 10.18632/oncotarget.11864
171. Subhash VV, Tan SH, Tan WL, Yeo MS, Xie C, Wong FY, et al. GTSE1 expression represses apoptotic signaling and confers cisplatin resistance in gastric cancer cells. *BMC Cancer.* (2015) 15:550. doi: 10.1186/s12885-015-1550-0
172. Liu J, Liu Y, Meng L, Liu K, Ji B. Targeting the PD-L1/DNMT1 axis in acquired resistance to sorafenib in human hepatocellular carcinoma. *Oncol Rep.* (2017) 38:899–907. doi: 10.3892/or.2017.5722

173. Tsang WP, Kwok TT. Riboregulator H19 induction of MDR1-associated drug resistance in human hepatocellular carcinoma cells. *Oncogene.* (2007) 26:4877–81. doi: 10.1038/sj.onc.1210266
174. Guijo M, Ceballos-Chavez M, Gomez-Marin E, Basurto-Cayuela L, Reyes JC. Expression of TDRD9 in a subset of lung carcinomas by CpG island hypomethylation protects from DNA damage. *Oncotarget.* (2018) 9:9618–31. doi: 10.18632/oncotarget.22709
175. Pan JX, Qu F, Wang FF, Xu J, Mu LS, Ye LY, et al. Aberrant SERPINE1 DNA methylation is involved in carboplatin induced epithelial-mesenchymal transition in epithelial ovarian cancer. *Arch Gynecol Obstet.* (2017) 296:1145–52. doi: 10.1007/s00404-017-4547-x
176. de Leon M, Cardenas H, Vieth E, Emerson R, Segar M, Liu Y, et al. Transmembrane protein 88 (TMEM88) promoter hypomethylation is associated with platinum resistance in ovarian cancer. *Gynecol Oncol.* (2016) 142:539–47. doi: 10.1016/j.ygyno.2016.06.017
177. Li D, Wu QJ, Bi FF, Chen SL, Zhou YM, Zhao Y, et al. Effect of the BRCA1-SIRT1-EGFR axis on cisplatin sensitivity in ovarian cancer. *Am J Transl Res.* (2016) 8:1601–8.
178. Iramaneerat K, Rattanatunyong P, Khemapech N, Triratanachat S, Mutirangura A. HERV-K hypomethylation in ovarian clear cell carcinoma is associated with a poor prognosis and platinum resistance. *Int J Gynecol Cancer.* (2011) 21:51–7. doi: 10.1097/IGC.0b013e3182021c1a
179. Lee PS, Teaberry VS, Bland AE, Huang Z, Whitaker RS, Baba T, et al. Elevated MAL expression is accompanied by promoter hypomethylation and platinum resistance in epithelial ovarian cancer. *Int J Cancer.* (2010) 126:1378–89. doi: 10.1002/ijc.24797
180. Barros-Silva D, Costa-Pinheiro P, Duarte H, Sousa EJ, Evangelista AF, Graca I, et al. MicroRNA-27a-5p regulation by promoter methylation and MYC signaling in prostate carcinogenesis. *Cell Death Dis.* (2018) 9:167. doi: 10.1038/s41419-017-0241-y
181. Liu T, Xu F, Du X, Lai D, Liu T, Zhao Y, et al. Establishment and characterization of multi-drug resistant, prostate carcinoma-initiating stem-like cells from human prostate cancer cell lines 22RV1. *Mol Cell Biochem.* (2010) 340:265–73. doi: 10.1007/s11010-010-0426-5
182. Luzhna L, Kovalchuk O. Modulation of DNA methylation levels sensitizes doxorubicin-resistant breast adenocarcinoma cells to radiation-induced apoptosis. *Biochem Biophys Res Commun.* (2010) 392:113–7. doi: 10.1016/j.bbrc.2009.12.093
183. Ter Brugge P, Kristel P, van der Burg E, Boon U, de Maaker M, Lips E, et al. Mechanisms of therapy resistance in patient-derived xenograft models of BRCA1-deficient breast cancer. *J Natl Cancer Inst.* (2016) 108:djw148. doi: 10.1093/jnci/djw148
184. Komiya Y, Habas R. Wnt signal transduction pathways. *Organogenesis.* (2008) 4:68–75. doi: 10.4161/org.4.2.5851
185. Nusse R, Clevers H. Wnt/beta-catenin signaling, disease, and emerging therapeutic modalities. *Cell.* (2017) 169:985–99. doi: 10.1016/j.cell.2017.05.016
186. MacDonald BT, Tamai K, He X. Wnt/beta-catenin signaling: components, mechanisms, and diseases. *Dev Cell.* (2009) 17:9–26. doi: 10.1016/j.devcel.2009.06.016
187. Shi J, Chi S, Xue J, Yang J, Li F, Liu X. Emerging role and therapeutic implication of wnt signaling pathways in autoimmune diseases. *J Immunol Res.* (2016) 2016:9392132. doi: 10.1155/2016/9392132
188. Lang CMR, Chan CK, Veltri A, Lien WH. Wnt signaling pathways in keratinocyte carcinomas. *Cancers.* (2019) 11:1216. doi: 10.3390/cancers11091216
189. Zhan T, Rindtorff N, Boutros M. Wnt signaling in cancer. *Oncogene.* (2017) 36:1461–73. doi: 10.1038/onc.2016.304
190. Ying Y, Tao Q. Epigenetic disruption of the WNT/beta-catenin signaling pathway in human cancers. *Epigenetics.* (2009) 4:307–12. doi: 10.4161/epi.4.5.9371
191. Cruciat CM, Niehrs C. Secreted and transmembrane wnt inhibitors and activators. *Cold Spring Harb Perspect Biol.* (2013) 5:a015081. doi: 10.1101/cshperspect.a015081
192. Choi HJ, Park H, Lee HW, Kwon YG. The Wnt pathway and the roles for its antagonists, DKKS, in angiogenesis. *IUBMB Life.* (2012) 64:724–31. doi: 10.1002/iub.1062
193. Ghosh N, Kazi M, Vora H, Gajjar K, Kobawala T. Frequent methylation of genes encoding wnt pathway antagonists: Secreted frizzled-related protein 1 and dickkopf 3 in invasive breast cancer. *Clin Cancer Invest J.* (2019) 8:106–13. doi: 10.4103/ccij.ccij_14_19
194. Tao L, Huang G, Chen Y, Chen L. DNA methylation of DKK3 modulates docetaxel chemoresistance in human nonsmall cell lung cancer cell. *Cancer Biother Radiopharm.* (2015) 30:100–6. doi: 10.1089/cbr.2014.1797
195. Guo Q, Qin W. DKK3 blocked translocation of beta-catenin/EMT induced by hypoxia and improved gemcitabine therapeutic effect in pancreatic cancer Bxpc-3 cell. *J Cell Mol Med.* (2015) 19:2832–41. doi: 10.1111/jcmm.12675
196. Ren J, Wang R, Song H, Huang G, Chen L. Secreted frizzled related protein 1 modulates taxane resistance of human lung adenocarcinoma. *Mol Med.* (2014) 20:164–78. doi: 10.2119/molmed.2013.00149
197. Zhu J, Wang Y, Duan J, Bai H, Wang Z, Wei L, et al. DNA Methylation status of Wnt antagonist SFRP5 can predict the response to the EGFR-tyrosine kinase inhibitor therapy in non-small cell lung cancer. *J Exp Clin Cancer Res.* (2012) 31:80. doi: 10.1186/1756-9966-31-80
198. Liu S, Chen X, Chen R, Wang J, Zhu G, Jiang J, et al. Diagnostic role of Wnt pathway gene promoter methylation in non small cell lung cancer. *Oncotarget.* (2017) 8:36354–67. doi: 10.18632/oncotarget.16754
199. Hu H, Wang T, Pan R, Yang Y, Li B, Zhou C, et al. Hypermethylated promoters of secreted frizzled-related protein genes are associated with colorectal cancer. *Pathol Oncol Res.* (2019) 25:567–75. doi: 10.1007/s12253-018-0505-6
200. Liu X, Fu J, Bi H, Ge A, Xia T, Liu Y, et al. DNA methylation of SFRP1, SFRP2, and WIF1 and prognosis of postoperative colorectal cancer patients. *BMC Cancer.* (2019) 19:1212. doi: 10.1186/s12885-019-6436-0
201. Su HY, Lai HC, Lin YW, Liu CY, Chen CK, Chou YC, et al. Epigenetic silencing of SFRP5 is related to malignant phenotype and chemoresistance of ovarian cancer through Wnt signaling pathway. *Int J Cancer.* (2010) 127:555–67. doi: 10.1002/ijc.25083
202. Ramachandran K, Speer C, Nathanson L, Claros M, Singal R. Role of DNA methylation in cabazitaxel resistance in prostate cancer. *Anticancer Res.* (2016) 36:161–8.
203. Hiltunen MO, Alhonen L, Koistinaho J, Myohanen S, Paakkonen M, Marin S, et al. Hypermethylation of the APC (*Adenomatous polyposis coli*) gene promoter region in human colorectal carcinoma. *Int J Cancer.* (1997) 70:644–8. doi: 10.1002/(SICI)1097-0215(19970317)70:6<644::AID-IJC3>3.0.CO;2-V
204. Aoki K, Taketo MM. Adenomatous polyposis coli (APC): a multi-functional tumor suppressor gene. *J Cell Sci.* (2007) 120:3327–35. doi: 10.1242/jcs.03485
205. Matuschek C, Bolke E, Lammering G, Gerber PA, Peiper M, Budach W, et al. Methylated APC and GSTP1 genes in serum DNA correlate with the presence of circulating blood tumor cells and are associated with a more aggressive and advanced breast cancer disease. *Eur J Med Res.* (2010) 15:277–86. doi: 10.1186/2047-783X-15-7-277
206. Stefanski CD, Keffler K, McClintock S, Milac L, Prosperi JR. APC loss affects DNA damage repair causing doxorubicin resistance in breast cancer cells. *Neoplasia.* (2019) 21:1143–50. doi: 10.1016/j.neo.2019.09.002
207. Fruman DA, Chiu H, Hopkins BD, Bagrodia S, Cantley LC, Abraham RT. The PI3K pathway in human disease. *Cell.* (2017) 170:605–35. doi: 10.1016/j.cell.2017.07.029
208. Tancredi R, Furlanetto J, Loibl S. Endocrine therapy in premenopausal hormone receptor positive/human epidermal growth receptor 2 negative metastatic breast cancer: between guidelines and literature. *Oncologist.* (2018) 23:974–81. doi: 10.1634/theoncologist.2018-0077
209. Phuong NT, Kim SK, Lim SC, Kim HS, Kim TH, Lee KY, et al. Role of PTEN promoter methylation in tamoxifen-resistant breast cancer cells. *Breast Cancer Res Treat.* (2011) 130:73–83. doi: 10.1007/s10549-010-1304-2
210. Ye L, Lin C, Wang X, Li Q, Li Y, Wang M, et al. Epigenetic silencing of SALL2 confers tamoxifen resistance in breast cancer. *EMBO Mol Med.* (2019) 11:e10638. doi: 10.15252/emmm.201910638
211. Spangle JM, Dreijerink KM, Groner AC, Cheng H, Ohlson CE, Reyes J, et al. PI3K/AKT signaling regulates H3K4 methylation in breast cancer. *Cell Rep.* (2016) 15:2692–704. doi: 10.1016/j.celrep.2016.05.046
212. Maeda M, Murakami Y, Watari K, Kuwano M, Izumi H, Ono M. CpG hypermethylation contributes to decreased expression of PTEN during

acquired resistance to gefitinib in human lung cancer cell lines. *Lung Cancer.* (2015) 87:265–71. doi: 10.1016/j.lungcan.2015.01.009

213. Cortes-Sempere M, de Miguel MP, Pernia O, Rodriguez C, de Castro Carpeno J, Nistal M, et al. IGFBP-3 methylation-derived deficiency mediates the resistance to cisplatin through the activation of the IGFIR/Akt pathway in non-small cell lung cancer. *Oncogene.* (2013) 32:1274–83. doi: 10.1038/onc.2012.146
214. Jung IL, Kang HJ, Kim KC, Kim IG. PTEN/pAkt/p53 signaling pathway correlates with the radioresponse of non-small cell lung cancer. *Int J Mol Med.* (2010) 25:517–23. doi: 10.3892/ijmm_00000372
215. Pappas G, Zumstein LA, Munshi A, Hobbs M, Meyn RE. Adenoviral-mediated PTEN expression radiosensitizes non-small cell lung cancer cells by suppressing DNA repair capacity. *Cancer Gene Ther.* (2007) 14:543–9. doi: 10.1038/sj.cgt.7701050
216. Geybels MS, Fang M, Wright JL, Qu X, Bibikova M, Klotzle B, et al. PTEN loss is associated with prostate cancer recurrence and alterations in tumor DNA methylation profiles. *Oncotarget.* (2017) 8:84338–48. doi: 10.18632/oncotarget.20940
217. Qian XJ, Li YT, Yu Y, Yang F, Deng R, Ji J, et al. Inhibition of DNA methyltransferase as a novel therapeutic strategy to overcome acquired resistance to dual PI3K/mTOR inhibitors. *Oncotarget.* (2015) 6:5134–46. doi: 10.18632/oncotarget.3016
218. Vojta A, Dobrinic P, Tadic V, Bockor L, Korac P, Julg B, et al. Repurposing the CRISPR-Cas9 system for targeted DNA methylation. *Nucleic Acids Res.* (2016) 44:5615–28. doi: 10.1093/nar/gkw159
219. Liu XS, Wu H, Ji X, Stelzer Y, Wu X, Czauderna S, et al. Editing DNA methylation in the mammalian genome. *Cell.* (2016) 167:233–47.e17. doi: 10.1016/j.cell.2016.08.056

Conflict of Interest: The authors declare that the research was conducted in the absence of any commercial or financial relationships that could be construed as a potential conflict of interest.

frontiers in Oncology

ORIGINAL RESEARCH
published: 16 September 2020
doi: 10.3389/fonc.2020.535449

KDM5c Promotes Colon Cancer Cell Proliferation Through the FBXW7-c-Jun Regulatory Axis

Haishan Lin[1†], Nina Ma[1†], Lei Zhao[1], Guowei Yang[2] and Bangwei Cao[1]*

[1] Cancer Center, Beijing Friendship Hospital, Capital Medical University, Beijing, China, [2] Department of Tropical Medicine, Beijing Friendship Hospital, Capital Medical University, Beijing, China

KDM5c is a histone demethylase that specifically demethylates trimethylated and dimethylated H3 Lys-4 to play a central role in transcriptional repression. C-Jun is a proto-oncogene and promotes cell proliferation when ectopically accumulated, but can be ubiquitinated by SCF (FBXW7), leading to its degradation. FBXW7 is an E3 ubiquitin ligase of c-Jun, and exhibits carcinostasis in colon cancer. Here, we report that overexpression of KDM5c in human colon cancer cells results in attenuated *FBXW7* transcription and accumulated c-Jun protein, leading to increased proliferation of colon cancer cells. We show that overexpression of KDM5c can result in increased c-Jun protein levels and decreased ubiquitin levels, with no significant change in mRNA levels of *c-Jun*. KDM5c overexpression blocks the ubiquitin-proteasome proteolytic pathway of c-Jun by down-regulating the expression of *FBXW7*. KDM5c down-regulation of *FBXW7* occurs by demethylation of H3K4me3 at TSS and downstream of the *FBXW7* gene. And interaction of KDM5c with H3K4me3 downstream of *FBXW7* gene may be followed by recruitment of DNMT3b to methylate the spatially close CpG island located near the *FBXW7* TSS. This methylation represses *FBXW7* gene expression, which can reduce c-Jun degradation via the ubiquitin-proteasome pathway. TCGA database analysis revealed high expression of KDM5c in colon cancer tissues. KDM5c expression in colon cancer was correlated with poor overall survival of patients in the first 7 years. Data from TCGA showed that high expression of KDM5c was correlated with high DNA methylation of the *FBXW7* gene, but was not positively correlated with methylation of the Jun gene. These results suggest that KDM5c regulation of colon cell proliferation is mainly mediated by the KDM5c-FBXW7-c-Jun axis.

Keywords: KDM5c, c-Jun oncogene, colon cancer cell, FBXW7, epigenetic modifier

OPEN ACCESS

Edited by:
Lei Chang,
Soochow University Medical College (SUMC), China

Reviewed by:
Jing Zhao,
The Ohio State University, United States
Rob Scott Illingworth,
University of Edinburgh, United Kingdom

***Correspondence:**
Bangwei Cao
oncology@ccmu.edu.cn

[†] These authors have contributed equally to this work

Specialty section:
This article was submitted to Molecular and Cellular Oncology, a section of the journal Frontiers in Oncology

Received: *16 February 2020*
Accepted: *18 August 2020*
Published: *16 September 2020*

Citation:
Lin H, Ma N, Zhao L, Yang G and Cao B (2020) KDM5c Promotes Colon Cancer Cell Proliferation Through the FBXW7-c-Jun Regulatory Axis. Front. Oncol. 10:535449. doi: 10.3389/fonc.2020.535449

INTRODUCTION

Colorectal cancer (CRC) is the third most prevalent malignancy and ranks second in mortality among solid tumors, representing a serious public health problem worldwide (1). Driver gene mutations account for a large proportion of colon malignant tumors cases, but mutated driver genes have not been identified for some colon cancer cases, suggesting that epigenetic changes act as an important supplement to genetic changes to cause tumors. During tumor development, abnormal epigenetic regulation can aggravate tumor proliferation and metastasis (2–4). Here, we applied an epigenetic perspective to investigate new potential therapeutic targets for colorectal cancer.

Recent evidence has indicated that epigenetic mutations are strongly involved in cancer initiation and progression (5). These mutations have been detected widely across the genome,

and are considered a more important contributor to tumor heterogeneity. Many epigenetic modifications play critical role in CRC including DNA methylation, histone modification, chromatin remodeling, microsatellite instability, and non-coding RNAs (6, 7). Thus, epigenetic mutations are promising targets for not only epidemiological and physiopathological studies, but also therapeutic response evaluation and drug design (8).

A member of the SMCY homolog family, KDM5c (also known as JARID1C) is an H3K4me2/3 demethylase that plays a central role in transcriptional repression (9). KDM5c was initially found to be important for brain development and function, and mutations of KDM5c can lead to X-linked mental retardation (10). KDM5c abnormality was subsequently correlated with development of various cancers. For example, KDM5c was significantly upregulated in breast cancer tissues compared with paired normal breast tissues, and was positively correlated with metastasis (11); loss of KDM5c results in the activation of a set of enhancers in human breast cancer cells (12); KDM5c acts in proliferation and invasion of gastric cancer cells, which may be partly associated with p53 expression (13); and KDM5 demethylase suppresses STING-induced innate immune response in tumor cells (14, 15). Despite these associations with various cancers types, the function of KDM5c in CRC progression has not been reported.

C-Jun is a proto-oncogene that accelerates cell proliferation (16). It is required for cell cycle progression through the G1 phase, and increased G1 arrest is detected in *c-Jun* null cells (17). The c-Jun protein is ubiquitinated by FBXW7 (F-box/WD repeat-containing protein 7), which belongs to the F-box protein family and functions as a receptor subunit for SCF (Skp1/Cullin/F-box protein) E3 ubiquitin ligases (18, 19). FBXW7 acts as an important tumor suppressor, and mutations in the *FBXW7* gene have been found in ovarian, lymphoma, and colorectal cancers (20, 21). However, whether FBXW7-mediated degradation of c-Jun is under strict control remains unknown.

In this study, we investigated the function and mechanism of KDM5c in colon cancer cell proliferation by disrupting KDM5c expression. Our results showed that KDM5c accelerated proliferation of colon cancer cells by down-regulating *FBXW7* transcription, thereby, reducing c-Jun degradation via the ubiquitin-proteasome pathway. We also observed regulation by KDM5c on *FBXW7* that may be mediated by binding of KDM5c to TSS and downstream of the *FBXW7* gene. We identified a DNA methylation site upstream of the *FBXW7* gene. And the interaction site of KDM5c and H3K4me3 in downstream of *FBXW7* gene may be spatially adjacent and interlinked by DNMT3/DNMT3L. Our study reveals novel roles of KDM5c in regulating colon cancer cell proliferation and suggests KDM5c as an attractive target for CRC treatment.

MATERIALS AND METHODS

Cell Culture

The human colon cancer cell lines RKO and HCT-8, containing the wild-type *FBXW7* gene, were cultured in Dulbecco's Modified Eagle Medium (DMEM) supplemented with 10% FBS, 1% penicillin-streptomycin, MEM vitamins (Media Tech), and MEM non-essential amino acids (Media Tech). Cells were grown on tissue culture-treated plates (Laboratory Product Sale) in a 37°C humidified incubator and an air atmosphere with 5% CO2. All cell lines were purchased from ATCC and routinely tested and authenticated via by assessing the cell morphology, proliferation rate, a panel of genetic markers, and checking for contamination. Cells were also tested for mycoplasma using the MycoAlert Detection Kit (Cambrex). Human interleukin 4 (IL4) and neutralizing IL4 antibody were purchased from Cell Signaling.

Transient Transfection

RKO and HCT-8 cells were transiently transfected with 30 nM KDM5c or a scrambled control siRNA using Lipofectamine 3000 (Thermo Fisher Scientific) following the manufacturer's protocol. For plasmid transfection, 3 μg plasmid was transfected using MSCV-dGFP-JARID1C (Promega) or MSCV-null (Mirus Bio). The cells were used for experiments 48 h after transfection, or as otherwise indicated.

Cell Proliferation Assay

RKO and HCT-8 cells were seeded in 96-well plates at a density of 2000 cells/well and allowed to attach for 8 h, and 0.5 mg/mL MTT (Sigma-Aldrich) was then added before another incubation of 4 h at 37°C. The violet MTT formazan precipitates were subsequently dissolved in 100 μL DMSO. Absorbance was measured at 570 and 670 nm and adjusted for background using a UQuant reader. The MTT assay was repeated at the same time on four consecutive days. For each group, five replicates and three independent experiments were performed.

Colony Formation Assay

For the colony formation assay, 1000 RKO or HCT-8 cells were seeded in 6-well plates and incubated overnight. The cells were then transfected with siRNA or mimic plasmid for 24 h. The medium was replaced with fresh medium every 3 days. When visible colonies formed, they were fixed with 4% paraformaldehyde and stained with 0.1% crystal violet. The numbers of colonies were counted using a Syngene G:BOX imaging system.

Flow Cytometry

Cell cycle progression was analyzed 48 h after transfection using propidium iodide (PI) as a stain to label the DNA content. The isolated cell pellet was washed twice with PBS supplemented with 1% FBS and resuspended in 70% cold ethanol for overnight fixation. The samples were then centrifuged for 10 min at 500 rcf at 4°C, and resuspended in cold PBS. Finally, the samples were centrifuged for 5 min at 300 rcf and 4°C, and then resuspended in DNA staining solution [0.1% Triton X-100 (Sigma Aldrich), 2% propidium iodide (Sigma Aldrich) in PBS]. Samples were then incubated for 30 min at room temperature, and flow cytometric analysis was performed on a BD FACSCalibur device (BD Biosciences). Flow cytometry was also used to confirm cell models were successfully established, with more than 90% of cells synchronized at each stage.

Immunofluorescence

Immunofluorescence was performed following the standard procedure. Briefly, RKO and HCT-8 cells were seeded on a 6-well plate 48 h after transfection. The cells were then fixed with 4% paraformaldehyde and permeabilized with 0.25% Triton X-100, blocked with 1% BSA in PBST, and probed with primary antibodies against c-Jun (Abcam). Alexa Fluor 488 tagged secondary antibody (Cell Signaling) was used for detection, and the nuclei were stained with DAPI (Sigma) and imaged by a Leica SP8 confocal microscope.

Chromatin Immunoprecipitation-Quantitative PCR (ChIP-qPCR)

Chromatin immunoprecipitation was performed to analyze the enrichment of select regions and confirm H3K4me3 binding at regions of interest using a True MicroChIP Kit (Diagenode) according to the manufacturer's protocol. A total of 1×10^6 cells were collected and crosslinked with 1% formaldehyde. Cells were disrupted by ultrasonication to fragment the DNA into 200–500 bp pieces. Specific antibodies to the protein of interest [anti-KDM5c (Abcam) and anti-H3K4me3 (Diagenode)] were added to bind target protein-DNA complexes, and incubated overnight. Protein A agarose was added to bind the antibody-target protein-DNA complexes, washed to remove non-specific binding, and then the enriched target protein-DNA complexes were eluted from the beads and the crosslinks were reversed. After purification, enriched DNA-fragments were subjected to qPCR analysis using fluorescence quantitative PCR. Goat IgG was used as the negative control. The fold change in the amount of the DNA fragment enriched by a specific antibody versus the total input was calculated by the following formula: % recovery = 100*2^[(Ct(input)-log%(x%)/log2)-Ct(sample)]. The primers used in the ChIP-PCR assays are listed in the **Table 1**.

TABLE 1 | The primers used in the ChIP-PCR assays.

Location	Primers
1# FBXW7 TSS (chromosome 4 152318937) F	5′-AGGTCCCAACAAGCATCAGA-3′
1# FBXW7 TSS (chromosome 4 152318937) R	5′-CCAGCTTTGTGTTTGAGGCT-3′
2# FBXW7 TSS (chromosome 4 152319177) F	5′-GGTGCTGGACTTTGATGTGG-3′
2# FBXW7 TSS (chromosome 4 152319177) R	5′-AACATCCTGCACCACTGAGA-3′
3# FBXW7 TSS (chromosome 4 152319971) F	5′-ACTCCCAGTGGCCAAACTTA-3′
3# FBXW7 TSS (chromosome 4 152319971) R	5′-GGCTCAAGTTTCAGTGGCAA-3′
4# FBXW7 TSS (chromosome 4 152320116) F	5′-TTGCCACTGAAACTTGAGCC-3′
4# FBXW7 TSS (chromosome 4 152320116) R	5′-TCTCCACAGAACAGGCAAGT-3′
5# FBXW7 (chromosome 4 152534873) F	5′-ACGTTTGTACTCAAGCCGCA-3′
5# FBXW7 (chromosome 4 152534873) F	5′-TTGGATAACGTGTGGTCGGG-3′
6# FBXW7 (chromosome 4 152535061) F	5′-GACCACACGTTATCCAACGC-3′
6# FBXW7 (chromosome 4 152535061) R	5′-CATTTGGCCCCAAACAGACC-3′
7# FBXW7 (chromosome 4 152535162) F	5′-GATCAGTCCGGCTTTTCGAG-3′
7# FBXW7 (chromosome 4 152535162) R	5′-GATCTTACCCCTGACCCGAG-3′
8# FBXW7 (chromosome 4 152539858) F	5′-CCACCATTCCCCTGTTGTAAGA-3′
8# FBXW7 (chromosome 4 152539858) R	5′-GACCTGAAGTTCCAAGAGCCA-3′
9# FBXW7 (chromosome 4 152540657) F	5′-TCTCGAAAGCTCCAAACCGT-3′
9# FBXW7 (chromosome 4 152540657) R	5′-TCCTCGCGCAGATTGTTAGG-3′
1# c-Jun TSS (chromosome 1 58778991) F	5′-GCAATGAACCCAAGGCTGAA-3′
1# c-Jun TSS (chromosome 1 58778991) R	5′-TCCTGTGAGAAGCATCGAGG-3′
2# c-Jun TSS (chromosome 1 58779638) F	5′-GCGTGACTTTATGCGAGTGT-3′
2# c-Jun TSS (chromosome 1 58779638) R	5′-CCGGTGTTAGTCTACTCCCC-3′
3# c-Jun TSS (chromosome 1 58780100) F	5′-GGAGACCGCCCCTAAACTTA-3′
3# c-Jun TSS (chromosome 1 58780100) R	5′-GAGGGGTGGTTGTTGTTTCC-3′
4# c-Jun (chromosome 1 58784487) F	5′-AACCTCAGCTCTGGGGAAATG-3′
4# c-Jun (chromosome 1 58784487) R	5′-CTGCTAATGAGCAAACAGCCC-3′
5# c-Jun (chromosome 1 58784705) F	5′-GTACCCAGTAGGTCTGGGAGT-3′
5# c-Jun (chromosome 1 58784705) R	5′-CCTTCCGGGTTGCTGACATC-3′
6# c-Jun (chromosome 1 58785088) F	5′-CACCACTCCCCAGTTTGCTT-3′
6# c-Jun (chromosome 1 58785088) R	5′-ACGATGTGTCACCAGCTTCAT-3′
7# c-Jun (chromosome 1 58785389) F	5′-AGCTGGTGACACATCGTCAT-3′
7# c-Jun (chromosome 1 58785389) R	5′-GAACTCTGGGAGGGTCGAAT-3′

Chromosome Conformation Capture (3C) Assay

A total of 1×10^6 cells were collected and crosslinked with 1% formaldehyde. After stopping the crosslinking via glycine, the cells were lysed using lysis buffer and centrifuged to remove cellular debris. The chromatin was then diluted 3-fold using a ChIP dilution buffer containing a protease inhibitor cocktail (Sigma-Aldrich) and digested overnight at 37°C with restriction enzymes including *Eco*NI, *Sna*BI, *Sal*I, and *Not*I (New England Biolabs). The digested chromatin was further diluted 6-fold into a T4 ligation buffer before ligation was performed for 4 h at room temperature using T4 DNA ligase and 0.5 mM ATP. DNA was purified with the QIAquick PCR Purification Kit (Qiagen) followed by CHIP-qPCR. For CHIP assay, anti-DNMT3 (Abcam) was used to bind target protein-DNA complexes. The primers used in the 3C-ChIP-PCR assays are listed in the **Table 2**.

Co-immunoprecipitation IP/Re-IP

Cells from a 10-cm plate were resuspended in lysis buffer supplemented with a protein inhibitor (PI). The lysate was then centrifuged to collect the supernatant, which was further incubated with primary antibodies (e.g., anti-c-Jun) via shaking at 4°C for 24 h. Then, a 50% slurry of Protein A/G Agarose Resin was added and incubated for two more hours. The resin was washed at least four times using a wash buffer with PI. Finally, the binding proteins were eluted using an SDS loading buffer. Re-IP was performed to re-enrich the antigen-antibody complex eluent

TABLE 2 | The primers used in the 3C-ChIP-PCR assays.

Location	Primers
P1 FBXW7 (chromosome 4 152534873) F	5′-ACGTTTGTACTCAAGCCGCA-3′
P1 FBXW7 (chromosome 4 152534873) R	5′-TTGGATAACGTGTGGTCGGG-3′
P2 FBXW7 (chromosome 4 152535162) F	5′-GATCAGTCCGGCTTTTCGAG-3′
P2 FBXW7 (chromosome 4 152535162) R	5′-GATCTTACCCCTGACCCGAG-3′
P3 FBXW7 (chromosome 4 152325958) F	5′-AGGAAACCGCTACAGACCAA-3′
P3 FBXW7 (chromosome 4 152325958) R	5′-GGGAAGAGGAAGTGGGGATC-3′
P4 FBXW7 (chromosome 4 152325311) F	5′-CCAAGACCAGAAGCTCTCGA-3′
P4 FBXW7 (chromosome 4 152325311) R	5′-CTCGCGCAGATTGTTAGGG-3′

TABLE 3 | BSP primers for DNA methylation.

Location	DNA methylation Primers
FBXW7 (chromosome 4 152325440) F	5′-AAAAATTTTTTAGTAATTTTTTAGAGG-3′
FBXW7 (chromosome 4 152325440) R	5′-TTAAATACAAAATCACAACCTAAATC-3′
FBXW7 (chromosome 4 152325675) F	5′-GTTTGTATTTTTATTATATTTTTTGAGTT-3′
FBXW7 (chromosome 4 152325675) R	5′-CCCTACAACCTAATCTACACCTACT-3′
FBXW7 (chromosome 4 152325974) F	5′-AGGAGTAGTTTTTATTTGTTTYGAAG-3′
FBXW7 (chromosome 4 152325974) R	5′-TCTATACRAAACTCTCRCCTCACTC-3′
c-Jun (chromosome 1 58779165) F	5′-GGAAAGTATATTTGGTTTTGTTAAA-3′
c-Jun (chromosome 1 58779165) R	5′-TTCATTTCCCTCATCTACAAAT-3′
c-Jun (chromosome 1 58779351) F	5′-TTTGTAGATGAGGGAAATGAAG-3′
c-Jun (chromosome 1 58779351) R	5′-TAAACTTCAAATCTCTACACTCCC-3′
c-Jun (chromosome 1 58779589) F	5′-AGTGTAGAGATTTGAAGTTTAGGTT-3′
c-Jun (chromosome 1 58779589) R	5′-TAACAAAATCCAAATAAAAACAA-3′
c-Jun (chromosome 1 58779949) F	5′-GGTGTAAYGGAGATTTAGTTGA-3′
c-Jun (chromosome 1 58779949) R	5′-TTTCCCCACTTATAAAACCC-3′
c-Jun (chromosome 1 58780320) F	5′-AAAATAATTGGTTAGGTTTTTTGG-3′
c-Jun (chromosome 1 58780320) R	5′-ATAACCCATAATATCACCCCAA-3′

obtained from IP using antibodies (e.g., anti-c-Jun) and Protein A/G Agarose Resin to reduce interference from non-chemical bond aggregation.

Assessment of DNA Methylation

Genomic DNA was extracted using a TIANamp Genomic DNA Kit (Tiangen) and treated with sodium bisulfate using an EZ DNA Methylation Kit (Zymo Research) according to the manufacturers' protocols. Three separate bisulfite (BSP) modification treatments were performed for each DNA sample. BSP primers (**Table 3**) were designed using the online MethPrimer software and 50 ng of genomic DNA was used for PCR amplification using Zymo Taq Premix (Zymo Research). A standard amplification program was used with annealing for 40 s at 50.4°C and extension for 30 s at 72°C (38 cycles). The PCR products were then sub-cloned into the pMD19-T vector (Takara) and different positive clones for each sample were randomly selected for sequencing (Sangon). Finally, the sequences were analyzed using online QUMA software.

TABLE 4 | Primers used for the RT-qPCR.

Location	DNA methylation Primers
GAPDH-CDS-F	5′-GGAGCGAGATCCCTCCAAAAT-3′
GAPDH-CDS-R	5′-GGCTGTTGTCATACTTCTCATGG-3′
C-JUNF-CDS-F	5′-TCCAAGTGCCGAAAAAGGAAG-3′
C-JUNR-CDS-R	5′-CGAGTTCTGAGCTTTCAAGGT-3′
FBWX7-CDS-F	5′-GGCCAAAATGATTCCCAGCAA-3′
FBWX7-CDS-R	5′-ACTGGAGTTCGTGACACTGTTA-3′
KDM5c-CDS-F	5′-GGGTCCGACGATTTCCTACC-3′
KDM5c-CDS-R	5′-ATGCCCGATTTCTCTGCGATG-3′
Cyclin D1-CDS-F	5′-GCTGCGAAGTGGAAACCATC-3′
Cyclin D1-CDS-R	5′-CCTCCTTCTGCACACATTTGAA-3′

Western Blot Analysis

Anti-KDM5c (1:1,000), anti-c-Jun (1:1,000), anti-FBXW7 (1:1,000), anti-Cyclin D1 (1:1,000), anti-H3K4me3 (1:1,000), anti-H3 (1:1000), and anti-β-actin (1:4,000) were used for Western blot analysis according to standard procedures.

Quantitative PCR (qPCR)

Total RNA was extracted using a Qiagen RNeasy Mini Kit (Qiagen) according to the manufacturer's protocol. A total amount of 2 μg RNA was used for reverse transcription using Superscript II (Invitrogen). Quantitative PCR (qPCR) was performed in triplicate on an ABI Prism 7500 real-time PCR system (Applied Biosystems) using SYBR Green Premix (Takara). GAPDH was used as the internal control. The relative expression of genes was calculated by the 2-($\Delta\Delta$Ct) method. Primers used for the RT-qPCR assays were designed using PrimerBank (**Table 4**).

Bioinformatics Analysis of the Association Between the KDM5c Expression and FBXW7/c-Jun Methylation Levels in Colon Cancer Patients

The gene expression data and DNA methylation data (BeadChip platform) from 464 samples were downloaded from TCGA website[1]. From these data, we extracted beta-values to evaluate the DNA methylation level of each probe. The annotations of probes to specific genes (e.g., KDM5c and c-Jun) were defined as probes located at the promoter region of genes. We used the "champ.DMP" function in the "ChAMP" package in R to identify differentially methylated probes. We defined probes with adjusted p-value ≤ 0.05 as differentially methylated probes. For the gene expression data, the KDM5C high expression group was defined as expression higher than 1.25 times the median expression and the low expression group was defined as expression lower than 0.75 times the median expression of KDM5c.

[1]https://portal.gdc.cancer.gov/

Bioinformatics Analysis of the Association Between KDM5c Gene Expression and Overall Survival in Patients With Colon Cancer

The association between the identified KDM5c gene expression and overall survival (OS) for colon cancer patients was assessed using data from TCGA. Kaplan-Meier plots were constructed to illustrate the relationship between gene expression levels of KDM5c and patient overall survival. The relationship was tested by log-rank test.

Statistical Analyses

Statistical analyses were performed using GraphPad Prism software (version 5.0). One-way ANOVA followed by Newman–Keuls *post hoc* analysis was used to determine differences between KDM5c-OE, empty vector, KDM5c-KD, and siControl. Tumor data were analyzed using a Student's *t*-test for comparison of two groups (KDM5c-OE and empty vector or KDM5c-KD and siControl). Any statistical data that did not pass the equal-variance test (Bartlett's test for equal variances) were logarithmically transformed and reanalyzed. The data presented are the mean ± standard error. The overall survival (OS) rates were analyzed via Kaplan-Meier survival analysis with the log-rank test. All data analyses and statistical correlations of TCGA datasets were performed using R software. A value of $p < 0.05$ is considered statistically significant.

RESULTS

KDM5c Is Required for Cell Proliferation and Cell Cycle Regulation in Colon Cancer Cells

Previous work has correlated KDM5c to various cancers, but whether KDM5c plays a role in colon cancer progression remains unknown. To answer this question, we first investigated if cell proliferation can be affected by altering expression of KDM5c. To do this, we increased the amount of KDM5c by transfected KDM5c plasmid and used western blot to confirm increased KDM5c protein level in both RKO and HCT-8 cells compared to the wild-type cells, but decreased H3K4me3 protein level, consistent with the demethylase function of KDM5c. Conversely, knockdown (KD) of KDM5c using short siRNAs in RKO/HCT-8 cells (with high endogenous KDM5c levels) reduced KDM5c protein level and increased H3K4me3 protein level (**Figures 1A,B**), which indicates the successful disruption of KDM5c expression in RKO/HCT-8 cells. Next, MTT assay using these cell lines showed that KDM5c overexpression (OE) significantly promoted HCT-8/RKO cell growth (**Figures 1C,E**). Consistent with this, KDM5c-KD obviously inhibited cell proliferation compared to the siControl group (**Figures 1D,F**), suggesting that KDM5c has an important role in colon cancer cell proliferation, which has not been previously reported. In addition, we performed a 2-D colony formation assay in KDM5c-OE HCT-8/RKO cells or KDM5c-KD HCT-8/RKO cells. The overexpression of KDM5c increased colony formation of HCT-8/RKO cells, whereas KDM5c-KD reduced colony formation in HCT-8/RKO cells (**Figures 1K,L**). These results were statistically significant (**Figures 1M,N**). To determine if KDM5C regulates the cell cycle, we next performed flow cytometry after cell cycle synchronization. The results showed that more than 90% of the cells were synchronized at each stage, indicating that the cell model was successfully established. In order to directly distinguish the M phase cells, flow cytometry assays were carried out with Propidium Iodide (PI) staining. For KDM5c-OE RKO/HCT-8 cells, there were more cells in G2/M phase and fewer cells in G1 phase and for KDM5c-KD RKO/HCT-8 cells, there were fewer G2/M phase cells and more G1 phase cells (**Figures 1G–J**), suggesting KDM5c is involved in cell cycle regulation. Together, these results indicate KDM5c is an important determinant of colon cancer cell proliferation and cell cycle.

KDM5c Promotes c-Jun Protein Accumulation but Downregulates *FBXW7* Expression

To investigate the mechanism underlying KDM5c regulation of RKO/HCT-8 cell growth, we used quantitative PCR (qPCR) and Western blot methods to examine changes of multiple cancer-related genes at the transcription and protein level when KDM5c expression was altered. Levels of c-Jun, FBXW7, and Cyclin D1 were measured with different amounts of KDM5c expression. When KDM5c was overexpressed, FBXW7 expression was significantly decreased compared to the level in the control group ($P < 0.05$), while in the KDM5c-KD group the FBXW7 mRNA level was much higher than that of the control group (**Figure 2C**). As shown by Western blot and qPCR results, the FBXW7 protein and RNA levels changed similarly in the different groups tested, indicating that KDM5c downregulates FBXW7 expression. However, there was no difference in the mRNA expression of c-Jun between the two groups (**Figure 2A**), but the protein level was much higher in KDM5c-OE and lower in the KDM5c-KD group relative to the level in the control. Furthermore, the downstream target of c-Jun, cyclin D1, exhibited the same changes in both mRNA and protein levels as c-Jun and KDM5c (**Figures 2A–F**). We tested the effects of expression of KDM5c fused to green fluorescence protein (GFP). The immunostaining results also showed increased c-Jun (red) levels in HCT-8 cells overexpressing the GFP-KDM5c fusion protein, with more than 40% of GFP-positive cells showing higher signal for c-Jun (**Figure 2I**). In contrast, c-Jun levels were quite stable in cells transfected with control vectors. These data indicate KDM5c promotes c-Jun protein accumulation but downregulates FBXW7 expression.

Co-localization of KDM5c and H3K4me3 in FBXW7

We next asked if KDM5c acts by binding directly to the *FXBW7* or *c-Jun* gene regions to regulate their expression. H3K4 trimethylation (H3K4me3) is a well-known epigenetic modification that promotes mRNA expression, and typically localizes close to the transcription start site (TSS) and up to

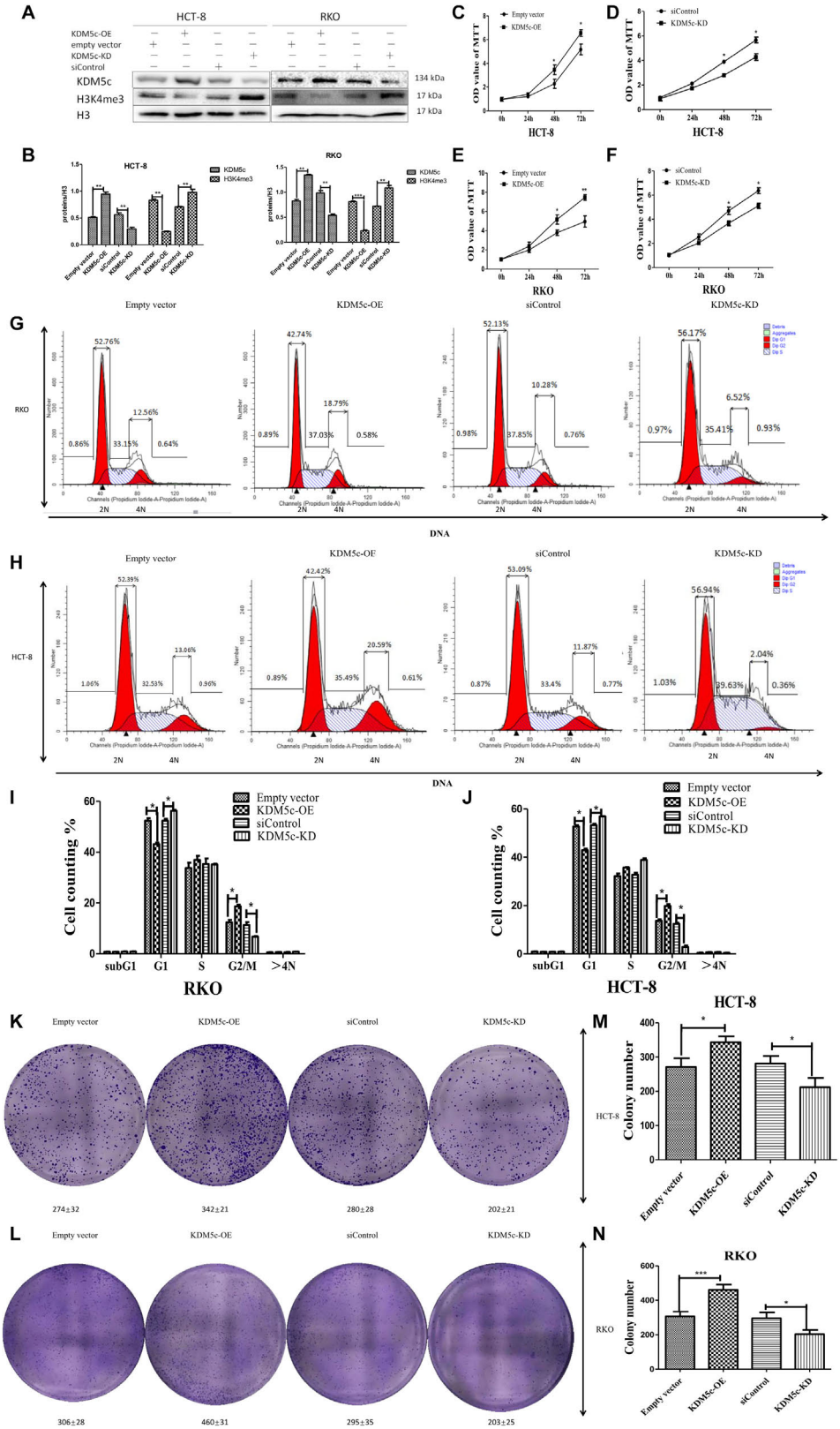

FIGURE 1 | Continued

FIGURE 1 | Effects of KDM5c overexpression and knock-down on H3K4me3 levels and colon cancer cell growth. **(A,B)** Representative Western blots **(A)** and quantification **(B)** showing the changes of the H3K4me3 levels in HCT-8 and RKO transfected with the empty vector, KDM5c-OE, siControl, and siKDM5c. H3 was detected as the loading control. **(C–F)** MTT assays to analyze the cell proliferation rates of HCT-8 and RKO 72 h after transfection with the empty vector, KDM5c-OE **(C,E)**, siControl, and siKDM5c **(D,F)**. **(G,H)** Representative flow plots of RKO (upper row) and HCT-8 (lower row) cells transfected with the empty vector, KDM5c-SMCV, siControl, and siKDM5c. Propidium iodide staining and flow cytometric analysis were performed to determine the fractions of G1 and G2/M cells. **(I,J)** The fraction of G2/M phase cells was increased in KDM5c-OE RKO (left) and HCT-8 (right) cells, while the fraction of G1 was decreased in siKDM5c RKO (left) and HCT-8 (right) cells. **(K,L)** Results of 2D colony formation assay showing differences in colony formation in HCT-8 **(K)** and RKO **(L)** cells transfected with the empty vector, KDM5c-OE, siControl, and siKDM5c. **(M,N)** The KDM5c-OE group showed increased colony formation as compared to the empty vector, but siKDM5c decreased colony formation as compared to siControl in HCT-8 **(M)** and RKO **(N)** cells. Each error bar represents the standard error of the mean (SEM). Statistical analysis was performed and *p*-values were calculated. This experiment was repeated three times with similar results. * Above the bars indicates significant difference; $^{*}P \leq 0.05$; $^{**}P \leq 0.01$; $^{***}P \leq 0.001$.

5 kb downstream on actively transcribed genes (ENCODE Project Consortium 2007). To do this, we performed ChIP-PCR in RKO cells overexpressing KDM5c to investigate KDM5c association with *FXBW7* and *c-Jun* genes and determine the potential correlation of KDM5c with H3K4me3 signals and transcriptional regulation. We probed the TSS and the surrounding sequence, up to 5 kb downstream (**Figures 3A,B**). The primers used for ChIP-qPCR assays were selected based on the H3K4me3 binding signal of the FBXW7 ChIP data in the ENCODE database, The primers used for ChIP-qPCR assays were selected based on the H3K4me3 binding signal of the FBXW7 ChIP data in the ENCODE database, which showed an obvious H3K4me3 peak in the TSS region of the *FBXW7* gene. Four primers were in TSS region and five primers downstream of the *FBXW7* gene. To confirm this, ChIP-PCR was performed to look at H3K4me3 binding and consistently with the ENCODE data (**Figure 3B**), revealed significant enrichments of H3K4me3 peaks in this same region. An obvious KDM5c enrichment was detected in the FBXW7 gene TSS between chromosome 4 152319971 and 152320116. And KDM5c signal was also observed in a region downstream of the FBXW7 transcription area at chromosome 4 152534873. Furthermore, a H3K4me3 peak was also tested in the *c-Jun* gene TSS between chromosome 1 58778991 and 58780100. While, no obvious KDM5c enrichment was teseted in the *c-Jun* gene TSS and within 2 kb of downstream sequence (**Figure 3C**). These data suggest that KDM5c does not directly control c-Jun expression, but promotes c-Jun accumulation by suppressing FBXW7 expression.

KDM5c Adjusts DNA Methylation Loci in the FBXW7 Gene Region

The online software MethPrimer[2] predicts that chromosome 4 152324318–152326358, which was between TSS and the first exon of the *FBXW7* gene, contains three CpG islands at −918/768, −683/498, and −384/129 (**Figure 4A**). And TSS of *c-Jun* (chromosome 158778791–58780791) also contains 3 CpG islands at −1420/641, −638/499, and −429/58 (**Figure 4D**). The sequences of FBXW7 CpG islands are presented in **Figure 4B**, with the methylation loci indicated in red letters and the primer-annealing positions boxed. The methylation patterns of these CpG sites were determined using bisulfite-assisted sequencing for RKO cells transfected with empty vector or KDM5c-SCMV in three individual trials. The same CpG sites were identified in all clones. The methylation percentages of all CpG sites in the three CpG islands were determined for the *FBXW7* and *c-Jun* RKO empty vector and KDM5c-OE and further assessed using QUMA software[3]. As shown in **Figure 4C**, the DNA methylation levels of (384/129) CpG island changed significantly between the empty vector and KDM5c-OE (34.2 ± 5.26% and 57.1 ± 6.95%). However, no methylation was detected for the other two CpG islands, (918/768) and (683/498), showed, suggesting that the (384/129) CpG island of the FBXW7 gene plays a major role in regulating the significantly higher DNA methylation levels adjusted by KDM5c. Furthermore, five primers were set up for detection the three CpG islands in the TSS of c-Jun gene (the sequence of CpG islands are presented in **Supplementary Material**), we found that KDM5c overexpression did not affect the methylation of CpG in *c-Jun* gene (**Figure 4E**), suggesting that KDM5c does not affect *c-Jun* gene expression by affecting DNA methylation.

DNMT3b May Mediate the Formation of DNA Looping Between CpG Islands Near the TSS and the H3K4me3 Peak Downstream of FBXW7

H3K4me3 in the TSS region is a recognized transcription initiation marker, which achieves transcriptional inhibition through histone and DNA bimodal methylation (22). However, we want to further explore how downstream H3K4me3 demethylation can achieve transcriptional inhibition. Despite their linear distance from each other, we hypothesized that the target sites of KDM5c and DNA demethylase might be brought physically into close proximity to each other by DNA looping. Based on previous studies that suggested DNMT3B expression might contribute to the CpG island methylator phenotype in colorectal cancer (23), we investigated DNMT3B as a DNA demethylase conformer member. If close together, KDM5c- and DNMT3B-binding fragments digested by the same restriction enzymes should be able to be ligated and detected by qPCR method. To test this hypothesis, we performed ChIP combined with chromosome conformation capture (ChIP-3C) assays in RKO cells. We designed two primers (P3 and P4) located in the promoter region flanking CpG island candidates. The binding site of P3 targets the position of CpG island near the TSS of FBXW7, which is the position where methylation is controlled by KDM5c (**Figure 4F**). In addition, we designed another two

[2]http://www.urogene.org/methprimer/

[3]http://quma.cdb.riken.jp/

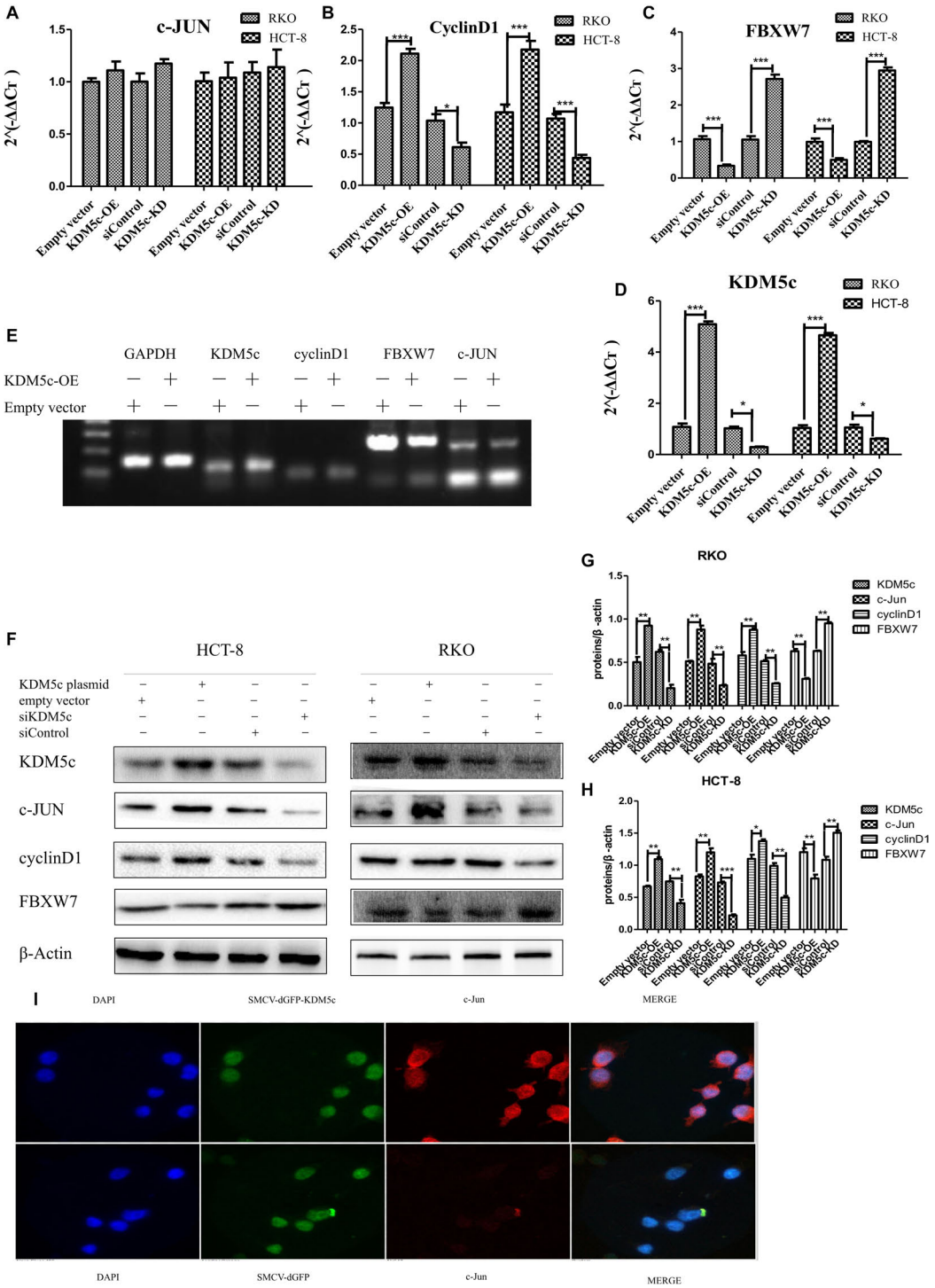

FIGURE 2 | KDM5c overexpression modified downstream gene expression. **(A–D)** Quantitative PCR (qPCR) data of c-Jun **(A)**, Cyclin D1 **(B)**, FBXW7 **(C)**, and KDM5c **(D)** expression in RKO and HCT-8 cells that were transfected with the empty vector (Control), KDM5c-SMCV (KDM5c-OE), siRNA (siControl), and siKDM5c. **(E)** RT-PCR results showing the kinetic transcription levels of KDM5c, cyclin D1, and FBXW7. **(F–H)** Western blot **(F)** and qualification **(G,H)** analysis showing that the overexpression of KDM5c in both RKO and HCT-8 cells increased c-Jun and cyclin D1 but reduced FBXW7 protein levels. The level ofβ-Actin was detected as the loading control. **(I)** Immunofluorescence indicates that HCT-8 cells transfected with MSCV-dGFP-KDM5c expressed more c-Jun than those transfected with MSCV-dGFP-null. The presented data are from two independent experiments. Upper panel: staining of HCT-8 overexpression of KDM5c. Lower panel: cell nucleus (blue), KDM5c (green), and c-Jun (red) staining of HCT-8 transfected with the empty vector. Merge: cell nucleus (blue), KDM5c (green), and c-Jun (red) overlap. Scale bar = 25 μm. Data indicate the mean ± SD from four technical replicates. Non-significant, $P > 0.05$; *$P \leq 0.05$; **$P \leq 0.01$; ***$P \leq 0.001$. This experiment was repeated three times with similar results.

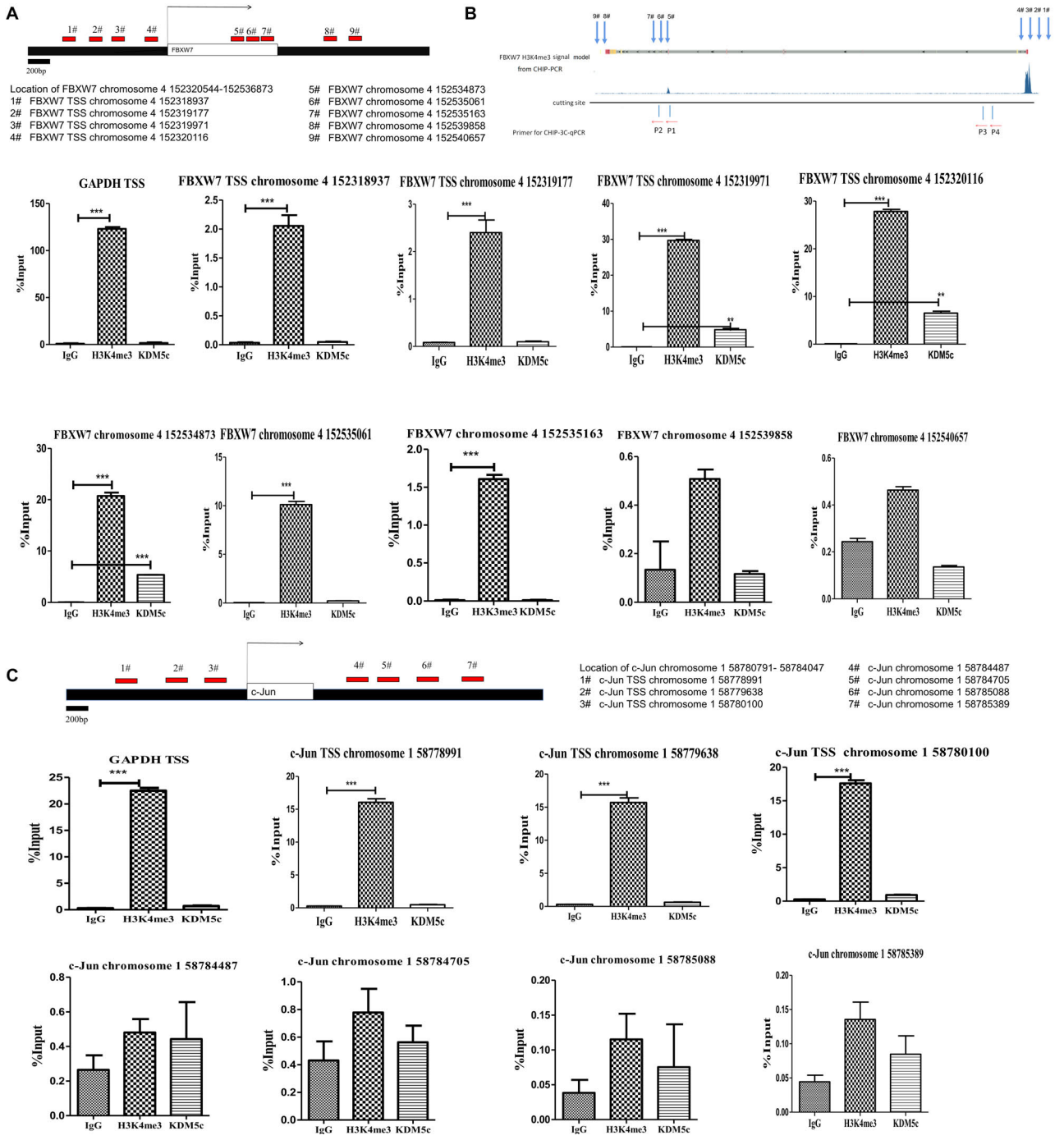

FIGURE 3 | H3K4me3 modification level and its binding proximity to KDM5c as determined by ChIP-qPCR assays. **(A,B)** Primer locations selected according to the H3K4me3 distribution patterns in the FBXW7 gene. The #1–4 primers, respectively, anneal to chromosome 4 152318937, 152319177, 152319971, and 152320116 in the TSS region of FBXW7; the #5–9 primers, respectively, anneal to chromosome 4 152534873, 152535061, 152535163, 152539858, and 152540657 in the downstream of the FBXW7 gene. The H3K4me3 peak distribution was determined by ChIP-qPCR using H3K4me3-specific antibodies. The location of KDM5c reciprocal DNA was determined by KDM5c-specific antibodies. The structure diagram shows the relationship between the loci and the anchor points in 3C-CHIP (showed in **Figure 4**) **(B)**. The ChIP-qPCR values are shown below. H3K4me3 enrichments were tested in #3–4 and #5–6 locations in FBXW7 gene. Enrichment of KDM5c was detected in the #3–4 and #5 locations in the FBXW7 gene. **(C)** Primer locations chosen according to the H3K4me3 distribution patterns in the c-Jun gene. The #1–3 primers, respectively, anneal to chromosome 1 58778991, 58779638, 58780100 in the TSS region of the c-Jun gene; the #4–7 primers, respectively, anneal to chromosome 1 58784487, 58784705, 58785088, and 58785389 in the downstream of the c-Jun genes. A H3K4me3 enrichment was tested in the #1–3 locations. And no obvious enrichment of KDM5c also was detected in the *c-Jun* gene. Experiments were repeated three times, each with three qPCR measurements, and the value for the representative experiment is shown as the mean ± SEM. * Above the bars indicates significant difference; $P > 0.05$; $^{*}P \leq 0.05$; $^{**}P \leq 0.01$; $^{***}P \leq 0.001$.

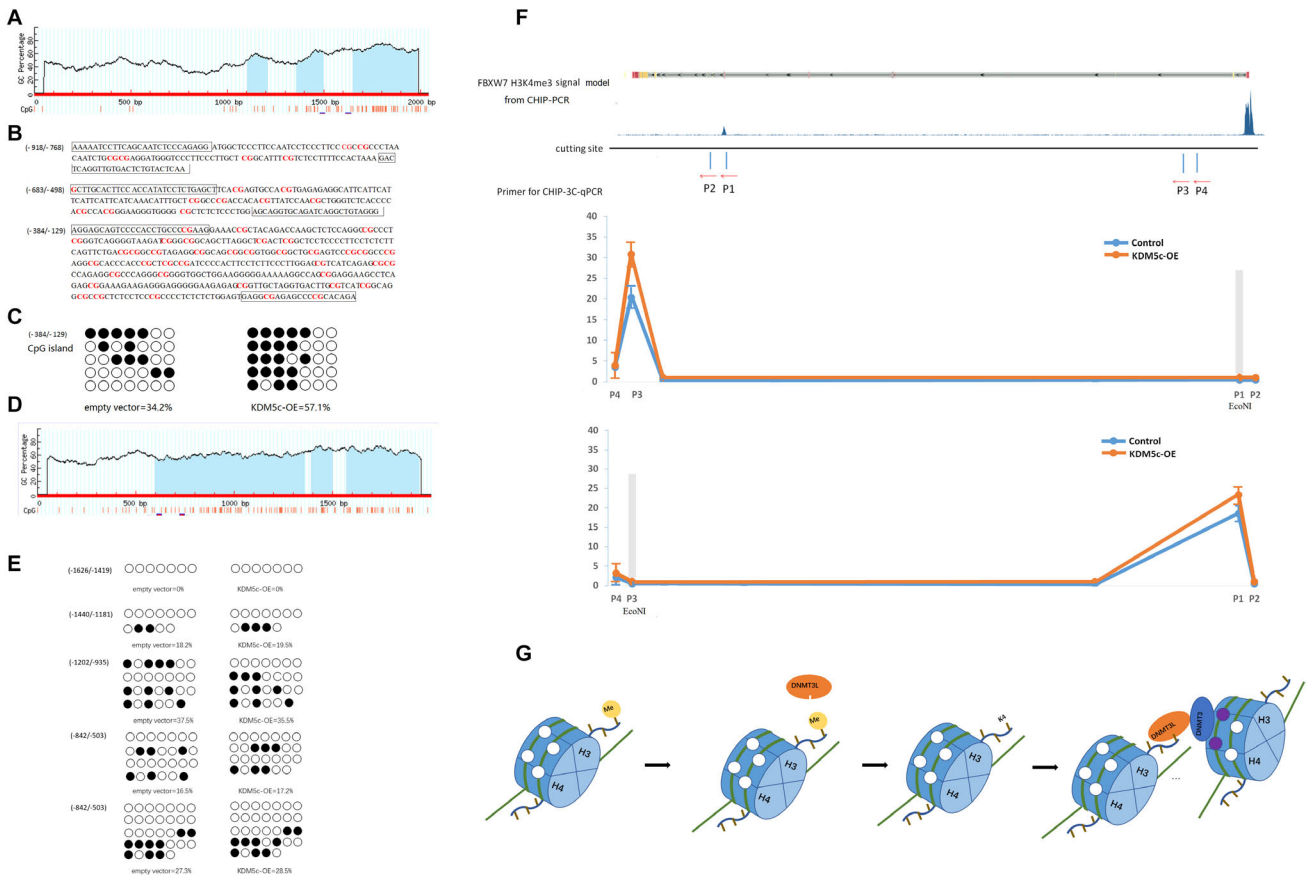

FIGURE 4 | KDM5c overexpression modifies the DNA methylation profile of the FBXW7 gene and its potential regulation. **(A)** Schematic representation of the FBXW7 promoter. The FBXW7 gene is located on chromosome 4, and a 2-kb promoter region spans from 152324318 to 152326358 (NCBI accession NG_029466). The GC percentage is indicated by blue background. The *x*-axis denotes the bp position in the 5′-untranslated region relative to the TSS. **(B)** Sequence of the CpG islands of the FBXW7 gene. The methylation loci are marked in red letters and the primer annealing positions are boxed. **(C)** The percentages of (384/129) CpG islands were analyzed using QUMA software. **(D)** Schematic representation of the c-Jun promoter. The c-Jun gene is located on chromosome 1, and a 2-kb promoter region spans from 58778791 to 58780791 (NCBI accession NC_000001.11). The GC percentage is indicated by. The *x*-axis denotes the bp position in the 5′-untranslated region relative to the TSS. **(E)** The percentages of *c-Jun* CpG islands were analyzed using QUMA software. **(F)** The relative association between the (384/129) CpG islands and the H3K4me3 peak interacting with KDM5c was detected by ChIP-3C-qPCR assays in RKO cells. The upper panel shows the H3K4me3 of the FBXW7 ChIP-seq signal in ENCODE, the *Eco*NI cleavage site, and the locations of primers used for ChIP-3C-qPCR assays. The lower panel shows the qPCR results. **(G)** Schematic figures showing how KDM5c adjusts the methylation of distant CpG islands.

primers (P1 and P2) downstream of FBXW7. P1 binds near the region of DNA bound by KDM5c. *Eco*NI restriction enzyme only acts on the DNA fragment amplified by P3 and P1, *Sna*BI only acts on the DNA fragment amplified by P3 and P2, *Sal*I only acts on the DNA fragment amplified by P4 and P1, and *Not*I only acts on the fragment produced by amplification by P3 and P2. As shown in **Figure 4D**, after cleaving the gene fragment with *Eco*NI restriction enzyme, the gene fragment enriched with DNMT3B antibody can be amplified by PCR detection using P1 and P3 primers. Thereby, we speculate that KDM5c demethylates H3K4me3 bound downstream of FBXW7 and recruits DNMT3 to remove the methylation of the DNA CpG island located upstream of the FBXW7 TSS, resulting in the downregulation of FBXW7 expression. All in all, KDM5c can increase the exposure of H3K4 by removing H3K4me3 methylation, recruit the DNMT3/DNMT3L complex containing, and induce demethylation of no matter linear distance proximity or spatially adjacent DNA CpG island to induce transcription initiation (**Figure 4G**).

KDM5c Overexpression Inhibits c-Jun Degradation via the Ubiquitin-Proteasome Pathway

Since FBXW7 is a ubiquitin ligase that targets c-Jun for proteasome-mediated degradation, we examined whether KDM5c overexpression decreases c-Jun ubiquitination by suppressing FBXW7 expression. Immuno-purified c-Jun was incubated with crude lysates of RKO cells transfected with wild-type KDM5c. Consistent with previous report, FBXW7-promoted formation of Ub-c-Jun conjugates, which were immunoprecipitated with anti-c-Jun antibody and detected

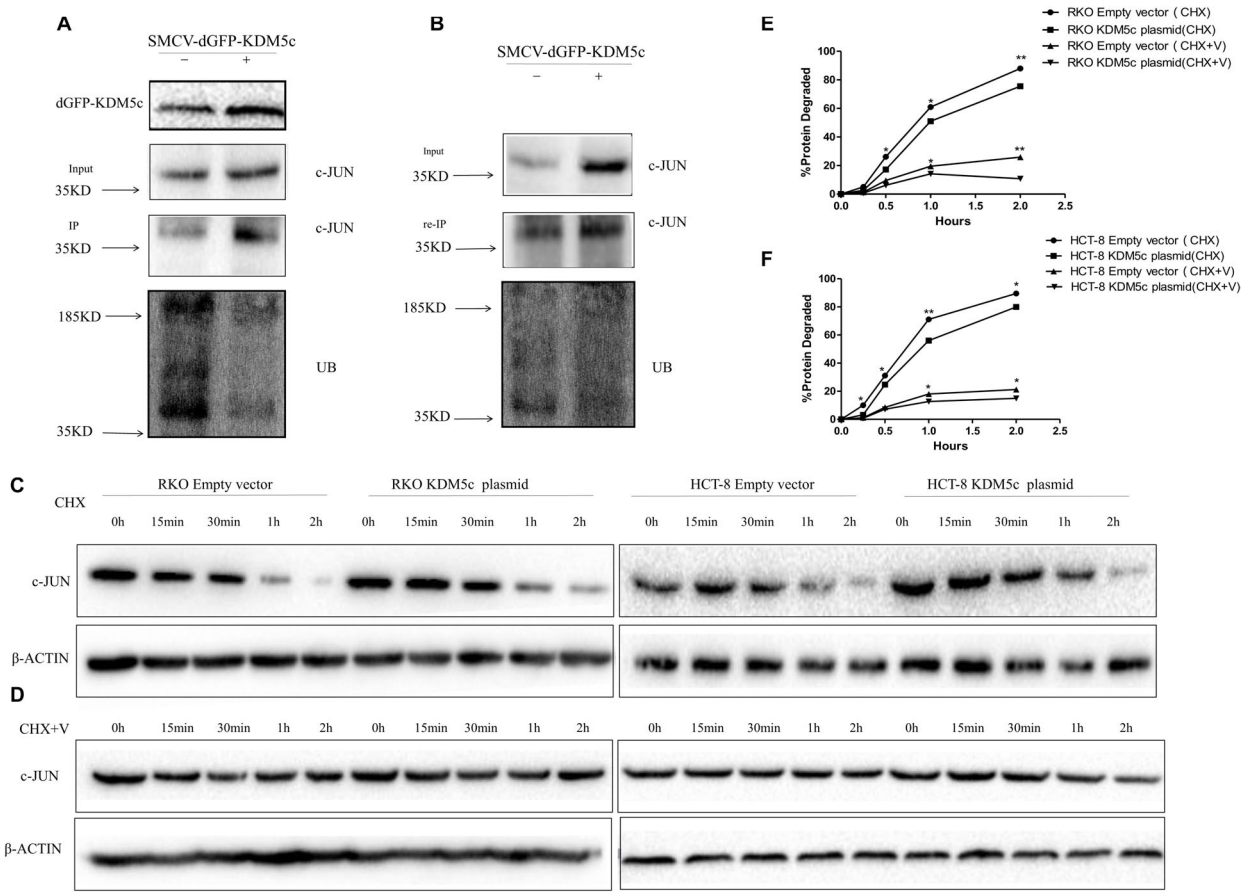

FIGURE 5 | KDM5c reduces proteasome-mediated c-Jun degradation. **(A)** KDM5c reduces the ubiquitination of c-Jun *in vivo*. RKO cells were transfected with an empty vector or vector encoding KDM5c-dGFP. After immunoprecipitation of c-Jun from lysates, the levels of c-Jun and ubiquitinated c-Jun were determined by Western blot using antibodies against c-Jun or Ub. **(B)** Re-immunoprecipitation of the ubiquitinated c-Jun. After the ubiquitination assay performed as in **(A)**, the proteins were eluted from the beads using SDS sample buffer, re-incubated with antic-c-Jun antibody, and then c-Jun ubiquitination was detected as in **(A)**. **(C)** Time course of c-Jun loss in either RKO or HCT-8 cells. Cells transfected with either the empty vector or KDM5cOE were treated with cycloheximide (CHX) (100 ug/ml) to inhibit protein biosynthesis before examination. The level of β-Actin was detected as the loading control. **(D)** Time course of c-Jun loss in the same cells as in **(C)** after the combined treatment of proteasome inhibitor VELCADE and CHX. Cells were first treated by 100 nM VELCADE for 12 h, then combined with 5 mg/ml CHX for another 2 h. β-Actin was detected as the loading control. **(E,F)** Quantitation of Western blots. Bands corresponding to c-Jun got from RKO **(E)** and HCT-8 **(F)** transfected with an empty vector or vector encoding KDM5c-dGFP and treated with CHX or CHX and VELCADE were quantified. C-JUN levels were normalized toβ-Actin. Data represent mean ± SD from two biological replicates. Non-significant, $P > 0.05$; $^{*}P \leq 0.05$; $^{**}P \leq 0.01$.

using an anti-ubiquitin antibody. Notably, in the c-Jun immunoprecipitates, the predominant ubiquitylated band was detected above 37 kDa (**Figure 5A**). The KDM5c-OE group exhibited lower ubiquitin level and higher c-Jun protein level. The putative ubiquitin-c-Jun conjugates were eluted from the beads using SDS sample buffer and re-immunoprecipitated with the anti-c-Jun antibody, indicating Ub is covalently conjugated to c-Jun (**Figure 5B**). To examine whether KDM5c overexpression can slow c-Jun metabolism, RKO cells were treated with CHX (1 μM) to inhibit protein synthesis, and then c-Jun protein dynamics were measured by western blot. The c-Jun protein level decreased gradually within the 2 h after CHX treatment (**Figure 5C**) and KDM5c-OE cells exhibited obviously reduced c-Jun degradation rate after CHX treatment. Moreover, the highly specific proteasome inhibitor VELCADE inhibited c-Jun degradation (**Figure 5D**), suggesting that the observed decrease in c-Jun content is largely due to degradation by the 26S proteasome. With combined treatment of CHX and VELCADE, KDM5c-OE cells further extended the c-Jun metabolic time. Interestingly, when colon cells were treated with both CHX and VELCADE, there was less of a difference of metabolic rate between KDM5c-OE colon cancer cells and control cells than that with CHX treatment alone. These data are statistically significant (**Figures 5E,F**) and suggest that KDM5c can inhibit the ubiquitin-26S proteasome degradation pathway of c-Jun.

KDM5c Promotes Cell Proliferation by Downregulating FBXW7 but Upregulating c-Jun in Colon Cancer Cells

The results described above suggest a mechanism in which KDM5c promotes cell proliferation by downregulating FBXW7

but upregulating c-Jun. To test this hypothesis, we next performed functional studies to measure cell proliferation and cell cycle progression. We co-transfected wild type KDM5c and FBXW7 as the KDM5c-OE/FBXW7-OE group (**Figures 1A,B**), which inhibited growth of RKO/HCT-8 cells (**Figures 6C,D**) and reduced colony formation (**Figures 6I–L**), with fewer G2/M phase cells and more G2 phase cells (**Figures 6E–H**). FBXW7 overexpression eliminated the oncogenicity of KDM5c, indicating downregulation of FBXW7 is necessary for tumorigenesis of KDM5c. However, colon cancer cells co-transfected with KDM5c, FBXW7, and c-Jun as KDM5c-OE/FBXW7-OE/c-Jun-OE cells, exhibited significantly increased cell growth and increased colony formation, with more G2/M phase cells and fewer G1 phase cells. The results show that C-JUN overexpression improves cell proliferation after FBXW7 overexpression, indicating that c-Jun is the downstream target of FBXW7.

TCGA Database Show High Expression of KDM5c in Colon Cancer Tissue Consistent With High Methylation in KDM5c DNA and Poor Overall Survival

To assess KDM5c expression levels in colon cancer, we first analyzed the expression of KDM5c mRNA in 464 colon cancer tissues samples from a TCGA dataset (The Cancer Genome Atlas)[4] and found that KDM5c expression was significantly increased in colon cancer tissue samples compared with normal tissue samples (**Figure 7A**). Patients with high expression of KDM5c exhibited decreased overall survival rates compared to those with low expression of KDM5c in the first 7 years, $p = 0.25$ (**Figure 7B**). The TCGA database DNA methylation analysis showed that higher methylation of FBXW7 DNA in colon cancer tissue correlated with high expression of KDM5c, ($p < 0.05$) but there was no association of JUN DNA methylation with KDM5c expression ($p > 0.05$) (**Figure 6C**). There were no direct differences for gender, pathological type, and tumor stage between the high and low KDM5c expression groups. The clinical information for all samples is provided in the **Supplementary Material**.

DISCUSSION

Colorectal cancer (CRC) is one of the leading causes of cancer death, but effective treatments remain limited, leading to a critical demand to identify and exploit novel therapeutic target. In this study, we identified the histone demethylase KDM5c as an interesting target candidate. KDM5c plays an important role in controlling human colon cancer cell proliferation. Specifically, KDM5c protein level can alter colon cancer cell growth by deregulating transcription of the cancer cell repressor gene FBXW7 (**Figure 2**), thereby, modulating c-Jun degradation via the ubiquitin-proteasome pathway (**Figure 4**). Thus, our work has revealed a novel function of KDM5c and the underlying mechanism of this function.

[4]http://ualcan.path.uab.edu/analysis.html

Colorectal cancer is a complex disease and was originally thought to result from genetic alterations in key regulatory genes and pathways (24). Later discoveries revealed that epigenetic modifications such as DNA methylation, histone modifications, and non-coding RNA play more essential roles in CRC pathogenesis (25). However, the relationship between these genetic and epigenetic contributions remains to be clarified. In this study, enhanced KDM5c expression increased c-Jun protein level and knock-down of KDM5c reduced c-Jun protein level (**Figure 2**), indicating strong association of KDM5c with c-Jun function. Modulation of c-Jun by KDM5c suggests epigenetic mechanisms target key gene regulators during CRC development. However, in a previous study, JARID1C promoted metastasis of breast cancer cells via down regulation of BRMS1 expression, and silencing of JARID1C dramatically increased BRMS1 expression, both at the mRNA and protein level (26). This is opposite to the way KDM5c regulates the c-Jun protein, suggesting different mechanisms may allow different functions of KDM5c in different cancer types. In the future, KDM5c inhibitor development, *in vivo* detection of KDM5c, and animal experiments can be applied to further investigate the importance of KDM5c as a target for CRC treatment.

As an important tumor suppressor by the negative regulation of many oncogenic proteins, FBXW7 is under tight control through various mechanisms, including non-coding RNA, methylation, and other genetic regulation (27). Our work here indicates that FBXW7 is a critical downstream target modulated by KDM5c, indicating a new regulatory mechanism by which FBXW7 is regulated. Whether this regulation is specific to CRC or also exists in other cancer types remains to be determined. As the histone methyltransferase EZH2 catalyzes H3K27me3 on FBXW7 (28), future research should investigate if EZH2 may counteract the action of KDM5c to balance the FBXW7 methylation level.

Histone methylation cooperates with DNA modification to modulate gene expression programming, despite the requirement of these two systems for different sets of enzymes to catalyze different chemical reactions (29). Histone methylation helps to direct DNA methylation patterns, and DNA methylation is facilitated by the DNMT3 binding partner, DNMT3L, which binds to chromatin by recognizing the K4 residue on histone H3 (30). If this histone moiety is methylated, the complex cannot bind and the underlying DNA region is thus protected from *de novo* methylation. Generally, H3K4me3 binds within the TSS region and up to 5 kb downstream from actively transcribed genes (31), but it is unclear how H3K4me3 downstream of transcription region affects DNA methylation in the TSS region. In this work, a H3K4me3 peak interacting with KDM5c is located downstream of the FBXW7 coding sequence, and the CpG island that exhibits increased methylation after KDM5c overexpression is located upstream of the TSS. If the H3K4me3 peak acts as the anchor of DNMT3L and recruits DNMT3 to methylate the CpG island in the TSS region, then the two sites, more than 16000 bp apart. As shown by our 3C-ChIP data, the CpG island in the FBXW7 gene TSS region and a H3K4me3 peak in the downstream portion of the FBXW7 gene are indeed physically close and connected by DNMT3 (**Figure 4**). Therefore, our

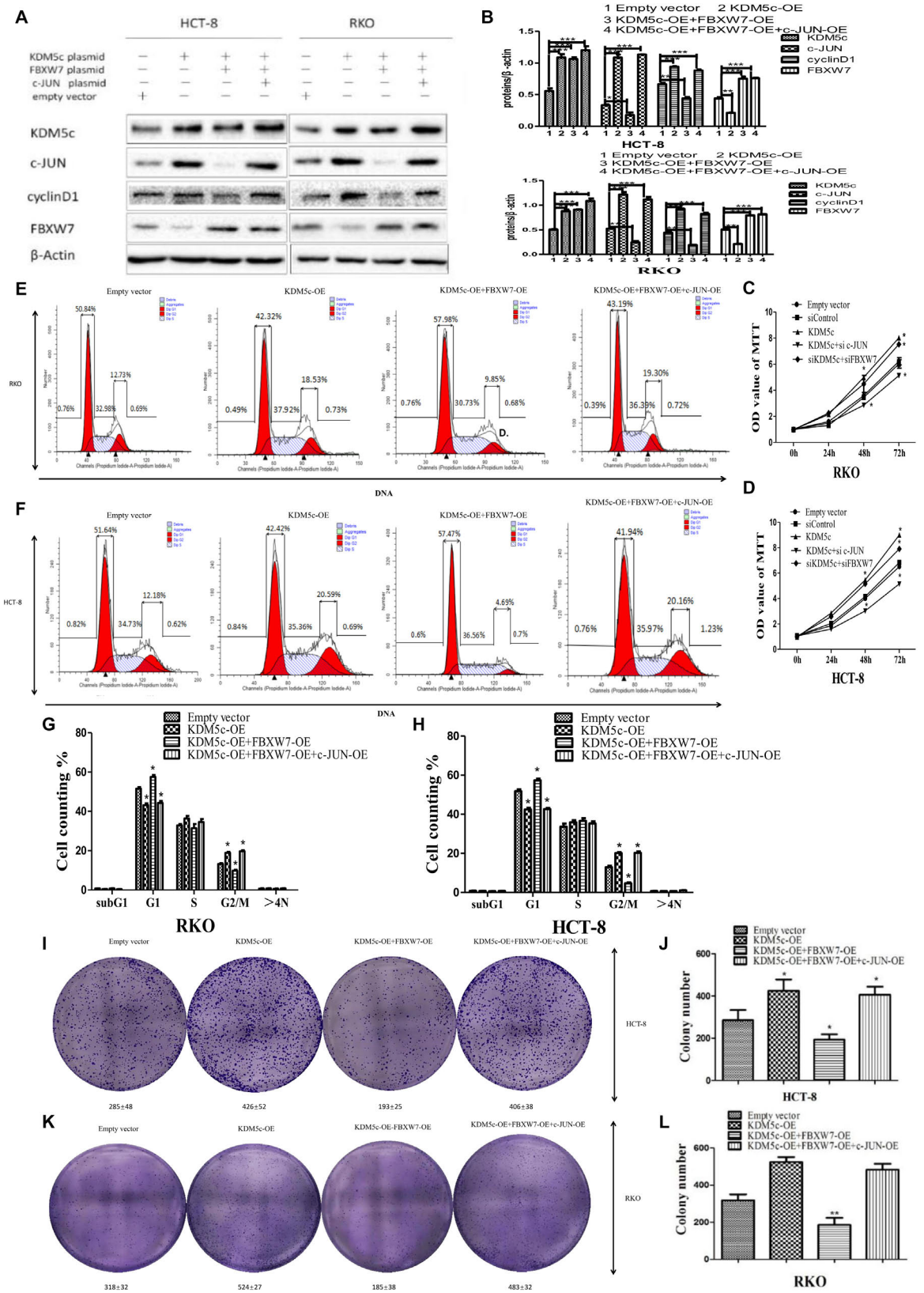

FIGURE 6 | Continued

FIGURE 6 | Overexpression of KDM5c promotes colon cancer cells by downregulating FBXW7 to indirectly change levels of the downstream regulator c-Jun. **(A,B)** Representative Western blots **(A)** and quantification **(B)** showing the protein levels of c-Jun, cyclin D1, and FBXW7 in either HCT-8 or RKO cells transfected by empty vector, KDM5c-OE, KDM5c-OE/FBXW7-OE or KDM5c-OE/FBXW7-OE/c-Jun-OE. **(C,D)** MTT assays to detect cell proliferation rates of the cell lines described in **(A)** 72 h after transfection. **(E,F)** Representative flow plots of the same cell lines as in **(A)**. **(G,H)** Statistical results showing that the fraction of G2/M phase cells was significantly increased in KDM5c-OE and KDM5c-OE + FBXW7-OE + c-Jun-OE and decreased in KDM5c-OE + FBXW7-OE RKO (left) and HCT-8 (right) cells. **(I)** 2-D colony formation assay showing colony formation changes in HCT-8 cells transfected by empty vector, KDM5c-OE, KDM5c-OE/FBXW7-OE, or KDM5c-OE/FBXW7-OE/c-Jun-OE. **(J)** In HCT-8 cells KDM5c-OE significantly increased colony formation compared to empty vector, and KDM5c-OE/FBXW7-OE significantly decreased colony formation compared to KDM5c-OE/FBXW7-OE/c-Jun-OE line. **(K)** 2-D colony formation assay showing colony formation changes in RKO cells transfected by empty vector, KDM5c-OE, KDM5c-OE/FBXW7-OE or KDM5c-OE/FBXW7-OE/c-Jun-OE. **(L)** In RKO cells, the KDM5c-OE group exhibited significantly increased colony formation compared to empty vector, while KDM5c-OE/FBXW7-OE exhibited significantly decreased colony formation compared to KDM5c-OE/FBXW7-OE/c-Jun-OE line. Column: mean; Error bar: standard error of the mean (SEM). Statistical analysis was performed and *p*-values were calculated. * Above the bars indicates significant difference; $^{*}P \leq 0.05$; $^{**}P \leq 0.01$; $^{***}P \leq 0.001$.

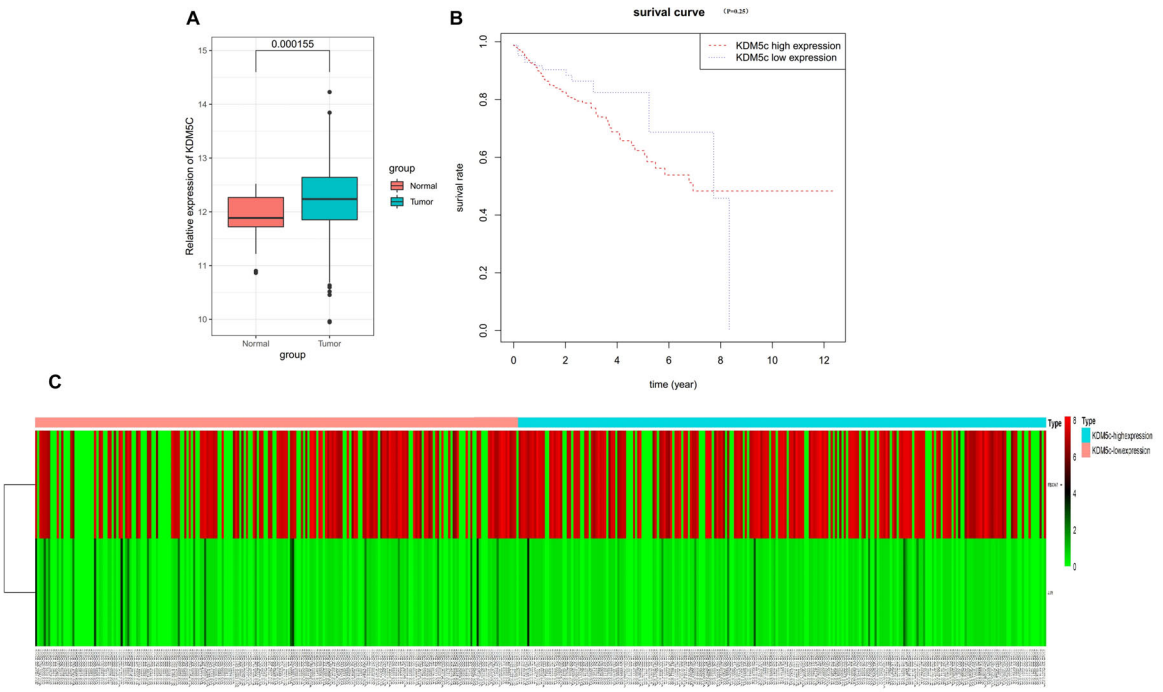

FIGURE 7 | TCGA database analysis. **(A)** TCGA dataset analysis revealed that the KDM5c mRNA levels were significantly increased in colon cancer, ($P < 0.05$). **(B)** Overall survival rates of patients with colon cancer stratified by the expression of KDM5c were analyzed via Kaplan-Meier survival analysis. **(C)** Heat map of the methylation levels of the FBXW7 and JUN genes in 473 human colon cancer tissues as sourced from TCGA. The upper panel shows that colon cancer tissues with higher KDM5c expression exhibit higher methylation levels in the FBXW7 gene. The lower panel shows that KDM5c expression in colon cancer tissue has no relationship with the methylation level in the c-Jun gene.

results provide insights into the coordination between histone methylation and DNA methylation.

CONCLUSION

In conclusion, KDM5c promotes *in vitro* colon cancer cell growth by a mechanism involving demethylation of H3K4me3 in the TSS and downstream of the tumor suppressor gene *FBXW7*. H3K4me3 demethylation may recruit DNMT3b, resulting in methylation of the CpG island located near the TSS. This causes downregulation of *FBXW7* expression, which reduces the ubiquitin-proteasome-mediated degradation of proto-oncogene c-Jun. The *in vivo* data from TCGA validate our conclusions. Our results demonstrate a novel epigenetic regulatory pathway in colon cancer and suggest KDM5c demethylase as an exciting potential target for colon cancer therapy.

DATA AVAILABILITY STATEMENT

All datasets generated for this study are included in the article/**Supplementary Material**.

ETHICS STATEMENT

Written informed consent was obtained from the individual(s) for the publication of any potentially identifiable images or data included in this article.

AUTHOR CONTRIBUTIONS

HL and BC designed the study. HL and NM developed the methodology, performed the analyses, and collected the data. LZ analyzed the data. HL and GY wrote the first draft. All the authors contributed to the review and revision of the manuscript, and read and approved the final manuscript.

FUNDING

This work was supported by the start-up fund from the Digestive Medical Coordinated Development Center of Beijing Hospitals Authority (No: XXT01 to BC), the Capital Health Research and Development of Special (2018-2-2022 to BC), the Beijing Key Clinical Specialty (2018-2020 to BC), the Pilot Project of Clinical Collaboration with Traditional Chinese Medicine and Western Medicine in Major Refractory Disease–Esophageal Cancer (to BC), the Beijing Municipal Administration of Hospitals' Youth Program (Code: QML20170102 to LZ), and the Beijing Natural Science Foundation (No. 7184200 to LZ).

ACKNOWLEDGMENTS

We thank the lab in Beijing Friendship Hospital for all the experimental facilities.

SUPPLEMENTARY MATERIAL

The Supplementary Material for this article can be found online at: https://www.frontiersin.org/articles/10.3389/fonc.2020.535449/full#supplementary-material

REFERENCES

1. Riley JM, Cross AW, Paulos CM, Rubinstein MP, Wrangle J, Camp ER. The clinical implications of immunogenomics in colorectal cancer: a path for precision medicine. *Cancer.* (2018) 124:1650–9. doi: 10.1002/cncr.31214
2. Hanley MP, Hahn MA, Li AX, Wu X, Lin J, Wang J, et al. Genome-wide DNA methylation profiling reveals cancer-associated changes within early colonic neoplasia. *Oncogene.* (2017) 35:5035–44. doi: 10.1038/onc.2017.130
3. Sugai T, Takahashi Y, Eizuka M, Ryo S, Fujita Y, Habano W, et al. Molecular profiling and genome-wide analysis based on somatic copy number alterations in advanced colorectal cancers. *Mol Carcinog.* (2018) 57:451–61. doi: 10.1002/mc.22769
4. Takane K, Akagi K, Fukuyo M, Yagi Y, Takayama T, Kaneda A. DNA methylation epigenotype and clinical features of NRAS-mutation (+) colorectal cancer. *Cancer Med.* (2017) 6:1023–35. doi: 10.1002/cam4.1061
5. Testa U, Pelosi E, Castelli G. Colorectal cancer: genetic abnormalities, tumor progression, tumor heterogeneity, clonal evolution and tumor-initiating cells. *Med Sci (Basel).* (2018) 6:31–6. doi: 10.3390/medsci6020031
6. Caretti A, Sirchia SM, Tabano S, Zulueta A, DallOlio F, Trinchera M. DNA methylation and histone modifications modulate the β1,3 galactosyltransferase β3Gal-T5 native promoter in cancer cells. *Int J Biochem Cell Biol.* (2012) 44:84–90. doi: 10.1016/j.biocel.2011.09.010
7. Hashimoto H, Vertino PM, Cheng X. Molecular coupling of DNA methylation and histone methylation. *Epigenomics.* (2010) 2:657–69. doi: 10.2217/epi.10.44
8. Herceg Z, Lambert MP, van Veldhoven K, Demetriou C, Vineis P, Smith MT, et al. Towards incorporating epigenetic mechanisms into carcinogen identification and evaluation. *Carcinogenesis.* (2013) 34:1955–67. doi: 10.1093/carcin/bgt212
9. Iwase S, Lan F, Bayliss P, de la Torre-Ubieta L, Huarte M, Qi HH, et al. The X-linked mental retardation gene SMCX/JARID1C defines a family of histone H3 lysine 4 demethylases. *Cell.* (2007) 128:1077–88. doi: 10.1016/j.cell.2007.02.017
10. Yap KL, Zhou MM. Structure and mechanisms of lysine methylation recognition by the chromodomain in gene transcription. *Biochemistry.* (2011) 29:1966–80. doi: 10.1021/bi101885m
11. DeVaux RS, Herschkowitz J. Beyond DNA: the role of epigenetics in the premalignant progression of breast cancer. *J Mammary Gland Biol Neoplasia.* (2018) 23:223–35. doi: 10.1007/s10911-018-9414-2
12. Spangle JM, Dreijerink KM, Groner AC, Cheng H, Ohlson CE, Lin CY, et al. PI3K/AKT signaling regulates H3K4 methylation in breast cancer. *Cell Rep.* (2016) 15:2692–704. doi: 10.1016/j.celrep.2016.05.046
13. Xu L, Wu W, Cheng G, Qian M, Hu K, Yin G, et al. Enhancement of proliferation and invasion of gastric cancer cell by KDM5C via decrease in p53 expression. *Technol Cancer Res Treat.* (2017) 16:141–9. doi: 10.1177/1533034616629261
14. Chang S, Yim S, Park H. The cancer driver genes IDH1/2, JARID1C/ KDM5C, and UTX/ KDM6A: crosstalk between histone demethylation and hypoxic reprogramming in cancer metabolism. *Exp Mol Med.* (2019) 51:66–71.
15. Wu L, Cao J, Cai WL, Lang SM, Horton JR, Jansen DJ, et al. KDM5 histone demethylases repress immune response via suppression of STING. *PLoS Biol.* (2018) 16:e2006134. doi: 10.1371/journal.pbio.2006134
16. Reinera J, Ye F, Kashikar ND, Datta PK. STRAP regulates c-Jun ubiquitin-mediated proteolysis and cellular proliferation. *Biochem Biophys Res Commun.* (2011) 407:372–7. doi: 10.1016/j.bbrc.2011.03.028
17. Wisdom R, Johnson RS, Moore C. c-Jun regulates cell cycle progression and apoptosis by distinct mechanisms. *EMBO J.* (1999) 18:188–97. doi: 10.1093/emboj/18.1.188
18. Li Y, Hu K, Xiao X, Wu W, Yan H, Chen H, et al. FBW7 suppresses cell proliferation and G2/M cell cycle transition via promoting γ-catenin K63-linked ubiquitylation. *Biochem Biophys Res Commun.* (2018) 497:473–9. doi: 10.1016/j.bbrc.2018.01.192
19. Nakayama S, Yumimoto K, Kawamura A, Nakayama KI. Degradation of the endoplasmic reticulum-anchored transcription factor MyRF by the ubiquitin ligase SCF^{Fbxw7} in a manner dependent on the kinase GSK-3. *J Biol Chem.* (2018) 293:5705–14. doi: 10.1074/jbc.ra117.000741
20. Csizmok V, Montecchio M, Lin H, Tyers M, Sunnerhagen M, Forman-Kay JD. Multivalent interactions with Fbw7 and Pin1 facilitate recognition of c-Jun by the SCF^{Fbw7} ubiquitin ligase. *Structure.* (2018) 26:28–39. doi: 10.1016/j.str.2017.11.003
21. Chen X, Li XY, Long M, Wang X, Gao ZW, Cui Y, et al. The FBXW7 tumor suppressor inhibits breast cancer proliferation and promotes apoptosis by targeting MTDH for degradation. *Neoplasma.* (2018) 65:201–9. doi: 10.4149/neo_2018_170228n149
22. Cedar H, Bergman Y. Linking DNA methylation and histone modification: patterns and paradigms. *Nat Rev Genet.* (2009) 10:295–304. doi: 10.1038/nrg2540
23. Nosho K, Shima K, Irahara N, Kure S, Baba Y, Kirkner GJ, et al. DNMT3B expression might contribute to CpG island methylator phenotype in colorectal cancer. *Clin Cancer Res.* (2009) 15:3663–71. doi: 10.1158/1078-0432.CCR-08-2383
24. Bien SA, Su YR, Conti DV, Harrison TA, Qu C, Guo X, et al. Genetic variant predictors of gene expression provide new insight into risk of colorectal cancer. *Hum Genet.* (2019) 138:307–26.
25. Bardhan K, Liu K. Epigenetics and colorectal cancer pathogenesis. *Cancers (Basel).* (2013) 5:676–713. doi: 10.3390/cancers5020676
26. Wang Q, Wei J, Su P, Gao P. Histone demethylase JARID1C promotes breast cancer metastasis cells via down regulating BRMS1 expression. *Biochem Biophys Res Commun.* (2015) 464:659–66. doi: 10.1016/j.bbrc.2015.07.049
27. Yeh CH, Bellon M, Nicot C. FBXW7: a critical tumor suppressor of human cancers. *Mol Cancer.* (2018) 17:115–24.

28. Jin X, Yang C, Fan P, Xiao J, Zhang W, Zhan S, et al. CDK5/FBW7-dependent ubiquitination and degradation of EZH2 inhibits pancreatic cancer cell migration and invasion. *J Biol Chem.* (2017) 292:6269–80. doi: 10.1074/jbc.m116.764407
29. Fyodorov D, Zhou BR, Skoultchi A, Bai Y. Emerging roles of linker histones in regulating chromatin structure and function. *Nat Rev Mol Cell Biol.* (2018) 19:192–206. doi: 10.1038/nrm.2017.94
30. Zhang ZM, Rui L, Wang P, Yu Y, Chen D, Gao L, et al. Structural basis for DNMT3A-mediated de novo DNA methylation. *Nature.* (2018) 554:387–91. doi: 10.1038/nature25477
31. Subhash S, Mishra K, Akhade VS, Kanduri M, Mondal T, Kanduri C. H3K4me2 and WDR5 enriched chromatin interacting long non-coding RNAs maintain transcriptionally competent chromatin at divergent transcriptional units. *Nucleic Acids Res.* (2018) 46:9384–400. doi: 10.1093/nar/gky635

Conflict of Interest: The authors declare that the research was conducted in the absence of any commercial or financial relationships that could be construed as a potential conflict of interest.

Advantages of publishing in Frontiers

OPEN ACCESS
Articles are free to read for greatest visibility and readership

FAST PUBLICATION
Around 90 days from submission to decision

HIGH QUALITY PEER-REVIEW
Rigorous, collaborative, and constructive peer-review

TRANSPARENT PEER-REVIEW
Editors and reviewers acknowledged by name on published articles

Frontiers
Avenue du Tribunal-Fédéral 34
1005 Lausanne | Switzerland

Visit us: www.frontiersin.org
Contact us: frontiersin.org/about/contact

REPRODUCIBILITY OF RESEARCH
Support open data and methods to enhance research reproducibility

DIGITAL PUBLISHING
Articles designed for optimal readership across devices

FOLLOW US
@frontiersin

IMPACT METRICS
Advanced article metrics track visibility across digital media

EXTENSIVE PROMOTION
Marketing and promotion of impactful research

LOOP RESEARCH NETWORK
Our network increases your article's readership